BRAIN PROTEIN AGING AND DEMENTIA CONTROL

EDITED BY: Gen Sobue and Naruhiko Sahara
PUBLISHED IN: Frontiers in Neuroscience and Frontiers in Neurology

frontiers Research Topics

frontiers

ISSN 1664-8714
ISBN 978-2-88945-872-1
DOI 10.3389/978-2-88945-872-1

About Frontiers

Frontiers is more than just an open-access publisher of scholarly articles: it is a pioneering approach to the world of academia, radically improving the way scholarly research is managed. The grand vision of Frontiers is a world where all people have an equal opportunity to seek, share and generate knowledge. Frontiers provides immediate and permanent online open access to all its publications, but this alone is not enough to realize our grand goals.

Frontiers Journal Series

The Frontiers Journal Series is a multi-tier and interdisciplinary set of open-access, online journals, promising a paradigm shift from the current review, selection and dissemination processes in academic publishing. All Frontiers journals are driven by researchers for researchers; therefore, they constitute a service to the scholarly community. At the same time, the Frontiers Journal Series operates on a revolutionary invention, the tiered publishing system, initially addressing specific communities of scholars, and gradually climbing up to broader public understanding, thus serving the interests of the lay society, too.

Dedication to Quality

Each Frontiers article is a landmark of the highest quality, thanks to genuinely collaborative interactions between authors and review editors, who include some of the world's best academicians. Research must be certified by peers before entering a stream of knowledge that may eventually reach the public - and shape society; therefore, Frontiers only applies the most rigorous and unbiased reviews.
Frontiers revolutionizes research publishing by freely delivering the most outstanding research, evaluated with no bias from both the academic and social point of view. By applying the most advanced information technologies, Frontiers is catapulting scholarly publishing into a new generation.

What are Frontiers Research Topics?

Frontiers Research Topics are very popular trademarks of the Frontiers Journals Series: they are collections of at least ten articles, all centered on a particular subject. With their unique mix of varied contributions from Original Research to Review Articles, Frontiers Research Topics unify the most influential researchers, the latest key findings and historical advances in a hot research area! Find out more on how to host your own Frontiers Research Topic or contribute to one as an author by contacting the Frontiers Editorial Office: researchtopics@frontiersin.org

BRAIN PROTEIN AGING AND DEMENTIA CONTROL

Topic Editors:
Gen Sobue, Nagoya University Graduate School of Medicine, Japan
Naruhiko Sahara, National Institute of Radiological Sciences, National Institutes for Quantum and Radiological Science and Technology, Japan

Citation: Sobue, G., Sahara, N., eds. (2019). Brain Protein Aging and Dementia Control. Lausanne: Frontiers Media. doi: 10.3389/978-2-88945-872-1

Table of Contents

frontiers in Neuroscience

EDITORIAL
published: 12 March 2019
doi: 10.3389/fnins.2019.00029

Editorial: Brain Protein Aging and Dementia Control

*Gen Sobue**

Nagoya University Graduate School of Medicine, Nagoya, Japan

Keywords: protein aging, dementia, toxicity, brain, neurodegeneration

Editorial on the Research Topic

Brain Protein Aging and Dementia Control

The prevention and control of dementia are challenging issues for medical sciences in the twenty-first century. Patients with neurodegenerative dementia including Alzheimer's disease, dementia with Lewy bodies, and frontotemporal lobar degeneration (FTLD) share abnormalities in brain proteins such as β amyloid, tau, TDP-43, FUS, and α-synuclein, which result in physiological dysfunction, loss of interaction with functional molecules, acquisition of toxicity and pathogenicity, and propagation associated with neural circuit breakdown.

However, issues concerning the aging of brain proteins and their acquisition of toxicity, the failure of neural circuits with resulting dementia, and the identification of therapeutic interventions that may prevent dementia have not been clarified. Since 2014, to address these crucial issues, we have defined toxicity-acquiring processes of functional proteins as "brain protein aging" and developed the novel research initiative "brain protein aging and dementia control" supported by a Grant-in-Aid for Scientific Research on Innovative Areas from MEXT.

"Brain protein aging" may be controlled and facilitated by various factors such as degradation, excretory mechanisms, stress, inflammation, and genetic factors. The process of brain aging, the expression of neural toxicity, and the mechanism of neural circuit breakdown remains to be elucidated. Therefore, our research initiative has established goals to clarify the mechanisms of initiation and pathologies of protein aging, to clarify the mechanisms of intercellular propagation of toxic proteins, and to develop novel biomarkers and drugs for each neurological disease.

"Brain protein aging" is a wide-ranged process that includes protein modifications, such as phosphorylation, glycation, and methylation, protein structural changes, aberrant liquid phase transition, common and rare variant transition leading to protein-protein and protein-RNA interaction, loss of protein physiological function, a gain of toxic function, and, eventually, neurodegeneration and dementia. To approach these problems, we generated three subgroups comprising "brain protein aging and neural circuit breakdown," "molecular basis of brain protein aging," and "development of therapies for brain protein aging. We have taken an extensive interdisciplinary and multidisciplinary approach to solve these complex problems from various angles at the molecular to individual levels controlled and facilitated by various factors such as degradation, excretory mechanisms, stress, inflammation, and genetic factors.

Based on these research strategies, we have obtained several results. We identified an impairment of RNA binding properties of RBPs, which leads to tau protein isoform disintegration (4 repeat tau to 3 repeat tau) resulting in FTLD type neurodegeneration. We reported the successful identification of toxic and propagation features of tau, TDP-43, and α-synuclein and successfully generated α-synuclein propagation models in mouse and marmoset. Finally, we demonstrated an association between autophagy and neurodegenerative diseases, the development of novel tau PET tracers, and the robustness and vulnerability of the autoregulatory system that maintains nuclear TDP-43 levels.

OPEN ACCESS

Edited by:
Einar M. Sigurdsson,
New York University, United States

Reviewed by:
Wendy Noble,
King's College London,
United Kingdom

***Correspondence:**
Gen Sobue
sobueg@med.nagoya-u.ac.jp

Specialty section:
This article was submitted to Neurodegeneration, a section of the journal Frontiers in Neuroscience

Received: *25 October 2018*
Accepted: *14 January 2019*
Published: *12 March 2019*

Citation:
Sobue G (2019) Editorial: Brain Protein Aging and Dementia Control. Front. Neurosci. 13:29. doi: 10.3389/fnins.2019.00029

This specific Topic for Frontiers in Neuroscience aims to integrate our achievements and improve the understanding of "brain protein aging." This Research Topic includes 22 articles by 99 researchers who are involved in the underlying molecular mechanisms, neurobiological processes, iPSC, model animals, PET, and brain network imaging. We also invited nine leading researchers (Drs. Jesús Avila, Laura J. Blair, Michel Goedert, Jürgen Götz, Tsuneya Ikezu, Michael J. Strong, and J. Paul Taylor) in the field related to "brain protein aging and dementia control" to submit review articles particularly on their recent work. These review articles are beneficial to the understanding of "brain protein aging." We believe that this research topic will provide current perspectives on the critical mechanisms, as well as theoretical, methodological, experimental, and clinical questions related to neurodegenerative dementia.

RESEARCH GROUPS

A01: Brain protein aging and neural circuit breakdown.
A01-1: Visualization of brain protein aging and clarification of the mechanisms of neural circuit breakdown.
A01-2: Elucidation of mechanisms for neural network disruption by protein-specific PET imaging.
A02: Molecular basis of brain protein aging.
A02-1: Mechanism of tau protein aging and toxicity.
A02-2: Molecular basis of pathogenic proteins and mechanisms of their propagation.
A02-3: Protein aging from perturbation of the robustness of nucleic acid metabolism and the elimination mechanism.
A03: Therapeutic development for brain protein aging.
A03-1: Establishment of brain protein aging models, human iPS cell models, and non-human primate models.
A03-2: Development of imaging-based diagnostic procedures for brain protein aging.
Director: Gen Sobue
Group Leaders; Gen Sobue (A01-1), Kazuhiko Yanai (A02-2), Akihiko Takashima (A02-1), Masato Hasegawa (A02-2), Osamu Onodera (A02-3), Hideyuki Okano (A03-1), Naruhiko Sahara (A03-2).

AUTHOR CONTRIBUTIONS

GS organized the project Brain Protein Aging and Dementia Control, and summarized the review articles by the all the members of the project.

Conflict of Interest Statement: The author declares that the research was conducted in the absence of any commercial or financial relationships that could be construed as a potential conflict of interest.

frontiers in Neuroscience

REVIEW
published: 12 July 2018
doi: 10.3389/fnins.2018.00473

Pathogenesis of Frontotemporal Lobar Degeneration: Insights From Loss of Function Theory and Early Involvement of the Caudate Nucleus

Gen Sobue, Shinsuke Ishigaki and Hirohisa Watanabe*

Nagoya University Graduate School of Medicine, Brain and Mind Center, Nagoya University, Nagoya, Japan

Frontotemporal lobar degeneration (FTLD) is a group of clinically, pathologically and genetically heterogeneous neurodegenerative disorders that involve the frontal and temporal lobes. Behavioral variant frontotemporal dementia (bvFTD), semantic dementia (SD), and progressive non-fluent aphasia (PNFA) are three major clinical syndromes. TDP-43, FUS, and tau are three major pathogenetic proteins. In this review, we first discuss the loss-of-function mechanism of FTLD. We focus on FUS-associated pathogenesis in which FUS is linked to tau by regulating its alternative splicing machinery. Moreover, FUS is associated with abnormalities in post-synaptic formation, which can be an early disease marker of FTLD. Second, we discuss clinical and pathological aspects of FTLD. Recently, FTLD and amyotrophic lateral sclerosis (ALS) have been recognized as the same disease entity; indeed, nearly all sporadic ALS cases show TDP-43 pathology irrespective of FTD phenotype. Thus, investigating early structural and network changes in the FTLD/ALS continuum can be useful for developing early diagnostic markers of FTLD. MRI studies have revealed the involvement of the caudate nucleus and its anatomical networks in association with the early phase of behavioral/cognitive decline in FTLD/ALS. In particular, even ALS patients with normal cognition have shown a significant decrease in structural connectivity between the caudate head networks. In pathological studies, FTLD/ALS has shown striatal involvement of both efferent system components and glutamatergic inputs from the cerebral cortices even in ALS patients. Thus, the caudate nucleus may be primarily associated with behavioral abnormality and cognitive involvement in FTLD/ALS. Although several clinical trials have been conducted, there is still no therapy that can change the disease course in patients with FTLD. Therefore, there is an urgent need to establish a strategy for predominant sporadic FTLD cases.

Keywords: frontotemporal lobar degeneration, loss of function, tau proteins, fused in sarcoma/translated in liposarcoma, amyotrophic lateral sclerosis, TDP-43 proteinopathies, caudate nucleus, marmoset

OPEN ACCESS

Edited by:
Sadayuki Hashioka, Shimane University, Japan

Reviewed by:
Rita Sattler, Barrow Neurological Institute (BNI), United States
Patrizia Longone, Fondazione Santa Lucia (IRCCS), Italy
Jesus Avila, Universidad Autonoma de Madrid, Spain

****Correspondence:***
Gen Sobue
sobueg@med.nagoya-u.ac.jp

Specialty section:
This article was submitted to Neurodegeneration, a section of the journal Frontiers in Neuroscience

Received: *31 January 2018*
Accepted: *21 June 2018*
Published: *12 July 2018*

Citation:
Sobue G, Ishigaki S and Watanabe H (2018) Pathogenesis of Frontotemporal Lobar Degeneration: Insights From Loss of Function Theory and Early Involvement of the Caudate Nucleus. Front. Neurosci. 12:473. doi: 10.3389/fnins.2018.00473

INTRODUCTION

Frontotemporal lobar degeneration (FTLD) is a clinically, genetically, and pathologically heterogeneous neurodegenerative disorder that causes selective neuronal loss and gliosis of the frontal and temporal lobes of the brain (Olney et al., 2017). "FTLD" is applied to patients whose diagnoses are genetically or pathologically confirmed. "Frontotemporal dementia (FTD)" is applied

to patients who have clinicoradiological abnormalities that correlate with FTLD but are not genetically or pathologically confirmed. Clinically, FTD patients exhibit progressive changes in behavior, language, and executive control. TAR DNA–binding protein 43 kDa (TDP–43), fused in sarcoma/translated in liposarcoma (FUS/TLS), and tau are three major causative proteins in FTLD. TDP-43 and FUS are classified as RNA-binding proteins. Interestingly, these proteins are associated with similar and consecutive clinicoradiological phenotypes.

Clarifying the upstream process of neurodegeneration and developing biomarkers for early diagnosis are essential for the future development of disease-modifying therapy for FTLD. In Asian countries, including Japan, familial FTLD is very rare (accounts for less than 10% of FTLD) (Fukuhara et al., 2014). In Western countries, more than half of FTLD patients have no family history of the disorder, although approximately 40% of patients have a familial trait. However, imaging and biological markers for sporadic FTLD, particularly those in prodromal cases, are very limited compared with the number available for Alzheimer's disease (AD) (Olsson et al., 2016) and dementia with Lewy bodies (DLB) (Iranzo et al., 2016).

Amyotrophic lateral sclerosis (ALS) has traditionally been considered a progressive neurodegenerative disorder in which the motor system is selectively involved (Hardiman et al., 2017). However, some ALS patients also present with the characteristic clinical findings of FTD during the early course of their illness (Tsujimoto et al., 2011; Masuda et al., 2016). Additionally, FTLD patients can also show upper and lower motor symptoms (Riku et al., 2014b). TDP-43, a major component of ubiquitinated inclusions, is a critically important pathogenic protein found in both sporadic FTLD and ALS (Neumann et al., 2006). Because nearly all sporadic ALS cases and more than half of sporadic FTLD cases have cytoplasmic inclusions consisting of the cleaved form of hyper-phosphorylated TDP-43 (Ling et al., 2013), TDP-43 proteinopathy was proposed as a concept that implicates FTLD-TDP and ALS as a continuous disease spectrum.

With respect to familial ALS and FTLD, a non-coding hexanucleotide repeat expansion (GGGGCC) mutation in the 50 non-coding region of the C9orf72 gene identified in familial ALS and FTLD in 2011 has provided important insights into the pathophysiological backgrounds of ALS and FTLD (DeJesus-Hernandez et al., 2011). In Western countries, the C9orf72 repeat expansion is the most common causative gene of familial ALS and FTLD. Up to 40% of patients with familial ALS, 25% with familial FTLD, especially, 88% with familial ALS-FTLD show the pathological repeat expansion (Van Mossevelde et al., 2017). Interestingly, even sporadic ALS and FTLD patients may also have the C9orf72 repeat expansion. Patients with C9orf72 repeat expansion are classified as TDP-43 pathology spectrum but show heterogeneous clinical and pathological characteristics. There are other major causal ALS genes such as SOD1, TARDBP, FUS, VCP, and PFN1. More recently, advancement of massive parallel sequencing approaches identified rare genetic variants (TBK1, CHCHD10, TUBA4A, CCNF, MATR3, NEK1, C21orf2, ANXA11, TIA1) (Nguyen et al., 2018). Pathogenic mutations of C9orf72, GRN, TBK1, and VCP are commonly linked to TDP-43 pathology. However, affected brain regions and clinical phenotype are highly variable among four mutations and are different from sporadic cases (Van Mossevelde et al., 2018).

In Japan, the frequency of the C9orf72 repeat expansion among ALS patients is much lower than that in Western populations (2/52 = 0.4% in Japan) (Ogaki et al., 2012). Twenty-eight known ALS-related genes were identified in only 3.0% of 251 Japanese sporadic ALS patients by next-generation sequencing (Nakamura et al., 2016). A pathological investigation showed that all consecutive 107 autopsied cases clinically diagnosed as sporadic ALS or progressive muscular atrophy showed TDP-43 pathology (Riku et al., 2014a). Thus, clinical and radiological factors associated with socio-cognitive decline in sporadic ALS may indicate that most sporadic ALS cases are associated with FTLD-TDP-related pathophysiology, although the continuity of the ALS/FTD spectrum remains unknown. Since sporadic cases are predominant in ALS/FTD spectrum even in Western countries, it would be crucial to identify the early structural and network changes associated with socio-cognitive decline in FTLD/ALS.

In this review, we introduce recent findings that can help detect the (1) key pathogenesis leading to neurodegeneration and (2) early structural and network changes related to early diagnosis in FTLD/ALS.

Loss-of-Function Mechanism of RNA-Binding Proteins in FTLD/ALS

Hypothesis of Loss-of-Function Theory in FTLD/ALS

Many genes have been identified in the development of ALS and FTLD, including TDP-43, FUS, and C9orf72, indicating that these two disorders comprise a spectrum of diseases (Seelaar et al., 2011; Renton et al., 2014; Riku et al., 2014b; Hayes and Rothstein, 2016). The cytoplasmic inclusion composing of TDP-43 and FUS in motor and/or cortical neurons is observed in FTLD/ALS as a major pathological hallmark, as observed in other neurodegenerative disorders (Neumann et al., 2006, 2009; Mackenzie and Neumann, 2012). There are two hypotheses for the pathomechanism of RNA-binding proteins such as TDP-43 or FUS: gain of toxicity and loss of function (Xu, 2012; Orozco and Edbauer, 2013). According to the first hypothesis, toxicity from the dislocated and aggregated protein is considered a possible cause of neuronal degeneration. According to the second hypothesis, impaired function of these nuclear proteins provoked by protein dislocation from the nucleus is considered to disturb neuronal function and lead to subsequent neuronal degeneration.

The latter hypothesis is supported by several pieces of evidence, including the fact that TDP-43 or FUS nuclear staining is decreased in the nuclei of neurons in both human FTLD/ALS tissue (Davidson et al., 2007; Neumann et al., 2009) and TDP-43-overexpressing mice (Wegorzewska et al., 2009; Igaz et al., 2011). Moreover, animal models involving the loss of either TDP-43 or FUS mimic the pathology of FTLD/ALS (Kabashi et al., 2011; Wang et al., 2011; Wu et al., 2012; Iguchi et al., 2013; Udagawa et al., 2015). Interestingly, the up- and down-regulation of TDP-43 in Drosophila produced highly similar transcriptome alterations (Vanden Broeck et al., 2013). The gene expression

profiles in neurons with simultaneous depletion of FUS and TAF15 were observed to be similar to those in ALS patient-derived neurons bearing the mutation of FUS^{R521G} (Kapeli et al., 2016). These findings indicate that loss of function and/or gain of toxicity of TDP-43 or FUS might influence wide-ranging RNA metabolism pathways in a similar manner.

However, recent evidence indicates that effects of loss of TDP-43 or FUS function on motor neurons are limited. Motor neuron-specific TDP-43 knock-out exhibited mild functional impairments in aged mice without prominent motor neuron loss (Iguchi et al., 2013). Similarly, the absence of FUS in motor neurons did not cause apparent ALS phenotypes in mice (Scekic-Zahirovic et al., 2016; Sharma et al., 2016). Thus, the absence of obvious neurodegeneration by FUS knock-out in motor neurons may indicate that loss of FUS function does not contribute to motor neuron degeneration in ALS. However, FUS knock-down or knock-out in hippocampal neurons and/or frontal lobe neurons exhibited behavioral impairments characterized by lack of anxiety, disinhibition, and hyperactivity but without apparent cognitive impairments in early disease stages (Kino et al., 2015; Udagawa et al., 2015; Ishigaki et al., 2017). Hippocampus-specific FUS silencing results in neuronal loss and hippocampal atrophy in aged mice (Ishigaki et al., 2017). These findings suggest that loss of FUS function in cerebral neurons could contribute to the neuronal dysfunction and neurodegeneration observed in FTLD.

The hippocampus is one of the most strongly affected regions in FTLD, similarly to Alzheimer's disease. Although the major function of the hippocampus is learning and memory, it has been shown that hippocampal lesions can cause emotional deficits, including hyperactivity, disinhibition, and anxiety (Bannerman et al., 2001; Barkus et al., 2010). A recent study further demonstrated that the specific subregions of the hippocampus are responsible for distinct behaviors; for example, the dorsal and ventral dentate gyri affect memory and anxiety, respectively (Kheirbek et al., 2013). Taken together with findings indicating that loss of FUS leads to neuronal cell death in Zebrafish and Drosophila (Kabashi et al., 2011; Wang et al., 2011), loss of FUS function in the hippocampus can explain the clinical and pathological features of FTLD.

Regulation of Tau Isoforms by FUS

Many neuronal function-related genes have been identified to be regulated by FUS (Ishigaki et al., 2012; Lagier-Tourenne et al., 2012; Rogelj et al., 2012; Honda et al., 2013; Nakaya et al., 2013). Intriguingly, FUS itself is auto-regulated by exon 7 skipping machinery that undergoes non-sense-mediated decay (NMD), indicating that the expression of FUS is tightly regulated and that dysregulation by disease-associated mutations is harmful to neurons (Zhou et al., 2013).

We and other groups have identified that FUS regulates an alternative splicing event of the *Mapt* gene at exon 10, which increases 4-repeat tau (4R-tau) but decreases 3-repeat tau (3R-tau) in neurons (Ishigaki et al., 2012; Lagier-Tourenne et al., 2012; Orozco et al., 2012; Rogelj et al., 2012; Fujioka et al., 2013). Loss of FUS functionality is relevant to the pathogenesis of FTLD/ALS by demonstrating that formation of the FUS intranuclear complex with splicing factor, proline-, and glutamine-rich (SFPQ), an RNA-binding protein, in neurons is compromised by FTLD/ALS-associated mutations (Ishigaki et al., 2017). SFPQ is involved in RNA splicing, DNA synthesis, gene expression, DNA repair, and cell survival (Shav-Tal and Zipori, 2002; Kameoka et al., 2004). Although FUS also binds to many other splicing factors in the crude nuclear extract, those proteins are mainly enriched in the small MW FUS complex of two FUS complexes with high MW and small MW. Thus, the high MW FUS complex and SFPQ are thought to compose the splicing machinery (Ishigaki et al., 2017). A recent study revealed novel variants of the SFPQ gene in familial ALS cases (Thomas-Jinu et al., 2017), supporting the idea that the quality loss of FUS function might be a key causal or pathological factor in FTLD/ALS. It has been previously proposed that a compromised RNA-binding protein machinery complex in the nucleus could be a cause of TDP-43- or FUS-associated FTLD/ALS (Tsuiji et al., 2013; Sun et al., 2015). Given that various RNA-binding proteins are genetically and pathologically linked to FTLD/ALS (Ling et al., 2013), our results also strengthen the hypothesis that functional disturbance of RNA metabolism in the nucleus of neurons is crucial for FTLD/ALS pathogenesis.

Because many splicing events are species-specific, it is necessary to confirm that the alternative splicing event for tau isoforms is regulated by FUS and SFPQ in human brain tissues. *MAPT* encodes tau protein, which is pathogenic for tauopathies, such as Alzheimer's disease and FTLD, both of which are characterized by an accumulation of phosphorylated tau in affected neurons. Pathologically, it is reported that a high 4R-tau/3R-tau ratio is observed in tauopathies, including FTLD (Hong et al., 1998; Yoshida, 2006; Umeda et al., 2013). Therefore, the impaired tau isoform ratio is likely to occur due to the dysregulation of the alternative splicing caused by dysfunction of the FUS-SFPQ complex in the pathogenesis of FTLD/ALS (Ishigaki et al., 2017). A recent case report of atypical FTLD family cases characterized by astrocyte-predominant tauopathy, an aberrant tau isoform ratio, and a Q140H substitution in the FUS gene (Ferrer et al., 2015) supports the notion of a pathophysiological link between FUS and tau in FTLD/ALS through the regulation of 4R-tau/3R-tau isoforms. Further pathological investigation is needed to clarify the role of FUS/SFPQ in the pathogenesis of FTLD/ALS and tauopathies.

Regulation of Synapse-Related Genes by FUS

FUS is an RNA-binding protein that is mainly located in the nucleus; however, it also occurs in neuronal processes. It has been reported that loss of FUS could lead to abnormal synaptic function and morphology (Fujii and Takumi, 2005; Aoki et al., 2012). FUS regulates the expressions of GluA1, a subunit of α-amino-3-hydroxy-5-methyl-4-isoxazolepropionic acid (AMPA) receptor, and SynGAP1 in the dendritic spines, and loss of FUS affects the function of dendritic spines and subsequent behavioral impairments (Udagawa et al., 2015; Yokoi et al., 2017). FUS binds GluA1 mRNA in the vicinity of the 3′ terminus and maintains its stability, likely via the control of poly(A) tail maintenance. GluA1 reduction upon FUS knock-down affects AMPA receptor surface expression and synaptic transmission in neurons (Udagawa et al., 2015). Similarly, FUS

regulates the expression of SynGAP isoform α2, which is critical for spine maturation and cognitive behavior. FUS cooperates with ELAVL and regulates SynGAP mRNA stability at its 3′UTR, resulting in a specific SynGAP isoform expression in a 3′UTR length-dependent manner (Yokoi et al., 2017). Moreover, the imbalance in tau isoforms and the increase in total amount of tau by loss of FUS/SFPQ can cause a redistribution of tau in the dendritic neuritis, which is also observed in tau transgenic models; thus, impairments in the post-synapse caused by FUS depletion might be a key pathogenesis leading to neurodegeneration (**Figure 1**).

Early Structural and Network Changes in FTLD/ALS Focusing on Caudate Nucleus

Caudate Nucleus and FTLD/ALS

Detection of early structural and network changes associated with behavioral and cognitive abnormality in FTLD/ALS is crucial for the development of disease-modifying therapy. Halabi et al. showed that patients with bvFTD had 20 and 23% lower caudate volumes on MRI than did healthy controls and individuals with AD, respectively (Halabi et al., 2013). A different group also found that MRI showed a significant volume reduction in the caudate (left 16%, right 11%) in a bvFTD group compared with that observed in controls (Macfarlane et al., 2015). In another study, 30% of FTD cases showed a significant reduction in FP-CIT SPECT uptake in the putamen and the caudate (Morgan et al., 2012). Atrophic changes of the caudate nucleus were also reported to be evident prior to extensive cortical changes in ALS-FTD patients (Masuda et al., 2016). Pathological results showed that even ALS patients exhibited significant efferent neuron loss in the caudate nucleus (Riku et al., 2016). Thus, the caudate nucleus may be primarily involved in the early phase of FTLD/ALS and associated with cognitive involvement in FTLD/ALS.

The caudate nucleus is associated with not only motor processes but also various non-motor functions, including set-shifting, planning cognitive self-initiated actions, rule learning, action contingency, and bilingualism (Provost et al., 2015). In particular, the impairment of inhibitory control, decision making, and the reward system are impaired in patients with FTLD. Thus, there is no contradiction regarding whether primary caudate nucleus lesions cause various behavioral disorders. Additionally, the caudate nucleus has widespread connections with the medial frontal cortex, anterior cingulate cortex, dorsolateral prefrontal cortex, lateral orbitofrontal cortex, and insular, all of which are affected in FTLD. Thus, mild but widespread involvement of the frontotemporal cortex may be associated with caudate nucleus abnormality. These primary and secondary changes may explain why the caudate nucleus is one of the most vulnerable subcortical structures and why lesions in this region are associated with cognitive decline in FTLD/ALS.

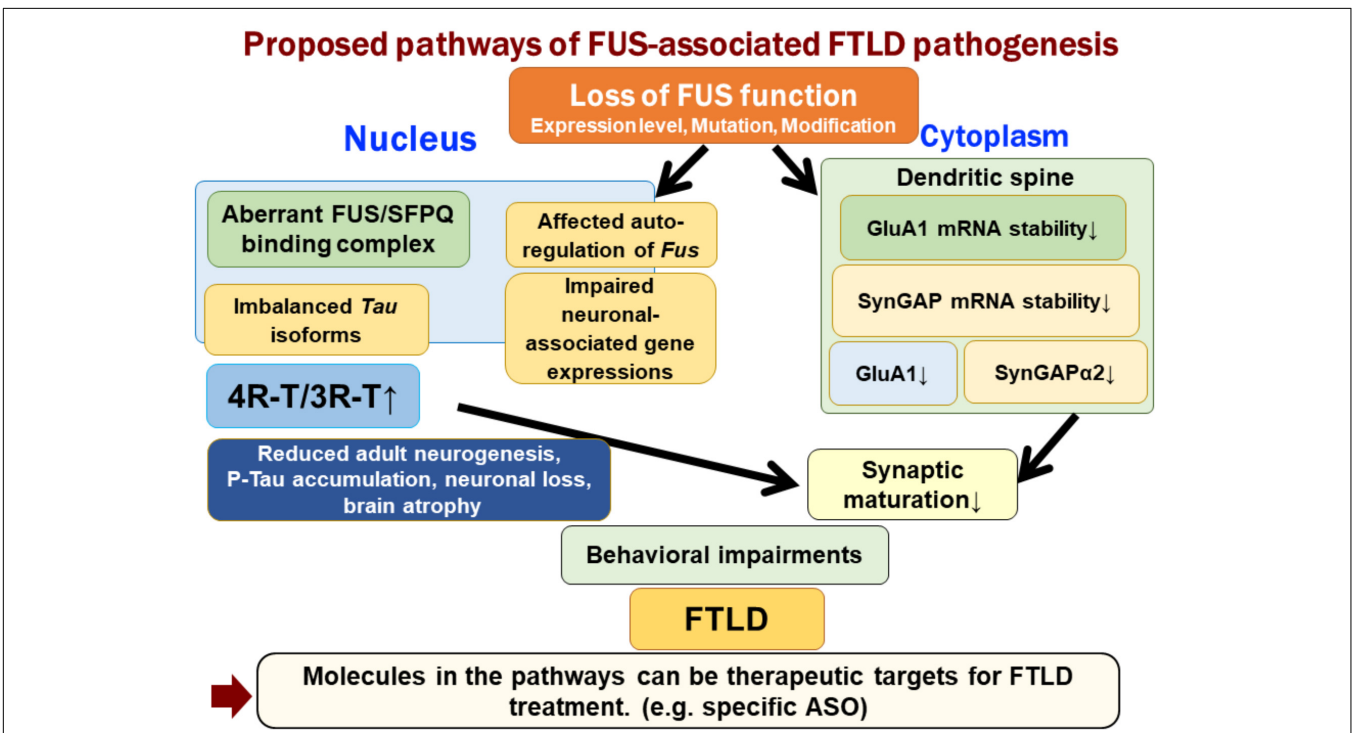

FIGURE 1 | Proposed pathways of FUS-associated FTLD pathogenesis. Loss of FUS function is involved in the early phenotypic pathomechanism of FTLD/ALS. Loss of FUS function in the nucleus, such as aberrant interaction with SFPQ, causes an imbalance in tau isoforms, which subsequently affects adult neurogenesis, phosphorylated tau accumulation, and neurodegeneration (Ishigaki et al., 2017). However, loss of FUS in the dendritic spine reduces the stability of GluA1 and SynGAP mRNA. This synaptic protein reduction impairs the maturation of spines (Udagawa et al., 2015; Yokoi et al., 2017). The two FUS-mediated molecular pathways lead to behavioral impairments, including emotional defects mimicking those observed in FTLD patients.

Interestingly, the caudate nucleus is involved in patients with not only FTLD-TDP but also FTLD-FUS and FTLD-tau (Kim et al., 2007; Seelaar et al., 2010; Bradfield et al., 2017). Although it is still unclear whether the caudate nucleus is the most vulnerable region in the context of cognitive impairment, there are some reports that atrophic changes in the caudate nucleus could be more prominent in patients with FTLD-tau and FTLD-FUS than in those with FTLD-TDP. ALS patients who were C9orf72 repeat expansion negative also showed significant volume reductions in the left caudate nucleus, left hippocampus, and right accumbens nucleus compared with healthy controls (Bede et al., 2013; Machts et al., 2015).

Caudate Nucleus Involvement Is an Early Event in Relation to Cognitive Decline in FTLD/ALS (Figure 2)

MR volumetry can provide common structural changes across the sporadic ALS and ALS-FTD continuum. Recent studies showed that patients with ALS could have widespread basal ganglia involvement (Bede et al., 2013), in accordance with neuropsychological impairments (Machts et al., 2015). Compared with controls, ALS-FTD showed atrophic changes in the following order of severity: caudate head, medial frontal gyrus, thalamus, amygdala, putamen, and cingulate gyrus. The caudate head atrophy was still significant at the cluster level using Family Wise Error (FWE) correction ($p < 0.05$) (Masuda et al., 2016).

Anatomical network analysis by diffusion tensor imaging with tract-based spatial statistics (TBSS) showed white matter involvements in the areas surrounding the caudate head, the internal capsule, and the anterior horn of the lateral ventricle in patients with ALS with cognitive deficiency (ALS-CD) and ALS-FTD (Masuda et al., 2016). Interestingly, probabilistic diffusion tractography showed a significant decrease in structural connectivity between the caudate head and the dorsomedial frontal cortex and the lateral orbitofrontal cortex in patients with not only ALS-CD and ALS-FTD but also ALS with normal cognitive function.

Striatal Efferent System Components in FTLD/ALS

According to recent pathological studies, patients with FTLD-TDP and ALS-TDP demonstrate frequent neuronal loss and/or TDP-43 inclusions in the striatum. In a study that investigated the striatal efferent system using 59 consecutively autopsied patients with sporadic FTLD-TDP or ALS-TDP (Riku et al., 2016), all patients showed markedly reduced striatal medium spiny neurons (efferent neurons) labeled by anti-calcineurin immunohistochemistry prominently in the caudate head. ALS patients revealed mild neuronal loss in the caudate head.

The axon terminals of striatal efferent neurons were immunohistochemically assessed in the substantia nigra pars reticulata (SNr) and globus pallidus interna (GPi) and externa (GPe). All patients with FTLD-TDP showed a distinct reduction in axon terminals in the SNr, GPi, and GPe, regardless of the duration of the illness. In particular, substance-P-positive projections to the SNr and GPi consistently showed severe depletion. Approximately 69.0% of the ALS-TDP patients showed similar but mild involvements compared with FTLD-TDP patients. A significant accumulation of phosphorylated TDP-43 was observed in striatal efferent neurons, efferent tracts, or their axon terminals in the SNr, GPi, and GPe in both FTLD-TDP and ALS-TDP.

These results indicate that there is a strong association between the severity of striatal efferent system involvement and the development of clinical FTD, suggesting that striatal efferent changes parallel the decline of socio-cognitive performance in sporadic FTLD-TDP patients.

Glutamatergic Inputs From the Cerebral Cortices Involvement in FTLD/ALS

Glutamatergic inputs from the cerebral cortices to the striatum were also exclusively involved in sporadic FTLD/ALS-TDP. Riku et al. demonstrated that striking depletions of vesicular glutamate transporter-1 (VGLUT-1)-positive axon terminals in the caudate head and putamen were observed in all 46 FTLD-TDP patients examined (31 with FTLD-TDP and 15 with ALS-TDP) (Riku et al., 2017). The ALS-TDP patients involved in the study also showed decreased VGLUT-1-positive axon terminals in the putamen, but those terminals were relatively spared in the caudate head.

A reduction in VGLUT-1-positive axon terminals could also result from a depletion of striatal neuronal density. However, an immunohistochemistry study did not show any association between changes in the expression of VGLUT-1 and synaptophysin. Thus, the severity of the involvement of both caudate nucleus predominant striatal efferent projections and striatal inputs from the cerebral cortices will become evident in association with the impairment in socio-cognitive performance in the TDP-43 proteinopathy spectrum.

Interestingly, confocal microscopy showed that phosphorylated TDP-43 accumulated in the VGLUT-1-positive axon terminals in the striatum of FTLD-TDP and ALS-TDP patients, indicating that aggregations of phosphorylated TDP-43 may play some role in the destruction of VGLUT-1-positive terminals.

Relationship Between Caudate Nucleus and Sequential Disease Spreading Demonstrated by Pathologically and Radiologically in FTLD/ALS

Many proteins associated with neurodegenerative diseases, such as TDP-43, tau, and a-synuclein, can show a stereotypical sequential distribution pattern with progression of the disease. Although subcortical structure analysis has not been fully investigated, cortical neural cytoplasmic inclusions in FTLD-TDP, FTLD-FUS, and FTLD-tau share a similar spatial pattern in the frontal and temporal cortex consistent with a "prion-like" spread of pathological proteins (Armstrong, 2017).

Pathological studies have reported evidence of sequential disease spreading in FTLD/ALS. ALS may disseminate in a sequential regional pattern during four disease stages: stage 1, phosphorylated TDP-43 (pTDP-43) pathology involving the agranular motor neocortex—Brodmann areas 4, 6, medulla oblongata at the level of nerve XII—bulbar somatomotor neurons of nerve XII, spinal cord layer 9—ventral horn a-motoneurons; stage 2, prefrontal neocortex (middle frontal gyrus), brainstem reticular formation, precerebellar nuclei, and red nucleus

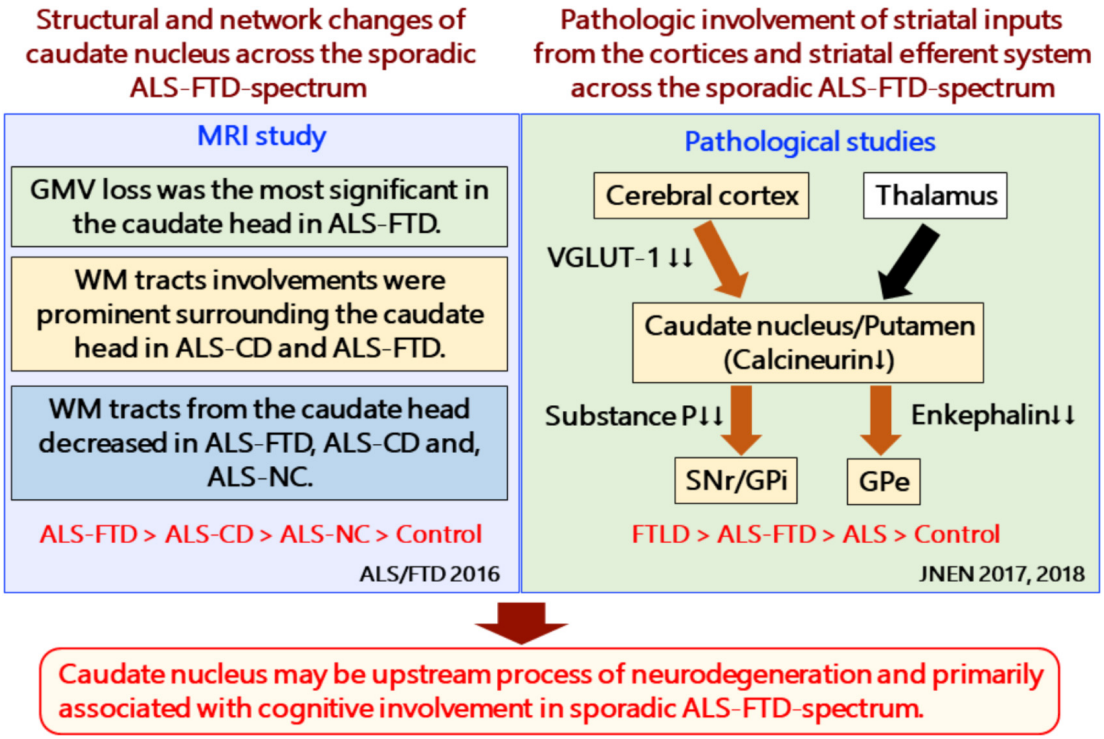

FIGURE 2 | Structural and network changes and pathologic involvement of glutamatergic striatal inputs from the cortices and striatal efferent system across the sporadic ALS-FTD spectrum. MRI studies demonstrated structural and network changes of caudate nucleus across the sporadic ALS-FTD-spectrum as follows: (1) Gray matter volume loss was the most significant in the caudate head in ALS-FTD patients relative to controls. (2) TBSS analysis showed significantly decreased FA values in widespread white matter, particularly surrounding the caudate nucleus in patients with ALS-CD and ALS-FTD, relative to controls (3) Probabilistic diffusion tractography from the head of the caudate nucleus showed extensive decreased connectivity in not only ALS-FTD and ALS-CD but also in ALS-NC. FTLD-TDP patients showed a significant reduction in the axon terminals of the glutamatergic cortical-striatal projection neurons at the caudate head and putamen, as quantified by VGLUT-1 immunohistochemistry. ALS patients showed decreased loss of VGLUT-1-positive axon terminals predominantly in the putamen. CN-positive efferent neurons from the striatum were markedly involved in the following order: ALS < FTD-MND < FTD. The striatal neuronal loss was more predominant in the caudate head than in the putamen. All FTLD-TDP patients exhibited a significant reduction in axon terminals of striatal efferent neurons immunohistochemically assessed by substance-P and enkephalin in the SNr/GPi and GPe. In particular, losses of substance-P-positive projections to the SNr and GPi were consistently severe. Similar findings were obtained in ALS-TDP patients but were mild to moderate. ALS-NC, ALS- normal cognitive; ALS-CD, ALS-cognitive deficiency; ALS-FTD, ALS with frontotemporal dementia; FTD, frontotemporal dementia; FWEc, family-wise error corrected at the cluster level for multiple comparisons; FA, fractional anisotropy; RD, radial diffusivity; TFCE, threshold-free cluster enhancement; TBSS, tensor-based spatial statistics. FTLD-TDP, TAR DNA-binding protein-43 kDa-related frontotemporal lobar degeneration (FTLD-TDP); ALS, amyotrophic lateral sclerosis; FTD, frontotemporal dementia; FTD-MND, FTD with motor neuron disease; VGLUT-1, anti-vesicular glutamate transporter-1; SNr, nigra pars reticulate; GP, globus pallidus (GP); GPi, internal segment of GP; GPe, external segment of GP; CN, calcineurin.

involvements; stage 3, striatum, gyrus rectus, and orbital gyri; and stage 4, anteromedial portions of the temporal lobe, including the hippocampus (Brettschneider et al., 2013).

This pTDP-43 staging pattern has recently been validated *in vivo* using a tract of interest (TOI)-based fiber-tracking approach. TOI analysis demonstrated sequential involvements of the corticospinal tract, the corticorubral and corticopontine tracts, the corticostriatal pathway, and the proximal portion of the perforant pathway in accordance with stages 1, 2, 3, and 4 in ALS (Kassubek et al., 2014). ALS patients with disinhibited behavior showed involvements of seed coordinates of the conticostriatal pathway located in the caudate head or higher (95% specificity and 100% sensitivity) (Lulé et al., 2018), suggesting a disconnect between the caudate head and prefrontal cortex associated with behavioral abnormality in ALS.

Similar sequential distributions of pTDP-43 pathology were also reported in bv FTD patients with TDP-43 Type A or Type B pathology: stage 1, orbital and amygdala; stage 2, additional frontal, temporal, and subcortical regions; stage 3, motor system involvement; and stage 4, visual cortex (Brettschneider et al., 2014). Longitudinal TOI analysis in FTLD also demonstrated a pattern of white matter pathway alterations consistent with patterns of pTDP-43 pathology: stages 1, uncinate fascicle; stage 2, corticostriatal pathway; stage 3, corticospinal tract; and stage 4, optic radiation (Kassubek et al., 2018).

However, whether all patients with ALS and bvFTD can show such a stereotypical sequential distribution pattern throughout the stages of pathology is yet to be determined. The greatest overlap in deposition of TDP-43 between ALS and bvFTD is observed in patients with type B TDP-43 pathology but not in those with type C (Burrell et al., 2016). Even in those with

type B, the spreading patterns vary between ALS and bvFTD. Although it may still be difficult to explain various clinical phenotypes and disease progressions based on stereotypical pathological progression, such a propagation theory provides several important insights into the early structural and network changes that occur in ALS and FTLD. The association between behavioral abnormalities and involvement of the corticostriatal tract seeded from the caudate head in ALS and bvFTD supports the view that the caudate head and its network can be the most important target for developing disease-modifying therapy.

Future Direction

A line of recent studies has suggested that loss of FUS and/or TDP-43 might contribute to early clinico-pathogenesis of FTLD/ALS. Pathological and imaging studies have also revealed that the caudate nucleus is the target candidate for early differential diagnosis between FTLD and AD. Because the caudate nucleus and the putamen are not distinguishable in rodents, it would be suitable to use non-human primates to investigate the pathophysiological relevancy of the caudate and FTLD.

Recently, an FTLD marmoset model was generated by silencing FUS gene using AAV encoding shRNA against the marmoset FUS gene (shFUS). The AAV encoding shFUS (AAV-shFUS) was introduced into the frontal cortex of young adult marmosets by stereotaxic injection, which enabled FUS expressions to be reduced by approximately 70–80%, with an increase in astrocytes and microglias (Endo et al., 2017). The non-human primate FTLD models of caudate-specific FUS-silencing may provide useful information about the importance of a loss-of-function model and the caudate nucleus in FTLD.

Further studies on animal behaviors, imaging studies, and clinic-pathological studies of patients are necessary to establish the caudate nuclei as an early-stage biomarker of FTLD.

CONCLUSION

In this review, we demonstrated the loss-of-function mechanism of FTLD, focusing on FUS-associated pathogenesis. Interestingly, FUS was linked to tau by regulating its alternative splicing machinery and was associated with abnormalities in post-synaptic formation that are expected to be an early disease marker of FTLD. We also introduced the involvement of the caudate nucleus and its network in FTLD/ALS, which is believed to be the key to determining the pathogenesis leading to neurodegeneration. We believe that elucidation of the upstream process of neurodegeneration and the development of imaging biomarkers for early diagnosis will allow for the future development of disease-modifying therapy for FTLD.

AUTHOR CONTRIBUTIONS

GS, SI, and HW: conceptualization, formal analysis, investigation, methodology, resources, visualization, writing – original draft, and writing – review and editing. SI and HW: data curation. GS: funding acquisition and supervision.

FUNDING

This research was supported in part by the following: a Grant-in-Aid from the Research Committee of Central Nervous System Degenerative Diseases by the Ministry of Health, Labor, and Welfare, Integrated Research on Neuropsychiatric Disorders project, carried out by SRBPS; a Grant-in-Aid for Scientific Research on Innovative Areas (Brain Protein Aging and Dementia Control) (26117002) from MEXT of Japan; Grant Number JP18dm0107059h and JP18dm0207015h supported by the Japan Agency for Medical Research and Development (AMED).

REFERENCES

Aoki, N., Higashi, S., Kawakami, I., Kobayashi, Z., Hosokawa, M., Katsuse, O., et al. (2012). Localization of fused in sarcoma (FUS) protein to the post-synaptic density in the brain. *Acta Neuropathol.* 124, 383–394. doi: 10.1007/s00401-012-0984-986

Armstrong, R. (2017). Neuronal cytoplasmic inclusions in tau, TDP-43, and FUS molecular subtypes of frontotemporal lobar degeneration share similar spatial patterns. *Folia Neuropathol.* 55, 85–192. doi: 10.5114/fn.2017.70482

Bannerman, D. M., Gilmour, G., Norman, G., Lemaire, M., Iversen, S. D., and Rawlins, J. N. (2001). The time course of the hyperactivity that follows lesions or temporary inactivation of the fimbria-fornix. *Behav. Brain Res.* 120, 1–11. doi: 10.1016/S0166-4328(00)00354-5

Barkus, C., McHugh, S. B., Sprengel, R., Seeburg, P. H., Rawlins, J. N., and Bannerman, D. M. (2010). Hippocampal NMDA receptors and anxiety: at the interface between cognition and emotion. *Eur. J. Pharmacol.* 626, 49–56. doi: 10.1016/j.ejphar.2009.10.014

Bede, P., Elamin, M., Byrne, S., McLaughlin, R. L., Kenna, K., Vajda, A., et al. (2013). Basal ganglia involvement in amyotrophic lateral sclerosis. *Neurology* 81, 2107–2115. doi: 10.1212/01.wnl.0000437313.80913.2c

Bradfield, N. I., McLean, C., Drago, J., Darby, D. G., and Ames, D. (2017). Rapidly progressive fronto-temporal dementia (FTD) associated with frontotemporal lobar degeneration (FTLD) in the presence of fused in sarcoma (FUS) protein: a rare, sporadic, and aggressive form of FTD. *Int. Psychogeriatr.* 29, 1743–1746. doi: 10.1017/S1041610217001193

Brettschneider, J., Del Tredici, K., Toledo, J. B., Robinson, J. L., Irwin, D. J., Grossman, M., et al. (2013). Stages of pTDP-43 pathology in amyotrophic lateral sclerosis. *Ann. Neurol.* 74, 20–38. doi: 10.1002/ana.23937

Brettschneider, J., Del Tredici, K., Irwin, D. J., Grossman, M., Robinson, J. L., Toledo, J. B., et al. (2014). Sequential distribution of pTDP-43 pathology in behavioral variant frontotemporal dementia (bvFTD). *Acta Neuropathol.* 127, 423–439. doi: 10.1007/s00401-013-1238-y

Burrell, J. R., Halliday, G. M., Kril, J. J., Ittner, L. M., Götz, J., Kiernan, M. C., et al. (2016). The frontotemporal dementia-motor neuron disease continuum. *Lancet* 388, 919–931. doi: 10.1016/S0140-6736(16)00737-736

Davidson, Y., Kelley, T., Mackenzie, I. R., Pickering-Brown, S., Du Plessis, D., Neary, D., et al. (2007). Ubiquitinated pathological lesions in frontotemporal lobar degeneration contain the TAR DNA-binding protein, TDP-43. *Acta Neuropathol.* 113, 521–533. doi: 10.1007/s00401-006-0189-y

DeJesus-Hernandez, M., Mackenzie, I. R., Boeve, B. F., Boxer, A. L., Baker, M., Rutherford, N. J., et al. (2011). Expanded GGGGCC hexanucleotide repeat in noncoding region of C9ORF72 causes chromosome 9p-linked FTD and ALS. *Neuron* 72, 245–56. doi: 10.1016/j.neuron.2011.09.011

Endo, K., Ishigaki, S., Masamizu, Y., Fujioka, Y., Watakabe, A., Yamamori. T., et al. (2017). Silencing of FUS in the common marmoset (*Callithrix jacchus*) brain via stereotaxic injection of an adeno-associated virus encoding shRNA. *Neurosci. Res.* 130, 56–64. doi: 10.1016/j.neures.2017.08.006

Ferrer, I., Legati, A., García-Monco, J. C., Gomez-Beldarrain, M., Carmona, M., Blanco, R., et al. (2015). Familial behavioral variant frontotemporal dementia associated with astrocyte-predominant tauopathy. *J. Neuropathol. Exp. Neurol.* 74, 370–379. doi: 10.1097/NEN.0000000000000180

Fujii, R., and Takumi, T. (2005). TLS facilitates transport of mRNA encoding an actin-stabilizing protein to dendritic spines. *J. Cell Sci.* 118(Pt 24), 5755–5765. doi: 10.1242/jcs.02692

Fujioka, Y., Ishigaki, S., Masuda, A., Iguchi, Y., Udagawa, T., Watanabe, H., et al. (2013). FUS-regulated region- and cell-type-specific transcriptome is associated with cell selectivity in ALS/FTLD. *Sci. Rep.* 3:2388. doi: 10.1038/srep02388

Fukuhara, R., Ghosh, A., Fuh, J. L., Dominguez, J., Ong, P. A., Dutt, A., et al. (2014). Family history of frontotemporal lobar degeneration in Asian international multi-center research. *Int. Psychogeriatr.* 26, 1967–1971. doi: 10.1017/S1041610214000635

Halabi, C., Halabi, A., Dean, D. L., Wang, P. N., Boxer, A. L., Trojanowski, J. Q., et al. (2013). Patterns of striatal degeneration in frontotemporal dementia. *Alzheimer Dis. Assoc. Disord.* 27, 74–83. doi: 10.1097/WAD.0b013e31824a7df4

Hardiman, O., Al-Chalabi, A., Chio, A., Corr, E. M., Logroscino, G., Robberecht, W., et al. (2017). Amyotrophic lateral sclerosis. *Nat. Rev. Dis. Primers* 3:17071. doi: 10.1038/nrdp.2017.71

Hayes, L. R., and Rothstein, J. D. (2016). C9ORF72-ALS/FTD: transgenic mice make a come-BAC. *Neuron* 90, 427–431. doi: 10.1016/j.neuron.2016.04.026

Honda, D., Ishigaki, S., Iguchi, Y., Fujioka, Y., Udagawa, T., Masuda, A., et al. (2013). The ALS/FTLD-related RNA-binding proteins TDP-43 and FUS have common downstream RNA targets in cortical neurons. *FEBS Open Bio* 4, 1–10. doi: 10.1016/j.fob.2013.11.001

Hong, M., Zhukareva, V., Vogelsberg-Ragaglia, V., Wszolek, Z., Reed, L., Miller, B. I., et al. (1998). Mutation-specific functional impairments in distinct tau isoforms of hereditary FTDP-17. *Science* 282, 1914–1917. doi: 10.1126/science.282.5395.1914

Igaz, L. M., Kwong, L. K., Lee, E. B., Chen-Plotkin, A., Swanson, E., Unger, T., et al. (2011). Dysregulation of the ALS-associated gene TDP-43 leads to neuronal death and degeneration in mice. *J. Clin. Invest.* 121, 726–738. doi: 10.1172/JCI44867

Iguchi, Y., Katsuno, M., Niwa, J., Takagi, S., Ishigaki, S., Ikenaka, K., et al. (2013). Loss of TDP-43 causes age-dependent progressive motor neuron degeneration. *Brain* 136(Pt 5), 1371–1382. doi: 10.1093/brain/awt029

Iranzo, A., Santamaria, J., and Tolosa, E. (2016). Idiopathic rapid eye movement sleep behaviour disorder: diagnosis, management, and the need for neuroprotective interventions. *Lancet Neurol.* 15, 405–419. doi: 10.1016/S1474-4422(16)00057-0

Ishigaki, S., Fujioka, Y., Okada, Y., Riku, Y., Udagawa, T., Honda, D., et al. (2017). Altered Tau isoform ratio caused by Los of FUS and SFPQ function leads to FTLD-like phenotypes. *Cell Rep.* 18, 1118–1131. doi: 10.1016/j.celrep.2017.01.013

Ishigaki, S., Masuda, A., Fujioka, Y., Iguchi, Y., Katsuno, M., Shibata, A., et al. (2012). Position-dependent FUS-RNA interactions regulate alternative splicing events and transcriptions. *Sci. Rep.* 2:529. doi: 10.1038/srep00529

Kabashi, E., Bercier, V., Lissouba, A., Liao, M., Brustein, E., Rouleau, G. A., et al. (2011). FUS and TARDBP but not SOD1 interact in genetic models of amyotrophic lateral sclerosis. *PLoS Genet.* 7:e1002214. doi: 10.1371/journal.pgen.1002214

Kameoka, S., Duque, P., and Konarska, M. M. (2004). p54(nrb) associates with the 5' splice site within large transcription/splicing complexes. *EMBO J.* 23, 1782–1791. doi: 10.1038/sj.emboj.7600187

Kassubek, J., Müller, H. P., Del Tredici, K., Brettschneider, J., Pinkhardt, E. H., Lulé, D., et al. (2014). Diffusion tensor imaging analysis of sequential spreading of disease in amyotrophic lateral sclerosis confirms patterns of TDP-43 pathology. *Brain* 137(Pt 6), 1733–1740. doi: 10.1093/brain/awu090

Kassubek, J., Müller, H. P., Del Tredici, K., Hornberger, M., Schroeter, M. L., Müller, K., et al. (2018). Longitudinal diffusion tensor imaging resembles patterns of pathology progression in behavioral variant frontotemporal dementia (bvFTD). *Front. Aging Neurosci.* 10:47. doi: 10.3389/fnagi.2018.00047

Kapeli, K., Pratt, G. A., Vu, A. Q., Hutt, K. R., Martinez, F. J., Sundararaman, B., et al. (2016). Distinct and shared functions of ALS-associated proteins TDP-43, FUS and TAF15 revealed by multisystem analyses. *Nat. Commun.* 7:12143. doi: 10.1038/ncomms12143

Kheirbek, M. A., Drew, L. J., Burghardt, N. S., Costantini, D. O., Tannenholz, L., Ahmari, S. E., et al. (2013). Differential control of learning and anxiety along the dorsoventral axis of the dentate gyrus. *Neuron* 77, 955–68. doi: 10.1016/j.neuron.2012.12.038

Kim, E. J., Rabinovici, G. D., Seeley, W. W., Halabi, C., Shu, H., Weiner, M. W., et al. (2007). Patterns of MRI atrophy in tau positive and ubiquitin positive frontotemporal lobar degeneration. *J. Neurol. Neurosurg. Psychiatry* 78, 1375–1378. doi: 10.1136/jnnp.2006.114231

Kino, Y., Washizu, C., Kurosawa, M., Yamada, M., Miyazaki, H., Akagi, T., et al. (2015). FUS/TLS deficiency causes behavioral and pathological abnormalities distinct from amyotrophic lateral sclerosis. *Acta Neuropathol. Commun.* 3:24. doi: 10.1186/s40478-015-0202-206

Lagier-Tourenne, C., Polymenidou, M., Hutt, K. R., Vu, A. Q., Baughn, M., Huelga, S. C., et al. (2012). Divergent roles of ALS-linked proteins FUS/TLS and TDP-43 intersect in processing long pre-mRNAs. *Nat. Neurosci.* 15, 1488–1497. doi: 10.1038/nn.3230

Ling, S. C., Polymenidou, M., and Cleveland, D. W. (2013). Converging mechanisms in ALS and FTD: disrupted RNA and protein homeostasis. *Neuron* 79, 416–438. doi: 10.1016/j.neuron.2013.07.033

Lulé, D., Böhm, S., Müller, H. P., Aho-Özhan, H., Keller, J., Gorges, M., et al. (2018). Cognitive phenotypes of sequential staging in amyotrophic lateral sclerosis. *Cortex* 101, 163–171. doi: 10.1016/j.cortex.2018.01.004

Macfarlane, M. D., Jakabek, D., Walterfang, M., Vestberg, S., Velakoulis, D., Wilkes, F. A., et al. (2015). Striatal atrophy in the behavioural variant of frontotemporal dementia: correlation with diagnosis, negative symptoms and disease severity. *PLoS One* 10:e0129692. doi: 10.1371/journal.pone.0129692

Mackenzie, I. R., and Neumann, M., (2012). FET proteins in frontotemporal dementia and amyotrophic lateral sclerosis. *Brain Res.* 1462, 40–3. doi: 10.1016/j.brainres.2011.12.010

Machts, J., Loewe, K., Kaufmann, J., Jakubiczka, S., Abdulla, S., Petri, S., et al. (2015). Basal ganglia pathology in ALS is associated with neuropsychological deficits. *Neurology* 85, 1301–1309. doi: 10.1212/WNL.0000000000002017

Masuda, M., Senda, J., Watanabe, H., Epifanio, B., Tanaka, Y., Imai, K., et al. (2016). Involvement of the caudate nucleus head and its networks in sporadic amyotrophic lateral sclerosis-frontotemporal dementia continuum. *Amyotroph. Lateral Scler. Frontotemporal Degener.* 17, 571–579. doi: 10.1080/21678421.2016.1211151

Morgan, S., Kemp, P., Booij, J., Costa, D. C., Padayachee, S., Lee, L., et al. (2012). Differentiation of frontotemporal dementia from dementia with Lewy bodies using FP-CIT SPECT. *J. Neurol. Neurosurg. Psychiatry* 83, 1063–70. doi: 10.1136/jnnp-2012-302577

Nakamura, R., Sone, J., Atsuta, N., Tohnai, G., Watanabe, H., Yokoi, D., et al. (2016). Japanese Consortium for Amyotrophic Lateral Sclerosis Research (JaCALS). Next-generation sequencing of 28 ALS-related genes in a Japanese ALS cohort. *Neurobiol. Aging* 39, 219.e1–219.e8. doi: 10.1016/j.neurobiolaging.2015.11.030

Nakaya, T., Alexiou, P., Maragkakis, M., Chang, A., and Mourelatos, Z. (2013). FUS regulates genes coding for RNA-binding proeins in neurons by binding to their highly conserved introns. *RNA* 19, 498–509. doi: 10.1261/rna.037804.112

Neumann, M., Sampathu, D. M., Kwong, L. K., Truax, A. C., Micsenyi, M. C., Chou, T. T., et al. (2006). Ubiquitinated TDP-43 in frontotemporal lobar degeneration and amyotrophic lateral sclerosis. *Science* 314, 130–133. doi: 10.1126/science.1134108

Neumann, M., Rademakers, R., Roeber, S., Baker, M., Kretzschmar, H. A., and Mackenzie, I. R. (2009). A new subtype of frontotemporal lobar degeneration with FUS pathology. *Brain* 132(Pt 11), 2922–2931. doi: 10.1093/brain/awp214

Nguyen, H. P., Van Broeckhoven, C., and van der Zee, J. (2018). ALS genes in the genomic Era and their implications for FTD. *Trends Genet.* 34, 404–423. doi: 10.1016/j.tig. 03.001

Ogaki, K., Li, Y., Atsuta, N., Tomiyama, H., Funayama, M., Watanabe, H., et al. (2012). Japanese Consortium for Amyotrophic Lateral Sclerosis research (JaCALS). Analysis of C9orf72 repeat expansion in 563 Japanese patients with amyotrophic lateral sclerosis. *Neurobiol. Aging* 33, 2527.e11–2527.e6. doi: 10.1016/j.neurobiolaging.2012.05.011

Olney, N. T., Spina, S., Miller, B. L. (2017). Frontotemporal dementia. *Neurol. Clin.* 35, 339–374. doi: 10.1016/j.ncl.2017.01.008

Olsson, B., Lautner, R., Andreasson, U., Öhrfelt, A., Portelius, E., Bjerke, M., et al. (2016). CSF and blood biomarkers for the diagnosis of Alzheimer's disease: a systematic review and meta-analysis. *Lancet Neurol.* 15, 673–684. doi: 10.1016/S1474-4422(16)00070-3

Orozco, D., and Edbauer, D. (2013). FUS-mediated alternative splicing in the nervous system: consequences for ALS and FTLD. *J. Mol. Med.* 91, 1343–1354. doi: 10.1007/s00109-013-1077-1072

Orozco, D., Tahirovic, S., Rentzsch, K., Schwenk, B. M., Haass, C., and Edbauer, D. (2012). Loss of fused in sarcoma (FUS) promotes pathological Tau splicing. *EMBO Rep.* 13, 759–764. doi: 10.1038/embor.2012.90

Provost, J. S., Hanganu, A., Monchi, O. (2015). Neuroimaging studies of the striatum in cognition Part I: healthy individuals. *Front. Syst. Neurosci.* 9:140. doi: 10.3389/fnsys.2015.00140

Renton, A. E., Chiò, A., Traynor, B. J. (2014). State of play in amyotrophic lateral sclerosis genetics. *Nat. Neurosci.* 17, 17–23. doi: 10.1038/nn.3584

Riku, Y., Atsuta, N., Yoshida, M., Tatsumi, S., Iwasaki, Y., Mimuro, M., et al. (2014a). Differential motor neuron involvement in progressive muscular atrophy: a comparative study with amyotrophic lateral sclerosis. *BMJ Open* 4:e005213. doi: 10.1136/bmjopen-2014-005213

Riku, Y., Watanabe, H., Yoshida, M., Tatsumi, S., Mimuro, M., Iwasaki, Y., et al. (2014b). Lower motor neuron involvement in TAR DNA-binding protein of 43 kDa-related frontotemporal lobar degeneration and amyotrophic lateral sclerosis. *JAMA Neurol.* 71, 172–179. doi: 10.1001/jamaneurol.2013.5489

Riku, Y., Watanabe, H., Yoshida, M., Mimuro, M., Iwasaki, Y., Masuda, M., et al. (2016). Marked involvement of the striatal efferent system in TAR DNA-binding protein 43 kDa-related frontotemporal lobar degeneration and amyotrophic lateral sclerosis. *J. Neuropathol. Exp. Neurol.* 75, 801–811. doi: 10.1093/jnen/nlw053

Riku, Y., Watanabe, H., Yoshida, M., Mimuro, M., Iwasaki, Y., Masuda, M., et al. (2017). Pathologic involvement of glutamatergic striatal inputs from the cortices in TAR DNA-binding protein 43 kDa-related frontotemporal lobar degeneration and amyotrophic lateral sclerosis. *J. Neuropathol. Exp. Neurol.* 76, 759–768. doi: 10.1093/jnen/nlx055

Rogelj, B., Easton, L. E., Bogu, G. K., Stanton, L. W., Rot, G., Curk, T., et al. (2012). Widespread binding of FUS along nascent RNA regulates alternative splicing in the brain. *Sci. Rep.* 2:603. doi: 10.1038/srep00603

Scekic-Zahirovic, J., Sendscheid, O., El Oussini, H., Jambeau, M., Sun, Y., Mersmann, S., et al. (2016). Toxic gain of function from mutant FUS protein is crucial to trigger cell autonomous motor neuron loss. *EMBO J.* 35, 1077–1097. doi: 10.15252/embj.201592559

Seelaar, H., Klijnsma, K. Y., de Koning, I., van der Lugt, A., Chiu, W. Z., et al. (2010). Frequency of ubiquitin and FUS-positive, TDP-43-negative frontotemporal lobar degeneration. *J. Neurol.* 257, 747–753. doi: 10.1007/s00415-009-5404-z

Seelaar, H., Rohrer, J. D., Pijnenburg, Y. A., Fox, N. C., van Swieten, J. C. (2011). Clinical, genetic and pathological heterogeneity of frontotemporal dementia: a review. *J. Neurol. Neurosurg. Psychiatry* 82, 476–486. doi: 10.1136/jnnp.2010.212225

Sharma, A., Lyashchenko, A. K., Lu, L., Nasrabady, S. E., Elmaleh, M., Mendelsohn, M., et al. (2016). ALS-associated mutant FUS induces selective motor neuron degeneration through toxic gain of function. *Nat. Commun.* 7:10465. doi: 10.1038/ncomms10465

Shav-Tal, Y., and Zipori, D. (2002). PSF and p54(nrb)/NonO–multi-functional nuclear proteins. *FEBS Lett.* 531, 109–114. doi: 10.1016/S0014-5793(02)03447-6

Sun, S., Ling, S. C., Qiu, J., Albuquerque, C. P., Zhou, Y., Tokunaga, S., et al. (2015). ALS-causative mutations in FUS/TLS confer gain and loss of function by altered association with SMN and U1-snRNP. *Nat. Commun.* 6:6171. doi: 10.1038/ncomms7171

Thomas-Jinu, S., Gordon, P. M., Fielding, T., Taylor, R., Smith, B. N., Snowden, V., et al. (2017). Non-nuclear pool of splicing factor SFPQ regulates axonal transcripts required for normal motor development. *Neuron* 94, 322.e5–336.e5. doi: 10.1016/j.neuron.2017.04.036

Tsuiji, H., Iguchi, Y., Furuya, A., Kataoka, A., Hatsuta, H., Atsuta, N., et al. (2013). Spliceosome integrity is defective in the motor neuron diseases ALS and SMA. *EMBO Mol. Med.* 5, 221–234. doi: 10.1002/emmm.201202303

Tsujimoto, M., Senda, J., Ishihara, T., Niimi, Y., Kawai, Y., Atsuta, N., et al. (2011). Behavioral changes in early ALS correlate with voxel-based morphometry and diffusion tensor imaging. *J. Neurol. Sci.* 307, 34–40. doi: 10.1016/j.jns.2011.05.025

Udagawa, T., Fujioka, Y., Tanaka, M., Honda, D., Yokoi, S., Riku, Y., et al. (2015). FUS regulates AMPA receptor function andFTLD/ALS-associated behaviour via GluA1 mRNA stabilization. *Nat. Commun.* 6:7098. doi: 10.1038/ncomms8098

Umeda, T., Yamashita, T., Kimura, T., Ohnishi, K., Takuma, H., Ozeki, T., et al. (2013). Neurodegenerative disorder FTDP-17-related tau intron 10 +16C → T mutation increases tau exon 10 splicing and causes tauopathy in transgenic mice. *Am. J. Pathol.* 183, 211–225. doi: 10.1016/j.ajpath.2013.03.015

Van Mossevelde, S., van der Zee, J., Cruts, M., Van Broeckhoven, C. (2017). Relationship between C9orf72 repeat size and clinical phenotype. *Curr. Opin. Genet. Dev.* 44, 117–124. doi: 10.1016/j.gde.02.008

Van Mossevelde. S., Engelborghs, S., van der Zee, J., Van Broeckhoven, C. (2018). Genotype-phenotype links in frontotemporal lobar degeneration. *Nat. Rev. Neurol.* 14, 363–378. doi: 10.1038/s41582-018-0009-8

Vanden Broeck, L., Naval-Sanchez, M., Adachi, Y., Diaper, D., Dourlen, P., Chapuis, J., et al. (2013). TDP-43 loss-of-function causes neuronal loss due to defective steroid receptor-mediated gene program switching in *Drosophila*. *Cell Rep.* 3, 160–172. doi: 10.1016/j.celrep.2012.12.014

Wang, J. W., Brent, J. R., Tomlinson, A., Shneider, N. A., and McCabe, B. D. (2011). The ALS-associated proteins FUS and TDP-43 function together to affect *Drosophila* locomotion and life span. *J. Clin. Invest.* 121, 4118–4126. doi: 10.1172/JCI57883

Wegorzewska, I., Bell, S., Cairns, N. J., Miller, T. M., and Baloh, R. H. (2009). TDP-43 mutant transgenic mice develop features of ALS and frontotemporal lobar degeneration. *Proc. Natl. Acad. Sci. U.S.A.* 106, 18809–18814. doi: 10.1073/pnas.0908767106

Wu, L. S., Cheng, W. C., and Shen, C. K. (2012). Targeted depletion of TDP-43 expression in the spinal cord motor neurons leads to the development of amyotrophic lateral sclerosis-like phenotypes in mice. *J. Biol. Chem.* 287, 27335–27344. doi: 10.1074/jbc.M112.359000

Yokoi, S., Udagawa, T., Fujioka, Y., Honda, D., Okado, H., Watanabe, H., et al. (2017). 3'UTR Length-dependent control of SynGAP isoform alpha2 mRNA by FUS and ELAV-like proteins promotes dendritic spine maturation and cognitive function. *Cell Rep.* 20, 3071–3084. doi: 10.1016/j.celrep.2017.08.100

Yoshida, M. (2006). Cellular tau pathology and immunohistochemical study of tau isoforms in sporadic tauopathies. *Neuropathology* 26, 457–470. doi: 10.1111/j.1440-1789.2006.00743.x

Xu, Z. S. (2012). Does a loss of TDP-43 function cause neurodegeneration? *Mol. Neurodegener.* 7:27. doi: 10.1186/1750-1326-7-27

Zhou, Y., Liu, S., Liu, G., Ozturk, A., and Hicks, G. G. (2013). ALS-associated FUS mutations result in compromised FUS alternative splicing and autoregulation. *PLoS Genet.* 9:e1003895. doi: 10.1371/journal.pgen.1003895

Conflict of Interest Statement: The authors declare that the research was conducted in the absence of any commercial or financial relationships that could be construed as a potential conflict of interest.

frontiers in Neuroscience

REVIEW
published: 21 August 2018
doi: 10.3389/fnins.2018.00585

Imaging Protein Misfolding in the Brain Using β-Sheet Ligands

*Ryuichi Harada[1], Nobuyuki Okamura[2], Shozo Furumoto[3] and Kazuhiko Yanai[1,3]**

[1] Department of Pharmacology, Tohoku University Graduate School of Medicine, Sendai, Japan, [2] Division of Pharmacology, Tohoku Medical and Pharmaceutical University, Sendai, Japan, [3] Cyclotron and Radioisotope Center, Tohoku University, Sendai, Japan

Neurodegenerative diseases characterized by pathological protein accumulation in cells are termed "proteinopathies." Although various protein aggregates share cross-β-sheet structures, actual conformations vary among each type of protein deposit. Recent progress in the development of radiotracers for positron emission tomography (PET) has enabled the visualization of protein aggregates in living brains. Amyloid PET tracers have been developed, and are widely used for the diagnosis of Alzheimer's disease and non-invasive assessment of amyloid burden in clinical trials of anti-dementia drugs. Furthermore, several tau PET tracers have been successfully developed and used in the clinical studies. However, recent studies have identified the presence of off-target binding of radiotracers in areas of tau deposition, suggesting that concomitant neuroinflammatory changes might affect tracer binding. In contrast to amyloid and tau PET, there are no established tracers for imaging Lewy bodies in the human brain. In this review, we describe lessons learned from the development of PET tracers and discuss the future direction of tracer development for protein misfolding diseases.

Keywords: proteinopathies, protein aggregates, β-sheet ligands, PET, tau

OPEN ACCESS

Edited by:
Gen Sobue,
Nagoya University, Japan

Reviewed by:
Michael D. Devous,
Avid Radiopharmaceuticals, Inc., United States
Jason Eriksen,
University of Houston, United States

***Correspondence:**
Kazuhiko Yanai
yanai@med.tohoku.ac.jp

Specialty section:
This article was submitted to Neurodegeneration, a section of the journal Frontiers in Neuroscience

Received: *28 November 2017*
Accepted: *06 August 2018*
Published: *21 August 2018*

Citation:
Harada R, Okamura N, Furumoto S and Yanai K (2018) Imaging Protein Misfolding in the Brain Using β-Sheet Ligands. Front. Neurosci. 12:585. doi: 10.3389/fnins.2018.00585

INTRODUCTION

Proteinopathies are neurodegenerative diseases characterized by pathological accumulation of amyloid-β (Aβ), tau, α-synuclein, and TDP-43 in the cells. Tauopathies, characterized by tau protein accumulation, include Alzheimer's disease (AD), some variants of frontotemporal lobar degeneration (FTLD), frontotemporal dementia with parkinsonism linked to chromosome-17 (FTLD-17), corticobasal degeneration (CBD), progressive supranuclear palsy (PSP), argyrophilic grain disease (AGD), and chronic traumatic encephalopathy (CTE). AD is a mixed proteinopathy characterized by abnormal accumulation of extracellular Aβ and intracellular tau protein. α-Synucleinopathies, characterized by pathological accumulation of α-synuclein, include Parkinson's disease (PD), Lewy bodies disease (LBD), and multiple system atrophy (MSA). TDP-43 proteinopathies include some variants of FTLD and amyotrophic lateral sclerosis (ALS). Genetic, pathological, and biochemical evidence strongly suggests that protein accumulation causes neurodegenerative disease, although the precise etiology and mechanisms underlying these processes remain unknown. Historically, these neuropathological lesions could only be identified by histopathological examination at autopsy. Neuropathologists described the distributions of these lesions in many patients and proposed a classification of their regional distribution (Thal et al., 2002; Braak et al., 2006a; Hyman et al., 2012). Braak staging, which is based on cross-sectional autopsy studies, represents the most commonly used classification system for Aβ, tau, α-synuclein, and TDP-43, (Braak and Braak, 1991; Braak et al., 2003; Brettschneider et al., 2013). Importantly,

the amount and spatial distribution of protein depositions is highly correlated with the severity of disease (Bierer et al., 1995; Braak et al., 2006b). Non-invasive detection of abnormal protein deposits would therefore be useful for accurate diagnosis, disease monitoring, and evaluation of the efficacy of anti-dementia treatments.

Positron emission tomography (PET) using specific radiotracers provides regional and pathophysiological information in a non-invasive manner in living human subjects. Although PET imaging is more expensive than examining body fluid biomarkers, such as blood and cerebrospinal fluid (CSF), it is advantageous because it enables the spatial assessment of brain lesions as well as accurate, reliable, and reproducible quantitative measurements. Following the successful imaging of amyloid with Pittsburgh compound B (PiB; Klunk et al., 2004), fluorinated alternatives have been developed in clinical studies and approved by the Food and Drug Administration (FDA) and European Medicines Agency (EMA; Mathis et al., 2017). These tracers are thioflavin and stilbene derivatives, which bind the cross-β-sheet structures of aggregated proteins. Many β-sheet binding compounds have been reported through the development of amyloid PET tracers (Furumoto et al., 2007). Several putative tau PET tracers have also been developed and evaluated in humans. In a clinical trial, these tracers demonstrated elevated retention in brain regions susceptible to tau deposition (Villemagne et al., 2015). However, tau pathology is more complicated than Aβ pathology, owing to its heterogeneous histopathology possibly resulting from isoform composition and ultrastructural conformation (for in depth review see Villemagne et al., 2012; Harada et al., 2016c). Furthermore, first generation tau tracers such as ^{11}C-PBB3, ^{18}F-AV1451 (also known as flortaucipir; T807), and ^{18}F-THK5351 result in off-target binding (Okamura and Yanai, 2017). Recently, ^{18}F-THK5351 was reported to bind with high affinity to monoamine oxidase-B (MAO-B), contributing to a high level of *in vivo* PET signal (Harada et al., 2017; Ng et al., 2017). In this review, we describe our experiences and lessons learned from the development of tau PET tracers, and discuss the future of radiotracer development for other proteinopathies.

CHARACTERISTICS OF PROTEIN AGGREGATES

Amyloid-β, tau, and α-synuclein are highly insoluble when accumulated in the diseased brain. They comprise amyloid, a filamentous protein which has a cross-β-sheet structure in which individual β-strands run perpendicular to the fiber axis (Serpell et al., 2000; **Figure 1**). In most cases, these protein aggregates can be stained with histological dyes, such as Congo red and thioflavin-S, which bind the cross-β-sheet structures. Tau aggregates are hyperphosphorylated, and form twisted filaments called paired helical filaments (PHFs), which have a diameter of 8–20 nm and a stereotypical periodicity of 80 nm as observed by electron microscopy (EM). X-ray diffraction of amyloid plaques and PHFs from AD brains reveals unique characteristics, including a sharp reflection at

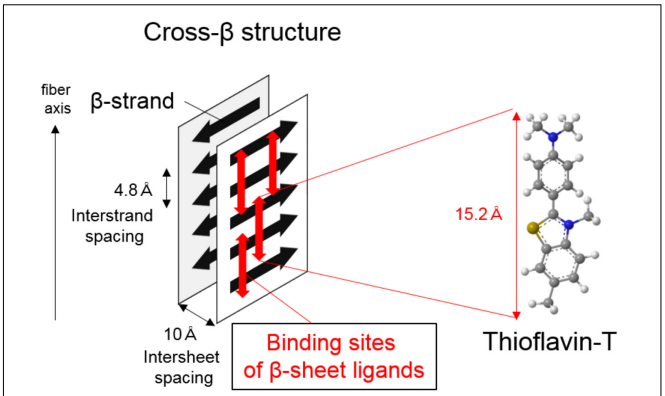

FIGURE 1 | Illustration of cross-β structure in protein aggregates and proposed binding mechanism of β-sheet ligands such as thioflavin-T.

4.76-Å spacing and a diffuse reflection at about 10.6-Å spacing (Kirschner et al., 1986). However, there are various isoforms of tau in the human brain, leading to diverse ultrastructures, spatial distributions, and clinical phenotypes in tauopathies. Tau deposits in neurodegenerative diseases contain different isoform compositions: 3 repeat (3R) and 4 repeat (4R) tau in AD, predominantly 4R tau in CBD and PSP, and 3R tau in Pick's disease. This leads to different affected cell types (e.g., neurons, astrocytes, oligodendrocytes) and histopathologies (e.g., neurofibrillary tangles and neuropil threads in AD, astrocytic plaques in CBD, tufted astrocytes in PSP, and Pick's bodies in Pick's disease). Ultrastructural and biochemical analyses reveal that the detailed composition and structure of tau deposits differ between CBD and PSP, despite both of these diseases being 4R tauopathies (Arai et al., 2004; Taniguchi-Watanabe et al., 2016). Because protein aggregates are highly insoluble, it is difficult to resolve the detailed structure of native aggregates in human brain tissue using conventional techniques such as X-ray crystallography and nuclear magnetic resonance (NMR). Thus, it is difficult to design rationally selective PET tracers. However, a recent study using a novel single particle cryo-EM approach revealed the detailed structure of native tau filaments from an AD brain (Fitzpatrick et al., 2017). The structure of the β-helix or the protofilament interface of PHF-tau may prove to be binding sites for selective tau PET ligands, owing to their specificities. Although the binding sites of tau PET ligands are complicated (Cai et al., 2016), this breakthrough may help in understanding ligand-protein interactions, and accelerate the development of new rationally designed PET tracers. Indeed, a Nobel Prize in chemistry was awarded for cryo-EM in 2017 (Bertozzi, 2017), supporting the potential of this technique to further the development of new tracers.

PROPERTIES REQUIRED FOR PET TRACERS

Protein aggregates consisting of Aβ, tau, and α-synuclein predominantly form cross-β sheet structures, laminated

assemblies of secondary structure β-sheets. Thus, β-sheet ligands such as thioflavin-T could be useful in the development of PET tracers for imaging protein aggregates. One of the most well-described β-sheet ligands is thioflavin-T, which is considered to bind with long axis of amyloid fibrils, having cross β-sheet structures in which individual β-strands run perpendicular to the fiber axis (**Figure 1**; Krebs et al., 2005). As described previously (Villemagne et al., 2012; Okamura et al., 2014b), useful neuroimaging radiotracers must possess the following chemical and pharmacological properties (summarized in **Table 1**): brain–blood barrier (BBB) permeability, ability to undergo rapid clearance from normal brain tissue and blood, and ability to bind with high affinity and specificity to targets.

Positron emission tomography radiotracers are often radiolabeled with ^{11}C or ^{18}F. In general, ^{11}C-labeled tracers are easier to design, as ^{11}C can be introduced into a methyl group. However, ^{11}C-labeled tracers must be radiolabeled in each PET center, owing to the short half-life of ^{11}C ($t_{1/2}$ = 20 min). On the other hand, ^{18}F has a longer half-life ($t_{1/2}$ = 110 min), allowing for easier commercial application.

Binding affinity of a ligand for its target is a critical factor in *in vivo* imaging. Binding sites (B_{max}) and binding affinity (dissociation constant; $K_{d,}$) can be predicted using *in vitro* saturation binding assays in homogenized tissue. At steady state, (B_{max}/K_d) is used to calculate the binding potential (BP), and can be estimated using PET data. The rate constants for dissociation (k_{off}; min^{-1}) and association (k_{on}; $nM^{-1}min^{-1}$) can also be predicted as an index of binding affinity and kinetics. The dissociation constant (K_d) is calculated as the ratio (k_{off}/k_{on}). High-affinity ligands are characterized by low k_{off} and high k_{on}, yielding a low K_d. These parameters serve as a good index of the binding properties of PET radiotracers. The most successful neuroimaging radiotracers for imaging amyloid possess a high binding affinity with K_d values of less than 10 nM (Mathis et al., 2003; Choi et al., 2009; Ni et al., 2013). However, reports of these parameters in the literature should be carefully interpreted as they largely depend on assay conditions. Dissociation constants (K_d) can also be assessed using *in vitro* autoradiography of human brain sections (Zhang et al., 2012; Maruyama et al., 2013; Xia et al., 2013). Binding inhibition constant (K_i) is alternatively estimated if test compounds are structurally related to one radioligand and could be a good indicator of binding affinity for the efficient screening of a number of non-radiolabeled candidate compounds (Furumoto et al., 2007). Recombinant proteins are widely used in binding assays for screening protein-ligand interactions (Mathis et al., 2003; Fodero-Tavoletti et al., 2007; Thompson et al., 2009). However, assays using native protein aggregates derived from human brain tissue represent a more reliable method for measuring the binding affinities of ligands.

Several misfolded proteins share cross β-sheet structures and are present in the neocortex in neurodegenerative diseases (e.g., Aβ and tau in AD, α-synuclein in LBD). In case of AD, there are far fewer tau aggregates than Aβ aggregates in the cortex (5–20 times fewer; Villemagne et al., 2012). Therefore, tau PET tracers require 20–50 times higher selectivity than Aβ, as estimated by simulation studies (Schafer et al., 2012). Further, the density of binding sites in α-synuclein and TDP-43 aggregates is much lower than that in tau and Aβ aggregates. *In vitro* autoradiography of human brain tissue is a reliable method to assess the binding selectivity of radioligands if the assays are performed at low nanomolar ligand concentrations, such as those achieved in brain tissue during a PET scan. *In vitro* autoradiography can also identify non-specific binding of radiotracers. However, a change in the assay conditions, such as washing and fixation procedures, can affect *in vitro* autoradiography results. For example, ethanol is commonly used in the differentiation process to mask non-specific and off-target binding. However, this treatment is not representative of physiological conditions and may damage the native structures of proteins. Fixation of brain tissue also affects autoradiography results. Pathologists generally use formalin-fixed paraffin embedded tissue for diagnostic procedures; however, the process of fixation may affect the native conformation of target and non-target proteins.

In order to allow for BBB penetration via passive diffusion, PET tracers should be small molecules (<450 Da). Useful PET radiotracers show initial brain uptake of more than 5% of an intravenously injected dose. Initial brain uptake depends not only on BBB penetration, but also blood flow, plasma radiotracer concentration, and free fraction of the radiotracer in the plasma and brain. Lipophilicity is a critical property that determines brain uptake. Ideally, a radiotracer should be moderately lipophilic, with an octanol-water partition coefficient (log*P* value) in the range of 0.9–2.5. Rapid clearance from normal tissues without non-specific binding is also desirable, as slower pharmacokinetics prolong the time it takes to reach steady state in a PET scan. In preclinical studies, the ratio of brain uptake 2–30 min after intravenous injection of tracers is a useful index of the clearance of tracers from normal tissues. Furthermore, radiotracers for neuroimaging should be stable and metabolized peripherally. Radiolabeled metabolites should be polar, and exhibit no brain entry or interaction with target proteins. In ^{18}F-labeled tracers, defluorination can cause the accumulation of ^{18}F in the bone, which could interfere with the visual assessment and quantification of radiotracer binding.

TABLE 1 | Properties required for PET tracers.

Properties	Requirements
High blood–brain barrier permeability	>4%ID/g at 2 min post injection in normal mice
Rapid clearance	2–30 min brain uptake ratio in mice > 10
High binding affinity	Kd or Ki < 20 nM for target(s)
Off-target binding	None
Reversible binding to target	Reversible binding to target(s)
Stability	No radiolabeled metabolites in the brain

SCREENING OF β-SHEET LIGANDS

As previously mentioned, small organic compounds that possess a high affinity for β-sheet structures are potential candidates

for PET tracers in the imaging of proteinopathies. Planar compounds potentially bind to the cross β-sheet structure of protein aggregates. Congo red, thioflavin-S, and thioflavin-T are histological dyes that have traditionally been used for the visualization of amyloid lesions. Therefore, much effort has been made to optimize derivatives of these in the development of amyloid PET tracers. The first successful radiotracer for Aβ is ^{11}C-PiB, a thioflavin-T derivative (Mathis et al., 2012). ^{18}F-labeled amyloid PET tracers such as Florbetapir (Amyvid^{TM}), Flutemetamol (Vizamyl^{TM}), and Florbetaben (NeuroCeq^{TM}) have also been developed and approved by the FDA and EMA. Identifying lead compounds for imaging proteinopathies other than Aβ has proven challenging, as most β-sheet binding ligands have a high affinity for Aβ fibrils. Although protein aggregates share a predominantly cross-β-sheet structure, they have distinct conformations. In fact, several fluorescent compounds display different emission spectra when bound to Aβ plaques and tau pathology in AD brain sections, suggesting that these compounds would interact with Aβ and tau aggregates differently (Harada et al., 2014). Fluorescence staining is useful for evaluating binding ability for initial screening processes. However, this method is very low throughput, and requires postmortem human brain samples. Previously, synthetic fibrils generated from recombinant proteins such as tau protein were used for the binding evaluation, but they cannot be expected to fully recapitulate the binding to native pathology. In fact, we have experienced the discrepancy of the binding data between synthetic fibrils and tissues containing native conformation of protein aggregates (Zhang et al., 2012; Okamura et al., 2013). Therefore, researchers have attempted to develop efficient and reliable high-throughput screening assays to identify lead compounds for imaging proteinopathies such as tau, α-synuclein, and TDP-43 aggregates. For example, tissue-based high throughput screening utilized with mass spectrometry imaging have been proposed (Yoshimi et al., 2015), but this field seems to be a big challenge.

DEVELOPMENT OF TAU PET TRACERS

Compared with the development of amyloid PET tracers, there was no lead compound available in the development of selective PET tracer for tau or α-synuclein. In the case of tau, Okamura et al. (2005) identified quinoline and styryl-benzimidazole derivatives that clearly stained neurofibrillary tangles, neuropil threads, and dystrophic neurites in AD brain sections. After successful identification of these derivatives, a quinoline derivative ^{11}C-BF158 was synthesized and evaluated in human brain sections. *In vitro* autoradiography of ^{11}C-BF158 revealed preferential binding in tau-rich regions over Aβ-rich regions (Okamura et al., 2005). In addition, ^{11}C-BF158 showed high BBB permeability in mice, suggesting that quinoline derivatives could be good candidates for tau PET tracers (**Figure 2**). Additionally, we synthesized the ^{18}F-quinoline derivative ^{18}F-THK523. Small animal PET studies have demonstrated higher tracer retention in rTg4510 tau transgenic mice compared to littermate controls (Fodero-Tavoletti et al., 2011). Direct comparison of ^{18}F-THK523 with ^{11}C-PiB, ^{18}F-BF227, and ^{18}F-FDDNP in AD brain sections revealed different binding distributions of ^{18}F-THK523, which co-localized with tau immunostaining and Gallyas Braak silver staining (Harada et al., 2013). A first-in-human study of ^{18}F-THK523 demonstrated significant tracer retention in the temporal parietal, orbitofrontal lobe, and hippocampus of AD patients, and different tracer retention compared to ^{11}C-PiB in the same subjects (Villemagne et al., 2014). However, ^{18}F-THK523 retention was significantly lower in gray matter than in white matter, suggesting insufficient binding affinity of this tracer to PHF-tau in the AD brain.

We further optimized the quinoline derivatives (Tago et al., 2014; Furumoto et al., 2017) and developed ^{18}F-THK5105 and ^{18}F-THK5117, which possess higher affinity for tau fibrils and better pharmacokinetics than ^{18}F-THK523 (Okamura et al., 2013; Lemoine et al., 2015). These tracers were evaluated in human studies (Okamura et al., 2014a; Harada et al., 2015). In these clinical studies, radiotracer retention was elevated in the inferior temporal lobe of patients with AD where tau pathology was frequently observed at autopsy. ^{18}F-THK5105 retention in the neocortex was significantly correlated with disease severity of AD patients (Okamura et al., 2014a). The spatial pattern of ^{18}F-THK5117 retention in AD was consistent with that of ^{18}F-THK5105, and different from that of ^{11}C-PiB. However, both ^{18}F-THK5105 and ^{18}F-THK5117 were retained in white matter. As observed in amyloid PET tracers, β-sheet ligands may bind to white matter in a non-specific manner, owing to the presence of β-sheet-rich myelin basic protein (Stankoff et al., 2011). Lipophilicity of compounds can strongly influence white matter binding. For example, increasing hydrophilicity via the introduction of nitrogen to a benzene ring can reduce non-specific binding of the tracer to white matter, as observed using ^{11}C-AZD2184, a pyridine derivative of ^{11}C-PiB (Johnson et al., 2009; Nyberg et al., 2009).

To reduce non-specific tracer retention in white matter, we additionally developed ^{18}F-THK5351, a pyridine derivative of ^{18}F-THK5117 (Harada et al., 2016b; Tago et al., 2016b). Indeed, ^{18}F-THK5351 is more hydrophilic than ^{18}F-THK5117 (Log P = 1.5 vs 2.3). As expected, ^{18}F-THK5351 showed less white matter binding and improved pharmacokinetics. A fluoropropanol side chain of THK5117 contains a chiral center. ^{18}F-THK5117 is a racemic compound with equal amounts of *S*- and *R*-enantiomers. In general, each enantiomer exhibits different biological properties including binding affinity, pharmacokinetics, and metabolism. In our analysis, *S*-enantiomers of THK compounds were superior to *R*-enantiomers with respect to pharmacokinetics, tolerance to defluorination, and binding affinity to human brain homogenates (Tago et al., 2016a,b). In ^{18}F-THK5351 PET study, we observed prominent tracer retention in the inferior temporal cortex of AD patients. ^{18}F-THK5351 successfully reduced non-specific retention in white matter and exhibited superior pharmacokinetics than ^{18}F-THK5117 (Harada et al., 2016b; Betthauser et al., 2017). The major radiolabeled metabolite of this tracer was a sulfate conjugate, which appears to be generated outside of (and does not enter into) the brain (Harada et al., 2016a).

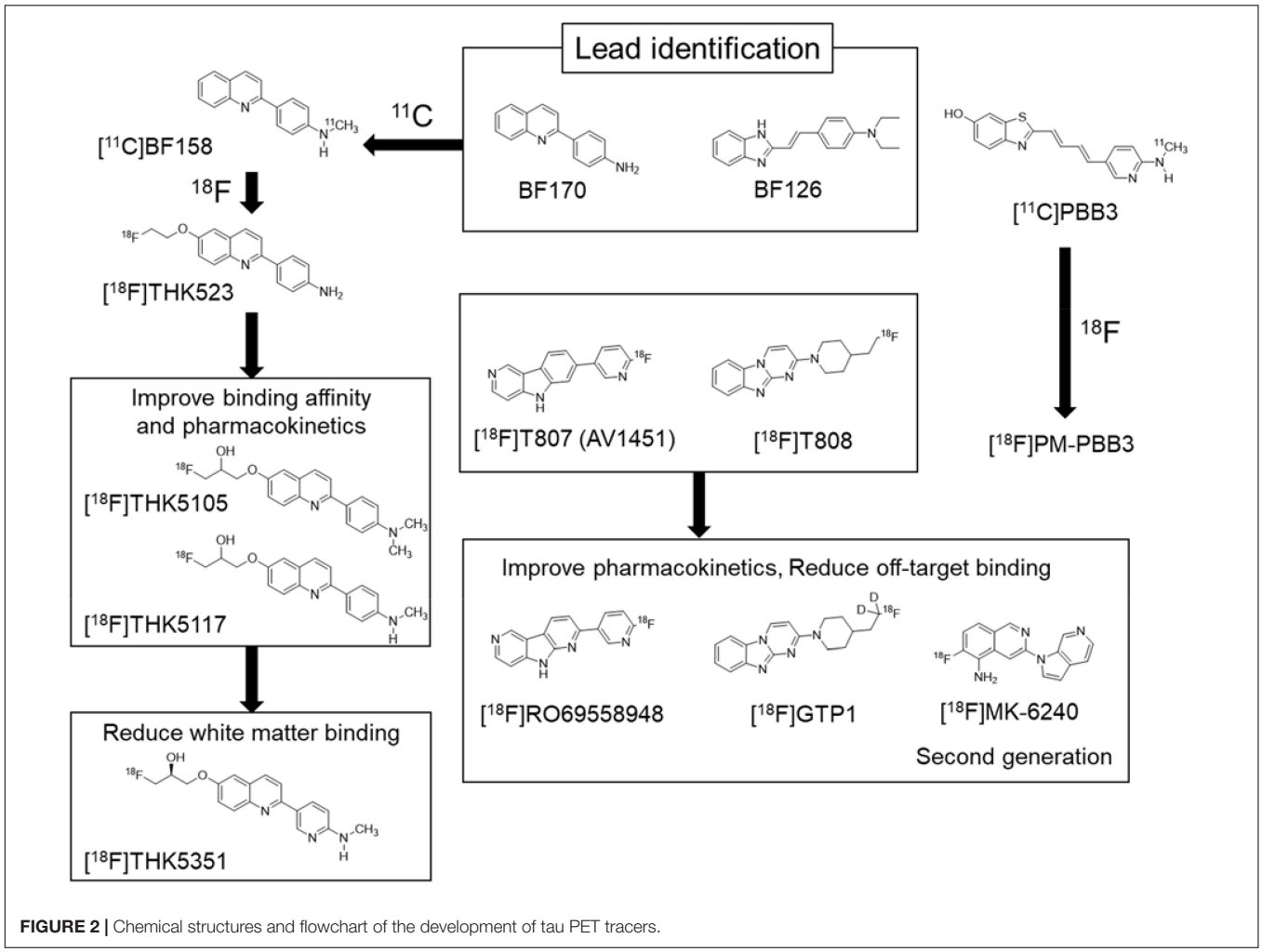

FIGURE 2 | Chemical structures and flowchart of the development of tau PET tracers.

In clinical studies of AD patients, regional tracer retention correlates well with glucose hypometabolism. and mirrors the clinical and neuroanatomical variability in AD variants (Chiotis et al., 2016; Saint-Aubert et al., 2016; Kang et al., 2017) as observed in ^{18}F-AV1451 PET studies (Ossenkoppele et al., 2016). Furthermore, prominent tracer retention is observed in sites susceptible to tau deposition in non-AD tauopathies such as CBD and PSP (Chiotis et al., 2016; Kikuchi et al., 2016; Ishiki et al., 2017). However, ^{18}F-THK5351 also accumulates in the temporal cortex in semantic variant primary progressive aphasia (svPPA), although notably, more than 90% of svPPA cases are FTLD-TDP type C pathology (Spinelli et al., 2017).

Since tau PET ligands recognize cross-β sheet structure of PHF-tau, they could detect extracellular ghost tangles as well as intracellular neurofibrillary tangles. However, they are not sensitive to non-argyrophilic pretangles that contain AT8-immunoreactive soluble tau (Braak et al., 1994; Sun et al., 2002). Tau immunohistochemistry and Gallyas Braak silver staining detect neurofibrillary pathology in layers II, III, and V of the neocortex in AD patients (Braak et al., 2006a). Interestingly, ^{3}H-THK5351 binds preferentially to neurofibrillary tangles in the pyramidal cell layer (V) compared to the granule cell layers (II/III), although the granule cell layers also contain neurofibrillary tangles. Similar binding characteristics were observed for ^{18}F-AV1451 (Lowe et al., 2016). These observations suggest variation in the structural conformation and maturity of neurofibrillary tangles in AD brains. As described by Lowe et al. (2016), this has very important implications on the sensitivity of tau PET imaging at different stages; tau PET ligands may detect more mature tangles than anticipated.

^{18}F-THK5351 satisfies the requirements for neuroimaging PET tracers. However, ^{18}F-THK5351 exhibits off-target binding in the basal ganglia and thalamus. Recent blocking studies have identified MAO-B as an off-target binding substrate of ^{18}F-THK5351. In a human study, a single oral dose (10 mg) of selegiline, an MAO-B inhibitor, reduced ^{18}F-THK5351 signal in the basal ganglia as well as neocortex (Ng et al., 2017). In addition, an autopsy imaging study of ^{18}F-THK5351 in an AD patient demonstrated significant correlation of *in vivo* ^{18}F-THK5351 signals with MAO-B levels (Harada et al., 2017). This indicates that ^{18}F-THK5351 is not a selective PET tracer for tau. In our previous studies, THK5351-MAO-B binding was overlooked in human brain sections because the formaldehyde-fixed sections had been used in autoradiography analyses

(Okamura et al., 2013; Harada et al., 2015, 2016b). Fixation of tissues with formalin, paraformaldehyde, or alcohol denatures native protein structures and deactivates native enzyme activity, while protein deposits such as neurofibrillary tangles and amyloid plaques are relatively stable. In fact, ^{3}H-THK5351 binding in the putamen disappears after fixation with 4% paraformaldehyde, while laminar THK5351 binding in the neocortex remains detectable even after fixation. Therefore, selectivity of radiotracers should be assessed in unfixed frozen tissue. A receptor panel screen (i.e., ligand binding assay) has also been utilized to identify off-target binding of tracer candidates. However, functional assays are commonly used to assess a compound's binding ability to a particular enzyme, and the panel screen was originally designed for the development of therapeutic drugs. In our experience, functional assays are less sensitive in the evaluation of the binding ability of a compound to an enzyme compared to ligand-binding assays.

^{18}F-AV1451 (also known as flortaucipir, T807) was developed as tau PET tracer (**Figure 2**). This tracer showed high binding affinity and specificity to tau deposits in AD brain sections. ^{18}F-AV1451 has been clinically evaluated in many PET centers (Villemagne et al., 2015) revealing a robust difference between AD patients and normal elderly controls. The spatial distribution of ^{18}F-AV1451 followed the known distribution of tau aggregates in the neocortex, glucose hypometabolism in FDG-PET, and cortical atrophy in MRI (Schwarz et al., 2016; Hanseeuw et al., 2017; Xia et al., 2017). ^{18}F-AV1451 PET studies have also demonstrated a distinct pattern of tracer binding in non-AD tauopathies such as PSP, CBD, and microtubule associated tau (MAPT) mutation carriers (Smith et al., 2016, 2017b; Cho et al., 2017a; Passamonti et al., 2017; Schonhaut et al., 2017; Spina et al., 2017). However, ^{18}F-AV1451 retention was also observed in non-tauopathies such as svPPA and MSA (Cho et al., 2017b; Makaretz et al., 2017). This is similar to the findings in studies of ^{18}F-THK5351 PET. Off-target binding of ^{18}F-AV1451 is observed in the basal ganglia, choroid plexus, and midbrain. Previous studies suggested that ^{18}F-AV1451 binds with high affinity to MAO-A and neuromelanin (Marquie et al., 2015; Vermeiren et al., 2015), although this fails to account for off-target retention of this tracer in the basal ganglia. A recent study demonstrated a lack of correlation between *in vivo* ^{18}F-AV1451 retention and tau pathology in cases with non-AD tauopathy (Josephs et al., 2016; Marquie et al., 2017; Smith et al., 2017a). While ^{18}F-AV1451 retention was elevated in the basal ganglia of PSP cases, *in vitro* assays failed to detect significant ^{18}F-AV1451 binding to 4R tau deposits in the basal ganglia of postmortem brains. It is speculated that these discrepancies are caused by the fixation of brain samples or the use of ethanol during differentiation, which can mask off-target and non-specific binding of radiotracer. Indeed, a recent autoradiography study successfully detected displaceable binding of ^{18}F-AV1451 in the basal ganglia without using ethanol (Walji et al., 2016). *In vitro* binding assays demonstrated that a MAO-A inhibitor blocked ^{18}F-AV1451 binding in the basal ganglia. However, the effect was relatively modest compared to that of self-blocking, indicating the presence of other off-target substrates of AV1451. ^{18}F-AV1451 PET in PD patients revealed no significant differences in tracer uptake between patients who received MAO-B inhibitors (selegiline and rasagiline) and those who did not (Hansen et al., 2017), indicating that MAO-B is not an off-target substrate of ^{18}F-AV1451 in the basal ganglia. Another frequent site of ^{18}F-AV1451 binding is the choroid plexus which is closely located to the hippocampus. Although tau protein deposits in epithelial cells may contribute to ^{18}F-AV1451 binding, it is still unclear why this tracer accumulates in the choroid plexus.

^{11}C-PBB3 was developed to visualize a broad range of tauopathies in the human brain. In clinical PET studies, significant ^{11}C-PBB3 retention has been detected in the hippocampus and neocortex of AD patients. ^{11}C-PBB3 retention was also observed in the striatum and midbrain of PSP patients, suggesting high binding affinity of this tracer to 4R tau deposits. Off-target binding of ^{11}C-PBB3 has been observed in the basal ganglia, the longitudinal sinus and the choroid plexus. The ^{18}F-labeled derivatives of PBB3 (^{18}F-AM-PBB3 and ^{18}F-PM-PBB3) have been newly developed and showed less off-target signals in the basal ganglia and higher specific signals than ^{11}C-PBB3. Recently, new-generation tau PET tracers have been developed to overcome the drawbacks of the first-generation tracers (Villemagne, 2017). ^{18}F-MK6240, ^{18}F-RO69558948, and ^{18}F-PI2620 (**Figure 2**) also showed excellent pharmacokinetics and high binding affinity selectivity for tau aggregates in AD brain tissue (Hostetler et al., 2016; Honer et al., 2018). Preclinical binding analysis also has suggested lower binding affinity of these second-generation tracers to MAO-A and MAO-B, than the binding affinity of the first-generation tracers such as ^{18}F-AV1451 and ^{18}F-THK5351. A recent first-in-human study showed no detectable signal in the basal ganglia and brainstem, suggesting high binding selectivity of these tracers to tau deposition in patients with AD (Villemagne, 2017; Lohith et al., 2018; Wong et al., 2018). Further validation studies are required to confirm the binding selectivity of these tracers.

CHALLENGES FOR IMAGING OTHER PROTEINOPATHIES

It is challenging to develop novel PET tracers for imaging other misfolded proteins such as α-synuclein and TDP-43, due to the density of binding sites of α-synuclein and TDP-43 aggregates in diseased brains is lower than that of Aβ and tau in AD brains. Like tau pathology, α-synuclein shows distinct cellular localization in synucleinopathies. Lewy bodies are observed in neurons in PD and dementia with Lewy bodies (DLB), while glial cytoplasmic inclusions (GCIs) are observed in oligodendrocytes of MSA (Shah et al., 2014). BF227 was originally developed for imaging Aβ in the brain (Kudo et al., 2007). However, this compound shows high binding affinity for recombinant α-synuclein fibrils. A ^{11}C-BF227 PET study demonstrated a significant increase in tracer retention in brain regions susceptible to α-synuclein deposition in MSA (Kikuchi et al., 2010). Recently, ^{11}C-PBB3 was also reported to have binding affinity to GCIs in a subset of MSA cases (Koga et al., 2017). ^{11}C-PBB3 PET demonstrated significant tracer retention in MSA patients compared to age-matched control subjects (Perez-Soriano et al., 2017). Currently,

no PET tracer is available for imaging Lewy bodies in the human brain. High binding affinity and selectivity for Lewy bodies are required to image Lewy pathology *in vivo*, because α-synuclein pathology is frequently concomitant with AD pathology.

Several groups have reported novel scaffold ligands that demonstrate affinity for α-synuclein aggregates. A phenothiazine derivative, ^{125}I-SIL23, showed binding affinity for *in vitro* generated α-synuclein as well as PD brain homogenates (Bagchi et al., 2013). ^{11}C- and ^{18}F-analogs of phenothiazine derivatives appear to demonstrate insufficient binding affinity for α-synuclein in PD brain tissues. ^{18}F-46a, which is a series of 3-(benzylidene)indolin-2-one, showed better selectivity for *in vitro* generated α-synuclein fibrils compared to Aβ and tau (Chu et al., 2015).

TDP-43 is frequently observed in some variants of FTLD and ALS as a primary histopathological feature. TDP-43 pathology is also concomitant with AD, PD-related disorders, Huntington's disease, and rare disorders such as Guam ALS, as a secondary histopathological feature (Chen-Plotkin et al., 2010). TDP-43 pathology is more complicated than other proteinopathies, because there are many histopathologic subtypes, including FTLD-TDP types 1-4 and ALS-TDP (Mackenzie et al., 2010). One concern in the development of TDP-43 tracers is the density of cross β-sheet structures in TDP-43 aggregates. Although partial peptides from TDP-43 can form amyloid structures (Shimonaka et al., 2016), most TDP-43 aggregates may not have cross β-sheet structures (Cairns et al., 2007). One study reported that thioflavin-S-positive skein-like inclusions are present in only 28% of ALS cases (Robinson et al., 2013), while another study found that thioflavin-S-positive TDP-43 inclusions were present in most FTLD-TDP and ALS cases (Bigio et al., 2013). Further validation studies are required to better understand the structure of TDP-43 aggregates. If the majority of TDP-43 aggregates do not contain cross β-sheet structures, other approaches will be required (i.e., non-β-sheet ligands). Bigio et al. (2013) also observed a high density of thioflavin-S-positive astrocytosis in the superficial frontal cortex of FTLD-TDP type A. Although the significance of thioflavin-S-positive astrocytosis remains unknown, proteins containing cross β-sheet conformation might be critical in understanding the histopathology of FTLD-TDP type A.

CONCLUSION

Here, we describe our experiences and lessons learned from the development of tau PET tracers, and discuss issues surrounding the development of new tracers for other proteinopathies. Advances in structural biology will aid in the development of novel PET tracers for imaging proteinopathies.

AUTHOR CONTRIBUTIONS

RH and NO wrote the manuscript. SF and KY revised the manuscript.

FUNDING

This study was supported by research funds from GE Healthcare, Grant-in-Aid for Scientific Research (B) (15H04900), and Grant-in-Aid for Scientific Research on Innovative Areas (Brain Protein Aging and Dementia Control) (26117003) from MEXT.

REFERENCES

Arai, T., Ikeda, K., Akiyama, H., Nonaka, T., Hasegawa, M., Ishiguro, K., et al. (2004). Identification of amino-terminally cleaved tau fragments that distinguish progressive supranuclear palsy from corticobasal degeneration. *Ann. Neurol.* 55, 72–79. doi: 10.1002/ana.10793

Bagchi, D. P., Yu, L., Perlmutter, J. S., Xu, J., Mach, R. H., Tu, Z., et al. (2013). Binding of the radioligand SIL23 to alpha-synuclein fibrils in Parkinson disease brain tissue establishes feasibility and screening approaches for developing a Parkinson disease imaging agent. *PLoS One* 8:e55031. doi: 10.1371/journal.pone.0055031

Bertozzi, C. (2017). Atoms out of blobs: CryoEM takes the Nobel prize in chemistry. *ACS Cent. Sci.* 3:1056. doi: 10.1021/acscentsci.7b00494

Betthauser, T. J., Lao, P. J., Murali, D., Barnhart, T. E., Furumoto, S., Okamura, N., et al. (2017). In vivo comparison of tau radioligands 18F-THK-5351 and 18F-THK-5317. *J. Nucl. Med.* 58, 996–1002. doi: 10.2967/jnumed.116.182980

Bierer, L. M., Hof, P. R., Purohit, D. P., Carlin, L., Schmeidler, J., Davis, K. L., et al. (1995). Neocortical neurofibrillary tangles correlate with dementia severity in Alzheimer's disease. *Arch. Neurol.* 52, 81–88. doi: 10.1001/archneur.1995.00540250089017

Bigio, E. H., Wu, J. Y., Deng, H. X., Bit-Ivan, E. N., Mao, Q., Ganti, R., et al. (2013). Inclusions in frontotemporal lobar degeneration with TDP-43 proteinopathy (FTLD-TDP) and amyotrophic lateral sclerosis (ALS), but not FTLD with FUS proteinopathy (FTLD-FUS), have properties of amyloid. *Acta Neuropathol.* 125, 463–465. doi: 10.1007/s00401-013-1089-6

Braak, E., Braak, H., and Mandelkow, E. M. (1994). A sequence of cytoskeleton changes related to the formation of neurofibrillary tangles and neuropil threads. *Acta Neuropathol.* 87, 554–567. doi: 10.1007/BF00293315

Braak, H., Alafuzoff, I., Arzberger, T., Kretzschmar, H., and Del Tredici, K. (2006a). Staging of Alzheimer disease-associated neurofibrillary pathology using paraffin sections and immunocytochemistry. *Acta Neuropathol.* 112, 389–404.

Braak, H., Rub, U., and Del Tredici, K. (2006b). Cognitive decline correlates with neuropathological stage in Parkinson's disease. *J. Neurol. Sci.* 248, 255–258.

Braak, H., and Braak, E. (1991). Neuropathological stageing of Alzheimer-related changes. *Acta Neuropathol.* 82, 239–259. doi: 10.1007/BF00308809

Braak, H., Del Tredici, K., Rub, U., De Vos, R. A., Jansen Steur, E. N., and Braak, E. (2003). Staging of brain pathology related to sporadic Parkinson's disease. *Neurobiol. Aging* 24, 197–211. doi: 10.1016/S0197-4580(02)00065-9

Brettschneider, J., Del Tredici, K., Toledo, J. B., Robinson, J. L., Irwin, D. J., Grossman, M., et al. (2013). Stages of pTDP-43 pathology in amyotrophic lateral sclerosis. *Ann. Neurol.* 74, 20–38. doi: 10.1002/ana.23937

Cai, L., Qu, B., Hurtle, B. T., Dadiboyena, S., Diaz-Arrastia, R., and Pike, V. W. (2016). Candidate PET radioligand development for neurofibrillary tangles: two distinct radioligand binding sites identified in postmortem Alzheimer's disease brain. *ACS Chem. Neurosci.* 7, 897–911. doi: 10.1021/acschemneuro.6b00051

Cairns, N. J., Neumann, M., Bigio, E. H., Holm, I. E., Troost, D., Hatanpaa, K. J., et al. (2007). TDP-43 in familial and sporadic frontotemporal lobar degeneration with ubiquitin inclusions. *Am. J. Pathol.* 171, 227–240. doi: 10.2353/ajpath.2007.070182

Chen-Plotkin, A. S., Lee, V. M., and Trojanowski, J. Q. (2010). TAR DNA-binding protein 43 in neurodegenerative disease. *Nat. Rev. Neurol.* 6, 211–220. doi: 10.1038/nrneurol.2010.18

Chiotis, K., Saint-Aubert, L., Savitcheva, I., Jelic, V., Andersen, P., Jonasson, M., et al. (2016). Imaging in-vivo tau pathology in Alzheimer's disease with THK5317 PET in a multimodal paradigm. *Eur. J. Nucl. Med. Mol. Imaging* 43, 1686–1699. doi: 10.1007/s00259-016-3363-z

Cho, H., Baek, M. S., Choi, J. Y., Lee, S. H., Kim, J. S., Ryu, Y. H., et al. (2017a). 18F-AV-1451 binds to motor-related subcortical gray and white matter in corticobasal syndrome. *Neurology* 89, 1170–1178. doi: 10.1212/WNL.0000000000004364

Cho, H., Choi, J. Y., Lee, S. H., Ryu, Y. H., Lee, M. S., and Lyoo, C. H. (2017b). 18 F-AV-1451 binds to putamen in multiple system atrophy. *Mov. Disord.* 32, 171–173. doi: 10.1212/WNL.0000000000004364

Choi, S. R., Golding, G., Zhuang, Z., Zhang, W., Lim, N., Hefti, F., et al. (2009). Preclinical properties of 18F-AV-45: a PET agent for Abeta plaques in the brain. *J. Nucl. Med.* 50, 1887–1894. doi: 10.2967/jnumed.109.065284

Chu, W., Zhou, D., Gaba, V., Liu, J., Li, S., Peng, X., et al. (2015). Design, synthesis, and characterization of 3-(Benzylidene)indolin-2-one derivatives as ligands for alpha-synuclein fibrils. *J. Med. Chem.* 58, 6002–6017. doi: 10.1021/acs.jmedchem.5b00571

Fitzpatrick, A. W. P., Falcon, B., He, S., Murzin, A. G., Murshudov, G., Garringer, H. J., et al. (2017). Cryo-EM structures of tau filaments from Alzheimer's disease. *Nature* 547, 185–190. doi: 10.1038/nature23002

Fodero-Tavoletti, M. T., Okamura, N., Furumoto, S., Mulligan, R. S., Connor, A. R., Mclean, C. A., et al. (2011). 18F-THK523: a novel in vivo tau imaging ligand for Alzheimer's disease. *Brain* 134, 1089–1100. doi: 10.1093/brain/awr038

Fodero-Tavoletti, M. T., Smith, D. P., Mclean, C. A., Adlard, P. A., Barnham, K. J., Foster, L. E., et al. (2007). In vitro characterization of Pittsburgh compound-B binding to Lewy bodies. *J. Neurosci.* 27, 10365–10371. doi: 10.1523/JNEUROSCI.0630-07.2007

Furumoto, S., Okamura, N., Iwata, R., Yanai, K., Arai, H., and Kudo, Y. (2007). Recent advances in the development of amyloid imaging agents. *Curr. Top. Med. Chem.* 7, 1773–1789. doi: 10.2174/156802607782507402

Furumoto, S., Tago, T., Harada, R., Kudo, Y., and Okamura, N. (2017). 18F-Labeled 2-Arylquinoline derivatives for tau imaging: chemical, radiochemical, biological and clinical features. *Curr. Alzheimer Res.* 14, 178–185. doi: 10.2174/1567205013666160620121811

Hanseeuw, B. J., Betensky, R. A., Schultz, A. P., Papp, K. V., Mormino, E. C., Sepulcre, J., et al. (2017). Fluorodeoxyglucose metabolism associated with tau-amyloid interaction predicts memory decline. *Ann. Neurol.* 81, 583–596. doi: 10.1002/ana.24910

Hansen, A. K., Brooks, D. J., and Borghammer, P. (2017). MAO-B inhibitors do not block in vivo flortaucipir([18F]-AV-1451) binding. *Mol. Imaging Biol.* 20, 356–360. doi: 10.1007/s11307-017-1143-1

Harada, R., Furumoto, S., Tago, T., Furukawa, K., Ishiki, A., Tomita, N., et al. (2016a). Characterization of the radiolabeled metabolite of tau PET tracer 18F-THK5351. *Eur. J. Nucl. Med. Mol. Imaging* 43, 2211–2218. doi: 10.1007/s00259-016-3453-y

Harada, R., Okamura, N., Furumoto, S., Furukawa, K., Ishiki, A., Tomita, N., et al. (2016b). 18F-THK5351: a novel PET radiotracer for imaging neurofibrillary pathology in Alzheimer disease. *J. Nucl. Med.* 57, 208–214. doi: 10.2967/jnumed.115.164848

Harada, R., Okamura, N., Furumoto, S., Tago, T., Yanai, K., Arai, H., et al. (2016c). Characteristics of tau and its ligands in PET imaging. *Biomolecules* 6:7. doi: 10.3390/biom6010007

Harada, R., Ishiki, A., Kai, H., Sato, N., Furukawa, K., Furumoto, S., et al. (2017). Correlations of ^{18}F-THK5351 PET with postmortem burden of tau and astrogliosis in Alzheimer's disease. *J. Nucl. Med.* 59, 671–674. doi: 10.2967/jnumed.117.197426

Harada, R., Okamura, N., Furumoto, S., Furukawa, K., Ishiki, A., Tomita, N., et al. (2015). [(18)F]THK-5117 PET for assessing neurofibrillary pathology in Alzheimer's disease. *Eur. J. Nucl. Med. Mol. Imaging* 42, 1052–1061. doi: 10.1007/s00259-015-3035-4

Harada, R., Okamura, N., Furumoto, S., Tago, T., Maruyama, M., Higuchi, M., et al. (2013). Comparison of the binding characteristics of [18F]THK-523 and other amyloid imaging tracers to Alzheimer's disease pathology. *Eur. J. Nucl. Med. Mol. Imaging* 40, 125–132. doi: 10.1007/s00259-012-2261-2

Harada, R., Okamura, N., Furumoto, S., Yoshikawa, T., Arai, H., Yanai, K., et al. (2014). Use of a benzimidazole derivative BF-188 in fluorescence multispectral imaging for selective visualization of tau protein fibrils in the Alzheimer's disease brain. *Mol. Imaging Biol.* 16, 19–27. doi: 10.1007/s11307-013-0667-2

Honer, M., Gobbi, L., Knust, H., Kuwabara, H., Muri, D., Koerner, M., et al. (2018). Preclinical evaluation of (18)F-RO6958948, (11)C-RO6931643, and (11)C-RO6924963 as novel PET radiotracers for imaging tau aggregates in Alzheimer disease. *J. Nucl. Med.* 59, 675–681. doi: 10.2967/jnumed.117.196741

Hostetler, E. D., Walji, A. M., Zeng, Z., Miller, P., Bennacef, I., Salinas, C., et al. (2016). Preclinical characterization of 18F-MK-6240, a promising PET tracer for in vivo quantification of human neurofibrillary tangles. *J. Nucl. Med.* 57, 1599–1606. doi: 10.2967/jnumed.115.171678

Hyman, B. T., Phelps, C. H., Beach, T. G., Bigio, E. H., Cairns, N. J., Carrillo, M. C., et al. (2012). National institute on aging-Alzheimer's association guidelines for the neuropathologic assessment of Alzheimer's disease. *Alzheimers Dement.* 8, 1–13. doi: 10.1016/j.jalz.2011.10.007

Ishiki, A., Harada, R., Okamura, N., Tomita, N., Rowe, C. C., Villemagne, V. L., et al. (2017). Tau imaging with [18 F]THK-5351 in progressive supranuclear palsy. *Eur. J. Neurol.* 24, 130–136. doi: 10.1111/ene.13164

Johnson, A. E., Jeppsson, F., Sandell, J., Wensbo, D., Neelissen, J. A., Jureus, A., et al. (2009). AZD2184: a radioligand for sensitive detection of beta-amyloid deposits. *J. Neurochem.* 108, 1177–1186. doi: 10.1111/j.1471-4159.2008.05861.x

Josephs, K. A., Whitwell, J. L., Tacik, P., Duffy, J. R., Senjem, M. L., Tosakulwong, N., et al. (2016). [18F]AV-1451 tau-PET uptake does correlate with quantitatively measured 4R-tau burden in autopsy-confirmed corticobasal degeneration. *Acta Neuropathol.* 132, 931–933. doi: 10.1007/s00401-016-1618-1

Kang, J. M., Lee, S. Y., Seo, S., Jeong, H. J., Woo, S. H., Lee, H., et al. (2017). Tau positron emission tomography using [18F]THK5351 and cerebral glucose hypometabolism in Alzheimer's disease. *Neurobiol. Aging* 59, 210–219. doi: 10.1016/j.neurobiolaging.2017.08.008

Kikuchi, A., Okamura, N., Hasegawa, T., Harada, R., Watanuki, S., Funaki, Y., et al. (2016). In vivo visualization of tau deposits in corticobasal syndrome by 18F-THK5351 PET. *Neurology* 87, 2309–2316. doi: 10.1212/WNL.0000000000003375

Kikuchi, A., Takeda, A., Okamura, N., Tashiro, M., Hasegawa, T., Furumoto, S., et al. (2010). In vivo visualization of alpha-synuclein deposition by carbon-11-labelled 2-[2-(2-dimethylaminothiazol-5-yl)ethenyl]-6-[2-(fluoro)ethoxy]benzoxazole positron emission tomography in multiple system atrophy. *Brain* 133, 1772–1778. doi: 10.1093/brain/awq091

Kirschner, D. A., Abraham, C., and Selkoe, D. J. (1986). X-ray diffraction from intraneuronal paired helical filaments and extraneuronal amyloid fibers in Alzheimer disease indicates cross-beta conformation. *Proc. Natl. Acad. Sci. U.S.A.* 83, 503–507. doi: 10.1073/pnas.83.2.503

Klunk, W. E., Engler, H., Nordberg, A., Wang, Y., Blomqvist, G., Holt, D. P., et al. (2004). Imaging brain amyloid in Alzheimer's disease with Pittsburgh Compound-B. *Ann. Neurol.* 55, 306–319. doi: 10.1002/ana.20009

Koga, S., Ono, M., Sahara, N., Higuchi, M., and Dickson, D. W. (2017). Fluorescence and autoradiographic evaluation of tau PET ligand PBB3 to alpha-synuclein pathology. *Mov. Disord.* 32, 884–892. doi: 10.1002/mds.27013

Krebs, M. R., Bromley, E. H., and Donald, A. M. (2005). The binding of thioflavin-T to amyloid fibrils: localisation and implications. *J. Struct. Biol.* 149, 30–37. doi: 10.1016/j.jsb.2004.08.002

Kudo, Y., Okamura, N., Furumoto, S., Tashiro, M., Furukawa, K., Maruyama, M., et al. (2007). 2-(2-[2-Dimethylaminothiazol-5-yl]ethenyl)-6-(2-[fluoro]ethoxy)benzoxazole: a novel PET agent for in vivo detection of dense amyloid plaques in Alzheimer's disease patients. *J. Nucl. Med.* 48, 553–561. doi: 10.2967/jnumed.106.037556

Lemoine, L., Saint-Aubert, L., Marutle, A., Antoni, G., Eriksson, J. P., Ghetti, B., et al. (2015). Visualization of regional tau deposits using (3)H-THK5117 in Alzheimer brain tissue. *Acta Neuropathol. Commun.* 3:40. doi: 10.1186/s40478-015-0220-4

Lohith, T. G., Bennacef, I., Vandenberghe, R., Vandenbulcke, M., Salinas-Valenzuela, C., Declercq, R., et al. (2018). First-in-human brain imaging of Alzheimer dementia patients and elderly controls with (18)F-MK-6240, a PET tracer targeting neurofibrillary tangle pathology. *J. Nucl. Med.* doi: 10.2967/jnumed.118.208215 [Epub ahead of print].

Lowe, V. J., Curran, G., Fang, P., Liesinger, A. M., Josephs, K. A., Parisi, J. E., et al. (2016). An autoradiographic evaluation of AV-1451 Tau PET in dementia. *Acta Neuropathol. Commun.* 4:58. doi: 10.1186/s40478-016-0315-6

Mackenzie, I. R., Rademakers, R., and Neumann, M. (2010). TDP-43 and FUS in amyotrophic lateral sclerosis and frontotemporal dementia. *Lancet Neurol.* 9, 995–1007. doi: 10.1016/S1474-4422(10)70195-2

Makaretz, S. J., Quimby, M., Collins, J., Makris, N., Mcginnis, S., Schultz, A., et al. (2017). Flortaucipir tau PET imaging in semantic variant primary progressive aphasia. *J. Neurol. Neurosurg. Psychiatry* doi: 10.1136/jnnp-2017-316409 [Epub ahead of print].

Marquie, M., Normandin, M. D., Meltzer, A. C., Siao Tick Chong, M., Andrea, N. V., Anton-Fernandez, A., et al. (2017). Pathological correlations of [F-18]-AV-1451 imaging in non-alzheimer tauopathies. *Ann. Neurol.* 81, 117–128. doi: 10.1002/ana.24844

Marquie, M., Normandin, M. D., Vanderburg, C. R., Costantino, I. M., Bien, E. A., Rycyna, L. G., et al. (2015). Validating novel tau positron emission tomography tracer [F-18]-AV-1451 (T807) on postmortem brain tissue. *Ann. Neurol.* 78, 787–800. doi: 10.1002/ana.24517

Maruyama, M., Shimada, H., Suhara, T., Shinotoh, H., Ji, B., Maeda, J., et al. (2013). Imaging of tau pathology in a tauopathy mouse model and in Alzheimer patients compared to normal controls. *Neuron* 79, 1094–1108. doi: 10.1016/j.neuron.2013.07.037

Mathis, C. A., Lopresti, B. J., Ikonomovic, M. D., and Klunk, W. E. (2017). Small-molecule PET tracers for imaging proteinopathies. *Semin. Nucl. Med.* 47, 553–575. doi: 10.1053/j.semnuclmed.2017.06.003

Mathis, C. A., Mason, N. S., Lopresti, B. J., and Klunk, W. E. (2012). Development of positron emission tomography beta-amyloid plaque imaging agents. *Semin. Nucl. Med.* 42, 423–432. doi: 10.1053/j.semnuclmed.2012.07.001

Mathis, C. A., Wang, Y., Holt, D. P., Huang, G. F., Debnath, M. L., and Klunk, W. E. (2003). Synthesis and evaluation of 11C-labeled 6-substituted 2-arylbenzothiazoles as amyloid imaging agents. *J. Med. Chem.* 46, 2740–2754. doi: 10.1021/jm030026b

Ng, K. P., Pascoal, T. A., Mathotaarachchi, S., Therriault, J., Kang, M. S., Shin, M., et al. (2017). Monoamine oxidase B inhibitor, selegiline, reduces 18F-THK5351 uptake in the human brain. *Alzheimers Res. Ther.* 9:25. doi: 10.1186/s13195-017-0253-y

Ni, R., Gillberg, P. G., Bergfors, A., Marutle, A., and Nordberg, A. (2013). Amyloid tracers detect multiple binding sites in Alzheimer's disease brain tissue. *Brain* 136, 2217–2227. doi: 10.1093/brain/awt142

Nyberg, S., Jonhagen, M. E., Cselenyi, Z., Halldin, C., Julin, P., Olsson, H., et al. (2009). Detection of amyloid in Alzheimer's disease with positron emission tomography using [11C]AZD2184. *Eur. J. Nucl. Med. Mol. Imaging* 36, 1859–1863. doi: 10.1007/s00259-009-1182-1

Okamura, N., Furumoto, S., Fodero-Tavoletti, M. T., Mulligan, R. S., Harada, R., Yates, P., et al. (2014a). Non-invasive assessment of Alzheimer's disease neurofibrillary pathology using 18F-THK5105 PET. *Brain* 137, 1762–1771. doi: 10.1093/brain/awu064

Okamura, N., Harada, R., Furumoto, S., Arai, H., Yanai, K., and Kudo, Y. (2014b). Tau PET imaging in Alzheimer's disease. *Curr. Neurol. Neurosci. Rep.* 14:500. doi: 10.1007/s11910-014-0500-6

Okamura, N., Furumoto, S., Harada, R., Tago, T., Yoshikawa, T., Fodero-Tavoletti, M., et al. (2013). Novel 18F-labeled arylquinoline derivatives for noninvasive imaging of tau pathology in Alzheimer disease. *J. Nucl. Med.* 54, 1420–1427. doi: 10.2967/jnumed.112.117341

Okamura, N., Suemoto, T., Furumoto, S., Suzuki, M., Shimadzu, H., Akatsu, H., et al. (2005). Quinoline and benzimidazole derivatives: candidate probes for in vivo imaging of tau pathology in Alzheimer's disease. *J. Neurosci.* 25, 10857–10862. doi: 10.1523/JNEUROSCI.1738-05.2005

Okamura, N., and Yanai, K. (2017). Brain imaging: applications of tau PET imaging. *Nat. Rev. Neurol.* 13, 197–198. doi: 10.1038/nrneurol.2017.38

Ossenkoppele, R., Schonhaut, D. R., Scholl, M., Lockhart, S. N., Ayakta, N., Baker, S. L., et al. (2016). Tau PET patterns mirror clinical and neuroanatomical variability in Alzheimer's disease. *Brain* 139, 1551–1567. doi: 10.1093/brain/aww027

Passamonti, L., Vazquez Rodriguez, P., Hong, Y. T., Allinson, K. S., Williamson, D., Borchert, R. J., et al. (2017). 18F-AV-1451 positron emission tomography in Alzheimer's disease and progressive supranuclear palsy. *Brain* 140, 781–791. doi: 10.1093/brain/aww340

Perez-Soriano, A., Arena, J. E., Dinelle, K., Miao, Q., Mckenzie, J., Neilson, N., et al. (2017). PBB3 imaging in Parkinsonian disorders: evidence for binding to tau and other proteins. *Mov. Disord.* 32, 1016–1024. doi: 10.1002/mds.27029

Robinson, J. L., Geser, F., Stieber, A., Umoh, M., Kwong, L. K., Van Deerlin, V. M., et al. (2013). TDP-43 skeins show properties of amyloid in a subset of ALS cases. *Acta Neuropathol.* 125, 121–131. doi: 10.1007/s00401-012-1055-8

Saint-Aubert, L., Almkvist, O., Chiotis, K., Almeida, R., Wall, A., and Nordberg, A. (2016). Regional tau deposition measured by [18F]THK5317 positron emission tomography is associated to cognition via glucose metabolism in Alzheimer's disease. *Alzheimers Res. Ther.* 8:38. doi: 10.1186/s13195-016-0204-z

Schafer, K. N., Kim, S., Matzavinos, A., and Kuret, J. (2012). Selectivity requirements for diagnostic imaging of neurofibrillary lesions in Alzheimer's disease: a simulation study. *Neuroimage* 60, 1724–1733. doi: 10.1016/j.neuroimage.2012.01.066

Schonhaut, D. R., Mcmillan, C. T., Spina, S., Dickerson, B. C., Siderowf, A., Devous, M. D., et al. (2017). 18 F-flortaucipir tau positron emission tomography distinguishes established progressive supranuclear palsy from controls and Parkinson disease: a multicenter study. *Ann. Neurol.* 82, 622–634. doi: 10.1002/ana.25060

Schwarz, A. J., Yu, P., Miller, B. B., Shcherbinin, S., Dickson, J., Navitsky, M., et al. (2016). Regional profiles of the candidate tau PET ligand 18F-AV-1451 recapitulate key features of Braak histopathological stages. *Brain* 139, 1539–1550. doi: 10.1093/brain/aww023

Serpell, L. C., Berriman, J., Jakes, R., Goedert, M., and Crowther, R. A. (2000). Fiber diffraction of synthetic alpha-synuclein filaments shows amyloid-like cross-beta conformation. *Proc. Natl. Acad. Sci. U.S.A.* 97, 4897–4902. doi: 10.1073/pnas.97.9.4897

Shah, M., Seibyl, J., Cartier, A., Bhatt, R., and Catafau, A. M. (2014). Molecular imaging insights into neurodegeneration: focus on alpha-synuclein radiotracers. *J. Nucl. Med.* 55, 1397–1400. doi: 10.2967/jnumed.113.136515

Shimonaka, S., Nonaka, T., Suzuki, G., Hisanaga, S., and Hasegawa, M. (2016). Templated aggregation of TAR DNA-binding protein of 43 kDa (TDP-43) by seeding with TDP-43 peptide fibrils. *J. Biol. Chem.* 291, 8896–8907. doi: 10.1074/jbc.M115.713552

Smith, R., Puschmann, A., Scholl, M., Ohlsson, T., Van Swieten, J., Honer, M., et al. (2016). 18F-AV-1451 tau PET imaging correlates strongly with tau neuropathology in MAPT mutation carriers. *Brain* 139, 2372–2379. doi: 10.1093/brain/aww163

Smith, R., Scholl, M., Honer, M., Nilsson, C. F., Englund, E., and Hansson, O. (2017a). Tau neuropathology correlates with FDG-PET, but not AV-1451-PET, in progressive supranuclear palsy. *Acta Neuropathol.* 133, 149–151. doi: 10.1007/s00401-016-1650-1

Smith, R., Scholl, M., Widner, H., Van Westen, D., Svenningsson, P., Hagerstrom, D., et al. (2017b). In vivo retention of 18F-AV-1451 in corticobasal syndrome. *Neurology* 89, 845–853. doi: 10.1212/WNL.0000000000004264

Spina, S., Schonhaut, D. R., Boeve, B. F., Seeley, W. W., Ossenkoppele, R., O'neil, J. P., et al. (2017). Frontotemporal dementia with the V337M MAPT mutation: tau-PET and pathology correlations. *Neurology* 88, 758–766. doi: 10.1212/WNL.0000000000003636

Spinelli, E. G., Mandelli, M. L., Miller, Z. A., Santos-Santos, M. A., Wilson, S. M., Agosta, F., et al. (2017). Typical and atypical pathology in primary progressive aphasia variants. *Ann. Neurol.* 81, 430–443. doi: 10.1002/ana.24885

Stankoff, B., Freeman, L., Aigrot, M. S., Chardain, A., Dolle, F., Williams, A., et al. (2011). Imaging central nervous system myelin by positron emission tomography in multiple sclerosis using [methyl-(1)(1)C]-2-(4′-methylaminophenyl)- 6-hydroxybenzothiazole. *Ann. Neurol.* 69, 673–680. doi: 10.1002/ana.22320

Sun, A., Nguyen, X. V., and Bing, G. (2002). Comparative analysis of an improved thioflavin-s stain, Gallyas silver stain, and immunohistochemistry for neurofibrillary tangle demonstration on the same sections. *J. Histochem. Cytochem.* 50, 463–472. doi: 10.1177/002215540205000403

Tago, T., Furumoto, S., Okamura, N., Harada, R., Adachi, H., Ishikawa, Y., et al. (2016a). Preclinical evaluation of [(18)F]THK-5105 enantiomers: effects of chirality on its effectiveness as a tau imaging radiotracer. *Mol. Imaging Biol.* 18, 258–266. doi: 10.1007/s11307-015-0879-8

Tago, T., Furumoto, S., Okamura, N., Harada, R., Adachi, H., Ishikawa, Y., et al. (2016b). Structure-activity relationship of 2-Arylquinolines as PET imaging tracers for tau pathology in Alzheimer disease. *J. Nucl. Med.* 57, 608–614. doi: 10.2967/jnumed.115.166652

Tago, T., Furumoto, S., Okamura, N., Harada, R., Ishikawa, Y., Arai, H., et al. (2014). Synthesis and preliminary evaluation of 2-arylhydroxyquinoline derivatives for tau imaging. *J. Labelled Comp. Radiopharm.* 57, 18–24. doi: 10.1002/jlcr.3133

Taniguchi-Watanabe, S., Arai, T., Kametani, F., Nonaka, T., Masuda-Suzukake, M., Tarutani, A., et al. (2016). Biochemical classification of tauopathies by immunoblot, protein sequence and mass spectrometric analyses of sarkosyl-insoluble and trypsin-resistant tau. *Acta Neuropathol.* 131, 267–280. doi: 10.1007/s00401-015-1503-3

Thal, D. R., Rub, U., Orantes, M., and Braak, H. (2002). Phases of A beta-deposition in the human brain and its relevance for the development of AD. *Neurology* 58, 1791–1800. doi: 10.1212/WNL.58.12.1791

Thompson, P. W., Ye, L., Morgenstern, J. L., Sue, L., Beach, T. G., Judd, D. J., et al. (2009). Interaction of the amyloid imaging tracer FDDNP with hallmark Alzheimer's disease pathologies. *J. Neurochem.* 109, 623–630. doi: 10.1111/j.1471-4159.2009.05996.x

Vermeiren, C., Mercier, J., Viot, D., Mairet-Coello, G., Hannestad, J., Courade, J.-P., et al. (2015). T807, a reported selective tau tracer, binds with nanomolar affinity to monoamine oxidase A. *Alzheimers Dement.* 11(Suppl. 7), 283. doi: 10.1016/j.jalz.2015.07.381

Villemagne, V. L. (2017). Selective tau imaging: *Der Stand der Dinge*. *J. Nucl. Med.* 59, 175–176. doi: 10.2967/jnumed.117.198325

Villemagne, V. L., Fodero-Tavoletti, M. T., Masters, C. L., and Rowe, C. C. (2015). Tau imaging: early progress and future directions. *Lancet Neurol.* 14, 114–124. doi: 10.1016/S1474-4422(14)70252-2

Villemagne, V. L., Furumoto, S., Fodero-Tavoletti, M. T., Harada, R., Mulligan, R. S., Kudo, Y., et al. (2012). The challenges of tau imaging. *Future Neurol.* 7, 409–421. doi: 10.2217/fnl.12.34

Villemagne, V. L., Furumoto, S., Fodero-Tavoletti, M. T., Mulligan, R. S., Hodges, J., Harada, R., et al. (2014). In vivo evaluation of a novel tau imaging tracer for Alzheimer's disease. *Eur. J. Nucl. Med. Mol. Imaging* 41, 816–826. doi: 10.1007/s00259-013-2681-7

Walji, A. M., Hostetler, E. D., Selnick, H., Zeng, Z., Miller, P., Bennacef, I., et al. (2016). Discovery of 6-(Fluoro-(18)F)-3-(1H-pyrrolo[2,3-c]pyridin-1-yl)isoquinolin-5-amine ([(18)F]-MK-6240): a positron emission tomography (PET) imaging agent for quantification of neurofibrillary tangles (NFTs). *J. Med. Chem.* 59, 4778–4789. doi: 10.1021/acs.jmedchem.6b00166

Wong, D. F., Comley, R., Kuwabara, H., Rosenberg, P. B., Resnick, S. M., Ostrowitzki, S., et al. (2018). First in-human PET study of 3 novel tau radiopharmaceuticals: [(11)C]RO6924963, [(11)C]RO6931643, and [(18)F]RO6958948. *J. Nucl. Med.* [Epub ahead of print].

Xia, C., Makaretz, S. J., Caso, C., Mcginnis, S., Gomperts, S. N., Sepulcre, J., et al. (2017). Association of in vivo [18F]AV-1451 tau PET imaging results with cortical atrophy and symptoms in typical and atypical Alzheimer disease. *JAMA Neurol.* 74, 427–436. doi: 10.1001/jamaneurol.2016.5755

Xia, C. F., Arteaga, J., Chen, G., Gangadharmath, U., Gomez, L. F., Kasi, D., et al. (2013). [(18)F]T807, a novel tau positron emission tomography imaging agent for Alzheimer's disease. *Alzheimers Dement.* 9, 666–676. doi: 10.1016/j.jalz.2012.11.008

Yoshimi, T., Kawabata, S., Taira, S., Okuno, A., Mikawa, R., Murayama, S., et al. (2015). Affinity imaging mass spectrometry (AIMS): high-throughput screening for specific small molecule interactions with frozen tissue sections. *Analyst* 140, 7202–7208. doi: 10.1039/c5an01381j

Zhang, W., Arteaga, J., Cashion, D. K., Chen, G., Gangadharmath, U., Gomez, L. F., et al. (2012). A highly selective and specific PET tracer for imaging of tau pathologies. *J. Alzheimers Dis.* 31, 601–612. doi: 10.3233/JAD-2012-120712

Conflict of Interest Statement: NO owns stock of CLINO Co. Ltd. NO and SF are scientific consultants for the CLINO Co. Ltd. RH and KY have no conflict of interest.

frontiers in Neuroscience

ORIGINAL RESEARCH
published: 01 March 2018
doi: 10.3389/fnins.2018.00124

Tau Depletion in APP Transgenic Mice Attenuates Task-Related Hyperactivation of the Hippocampus and Differentially Influences Locomotor Activity and Spatial Memory

Misato Yoshikawa[1,2], *Yoshiyuki Soeda*[1,3], *Makoto Michikawa*[4], *Osborne F. X. Almeida*[5] and *Akihiko Takashima*[1,6]*

[1] Department of Aging Neurobiology, National Center for Geriatrics and Gerontology, Obu, Japan, [2] Department of Pharmacology, Shujitsu University, Okayama, Japan, [3] Clinical Research Center, Fukushima Medical University, Fukushima, Japan, [4] Department of Biochemistry, School of Medicine, Nagoya City University, Nagoya, Japan, [5] Department of Stress Neurobiology and Neurogenetics, Max Planck Institute of Psychiatry, Munich, Germany, [6] Laboratory for Alzheimer's Disease, Department of Life Science, Faculty of Science, Gakushuin University, Tokyo, Japan

OPEN ACCESS

Edited by:
Naruhiko Sahara, National Institute of Radiological Sciences (NIRS), Japan

Reviewed by:
Ioannis Sotiropoulos, University of Minho, Portugal
Luc Buee, Institut National de la Santé et de la Recherche Médicale (INSERM), France

***Correspondence:**
Akihiko Takashima
akihiko.takashima@gakushuin.ac.jp

Specialty section:
This article was submitted to Neurodegeneration, a section of the journal Frontiers in Neuroscience

Received: *13 December 2017*
Accepted: *15 February 2018*
Published: *01 March 2018*

Citation:
Yoshikawa M, Soeda Y, Michikawa M, Almeida OFX and Takashima A (2018) Tau Depletion in APP Transgenic Mice Attenuates Task-Related Hyperactivation of the Hippocampus and Differentially Influences Locomotor Activity and Spatial Memory. Front. Neurosci. 12:124. doi: 10.3389/fnins.2018.00124

Hippocampal hyperactivity, ascribed to amyloid β (Aβ)-induced imbalances in neural excitation and inhibition, is found in patients with mild cognitive impairment, a prodromal stage of Alzheimer's disease (AD). To better understand the relationship between hippocampal hyperactivity and the molecular triggers of behavioral impairments in AD, we used Mn-enhanced MRI (MEMRI) to assess neuronal activity after subjecting mice to a task requiring spatial learning and memory. Depletion of endogenous tau in an amyloid precursor protein (APP) transgenic (J20) mouse line was shown to ameliorate hippocampal hyperactivity in J20 animals, tau depletion failed to reverse memory deficits associated with APP/Aβ overproduction. On the other hand, deletion of tau alleviated the hyperlocomotion displayed by APP transgenics, suggesting that the functional effects of Aβ-tau interactions reflect the temporal appearance of these molecules in individual brain areas.

Keywords: tau, amyloid beta-peptides, hippocampus, hyperexcitation, Dementia

INTRODUCTION

Gradual worsening of memory and eventual impairments of executive functions are the main clinical features of both sporadic and familial Alzheimer disease (AD). The neuropathological correlates of these phenotypic characteristics include extracellular deposits of amyloid β (Aβ) that eventually form senile plaques and intracellular hyperphosphorylated tau that aggregates into neurofibrillary tangles (NFTs). Both Aβ and tau pathology are thought to contribute to the massive neuronal atrophy seen in the AD brain (Crimins et al., 2013) and genes that result in Aβ overproduction display have 100% penetrance in affected individuals (Tanzi, 2012). Treatments aimed to reduce the generation or deposits of Aβ with β–and γ-secretase inhibitors or antibodies against Aβ were shown to restore memory in mutant mouse models of AD, albeit without reversing the neuronal loss usually associated with Aβ overproduction

(Janus et al., 2000; Fukumoto et al., 2010; Netzer et al., 2010). Thus, Aβ disrupts mnemonic functions, apparently by interfering with the function of brain circuits (Palop and Mucke, 2010), e.g., the ability to induce synaptic long term potentiation (LTP) (Walsh et al., 2002). In an extension of those studies, Roberson et al. implicated tau protein in Aβ-induced memory impairment; these authors found an amelioration of memory deficits (and survival) when *amyloid precursor protein* transgenic (*APP* Tg) mice were cross-bred with *tau* knockout mice (Roberson et al., 2007). Moreover, tau deletion resulted in a recovery of LTP in *APP* Tg mice (Shipton et al., 2011). These preclinical findings are consistent with those of a recent cross-sectional study strongly suggested a causal link between NFT lesions, rather than Aβ deposits, with cognitive decline (Brier et al., 2016); the latter may explain why Aβ-targeted therapies have generally proven ineffective at halting disease progression in subjects with mild cognitive impairment (MCI), a precursor of early-to-moderate AD (Holmes et al., 2008).

An abundance of evidence suggests that Aβ and tau AD pathology appear to mutually drive each other (Jack et al., 2013; Musiek and Holtzman, 2015) and that neuronal activation may increase either the aggregation, deposition and/or propagation of Aβ and tau (Bakker et al., 2012; Wu et al., 2016). Nevertheless, understanding the specific roles and sites and mechanisms of action of these molecules is essential for progress toward the development of targeted AD therapies. Complementing previous studies in mice that described (epileptiform) hyperactivity of hippocampal neurons in *APP* Tg mice (Palop et al., 2007; Busche et al., 2012), aged human subjects with a significant Aβ burden, but who were nonetheless cognitively healthy, were found to display increased hippocampal activity, as measured by functional magnetic resonance imaging (fMRI) (Mormino et al., 2012). A more recent fMRI (cross-sectional) study in healthy older humans found an association between Aβ tau pathology, neuronal atrophy and aberrant hyperactivation of the hippocampus during memory encoding (Marks et al., 2017); subsequent mediation analysis of those data revealed causality between hippocampal tau and hyperactivation. In this study, manganese-enhanced MRI (MEMRI) was used to re-investigate the relationship between neuronal hyperactivation, APP overexpression, tau and memory performance in mice.

MATERIALS AND METHODS

Animals

Transgenic (J20) mice express human amyloid precursor protein (hAPP) with the Swedish (K670N, M671L) and Indiana (V717F) mutations under the control of the PDGF β-chain promoter (Mucke et al., 2000). J20 mice were crossed with a *tau*-deficient (*tau* KO) mouse (provided from Dr. Vitek, Duke University) (Dawson et al., 2001) to produce J20/tau KO mice. We used 8- to 13-month-old WT ($n = 22$), J20 ($n = 19$), tau KO ($n = 17$), and J20/tau KO ($n = 26$) mice in this study. All studies were approved by the local ethical board and complied with the guidelines for animal experimentation of the National Center for Geriatrics and Gerontology. Mice were kept in a 12 h light/dark cycle and had free access to food and water.

Behavioral Tests

Exploration of an open-field was assessed by placing mice in a clear Perspex cylinder (30 cm diameter) for 30 min. using video recordings. Spontaneous alternation was assessed in a Y-maze (40 cm arm lengths) and monitored with a CCD camera. Mice were placed at the end of one arm and allowed to freely explore the arms for 15 min. *Spontaneous alternation* (%), defined as a consecutive entry in any of three arms of the maze, was calculated using the formula: No. of alternations/(Σ no. of entries – 2) * 100. Real-time recorded images (sampled at 2 Hz) were evaluated using the public domain NHI Image J software (http://rsb.info.nih.gov/nih-image/).

Spatial memory was evaluated using the Morris water maze (MWM) (1 m diameter) test, as described previously (Kimura et al., 2007). Briefly, for hidden platform training, a platform (10 cm diameter) was placed 1 cm below the surface of the water (constant location in within-trials training, but randomly located in between-trials testing. Each mouse received 3 daily training sessions at 30 min intervals over 9 consecutive days. Mice that did not find the platform within 60 s were guided to it and allowed to stay on it for 10 s. For the probe test (10th day), mice had to swim for 60 s in the maze from which the platform was removed. An error score was calculated by measuring the total distance traveled to reach the quadrant in which the platform was anticipated.

Acquired images were analyzed using a customized Matlab-based software in conjunction with an image analysis tool box (Mathworks Co. Ltd.).

Mn-Enhanced MRI (MEMRI)

Body weight of mice was measured (**Supplementary Figure 3**). Mice received $MnCl_2$ (20 mg/kg i.p.), returned to their home cages for 30 min before exposure to a novel environment (clear Perspex cylinder, 30 cm diameter) for a period of 2 h (cylinder moved every 30 min to prevent habituation), after which they were again returned to their home cages (90 min) before MRI scanning. Anesthesia was induced with 3.0% isoflurane/air and maintained with 0.5–1.5% isoflurane/air; throughout, deep core temperature and heart rate were monitored (SA Instruments, Inc., USA). Scanning was performed (4 h after $MnCl_2$ injection) in a 4.7T AVANCE III PharmaScan (Bruker BioSpin, Germany). RF transmission and reception were applied with a 23 mm inner diameter birdcage volume coil. Images were acquired with 3D Fast Imaging using a Steady-State Free Precession (FISP) sequence [repetition time (TR) = 8 ms, echo time (TE) = 4 ms, flip angle = 20°, number of acquisition = 7, matrix = 160 × 160 × 160, field of view (FOV) = 20 × 20 × 20 mm, and voxel size = 0.125 × 0.125 × 0.125 mm]. The total acquisition time was 31 min. MRI data analysis was performed as described previously (Kimura et al., 2007), with the aid of a custom-developed Matlab function (2012a, MathWorks). Brain slices were aligned with reference to Bregma. MR images were realigned and registered non-rigidly to the mouse brain template constructed by aligning and averaging 10 subject images. All voxel data were smoothed using a 3-dimensional Gaussian filter (Matlab image processing tool box, version 5.02, Mathworks). Image intensities were normalized to the mean signal in the whole

brain of each individual mouse. MR images were visualized with Osirix (version 5.0.2), an open-source software for navigating multidimensional DICOM images.

Statistical Analysis

All numerical data are presented as mean ± SEM. The significance of differences between two groups was assessed by Student's *t*-test, and differences between multiple groups were assessed using 1-way ANOVA, followed by Tukey's multiple comparisons test. Statistical analyses was performed using PRISM4 software (GraphPad Software Inc., La Jolla, CA). Differences were considered significant when $p < 0.05$.

RESULTS

Optimization of $MnCl_2$ Dose

MEMRI exploits the paramagnetic properties of manganese (Mn^{2+}) to enhance tissue contrast of the MRI signal. Cellular uptake of the contrast agent, whose radius and chemical properties resemble those of calcium (Ca^{2+}), is facilitated by Ca^{2+} channels; this allows it to be used as a reporter of neuronal activity (Silva and Bock, 2008). Although Mn^{2+} only poorly penetrates the blood-brain-barrier, excessive dosage can induce manganism with Parkinsonian-like symptoms (Sepúlveda et al., 2012) which present a potential confound in the interpretation of behavioral assays. Therefore, we initially determined the optimal dose of $MnCl_2$ (i.p.) in wildtype (WT) mouse. As shown in **Figure 1A**, there was a dose-dependent increase in the mean intensity of MRI signal in mouse, with doses >20 mg/kg resulting in gradual decreases in locomotor activity **Figure 1B**. Accordingly, $MnCl_2$ was administered at 20 mg/kg i.p. in all subsequent experiments.

App Overexpression Is Associated With Hippocampal Hyperactivity

Place learning (vs. home cage) produced strong MEMRI signals in the accumbens, motor cortex, and hippocampus of WT mice (**Figure 2A**). Compared to age-matched WT mice, APP-overexpressing J20 mice displayed increased hippocampal activity (2% normalized mean MEMRI intensity signal; $P = 0.0134$, Tukey's multiple comparison test) immediately after place learning (**Figure 2B**); on the other hand, the behavioral task did not alter signal intensities in the accumbens and motor cortex.

Hippocampal Hyperactivity, but Not mPFC Hypoactivity, Is Attenuated by Deletion of Tau

A pioneer study demonstrated that memory impairments in APP-overexpressing (J20) mice can be rescued by tau deletion; it was suggested that tau depletion results in an amelioration of APP-induced hyperactivity of hippocampal neurons and therefore, cognitive improvement (Roberson et al., 2007). In a replication of that study, we here cross-bred J20 with tau knockout mice and confirmed the original observation by MEMRI scanning of mice that had performed the place learning task: specifically, whereas MEMRI signal intensity in the hippocampus did not differ between WT and tau KO mice, and J20 mice displayed approximately 2% higher intensities than wildtype and tau KO mice, MEMRI signals were similar between J20/tau KO, tau KO, and WT mice (**Figure 2B**). In contrast, MEMRI signal intensity in medial prefrontal cortex (mPFC) of J20 mice was lower than that observed in WT and Tau KO mice, an effect that was not reversible by depletion of tau (**Figure 2C**). Thus, tau contributes to the increased neural activity in the hippocampus, but not the mPFC, in APP-overexpressing J20 mice.

Behavioral Correlates of Hippocampal Hyperactivity and Its Reversal by Deletion of Tau

As mentioned above, Roberson et al. (2007) implicated tau in the parallel display of hippocampal hyperactivity and memory deficits by APP-overexpressing mice. Since those observations have not been corroborated thus far, we here investigated the role of tau (and its absence) on memory formation. To this end, WT, J20, tau KO, and J20/tau KO mice were trained to

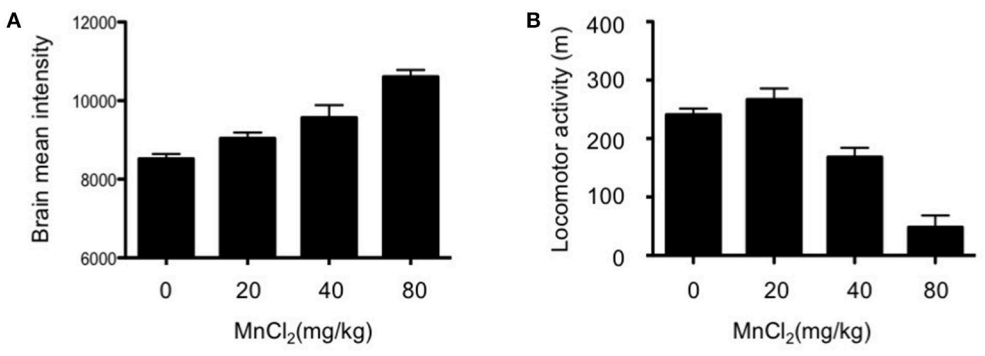

FIGURE 1 | Dose-dependent increases in the mean intensity of MEMRI signal after application of $MnCl_2$. **(A)** Mean signal intensity in whole brain 4 h after $MnCl_2$ injections at doses indicated (0 and 20 mg/kg: $n = 5$/group; 40 and 80 mg/kg: $n = 5$/group). **(B)** Locomotor activity in C57BL/6 mice (5–8 months old), measured in an open-field for 30 min following i.p. injections with the indicated doses of $MnCl_2$ (0 mg/kg: $n = 6$/group; 20, 40, and 80 mg/kg: $n = 5$/group).

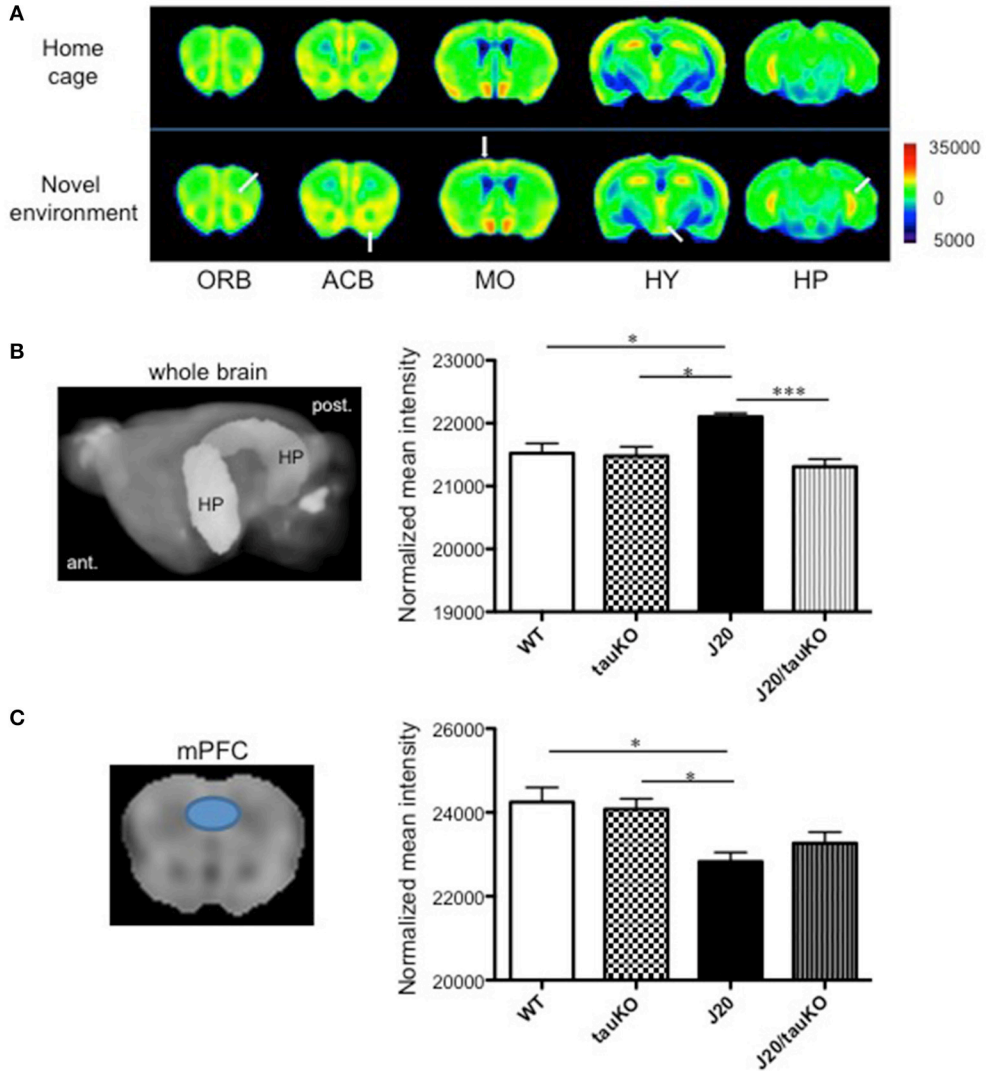

FIGURE 2 | Differential brain area-specific and genotype-specific neural activation after place/contextual learning. **(A)** Shown are coronal brain sections from mice (C57BL/6 background) aged 5–8 months old, in their home cage (*upper*) or new (*lower*) environments. Relative MRI signal intensities, after normalization to mean signal intensity in the whole brain), are depicted (see color spectrum scale bar); in *lower* panel, white arrows indicate activation in regions of interest. In WT mice, neural activity in the orbito-frontal cortex (ORB), accumbens (ACB), motor cortex (MO), and hippocampus (HP) was enhanced after exposure to a new environment ($n = 5$) vs. home cage setting ($n = 6$). Place learning also increased activity in the hypothalamus (HY) of WT mice. **(B**,**C)** *left-hand panel* shows the hippocampus **(B)** and medial prefrontal cortex (mPFC) **(C)** as region of interest (based in Allen Mouse Brain Atlas) used to quantify MEMRI signal intensities to obtain the normalized data depicted in the *right-hand panel* where comparisons are made between WT ($n = 6$–7), J20 ($n = 6$–7), tau KO ($n = 7$), and J20/tau KO ($n = 8$) mice (aged 8–11 months) exposed to the place/contextual learning paradigm immediately before scanning. $^{*}P < 0.05$, $^{***}P < 0.001$.

navigate to an invisible platform in a MWM. Error scores after 9 consecutive days of training were lower in all groups as compared to scores during the first learning session (**Figure 3A**). A probe test of memory revealed that whereas the WT and tau KO groups spent significantly >25% of the time in the target quadrant, both the J20 and J20/tau KO mice were markedly poor in locating the quadrant with the escape platform (**Figure 3B**). Thus, tau depletion failed to reverse the memory impairment induced by over-production of APP.

Next, we used the Y-maze test to investigate alternation behavior in the four genotypes. Although all mouse lines groups alternated between the two arms of the maze at similar rates, around 50% (**Figure 3C**), the APP-overexpressing J20 made significantly more arm entries (**Figure 3D**) than either the WT, tau KO or J20/tau KO lines**.** Together, these data suggested a role for tau in locomotor activity. This interpretation was supported by data showing that the locomotor activity of J20 mice in an open field arena is significantly higher than that of any of the other genotypes (WT, tau KO, and J20/tau KO) tested (**Figure 3E**). Together, this set of experiments indicates that, in J20 mice, the behavioral correlate of hippocampal hyperactivity is locomotor activity rather than place learning and memory.

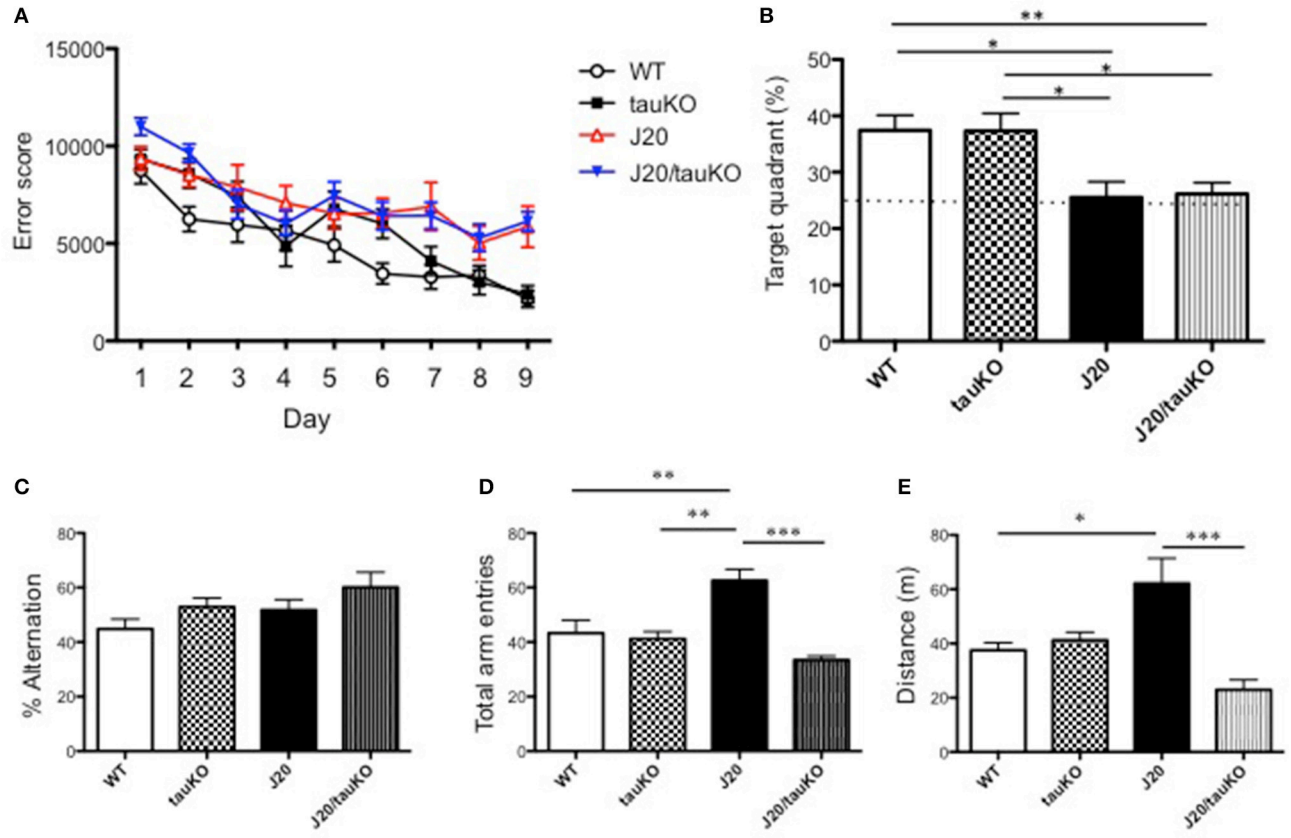

FIGURE 3 | Depletion of tau reverses hyperlocomotor behavior but not place memory deficits in J20 mice. **(A)** Place memory was tested in the MWM in mice aged 8–12 months. Acquisition profiles, showing error scores during daily training trials (9 consecutive days) are shown. **(B)** Shows performance (time spent in target quadrant) in a probe test on day 10. Experimental groups in **(A,B)** were WT ($n = 15$), J20 ($n = 12$), tau KO ($n = 10$), and J20/tau KO ($n = 18$). In the Y-maze, alternations between the two arms of the maze (% time) ($P = 0.4497$, WT vs. tauKO; $P = 0.6388$, WT vs. J20; $P = 0.0728$, WT vs. J20/tauKO; $P = 0.9969$, tauKO vs. J20; $P = 0.5895$, tauKO vs. J20/tauKO; $P = 0.5328$, J20 vs. J20/tauKO). **(C)** Number of entries into the arms of the maze **(D)** were monitored in WT ($n = 6$), J20 ($n = 5$), tau KO ($n = 7$), and J20/tau KO ($n = 5$) mice (aged 10–13 months). Panel **(E)** shows distance in WT ($n = 7$), J20 ($n = 7$), tau KO ($n = 7$), and J20/tau KO ($n = 6$) mice during the first 5 min exploration of an open field arena. $^*P < 0.05$, $^{**}P < 0.01$, $^{***}P < 0.001$.

DISCUSSION

Hippocampal hyperactivity is observed in patients with mild cognitive impairment (MCI) (Dickerson et al., 2005) but also in non-demented elderly subjects (Miller et al., 2008; Yassa et al., 2011). High levels of APP-derived amyloid β (Aβ) have long been linked to aberrant synaptic activity (Nitsch et al., 1993; Kamenetz et al., 2003) and strong associations have been established between Aβ, hippocampal activation and memory decline in otherwise cognitively-normal older humans (Mormino et al., 2012; Elman et al., 2014; Leal et al., 2017); accordingly, hippocampal hyperactivity may be a physiological accompaniment of aging in the mouse. Importantly, both cognitively-healthy aging humans (Sperling et al., 2003) and aged wildtype mice (**Supplementary Figure 1**) display reduced task-induced deactivation of the hippocampus. Interestingly, low doses of the anti-epileptic drug levetiracetam decrease hippocampal hyperactivity and improve memory in MCI patients (Bakker et al., 2012) and mouse models of AD (Palop et al., 2007); thus, memory deficits in AD patients and age-related cognitive decline are likely to be the consequence of shifts in the balance between excitation and inhibition of hippocampal neurons (see Busche and Konnerth, 2016).

Two recent positron emission tomography (PET) studies provide critical support that deposition of tau protein tracks and predicts cognitive decline during healthy aging (Marks et al., 2017) and in AD patients (Brier et al., 2016) better than Aβ. Tau, better known as a cytoskeletal protein, is now known to be located at synapses (Kimura et al., 2013; Kobayashi et al., 2017) where its potential to regulate neuroplastic events related to learning and memory has generated much interest. Clearly, tau pathology occurs downstream of Aβ (Jack et al., 2013) and a pioneering study by Roberson et al. (2007) implicated the essential role for tau in Aβ-associated memory deficits in the mouse. In this study, we confirmed that APP overexpression in J20 mice is accompanied by hippocampal hyperactivity; the latter was measured in mice aged 8 months

old, an age at which Aβ deposition is seen in the hippocampus, prefrontal cortex and entorhinal cortex and when significant deficits in spatial memory are detectable in this mouse line (Mucke et al., 2000; Escribano et al., 2010; Wright et al., 2013). Further, we confirmed that tau contributes to hippocampal hyperactivity in J20 mice (cf. Roberson et al., 2007); briefly, J20 mice cross-bred to mice deficient in tau (tau KO) showed levels of hippocampal activity that were similar to those displayed by WT mice. Earlier authors proposed that the hyperexcitability observed in J20 mice results from Aβ -induced Fyn-mediated NMDA receptor activation (Ittner et al., 2010; Roberson et al., 2011) this interpretation is supported by reports that most APP transgenic mice exhibit spontaneous seizures and/or increased epileptiform EEG activity (Ziyatdinova et al., 2016).

Besides the aforementioned clinical studies, numerous studies in mice document a strong association between hAPP expression and impaired performance in the MWM (e.g., Palop et al., 2003; Galvan et al., 2006); the latter reports are supported by the demonstration that immunization against Aβ rescues learning and memory deficits in hAPP transgenic mice (Schenk et al., 1999; Janus et al., 2000) as well as the observation that hAPP mice display reduced synapse numbers and reduced inducibility of LTP (Shipton et al., 2011; Wright et al., 2013; Vega-Flores et al., 2014). Notably, our results do not conform with those of Roberson et al. (2011) who found that depletion of tau abrogates learning/memory impairments in hAPP mice tested in the MWM. As shown in **Figure 2B**, depletion of tau in J20 mice failed to reverse APP-induced memory impairments when the same test paradigm as that described by Roberson et al. (2011) was used; likewise, tau depletion did not improve cognitive performance by J20 mice in a variation of the MWM in which the escape platform is submerged (**Supplementary Figure 2**). While the discrepant findings on learning and memory performance in the MWM cannot be readily explained at present, it is worth noting that memory encoding and retrieval is regulated through reciprocal communication between the medial prefrontal cortex (mPFC) and hippocampus (see Eichenbaum, 2017) which, in turn, are likely modulated by dynamic spatio-temporal interactions between Aβ, tau and synaptic activity (see Leal et al., 2017; Marks et al., 2017). Since damage to the mPFC reportedly results in longer escape latencies in the MWM (de Bruin et al., 1997), the reduction in mPFC activity in J20 mice (**Figure 2C**) suggests that spatial recognition in the MWM test depends on both, hypoactivity in the mPFC and hyperactivity in the hippocampus. Inter-dependence between different brain areas (see Lalonde, 2002) and the potential for compensatory mechanisms is supported by the finding that there were no genotype-specific differences in alternation behavior.

Whereas tau depletion did not reverse the impaired memory phenotype of J20 mice, the hyperlocomotor behavior displayed by J20 mice was significantly reduced in the absence of tau. We recently reported that glutamate receptor stimulation induces AMPA/NMDA receptor- and GSK-3β-dependent local translation of tau in the somatodendritic compartment (Kobayashi et al., 2017). Since glutamate is the major fast excitatory transmitter in the brain, and because Aβ increases transmitter release (Abramov et al., 2009), it is plausible that Aβ enhances synaptic tau levels in the hippocampus and thus, hyperexcitation. Importantly, mPFC hypoexcitation in the J20 mouse does not appear to be tau-dependent, suggesting that Aβ modifies neuronal excitability and behavioral outputs through tau-dependent (hippocampus) and tau-independent (mPFC) mechanisms.

ETHICS STATEMENT

This study was carried out in accordance with the recommendations of NCGG of guidelines, NCGG animal experiment committee. The protocol was approved by the NCGG animal experiment committee.

AUTHOR CONTRIBUTIONS

The study was conceptualized and designed by MY, YS, and AT; MY and YS performed experiments and analyzed the data; MM provided experimental animals; MY, OA, and AT interpreted the results; MY, YS, OA, and AT wrote the manuscript. All authors read and approved the manuscript.

ACKNOWLEDGMENTS

This work was supported by Mext Grant–in-aid project, Scientific Research on Innovation Area, [Brain Protein Aging and Dementia control (to AT)]. OA was supported by the Max Planck Society and a fellowship from the Japan Society for the Advancement of Science (JSPS).

SUPPLEMENTARY MATERIAL

The Supplementary Material for this article can be found online at: https://www.frontiersin.org/articles/10.3389/fnins.2018.00124/full#supplementary-material

Supplementary Figure 1 | Hippocampal hyperactivity is accentuated during aging. Wildtype mice (C57BL/6 strain), aged 10 ($n = 5$) or 20–23 ($n = 6$) months were scanned using MEMRI following placement in a novel environment. Note the reduced ability of the older group to display task-induced deactivation of the hippocampus. $^{**}P < 0.01$.

Supplementary Figure 2 | Tau depletion does not improve performance in MWM with invisible escape platform. Following training and testing (3 d) with a visible escape platform, WT ($n = 9$), J20 ($n = 9$), tau KO ($n = 7$), and J20/tau KO ($n = 8$) mice (aged 7–10 months) were then exposed to 5 daily sessions during which the platform was submerged. **(A)** Acquisition profiles showing error scores during training trials (visible and submerged platforms). **(B)** Probe test results depicting performance on the 4th session with a hidden platform. $^{*}P < 0.05$.

Supplementary Figure 3 | Tau depletion elevates body weight. Body weight was measured in WT ($n = 7$), J20 ($n = 8$), tau KO ($n = 7$), and J20/tau KO ($n = 8$) mice (aged 8–11 months) before MEMRI.

REFERENCES

Abramov, E., Dolev, I., Fogel, H., Ciccotosto, G. D., Ruff, E., and Slutsky, I. (2009). Amyloid-β as positive endogenous regulator of release probability at hippocampal synapses. *Nat. Neurosci.* 12, 1567–1576. doi: 10.1038/nn.2433

Bakker, A., Krauss, G. L., Albert, M. S., Speck, C. L., Jones, L. R., Stark, C. E., et al. (2012). Report reduction of hippocampal hyperactivity improves cognition in amnestic mild cognitive impairment. *Neuron* 74, 467–474. doi: 10.1016/j.neuron.2012.03.023

Brier, M. R., Gordon, B., Friedrichsen, K., McCarthy, J., Stern, A., Christensen, J., et al. (2016). Tau and Aβ imaging, CSF measures, and cognition in Alzheimer's disease. *Sci. Transl. Med.* 8:338ra66. doi: 10.1126/scitranslmed.aaf2362

Busche, M. A., Chen, X., Henning, H. A., Reichwald, J., Staufenbiel, M., Sakmann, B., et al. (2012). Critical role of soluble amyloid-β for early hippocampal hyperactivity in a mouse model of Alzheimer's disease. *Proc. Natl. Acad. Sci. U.S.A.* 109, 8740–8745. doi: 10.1073/pnas.1206171109

Busche, M. A., and Konnerth, A. (2016). Impairments of neural circuit function in Alzheimer's disease. *Philos. Trans. R. Soc. Lond. B Biol. Sci.* 371:20150429. doi: 10.1098/rstb.2015.0429

Crimins, J. L., Pooler, A., Polydoro, M., Luebke, J. I., and Spires-Jones, T. L. (2013). The intersection of amyloid β and tau in glutamatergic synaptic dysfunction and collapse in Alzheimer's disease. *Ageing Res. Rev.* 12, 757–763. doi: 10.1016/j.arr.2013.03.002

Dawson, H. N., Ferreira, A., Eyster, M. V., Ghoshal, N., Binder, L. I., and Vitek, M. P. (2001). Inhibition of neuronal maturation in primary hippocampal neurons from tau deficient mice. *J. Cell Sci.* 114, 1179–1187.

de Bruin, J. P., Swindles, W. A., and de Brander, J. M. (1997). Response learning of rats in a Morris water maze: involvement of the medical prefrontal cortex. *Behav. Brain Res.* 85,47–55.

Dickerson, B. C., Salat, D. H., Greve, D. N., Chua, E. F., Rand-Giovannetti, E., Rentz, D. M., et al. (2005). Increased hippocampal activation in mild cognitive impairment compared to normal aging and AD. *Neurology* 65, 404–411. doi: 10.1212/01.wnl.0000171450.97464.49

Eichenbaum, H. (2017). Prefrontal-hippocampal interactions in episodic memory. *Nat. Rev. Neurosci.* 18, 547–558. doi: 10.1038/nrn.2017.74

Elman, J. A., Oh, H., Madison, C. M., Baker, S. L., Vogel, J. W., Marks, S. M., et al. (2014). Neural compensation in older people with brain amyloid-β deposition. *Nat. Neurosci.* 17, 1316–1318. doi: 10.1038/nn.3806

Escribano, L., Simón, A. M., Gimeno, E., Cuadrado-Tejedor, M., López de Maturana, R., García-Osta, A., et al. (2010). Rosiglitazone rescues memory impairment in Alzheimer's transgenic mice: mechanisms involving a reduced amyloid and tau pathology. *Neuropsychopharmacology* 35, 1593–1604. doi: 10.1038/npp.2010.32

Fukumoto, H., Takahashi, H., Tarui, N., Matsui, J., Tomita, T., Hirode, M., et al. (2010). A noncompetitive BACE1 inhibitor TAK-070 ameliorates Aβ pathology and behavioural deficits in a mouse model of Alzheimer's disease. *J. Neurosci.* 6, 11157–11166. doi: 10.1523/JNEUROSCI.2884-10.2010

Galvan, V., Gorostiza, O. F., Banwait, S., Ataie, M., Logvinova, A. V., Sitaraman, S., et al. (2006). Reversal of Alzheimer's-like pathology and behavior in human APP transgenic mice by mutation of Asp664. *Proc. Natl. Acad. Sci. U.S.A.* 103, 7130–7135. doi: 10.1073/pnas.0509695103

Holmes, C., Boche, D., Wilkinson, D., Yadegarfar, G., Hopkins, V., Bayer, A., et al. (2008). Long-term effects of Abeta42 immunisation in Alzheimer's disease: follow-up of a randomised, placebo-controlled phase I trial. *Lancet* 372, 216–223. doi: 10.1016/S0140-6736(08)61075-2

Ittner, L. M., Ke, Y. D., Delerue, F., Bi, M., Gladbach, A., van Eersel, J., et al. (2010). Dendritic function of tau mediates amyloid- b toxicity in Alzheimer's disease mouse models. *Cell* 142, 387–397. doi: 10.1016/j.cell.2010.06.036

Jack, C. R. Jr., Knopman, D. S., Jagust, W. J., Petersen, R. C., Weiner, M. W., Aisen, P. S., et al. (2013). Tracking pathophysiological processes in Alzheimer's disease: an updated hypothetical model of dynamic biomarkers. *Lancet Neurol.* 12, 207–216. doi: 10.1016/S1474-4422(12)70291-0

Janus, C., Pearson, J., McLaurin, J., Mathews, P. M., Jiang, Y., Schmidt, S. D., et al. (2000). Aβ peptide immunization reduces behavioural impairment and plaques in a model of Alzheimer's disease. *Nature* 408, 979–982. doi: 10.1038/35050110

Kamenetz, F., Tomita, T., Hsieh, H., Seabrook, G., Borchelt, D., Iwatsubo, T., et al. (2003). APP processing and synaptic function. *Neuron* 37, 925–937. doi: 10.1016/S0896-6273(03)00124-7

Kimura, T., Whitcomb, D. J., Jo, J., Regan, P., Piers, T., Heo, S., et al. (2013). Microtubule-associated protein tau is essential for long-term depression in the hippocampus. *Philos. Trans. R. Soc. Lond. B Biol. Sci.* 369:20130144. doi: 10.1098/rstb.2013.0144

Kimura, T., Yamashita, S., Fukuda, T., Park, J. M., Murayama, M., Mizoroki, T., et al. (2007). Hyperphosphorylated tau in parahippocampal cortex impairs place learning in aged mice expressing wild-type human tau. *EMBO J.* 26, 5143–5152. doi: 10.1038/sj.emboj.7601917

Kobayashi, S., Tanaka, T., Soeda, Y., Almeida, O. F. X., and Takashima, A. (2017). Local somatodendritic translation and hyperphosphorylation of tau protein triggered by AMPA and NMDA receptor stimulation. *EBioMedicine* 20, 120–126. doi: 10.1016/j.ebiom.2017.05.012

Lalonde, R. (2002). The neurobiological basis of spontaneous alternation. *Neurosci. Biobehav. Rev.* 26, 91–104. doi: 10.1016/S0149-7634(01)00041-0

Leal, S. L., Landau, S. M., Bell, R. K., and Jagust, W. J. (2017). Hippocampal activation is associated with longitudinal amyloid accumulation and cognitive decline. *Elife* 6:e22978. doi: 10.7554/eLife.22978

Marks, S. M., Lockhart, S. N., Baker, S. L., and Jagust, W. J. (2017). Tau and β-Amyloid are associated with medial temporal lobe structure, function, and memory encoding in normal aging. *J. Neurosci.* 37, 3192–3201. doi: 10.1523/JNEUROSCI.3769-16.2017

Miller, S. L., Celone, K., DePeau, K., Diamond, E., Dickerson, B. C., Rentz, D., et al. (2008). Age-related memory impairment associated with loss of parietal deactivation but preserved hippocampal activation. *Proc. Natl. Acad. Sci. U.S.A.* 105, 2181–2186. doi: 10.1073/pnas.0706818105

Mormino, E. C., Brandel, M. G., Madison, C. M., Marks, S., Baker, S. L., and Jagust, W. J. (2012). Aβ deposition in aging is associated with increases in brain activation during successful memory encoding. *Cereb. Cortex* 22, 1813–1823. doi: 10.1093/cercor/bhr255

Mucke, L., Masliah, E., Yu, G. Q., Mallory, M., Rockenstein, E. M., Tatsuno, G., et al. (2000). High-level neuronal expression of $A\beta_{1-42}$ in wild-type human amyloid protein precursor transgenic mice: synaptotoxicity without plaque formation. *J. Neurosci.* 20, 4050–4058.

Musiek, E. S., and Holtzman, D. M. (2015). Three dimensions of the amyloid hypothesis: time, space and 'wingmen'. *Nat. Neurosci.* 18, 800–806. doi: 10.1038/nn.4018

Netzer, W. J., Powell, C., Nong, Y., Blundell, J., Wong, L., Duff, K., et al. (2010). Lowering β-amyloid levels rescues learning and memory in a down syndrome mouse model. *PLoS ONE* 6:e10943. doi: 10.1371/journal.pone.0010943

Nitsch, R. M., Farber, S. A., Growdon, J. H., and Wurtman, R. J. (1993). Release of amyloid beta-protein precursor derivatives by electrical depolarization of rat hippocampal slices. *Proc. Natl. Acad. Sci. U.S.A.* 90, 5191–5193. doi: 10.1073/pnas.90.11.5191

Palop, J. J., Chin, J., Roberson, E. D., Wang, J., Thwin, M. T., Bien-Ly, N., et al. (2007). Aberrant excitatory neuronal activity and compensatory remodeling of inhibitory hippocampal circuits in mouse models of Alzheimer's disease. *Neuron* 55, 697–711. doi: 10.1016/j.neuron.2007.07.025

Palop, J. J., Jones, B., Kekonius, L., Chin, J., Yu, G. Q., Raber, J., et al. (2003). Neuronal depletion of calcium-dependent proteins in the dentate gyrus is tightly linked to Alzheimer's disease-related cognitive deficits. *Proc. Natl. Acad. Sci. U.S.A.* 100, 9572–9577. doi: 10.1073/pnas.1133381100

Palop, J. J., and Mucke, L. (2010). Amyloid-β induced neuronal dysfunction in Alzheimer's disease: from synapses toward neural networks. *Nat. Neurosci.* 13, 812–818. doi: 10.1038/nn.2583

Roberson, E. D., Halabisky, B., Yoo, J. W., Yao, J., Chin, J., Yan, F., et al. (2011). Amyloid-β/Fyn-induced synaptic, network, and cognitive impairments depend on tau levels in multiple mouse models of Alzheimer's disease. *J. Neurosci.* 31, 700–711. doi: 10.1523/JNEUROSCI.4152-10.2011

Roberson, E. D., Scearce-Levie, K., Palop, J. J., Yan, F., Cheng, I. H., Wu, T., et al. (2007). Reducing endogenous tau ameliorates amyloid beta-induced deficits in an Alzheimer's disease mouse model. *Science* 316, 750–754. doi: 10.1126/science.1141736

Schenk, D., Barbour, R., Dunn, W., Gordon, G., Grajeda, H., Guido, T., et al. (1999). Immunization with amyloid-beta attenuates Alzheimer-disease-like pathology in the PDAPP mouse. *Nature* 400, 173–177. doi: 10.1038/22124

Sepúlveda, M. R., Dresselaers, T., Vangheluwe, P., Everaerts, W., Himmelreich, U., Mata, A. M., et al. (2012). Evaluation of manganese uptake and toxicity in

mouse brain during continuous $MnCl_2$ administration using osmotic pumps. *Contrast Media Mol. Imaging* 7, 426–434. doi: 10.1002/cmmi.1469

Shipton, O. A., Leitz, J. R., Dworzak, J., Acton, C. E. J., Tunbridge, E. M., Denk, F., et al. (2011). Tau protein is required for amyloid-induced impairment of hippocampal long-term potentiation. *J. Neurosci.* 31, 1688–1692. doi: 10.1523/JNEUROSCI.2610-10.2011

Silva, A. C., and Bock, N. A. (2008). Manganense-enhanced MRI: an exceptional tool in translational neuroimaging. *Schizophr. Bull.* 34, 595–604. doi: 10.1093/schbul/sbn056

Sperling, R. A., Bates, J. F., Chua, E. F., Cocchiarella, A. J., Rentz, D. M., Rosen, B. R., et al. (2003). fMRI studies of associative encoding in young and elderly controls and mild Alzheimer's disease. *J. Neurol. Neurosurg. Psychiatry* 74, 44–50. doi: 10.1136/jnnp.74.1.44

Tanzi, R. E. (2012). The genetics of Alzheimer disease. *Cold Spring Harb. Perspect. Med.* 2:a006296. doi: 10.1101/cshperspect.a006296

Vega-Flores, G., Rubio, S. E., Jurado-Parras, M. T., Gómez-Climent, M. Á., Hampe, C. S., Manto, M., et al. (2014). The GABAergic septohippocampal pathway is directly involved in internal processes related to operant reward learning. *Cereb. Cortex* 24, 2093–2107. doi: 10.1093/cercor/bht060

Walsh, D. M., Klyubin, I., Fadeeva, J. V., Cullen, W. K., Anwyl, R., Wolfe, M. S., et al. (2002). Naturally secreted oligomers of amyloid beta protein potently inhibit hippocampal long-term potentiation *in vivo*. *Nature* 416, 535–539. doi: 10.1038/416535a

Wright, A. L., Zinn, R., Hohensinn, B., Konen, L. M., Beynon, S. B., Tan, R. P., et al. (2013). Neuroinflammation and neuronal loss precede Aβ plaque deposition in the hAPP-J20 mouse model of Alzheimer's disease. *PLoS ONE* 8:e59586. doi: 10.1371/journal.pone.0059586

Wu, J. W., Hussaini, S. A., Bastille, I. M., Rodriguez, G. A., Mrejeru, A., Rilett, K., et al. (2016). Neuronal activity enhances tau propagation and tau pathology *in vivo*. *Nat. Neurosci.* 19, 1085–1092. doi: 10.1038/nn.4328

Yassa, M. A., Lacy, J. W., Stark, S. M., Albert, M. S., Gallagher, M., and Stark, C. E. (2011). Pattern separation deficits associated with increased hippocampal CA3 and dentate gyrus activity in nondemented older adults. *Hippocampus* 21, 968–979. doi: 10.1002/hipo.20808

Ziyatdinova, S., Rönnbäck, A., Gurevicius, K., Miszczuk, D., Graff, C., Winblad, B., et al. (2016). Increased epileptiform EEG activity and decreased seizure threshold in arctic APP transgenic mouse model of Alzheimer's disease. *Curr. Alzheimer Res.* 13, 817–830. doi: 10.2174/1567205013666160129095508

Conflict of Interest Statement: The authors declare that the research was conducted in the absence of any commercial or financial relationships that could be construed as a potential conflict of interest.

frontiers in Neuroscience

REVIEW
published: 30 January 2018
doi: 10.3389/fnins.2018.00025

Reconsideration of Amyloid Hypothesis and Tau Hypothesis in Alzheimer's Disease

Fuyuki Kametani and Masato Hasegawa**

Department of Dementia and Higher Brain Function, Tokyo Metropolitan Institute of Medical Science, Tokyo, Japan

The so-called amyloid hypothesis, that the accumulation and deposition of oligomeric or fibrillar amyloid β (Aβ) peptide is the primary cause of Alzheimer's disease (AD), has been the mainstream concept underlying AD research for over 20 years. However, all attempts to develop Aβ-targeting drugs to treat AD have ended in failure. Here, we review recent findings indicating that the main factor underlying the development and progression of AD is tau, not Aβ, and we describe the deficiencies of the amyloid hypothesis that have supported the emergence of this idea.

Keywords: Alzheimer's disease, Aβ, APP, amyloid, tau, PHF

OPEN ACCESS

Edited by:
Naruhiko Sahara, National Institute of Radiological Sciences (NIRS), Japan

Reviewed by:
Felix Hernandez, Consejo Superior de Investigaciones Científicas (CSIC), Spain
Tetsuaki Arai, University of Tsukuba, Japan

****Correspondence:***
Fuyuki Kametani
kametani-fy@igakuken.or.jp
Masato Hasegawa
hasegawa-ms@igakuken.or.jp

Specialty section:
This article was submitted to Neurodegeneration, a section of the journal Frontiers in Neuroscience

Received: *08 November 2017*
Accepted: *12 January 2018*
Published: *30 January 2018*

Citation:
Kametani F and Hasegawa M (2018) Reconsideration of Amyloid Hypothesis and Tau Hypothesis in Alzheimer's Disease. Front. Neurosci. 12:25. doi: 10.3389/fnins.2018.00025

INTRODUCTION

Alzheimer's disease (AD) is said to account for about 70% of dementia. The affected brain exhibits astroglyosis, nerve cell atrophy and neuronal loss, and is characterized by the extensive distribution of two kinds of abnormal structures: so-called senile plaques and neurofibrillary tangles (NFTs). In the 1980's, it was shown that senile plaque consists of amyloid fibrils composed of the amyloid β (Aβ) peptide (Glenner and Wong, 1984; Masters et al., 1985), while NFT contain bundles of paired helical filaments of the microtubule-associated protein tau by immunochemically (Brion et al., 1985; Grundke-Iqbal et al., 1986; Nukina and Ihara, 1986) and biochemically (Goedert et al., 1988; Kondo et al., 1988; Kosik et al., 1988; Wischik et al., 1988b).

Aβ is a peptide consisting of about 40 amino acids, formed by sequential cleavages of amyloid β precursor protein (APP, http://www.uniprot.org/uniprot/P05067) by β-secretase (BACE 1) and γ-secretase (a complex containing presenilin 1), as illustrated in **Figure 1**. APP is a transmembrane protein associated with neuronal development, neurite outgrowth, and axonal transport (Kang et al., 1987). On the other hand, tau is a microtubule-associated protein that promotes microtubule polymerization and stabilization, and the abilities are regulated by phosphorylation (http://www.uniprot.org/uniprot/P10636).

Studies of AD pathogenesis have mostly been focused on how Aβ and tau form senile plaques and NFTs, respectively, and how these abnormal structures induce neural degeneration and neuronal loss.

THE AMYLOID HYPOTHESIS

The amyloid hypothesis (also known as the amyloid cascade hypothesis, the Aβ hypothesis, etc.) has been the mainstream explanation for the pathogenesis of AD for over 25 years (Hardy and Allsop, 1991; Selkoe, 1991; Hardy and Higgins, 1992; Hardy and Selkoe, 2002), and may be briefly summarized as follows (**Figure 1**). In normal subjects, Aβ is excised from APP by β- and γ-secretase and released outside the cell, where it is rapidly

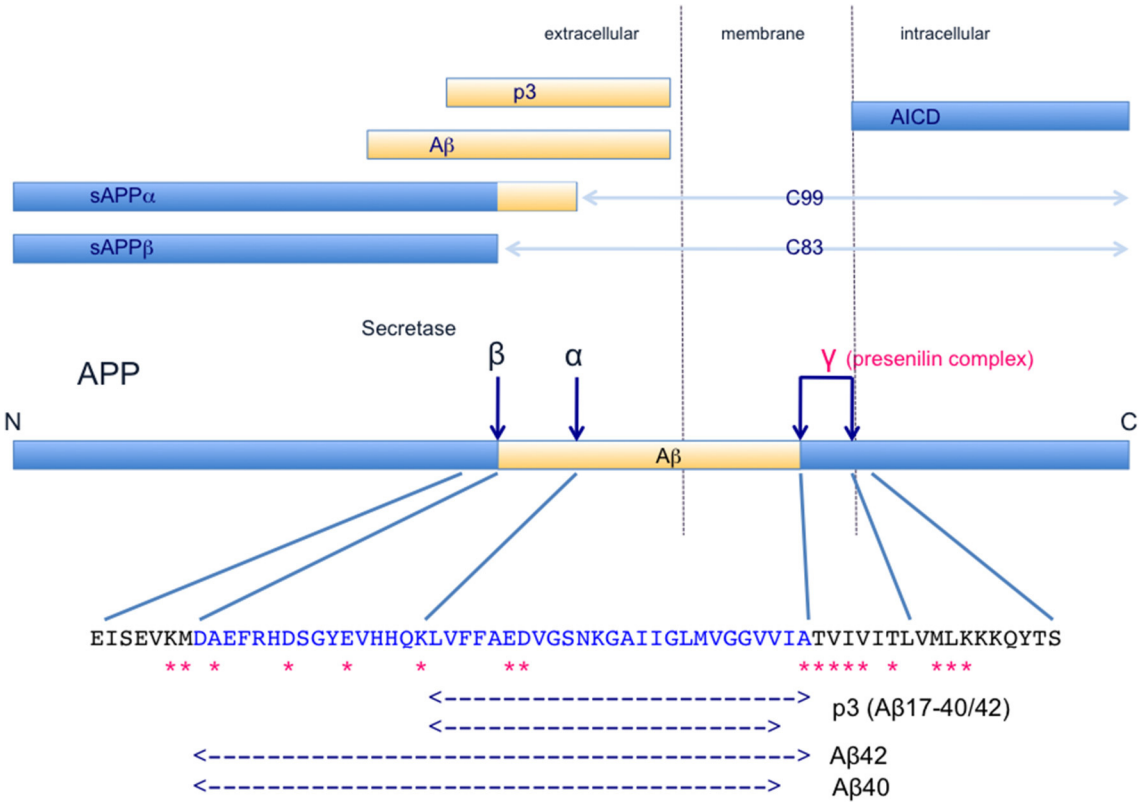

FIGURE 1 | Schematic illustration of the structure and metabolism of APP and its derivatives. Dark blue arrows indicate cleavage sites. α-Secretase (TACE/ADAM) (Buxbaum et al., 1998; Lammich et al., 1999) cleaves the α-site and β-secretase (BACE1, Vassar et al., 1999) cleaves the β-site, affording N-terminal fragments, sAPPα and sAPP β, and C-terminal fragments, C83 and C99, respectively. C83 and C99 are further cleaved at the γ-sites by γ-secretase complex, which includes presenilin-1, nicastrin, Aph-1 and Pen2 (Capell et al., 1998; De Strooper et al., 1998; Yu et al., 2000; Francis et al., 2002; Goutte et al., 2002; Takasugi et al., 2003). AICD and p3/Aβ are produced and released from the membrane. In the normal physiological state, α-secretase cleaves 90% or more of APP and the remaining APP is cleaved by β-secretase. Therefore, the major products in this APP metabolic pathway are sAPPα, C83, p3, and AICD, and Aβ is a minor product. AICD is rapidly degraded (Cupers et al., 2001; Kopan and Ilagan, 2004; Kametani and Haga, 2015). Thus, mutations found in familial AD, especially presenilin mutations, may affect the formation and processing of a variety of products. A part of APP sequence including Aβ is shown. Asterisks indicate APP mutations that have been identified in familial AD. These pathogenetic mutations of APP cluster near the α-secretase, β-secretase and γ-secretase cleavage sites. These mutations cause accumulation of APP C-terminal fragments (Tesco et al., 2005; Wiley et al., 2005; Xu et al., 2016a), and such accumulation has been found even in sporadic AD brains (Pera et al., 2013). Furthermore, mutations in presenilin, a constitutive protein of the γ-secretase complex, reduce γ-secretase activity (Chen et al., 2002; Walker et al., 2005; Bentahir et al., 2006; Shen and Kelleher, 2007; Xia et al., 2015). Decrease in the catalytic capacity of γ-secretase, which would lead to an increase of APP C-terminal fragments, facilitates the pathogenesis in sporadic and familial AD (Svedruzic et al., 2015).

degraded or removed. However, in aged subjects or under pathological conditions, the metabolic ability to degrade Aβ is decreased, and Aβ peptides may be accumulated. Aβ 40 and Aβ 42 (more hydrophobic than Aβ 40), containing 40 and 42 amino acid residues, respectively, are major components of the accumulated Aβ (**Figure 1**). An increase in the level of Aβ 42 or an increase in the ratio of Aβ 42 induces Aβ amyloid fibril formation, and the accumulated Aβ amyloid fibrils develop into senile plaque, causing neurotoxicity and induction of tau pathology, leading to neuronal cell death and neurodegeneration.

The APP gene is on chromosome 21 (Kang et al., 1987), and the discovery of genetic mutations of APP in early-onset familial AD (http://www.alzforum.org/mutations), as shown in **Figure 1**, appeared to support the amyloid hypothesis. These pathogenetic mutations of APP are clustered near β-secretase or γ-secretase cleavage sites, and are associated with an increase in Aβ42 production and/or a change in the ratio of Aβ42 formation. Interestingly, Down's syndrome patients with trisomy 21 exhibit AD-like pathology by about 40 years of age (Kolata, 1985), and this was thought to be due to the fact that the amount of APP in the brain was increased to 1.5 times the normal amount and the amount of Aβ was also increased (Kolata, 1985). In addition, APP locus duplication causes autosomal-dominant early-onset AD with cerebral amyloid angiopathy, with accumulation of large amounts of Aβ peptides (Delabar et al., 1987; Rovelet-Lecrux et al., 2006). Moreover, other familial AD mutations have been identified in presenilin 1/2, which is a component of γ-secretase (http://www.alzforum.org/mutations) (**Figure 1**). These mutations in APP and presenilin are closely linked to the Aβ production process, providing a rational basis for the idea that Aβ production and/or Aβ amyloid fibril formation represent the

central pathogenic cause of AD (Hardy and Allsop, 1991; Selkoe, 1991; Hardy and Higgins, 1992; Hardy and Selkoe, 2002).

PROBLEMS WITH THE AMYLOID HYPOTHESIS

To investigate the pathogenesis of AD, a number of genetically modified mouse models were produced in which Aβ is deposited in the brain. However, although senile plaques (accumulation of Aβ amyloid fibrils) are formed in these mice, NFT formation (accumulation of tau) and nerve cell death have not been observed (Bryan et al., 2009) (http://www.alzforum.org/research-models/alzheimers-disease). This suggested that extracellular accumulation of Aβ fibrils is not intrinsically cytotoxic, and also that Aβ does not induce tau accumulation. As Aβ is a normal metabolic product of APP and is not itself toxic under normal physiological conditions, the idea developed that Aβ oligomers (multimers) were the key toxic agents.

It has been reported that synaptic failures occur from an early stage in the AD brain and that the levels of synaptic proteins change (Masliah et al., 2001). Also, a drastic decrease in the number of synapses is characteristically observed in AD (Davies et al., 1987). Therefore, it was suggested that Aβ, which is present abundantly at an early stage after birth in AD model mice, causes synaptic impairment (William et al., 2012). Furthermore, it was reported that decrease of dendritic spines, inhibition of long-term potentiation, promotion of long-term suppression, and impairment of memory learning occur when Aβ oligomers (dimers) obtained from AD patients' brains were directly transferred to hippocampus of mouse brain (Shankar et al., 2008). However, although Aβ oligomers and Aβ amyloid fibrils were present in Aβ42-overexpressing BRI2-Aβ mice, and amyloid deposits and formation of senile plaques were observed in the brain, degeneration of nerve cells and neuronal loss were not observed, and there was no impairment of cognitive functions (Kim et al., 2007, 2013). These results indicate that Aβ42, including its oligomers and amyloid fibrils, is not cytotoxic. In addition, various immunotherapies targeting Aβ in AD model mice were effective in decreasing Aβ deposition in the brains, but it did not lead to improvement of actual symptoms or accumulation of tau (Ostrowitzki et al., 2012; Giacobini and Gold, 2013; Doody et al., 2014; Salloway et al., 2014).

Recent advances in amyloid imaging have made it possible to observe Aβ amyloid accumulation in the patient's brain. As a result, it has been found that there are many normal patients with amyloid deposits, and also AD patients with very few amyloid deposits (Edison et al., 2007; Li et al., 2008). Further, in the brain of elderly non-demented patients, the distribution of senile plaques is sometimes as extensive as that of dementia patients (Davis et al., 1999; Fagan et al., 2009; Price et al., 2009; Chetelat et al., 2013). This suggests that Aβ amyloid deposition is a phenomenon of aging, and has no direct relation with the onset of AD.

Taking these facts into account, it appears that neurodegeneration/neuronal loss and amyloid deposition are independent, unrelated phenomena (Chetelat, 2013), contrary to the amyloid hypothesis.

RECONSIDERATION OF APP AND PRESENILIN (PS) MUTATIONS IN FAMILIAL AD

In this section, we will focus on the nature and effects of mutations that are reported to be associated with familial AD.

In the normal physiological state, α-secretase cleaves 90% or more of APP and the remaining APP is cleaved by β-secretase, then γ-secretase cleaves the C-terminal region, as shown in **Figure 1**. The major products of this APP metabolic pathway are sAPPα, C83, p3, and APP intracellular domain (AICD), and Aβ is a minor product. Moreover, AICD is rapidly degraded (Cupers et al., 2001; Kopan and Ilagan, 2004; Kametani and Haga, 2015), suggesting that APP C-terminal fragments (C83, C99, and AICD) may be toxic and need to be removed (Kametani, 2008; Robakis and Georgakopoulos, 2014). Thus, when considering the effects of familial AD mutations, the effects on all the major products of APP metabolism should be considered.

AD-associated mutations in PS (PS1), a constituent protein of the γ-secretase complex, reduce γ-secretase activity, leading to decreased production of Aβ, especially Aβ40 (Chen et al., 2002; Walker et al., 2005; Bentahir et al., 2006; Shen and Kelleher, 2007; Xia et al., 2015). But, as a result, the proportion of Aβ42 increases and Aβ amyloid is formed. At the same time, APP C-terminal fragments that should be cleaved by γ-secretase are not cleaved, and accumulate in the cell membrane (Chen et al., 2002; Kametani, 2008; Robakis and Georgakopoulos, 2014).

It has also been reported that APP mutation causes accumulation of APP C-terminal fragments (Tesco et al., 2005, p.181; Wiley et al., 2005, p. 205; Xu et al., 2016a) and that the production of APP C-terminal fragment by β-secretase increases in the brain of patients with sporadic AD (Pera et al., 2013). Moreover, decrease in the catalytic capacity of γ-secretase, which would promote accumulation of APP C-terminal fragments, might facilitate the development of both sporadic and familial AD with APP mutation (Svedruzic et al., 2015).

Further, γ-secretase inhibitor may accelerate accumulation of APP C-terminal fragments in brain, if it is used as a therapeutic agent to suppress Aβ production in AD patients. Notably, the symptoms of AD worsened in a clinical trial of γ-secretase inhibitor (Doody et al., 2013).

These indicate that APP C-terminal fragment accumulation closely links to pathogenesis of sporadic and familial AD.

It was previously reported that APP or APP fragments accumulated in dystrophic neurites in AD brains (Ishii et al., 1989) and that the accumulation of APP and its metabolic fragments induced neurotoxicity and vesicular trafficking impairment (Yoshikawa et al., 1992; Kametani et al., 2004; Roy et al., 2005). It has also been reported that synaptic disorders and dendritic dysplasia occur in the absence of Aβ amyloid deposition (Boncristiano et al., 2005), and that C-terminal fragments of APP cause synaptic failure and memory impairment (Tamayev et al., 2012). Furthermore, transgenic mice expressing the C-terminal intracellular domain of APP (AICD) developed Alzheimer's-like symptoms, such as accumulation of phosphorylated tau and memory impairment (Ghosal et al., 2009). Also, accumulation of APP C-terminal fragments triggers the hydrolysis of cAMP, causing impairment of the cAMP/PKA/CREB pathway

(Kametani and Haga, 2015). Moreover, APP C-terminal fragment accumulation alters the subcellular localization of APP and the distribution of Rab11, and decreases endocytosis and soma-to-axon transcytosis of LDL (Woodruff et al., 2016), and this affects axonal vesicle trafficking (Szpankowski et al., 2012; Fu and Holzbaur, 2013; Gunawardena et al., 2013). These findings support the idea that APP C-terminal fragment accumulation causes neuronal impairment.

In addition, sAPPα is involved in neurite outgrowth and has a neuroprotective effect (Baratchi et al., 2012), and AICD is involved in signal transduction (Cao and Sudhof, 2001). Thus, multiple APP domains, including the C-terminus, are required for normal nervous system function (Klevanski et al., 2015). Therefore, since APP metabolites play a variety of functions in the brain, impaired APP metabolism may have a range of effects.

Overall, these findings suggest that the trigger of AD are closely linked to impairments of APP metabolism and accumulation of APP C-terminal fragments, rather than Aβ production and Aβ amyloid formation.

THE TAU HYPOTHESIS

Tau is one of the microtubule-associated proteins that regulate the stability of tubulin assemblies. The human tau gene is localized in chromosome 17. Six tau isoforms are expressed in the adult human brain as a result of mRNA alternative splicing, with or without exons 2, 3, and 10 (Goedert et al., 1989a; **Figure 2**). Exon 10 contains the microtubule-binding region. Insertion of exon 10 affords 4-repeat (4R) tau isoforms, while 3-repeat (3R) tau isoforms are produced without exon 10 (**Figure 2**). Adult human brain expresses both 3R and 4R tau isoforms, which are located mainly in axons of adult neurons under normal physiological conditions. The tau hypothesis is that the principle causative substance of AD is tau.

In AD brains, 3R and 4R tau is accumulated in a hyperphosphorylated state in the pathological inclusions (Goedert, 1993; Goedert et al., 1996; Serrano-Pozo et al., 2011; Iqbal et al., 2016). Ultrastructurally, unique twisted fibrils with ∼80 nm periodicity appearing as paired helical filaments (PHFs) or related straight filaments (SFs) are observed (Crowther and Wischik, 1985; Wischik et al., 1988a,b; Crowther et al., 1989; Goedert et al., 1989b; Greenberg and Davies, 1990; Lee et al., 1991). These pathological inclusions are referred to as neurofibrillary tangles (NFTs) if they are formed in neuronal cell bodies, while they are referred to as threads if they are formed in dendrites or axons. These findings suggested that mis-sorting of tau might induce tau pathology (Zempel and Mandelkow, 2014).

Tau pathology is staged according to Braak and Braak (Braak and Braak, 1991), and appears first in the transentorhinal region (stages I and II), then spreads to the limbic region (stages III and IV) and neocortical areas (stages V and IV). This spreading of tau pathology is strongly correlated with the extent of cognitive and clinical symptoms. Recent PET studies have shown that the spatial patterns of tau tracer binding are closely linked to the patterns of neurodegeneration and the clinical presentation in AD patients (Bejanin et al., 2017; Okamura and Yanai, 2017) and that subjective cognitive decline is indicative of early tauopathy in the medial temporal lobe, specifically in the entorhinal cortex, and to a lesser extent with elevated global levels of Aβ (Scholl et al., 2016; Schwarz et al., 2016; Buckley et al., 2017). Furthermore, it has been reported that tau lesions occurred earlier than Aβ accumulation (Braak and Del Tredici, 2014; Johnson et al., 2015). Thus, progression of AD is strongly associated with tau pathology, rather than Aβ amyloid accumulation.

Tau pathologies are also seen in other neurodegenerative dementing disorders, such as frontotemporal dementia and parkinsonism linked to chromosome 17 (FTDP-17), Pick's disease (PiD), progressive supranuclear palsy (PSP), corticobasal degeneration (CBD), argyrophilic grain disease (AGD), tangle-only dementia, and chronic traumatic encephalopathies (CTE) (Iwatsubo et al., 1994; Spillantini et al., 1997, 1998; Hutton et al., 1998; Poorkaj et al., 1998; Buee and Delacourte, 1999; Goedert and Hasegawa, 1999; Lee et al., 2001; Kovacs, 2015) In particular, FTDP-17 patients exhibit many exonic and intronic mutations in the tau gene (http://www.alzforum.org/mutations), resulting in tau accumulation (Spillantini et al., 1997, 1998; Hutton et al., 1998; Poorkaj et al., 1998). These findings suggest that tau abnormalities cause accumulation of tau and degeneration of neurons. In other sporadic cases of tauopathies, including AD, the initial trigger is unclear, but wild-type tau is accumulated.

What is the tau-induced neurodegeneration? In FTDP-17, the disease causing tau-mutations cluster near the C-terminal microtubule binding repeat and impair the ability of tau to bind microtubules (Hasegawa et al., 1998), suggesting impairment of the microtubule regulation. Mis-localized tau also induces impairment of microtubule regulation (Zempel and Mandelkow, 2014). These taus form aggregation and fibril seed, and were hyperphosphorylated as described above. Furthermore, the stability of mutant and hyperphosphorylated tau increases compared to the normal tau (Yamada et al., 2015; Bardai et al., 2018). Aberrant interaction of stabilized tau with filamentous actin induces mis-stabilization of actin (Fulga et al., 2007), synaptic impairment (Cabrales Fontela et al., 2017; Zhou et al., 2017; Bardai et al., 2018), and defects in mitochondrial integrity (DuBoff et al., 2012). Therefore, tau pathology causes extensive damage in the cell, such as transport system, cytoskeletal system, signaling system, and mitochondrial integrity.

PROPAGATION OF TAU PATHOLOGY

In an experimental model of cultured cells and mice, abnormal tau (amyloid-like fibril tau) converts normal tau to an abnormal type. Therefore, it has been hypothesized that tau aggregates form first in a small number of brain cells, from where they propagate to other regions, resulting in neurodegeneration and disease. This hypothesis has recently gained attention because it has been confirmed that tau proliferates and propagates between

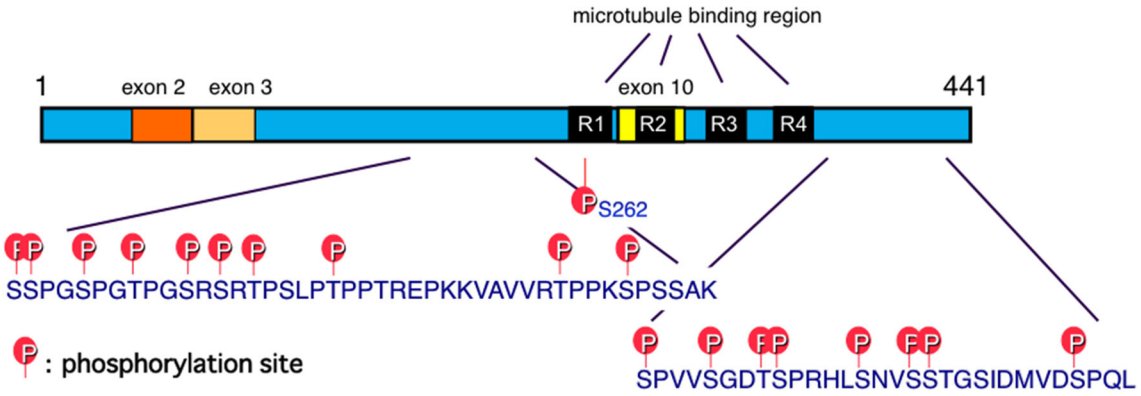

FIGURE 2 | Schematic illustration of functional sites of tau. Six tau isoforms are expressed in the adult human brain as a result of mRNA alternative splicing, with or without exons 2, 3, and 10. Exon 10 contains the microtubule-binding region. Insertion of exon 10 affords 4-repeat (4R) tau isoforms, while 3-repeat (3R) tau isoforms are produced without exon 10 (Goedert et al., 1989a). Major tau phosphorylation sites identified in PHF-tau from AD brains are shown. Microtubule binding regions R3 and R4 form the core of tau fibrils (PHF and SF) (Taniguchi-Watanabe et al., 2016; Fitzpatrick et al., 2017).

cells (Clavaguera et al., 2009, 2013; Nonaka et al., 2010; Hasegawa, 2016; Goedert and Spillantini, 2017). The existence of several human tauopathies with distinct fibril morphologies has led to the suggestion that different molecular conformers (or strains) of aggregated tau exist (Goedert and Spillantini, 2017). Although the transmission mechanism of tau aggregates from cell to cell is still not clear, tau pathology does spread in the brain in a well-defined manner; its distribution can be correlated with the clinical stages of disease (Braak and Braak, 1991), and it is considered that tau pathology correlates better than Aβ pathology with clinical features of dementia. Recently, we found that increase APP with or without familial AD mutations, not Aβ, may work as a receptor of abnormal tau fibrils and promote intracellular tau aggregation (Takahashi et al., 2015), suggesting that APP rather than Aβ may accelerate tau accumulation and propagation.

AD RISK FACTORS, ApoE4 AND TREM2

Apolipoprotein E (ApoE) is one of the major apolipoproteins (http://www.uniprot.org/uniprot/P02649). The *ApoE* gene has three alleles, *ε2*, *ε3*, and *ε4*, corresponding to isoforms E2, E3, and E4, respectively. In the central nervous system, ApoE produced and secreted by astrocytes and microglia binds to lipoprotein and is taken up into nerve cells via the ApoE receptor during the developmental stage of the central nervous system and the repair period after neuronal damage.

The *ApoE4* allele is a genetic risk factor for sporadic AD (Corder et al., 1993). As the number of *ε4* genes increases, the age of onset of AD declines and the incidence of AD increases (Maestre et al., 1995), and there is an increased risk of 3–4 and 8–12 times for one or two copies of the allele, respectively. It is considered that impaired apoE4 function affects the clearance pathway of Aβ (Zlokovic, 2013; Robert et al., 2017) and modulates Aβ-induced effects on inflammatory receptor signaling, including amplification of detrimental pathways and suppression of beneficial pathways (Chan et al., 2015; Tai et al., 2015). To examine the role of ApoE, human ApoE targeted replacement mice were crossed with mutant human amyloid precursor protein (APP) mice. In this context, ApoE genotypes only modulate Aβ-mediated insulin signaling impairment (Chan et al., 2015). Recently, however, P301S tau transgenic mice were generated on either a human ApoE knock-in (KI) or ApoE knockout (KO) background, and developed significant brain atrophy primarily in the hippocampus, piriform/entorhinal cortex, and amygdala, accompanied by significant lateral ventricular enlargement (Shi et al., 2017). ApoE plays an important role in regulating tau-mediated neurodegeneration and neuroinflammation, with ApoE4 causing more severe damage and the absence of ApoE being protective (Shi et al., 2017). These findings indicate that ApoE4 affects neurodegeneration independently of Aβ and Aβ amyloid in the context of tau pathology (Shi et al., 2017).

Triggering receptor expressed on myeloid cells 2 (TREM2) is expressed on the membranes of microglia and is critical for the response to injury and AD pathology (http://www.uniprot.org/uniprot/Q9NZC2). TREM2 recognizes lipoproteins including ApoE, phospholipid and apoptotic cells and is implicated in microglial phagocytosis. Variants in the *TREM2* gene increase the risk of getting AD. Initially, this was thought to be related to the elimination of Aβ plaque. TREM2 deficiency in the setting of pure tauopathy limits gliosis and neuroinflammation, as well as protecting against brain atrophy, suggesting that TREM2 facilitates a microglial response to tau pathology and/or tau-mediated damage in the brain (Bemiller et al., 2017; Leyns et al., 2017). These results are consistent with the findings of strikingly reduced inflammation and neurodegeneration in mice lacking ApoE, as described above. Therefore, the TREM2-ApoE pathway is important for facilitating the microglial response to damage in the brain, and a functional consequence of activation of the TREM2-ApoE pathway is that microglia lose the ability to regulate brain homeostasis (Krasemann et al., 2017; Ulland et al., 2017). Microglial inflammation promotes

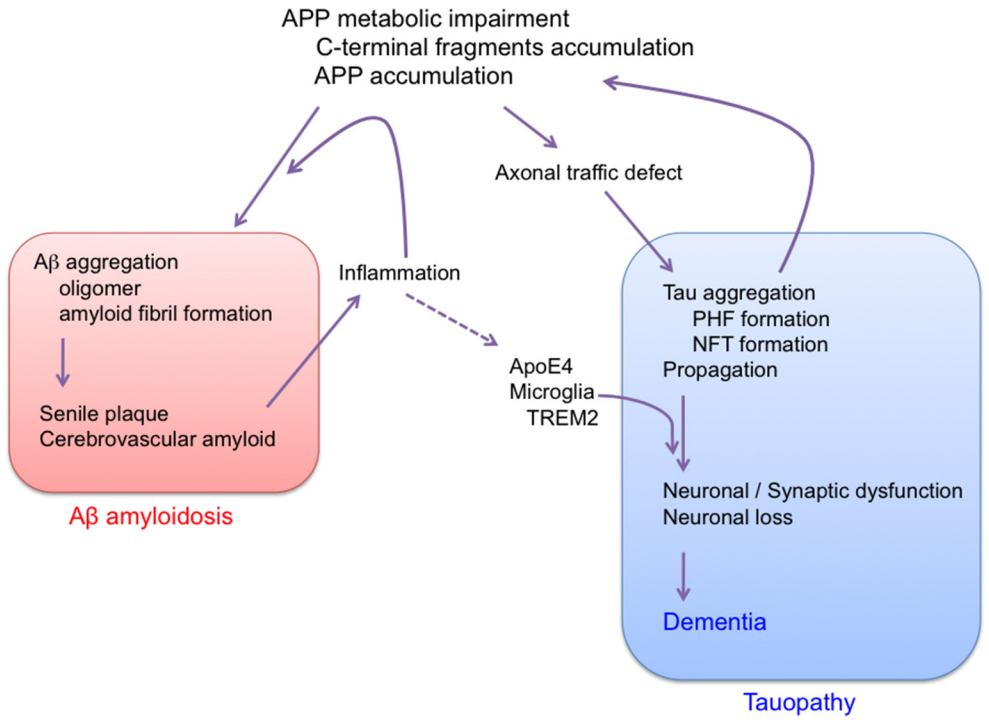

FIGURE 3 | Proposed sequence of major pathogenic events leading to AD. Aβ amyloidosis and tau pathology are regarded as independent pathological events. AD is APP trigger tauopathy.

tau-dependent degeneration independently of Aβ and Aβ amyloid.

APP TRIGGER TAUOPATHY

APP turn over rapidly and easily metabolize (Oltersdorf et al., 1990; Weidemann et al., 2002). Therefore, impairment of APP metabolism has a serious effect on cells. Increased APP and/or its C-terminal fragments induce axonal and synaptic defects (Rusu et al., 2007; Rodrigues et al., 2012; Deyts et al., 2016; Xu et al., 2016b), thereby triggering the mis-localization of tau (Blurton-Jones and Laferla, 2006; Hochgrafe et al., 2013). This protein modulates motility in a motor-specific manner to direct intracellular transport (Chaudhary et al., 2017). Mis-localized tau proteins accumulate, form fibril seeds and propagate (He et al., 2017). The pathological tau induce further transport dysfunction (Goldsbury et al., 2006; Rusu et al., 2007), creating a vicious circle and leading to tau accumulation. Moreover, since overexpression of APP promoted the seed aggregation of intracellular tau in cultured cell, suggesting that APP may function as a receptor of abnormal tau fibrils (Takahashi et al., 2015). Thus, increased APP may accelerate pathological incorporation and propagation.

Overall, the results described above suggest that AD is a disorder that is triggered by impairment of APP metabolism, and that progresses through tau pathology (**Figure 3**). It is well-known that Aβ amyloidosis due to APP metabolic impairment leads to neuroinflammation, which may further affect the progression of tau pathology (Leyns and Holtzman, 2017). So far, there is no evidence that Aβ itself directly affects tau pathology. We cannot rule out the possibility that APP metabolic impairment and tau pathology might be initiated independently in sporadic AD. In any event, there is now convincing evidence that the main factor causing progression of AD is tau, not Aβ, and that Aβ amyloidosis and tau pathology should be regarded as independent pathological events. Indeed, it was recently shown that the AD risk factors ApoE4 and TREM2 are linked to tau pathology (Bemiller et al., 2017; Leyns et al., 2017; Shi et al., 2017). Moreover, the incidence of type 2 diabetes is increased in AD patients (Janson et al., 2004), and it was recently shown that tau protein is involved in the control of brain insulin signaling (Marciniak et al., 2017). Furthermore, the brains of patients with primary age-related tauopathy (PART) contain NFTs that are indistinguishable from those of AD, in the absence of Aβ amyloid plaques (Crary et al., 2014; Duyckaerts et al., 2015; Jellinger et al., 2015). Therefore, tau could contribute to the cognitive and metabolic alterations in patients with AD.

The unexpected failures of all trials of AD treatment candidate drugs targeting Aβ can easily be understood if the main factor causing progression of AD is tau, not Aβ. Indeed, it has already been reported that the suppression or deletion of tau has a profound protective effect against brain damage and neurological deficits (Rapoport et al., 2002; SantaCruz et al., 2005; Roberson et al., 2007; Miao et al., 2010; Shipton et al., 2011; Bi et al., 2017).

Thus, suppression of tau production currently seems to be the most promising target for development of AD therapeutic drugs.

CONCLUSION

The amyloid hypothesis has been the mainstream concept underlying AD research for over 20 years. However, reconsideration of APP and presenilin (PS) mutations in familial AD indicate that the trigger of AD is closely linked to impairments of APP metabolism and accumulation of APP C-terminal fragments, rather than Aβ production and Aβ amyloid formation. Furthermore, all attempts to develop Aβ-targeting drugs to treat AD have ended in failure and recent findings indicating that the main factor underlying the development and progression of AD is tau, not Aβ. Therefore, AD is a disorder that is triggered by impairment of APP metabolism, and progresses through tau pathology, not Aβ amyloid.

AUTHOR CONTRIBUTIONS

FK and MH, data collection, literature review, manuscript writing.

ACKNOWLEDGMENTS

This work was supported by Grants-in-Aid for Scientific Research (KAKENHI) JP26117005 (to MH) and JP26293084 (to FK) from the Ministry of Education, Culture, Sports, Science, and Technology, as well as a Grant-in-Aid for Scientific Research (KAKENHI) JP23228004 (to MH) from the Japan Society for the Promotion of Science, and a Grant-in-Aid for Research on Brain Mapping by Integrated Neurotechnologies for Disease Studies (Brain/MINDS) from the Japan Agency for Medical Research and Development (AMED) JP14533254 (to MH).

REFERENCES

Baratchi, S., Evans, J., Tate, W. P., Abraham, W. C., and Connor, B. (2012). Secreted amyloid precursor proteins promote proliferation and glial differentiation of adult hippocampal neural progenitor cells. *Hippocampus* 22, 1517–1527. doi: 10.1002/hipo.20988

Bardai, F. H., Wang, L., Mutreja, Y., Yenjerla, M., Gamblin, T. C., and Feany, M. B. (2018). A conserved cytoskeletal signaling cascade mediates neurotoxicity of FTDP-17 tau mutations *in vivo*. *J. Neurosci.* 38, 108–119. doi: 10.1523/JNEUROSCI.1550-17.2017

Bejanin, A., Schonhaut, D. R., La Joie, R., Kramer, J. H., Baker, S. L., Sosa, N., et al. (2017). Tau pathology and neurodegeneration contribute to cognitive impairment in Alzheimer's disease. *Brain* 140, 3286–3300. doi: 10.1093/brain/awx243.

Bemiller, S. M., McCray, T. J., Allan, K., Formica, S. V., Xu, G., Wilson, G., et al. (2017). TREM2 deficiency exacerbates tau pathology through dysregulated kinase signaling in a mouse model of tauopathy. *Mol. Neurodegener.* 12:74. doi: 10.1186/s13024-017-0216-6

Bentahir, M., Nyabi, O., Verhamme, J., Tolia, A., Horré, K., Wiltfang, J., et al. (2006). Presenilin clinical mutations can affect gamma-secretase activity by different mechanisms. *J. Neurochem.* 96, 732–742. doi: 10.1111/j.1471-4159.2005.03578.x

Bi, M., Gladbach, A., Van Eersel, J., Ittner, A., Przybyla, M., Van Hummel, A., et al. (2017). Tau exacerbates excitotoxic brain damage in an animal model of stroke. *Nat. Commun.* 8, 473. doi: 10.1038/s41467-017-00618-0

Boncristiano, S., Calhoun, M. E., Howard, V., Bondolfi, L., Kaeser, S. A., Wiederhold, K. H., et al. (2005). Neocortical synaptic bouton number is maintained despite robust amyloid deposition in APP23 transgenic mice. *Neurobiol. Aging* 26, 607–613. doi: 10.1016/j.neurobiolaging.2004.06.010

Blurton-Jones, M., and Laferla, F. M. (2006). Pathways by which Abeta facilitates tau pathology. *Curr. Alzheimer Res.* 3, 437–448. doi: 10.2174/156720506779025242

Braak, H., and Braak, E. (1991). Neuropathological stageing of Alzheimer-related changes. *Acta Neuropathol.* 82, 239–259. doi: 10.1007/BF00308809

Braak, H., and Del Tredici, K. (2014). Are cases with tau pathology occurring in the absence of Abeta deposits part of the AD-related pathological process? *Acta Neuropathol.* 128, 767–772. doi: 10.1007/s00401-014-1356-1

Brion, J. P., Passareiro, H., Nunez, J., and Flament-Durand, J., (1985). Mise en évidence immunologique de la protéine tau au niveau deslésions de dégénérescence neurofibrillaire de la maladie d'Alzheimer. *Arch. Biol.* 95, 229–235.

Bryan, K. J., Lee, H., Perry, G., Smith, M. A., and Casadesus, G. (2009). *Transgenic Mouse Models of Alzheimer's Disease: Behavioral Testing and Considerations Methods of Behavior Analysis in Neuroscience*. Boca Raton, FL: Taylor & Francis Group, LLC.

Buckley, R. F., Hanseeuw, B., Schultz, A. P., Vannini, P., Aghjayan, S. L., Properzi, M. J., et al. (2017). Region-specific association of subjective cognitive decline with tauopathy independent of global beta-amyloid burden. *JAMA Neurol.* 74, 1455–1463. doi: 10.1001/jamaneurol.2017.2216

Buée, L., and Delacourte, A. (1999). Comparative biochemistry of tau in progressive supranuclear palsy, corticobasal degeneration, FTDP-17 and Pick's disease. *Brain Pathol.* 9, 681–693. doi: 10.1111/j.1750-3639.1999.tb00550.x

Buxbaum, J. D., Liu, K. N., Luo, Y., Slack, J. L., Stocking, K. L., Peschon, J. J., et al. (1998). Evidence that tumor necrosis factor alpha converting enzyme is involved in regulated alpha-secretase cleavage of the Alzheimer amyloid protein precursor. *J. Biol. Chem.* 273, 27765–27767. doi: 10.1074/jbc.273.43.27765

Cabrales Fontela, Y., Kadavath, H., Biernat, J., Riedel, D., Mandelkow, E., and Zweckstetter, M. (2017). Multivalent cross-linking of actin filaments and microtubules through the microtubule-associated protein Tau. *Nat. Commun.* 8, 1981. doi: 10.1038/s41467-017-02230-8

Cao, X., and Südhof, T. C. (2001). A transcriptionally active complex of APP with Fe65 and histone acetyltransferase Tip60. *Science* 293, 115–120. doi: 10.1126/science.1058783

Capell, A., Grünberg, J., Pesold, B., Diehlmann, A., Citron, M., Nixon, R., et al. (1998). The proteolytic fragments of the Alzheimer's disease-associated presenilin-1 form heterodimers and occur as a 100-150-kDa molecular mass complex. *J. Biol. Chem.* 273, 3205–3211. doi: 10.1074/jbc.273.6.3205

Chan, E. S., Chen, C., Cole, G. M., and Wong, B. S. (2015). Differential interaction of Apolipoprotein-E isoforms with insulin receptors modulates brain insulin signaling in mutant human amyloid precursor protein transgenic mice. *Sci. Rep.* 5:13842. doi: 10.1038/srep13842

Chaudhary, A. R., Berger, F., Berger, C. L., and Hendricks, A. G. (2017). Tau directs intracellular trafficking by regulating the forces exerted by kinesin and dynein teams. *Traffic*. doi: 10.1111/tra.12537. [Epub ahead of print].

Chen, F., Gu, Y., Hasegawa, H., Ruan, X., Arawaka, S., Fraser, P., et al. (2002). Presenilin 1 mutations activate gamma 42-secretase but reciprocally inhibit epsilon -secretase cleavage of amyloid precursor protein (APP) and S3-Cleavage of Notch. *J. Biol. Chem.* 277, 36521–36526. doi: 10.1074/jbc.M205093200

Chételat, G. (2013). Alzheimer disease: Abeta-independent processes-rethinking preclinical AD. *Nat. Rev. Neurol.* 9, 123–124. doi: 10.1038/nrneurol.2013.21

Chételat, G., La Joie, R., Villain, N., Perrotin, A., De La Sayette, V., Eustache, F., et al. (2013). Amyloid imaging in cognitively normal individuals, at-risk populations and preclinical Alzheimer's disease. *Neuroimage Clin.* 2, 356–365. doi: 10.1016/j.nicl.2013.02.006

Clavaguera, F., Akatsu, H., Fraser, G., Crowther, R. A., Frank, S., Hench, J., et al. (2013). Brain homogenates from human tauopathies induce tau

inclusions in mouse brain. *Proc. Natl. Acad. Sci. U.S.A.* 110, 9535–9540. doi: 10.1073/pnas.1301175110

Clavaguera, F., Bolmont, T., Crowther, R. A., Abramowski, D., Frank, S., Probst, A., et al. (2009). Transmission and spreading of tauopathy in transgenic mouse brain. *Nat. Cell Biol.* 11, 909–913. doi: 10.1038/ncb1901

Corder, E. H., Saunders, A. M., Strittmatter, W. J., Schmechel, D. E., Gaskell, P. C., Small, G. W., et al. (1993). Gene dose of apolipoprotein E type 4 allele and the risk of Alzheimer's disease in late onset families. *Science* 261, 921–923. doi: 10.1126/science.8346443

Crary, J. F., Trojanowski, J. Q., Schneider, J. A., Abisambra, J. F., Abner, E. L., Alafuzoff, I., et al. (2014). Primary age-related tauopathy (PART): a common pathology associated with human aging. *Acta Neuropathol.* 128, 755–766. doi: 10.1007/s00401-014-1349-0

Crowther, R. A., and Wischik, C. M. (1985). Image reconstruction of the Alzheimer paired helical filament. *EMBO J.* 4, 3661–3665.

Crowther, T., Goedert, M., and Wischik, C. M. (1989). The repeat region of microtubule-associated protein tau forms part of the core of the paired helical filament of Alzheimer's disease. *Ann. Med.* 21, 127–132. doi: 10.3109/07853898909149199

Cupers, P., Orlans, I., Craessaerts, K., Annaert, W., and De Strooper, B. (2001). The amyloid precursor protein (APP)-cytoplasmic fragment generated by gamma-secretase is rapidly degraded but distributes partially in a nuclear fraction of neurones in culture. *J. Neurochem.* 78, 1168–1178. doi: 10.1046/j.1471-4159.2001.00516.x

Davies, C. A., Mann, D. M., Sumpter, P. Q., and Yates, P. O. (1987). A quantitative morphometric analysis of the neuronal and synaptic content of the frontal and temporal cortex in patients with Alzheimer's disease. *J. Neurol. Sci.* 78, 151–164. doi: 10.1016/0022-510X(87)90057-8

Davis, D. G., Schmitt, F. A., Wekstein, D. R., and Markesbery, W. R. (1999). Alzheimer neuropathologic alterations in aged cognitively normal subjects. *J. Neuropathol. Exp. Neurol.* 58, 376–388. doi: 10.1097/00005072-199904000-00008

De Strooper, B., Saftig, P., Craessaerts, K., Vanderstichele, H., Guhde, G., Annaert, W., et al. (1998). Deficiency of presenilin-1 inhibits the normal cleavage of amyloid precursor protein. *Nature* 391, 387–390. doi: 10.1038/34910

Delabar, J. M., Goldgaber, D., Lamour, Y., Nicole, A., Huret, J. L., De Grouchy, J., et al. (1987). Beta amyloid gene duplication in Alzheimer's disease and karyotypically normal Down syndrome. *Science* 235, 1390–1392. doi: 10.1126/science.2950593

Deyts, C., Clutter, M., Herrera, S., Jovanovic, N., Goddi, A., and Parent, A. T. (2016). Loss of presenilin function is associated with a selective gain of APP function. *Elife* 5:e15645. doi: 10.7554/eLife.15645

Doody, R. S., Raman, R., Farlow, M., Iwatsubo, T., Vellas, B., Joffe, S., et al. (2013). A phase 3 trial of semagacestat for treatment of Alzheimer's disease. *N. Engl. J. Med.* 369, 341–350. doi: 10.1056/NEJMoa1210951

Doody, R. S., Thomas, R. G., Farlow, M., Iwatsubo, T., Vellas, B., Joffe, S., et al. (2014). Phase 3 trials of solanezumab for mild-to-moderate Alzheimer's disease. *N. Engl. J. Med.* 370, 311–321. doi: 10.1056/NEJMoa1312889

DuBoff, B., Götz, J., and Feany, M. B. (2012). Tau promotes neurodegeneration via DRP1 mislocalization *in vivo*. *Neuron* 75, 618–632. doi: 10.1016/j.neuron.2012.06.026

Duyckaerts, C., Braak, H., Brion, J.-P., Buée, L., Del Tredici, K., Goedert, M., et al. (2015). PART is part of Alzheimer disease. *Acta Neuropathol.* 129, 749–756. doi: 10.1007/s00401-015-1390-7

Edison, P., Archer, H. A., Hinz, R., Hammers, A., Pavese, N., Tai, Y. F., et al. (2007). Amyloid, hypometabolism, and cognition in Alzheimer disease: An [11C]PIB and [18F]FDG PET study. *Neurology* 68, 501–508. doi: 10.1212/01.wnl.0000244749.20056.d4

Fagan, A. M., Mintun, M. A., Shah, A. R., Aldea, P., Roe, C. M., Mach, R. H., et al. (2009). Cerebrospinal fluid tau and ptau(181) increase with cortical amyloid deposition in cognitively normal individuals: implications for future clinical trials of Alzheimer's disease. *EMBO Mol. Med.* 1, 371–380. doi: 10.1002/emmm.200900048

Fitzpatrick, A. W. P., Falcon, B., He, S., Murzin, A. G., Murshudov, G., Garringer, H. J., et al. (2017). Cryo-EM structures of tau filaments from Alzheimer's disease. *Nature* 547, 185–190. doi: 10.1038/nature23002

Francis, R., McGrath, G., Zhang, J., Ruddy, D. A., Sym, M., Apfeld, J., et al. (2002). aph-1 and pen-2 are required for Notch pathway signaling, gamma-secretase cleavage of betaAPP, and presenilin protein accumulation. *Dev. Cell* 3, 85–97. doi: 10.1016/S1534-5807(02)00189-2

Fu, M. M., and Holzbaur, E. L. (2013). JIP1 regulates the directionality of APP axonal transport by coordinating kinesin and dynein motors. *J. Cell Biol.* 202, 495–508. doi: 10.1083/jcb.201302078

Fulga, T. A., Elson-Schwab, I., Khurana, V., Steinhilb, M. L., Spires, T. L., Hyman, B. T., et al. (2007). Abnormal bundling and accumulation of F-actin mediates tau-induced neuronal degeneration *in vivo*. *Nat. Cell Biol.* 9, 139–148. doi: 10.1038/ncb1528

Ghosal, K., Vogt, D. L., Liang, M., Shen, Y., Lamb, B. T., and Pimplikar, S. W. (2009). Alzheimer's disease-like pathological features in transgenic mice expressing the APP intracellular domain. *Proc. Natl. Acad. Sci. U.S.A.* 106, 18367–18372. doi: 10.1073/pnas.0907652106

Giacobini, E., and Gold, G. (2013). Alzheimer disease therapy[mdash]moving from amyloid-[beta] to tau. *Nat. Rev. Neurol.* 9, 677–686. doi: 10.1038/nrneurol.2013.223

Glenner, G. G., and Wong, C. W. (1984). Alzheimer's disease: INITIAL report of the purification and characterization of a novel cerebrovascular amyloid protein. *Biochem. Biophys. Res. Commun.* 120, 885–890. doi: 10.1016/S0006-291X(84)80190-4

Goedert, M. (1993). Tau protein and the neurofibrillary pathology of Alzheimer's disease. *Trends Neurosci.* 16, 460–465. doi: 10.1016/0166-2236(93)90078-Z

Goedert, M., and Hasegawa, M. (1999). The tauopathies: toward an experimental animal model. *Am. J. Pathol.* 154, 1–6. doi: 10.1016/S0002-9440(10)65242-X

Goedert, M., and Spillantini, M. G. (2017). Propagation of Tau aggregates. *Mol. Brain* 10, 18. doi: 10.1186/s13041-017-0298-7

Goedert, M., Spillantini, M. G., Hasegawa, M., Jakes, R., Crowther, R. A., and Klug, A. (1996). Molecular dissection of the neurofibrillary lesions of Alzheimer's disease. *Cold Spring Harb. Symp. Quant. Biol.* 61, 565–573. doi: 10.1101/SQB.1996.061.01.057

Goedert, M., Spillantini, M. G., Jakes, R., Rutherford, D., and Crowther, R. A. (1989a). Multiple isoforms of human microtubule-associated protein tau: sequences and localization in neurofibrillary tangles of Alzheimer's disease. *Neuron* 3, 519–526. doi: 10.1016/0896-6273(89)90210-9

Goedert, M., Spillantini, M. G., Potier, M. C., Ulrich, J., and Crowther, R. A. (1989b). Cloning and sequencing of the cDNA encoding an isoform of microtubule-associated protein tau containing four tandem repeats: differential expression of tau protein mRNAs in human brain. *EMBO J.* 8, 393–399.

Goedert, M., Wischik, C. M., Crowther, R. A., Walker, J. E., and Klug, A. (1988). Cloning and sequencing of the cDNA encoding a core protein of the paired helical filament of Alzheimer disease: identification as the microtubule-associated protein tau. *Proc. Natl. Acad. Sci. U.S.A.* 85, 4051–4055. doi: 10.1073/pnas.85.11.4051

Goldsbury, C., Mocanu, M. M., Thies, E., Kaether, C., Haass, C., Keller, P., et al. (2006). Inhibition of APP trafficking by tau protein does not increase the generation of amyloid-beta peptidesPresenilin/gamma-secretase activity regulates protein clearance from the endocytic recycling compartment Presenilin-1-mediated retention of APP derivatives in early biosynthetic compartments A partial failure of membrane protein turnover may cause Alzheimer's disease: a new hypothesis. *Traffic* 7, 873–888. doi: 10.1111/j.1600-0854.2006.00434.x

Goutte, C., Tsunozaki, M., Hale, V. A., and Priess, J. R. (2002). APH-1 is a multipass membrane protein essential for the Notch signaling pathway in Caenorhabditis elegans embryos. *Proc. Natl. Acad. Sci. U.S.A.* 99, 775–779. doi: 10.1073/pnas.022523499

Greenberg, S. G., and Davies, P. (1990). A preparation of Alzheimer paired helical filaments that displays distinct tau proteins by polyacrylamide gel electrophoresis. *Proc. Natl. Acad. Sci. U.S.A.* 87, 5827–5831. doi: 10.1073/pnas.87.15.5827

Grundke-Iqbal, I., Iqbal, K., Tung, Y. C., Quinlan, M., Wisniewski, H. M., and Binder, L. I. (1986). Abnormal phosphorylation of the microtubule-associated protein tau (tau) in Alzheimer cytoskeletal pathology. *Proc. Natl. Acad. Sci. U.S.A.* 83, 4913–4917. doi: 10.1073/pnas.83.13.4913

Gunawardena, S., Yang, G., and Goldstein, L. S. (2013). Presenilin controls kinesin-1 and dynein function during APP-vesicle transport *in vivo*. *Hum. Mol. Genet.* 22, 3828–3843. doi: 10.1093/hmg/ddt237

Hardy, J., and Allsop, D. (1991). Amyloid deposition as the central event in the aetiology of Alzheimer's disease. *Trends Pharmacol. Sci.* 12, 383–388. doi: 10.1016/0165-6147(91)90609-V

Hardy, J., and Selkoe, D. J. (2002). The Amyloid hypothesis of Alzheimer's Disease: progress and problems on the road to therapeutics. *Science* 297, 353–356. doi: 10.1126/science.1072994

Hardy, J. A., and Higgins, G. A. (1992). Alzheimer's disease: the amyloid cascade hypothesis. *Science* 256, 184–185. doi: 10.1126/science.1566067

Hasegawa, M. (2016). Molecular mechanisms in the pathogenesis of alzheimer's disease and tauopathies-prion-like seeded aggregation and phosphorylation. *Biomolecules* 6:e24. doi: 10.3390/biom6020024

Hasegawa, M., Smith, M. J., and Goedert, M. (1998). Tau proteins with FTDP-17 mutations have a reduced ability to promote microtubule assembly. *FEBS Lett.* 437, 207–210. doi: 10.1016/S0014-5793(98)01217-4

He, Z., Guo, J. L., McBride, J. D., Narasimhan, S., Kim, H., Changolkar, L., et al. (2017). Amyloid-beta plaques enhance Alzheimer's brain tau-seeded pathologies by facilitating neuritic plaque tau aggregation. *Nat. Med.* 24, 29–38. doi: 10.1038/nm.4443

Hochgräfe, K., Sydow, A., and Mandelkow, E. M. (2013). Regulatable transgenic mouse models of Alzheimer disease: onset, reversibility and spreading of Tau pathology. *FEBS J.* 280, 4371–4381. doi: 10.1111/febs.12250

Hutton, M., Lendon, C. L., Rizzu, P., Baker, M., Froelich, S., Houlden, H., et al. (1998). Association of missense and 5'-splice-site mutations in tau with the inherited dementia FTDP-17. *Nature* 393, 702–705. doi: 10.1038/31508

Iqbal, K., Liu, F., and Gong, C. X. (2016). Tau and neurodegenerative disease: the story so far. *Nat. Rev. Neurol.* 12, 15–27. doi: 10.1038/nrneurol.2015.225

Ishii, T., Kametani, F., Haga, S., and Sato, M. (1989). The immunohistochemical demonstration of subsequences of the precursor of the amyloid A4 protein in senile plaques in Alzheimer's disease. *Neuropathol. Appl. Neurobiol.* 15, 135–147. doi: 10.1111/j.1365-2990.1989.tb01216.x

Iwatsubo, T., Hasegawa, M., and Ihara, Y. (1994). Neuronal and glial tau-positive inclusions in diverse neurologic diseases share common phosphorylation characteristics. *Acta Neuropathol.* 88, 129–136. doi: 10.1007/BF00294505

Janson, J., Laedtke, T., Parisi, J. E., O'Brien, P., Petersen, R. C., and Butler, P. C. (2004). Increased risk of type 2 diabetes in Alzheimer disease. *Diabetes* 53, 474–481. doi: 10.2337/diabetes.53.2.474

Jellinger, K. A., Alafuzoff, I., Attems, J., Beach, T. G., Cairns, N. J., Crary, J. F., et al. (2015). PART, a distinct tauopathy, different from classical sporadic Alzheimer disease. *Acta Neuropathol.* 129, 757–762. doi: 10.1007/s00401-015-1407-2

Johnson, K. A., Schultz, A., Betensky, R. A., Becker, J. A., Sepulcre, J., Rentz, D., et al. (2015). Tau PET imaging in aging and early Alzheimer's disease. *Ann. Neurol.* 79, 110–119. doi: 10.1002/ana.24546

Kametani, F. (2008). epsilon-Secretase: reduction of amyloid precursor protein epsilon-site cleavage in Alzheimer's disease. *Curr. Alzheimer Res.* 5, 165–171. doi: 10.2174/156720508783954776

Kametani, F., and Haga, S. (2015). Accumulation of carboxy-terminal fragments of APP increases phosphodiesterase 8B. *Neurobiol. Aging* 36, 634–637. doi: 10.1016/j.neurobiolaging.2014.09.029

Kametani, F., Usami, M., Tanaka, K., Kume, H., and Mori, H. (2004). Mutant presenilin (A260V) affects Rab8 in PC12D cell. *Neurochem. Int.* 44, 313–320. doi: 10.1016/S0197-0186(03)00176-1

Kang, J., Lemaire, H. G., Unterbeck, A., Salbaum, J. M., Masters, C. L., Grzeschik, K. H., et al. (1987). The precursor of Alzheimer's disease amyloid A4 protein resembles a cell-surface receptor. *Nature* 325, 733–736. doi: 10.1038/325733a0

Kim, J., Chakrabarty, P., Hanna, A., March, A., Dickson, D. W., Borchelt, D. R., et al. (2013). Normal cognition in transgenic BRI2-Abeta mice. *Mol. Neurodegener.* 8, 15. doi: 10.1186/1750-1326-8-15

Kim, J., Onstead, L., Randle, S., Price, R., Smithson, L., Zwizinski, C., et al. (2007). Abeta40 inhibits amyloid deposition *in vivo*. *J. Neurosci.* 27, 627–633. doi: 10.1523/JNEUROSCI.4849-06.2007

Klevanski, M., Herrmann, U., Weyer, S. W., Fol, R., Cartier, N., Wolfer, D. P., et al. (2015). The APP intracellular domain is required for normal synaptic morphology, synaptic plasticity, and hippocampus-dependent behavior. *J. Neurosci.* 35, 16018–16033. doi: 10.1523/JNEUROSCI.2009-15.2015

Kolata, G. (1985). Down syndrome–Alzheimer's linked. *Science* 230, 1152–1153. doi: 10.1126/science.2933807

Kondo, J., Honda, T., Mori, H., Hamada, Y., Miura, R., Ogawara, M., et al. (1988). The carboxyl third of tau is tightly bound to paired helical filaments. *Neuron* 1, 827–834. doi: 10.1016/0896-6273(88)90130-4

Kopan, R., and Ilagan, M. X. (2004). Gamma-secretase: proteasome of the membrane? *Nat. Rev. Mol. Cell Biol.* 5, 499–504. doi: 10.1038/nrm1406

Kosik, K. S., Orecchio, L. D., Binder, L., Trojanowski, J. Q., Lee, V. M., and Lee, G. (1988). Epitopes that span the tau molecule are shared with paired helical filaments. *Neuron* 1, 817–825. doi: 10.1016/0896-6273(88)90129-8

Kovacs, G. G. (2015). Invited review: neuropathology of tauopathies: principles and practice. *Neuropathol. Appl. Neurobiol.* 41, 3–23. doi: 10.1111/nan.12208

Krasemann, S., Madore, C., Cialic, R., Baufeld, C., Calcagno, N., El Fatimy, R., et al. (2017). The TREM2-APOE pathway drives the transcriptional phenotype of dysfunctional microglia in neurodegenerative diseases. *Immunity* 47, 566–581.e569. doi: 10.1016/j.immuni.2017.08.008

Lammich, S., Kojro, E., Postina, R., Gilbert, S., Pfeiffer, R., Jasionowski, M., et al. (1999). Constitutive and regulated alpha-secretase cleavage of Alzheimer's amyloid precursor protein by a disintegrin metalloprotease. *Proc. Natl. Acad. Sci. U.S.A.* 96, 3922–3927. doi: 10.1073/pnas.96.7.3922

Lee, V. M., Balin, B. J., Otvos, L. Jr., and Trojanowski, J. Q. (1991). A68: a major subunit of paired helical filaments and derivatized forms of normal Tau. *Science* 251, 675–678. doi: 10.1126/science.1899488

Lee, V. M., Goedert, M., and Trojanowski, J. Q. (2001). Neurodegenerative tauopathies. *Annu. Rev. Neurosci.* 24, 1121–1159. doi: 10.1146/annurev.neuro.24.1.1121

Leyns, C. E. G., and Holtzman, D. M. (2017). Glial contributions to neurodegeneration in tauopathies. *Mol. Neurodegener.* 12, 50. doi: 10.1186/s13024-017-0192-x

Leyns, C. E. G., Ulrich, J. D., Finn, M. B., Stewart, F. R., Koscal, L. J., Remolina Serrano, J., et al. (2017). TREM2 deficiency attenuates neuroinflammation and protects against neurodegeneration in a mouse model of tauopathy. *Proc. Natl. Acad. Sci. U.S.A.* 114, 11524–11529. doi: 10.1073/pnas.1710311114

Li, Y., Rinne, J. O., Mosconi, L., Pirraglia, E., Rusinek, H., Desanti, S., et al. (2008). Regional analysis of FDG and PIB-PET images in normal aging, mild cognitive impairment, and Alzheimer's disease. *Eur. J. Nuclear Med. Mol. Image* 35, 2169–2181. doi: 10.1007/s00259-008-0833-y

Maestre, G., Ottman, R., Stern, Y., Gurland, B., Chun, M., Tang, M. X., et al. (1995). Apolipoprotein E and Alzheimer's disease: ethnic variation in genotypic risks. *Ann. Neurol.* 37, 254–259. doi: 10.1002/ana.410370217

Marciniak, E., Leboucher, A., Caron, E., Ahmed, T., Tailleux, A., Dumont, J., et al. (2017). Tau deletion promotes brain insulin resistance. *J. Exp. Med.* 214, 2257–2269. doi: 10.1084/jem.20161731

Masliah, E., Mallory, M., Alford, M., DeTeresa, R., Hansen, L. A., Mckeel, D. W. Jr., et al. (2001). Altered expression of synaptic proteins occurs early during progression of Alzheimer's disease. *Neurology* 56, 127–129. doi: 10.1212/WNL.56.1.127

Masters, C. L., Simms, G., Weinman, N. A., Multhaup, G., McDonald, B. L., and Beyreuther, K. (1985). Amyloid plaque core protein in Alzheimer disease and Down syndrome. *Proc. Natl. Acad. Sci. U.S.A.* 82, 4245–4249. doi: 10.1073/pnas.82.12.4245

Miao, Y., Chen, J., Zhang, Q., and Sun, A. (2010). Deletion of tau attenuates heat shock-induced injury in cultured cortical neurons. *J. Neurosci. Res.* 88, 102–110. doi: 10.1002/jnr.22188

Nonaka, T., Watanabe, S. T., Iwatsubo, T., and Hasegawa, M. (2010). Seeded aggregation and toxicity of {alpha}-synuclein and tau: cellular models of neurodegenerative diseases. *J. Biol. Chem.* 285, 34885–34898. doi: 10.1074/jbc.M110.148460

Nukina, N., and Ihara, Y. (1986). One of the antigenic determinants of paired helical filaments is related to tau protein. *J. Biochem.* 99, 1541–1544. doi: 10.1093/oxfordjournals.jbchem.a135625

Okamura, N., and Yanai, K. (2017). Brain imaging: applications of tau PET imaging. *Nat. Rev. Neurol.* 13, 197–198. doi: 10.1038/nrneurol.2017.38

Oltersdorf, T., Ward, P. J., Henriksson, T., Beattie, E. C., Neve, R., Lieberburg, I., et al. (1990). The Alzheimer amyloid precursor protein. Identification of a stable intermediate in the biosynthetic/degradative pathway. *J. Biol. Chem.* 265, 4492–4497.

Ostrowitzki, S., Deptula, D., Thurfjell, L., Barkhof, F., Bohrmann, B., Brooks, D. J., et al. (2012). Mechanism of amyloid removal in patients with

Alzheimer disease treated with gantenerumab. *Arch. Neurol.* 69, 198–207. doi: 10.1001/archneurol.2011.1538

Pera, M., Alcolea, D., Sánchez-Valle, R., Guardia-Laguarta, C., Colom-Cadena, M., Badiola, N., et al. (2013). Distinct patterns of APP processing in the CNS in autosomal-dominant and sporadic Alzheimer disease. *Acta Neuropathol.* 125, 201–213. doi: 10.1007/s00401-012-1062-9

Poorkaj, P., Bird, T. D., Wijsman, E., Nemens, E., Garruto, R. M., Anderson, L., et al. (1998). Tau is a candidate gene for chromosome 17 frontotemporal dementia. *Ann. Neurol.* 43, 815–825. doi: 10.1002/ana.410430617

Price, J. L., Mckeel, D. W. Jr., Buckles, V. D., Roe, C. M., Xiong, C., Grundman, M., et al. (2009). Neuropathology of nondemented aging: presumptive evidence for preclinical Alzheimer disease. *Neurobiol. Aging* 30, 1026–1036. doi: 10.1016/j.neurobiolaging.2009.04.002

Rapoport, M., Dawson, H. N., Binder, L. I., Vitek, M. P., and Ferreira, A. (2002). Tau is essential to β-amyloid-induced neurotoxicity. *Proc. Natl. Acad. Sci. U.S.A.* 99, 6364–6369. doi: 10.1073/pnas.092136199

Robakis, N. K., and Georgakopoulos, A. (2014). Allelic interference: a mechanism for trans-dominant transmission of loss of function in the neurodegeneration of Familial Alzheimer's Disease. *Neurodegener. Dis.* 13, 126–130. doi: 10.1159/000354241

Roberson, E. D., Scearce-Levie, K., Palop, J. J., Yan, F., Cheng, I. H., Wu, T., et al. (2007). Reducing endogenous tau ameliorates Amyloid ß-Induced Deficits in an Alzheimer's disease mouse model. *Science* 316, 750–754. doi: 10.1126/science.1141736

Robert, J., Button, E. B., Yuen, B., Gilmour, M., Kang, K., Bahrabadi, A., et al. (2017). Clearance of beta-amyloid is facilitated by apolipoprotein E and circulating high-density lipoproteins in bioengineered human vessels. *Elife* 6:e29595. doi: 10.7554/eLife.29595

Rodrigues, E. M., Weissmiller, A. M., and Goldstein, L. S. (2012). Enhanced beta-secretase processing alters APP axonal transport and leads to axonal defects. *Hum. Mol. Genet.* 21, 4587–4601. doi: 10.1093/hmg/dds297

Rovelet-Lecrux, A., Hannequin, D., Raux, G., Meur, N. L., Laquerrière, A., Vital, A., et al. (2006). APP locus duplication causes autosomal dominant early-onset Alzheimer disease with cerebral amyloid angiopathy. *Nat. Genet.* 38, 24–26. doi: 10.1038/ng1718

Roy, S., Zhang, B., Lee, V. M.-Y., and Trojanowski, J. Q. (2005). Axonal transport defects: a common theme in neurodegenerative diseases. *Acta Neuropathol.* 109, 5–13. doi: 10.1007/s00401-004-0952-x

Rusu, P., Jansen, A., Soba, P., Kirsch, J., Löwer, A., Merdes, G., et al. (2007). Axonal accumulation of synaptic markers in APP transgenic Drosophila depends on the NPTY motif and is paralleled by defects in synaptic plasticity. *Eur. J. Neurosci.* 25, 1079–1086. doi: 10.1111/j.1460-9568.2007.05341.x

Salloway, S., Sperling, R., Fox, N. C., Blennow, K., Klunk, W., Raskind, M., et al. (2014). Two phase 3 trials of bapineuzumab in mild-to-moderate Alzheimer's disease. *N. Engl. J. Med.* 370, 322–333. doi: 10.1056/NEJMoa1304839

SantaCruz, K., Lewis, J., Spires, T., Paulson, J., Kotilinek, L., Ingelsson, M., et al. (2005). Tau suppression in a neurodegenerative mouse model improves memory function. *Science* 309, 476–481. doi: 10.1126/science.1113694

Schöll, M., Lockhart, S. N., Schonhaut, D. R., O'neil, J. P., Janabi, M., Ossenkoppele, R., et al. (2016). PET imaging of tau deposition in the aging human brain. *Neuron* 89, 971–982. doi: 10.1016/j.neuron.2016.01.028

Schwarz, A. J., Yu, P., Miller, B. B., Shcherbinin, S., Dickson, J., Navitsky, M., et al. (2016). Regional profiles of the candidate tau PET ligand 18F-AV-1451 recapitulate key features of Braak histopathological stages. *Brain* 139, 1539–1550. doi: 10.1093/brain/aww023

Selkoe, D. J. (1991). The molecular pathology of Alzheimer's disease. *Neuron* 6, 487–498. doi: 10.1016/0896-6273(91)90052-2

Serrano-Pozo, A., Frosch, M. P., Masliah, E., and Hyman, B. T. (2011). Neuropathological alterations in Alzheimer disease. *Cold Spring Harb. Perspect. Med.* 1, a006189. doi: 10.1101/cshperspect.a006189

Shankar, G. M., Li, S., Mehta, T. H., Garcia-Munoz, A., Shepardson, N. E., Smith, I., et al. (2008). Amyloid-beta protein dimers isolated directly from Alzheimer's brains impair synaptic plasticity and memory. *Nat. Med.* 14, 837–842. doi: 10.1038/nm1782

Shen, J., and Kelleher, R. J., III (2007). The presenilin hypothesis of Alzheimer's disease: evidence for a loss-of-function pathogenic mechanism. *Proc. Natl. Acad. Sci. U.S.A.* 104, 403–409. doi: 10.1073/pnas.0608332104

Shi, Y., Yamada, K., Liddelow, S. A., Smith, S. T., Zhao, L., Luo, W., et al. (2017). ApoE4 markedly exacerbates tau-mediated neurodegeneration in a mouse model of tauopathy. *Nature* 549, 523–527. doi: 10.1038/nature24016

Shipton, O. A., Leitz, J. R., Dworzak, J., Acton, C. E. J., Tunbridge, E. M., Denk, F., et al. (2011). Tau Protein Is Required for Amyloid β-induced impairment of hippocampal long-term potentiation. *J. Neurosci.* 31, 1688–1692. doi: 10.1523/JNEUROSCI.2610-10.2011

Spillantini, M. G., Goedert, M., Crowther, R. A., Murrell, J. R., Farlow, M. R., and Ghetti, B. (1997). Familial multiple system tauopathy with presenile dementia: a disease with abundant neuronal and glial tau filaments. *Proc. Natl. Acad. Sci. U.S.A.* 94, 4113–4118. doi: 10.1073/pnas.94.8.4113

Spillantini, M. G., Murrell, J. R., Goedert, M., Farlow, M. R., Klug, A., and Ghetti, B. (1998). Mutation in the tau gene in familial multiple system tauopathy with presenile dementia. *Proc. Natl. Acad. Sci. USA.* 95, 7737–7741. doi: 10.1073/pnas.95.13.7737

SvedruŽić, Ž. M., Popović, K., and Šendula-Jengić, V. (2015). Decrease in catalytic capacity of gamma-secretase can facilitate pathogenesis in sporadic and Familial Alzheimer's disease. *Mol. Cell. Neurosci.* 67, 55–65. doi: 10.1016/j.mcn.2015.06.002

Szpankowski, L., Encalada, S. E., and Goldstein, L. S. (2012). Subpixel colocalization reveals amyloid precursor protein-dependent kinesin-1 and dynein association with axonal vesicles. *Proc. Natl. Acad. Sci. U.S.A.* 109, 8582–8587. doi: 10.1073/pnas.1120510109

Tai, L. M., Ghura, S., Koster, K. P., Liakaite, V., Maienschein-Cline, M., Kanabar, P., et al. (2015). APOE-modulated Aβ-induced neuroinflammation in Alzheimer's disease: current landscape, novel data, and future perspective. *J. Neurochem.* 133, 465–488. doi: 10.1111/jnc.13072

Takahashi, M., Miyata, H., Kametani, F., Nonaka, T., Akiyama, H., Hisanaga, S.-I., et al. (2015). Extracellular association of APP and tau fibrils induces intracellular aggregate formation of tau. *Acta Neuropathol.* 129, 895–907. doi: 10.1007/s00401-015-1415-2

Takasugi, N., Tomita, T., Hayashi, I., Tsuruoka, M., Niimura, M., Takahashi, Y., et al. (2003). The role of presenilin cofactors in the gamma-secretase complex. *Nature* 422, 438–441. doi: 10.1038/nature01506

Tamayev, R., Matsuda, S., Arancio, O., and D'adamio, L. (2012). beta- but not gamma-secretase proteolysis of APP causes synaptic and memory deficits in a mouse model of dementia. *EMBO Mol. Med.* 4, 171–179. doi: 10.1002/emmm.201100195

Taniguchi-Watanabe, S., Arai, T., Kametani, F., Nonaka, T., Masuda-Suzukake, M., Tarutani, A., et al. (2016). Biochemical classification of tauopathies by immunoblot, protein sequence and mass spectrometric analyses of sarkosyl-insoluble and trypsin-resistant tau. *Acta Neuropathol.* 131, 267–280. doi: 10.1007/s00401-015-1503-3

Tesco, G., Ginestroni, A., Hiltunen, M., Kim, M., Dolios, G., Hyman, B. T., et al. (2005). APP substitutions V715F and L720P alter PS1 conformation and differentially affect Abeta and AICD generation. *J. Neurochem.* 95, 446–456. doi: 10.1111/j.1471-4159.2005.03381.x

Ulland, T. K., Song, W. M., Huang, S. C.-C., Ulrich, J. D., Sergushichev, A., Beatty, W. L., et al. (2017). TREM2 maintains microglial metabolic fitness in Alzheimer's Disease. *Cell* 170, 649–663.e613. doi: 10.1016/j.cell.2017.07.023

Vassar, R., Bennett, B. D., Babu-Khan, S., Kahn, S., Mendiaz, E. A., Denis, P., et al. (1999). Beta-secretase cleavage of Alzheimer's amyloid precursor protein by the transmembrane aspartic protease BACE. *Science* 286, 735–741. doi: 10.1126/science.286.5440.735

Walker, E. S., Martinez, M., Brunkan, A. L., and Goate, A. (2005). Presenilin 2 familial Alzheimer's disease mutations result in partial loss of function and dramatic changes in Abeta 42/40 ratios. *J. Neurochem.* 92, 294–301. doi: 10.1111/j.1471-4159.2004.02858.x

Weidemann, A., Eggert, S., Reinhard, F. B., Vogel, M., Paliga, K., Baier, G., et al. (2002). A novel epsilon-cleavage within the transmembrane domain of the Alzheimer amyloid precursor protein demonstrates homology with Notch processing. *Biochemistry* 41, 2825–2835. doi: 10.1021/bi015794o

Wiley, J. C., Hudson, M., Kanning, K. C., Schecterson, L. C., and Bothwell, M. (2005). Familial Alzheimer's disease mutations inhibit gamma-secretase-mediated liberation of beta-amyloid precursor protein carboxy-terminal fragment. *J. Neurochem.* 94, 1189–1201. doi: 10.1111/j.1471-4159.2005.03266.x

William, C. M., Andermann, M. L., Goldey, G. J., Roumis, D. K., Reid, R. C., Shatz, C. J., et al. (2012). Synaptic plasticity defect following visual deprivation

in Alzheimer's disease model transgenic mice. *J. Neurosci.* 32, 8004–8011. doi: 10.1523/JNEUROSCI.5369-11.2012

Wischik, C. M., Novak, M., Edwards, P. C., Klug, A., Tichelaar, W., and Crowther, R. A. (1988a). Structural characterization of the core of the paired helical filament of Alzheimer disease. *Proc. Natl. Acad. Sci. U.S.A.* 85, 4884–4888. doi: 10.1073/pnas.85.13.4884

Wischik, C. M., Novak, M., Thøgersen, H. C., Edwards, P. C., Runswick, M. J., Jakes, R., et al. (1988b). Isolation of a fragment of tau derived from the core of the paired helical filament of Alzheimer disease. *Proc. Natl. Acad. Sci. U.S.A.* 85, 4506–4510. doi: 10.1073/pnas.85.12.4506

Woodruff, G., Reyna, S. M., Dunlap, M., Van Der Kant, R., Callender, J. A., Young, J. E., et al. (2016). Defective transcytosis of APP and lipoproteins in human iPSC-derived neurons with familial Alzheimer's disease mutations. *Cell Rep.* 17, 759–773. doi: 10.1016/j.celrep.2016.09.034

Xia, D., Watanabe, H., Wu, B., Lee, S. H., Li, Y., Tsvetkov, E., et al. (2015). Presenilin-1 knockin mice reveal loss-of-function mechanism for familial Alzheimer's disease. *Neuron* 85, 967–981. doi: 10.1016/j.neuron.2015.02.010

Xu, T. H., Yan, Y., Kang, Y., Jiang, Y., Melcher, K., and Xu, H. E. (2016a). Alzheimer's disease-associated mutations increase amyloid precursor protein resistance to gamma-secretase cleavage and the Abeta42/Abeta40 ratio. *Cell Discov.* 2:16026. doi: 10.1038/celldisc.2016.26

Xu, W., Weissmiller, A. M., White, J. A. II., Fang, F., Wang, X., Wu, Y., et al. (2016b). Amyloid precursor protein-mediated endocytic pathway disruption induces axonal dysfunction and neurodegeneration. *J. Clin. Invest.* 126, 1815–1833. doi: 10.1172/JCI82409

Yamada, K., Patel, T. K., Hochgräfe, K., Mahan, T. E., Jiang, H., Stewart, F. R., et al. (2015). Analysis of *in vivo* turnover of tau in a mousemodel of tauopathy. *Mol. Neurodegener.* 10, 55. doi: 10.1186/s13024-015-0052-5

Yoshikawa, K., Aizawa, T., and Hayashi, Y. (1992). Degeneration *in vitro* of post-mitotic neurons overexpressing the Alzheimer amyloid protein precursor. *Nature* 359, 64–67. doi: 10.1038/359064a0

Yu, G., Nishimura, M., Arawaka, S., Levitan, D., Zhang, L., Tandon, A., et al. (2000). Nicastrin modulates presenilin-mediated notch/glp-1 signal transduction and betaAPP processing. *Nature* 407, 48–54. doi: 10.1038/35024009

Zempel, H., and Mandelkow, E. (2014). Lost after translation: missorting of Tau protein and consequences for Alzheimer disease. *Trends Neurosci.* 37, 721–732. doi: 10.1016/j.tins.2014.08.004

Zhou, L., McInnes, J., Wierda, K., Holt, M., Herrmann, A. G., Jackson, R. J., et al. (2017). Tau association with synaptic vesicles causes presynaptic dysfunction. *Nat. Commun.* 8:15295. doi: 10.1038/ncomms15295

Zlokovic, B. V. (2013). Cerebrovascular effects of apolipoprotein e: implications for alzheimer disease. *JAMA Neurol.* 70, 440–444. doi: 10.1001/jamaneurol.2013.2152

Conflict of Interest Statement: The authors declare that the research was conducted in the absence of any commercial or financial relationships that could be construed as a potential conflict of interest.

frontiers in Neuroscience

HYPOTHESIS AND THEORY
published: 01 February 2018
doi: 10.3389/fnins.2018.00028

Robustness and Vulnerability of the Autoregulatory System That Maintains Nuclear TDP-43 Levels: A Trade-off Hypothesis for ALS Pathology Based on *in Silico* Data

Akihiro Sugai[1]*, *Taisuke Kato*[2], *Akihide Koyama*[3], *Yuka Koike*[1], *Sou Kasahara*[1], *Takuya Konno*[1], *Tomohiko Ishihara*[4] *and Osamu Onodera*[1]*

[1] Department of Neurology, Clinical Neuroscience Branch, Brain Research Institute, Niigata University, Niigata, Japan, [2] Department of System Pathology for Neurological Disorders, Brain Science Branch, Center for Bioresource-Based Research, Brain Research Institute, Niigata University, Niigata, Japan, [3] Division of Legal Medicine, Graduate School of Medicine and Dental Science, Niigata University, Niigata, Japan, [4] Department of Molecular Neuroscience, Resource Branch for Brain Disease Research, Center for Bioresource-based Research, Brain Research Institute, Niigata University, Niigata, Japan

OPEN ACCESS

Edited by:
Naruhiko Sahara,
National Institute of Radiological Sciences (NIRS), Japan

Reviewed by:
Hisao Moriya,
Okayama University, Japan
Rita Sattler,
Barrow Neurological Institute (BNI), United States
Sami Barmada,
University of Michigan, United States

***Correspondence:**
Akihiro Sugai
akihiro.sugai@bri.niigata-u.ac.jp
Osamu Onodera
onodera@bri.niigata-u.ac.jp

Specialty section:
This article was submitted to Neurodegeneration, a section of the journal Frontiers in Neuroscience

Received: 30 October 2017
Accepted: 15 January 2018
Published: 01 February 2018

Citation:
Sugai A, Kato T, Koyama A, Koike Y, Kasahara S, Konno T, Ishihara T and Onodera O (2018) Robustness and Vulnerability of the Autoregulatory System That Maintains Nuclear TDP-43 Levels: A Trade-off Hypothesis for ALS Pathology Based on in Silico Data. Front. Neurosci. 12:28. doi: 10.3389/fnins.2018.00028

Abnormal accumulation of TAR DNA-binding protein 43 (TDP-43) in the cytoplasm and its disappearance from the nucleus are pathological features of amyotrophic lateral sclerosis and frontotemporal dementia (ALS/FTD) and are directly involved in the pathogenesis of these conditions. TDP-43 is an essential nuclear protein that readily aggregates in a concentration-dependent manner. Therefore, cells must strictly maintain an appropriate amount of nuclear TDP-43. In one relevant maintenance mechanism, TDP-43 binds to its pre-mRNA and promotes alternative splicing, resulting in mRNA degradation via nonsense-mediated mRNA decay. The level of nuclear TDP-43 is tightly regulated by these mechanisms, which control the amount of mRNA that may be translated. Based on the results of previous experiments, we developed an *in silico* model that mimics the intracellular dynamics of TDP-43 and examined TDP-43 metabolism under various conditions. We discovered an inherent trade-off in this mechanism between transcriptional redundancy, which maintains the robustness of TDP-43 metabolism, and vulnerability to specific interfering factors. These factors include an increased tendency of TDP-43 to aggregate, impaired nuclear-cytoplasmic TDP-43 transport, and a decreased efficiency of degrading abnormal proteins, all of which are functional abnormalities related to the gene that causes familial ALS/FTD. When these conditions continue at a certain intensity, the vulnerability of the autoregulatory machinery becomes apparent over time, and transcriptional redundancy enters a vicious cycle that ultimately results in TDP-43 pathology. The results obtained using this *in silico* model reveal the difference in TDP-43 metabolism between normal and disease states. Furthermore, using this model, we simulated the effect of a decrease in TDP-43 transcription and found that this decrease improved TDP-43 pathology and suppressed the abnormal propagation of TDP-43. Therefore, we propose a potential therapeutic strategy to suppress transcriptional redundancy, which is the driving force of the pathological condition caused by the specific

factors described above, in patients with ALS presenting with TDP-43 pathology. An ALS animal model exhibiting TDP-43 pathology without overexpression of exogenous TDP-43 should be developed to investigate the effect of alleviating the transcriptional redundancy of *TARDBP*.

Keywords: amyotrophic lateral sclerosis, TDP-43, *TARDBP*, autoregulation, robustness, systems biology

INTRODUCTION

Amyotrophic lateral sclerosis (ALS) is a devastating neurological disease characterized by the degeneration of upper and lower motor neurons. ALS leads to death within 2–5 years as a result of muscle weakness, including respiratory dysfunction. Up to 50% of patients with ALS develop cognitive and behavioral abnormalities, and approximately 13% of patients with ALS present with concomitant behaviorally variant frontotemporal dementia (FTD) (van Es et al., 2017). These two neurodegenerative diseases have a common pathological background caused by the abnormal accumulation of TAR DNA-binding protein 43 (TDP-43). This feature occurs in nearly all patients with ALS and in up to 50% of patients with FTD (Arai et al., 2006; Neumann et al., 2006). The accumulation of TDP-43 correlates with the spread of neurodegeneration, suggesting that pathological conditions progress between cells through the propagation of abnormal TDP-43 accumulation (Polymenidou and Cleveland, 2011; Braak et al., 2013; Brettschneider et al., 2013; Nonaka et al., 2013). A mutation in the *TARDBP* gene, which encodes TDP-43, is present in 1–5% of patients with familial ALS, and these patients exhibit TDP-43 pathology similar to individuals with sporadic ALS. The same TDP-43 pathology has also been identified in patients with mutations in many ALS-causative genes, including hexanucleotide repeat expansions in *C9ORF72*, a major genetic cause of ALS/FTD (van Es et al., 2017). Based on these findings, abnormalities in TDP-43 are directly involved in the pathogenesis of ALS/FTD.

TDP-43 is a nuclear protein that moves between the nucleus and cytoplasm through a nuclear localization signal and a nuclear export signal, respectively (Ayala et al., 2008; Winton et al., 2008). TDP-43 also contains RNA recognition motifs, binds to RNAs, and affects a wide range of RNA metabolic processes, including pre-mRNA processing, microRNA regulation, and the control of long noncoding RNA and mRNA transport (Ling et al., 2013; Ratti and Buratti, 2016). In addition, TDP-43 contains a prion-like domain and regulates the formation and dynamics of stress granules (McDonald et al., 2011; Sun and Chakrabartty, 2017). Stress granules are membraneless organelles that are involved in the transient and reversible sequestration of undesirable transcripts. RNA-binding proteins that contain prion-like domains undergo liquid-liquid phase separation, which underlies the formation of these membraneless organelles (Molliex et al., 2015; Sun and Chakrabartty, 2017). The properties of TDP-43, an aggregation-prone protein, contribute to stress granule formation.

As TDP-43 is extensively involved in RNA metabolism and tends to aggregate, cell function and survival depend on the strict control of TDP-43 levels (Lee et al., 2012; Ling et al., 2013). TDP-43 knockout mice display embryonic lethality (Kraemer et al., 2010; Sephton et al., 2010). Adult mice in which TDP-43 is conditionally deleted also die shortly after the loss of TDP-43 expression (Chiang et al., 2010), and the motor neuron-specific loss of TDP-43 leads to age-dependent motor neuron degeneration (Wu et al., 2012; Iguchi et al., 2013). Moreover, TDP-43 overexpression leads to neuronal degeneration and death in a dose-dependent manner (McGoldrick et al., 2013). However, TDP-43 expression is increased in the central nervous system, cerebrospinal fluid, and plasma of patients with ALS (Kasai et al., 2009; Swarup et al., 2011b; Verstraete et al., 2012; Iguchi et al., 2016). Additionally, in patients with ALS/FTD, TDP-43 diminishes or disappears from the nucleus and forms inclusion bodies with fragmented products in the cytoplasm (Arai et al., 2006; Neumann et al., 2006). Currently, the functional losses caused by the disappearance of nuclear TDP-43 and the toxicity caused by the formation of aggregates in the cytoplasm are both postulated to contribute to the pathogenesis of ALS/FTD (Lee et al., 2012; Ling et al., 2013).

Similar to many RNA-binding proteins (Huelga et al., 2012; Zhou et al., 2013), TDP-43 autoregulates its own expression through a negative feedback mechanism that depends on nuclear TDP-43 (Ayala et al., 2011; Polymenidou et al., 2011). The *TARDBP* pre-mRNA contains multiple alternative introns and polyadenylation signals in its last exon (Avendaño-Vázquez et al., 2012; Koyama et al., 2016). In the nucleus, TDP-43 binds to the 3′-UTR of its pre-mRNA, resulting in the use of distal poly A sites (alternative polyadenylation) (Avendaño-Vázquez et al., 2012; Koyama et al., 2016). Multiple alternative introns are then consecutively spliced (Koyama et al., 2016). The resulting isoform has an additional termination codon located more than 50 nucleotides upstream of the final exon junction complex. These alternatively spliced variants are susceptible to nonsense-mediated mRNA decay (Polymenidou et al., 2011; Koyama et al., 2016). However, some RNAs avoid alternative splicing, despite the use of distal poly A sites. These RNAs tend to localize in the nucleus and therefore do not contribute to translation in the cytoplasm (Koyama et al., 2016). Thus, by processing its pre-mRNA, the amount of nuclear TDP-43 precisely regulates the intracytoplasmic *TARDBP* mRNA level (**Figure 1**).

Notably, major ALS-related RNA-binding proteins with a prion-like domain have an autoregulatory mechanism (Le Guiner et al., 2001; Zhou et al., 2013; Suzuki and Matsuoka, 2017). Several ALS-causing mutations in *FUS* and *hnRNPA1* disrupt the nuclear localization sequence and thus increase the amount of these factors in the cytoplasm (Dormann et al., 2010; Liu et al., 2016). When nuclear-cytoplasmic transport is impaired, the autoregulatory mechanism enhances mRNA expression by reducing the nuclear protein level, leading to a further increase

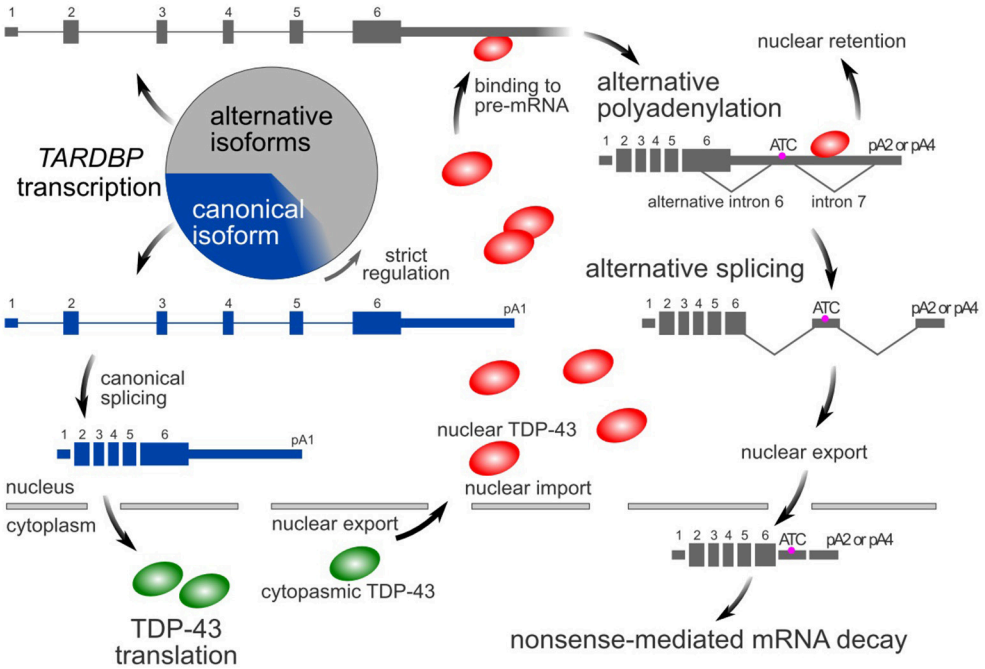

FIGURE 1 | TDP-43 autoregulatory mechanism. In the canonical isoform (blue box) of the *TARDBP* mRNA, pA1 is used as a poly A site, and introns 6 and 7 are not spliced. In its alternative isoforms (gray boxes), pA2 or pA4 is used as a poly A site, and introns 6 and 7 are spliced. The amount of nuclear TDP-43 determines the ratio of these isoforms. Because the alternative isoforms are ultimately destined to undergo rapid degradation via nonsense-mediated mRNA decay, only a small amount of these forms is typically detected. However, these alternatively spliced isoforms comprise more than half of the transcripts. The circle represents the total amount of transcribed *TARDBP* mRNA.

in the amount of the protein in the cytoplasm (Zhou et al., 2013). ALS-related RNA-binding proteins such as FUS, hnRNPA1, TIA1, and TDP-43 have been reported to undergo liquid-liquid phase separation through a mechanism that involves a prion-like domain (Molliex et al., 2015; Gopal et al., 2017; Mackenzie et al., 2017). This liquid-liquid phase transition strongly depends on the local concentrations of RNA-binding proteins (Molliex et al., 2015; Boeynaems et al., 2016). Therefore, the entanglement of the mechanisms of autoregulation with the mechanisms of RNA granule formation involving these RNA-binding proteins may contribute to the pathogenesis of ALS.

Here, we created an *in silico* model mimicking the intracellular dynamics of TDP-43 to determine the vulnerability of the mechanism regulating TDP-43 levels in the nucleus. Using this model, we show that robustness in the maintenance of nuclear TDP-43 by autoregulation conversely results in a decrease in nuclear TDP-43 and enhances aggregate accumulation through a pathological spiral driven by redundant transcription under several specific conditions. The role of TDP-43 in the formation of membraneless organelles and the mechanism that strictly controls the amount of nuclear TDP-43 through transcriptional redundancy may conflict in motor neurons in patients with ALS. Based on this hypothesis, we focus on the role of *TARDBP* transcriptional redundancy in the pathogenesis of ALS and propose a treatment strategy to control abnormal TDP-43 metabolism in patients with ALS.

ESTABLISHING THE *IN SILICO* MODEL OF TDP-43 DYNAMICS IN CELLS

What is the weak point in the mechanism that controls TDP-43 levels? Moreover, how do pathological abnormalities in TDP-43, including its cytoplasmic translocation, fragmentation, and aggregation, occur? We applied an *in silico* model that simulates the intracellular dynamics of TDP-43 in CellDesigner (v4.4; Systems Biology Institute, Tokyo, Japan), a structured diagram editor used to draw gene-regulatory and biochemical networks (Funahashi et al., 2003), to investigate these issues. For our research purposes, we presumed that a description of the absolute quantity and absolute timing of each element and its variation in the cell was unnecessary. Therefore, a relative amount and relative time were applied to descriptions of each element and its variation. In the normal state where no disturbance was applied, each element was assumed to be static without fluctuations. Each setting of the model was designed to maintain consistency with our experimental results as described below and with the findings reported in previous experiments. In addition, the settings of the model were adjusted to be consistent with the results from animal models described below, and finally the adequacy of the model was confirmed (Supplementary Tables 1–3, Data Sheet 1).

Autoregulation

TDP-43 binds to its pre-mRNA in the nucleus to negatively control cytoplasmic mRNA levels (negative autoregulation;

NAR). The *TARDBP* pre-mRNA is transcribed above the level required for normal conditions, and the extra mRNA is degraded via nonsense-mediated mRNA decay through alternative splicing (**Figure 1**). A decrease in TDP-43 protein and mRNA levels does not occur in the central nervous system of *TARDBP* heterozygous knockout mice (Kraemer et al., 2010; Sephton et al., 2010; Ricketts et al., 2014). Thus, the transcription of the *TARDBP* mRNA displays at least twice as much redundancy as the normal state and at least 50% of the *TARDBP* pre-mRNA is alternatively spliced. In addition, in the analysis of mouse embryonic stem (ES) cells expressing human TDP-43 cDNA under the control of the endogenous mouse *TARDBP* promoter, the amount of TDP-43 protein increases approximately 3-fold in the absence of the *TARDBP* 3′-UTR, which is essential for autoregulation (Stribl et al., 2014). Furthermore, following the silencing of endogenous TDP-43 with siRNAs in HEK293T cells, alternative splicing of the minigene containing the last exon of human *TARDBP* is markedly diminished, resulting in a 3- to 4-fold increase in the canonical mRNA level of the minigene (Koyama et al., 2016). Based on this result, 67–75% of the pre-mRNA of the human *TARDBP* minigene is alternatively spliced.

Alternative Splicing of the *TARDBP* mRNA in the Mouse Cerebrum

We extracted total RNA from the cerebrum of wild-type mice (C57BL/6NCrl) using NucleoSpin RNA II (TaKaRa Bio, Japan) to confirm the percentage of the *TARDBP* pre-mRNA that undergoes alternative splicing *in vivo*. The percentage of alternatively spliced isoforms among all isoforms of the *TARDBP* mRNA was examined using the Droplet Digital PCR method (**Figure 2A**). Since Droplet Digital PCR enables the absolute quantification of target RNAs, the expression ratio of each isoform was determined. The primers and probe sequences used for Droplet Digital PCR are shown in Supplemental Table 4. The average percentages of isoforms lacking alternative intron 6 of the *TARDBP* mRNA in the cerebrum of 7-day-old and 11-week-old mice were 44 and 36%, respectively (**Figure 2B**). For most of the mRNA in which alternative intron 6 is spliced, alternative intron 7 is also spliced, and this isoform undergoes degradation through nonsense-mediated mRNA decay (Koyama et al., 2016). The percentage of the *TARDBP* pre-mRNA that underwent alternative splicing was calculated by determining the rate of degradation of isoforms lacking the alternative intron 6. We were not able to accurately determine the rate of degradation of *TARDBP* mRNA isoforms that were alternatively spliced in the mouse cerebrum. However, when the degradation rate was assumed to be only 3–5 times greater than the rate of the canonical *TARDBP* mRNA, which may be lower than the general degradation rate due to nonsense-mediated mRNA decay (Tani et al., 2012), the percentage of alternatively spliced *TARDBP* pre-mRNA (**Figure 2C**; Y axis) was estimated to be 63% to 74% in the cerebrum of adult mice. After defining transcriptional redundancy as 100/(100-Y), where Y indicates the percentage of pre-mRNA that has undergone alternative splicing, the redundancy of *TARDBP* transcription in the adult mouse cerebrum was estimated to be 2.7–3.8 (**Figure 2C**; R axis). The results from the mouse cerebrum analysis are consistent with the findings from previous studies (Kraemer et al., 2010; Sephton et al., 2010; Ricketts et al., 2014; Stribl et al., 2014; Koyama et al., 2016).

Based on these experimental results and previous findings, we hypothesized that at least 50%, and potentially 60–80%, of the transcribed *TARDBP* RNA is degraded by nonsense-mediated mRNA decay. This transcriptional redundancy may be influenced by several conditions, including conditions within the tissue or cell (Kraemer et al., 2010; Sephton et al., 2010), environmental factors, and age (**Figure 2B**). Therefore, in our model, parameters representing the efficiency of autoregulation were initially determined by estimating that 65% of the transcribed RNA was degraded by nonsense-mediated mRNA decay. The rate at which the canonical mRNA was produced was approximated using the Hill function (Supplementary Table 1). In this function, the product of the pre-mRNA and the coefficient (k2) define the maximum amount of canonical mRNA expression. The initial amount of the pre-mRNA is a constant. The suppression coefficient (Knar) indicates the concentration of nuclear TDP-43 that suppresses the maximal production of canonical mRNA by 50%. Knar is assumed to depend on the affinity of TDP-43 for the TDP-43-binding region of the *TARDBP* 3′-UTR and represents the efficiency of the autoregulatory mechanism.

Nuclear and Cytoplasmic TDP-43 Levels

TDP-43 is shuttled between the nucleus and cytoplasm (Ayala et al., 2008; Winton et al., 2008). Immunohistochemistry for TDP-43 revealed a cytoplasmic/nuclear ratio of TDP-43 of 0.05–0.2 under normal conditions (Matsukawa et al., 2016; Khosravi et al., 2017; Woo et al., 2017). Therefore, in our model, the ratio of cytoplasmic/nuclear TDP-43 was set to 0.15. The half-life of TDP-43 lacking a nuclear export signal is sufficiently longer than the half-life of TDP-43 lacking a nuclear localization signal (Watanabe et al., 2012). Therefore, in this model, the degradation rate for cytoplasmic TDP-43 was set to 5-times the degradation rate for nuclear TDP-43. In experiments with SH-SY5Y cells, the half-life of the TDP-43 protein is approximately 20 times the half-life of the mRNA (Scotter et al., 2014). Thus, in this model, the degradation rate of nuclear TDP-43 was set to 0.05 times the mRNA degradation rate.

Aggregation and Fragmentation

The TDP-43 protein is intrinsically disordered and prone to aggregation because it contains a low-complexity prion-like domain at its C-terminus (Johnson et al., 2009; Budini et al., 2012). The TDP-43 concentration strongly affects this aggregation-prone property. TDP-43 accumulates in cytoplasmic stress granules, and the formation of these puncta is thought to be caused by a phenomenon referred to as the phase transition, which depends on the concentration of the protein in the cytoplasm (Molliex et al., 2015; Sun and Chakrabartty, 2017). Therefore, in our model, the rate of aggregate formation was defined based on the amount of TDP-43 in the cytoplasm (**Figure 3A**). Treatment of SH-SY5Y cells with the proteasome

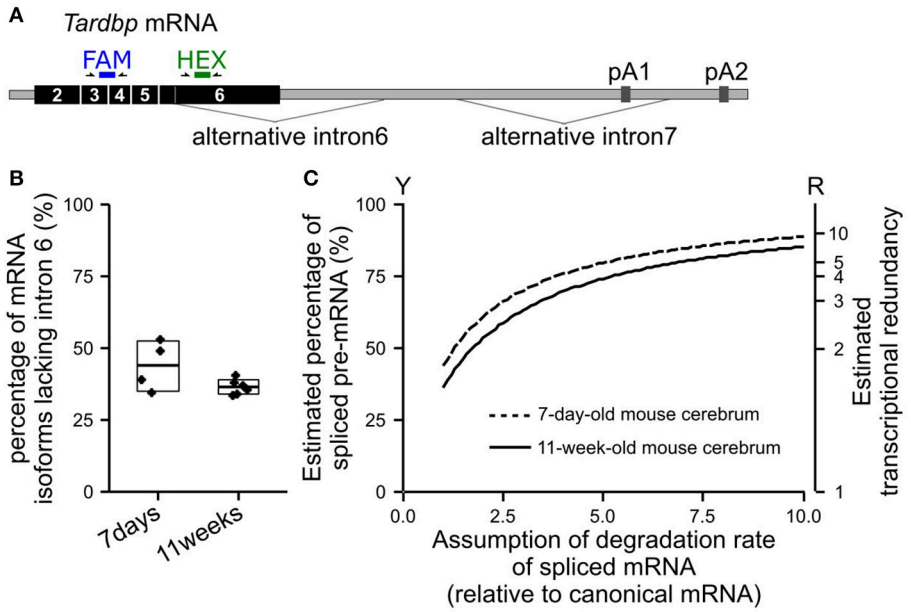

FIGURE 2 | Estimated percentage of alternatively spliced pre-mRNAs in the mouse cerebrum. **(A)** The positions of the primers and probes used for Droplet Digital PCR to determine the percentage of isoforms lacking alternative intron 6 among all *TARDBP* mRNA isoforms are shown. The FAM probe detects all isoforms of the *TARDBP* mRNA, and the HEX probe detects isoforms that retain alternative intron 6. **(B)** The percentages of isoforms lacking alternative intron 6 in the cerebrum of 7-day-old and 11-week-old wild-type mice (C57BL/6NCrl) are shown. The upper and lower sides of the box indicate the standard deviation. The lines in the box indicate the average. **(C)** Estimated percentage of alternatively spliced pre-mRNAs among the total transcribed *TARDBP* pre-mRNA is shown; the degradation rate of the isoforms lacking alternative intron 6 relative to the canonical mRNA was estimated (horizontal axis). Transcriptional redundancy (R) is represented by the equation $R = 100/(100\text{-}Y)$, where Y indicates the percentage of pre-mRNA that has undergone alternative splicing among all transcribed pre-mRNAs.

inhibitor MG132 induces the formation of aggregates and increases the amount of high molecular weight, urea-soluble TDP-43. Although the half-life of the 43 kDa TDP-43 protein in this cultured cell line is approximately 30 h, the level of urea-soluble TDP-43 remains slightly reduced 48 h after MG132 wash out (Scotter et al., 2014). Therefore, in this model, the degradation rate of aggregates was assumed to be 0.2 times the degradation rate of nuclear TDP-43.

TDP-43 fragmentation is a biochemical characteristic of ALS/FTD. Although TDP-43 fragmentation occurs under normal conditions, it increases in the presence of an excessive amount of TDP-43 (Hasegawa et al., 2008; Kabashi et al., 2008; Xu et al., 2010). In addition, an excess amount of fragmented TDP-43 products has been reported to induce and promote aggregation by trapping the normal TDP-43 protein, and this aggregate may be fragmented (Igaz et al., 2009; Nonaka et al., 2009; Furukawa et al., 2011). Therefore, in this model, the extent of TDP-43 fragmentation was based on the amount of cytoplasmic TDP-43, and the rate of aggregate formation was modified by the amount of accumulated fragmented TDP-43 (**Figure 3A**). Based on experiments using SH-SY5Y and HEK293 cells, the TDP-43 C-terminal fragment degrades more quickly than wild-type TDP-43, and its half-life was approximately one-third the half-life of wild-type TDP-43 (Scotter et al., 2014). Thus, in this model, the degradation rate of fragments was set to 3 times the degradation rate of cytoplasmic TDP-43. For both aggregated and fragmented TDP-43, the parameters related to the initial value, production efficiency, and decomposition efficiency were set based on the assumption that only a trace amount of fragments exist in the normal state (**Figure 3B**).

VALIDATION OF THE *IN SILICO* MODEL

TARDBP Heterozygous Knockout Model

We initially assessed a *TARDBP* heterozygous knockout model in which the transcription of *TARDBP* is reduced by half to determine whether our *in silico* model designed to investigate TDP-43 autoregulation produces results consistent with the findings from previous studies (**Figure 3C**). In this model, the level of transcription is reduced because only one allele is present, and in the level of the *TARDBP* mRNA is initially decreased. However, the level of *TARDBP* mRNA is restored by an autoregulatory mechanism and eventually stabilizes at 79% of the initial value. In addition, the amount of TDP-43 in the nucleus is not reduced by half and is maintained at 82% of the initial value. In experimental analyses of *TARDBP* heterozygous knockout mice, TDP-43 expression is not different from the level of the mRNA or protein observed in wild-type mice (Kraemer et al., 2010; Sephton et al., 2010; Ricketts et al., 2014). However, because the efficiency of the alternative splicing of *SORT1* and *PDP1* pre-mRNAs, which are target RNAs of TDP-43, is decreased, we suggest that

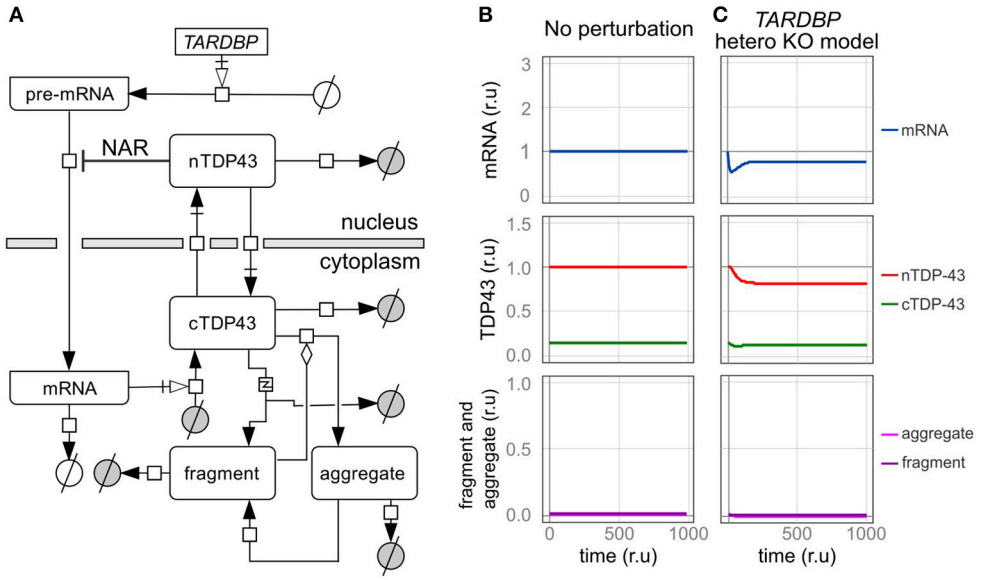

FIGURE 3 | An *in silico* model of TDP-43 metabolism. **(A)** Graphic representation of TDP-43 metabolism in cells with TDP-43-negative autoregulation (NAR). nTDP43 and cTDP43 represent nuclear and cytoplasmic TDP-43, respectively. mRNA represents the canonical *TARDBP* mRNA that is translated in the cytoplasm. The gray and white circles represent amino acids and nucleic acids, respectively. The squares represent each reaction. Black arrows represent state transitions. White arrows with squares represent transcription or translation. The diamond represents modulation. The square including "z" represents truncation. **(B,C)** Changes in the level of each element are shown for a case in which no disturbance was added to the cell over time and **(B)** a case in which the amount of transcription was reduced by half **(C)**. The mRNA level is expressed relative to the initial level. Levels of nuclear TDP-43, cytoplasmic TDP-43, and fragmented and aggregated TDP-43 are expressed relative to the initial level of nuclear TDP-43 (r.u., relative unit).

TDP-43 expression is only slightly reduced, as the western blot results did not reveal differences (Ricketts et al., 2014). Thus, the results obtained using the dynamics established in this model display good agreement with the results of previous analyses of this *TARDBP* heterozygous knockout mouse line.

TARDBP Transgenic Model

We subsequently examined a model in which the *TARDBP* mRNA was exogenously expressed. In most previous experiments, an exogenous *TARDBP* mRNA lacking the 3′-UTR, which is important for autoregulation, was employed. Therefore, this exogenous *TARDBP* mRNA is not autoregulated (**Figure 4A**, Supplementary Tables 5–7).

First, fluctuations in each factor were examined when the exogenous mRNA was expressed at a level equivalent to the initial level of the endogenous mRNA (**Figure 4B**). Upon the expression of exogenous TDP-43, the level of the endogenous mRNA was decreased by the autoregulatory mechanism, which was followed by a decrease in endogenous TDP-43 until the level ultimately stabilized at 39% of the initial value (**Figure 4B**). The total amount of exogenous and endogenous nuclear TDP-43 was 138% of the initial amount of endogenous TDP-43 in the nucleus, which subsequently stabilized. These dynamics are consistent with the results of various previous experiments (Arnold et al., 2013; Koyama et al., 2016).

Next, we changed the expression level of exogenous TDP-43 and investigated the levels of endogenous TDP-43 and its aggregates (**Figure 4C**). As the level of exogenous TDP-43 increased, the level of endogenous TDP-43 in the nucleus decreased and more TDP-43 aggregates formed. These results are consistent with the results of previous studies in which the overexpression of exogenous TDP-43 reduced endogenous TDP-43 levels and caused aggregates to form in both cell lines and animal models (Xu et al., 2010; Swarup et al., 2011a; McGoldrick et al., 2013).

Intercellular Propagation Model of Aggregated and Fragmented TDP-43

TDP-43 fragmentation is a biochemical property of ALS/FTD, conditions in which TDP-43 is more prone to aggregate, and endogenous TDP-43 may be sequestered with fragmented TDP-43 to form aggregates in affected individuals (Chen et al., 2010; Furukawa et al., 2011). Based on the results of several previous studies using cells cultured in medium supplemented with fragmented TDP-43, the fragmented TDP-43 is transferred into the cells where it forms aggregates with endogenous TDP-43 (Nonaka et al., 2013; Ding et al., 2015; Feiler et al., 2015; Iguchi et al., 2016). We subsequently evaluated this phenomenon using our model. In this model, fragmented TDP-43 was placed outside of the cells, and we set the parameters of the model to ensure that a certain amount of fragmented TDP-43 would be transferred into the cells (Supplementary Table 8). Under these conditions, aggregate formation was promoted when the amount of fragmented TDP-43 reached a certain level, and endogenous

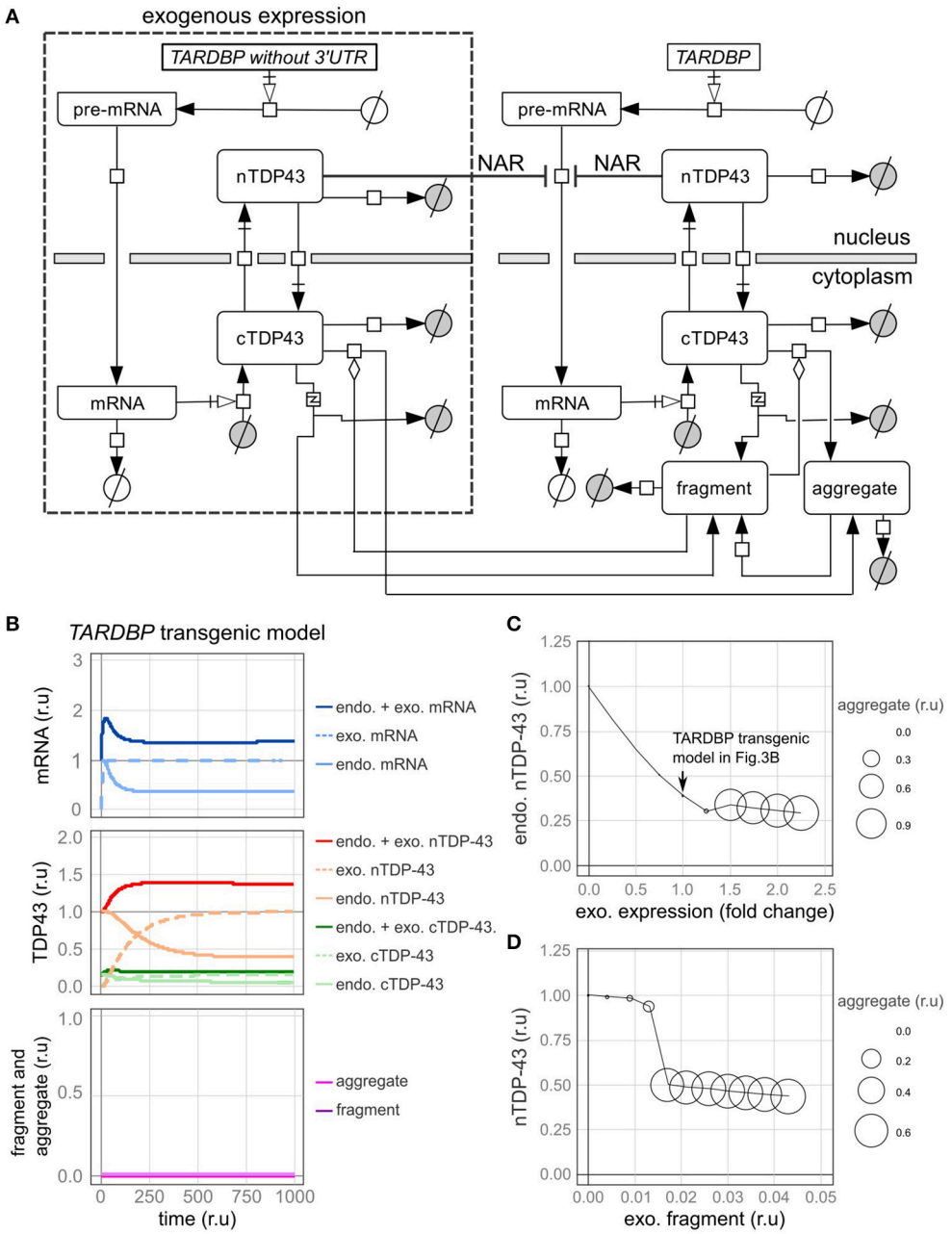

FIGURE 4 | A model of transgenic *TARDBP* expression and a model involving exogenous TDP-43 fragments. **(A)** Graphic representation of TDP-43 metabolism in cells expressing a *TARDBP* transgene that lacks a 3'-UTR. **(B)** Changes in the level of each element over time when exogenous *TARDBP* mRNA was expressed at a level equivalent to the initial level of the endogenous *TARDBP* mRNA. **(C)** The relative amounts of endogenous TDP-43 in the nucleus (vertical axis) and aggregates (area of circle) are shown when exogenous *TARDBP* expression was increased in a stepwise manner (horizontal axis). **(D)** The relative amounts of endogenous nuclear TDP-43 (vertical axis) and aggregates (area of the circle) compared with the relative amount of extracellular fragmented TDP-43 (horizontal axis) are shown.

intranuclear TDP-43 levels were decreased, similar to the findings in cells from patients affected by ALS/FTD (**Figure 4D**).

The Half-Life of TDP-43

The half-life of total TDP-43 analyzed by stopping translation was 110 relative time units in this model (Supplementary Figure 1). In previous experiments, estimates of the half-life of TDP-43 in cultured cells ranged from 4 to over 34 h, depending on the experimental conditions (Ling et al., 2010; Pesiridis et al., 2011; Watanabe et al., 2012; Scotter et al., 2014). Thus, in our model, the value of 100 relative time units corresponds to a range from 3.6 to over 31 h. Since evidence is not available to determine the half-life of TDP-43 in motor neurons *in vivo*, relative units were also used in the subsequent analysis.

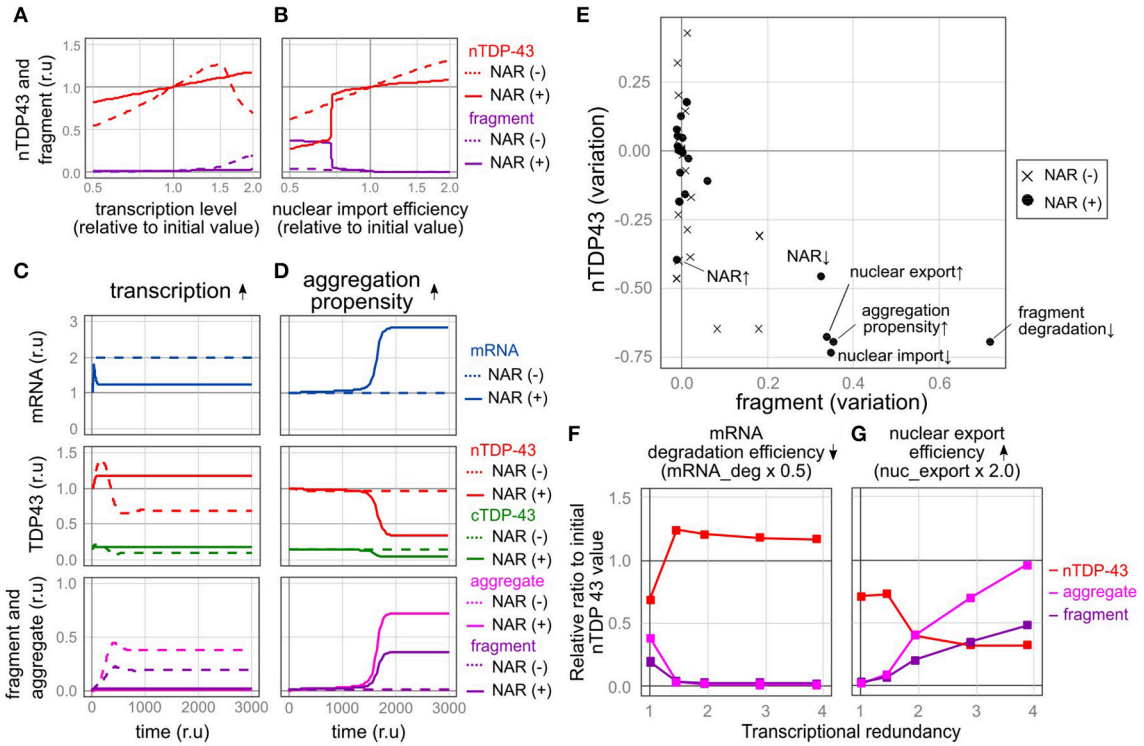

FIGURE 5 | Robustness and fragility of the TDP-43 autoregulatory mechanism. **(A,B)** Plot of the relative amounts of nuclear TDP-43 (red line) and fragments (purple line) that finally stabilized when each parameter was varied (**A**, transcription level; **B**, nuclear import rate) by 100 steps from half to twice the initial value. The dotted line shows the NAR (–) model, and the solid line shows the NAR (+) model. **(C,D)** Changes in the level of each element over time when TDP-43 transcription was increased 2-fold **(C)** or aggregate formation was increased (the parameter agg_K was 0.6 times the initial value) **(D)**. **(E)** The extent of changes in the initial levels of nuclear TPP-43 (vertical axis) and fragmented TDP-43 (horizontal axis) when each parameter was changed to half or twice the initial level is shown. The change in each parameter is indicated by a black circle [NAR (+)] or a cross [NAR (–)]. **(F,G)** Transcriptional redundancy depends on changes in the levels of nuclear TDP-43, aggregates and fragments when each parameter is changed to half or twice the initial level. Representative plots from Supplementary Figure 4 are shown.

ANALYSIS OF THE *IN SILICO* MODEL

Robustness and Fragility of TDP-43 Autoregulation

We subsequently examined the fragility of this autoregulatory mechanism by investigating how each element behaves when each parameter was varied. For this analysis, we compared a model with autoregulation [negative autoregulation, NAR (+)] to a model without autoregulation [NAR (–)]. In the NAR (–) model, only the level of transcription was adjusted, which indicates that the initial expression level of the *TARDBP* mRNA was the same as that in the NAR (+) model. Therefore, in a state in which no disturbance was applied, the levels of the *TARDBP* mRNA, nuclear TDP-43, cytoplasmic TDP-43, aggregates, and fragments were equal between these two models. We recorded the amount of each element that stabilized when each parameter was varied from half to twice its initial level.

The autoregulatory mechanism that controls TDP-43 robustly maintains the nuclear TDP-43 level, even when the levels of many factors were altered. For example, in the NAR (–) model, the level of nuclear TDP-43 decreased as its transcription level decreased, reaching approximately half of the initial value under conditions that mimic the *TARDBP* heterozygous knockout mouse model (**Figure 5A**). When the transcriptional level increased, the production of TDP-43 increased, and the nuclear TDP-43 level temporarily increased (**Figure 5C**). The level of cytoplasmic TDP-43 also subsequently increased, resulting in an increase in the levels of fragmented or aggregated TDP-43 accompanied by a decrease in nuclear TDP-43 levels (**Figure 5C**). However, in the NAR (+) model, regardless of whether transcription was decreased or increased, the nuclear TDP-43 level remained relatively stable (**Figures 5A,C**). Similar results were obtained when levels of other factors changed (e.g., RNA degradation efficiency, translation efficiency, and TDP-43 degradation efficiency) (**Figure 5E** and Supplementary Figures 2A, 3A). Thus, the autoregulatory mechanism that maintains the nuclear TDP-43 content is robust.

In contrast, when some factors were changed, the autoregulatory mechanism caused an extreme decrease in the amount of nuclear TDP-43 and an increase in TDP-43 fragmentation, indicating that the autoregulatory mechanism is vulnerable to these factors. For example, the mechanism was vulnerable to a reduction in the nuclear import of TDP-43. In the NAR (–) model, changes in the degree of nuclear import

altered the nuclear TDP-43 level; however, these changes did not increase the fragmentation of TDP-43. In the NAR (+) model, the amount of nuclear TDP-43 remained robust until nuclear import was reduced to approximately three-quarters of the initial setting (**Figure 5B**). When nuclear import fell below this level, the amount of nuclear TDP-43 substantially decreased, whereas the level of fragmented TDP-43 increased (**Figure 5B**). The mechanism was also vulnerable to an increase in the tendency of TDP-43 to aggregate. In this scenario, a slight but sustained increase in levels of aggregated and fragmented TDP-43 was initially observed; however, the amount of nuclear TDP-43 was strictly maintained for a certain period. At a certain point, the nuclear TDP-43 levels rapidly decreased in parallel with marked increases in the amounts of aggregated TDP-43 and the *TARDBP* mRNA (**Figure 5D**). In the NAR (–) model, the amount of nuclear TDP-43 remained constant, and no clear increase in levels of aggregation/fragmentation products was identified under the same TDP-43 aggregation-prone conditions (**Figure 5D**). As the aggregation tendency increases, the nuclear TDP-43 level decreases and nuclear TDP-43 aggregate/fragment accumulation increases in the NAR (–) model; however, the degree of aggregate/fragment accumulation is limited (Supplementary Figure 2B). Similarly, the NAR (+) model exhibited more fragility than the NAR (–) model when the parameters were set such that the efficiency of the degradation of fragmented proteins decreased (**Figure 5E** and Supplementary Figures 2B, 3B).

A Vicious Cycle Induced by Transcriptional Redundancy Accelerates TDP-43 Pathology

The model in the present study, which was designed to accumulate aggregates depending on the amount of TDP-43 in the cytoplasm, displays bi-stability between healthy and pathological states, depending on the intracellular disturbance. The autoregulatory mechanism, which originally functions to robustly maintain the amount of TDP-43, promotes separation into these two states as the driving force underlying the shift toward TDP-43 pathology when disturbances in specific factors reach or exceed a certain level. Under these conditions, the autoregulatory mechanism is expected to increase the expression of the canonical *TARDBP* mRNA and subsequently exacerbate TDP-43-related pathology (**Figure 5D**). Indeed, higher expression of the canonical *TARDBP* mRNA is detected in the cytoplasm in the motor neurons from patients with ALS, specifically in motor neurons in which nuclear TDP-43 has been eliminated and inclusion bodies have formed in the cytoplasm (Koyama et al., 2016).

Trade-off between the Robustness and Fragility of Nuclear TDP-43 Homeostasis

We subsequently altered the transcriptional redundancy in five stages to investigate how transcriptional redundancy is involved in TDP-43 metabolism (Supplementary Table 9). We halved or doubled the parameters and subsequently examined the resulting changes in the nuclear TDP-43 levels and the accumulation of aggregates and fragments at each stage (**Figures 5F,G** and Supplementary Figure 4).

The observed perturbations divided the factors into two types (**Figures 5F,G**, Supplementary Figures 4A,B). Alterations in one type of factor stabilized the nuclear TDP-43 level as transcriptional redundancy increased (**Figure 5F** and Supplementary Figure 4A), whereas alterations in the other type of factor led to a marked change in nuclear TDP-43 levels and an increase in TDP-43 aggregates as transcriptional redundancy increased (**Figure 5G** and Supplementary Figure 4B). The latter type of factors that increased system fragility were the promotion of TDP-43 aggregation, impaired nuclear-cytoplasmic TDP-43 transport, decreased the efficiency of abnormal protein degradation, and reduced efficiency of autoregulation. Thus, the robust autoregulatory mechanism that controls nuclear TDP-43 levels, which is based on transcriptional redundancy, is susceptible to specific factors, potentially because this mechanism is so robust. Therefore, a trade-off between the robustness and fragility of this relationship exists.

The Pathogenesis of Hereditary ALS Is Caused by the Fragility of the TDP-43 Autoregulatory Mechanism

The fragility of the TDP-43 autoregulatory mechanism is manifested by the tendency of TDP-43 to aggregate, impairments in nuclear-cytoplasmic TDP-43 transport, a decrease in the efficiency of the degradation of fragments, and a reduction in autoregulatory efficiency (**Figures 5E**). Therefore, TDP-43 pathology is triggered if a disorder in one of these factors persistently exceeds a threshold. We therefore suggest that mutations that cause this condition may also cause ALS/FTD.

The causative genes that underlie familial ALS/FTD are intimately associated with these factors. Mutations in the C-terminal low complex region of TDP-43 increase its aggregation-prone nature (Johnson et al., 2009). In cells with an expansion of the GGGGCC repeat at *C9ORF72*, nuclear-cytoplasmic transport is inhibited (Freibaum et al., 2015; Zhang et al., 2015; Boeynaems et al., 2016). Moreover, mutations in *VCP, UBQLNl, SQSTMl, GRN,* and *TBKl* are thought to result in a failure of the degradation machinery, leading to the accumulation of TDP-43 in the cytoplasm (Taylor et al., 2016; Chang et al., 2017; Ramesh and Pandey, 2017).

TDP-43 Pathology May Be Treated by Reductions in Transcriptional Redundancy

In the present study, we propose that transcriptional redundancy, which is important for the strict regulation of TDP-43, is the driving force underlying the formation and progression of TDP-43 pathology in patients with ALS. We therefore hypothesize that strategies that reduce transcriptional redundancy may affect TDP-43 pathology in patients with ALS. We evaluated this possibility using the model developed by our group described below.

First, we modeled the conditions under which the formation of TDP-43 aggregates is continuously increased by the mutation of *TARDBP* and the formation of stress granules is promoted.

TARDBP mRNA levels increased, nuclear TDP-43 levels decreased, and aggregated/fragmented TDP-43 accumulation increased over time, as shown in **Figure 5D**. However, after the transcription of the *TARDBP* mRNA decreased to 40%, nuclear TDP-43 levels increased, fragmented TDP-43 levels decreased and subsequently disappeared, and the *TARDBP* mRNA level returned to a nearly normal value (**Figure 6A**). Based on these results, TDP-43 pathology may be rescued by reducing the redundancy of *TARDBP* transcription.

Impaired nuclear-cytoplasmic TDP-43 transport, decreased efficiency of abnormal protein degradation, and reduced autoregulatory efficiency also shift the system to a disease state [**Figure 6B**, from a healthy state (light blue) to a disease state (pale red)]. However, the bi-stability of healthy and disease states stratified by the absence or presence of these disturbances became ambiguous when transcriptional redundancy was reduced. Therefore, disease conditions induced by these disturbances were improved (**Figure 6B**, from a disease state (pale red) to a healthy state (light blue); and Supplementary Figure 5). Although the factors that cause sporadic ALS in humans remain obscure, strategies that reduce transcriptional redundancy may represent a treatment option for ALS in patients with TDP-43 pathology initiated by any of the factors implicated in this model.

Reduced Transcription Inhibits the Propagation of TDP-43 Pathology

We speculated that a reduced transcription level would reduce the formation of new TDP-43 aggregates and fragments and subsequently suppress the propagation of pathological TDP-43 to other neurons. We therefore evaluated this hypothesis using the model developed by our group.

In this model, fragmented TDP-43 was assumed to be continuously propagated to other neurons to a certain extent, regardless of its propagation pattern. As shown in **Figure 4D**, TDP-43 pathology subsequently developed in the receiving neuron. When the transcription of TDP-43 was reduced to half in the receiving neuron, nuclear TDP-43 levels increased, the numbers of TDP-43 aggregates and fragments decreased, and the mRNA level recovered to near-normal values in the receiving neuron (**Figure 6C**). Thus, the spread of TDP-43 lesions mediated by fragmented TDP-43 was also rescued by decreasing its transcription.

We predicted that the spread of this pathological state would be affected by the amount of extracellular fragmented TDP-43. Therefore, we examined the extent of extracellular fragmentation of TDP-43 at six concentrations and determined the extent of the spread of the pathological state to receiving cells (**Figures 6D,E** and Supplementary Figure 6). When relatively small amounts of extracellular TDP-43 fragments were present, the receiving cell did not exhibit a pathological state (Supplementary Figures 6A–C). However, when the amount of extracellular TDP-43 fragments exceeded a certain level, the nuclear TDP-43 level decreased, and TDP-43 aggregates accumulated in the cytoplasm of the receiving cell (Supplementary Figures 6D–F). However, depending on the extent of the reduction in transcription in the receiving cell, the transition to this pathological condition was impeded (**Figure 6E** and Supplementary Figure 6). Thus, a therapeutic strategy designed to reduce the transcriptional redundancy of TDP-43 would prevent not only the accumulation and supply of aggregates and fragments of TDP-43 but also the spread of the disease state between cells.

DISCUSSION

In the present study, we attempted to identify specific factors related to the fragility of the TDP-43 autoregulatory mechanism using an *in silico* model mimicking the intracellular dynamics of TDP-43. TDP-43 autoregulation involves transcriptional redundancy and is robust to disturbances in many factors (**Figure 7**, left panel). However, when specific factors exceed a certain threshold for a certain period, the fragility of the autoregulatory mechanism becomes apparent. This robust autoregulatory mechanism based on transcriptional redundancy shows vulnerability under specific pathological conditions and is prone to falling into a vicious cycle in which the TDP-43 pathology continuously accelerates and deteriorates (**Figure 7**, center panel). Therefore, the system controlling TDP-43 levels shows bi-stability between healthy and disease states, according to the circumstances, and these properties of robustness and fragility may underlie the pathogenesis of TDP-43 pathology.

An appropriate amount of nuclear TDP-43 must be constantly maintained to establish homeostasis of RNA metabolism. In motor neurons, the intracellular environment may be disturbed by various factors; thus, motor neurons likely require a system that is robust to these disturbing factors. The model of cellular TDP-43 metabolism proposed here robustly maintains the amount of TDP-43 in the nucleus at a constant level in the presence of several types of disturbances, including disturbances in transcription, RNA degradation, translation, and the efficiency of degradation of the TDP-43 protein. In addition, the system was stable when fluctuations in nuclear-cytoplasmic TDP-43 transport and the increase in the tendency of the protein to aggregate were mild or persisted for a short time. However, when these disturbances were intense and sufficiently prolonged, the vulnerability of the autoregulatory system became apparent. According to several studies, TDP-43 expression increases under stress conditions, such as neuronal injury (Moisse et al., 2009), or in response to neural activity (Wang et al., 2008); however, the mechanism underlying this context-dependent change in TDP-43 expression has not been elucidated. Due to the existence of the TDP-43 autoregulatory mechanism, fluctuations in its transcription, translation efficiency, and protein degradation efficiency are less likely to affect its expression level. Therefore, in these cell states, a decrease in the efficiency of the autoregulatory mechanism itself may increase TDP-43 expression. Further studies are required to investigate whether transcriptional redundancy also contributes to the rapid increase in expression required depending on the situation within the cell. Based on the results obtained from the *in silico* model, the system will eventually shift to a disease state as the efficiency of the autoregulatory mechanism decreases and transcriptional redundancy persists. The relationship between environmental

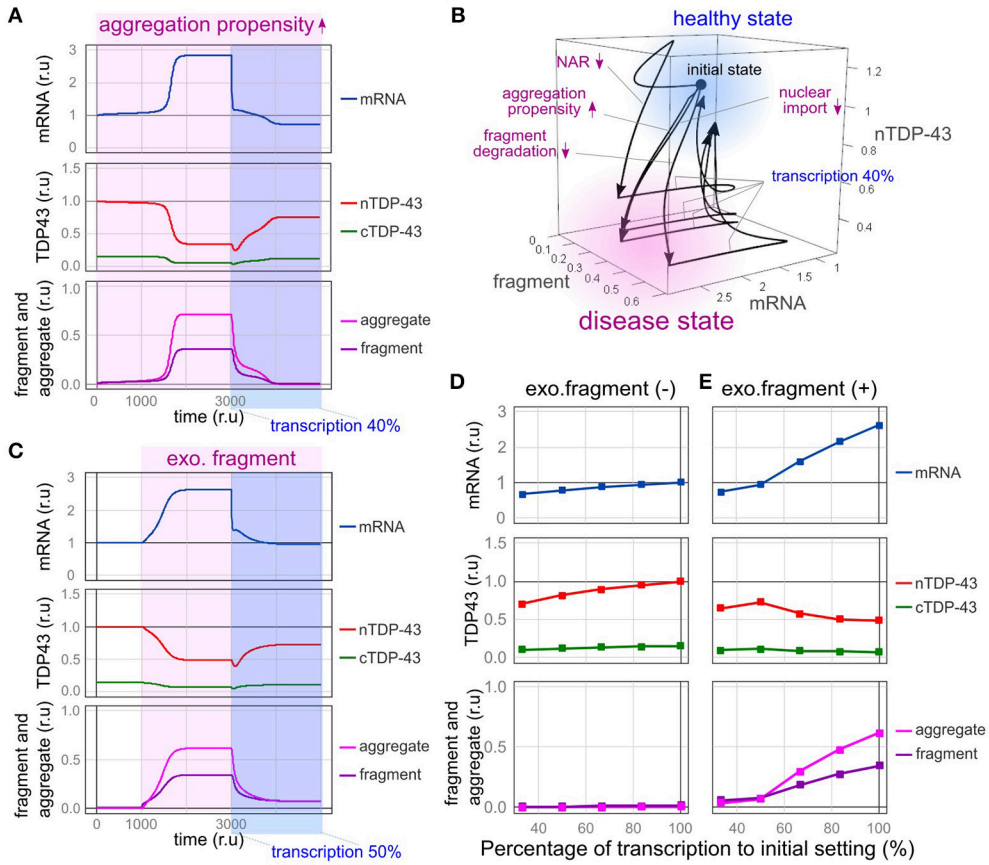

FIGURE 6 | Therapeutic effects of reducing the transcriptional redundancy of TDP-43. **(A)** Changes in the level of each element over time are shown when transcription is reduced to 40% in a state in which TDP-43 tends to aggregate. **(B)** Due to the disturbance shown in the figure, the system enters a disease state (pale red region) exhibiting an increase in mRNA levels, a decrease in nuclear TDP-43 levels, and an increase in fragment levels. When transcription is reduced to 40%, the system returns to a healthy state (light blue region). **(C)** Changes in the level of each element over time are shown when transcription is reduced to 50% in a state in which the amount of extracellular fragments is increased. **(D,E)** Changes in each element related to the decrease in transcription are shown under the condition in which the same amount of extracellular fragments depicted in **C** is present **(E)** or absent **(D)**.

factors in motor neurons and the efficiency of the TDP-43 autoregulatory mechanism should be investigated.

At this stage, we propose that TDP-43 pathology involves a vicious cycle in which excessive TDP-43 is continuously produced as a result of an autoregulatory mechanism. As shown in a previous study, motor neurons from subjects with ALS displaying abnormal TDP-43 accumulation exhibit an increase in the amount of *TARDBP* mRNA in the cytoplasm (Koyama et al., 2016), whereas other studies have observed higher amounts of TDP-43 in the cerebrospinal fluid and brain-derived exosomes obtained from patients with ALS (Kasai et al., 2009; Iguchi et al., 2016). The genetic background that results in impaired control of TDP-43 levels has not been sufficiently investigated. A family with ALS presenting with a mutation in the *TARDBP* 3′-UTR that leads to an increase in *TARDBP* mRNA levels has been identified. This mutation is located near the splice site of intron 7, which plays an important role in autoregulation, and it would be interesting to determine whether the mechanism that causes this increase involves the autoregulatory capacity of this gene (Gitcho et al., 2009). Interestingly, mutations in the *TARDBP* gene associated with ALS are frequently identified in intron 6 (Onodera et al., 2013), which undergoes alternative splicing and plays an important role in autoregulation (Koyama et al., 2016). These mutations may result in changes in the sequence motif to which the splicing factor binds, potentially causing autoregulatory abnormalities resulting from changes in the splicing efficiency or aberrations in cis factors. This possibility should be explored in the future. Furthermore, the genes that have been identified to date as causing familial ALS with TDP-43 pathology (*TARDBP, C9ORF72*, *VCP, UBQLNl, SQSTMl, GRN,* and *TBKl*) are related to disturbances in the factors that lead to the vicious cycle of the autoregulatory system. Therefore, examinations of the TDP-43 metabolism and specifically the expression of *TARDBP* mRNA in model animals with mutations in these causative genes are necessary.

Using this model, TDP-43 pathology was reversed and abnormal TDP-43 propagation was suppressed when the transcription of the *TARDBP* mRNA was suppressed (**Figure 7**,

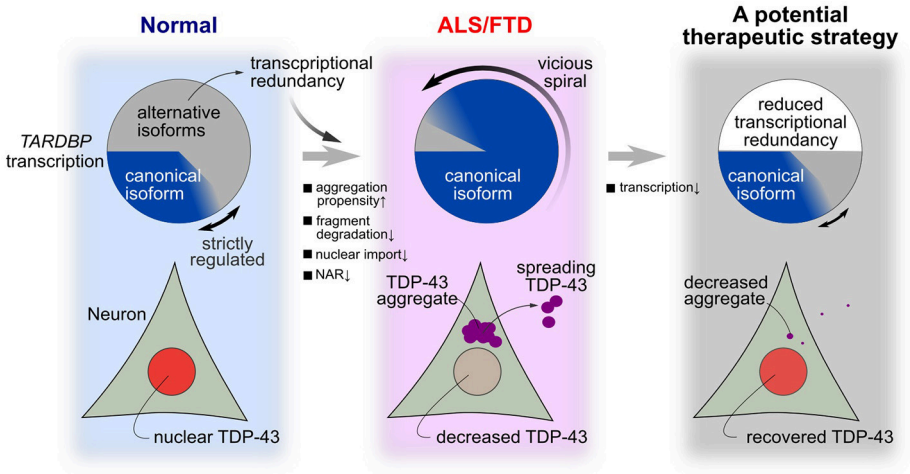

FIGURE 7 | A hypothesis for the mechanism of TDP-43 pathology in ALS and a potential treatment strategy. In a normal state, many transcribed RNAs are ultimately rapidly degraded via nonsense-mediated mRNA decay. Strict autoregulation is maintained by changing the ratios of alternatively spliced isoforms according to the amount of TDP-43 present in the nucleus. However, this robust mechanism for maintaining nuclear TDP-43 levels becomes fragile when certain intracellular lesions persist at a constant intensity. In these cases, the level of nuclear TDP-43 substantially decreases, aggregation/fragmentation increases, and the level of canonical *TARDBP* mRNA increases until the model enters the pathological state of ALS/FTD. Transcriptional redundancy promotes the transition to this pathological condition. A therapeutic strategy that reduces transcription by approximately one-half abolishes transcriptional redundancy and may reverse the morbidity observed in patients with ALS.

right panel). Mice conditionally overexpressing the TDP-43 mutant that lacked a nuclear localization signal showed TDP-43 pathology and neurological symptoms; however, when protein expression was terminated, the TDP-43 pathology was reversed and the loss of neurological function was abolished (Walker et al., 2015). Similar results were reported in mice that conditionally overexpressed TDP-43 containing an ALS-related mutation (Ke et al., 2015). Based on these findings, strategies alleviating TDP-43 overexpression ameliorate the disease state. We should validate this therapeutic strategy of reducing *TARDBP* mRNA levels under the pathological condition of persistent *TARDBP* mRNA expression driven by transcriptional redundancy. An animal model that maintains the autoregulatory mechanism that controls TDP-43 levels is necessary to provide supporting evidence for this treatment strategy. In this type of animal model, the endogenous *TARDBP* mRNA, but not exogenous *TARDBP*, should be overexpressed, as observed in motor neurons from patients with ALS (Koyama et al., 2016). This animal model should ideally be accompanied by a perturbation that induces the fragility of the TDP-43 autoregulatory system due to mutations in ALS causative genes. Once this ALS animal model is established, we can test the therapeutic effectiveness of strategies designed to reduce the transcriptional redundancy of *TARDBP* mRNA in ALS. Specifically, a strategy that employs an antisense oligonucleotide or CRISPR-dCas9 system to decrease the *TARDBP* mRNA level would conceivably be successful. A decrease in TDP-43 levels induces a loss in TDP-43 function, which may be detrimental to cell survival and function. However, because *TARDBP* expression is transcriptionally redundant, a 50% reduction in its transcription does not affect protein levels (Kraemer et al., 2010; Sephton et al., 2010; Ricketts et al., 2014). Moreover, *TARDBP* heterozygous knockout mice have normal survival times (Ricketts et al., 2014). Therefore, treatments that target *TARDBP* mRNA levels might be effective.

The pathophysiology of neurodegenerative diseases is particularly difficult to understand due to the complexity, multifactorial, and dynamic aspects of the central nervous system. Approaches using systems biology may be useful for integrating all aspects of a given phenomenon and may constitute promising strategies. However, models of any scale have advantages and limitations (Vujasinovic et al., 2010). We have created a small-scale, simple model that focuses on the dynamics of TDP-43 and does not contain other related molecules. In reality, however, intracellular metabolism, including TDP-43 metabolism, may occur while many unidentified molecules interact. Extracellular factors, including the mechanism of TDP-43 propagation between cells, are also poorly understood. Therefore, we cannot accurately model all of these factors at this stage. In addition, previous experimental results on the temporal aspects of each element, such as the half-life of the wild-type TDP-43 protein, vary greatly, depending on the cell type and conditions used in the experiment. We thus adopted relative times because we were concerned that descriptions of models incorporating absolute times would lead to erroneous interpretations. A decrease in the abstraction level or an increase the scale of the model by increasing the number of factors in the model increases the difficulty of setting appropriate parameters in the model and may result in a misinterpretation of the results. Meanwhile, even if many other factors are involved, we rationally presume that these factors ultimately act on the dynamics of TDP-43 and are responsible for the development of ALS-related TDP-43 pathology. Therefore, we postulate that

the scale and abstraction level of this model are suitable for the research purpose to reveal hidden vulnerabilities in the robustness of the TDP-43 autoregulatory mechanism. However, changes in the intracellular environment may influence multiple factors that determine the dynamics of TDP-43. In addition, since secondary impairments in nuclear-cytoplasmic TDP-43 transport due to the accumulation of aggregates have been reported (Woerner et al., 2015), disturbances in multiple factors may occur continuously. Despite this evidence, the present study did not analyze pathological conditions involving these multiple factors. The hypothesis and treatment strategy for TDP-43 pathology proposed based on this model should be experimentally verified as discussed above. In addition, the relationship of each element and the scale of the model can be corrected based on accumulating results from biological experiments.

CONCLUSION

Why does TDP-43 accumulate abnormally in the cytoplasm in patients with ALS/FTD when a mechanism that precisely maintains its expression exists? Studies aiming to resolve this issue are important to enhance our understanding of the pathology of sporadic ALS, which accounts for most ALS cases, and to promote the development of methods to treat this disease. Therefore, in the present study, we modeled and simulated TDP-43 dynamics within the cell. The trade-off relationship between the vulnerability and robustness of the mechanism that maintains nuclear TDP-43 levels might underlie TDP-43 pathology. Once this vulnerability is triggered, the redundancy of *TARDBP* transcription that is intended to maintain nuclear TDP-43 levels becomes the driving force that leads to TDP-43 pathology. This hypothesis answers several questions: why do ALS motor neurons enter a pathological state from which they cannot escape; why do many different ALS causative genes result in TDP-43 pathology; and why does TDP-43 pathology propagate between cells, thereby resulting in progression? Furthermore, based on our model, therapies for ALS targeting specific molecules are a possibility. In the future, an ideal animal model of this disease should be established to explore this hypothesis.

AUTHOR CONTRIBUTIONS

AS and OO designed the study. AS, TKA, and AK performed the biological experiments using the mouse cerebrum and investigated the results of previous experiments to create our model. AS analyzed the results. YK, SK, TKO, and TI contributed to the interpretation of the findings. AS and OO drafted the manuscript. All authors critically revised the draft and approved the final version.

FUNDING

This research was supported by a grant-in-aid for Scientific Research on Innovative Areas (Brain Protein Aging and Dementia Control; 26117006) from MEXT; grants-in-aid for Scientific Research (A) (26250017 and 25253065) and a grant-in-aid for Scientific Research (C) (17K09751) from the Japan Society for the Promotion of Science; a grant-in-aid from the Research Committee of CNS Degenerative Diseases and Comprehensive Research on Disability, Health, and Welfare (13230021) from the Japanese Ministry of Health, Labor, and Welfare of Japan; and a grant-in-aid from the Takeda Science Foundation.

SUPPLEMENTARY MATERIAL

The Supplementary Material for this article can be found online at: https://www.frontiersin.org/articles/10.3389/fnins.2018.00028/full#supplementary-material

REFERENCES

Arai, T., Hasegawa, M., Akiyama, H., Ikeda, K., Nonaka, T., Mori, H., et al. (2006). TDP-43 is a component of ubiquitin-positive tau-negative inclusions in frontotemporal lobar degeneration and amyotrophic lateral sclerosis. *Biochem. Biophys. Res. Commun.* 351, 602–611. doi: 10.1016/j.bbrc.2006.10.093

Arnold, E. S., Ling, S.-C., Huelga, S. C., Lagier-tourenne, C., Polymenidou, M., Ditsworth, D., et al. (2013). ALS-linked TDP-43 mutations produce aberrant RNA splicing and adult-onset motor neuron disease without aggregation or loss of nuclear TDP-43. *Proc. Natl. Acad. Sci. U.S.A.* 110, E736–E745. doi: 10.1073/pnas.1222809110

Avendaño-Vázquez, S. E., Dhir, A., Bembich, S., Buratti, E., Proudfoot, N., Baralle, F. E., et al. (2012). Autoregulation of TDP-43 mRNA levels involves interplay between transcription, splicing, and alternative polyA site selection. *Genes Dev.* 26, 1679–1684. doi: 10.1101/gad.194829.112

Ayala, Y. M., De Conti, L., Avendaño-Vázquez, S. E., Dhir, A., Romano, M., D'Ambrogio, A., et al. (2011). TDP-43 regulates its mRNA levels through a negative feedback loop. *EMBO J.* 30, 277–288. doi: 10.1038/emboj.2010.310

Ayala, Y. M., Zago, P., D'Ambrogio, A., Xu, Y.-F., Petrucelli, L., Buratti, E., et al. (2008). Structural determinants of the cellular localization and shuttling of TDP-43. *J. Cell Sci.* 121, 3778–3785. doi: 10.1242/jcs.038950

Boeynaems, S., Bogaert, E., Van Damme, P., and Van Den Bosch, L. (2016). Inside out: the role of nucleocytoplasmic transport in ALS and FTLD. *Acta Neuropathol.* 132, 159–173. doi: 10.1007/s00401-016-1586-5

Braak, H., Brettschneider, J., Ludolph, A. C., Lee, V. M., Trojanowski, J. Q., and Del Tredici, K., (2013). Amyotrophic lateral sclerosis—a model of corticofugal axonal spread. *Nat. Rev. Neurol.* 9, 708–714. doi: 10.1038/nrneurol.2013.221

Brettschneider, J., Del Tredici, K., Toledo, J. B., Robinson, J. L., Irwin, D. J., Grossman, M., et al. (2013). Stages of pTDP-43 pathology in amyotrophic lateral sclerosis. *Ann. Neurol.* 74, 20–38. doi: 10.1002/ana.23937

Budini, M., Buratti, E., Stuani, C., Guarnaccia, C., Romano, V., De Conti, L., et al. (2012). Cellular model of TAR DNA-binding Protein 43 (TDP-43) aggregation based on its C-terminal Gln/Asn-rich region. *J. Biol. Chem.* 287, 7512–7525. doi: 10.1074/jbc.M111.288720

Chang, M. C., Srinivasan, K., Friedman, B. A., Suto, E., Modrusan, Z., Lee, W. P., et al. (2017). Progranulin deficiency causes impairment of autophagy and TDP-43 accumulation. *J. Exp. Med.* 214, 2611–2628. doi: 10.1084/jem.20160999

Chen, A. K., Lin, R. Y., Hsieh, E. Z., Tu, P. H., Chen, R. P., Liao, T. Y., et al. (2010). Induction of amyloid fibrils by the C-terminal fragments of TDP-43 in amyotrophic lateral sclerosis. *J. Am. Chem. Soc.* 132, 1186–1187. doi: 10.1021/ja9066207

Chiang, P., Ling, J., Ha, Y., Price, D. L., Aja, S. M., and Wong, P. C. (2010). Deletion of TDP-43 down-regulates Tbc1d1, a gene linked to obesity, and

alters body fat metabolism. *Proc. Natl. Acad. Sci. U.S.A.* 107, 16320–16324. doi: 10.1073/pnas.1002176107

Ding, X., Ma, M., Teng, J., Teng, R. K. F., Zhou, S., Yin, J., et al. (2015). Exposure to ALS-FTD-CSF generates TDP-43 aggregates in glioblastoma cells through exosomes and TNTs-like structure. *Oncotarget* 6, 24178–24191. doi: 10.18632/oncotarget.4680

Dormann, D., Rodde, R., Edbauer, D., Bentmann, E., Fischer, I., Hruscha, A., et al. (2010). ALS-associated fused in sarcoma (*FUS*) mutations disrupt Transportin-mediated nuclear import. *EMBO J.* 29, 2841–2857. doi: 10.1038/emboj.2010.143

Feiler, M. S., Strobel, B., Freischmidt, A., Helferich, A. M., Kappel, J., Brewer, B. M., et al. (2015). TDP-43 is intercellularly transmitted across axon terminals. *J. Cell Biol.* 211, 897–911. doi: 10.1083/jcb.201504057

Freibaum, B. D., Lu, Y., Lopez-Gonzalez, R., Kim, N. C., Almeida, S., Lee, K.-H., et al. (2015). GGGGCC repeat expansion in *C9orf72* compromises nucleocytoplasmic transport. *Nature* 525, 129–133. doi: 10.1038/nature14974

Funahashi, A., Morohashi, M., Kitano, H., and Tanimura, N. (2003). CellDesigner: a process diagram editor for gene-regulatory and biochemical networks. *Biosilico* 1, 159–162. doi: 10.1016/S1478-5382(03)02370-9

Furukawa, Y., Kaneko, K., Watanabe, S., Yamanaka, K., and Nukina, N. (2011). A seeding reaction recapitulates intracellular formation of sarkosyl-insoluble transactivation response element (TAR) DNA-binding protein-43 inclusions. *J. Biol. Chem.* 286, 18664–18672. doi: 10.1074/jbc.M111.231209

Gitcho, M. A., Bigio, E. H., Mishra, M., Johnson, N., Weintraub, S., Mesulam, M., et al. (2009). *TARDBP* 3'-UTR variant in autopsy-confirmed frontotemporal lobar degeneration with TDP-43 proteinopathy. *Acta Neuropathol.* 118, 633–645. doi: 10.1007/s00401-009-0571-7

Gopal, P. P., Nirschl, J. J., Klinman, E., and Holzbaur, E. L. F. (2017). Amyotrophic lateral sclerosis-linked mutations increase the viscosity of liquid-like TDP-43 RNP granules in neurons. *Proc. Natl. Acad. Sci. U.S.A.* 114, E2466–E2475. doi: 10.1073/pnas.1614462114

Hasegawa, M., Arai, T., Nonaka, T., Kametani, F., Yoshida, M., Hashizume, Y., et al. (2008). Phosphorylated TDP-43 in frontotemporal lobar degeneration and amyotrophic lateral sclerosis. *Ann. Neurol.* 64, 60–70. doi: 10.1002/ana.21425

Huelga, S. C., Vu, A. Q., Arnold, J. D., Liang, T. D., Liu, P. P., Yan, B. Y., et al. (2012). Integrative genome-wide analysis reveals cooperative regulation of alternative splicing by hnRNP proteins. *Cell Rep.* 1, 167–178. doi: 10.1016/j.celrep.2012.02.001

Igaz, L. M., Kwong, L. K., Chen-plotkin, A., Winton, M. J., Unger, T. L., Xu, Y., et al. (2009). Expression of TDP-43 C-terminal fragments *in vitro* recapitulates pathological features of TDP-43 Proteinopathies. *J. Biol. Chem.* 284, 8516–8524. doi: 10.1074/jbc.M809462200

Iguchi, Y., Eid, L., Parent, M., Soucy, G., Bareil, C., Riku, Y., et al. (2016). Exosome secretion is a key pathway for clearance of pathological TDP-43. *Brain* 139, 3187–3201. doi: 10.1093/brain/aww237

Iguchi, Y., Katsuno, M., Niwa, J. I., Takagi, S., Ishigaki, S., Ikenaka, K., et al. (2013). Loss of TDP-43 causes age-dependent progressive motor neuron degeneration. *Brain* 136, 1371–1382. doi: 10.1093/brain/awt029

Johnson, B. S., Snead, D., Lee, J. J., McCaffery, J. M., Shorter, J., and Gitler, A. D. (2009). TDP-43 is intrinsically aggregation-prone, and amyotrophic lateral sclerosis-linked mutations accelerate aggregation and increase toxicity. *J. Biol. Chem.* 284, 20329–20339. doi: 10.1074/jbc.M109.010264

Kabashi, E., Valdmanis, P. N., Dion, P., Spiegelman, D., McConkey, B. J., Vande Velde, C., et al. (2008). *TARDBP* mutations in individuals with sporadic and familial amyotrophic lateral sclerosis. *Nat. Genet.* 40, 572–574. doi: 10.1038/ng.132

Kasai, T., Tokuda, T., Ishigami, N., Sasayama, H., Foulds, P., Mitchell, D. J., et al. (2009). Increased TDP-43 protein in cerebrospinal fluid of patients with amyotrophic lateral sclerosis. *Acta Neuropathol.* 117, 55–62. doi: 10.1007/s00401-008-0456-1

Ke, Y. D., van Hummel, A., Stevens, C. H., Gladbach, A., Ippati, S., Bi, M., et al. (2015). Short-term suppression of A315T mutant human TDP-43 expression improves functional deficits in a novel inducible transgenic mouse model of FTLD-TDP and ALS. *Acta Neuropathol.* 130, 661–678. doi: 10.1007/s00401-015-1486-0

Khosravi, B., Hartmann, H., May, S., Möhl, C., Ederle, H., Michaelsen, M., et al. (2017). Cytoplasmic poly-GA aggregates impair nuclear import of TDP-43 in *C9orf72* ALS/FTLD. *Hum. Mol. Genet.* 26, 790–800. doi: 10.1093/hmg/ddw432

Koyama, A., Sugai, A., Kato, T., Ishihara, T., Shiga, A., Toyoshima, Y., et al. (2016). Increased cytoplasmic *TARDBP* mRNA in affected spinal motor neurons in ALS caused by abnormal autoregulation of TDP-43. *Nucleic Acids Res.* 44, 5820–5836. doi: 10.1093/nar/gkw499

Kraemer, B. C., Schuck, T., Wheeler, J. M., Robinson, L. C., Trojanowski, J. Q., Lee, V. M. Y., et al. (2010). Loss of murine TDP-43 disrupts motor function and plays an essential role in embryogenesis. *Acta Neuropathol.* 119, 409–419. doi: 10.1007/s00401-010-0659-0

Lee, E. B., Lee, V. M.-Y., and Trojanowski, J. Q. (2012). Gains or losses: molecular mechanisms of TDP43-mediated neurodegeneration. *Nat. Rev. Neurosci.* 13, 38–50. doi: 10.1038/nrn3121

Le Guiner, C., Lejeune, F., Galiana, D., Kister, L., Breathnach, R., Stévenin, J., et al. (2001). TIA-1 and TIAR Activate Splicing of Alternative Exons with Weak 5′ Splice Sites followed by a U-rich Stretch on Their Own Pre-mRNAs. *J. Biol. Chem.* 276, 40638–40646. doi: 10.1074/jbc.M105642200

Ling, S., Albuquerque, C. P., Seok, J., Lagier-tourenne, C., and Tokunaga, S. (2010). ALS-associated mutations in TDP-43 increase its stability and promote TDP-43 complexes with FUS/TLS. *Proc. Natl. Acad. Sci. U.S.A.* 107, 13318–13323. doi: 10.1073/pnas.1008227107

Ling, S.-C., Polymenidou, M., and Cleveland, D. W. (2013). Converging mechanisms in ALS and FTD: disrupted RNA and protein homeostasis. *Neuron* 79, 416–438. doi: 10.1016/j.neuron.2013.07.033

Liu, Q., Shu, S., Wang, R. R., Liu, F., Cui, B., Guo, X. N., et al. (2016). Whole-exome sequencing identifies a missense mutation in *hnRNPA1* in a family with flail arm ALS. *Neurology* 87, 1763–1769. doi: 10.1212/WNL.0000000000003256

Mackenzie, I. R., Nicholson, A. M., Sarkar, M., Boylan, K. B., Taylor, J. P., and Rademakers, R. (2017). TIA1 mutations in amyotrophic lateral sclerosis and frontotemporal dementia promote phase separation and alter stress granule dynamics. *Neuron* 95, 808–816. doi: 10.1016/j.neuron.2017.07.025

Matsukawa, K., Hashimoto, T., Matsumoto, T., Ihara, R., Chihara, T., Miura, M., et al. (2016). Familial Amyotrophic lateral sclerosis-linked mutations in profilin 1 exacerbate TDP-43-induced degeneration in the retina of *Drosophila melanogaster* through an increase in the cytoplasmic localization of TDP-43. *J. Biol. Chem.* 291, 23464–23476. doi: 10.1074/jbc.M116.729152

McDonald, K. K., Aulas, A., Destroismaisons, L., Pickles, S., Beleac, E., Camu, W., et al. (2011). TAR DNA-binding protein 43 (TDP-43) regulates stress granule dynamics via differential regulation of G3BP and TIA-1. *Hum. Mol. Genet.* 20, 1400–1410. doi: 10.1093/hmg/ddr021

McGoldrick, P., Joyce, P. I., Fisher, E. M. C., and Greensmith, L. (2013). Rodent models of amyotrophic lateral sclerosis. *Biochim. Biophys. Acta* 1832, 1421–1436. doi: 10.1016/j.bbadis.2013.03.012

Moisse, K., Volkening, K., Leystra-Lantz, C., Welch, I., Hill, T., and Strong, M. J. (2009). Divergent patterns of cytosolic TDP-43 and neuronal progranulin expression following axotomy: implications for TDP-43 in the physiological response to neuronal injury. *Brain Res.* 1249, 202–211. doi: 10.1016/j.brainres.2008.10.021

Molliex, A., Temirov, J., Lee, J., Coughlin, M., Kanagaraj, A. P., Kim, H. J., et al. (2015). Phase separation by low complexity domains promotes stress granule assembly and drives pathological fibrillization. *Cell* 163, 123–133. doi: 10.1016/j.cell.2015.09.015

Neumann, M., Sampathu, D. M., Kwong, L. K., Truax, A. C., Micsenyi, M. C., Chou, T. T., et al. (2006). Ubiquitinated TDP-43 in frontotemporal lobar degeneration and amyotrophic lateral sclerosis. *Science* 314, 130–133. doi: 10.1126/science.1134108

Nonaka, T., Kametani, F., Arai, T., Akiyama, H., and Hasegawa, M. (2009). Truncation and pathogenic mutations facilitate the formation of intracellular aggregates of TDP-43. *Hum. Mol. Genet.* 18, 3353–3364. doi: 10.1093/hmg/ddp275

Nonaka, T., Masuda-Suzukake, M., Arai, T., Hasegawa, Y., Akatsu, H., Obi, T., et al. (2013). Prion-like properties of pathological TDP-43 aggregates from diseased brains. *Cell Rep.* 4, 1–11. doi: 10.1016/j.celrep.2013.06.007

Onodera, O., Sugai, A., Konno, T., and Et, A. L. (2013). What is the key player in TDP-43 pathology in ALS: disappearance from the nucleus or inclusion formation in the cytoplasm? *Neurol. Clin. Neurosci.* 1, 11–17. doi: 10.1002/ncn3.9

Pesiridis, G. S., Tripathy, K., Tanik, S., Trojanowski, J. Q., Lee, V. M.-Y., Lee, M., et al. (2011). A "two-hit" hypothesis for inclusion formation by carboxyl-terminal fragments of TDP-43 protein linked to RNA depletion and

impaired microtubule-dependent transport. *J. Biol. Chem.* 286, 18845–18855. doi: 10.1074/jbc.M111.231118

Polymenidou, M., and Cleveland, D. W. (2011). The seeds of neurodegeneration: prion-like spreading in ALS. *Cell* 147, 498–508. doi: 10.1016/j.cell.2011.10.011

Polymenidou, M., Lagier-tourenne, C., Hutt, K. R., Stephanie, C., Moran, J., Liang, T. Y., et al. (2011). Long pre-mRNA depletion and RNA missplicing contribute to neuronal vulnerability from loss of TDP-43. *Nat. Neurosci.* 14, 459–468. doi: 10.1038/nn.2779

Ramesh, N., and Pandey, U. B. (2017). Autophagy dysregulation in ALS: when protein aggregates get out of hand. *Front. Mol. Neurosci.* 10:263. doi: 10.3389/fnmol.2017.00263

Ratti, A., and Buratti, E. (2016). Physiological functions and pathobiology of TDP-43 and FUS/TLS proteins. *J. Neurochem.* 138, 95–111. doi: 10.1111/jnc.13625

Ricketts, T., McGoldrick, P., Fratta, P., de Oliveira, H. M., Kent, R., Phatak, V., et al. (2014). A nonsense mutation in mouse *Tardbp* Affects TDP43 alternative splicing activity and causes limb-clasping and body tone defects. *PLoS ONE* 9:e85962. doi: 10.1371/journal.pone.0085962

Scotter, E. L., Vance, C., Nishimura, A. L., Lee, Y.-B., Chen, H.-J., Urwin, H., et al. (2014). Differential roles of the ubiquitin proteasome system and autophagy in the clearance of soluble and aggregated TDP-43 species. *J. Cell Sci.* 127, 1263–1278. doi: 10.1242/jcs.140087

Sephton, C. F., Good, S. K., Atkin, S., Dewey, C. M., Iii, P. M., Herz, J., et al. (2010). TDP-43 is a developmentally regulated protein essential for early embryonic development. *J. Biol. Chem.* 285, 6826–6834. doi: 10.1074/jbc.M109.061846

Stribl, C., Samara, A., Trümbach, D., Peis, R., Neumann, M., Fuchs, H., et al. (2014). Mitochondrial dysfunction and decrease in body weight of a transgenic knock-in mouse model for TDP-43. *J. Biol. Chem.* 289, 10769–10784. doi: 10.1074/jbc.M113.515940

Sun, Y., and Chakrabartty, A. (2017). Phase to phase with TDP-43. *Biochemistry* 56, 809–823. doi: 10.1021/acs.biochem.6b01088

Suzuki, H., and Matsuoka, M. (2017). hnRNPA1 autoregulates its own mRNA expression to remain non-cytotoxic. *Mol. Cell. Biochem.* 427, 123–131. doi: 10.1007/s11010-016-2904-x

Swarup, V., Phaneuf, D., Bareil, C., Robertson, J., Rouleau, G. A., Kriz, J., et al. (2011a). Pathological hallmarks of amyotrophic lateral sclerosis/frontotemporal lobar degeneration in transgenic mice produced with TDP-43 genomic fragments. *Brain* 134, 2610–2626. doi: 10.1093/brain/awr159

Swarup, V., Phaneuf, D., Dupré, N., Petri, S., Strong, M., Kriz, J., et al. (2011b). Deregulation of TDP-43 in amyotrophic lateral sclerosis triggers nuclear factor κB-mediated pathogenic pathways. *J. Exp. Med.* 208, 2429–2447. doi: 10.1084/jem.20111313

Tani, H., Imamachi, N., Salam, K. A., Mizutani, R., Ijiri, K., Irie, T., et al. (2012). Identification of hundreds of novel UPF1 target transcripts by direct determination of whole transcriptome stability. *RNA Biol.* 9, 1370–1379. doi: 10.4161/rna.22360

Taylor, J. P., Brown, R. H., and Cleveland, D. W. (2016). Decoding ALS: from genes to mechanism. *Nature* 539, 197–206. doi: 10.1038/nature20413

van Es, MA., Van Hardiman, O., Chio, A., Al-chalabi, A., Pasterkamp, R. J., Veldink, J. H., et al. (2017). Amyotrophic lateral sclerosis. *Lancet* 390, 2084–2098. doi: 10.1016/S0140-6736(17)31287-4

Verstraete, E., Kuiperij, H. B., van Blitterswijk, M. M., Veldink, J. H., Schelhaas, H. J., van den Berg, L. H., et al. (2012). TDP-43 plasma levels are higher in amyotrophic lateral sclerosis. *Amyotroph. Lateral Scler.* 13, 446–451. doi: 10.3109/17482968.2012.703208

Vujasinovic, T., Zampera, A. S., Jackers, P., Sanoudou, D., and Depaulis, A. (2010). In silico dynamic molecular interaction networks for the discovery of new therapeutic targets. *Curr. Pharm. Des.* 16, 2241–2251. doi: 10.2174/138161210791792822

Walker, A. K., Spiller, K. J., Ge, G., Zheng, A., Xu, Y., Zhou, M., et al. (2015). Functional recovery in new mouse models of ALS/FTLD after clearance of pathological cytoplasmic TDP-43. *Acta Neuropathol.* 130, 643–660. doi: 10.1007/s00401-015-1460-x

Wang, I., Wu, L., Chang, H., and Shen, C. J. (2008). TDP-43, the signature protein of FTLD-U, is a neuronal activity-responsive factor. *J. Neurochem.* 105, 797–806. doi: 10.1111/j.1471-4159.2007.05190.x

Watanabe, S., Kaneko, K., and Yamanaka, K. (2012). Accelerated disease onset with stabilized familial Amyotrophic Lateral Sclerosis (ALS)-linked TDP-43 mutations. *J. Biol. Chem.* 288, 3641–3654. doi: 10.1074/jbc.M112.433615

Winton, M. J., Igaz, L. M., Wong, M. M., Kwong, L. K., Trojanowski, J. Q., and Lee, V. M. Y. (2008). Disturbance of nuclear and cytoplasmic TAR DNA-binding protein (TDP-43) induces disease-like redistribution, sequestration, and aggregate formation. *J. Biol. Chem.* 283, 13302–13309. doi: 10.1074/jbc.M800342200

Woerner, A. C., Frottin, F., Hornburg, D., and Feng, L. R. (2015). Cytoplasmic protein aggregates interfere with nucleo-cytoplasmic transport of protein and RNA. *Science* 351, 173–177. doi: 10.1126/science.aad2033

Woo, J. -A., Liu, T., Trotter, C., Fang, C. C., De Narvaez, E., LePochat, P., et al. (2017). Loss of function *CHCHD10* mutations in cytoplasmic TDP-43 accumulation and synaptic integrity. *Nat. Commun.* 8:15558. doi: 10.1038/ncomms15558

Wu, L. S., Cheng, W. C., and Shen, C. K. J. (2012). Targeted depletion of TDP-43 expression in the spinal cord motor neurons leads to the development of amyotrophic lateral sclerosis-like phenotypes in mice. *J. Biol. Chem.* 287, 27335–27344. doi: 10.1074/jbc.M112.359000

Xu, Y.-F., Gendron, T. F., Zhang, Y.-J., Lin, W.-L., D'Alton, S., Sheng, H., et al. (2010). Wild-type human TDP-43 expression causes TDP-43 phosphorylation, mitochondrial aggregation, motor deficits, and early mortality in transgenic mice. *J. Neurosci.* 30, 10851–10859. doi: 10.1523/JNEUROSCI.1630-10.2010

Zhang, K., Donnelly, C. J., Haeusler, A. R., Grima, J. C., Machamer, J. B., Steinwald, P., et al. (2015). The *C9orf72* repeat expansion disrupts nucleocytoplasmic transport. *Nature* 525, 56–61. doi: 10.1038/nature14973

Zhou, Y., Liu, S., Liu, G., Öztürk, A., Hicks, G. G., and Splicing, A. (2013). ALS-Associated *FUS* mutations result in compromised *FUS* alternative splicing and autoregulation. *PLoS Genet.* 9:e1003895. doi: 10.1371/journal.pgen.1003895

Conflict of Interest Statement: The authors declare that the research was conducted in the absence of any commercial or financial relationships that could be construed as a potential conflict of interest.

frontiers in Neuroscience

ORIGINAL RESEARCH
published: 22 January 2018
doi: 10.3389/fnins.2017.00751

Nitrative Stress and Tau Accumulation in Amyotrophic Lateral Sclerosis/Parkinsonism-Dementia Complex (ALS/PDC) in the Kii Peninsula, Japan

Yukiko Hata[1], Ning Ma[2], Misao Yoneda[3], Satoru Morimoto[4,5,6], Hideyuki Okano[5], Shigeo Murayama[6], Shosuke Kawanishi[7], Shigeki Kuzuhara[8] and Yasumasa Kokubo[9]**

[1] Department of Neurology, Graduate School of Medicine, Mie University, Mie, Japan, [2] Division of Health Science, Graduate School of Health Science, Suzuka University of Medical Science, Mie, Japan, [3] Department of Medical Welfare, Suzuka University of Medical Science, Mie, Japan, [4] Department of Oncologic Pathology, Graduate School of Medicine, Mie University, Mie, Japan, [5] Department of Physiology, Keio University School of Medicine, Tokyo, Japan, [6] Department of Neuropathology, Metropolitan Geriatric Hospital and Institute of Gerontology, Tokyo, Japan, [7] Faculty of Pharmaceutical Sciences, Suzuka University of Medical Science, Mie, Japan, [8] Department of Neurology and Medicine, School of Nursing, Suzuka University of Medical Science, Mie, Japan, [9] Kii ALS/PDC Research Center, Graduate School of Regional Innovation studies, Mie University, Mie, Japan

OPEN ACCESS

Edited by:
Naruhiko Sahara,
National Institute of Radiological Sciences (NIRS), Japan

Reviewed by:
Patrizia Longone,
Fondazione Santa Lucia (IRCCS), Italy
Jenny Sassone,
Vita-Salute San Raffaele University, Italy

***Correspondence:**
Hideyuki Okano
hidokano@a2.keio.jp
Yasumasa Kokubo
ktyktykty@me.com

Specialty section:
This article was submitted to Neurodegeneration, a section of the journal Frontiers in Neuroscience

Received: 30 September 2017
Accepted: 26 December 2017
Published: 22 January 2018

Citation:
Hata Y, Ma N, Yoneda M, Morimoto S, Okano H, Murayama S, Kawanishi S, Kuzuhara S and Kokubo Y (2018) Nitrative Stress and Tau Accumulation in Amyotrophic Lateral Sclerosis/Parkinsonism-Dementia Complex (ALS/PDC) in the Kii Peninsula, Japan. Front. Neurosci. 11:751. doi: 10.3389/fnins.2017.00751

Objective: The Kii Peninsula of Japan is known to be a high incidence area of amyotrophic lateral sclerosis/parkinsonism-dementia complex (Kii ALS/PDC) with tauopathy. Nitrative stress and oxidative stress on ALS/PDC and their relationship to tau pathology were clarified.

Methods: Seven patients with Kii ALS/PDC (3 males and 4 females, average age 70.7 years, 3 with ALS, 2 with ALS with dementia, and 2 with PDC) were analyzed in this study. Five patients with Alzheimer's disease and five normal aged subjects were used as controls. Immunohistochemical analysis was performed on formalin-fixed, paraffin-embedded temporal lobe sections (the hippocampal area including hippocampus, prosubiculum, subiculum, presubiculum, and parahippocampal gyri) using antibodies to detect phosphorylated tau (anti-AT-8), nitrated guanine (anti-8-NG), anti-iNOS, anti-NFκB, and oxidized guanine (anti-8-OHdG) antibodies.

Results: Most hippocampal neurons of Kii ALS/PDC patients were stained with anti-8-NG, anti-iNOS, anti-NFκB, and anti-8-OHdG antibodies and some AT-8 positive neurons were co-stained with anti-8-NG antibody. The numbers of 8-NG positive neurons and 8-OHdG positive neurons were greater than AT-8 positive neurons and the number of 8-NG positive neurons was larger in patients with Kii ALS/PDC than in controls.

Conclusion: Nitrative and oxidative stress may take priority over tau accumulation and lead to the neurodegeneration in Kii ALS/PDC.

Keywords: amyotrophic lateral sclerosis, parkinsonism-dementia complex, Kii Peninsula, tau, nitrative stress, oxidative stress

INTRODUCTION

The Kii Peninsula is the high-incidence focus of amyotrophic lateral sclerosis (ALS) and parkinsonism-dementia complex (PDC) in Japan (Kokubo and Kuzuhara, 2001). ALS and PDC occur concomitantly on Guam and in the Kii Peninsula and share common neuropathological features characterized by the presence of many neurofibrillary tangles in the central nervous system (Kokubo and Kuzuhara, 2001, 2004; Kuzuhara, 2004; Kuzuhara and Kokubo, 2005). Kii ALS shows typical ALS symptoms and Kii PDC shows parkinsonism, dementia especially abulia and/or ALS symptoms. Lately Kii ALS/PDC has been revealed multiple proteinopathy including tauopathy, α-synucleinopathy and TDP-43 proteinopathy (Mimuro et al., 2017). Although the pathogenesis of Kii ALS/PDC remains unclear, interaction of environmental factors and genetic factors are surmised to cooperate in the development of the disease.

Oxidative stress (OS) and nitrative stress (NS) are involved in many neurodegenerative diseases, such as Parkinson's disease (PD), Alzheimer's disease (AD), and ALS (Jesberger and Richardson, 1991; de la Monte et al., 2000; Giasson et al., 2002; Kikuchi et al., 2002; Nunomura et al., 2004; Imaizumi et al., 2012). We have reported an increased ration of urinary 8-hydroxydeoxyguanosine (8-OHdG)/creatinine in Kii ALS/PDC patients (Morimoto et al., 2009). In this study, we investigated the interaction between OS, NS, and tau in the pathogenesis of Kii ALS/PDC using immunohistological analyses with the following five antibodies: anti-8-nitroguanine (8-NG), which detects nitrated guanine in DNA and RNA (Ma et al., 2004, 2006; Pinlaor et al., 2004a,b), anti-8-OHdG, which detects oxidized guanine in RNA (Kikuchi et al., 2002; Nunomura et al., 2004), anti-inducible nitric oxide synthase (iNOS) (Levecque et al., 2003; Fernández-Vizarra et al., 2004; Ma et al., 2004, 2006; Pinlaor et al., 2004a,b), anti-NFκB which induces iNOS, and anti-AT-8 antibody, which detects phosphorylated tau (p-tau). We found that OS and especially NS, were concerned with tau deposition in the Kii ALS/PDC patients' brains.

MATERIALS AND METHODS

Patient Tissue

The brains from seven patients with Kii ALS/PDC, five from patients with AD and five normal aged control subjects were analyzed (Wilcoxon test for age: Control vs. AD; $p = 0.1172$, Control vs. Kii ALS/PDC; $p = 0.1062$). Informed consents were obtained from the families of all patients who participated in the present study in the written form. The present study was approved by the Ethical Committee of Mie University Hospital, Mie, Japan (approval number; 2592) and Tokyo Metropolitan Geriatric Hospital, Tokyo, Japan (approval number; 2014-11, 2014-12). The profiles of these patients are summarized in **Table 1**. The clinical and neuropathological findings of Kii ALS/PDC have been described in previous reports (Kuzuhara et al., 2001; Mimuro et al., 2017). Neuropathological diagnosis of AD was obtained based on the following criteria: (1) Braak neurofibrillary tangle stage IV or above and (2) amyloid deposits of Braak stage C.

TABLE 1 | The quantitative assessment summary of the immunohistochemistry in the hippocampus of Kii ALS/PDC patients, Alzheimer's disease patients and controls.

Case	Range of age at death	Clinical phenotype	AT-8	8-NG	iNOS	NF-κB	8-OHdG
Kii ALS/PDC-1	61–65	ALS	+	++	++	+	+
Kii ALS/PDC-2	81–85	ALS	++	+++	++	+	+++
Kii ALS/PDC-3	66–70	ALS	++	++++++	++	+	
Kii ALS/PDC-4	71–75	ALS with D	+++	+++++++++		++	
Kii ALS/PDC-5	61–65	ALS with D	+++++++++		++		++
Kii ALS/PDC-6	66–70	PDC	+	+	+	+	−
Kii ALS/PDC-7	71–75	PDC	++	+++++++++		++	
AD-1	76–80	D	++	+	++	+	+
AD-2	81–85	D	++	++	++	++	+
AD-3	86–90	D	+++	+	+	+	++
AD-4	86–90	D	+++	++	++	++	++
AD-5	76–80	D	+++	++	++	++	++
Control-1	51–55	−	−	−	−	−	−
Control-2	61–65	−	−	−	−	−	+
Control-3	96–100	−	−	+	+	−	+
Control-4	66–70	−	−	+	+	+	+
Control-5	56–60	−	−	+	+	+	+

Immunohistochemical grading was performed based on frequency of the staining results, as described previously. The frequency of positive cells in a section was scored as negative (–), less than 25% (+), 26–50% (++), 51–75% (+++), or more than 76% (++++). AD, Alzheimer's disease; ALS, amyotrophic lateral sclerosis; D, dementia; PDC, Parkinsonism-Dementia Complex; 8-NG, 8-Nitroguanine; 8-OHdG, 8-hydroxy-2′-deoxyguanosine; iNOS, inducible nitric oxide synthase; NF-κB, nuclear factor-kappa B.

Immunohistochemical Study

For immunohistochemical analyses, paraffin-embedded, 6 μm sections from the hippocampal area including hippocampus, prosubiculum, subiculum, presubiculum, and parahippocampal gyri were cut and incubated with a range of antibodies as follows: rabbit polyclonal anti-8-NG antibody (1:100, provided by Dr. Ma, Suzuka University of Medical Science, Mie, Japan) for specific detection of nitrated guanine in DNA and RNA, the production and properties of which were reported previously (Ma et al., 2004, 2006; Pinlaor et al., 2004a,b), anti-8-OHdG antibody, a mouse monoclonal antibody for detection of oxidized guanine in RNA (1:30; Trevigen, Gaithersburg, MD, USA) (Kikuchi et al., 2002), anti-iNOS antibody for detection of the inducible form of nitric oxide synthase (1:500; Sigma-Aldrich Japan, Tokyo, Japan) (Levecque et al., 2003; Fernández-Vizarra et al., 2004; Ma et al., 2004, 2006; Pinlaor et al., 2004a,b), anti-NF-κB antibody, a mouse monoclonal antibody against the p65 subunit (1:400; Sigma) (Sugiura et al., 2013) and anti-AT-8, a mouse monoclonal anti-phosphorylated tau antibody [1:100; Innogenetics (Fujirebio Europe N.V.), Ghent, Belgium].

Double Immunofluorescence labeling were performed on sections from paraffin-embedded brain samples that had

been fixed in 4% paraformaldehyde or in 10% formalin. For immunostaining, following de-paraffinization with xylene, sections were hydrated through graded ethanol concentrations. After washing three times with phosphate buffered saline (PBS), the brain sections were treated with 1% skim milk in PBS for 30 min to block non-specific bindings. Subsequently, section was treated with 8-NG and/or iNOS, NF-κB, 8-OHdG, AT-8 for overnight at room temperature. And then treated with Alexa 594-labeled goat antibody against rabbit IgG and Alexa 488-labeled goat antibody against mouse IgG (1:400 diluted in PBS, Molecular Probes, Eugene, OR, USA) for 3 hours. The nuclei were stained with DAPI (Dapi FluoromountG, Birmingham, AL, USA). The stained sections were examined under a fluorescence microscope (BX53, Olympus, Tokyo, Japan).

According to previous reports (Ma et al., 2011; Thanan et al., 2013), immunohistochemical grading was defined based on frequency derived from the staining results. The frequency of positive cells in a section was scored as negative (−), less than 25% (+), 26–50% (++), 51–75% (+ + +), or more than 76% (+ + + +).

RESULTS

Seven Kii ALS/PDC patients showed positive staining for AT-8, 8-NG, iNOS, and NF-κB (100%), and six patients showed positive staining for 8-OHdG (86%). Five AD patients also showed positive staining for AT-8, 8-NG, iNOS, NF-κB, and 8-OHdG (100%). Three control subjects showed positive staining for 8-NG and iNOS (60%), two controls showed positive staining for NF-κB (40%), and four controls showed positive staining for 8-OHdG (80%).

The number of neurons positive for AT-8, 8-NG, iNOS, NF-κB, and 8-OHdG in the patients with Kii ALS/PDC or AD was greater than that in the control subjects (**Table 1**). Additionally, comparing the grouped (−) and (+) against the grouped (++), (+ + +), and (+ + + +) in the score for the frequency of positive cells, statistical analysis using two-sided Fisher's exact test showed the following; AT-8 (Control vs. AD: $p = 0.0079$, Control vs. Kii ALS/PDC: $p = 0.0278$), 8-NG (Control vs. AD: $p = 0.1667$, Control vs. Kii ALS/PDC: $p = 0.0152$, iNOS (Control vs. AD: $p = 0.0476$, Control vs. Kii ALS/PDC: $p = 0.0152$), NF-κB (Control vs. AD: $p = 0.1667$, Control vs. Kii ALS/PDC: $p = 0.0808$), and 8-OHdG (Control vs. AD: $p = 0.1667$, Control vs. Kii ALS/PDC: $p = 0.0808$).

Double immunofluorescence staining of AT-8 and 8-NG showed that some neurons with co-staining of both antibodies in Kii ALS/PDC brains (**Figure 1**). The number of anti-8-NG antibody positive neurons in each patient was greater than that of AT-8 positive neurons (**Figure 1A**). Double immunofluorescence staining of AT-8 and 8-OHdG, and AT-8 and iNOS, showed that most of the AT-8 positive neurons were also co-stained with anti-8-OHdG or anti-iNOS antibodies (**Figures 1B,C**). Double immunofluorescence staining with each pair of antibodies; 8-NG and iNOS, 8-NG and NF-κB, and 8-NG and 8-OHdG, showed co-staining in control and Kii ALS/PDC brains (**Figure 2**). Overall, the positive expression of 8-NG, iNOS, NF-κB and 8-OHdG was 100, 100, 100, and 86% of cells, respectively, in the hippocampal area including hippocampus, prosubiculum, subiculum, presubiculum, and parahippocampal gyri in the cerebrum of the Kii ALS/PDC patients.

DISCUSSION

Regarding the pathomechanism of Kii ALS/PDC, environmental factors such as mineral deficiency have been proposed. Yase (1972) advocated that a combination of hypo-calcium and hypo-magnesium in the drinking water induces secondary hypoparathyroidism, leading to mineral deposition and neuronal cell death. Morimoto et al. (2009) revealed an increase in the ratio of urinary 8-OHdG versus creatinine in Kii ALS/PDC patients, while Kihira et al. suggested OS associated with lifestyle changes might be related to the decrease of Kii ALS/PDC (Kihira et al., 2017). Kokubo et al. (2012) reported that the free radical scavenger, Edaravon, improved volition in patients with ALS/PDC.

The anti-8-NG antibody recognizes the nitrated guanine in DNA and RNA, reflecting NS. The present study revealed that OS and NS are highly involved in the pathogenic mechanism of Kii ALS/PDC, and the nitration could be induced by NO generated via iNOS. Under the condition with acceleration of their production or impairment of the normal reduction, OS and NS can be arise and accelerated or when the mechanisms involved in maintaining the normal reductive cellular environment are impaired. The summation of oxidative and nitrative modifications changes the conformation of key proteins, which contributes to neuronal cell death throughout neuronal dysfunction (Giasson et al., 2002; **Figure 3**). The physiological changes induced by aging may facilitate the accumulation of abnormal proteins through OS and NS (Oliver et al., 1987; Harman, 1992; Stadtman, 1992; Ames et al., 1993; Reiter, 1995; Giasson et al., 2002). While OS and NS has been implicated in many diseases like AD, PD, ALS (Bergeron, 1995; Good et al., 1996; Jenner and Olanow, 1996; Giasson et al., 2002) and Kii ALS/PDC (Morimoto et al., 2009), OS and NS may be promoted by genetic predisposition and/or environmental factors accumulated in the high incidence area or lower the cellular capacity to compensate for such insults.

Nitrative stress and oxidative stress can be exceedingly toxic to neurons. In a state of neurodegeneration, which progress over many years, the aberrant and continuous nitrative and oxidative stress may lead to the accumulation of abnormal proteins and cell death (Giasson et al., 2002). The 8-NG anion radical is formed by NADPH/P450 reductase. Generation of Superoxide ($O2^{-\cdot}$) from NOSs is stimulated by 8-NG and 8-NG prompts $O2^{-\cdot}$ generation by means of reductive activation of NOSs at the reductase domain. The previous study shows that NOS uncoupling, and thereby formation of $O2^{-\cdot}$, might be related to many disorders through the

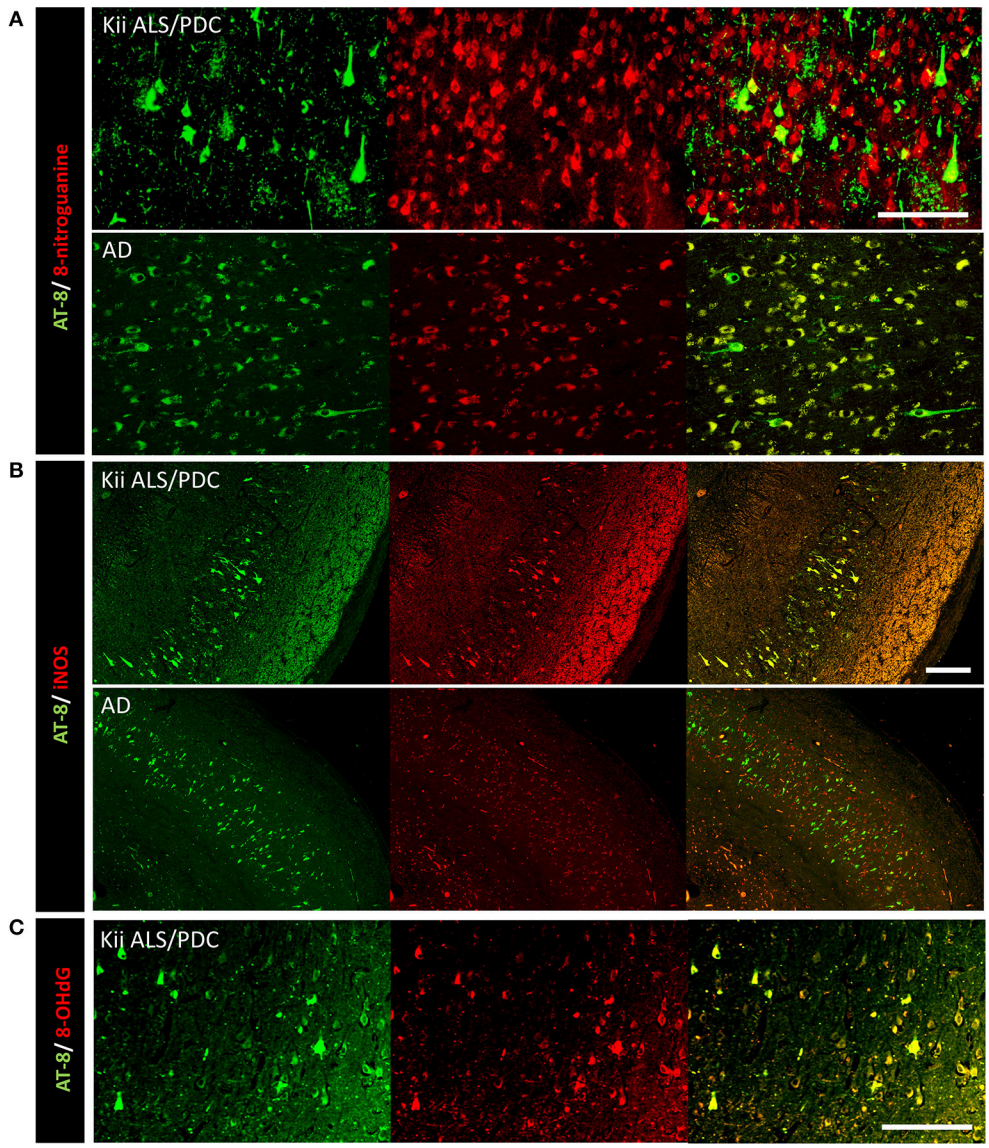

FIGURE 1 | Double immunofluorescence staining in the hippocampus of patients with Kii ALS/PDC and Alzheimer's disease. **(A)** AT-8 and anti-8-NG antibody. **(B)** AT-8 and anti-iNOS antibody. **(C)** AT-8 and anti- 8-OHdG antibody. **(A**: ×200, **B**: ×100, **C**: ×200, scale bars represent 50 μm).

following mechanisms: (1) production of reactive metabolites including hydrogen peroxide, (2) consumption of NO via the rapid reaction with $O2^{-\cdot}$ to form peroxynitrite (ONOO−), and (3) peroxynitrite-induced oxidative and nitrative injuries (Sawa et al., 2003).

Next, we mention the relationship between OS/NS and tau protein. Some studies revealed that chronic OS leaded to increased phosphorylation of tau in culture neurons (Zhu et al., 2005; Su et al., 2010). Furthermore, carbonyl-4-hydroxy-2-nonenal (4-HNE) facilitates aggregation of p-tau *in vitro* (Pérez et al., 2000) and induces hyperphosphorylation of tau (Gómez-Ramos et al., 2003; Liu et al., 2005). In primary cortical neuron cultures of rat treated with cuprizone (a copper chelator in combination with oxidant agents Fe^{2+} and H_2O_2), Glycogen synthase kinase-3 beta (GSK-3β) activity and pathologic hyperphosphorylation of tau significantly increased (Lovell et al., 2004; Lee et al., 2007). Particularly, some tau kinases belong to the family of stress-activated protein kinases, which are activated in response to OS (Goedert et al., 1997; Atzori et al., 2001). Interestingly, HNE directly activates two members of the stress-activated kinase family (JNK and p38) in NT2 neuronal cells (Tamagno et al., 2005). Another pathologic link between abnormal phosphorylation of tau and OS is peptidyl prolyl cis-trans isomerase 1 (PPIase1) or Pin1. This enzyme is significantly downregulated and oxidized in hippocampus of AD patients. Because Pin1 relates to de-phosphorylation of tau, *in vivo* oxidative modifications of Pin1 found in hippocampus of AD patients reduce

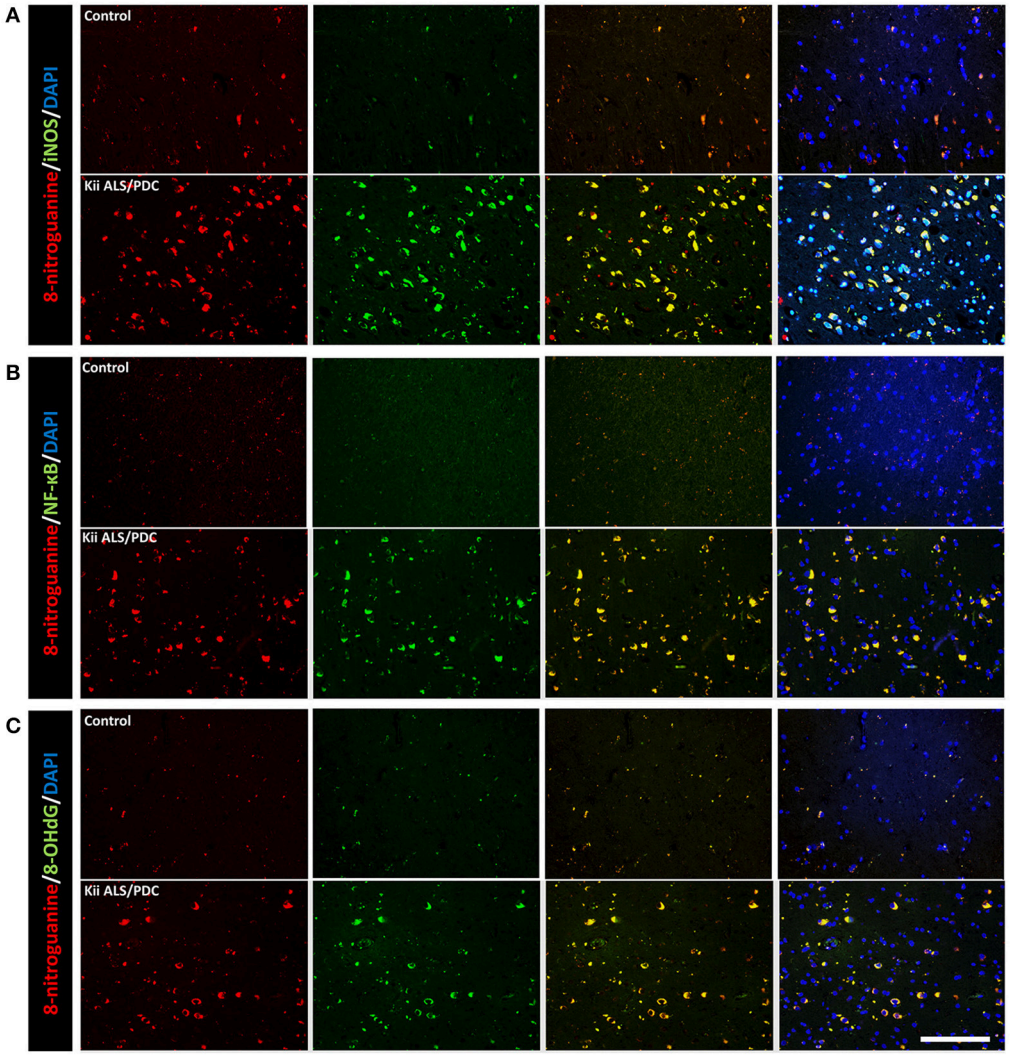

FIGURE 2 | Double immunofluorescence staining in the hippocampus of control and Kii ALS/PDC patients. **(A)** Anti-8-NG antibody and anti-OHdG antibody. **(B)** Anti-8-NG antibody and anti-NF-κB antibody. **(C)** Anti-8-NG antibody and anti- iNOS antibody (all images ×200, scale bar represents 50 μm).

Pin1 activity, leading to increased phosphorylation of tau (Sultana et al., 2006). Additionally, mitochondrial oxidative stress causes hyperphosphorylation of tau (Melov et al., 2007).

On the other hand, there is also substantial evidence for nitrative damage as revealed by immunostaining of NFTs for 3-nitrotyrosine (3-NT) (Good et al., 1996; Smith et al., 1997). Moreover, levels of 3-NT and o-o-dityrosine detected analytically are greatly increased in AD brains (Hensley et al., 1998), which is consistent with the increase in 3-NT cytoplasmic immunoreactivity in many neurons (Smith et al., 1997). Interestingly, astrocytic nitric oxide triggers tau hyperphosphorylation in hippocampal neurons (Saez et al., 2004). Nitrated and Thioflavin-S-positive tau aggregates were produced in a oligodendrocytic cell line treated with peroxynitrite, so this finding implies that nitrative injury is directly linked to the formation of filamentous inclusions of tau (Horiguchi et al., 2003). As another hypothesis, CAPON (carboxy-terminal PDZ ligand of nNOS), a cytoplasmic protein whose C terminus binds to the PDZ domain of nNOS (Jaffrey et al., 1998), may prompt tau phosphorylation and multimerization.

Overall, regarding tau, OS and NS, OS and NS increases oligomerization of truncated tau and hyperphosphorylation of tau which may facilitate tau accumulation in neurons and speed up the process of neurodegeneration (Thanan et al., 2008; Filipcik et al., 2009).

There is other important evidence that the pathogenesis of some neurodegenerative disorders, including AD, PD, and ALS might be involved in the generation of reactive oxygen species (ROS) and/or reactive nitrogen species (RNS), which are related to mitochondrial abnormality. Such defects in respiratory complex activities are possibly related to imbalance of oxidant

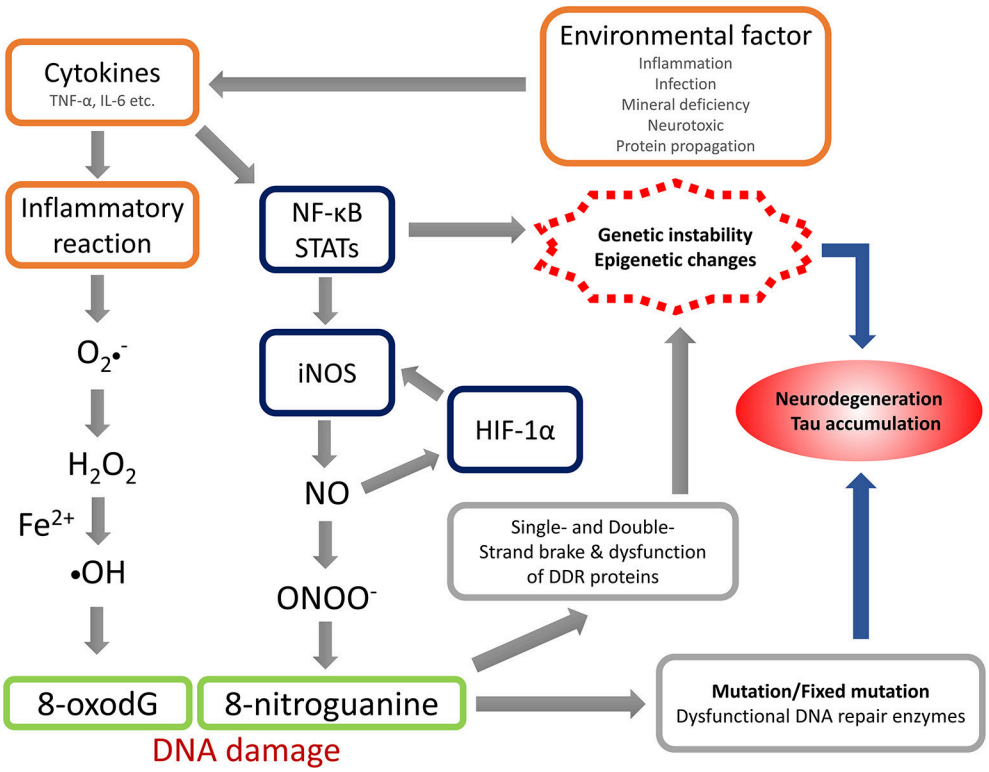

FIGURE 3 | Hypothesis of nitrative stress in the pathomechanism of Kii ALS/PDC. TNF-α, tumor necrosis factor-α; IL-6, interleukin-6; NF-κB, nuclear factor-kappa B; STATs, signal transducers and activators of transcriptions; iNOS, inducible nitric oxide synthase; HIF-1α, hypoxia Inducible Factor-1α; NO, nitric oxide; DDR, DNA damage response.

and antioxidant, and they are said to underlie abnormalities in energy metabolism and induce degeneration of cells (Good et al., 1996; Stewart et al., 2000; Dhir et al., 2008). Mitochondria have multifarious functions and might be essentially significant for adult-onset neurodegenerative disorders including ALS, AD, and PD (Nicholls, 2002). For example, an increased hyperphosphorylation of tau parallels mitochondrial dysfunction and OS in deficient mice in mitochondrial SOD-2 (Melov et al., 2007). As well as cell models and animal models of the neurodegenerative disorders, morphological and biochemical data from analyses of human CNS autopsy, imply that mitochondrial abnormality is a trigger or a propagator of neurodegeneration. New pathomechanisms for mitochondrial disorders and neurodegeneration might be involved in 1-methyl-4-phenyl-1,2,3,6-tetrahydropyridine (mPTP). There is precedence for this logic in mouse models of AD (Du et al., 2008) and ALS (Martin et al., 2009). mPTP involves actively in the pathomechanisms of motor neuronal cell death in ALS mice in a gender-preferential intergenerational pattern (Martin et al., 2009). Therefore, activation of mPTP is a possible trigger for degeneration of motor neurons, and selective vulnerability of motor neurons in ALS might be associated with the trafficking, amount, and composition of mitochondria in the cells.

The results of this study suggest Kii ALS/PDC, other neurodegenerative disorders and aging may have similar mechanisms which associated to the etiology. Furthermore, the increase of OS and NS seen in the Kii ALS/PDC autopsy brain should be reproduced in induced pluripotent stem cells (iPSCs)-derived neurons of Kii ALS/PDC patients as shown in our recent report (Imaizumi et al., 2012), if the Kii ALS/PDC patients have genetic factors underlying the disease development. This is our important future task.

CONCLUSION

NS and/or OS may result in different mechanisms of modification of tau protein which influence the stable tau fibrils formation. Given that markers of NS and OS were highly expressed in the brains of Kii ALS/PDC patients, it suggests the involvement of NS and OS in the disease mechanism.

AUTHOR CONTRIBUTIONS

YH: Research project: Conception and Execution; Manuscript: Writing of the first draft; NM: Research project: Conception and Execution; Manuscript: Writing of the first draft; MY: Research project: Execution; SaM: Research project: Execution; Manuscript: Review and Critique; HO: Research project: Execution; ShM: Research project: Execution; ShoK: Research project: Execution; ShiK: Research project: Conception and

Organization; YK: Research project: Conception; Organization and Execution; Manuscript: Review and Critique.

FUNDING

This work was partly supported by grants-in-aid from the Mie Medical Fund (to SM, YK), the Japan Foundation for Neuroscience and Mental Health (to YK), the Research Committee of CNS Degenerative Diseases (to YK, H26-Nanchi- Ippan-085, collaborator, 2014–2016) and the Research Committee of Muro disease (Kii ALS/PDC) (to YK, 21210301, Chair, 2009–2014), Ministry of Health, Labor and Welfare (MHLW), Japan, by a grant-in-aid for the Scientific Research from the Ministry of Education, Culture, Sports, Science and Technology (MEXT; to YK, 25305030, Chair, 2013–2017), and the Research Consortium of Kii ALS/PDC from the Japan Agency for Medical Research and Development, AMED (to YK, Chair, 17ek0109139h0003, 2015–2017), Japan.

ACKNOWLEDGMENTS

The authors thank Dr. Akihiko Nunomura for providing antibody, Ms. Hisami Akatsuka for the excellent technical assistance in the preparation of tissues for histopathological examination, and Dr. Kazushi Okamoto for supporting statistical analysis. We thank Ann Turnley, Ph.D., from Edanz Group (www.edanzediting.com/ac) for editing a draft of this manuscript.

REFERENCES

Ames, B. N., Shigenaga, M. K., and Hagen, T. M. (1993). Oxidants, antioxidants, and the degenerative diseases of aging. *Proc. Natl. Acad. Sci. U.S.A.* 90, 7915–7922. doi: 10.1073/pnas.90.17.7915

Atzori, C., Ghetti, B., Piva, R., Srinivasan, A. N., Zolo, P., Delisle, M. B., et al. (2001). Activation of the JNK/p38 pathway occurs in diseases characterized by tau protein pathology and is related to tau phosphorylation but not to apoptosis. *J. Neuropathol. Exp. Neurol.* 60, 1190–1197. doi: 10.1093/jnen/60.12.1190

Bergeron, C. (1995). Oxidative stress: its role in the pathogenesis of amyotrophic lateral sclerosis. *J. Neurol. Sci.* 129, S81–S84. doi: 10.1016/0022-510X(95)00071-9

de la Monte, S. M., Ganju, N., Feroz, N., Luong, T., Banerjee, K., Cannon, J., et al. (2000). Oxygen free radical injury is sufficient to cause some Alzheimer-type molecular abnormalities in human CNS neuronal cells. *J. Alzheimers Dis.* 2, 261–281. doi: 10.3233/JAD-2000-23-406

Dhir, A., Akula, K. K., and Kulkarni, S. K. (2008). Tiagabine, a GABA uptake inhibitor, attenuates 3-nitropropionic acid-induced alterations in various behavioral and biochemical parameters in rats. *Prog. Neuropsychopharmacol. Biol. Psychiatry* 32, 835–843. doi: 10.1016/j.pnpbp.2007.12.017

Du, H., Guo, L., Fang, F., Chen, D., Sosunov, A. A., McKhann, G. M., et al. (2008). Cyclophilin D deficiency attenuates mitochondrial and neuronal perturbation and ameliorates learning and memory in Alzheimer's disease. *Nat. Med.* 14, 1097–1105. doi: 10.1038/nm.1868

Fernández-Vizarra, P., Fernández, A. P., Castro-Blanco, S., Encinas, J. M., Serrano, J., Bentura, M. L., et al. (2004). Expression of nitric oxide system in clinically evaluated cases of Alzheimer's disease. *Neurobiol. Dis.* 15, 287–305. doi: 10.1016/j.nbd.2003.10.010

Filipcik, P., Cente, M., Krajciova, G., Vanicky, I., and Novak, M. (2009). Cortical and hippocampal neurons from truncated tau transgenic rat express multiple markers of neurodegeneration. *Cell. Mol. Neurobiol.* 29, 895–900. doi: 10.1007/s10571-009-9372-8

Giasson, B. I., Ischiropoulos, H., Lee, V. M., and Trojanowski, J. Q. (2002). The relationship between oxidative/nitrative stress and pathological inclusions in Alzheimer's and Parkinson's diseases. *Free Radic. Biol. Med.* 32, 1264–1275. doi: 10.1016/S0891-5849(02)00804-3

Goedert, M., Hasegawa, M., Jakes, R., Lawler, S., Cuenda, A., and Cohen, P. (1997). Phosphorylation of microtubule-associated protein tau by stress-activated protein kinases. *FEBS Lett.* 409, 57–62. doi: 10.1016/S0014-5793(97)00483-3

Gómez-Ramos, A., Díaz-Nido, J., Smith, M. A., Perry, G., and Avila, J. (2003). Effect of the lipid peroxidation product acrolein on tau phosphorylation in neural cells. *J. Neurosci. Res.* 71, 863–870. doi: 10.1002/jnr.10525

Good, P. F., Werner, P., Hsu, A., Olanow, C. W., and Perl, D. P. (1996). Evidence of neuronal oxidative damage in Alzheimer's disease. *Am. J. Pathol.* 149, 21–28.

Harman, D. (1992). Free radical theory of aging. *Mutat. Res.* 275, 257–266. doi: 10.1016/0921-8734(92)90030-S

Hensley, K., Maidt, M. L., Yu, Z., Sang, H., Markesbery, W. R., and Floyd, R. A. (1998). Electrochemical analysis of protein nitrotyrosine and dityrosine in the Alzheimer brain indicates region-specific accumulation. *J. Neurosci.* 18, 8126–8132.

Horiguchi, T., Uryu, K., Giasson, B. I., Ischiropoulos, H., LightFoot, R., Bellmann, C., et al. (2003). Nitration of tau protein is linked to neurodegeneration in tauopathies. *Am. J. Pathol.* 163, 1021–1031. doi: 10.1016/S0002-9440(10)63462-1

Imaizumi, Y., Okada, Y., Akamatsu, W., Koike, M., Kuzumaki, N., Hayakawa, H., et al. (2012). Mitochondrial dysfunction associated with increased oxidative stress and α-synuclein accumulation in PARK2 iPSC-derived neurons and postmortem brain tissue. *Mol. Brain* 5:35. doi: 10.1186/1756-6606-5-35

Jaffrey, S. R., Snowman, A. M., Eliasson, M. J., Cohen, N. A., and Snyder, S. H. (1998). CAPON: a protein associated with neuronal nitric oxide synthase that regulates its interactions with PSD95. *Neuron* 20, 115–124. doi: 10.1016/S0896-6273(00)80439-0

Jenner, P., and Olanow, C. W. (1996). Oxidative stress and the pathogenesis of Parkinson's disease. *Neurology* 47(6 Suppl. 3), S161–S170. doi: 10.1212/WNL.47.6_Suppl_3.161S

Jesberger, J. A., and Richardson, J. S. (1991). Oxygen free radicals and brain dysfunction. *Int. J. Neurosci.* 57, 1–17. doi: 10.3109/00207459109150342

Kihira, T., Okamoto, K., Sakurai, I., Arakawa, Y., Wakayama, I., Takamiya, K., et al. (2017). Lifestyle changes and oxidative stress in a high-incidence area of amyotrophic lateral sclerosis in the Southwestern Kii Peninsula, Japan. *Int. Med.* 56, 1497–1506. doi: 10.2169/internalmedicine.56.8038

Kikuchi, A., Takeda, A., Onodera, H., Kimpara, T., Hisanaga, K., Sato, N., et al. (2002). Systemic increase of oxidative nucleic acid damage in Parkinson's disease and multiple system atrophy. *Neurobiol. Dis.* 9, 244–248. doi: 10.1006/nbdi.2002.0466

Kokubo, Y., and Kuzuhara, S. (2001). Neurological and neuropathological studies of amyotrophic lateral sclerosis/parkinsonism-dementia complex in the Kii peninsula of Japan. *Rinsho Shinkeigaku* 41, 769–774.

Kokubo, Y., and Kuzuhara, S. (2004). Neurofibrillary tangles in ALS and Parkinsonism-dementia complex focus in Kii, Japan. *Neurology* 63, 2399–2401. doi: 10.1212/01.WNL.0000147241.52694.6A

Kokubo, Y., Morimoto, S., Nakagawa, T., Morimoto, S., and Kuzuhara, S. (2012). Clinical trial of edaravone in amyotrophic lateral sclerosis/parkinsonism-dementia complex of the Kii peninsula of Japan. *Neurol. Ther.* 29:670.

Kuzuhara, S. (2004). Amyotrophic lateral sclerosis-parkinsonism-dementia complex of the Kii peninsula of Japan, Nippon *Rinsho Shinkeigaku* 62, S141–S146.

Kuzuhara, S., and Kokubo, Y. (2005). Atypical parkinsonism of Japan: amyotrophic lateral sclerosis-parkinsonism-dementia complex of the Kii peninsula of Japan (Muro disease): an update. *Mov. Disord. Suppl.* 12, S108–S113. doi: 10.1002/mds.20548

Kuzuhara, S., Kokubo, Y., Sasaki, R., Narita, Y., Yabana, T., Hasegawa, M., et al. (2001). Familial amyotrophic lateral sclerosis and parkinsonism-dementia

complex of the Kii peninsula of Japan: clinical and neuropathological study and tau analysis. *Ann. Neurol.* 49, 501–511. doi: 10.1002/ana.100

Lee, K. Y., Koh, S. H., Noh, M. Y., Park, K. W., Lee, Y. J., and Kim, S. H. (2007). Glycogen synthase kinase-3beta activity plays very important roles in determining the fate of oxidative stress-inflicted neuronal cells. *Brain Res.* 1129, 89–99. doi: 10.1016/j.brainres.2006.10.055

Levecque, C., Elbaz, A., Clavel, J., Richard, F., Vidal, J. S., Amouyel, P., et al. (2003). Association between Parkinson's disease and polymorphisms in the nNOS and iNOS genes in a community-based case-control study. *Hum. Mol. Genet.* 12, 79–86. doi: 10.1093/hmg/ddg009

Liu, Q., Smith, M. A., Avilá, J., DeBernardis, J., Kansal, M., Takeda, A., et al. (2005). Alzheimer-specific epitopes of tau represent lipid peroxidation-induced conformations. *Free Radic. Biol. Med.* 38, 746–754. doi: 10.1016/j.freeradbiomed.2004.11.005

Lovell, M. A., Xiong, S., Xie, C., Davies, P., and Markesbery, W. R. (2004). Induction of hyperphosphorylated tau in primary rat cortical neuron cultures mediated by oxidative stress and glycogen synthase kinase-3. *J. Alzheimers Dis.* 6, 659–671. doi: 10.3233/JAD-2004-6610

Ma, N., Adachi, Y., Hiraku, Y., Horiki, N., Horiike, S., Imoto, I., et al. (2004). Accumulation of 8-nitroguanine in human gastric epithelium induced by Helicobacter pylori infection. *Biochem. Biophys. Res. Commun.* 319, 506–510. doi: 10.1016/j.bbrc.2004.04.193

Ma, N., Tagawa, T., Hiraku, Y., Murata, M., Ding, X., and Kawanishi, S. (2006). 8-Nitroguanine formation in oral leukoplakia, a premalignant lesion. *Nitric Oxide* 14, 137–143. doi: 10.1016/j.niox.2005.09.012

Ma, N., Thanan, R., Kobayashi, H., Hammam, O., Wishahi, M., El Leithy, T., et al. (2011). Nitrative DNA damage and Oct3/4 expression in urinary bladder cancer with *Schistosomahaematobium* infection. *Biochem. Biophys. Res. Commun.* 414, 344–349. doi: 10.1016/j.bbrc.2011.09.073

Martin, L. J., Gertz, B., Pan, Y., Price, A. C., Molkentin, J. D., and Chang, Q. (2009). The mitochondrial permeability transition pore in motor neurons: involvement in the pathobiology of ALS mice. *Exp. Neurol.* 218, 333–346. doi: 10.1016/j.expneurol.2009.02.015

Melov, S., Adlard, P. A., Morten, K., Johnson, F., Golden, T. R., Hinerfeld, D., et al. (2007). Mitochondrial oxidative stress causes hyperphosphorylation of tau. *PLoS One*. 2:e536. doi: 10.1371/journal.pone.0000536

Mimuro, M., Yoshida, M., Kuzuhara, S., and Kokubo, Y. (2017). Amyotrophic lateral sclerosis and parkinsonism-dementia complex of the Kii peninsula: a multiple proteinopathy. *Neuropathology.* doi: 10.1111/neup.12434. [Epub ahead of print].

Morimoto, S., Kuzuhara, S., and Kokubo, Y. (2009). Increased oxidative stress in patients with amyotrophic lateral sclerosis/Parkinsonism-dementia complex in the Kii peninsula, Japan. *Mov. Disord.* 24, 123–126. doi: 10.1002/mds.22362

Nicholls, D. G. (2002). Mitochondrial function and dysfunction in the cell: its relevance to aging and aging-related disease. *Int. J. Biochem. Cell Biol.* 34, 1372–1381. doi: 10.1016/S1357-2725(02)00077-8

Nunomura, A., Chiba, S., Lippa, C. F., Cras, P., Kalaria, R. N., Takeda, A., et al. (2004). Neuronal RNA oxidation is a prominent feature of familial Alzheimer's disease. *Neurobiol. Dis.* 17, 108–113. doi: 10.1016/j.nbd.2004.06.003

Oliver, C. N., Ahn, B. W., Moerman, E. J., Goldstein, S., and Stadtman, E. R. (1987). Age-related changes in oxidized proteins. *J. Biol. Chem.* 262, 5488–5491.

Pérez, M., Cuadros, R., Smith, M. A., Perry, G., and Avila, J. (2000). Phosphorylated, but not native, tau protein assembles following reaction with the lipid peroxidation product, 4-hydroxy-2-nonenal. *FEBS Lett.* 486, 270–274. doi: 10.1016/S0014-5793(00)02323-1

Pinlaor, S., Hiraku, Y., Ma, N., Yongvanit, P., Semba, R., Oikawa, S., et al. (2004a). Mechanism of NO-mediated oxidative and nitrative DNA damage in hamsters infected with *Opisthorchis viverrini*: a model of inflammation-mediated carcinogenesis. *Nitric Oxide* 11, 175–183. doi: 10.1016/j.niox.2004.08.004

Pinlaor, S., Ma, N., Hiraku, Y., Yongvanit, P., Semba, R., Oikawa, S., et al. (2004b). Repeated infection with *Opisthorchis viverrini* induces accumulation of 8-nitroguanine and 8-oxo-7,8-dihydro-2′-deoxyguanine in the bile duct of hamsters via inducible nitric oxide synthase. *Carcinogenesis* 25, 1535–1542. doi: 10.1093/carcin/bgh157

Reiter, R. J. (1995). Oxidative processes and antioxidative defense mechanisms in the aging brain. *FASEB J.* 9, 526–533.

Saez, T. E., Pehar, M., Vargas, M., Barbeito, L., and Maccioni, R. B. (2004). Astrocytic nitric oxide triggers tau hyperphosphorylation in hippocampal neurons. *In Vivo* 18, 275–280.

Sawa, T., Akaike, T., Ichimori, K., Akuta, T., Kaneko, K., Nakayama, H., et al. (2003). Superoxide generation mediated by 8-nitroguanosine, a highly redox-active nucleic acid derivative. *Biochem. Biophys. Res. Commun.* 311, 300–306. doi: 10.1016/j.bbrc.2003.10.003

Smith, M. A., Richey Harris, P. L., Sayre, L. M., Beckman, J. S., and Perry, G. (1997). Widespread peroxynitrite-mediated damage in Alzheimer's disease. *J. Neurosci.* 17, 2653–2657.

Stadtman, E. R. (1992). Protein oxidation and aging. *Science* 257 1220–1224.

Stewart, V. C., Sharpe, M. A., Clark, J. B., and Heales, S. J. (2000). Astrocyte-derived nitric oxide causes both reversible and irreversible damage to the neuronal mitochondrial respiratory chain. *J. Neurochem.* 75, 694–700. doi: 10.1046/j.1471-4159.2000.0750694.x

Su, B., Wang, X., Lee, H. G., Tabaton, M., Perry, G., Smith, M. A., et al. (2010). Chronic oxidative stress causes increased tau phosphorylation in M17 neuroblastoma cells. *Neurosci Lett.* 468, 267–271. doi: 10.1016/j.neulet.2009.11.010

Sugiura, H., Okita, S., Kato, T., Naka, T., Kawanishi, S., Ohnishi., S., et al. (2013). Protection by taurine against INOS-dependent DNA damage in heavily exercised skeletal muscle by inhibition of the NF-κB signaling pathway. *Adv. Exp. Med. Biol.* 775, 237–246. doi: 10.1007/978-1-4614-6130-2_20

Sultana, R., Boyd-Kimball, D., Poon, H. F., Cai, J., Pierce, W. M., Klein, J. B., et al. (2006). Oxidative modification and down-regulation of Pin1 in Alzheimer's disease hippocampus: a redox proteomics analysis. *Neurobiol. Aging* 27, 918–925. doi: 10.1016/j.neurobiolaging.2005.05.005

Tamagno, E., Parola, M., Bardini, P., Piccini, A., Borghi, R., Guglielmotto, M., et al. (2005). Beta-site APP cleaving enzyme up-regulation induced by 4-hydroxynonenal is mediated by stress-activated protein kinases pathways. *J. Neurochem.* 92, 628–636. doi: 10.1111/j.1471-4159.2004.02895.x

Thanan, R., Murata, M., Ning, M., Hammam, O., Wishahi, M., Leithy, T. E., et al. (2008). Generation, accumulation and degradation of aberrant tau proteins in cortical neurons of transgenic rat during pathogenesis of chronic neurodegenerative disease. *FASEB J.* 22:324.

Thanan, R., Pairojkul, C., Pinlaor, S., Khuntikeo, N., Wongkham, C., Sripa, B., et al. (2013). Inflammation-related DNA damage and expression of CD133 and Oct3/4 in cholangiocarcinoma patients with poor prognosis. *Free Radic. Biol. Med.* 65, 464–472. doi: 10.1016/j.freeradbiomed.2013.07.034

Yase, Y. (1972). The pathogenesis of amyotrophic lateral sclerosis. *Lancet* 12, 292–296. doi: 10.1016/S0140-6736(72)92903-0

Zhu, X., Lee, H. G., Casadesus, G., Avila, J., Drew, K., Perry, G., et al. (2005). Oxidative imbalance in Alzheimer's disease. *Mol. Neurobiol.* 31, 205–217. doi: 10.1385/MN:31:1-3:205

Conflict of Interest Statement: The authors declare that the research was conducted in the absence of any commercial or financial relationships that could be construed as a potential conflict of interest.

The reviewer JS declared a past co-authorship with one of the authors HO to the handling Editor.

frontiers in Neurology

MINI REVIEW
published: 07 December 2017
doi: 10.3389/fneur.2017.00663

In Vivo Tau Imaging for a Diagnostic Platform of Tauopathy Using the rTg4510 Mouse Line

Naruhiko Sahara[1], Masafumi Shimojo[1], Maiko Ono[1], Hiroyuki Takuwa[1], Marcelo Febo[2], Makoto Higuchi[1] and Tetsuya Suhara[1]*

[1] Department of Functional Brain Imaging Research, National Institute of Radiological Sciences, National Institutes for Quantum and Radiological Science and Technology, Chiba, Japan, [2] Department of Psychiatry and Neuroscience, University of Florida College of Medicine, Gainesville, FL, United States

Association of tau deposition with neurodegeneration in Alzheimer's disease (AD) and related tau-positive neurological disorders collectively referred to as tauopathies indicates contribution of tau aggregates to neurotoxicity. The discovery of tau gene mutations in FTDP-17-*tau* kindreds has provided unequivocal evidence that tau abnormalities alone can induce neurodegenerative disorders. Therefore, visualization of tau accumulation would offer a reliable, objective index to aid in the diagnosis of tauopathy and to assess the disease progression. Positron emission tomography (PET) imaging of tau lesions is currently available using several tau PET ligands. Because most tau PET ligands have the property of an extrinsic fluorescent dye, these ligands are considered to be useful for both PET and fluorescence imaging. In addition, small-animal magnetic resonance imaging (MRI) is available for both structural and functional imaging. Using these advanced imaging techniques, *in vivo* studies on a mouse model of tauopathy will provide significant insight into the translational research of neurodegenerative diseases. In this review, we will discuss the utilities of PET, MRI, and fluorescence imaging for evaluating the disease progression of tauopathy.

Keywords: tau protein, transgenic mouse, positron emission tomography, magnetic resonance imaging, two-photon microscopy

OPEN ACCESS

Edited by:
Jesus Avila, Universidad Autonoma de Madrid, Spain

Reviewed by:
Felix Hernandez, Consejo Superior de Investigaciones Científicas (CSIC), Spain
Mar Perez, Universidad Autonoma de Madrid, Spain

****Correspondence:***
Naruhiko Sahara
sahara.naruhiko@qst.go.jp

Specialty section:
This article was submitted to Neurodegeneration, a section of the journal Frontiers in Neurology

Received: *16 October 2017*
Accepted: *23 November 2017*
Published: *07 December 2017*

Citation:
Sahara N, Shimojo M, Ono M, Takuwa H, Febo M, Higuchi M and Suhara T (2017) In Vivo Tau Imaging for a Diagnostic Platform of Tauopathy Using the rTg4510 Mouse Line. Front. Neurol. 8:663. doi: 10.3389/fneur.2017.00663

INTRODUCTION

Dementia is a leading cause of death in developed countries. Increasing age is the greatest risk factor for dementia. About 46 million people in the world are estimated to be suffering from dementia, and this figure is expected to rise to 135 million by 2050. Alzheimer's disease (AD) is the most common type of dementia. The global impact of AD will strikingly affect social and economic costs. Distinctive features of AD are the deposited accumulations of β-amyloid (Aβ) protein fragments and intracellular neurofibrillary tangles (NFTs) (1). NTFs are closely associated with the severity of brain function loss in AD (2). Therefore, making tau protein a target in the treatment of AD has become a major therapeutic strategy.

Recent advances in positron emission tomography (PET) imaging research have led to significant breakthroughs with the application of newly developed tracers for visualizing regional tau depositions (3–8). This technology allows us to non-invasively evaluate the progression of tau pathology in living brains. PBB3 was developed as a novel PET tracer that binds with tau for the diagnosis of AD and other neurodegenerative diseases regarded as tauopathies (4, 9). PET imaging using [^{11}C]PBB3

(radiotracer) is superior in detecting tau deposits, and it is closely aligned with disease symptoms. This was also confirmed by our tauopathy mouse models (4; Ishikawa, forthcoming[1]). ^{11}C-labeled tracers, due to their short half-life, are generally unsuitable for clinical practice, but [^{11}C]PBB3 can be used to evaluate certain tau conditions including AD (4, 10). The fluorescent quality of PBB3 makes it especially useful for multimodal imaging, allowing us to assess its binding by microscopic observation of related cells and tissues.

Animal models of tauopathy are essential for preclinical studies of AD and related dementias. The rTg4510 mouse line was developed to model aspects of tauopathy through forebrain expression of the P301L mutated human tau (11). Expression of human tau is controlled by the tetracycline transactivator transgene under the CaMKIIα promoter. This mouse line develops progressive intracellular tau aggregations in corticolimbic areas and forebrain atrophy (11). The age-dependent tau pathology of rTg4510 mice has been investigated in detail by immunohistochemical and biochemical examinations (12–14). These postmortem brain-based studies showed an extensive increase of pathological tau inclusions in the cerebral cortex and hippocampus between 4 and 6 months of age. Now, for both current and therapeutic strategies, rather than endpoint measurements, researchers are eagerly involved in the development of new *in vivo* protocols for tracking the progressive pathological status in living animals.

Taking advantage of the multimodality of the PBB3 ligand, *in vivo* monitoring of NFT formation is now available for possible in tauopathy mouse models, including the rTg4510 mouse. In addition, advanced brain magnetic resonance imaging (MRI) techniques have enabled us to visualize neuronal dysfunction and the structural changes related to neurodegenerative processes in living animals. Here, we will introduce *in vivo* multimodal imaging technologies, including PET, MRI, and fluorescence imaging to investigate the real-time events of tau-related neuropathology.

MRI STUDIES FOR A MOUSE MODEL OF TAUOPATHY

Magnetic resonance imaging-based volumetry is a valuable tool for assessing disease progression in humans (15–19). As translational research of neurodegenerative diseases, several groups have reported studies using volumetric MRI in mouse models (20–25). Age-dependent volume reduction in both cerebral cortex and hippocampus of the rTg4510 mouse line was clearly demonstrated on MRI (24, 25). The volume (size) of the cerebral cortex from 5 to 8-month-old rTg4510 mice was significantly less (by approximately 20%) than that of age-matched non-transgenic (non-tg) mice (24). Brain atrophy in rTg4510 mice as examined by MRI was in agreement with previous histopathology findings (13, 26). A gender difference showing more severe phenotype in female rTg4510 mice compared with males (27) was confirmed by volumetric MRI study (24).

In addition to volumetric MRI, MR-based *in vivo* imaging techniques, including MR spectroscopy (MRS), manganese-enhanced MRI (MEMRI), arterial spin labeling, amide proton transfer imaging, and diffusion tensor imaging (DTI), have been tested to evaluate brain functions and microstructural changes in living rTg4510 mice (24, 25, 28–32). MEMRI is a technique for measuring neuronal function, because the manganese ion (Mn^{2+}) accumulates in actively firing neurons through voltage-gated Ca^{2+} channels and serves as a positive contrast agent in T1-weighted brain images (33, 34). Using this technique, Perez et al. observed a reduction in both neuronal activity and volume in the hippocampus of 6-month-old rTg4510 mice (25). Fontaine et al. demonstrated neuronal dysfunction in the CA3 and CA1 regions of 3-month-old rTg4510 mice (32). Together, these studies illustrate the importance of the MEMRI method as a diagnostic research tool for the early detection of neuronal dysfunction in rTg4510 mice.

Diffusion tensor imaging is another MR-based imaging technique, which is applied to assess the integrity and organization of myelinated structures such as axons in white matter (WM) and also in gray matter regions (35). For this purpose, we used DTI to examine age-related alterations in WM diffusion anisotropy in rTg4510 and non-tg control mice (29). Our results indicated that 8-month-old rTg4510 mice show significant reductions in fractional anisotropy (FA) in WM structures compared with control non-tg and young (2.5-month-old) rTg4510 mice. The microstructural changes contributing to these age- and tauopathy-associated WM changes were supported by electron microscopic evidence of disorganized axonal processes and the presence of interprocess spaces, which could explain the reduced FA in aged rTg4510 mice (29). Reduced FA at a later age (over 7.5 months) was confirmed by another research group (30, 31). Since, reduced FA values in WM were mostly observed at an age that included the presence of significant atrophy and tau pathology, this standard method may be useful for assessing the therapeutic efficacy of treatments that may be used to reduce or prevent neurodegenerative progression. On the other hand, examination with additional diffusion anisotropy indices such as the mode of anisotropy allowed us to detect early signs (at 2.5 months old) of WM disorganization (29). Although disorganization of myelin morphology at this age was not determined, WM degeneration may be one of the early signs of tauopathy. Nevertheless, reduced WM integrity associated with tau pathology was confirmed by *in vivo* DTI studies.

TAU PET TRACERS

Current tau PET tracers are mostly designed by β-sheet binding properties. In principle, filamentous tau aggregates (e.g., NFTs, neuropile threads, tufted astrocytes, astrocytic plaques, and coiled bodies) will be labeled by these tracers with distinct specificity and selectivity. Up to date, three types of radiotracers have been widely tested for the clinical assessment of patients with tauopathy [reviewed in Ref. (36)]. These tracers include the arcyquinoline derivative THK5351 (37), the pyrido-indole derivative AV-1451

[1] Ishikawa I, Tokunaga M, Maeda J, Minamihisamatsu T, Shimojo M, Takuwa H, et al. In vivo visualization of tau accumulation, microglial activation and brain atrophy in a mouse model of tauopathy rTg4510. *J Alzheimers Dis* (2018, Forthcoming).

(38, 39), and the phenyl/pyridinyl-butadienyl-benzothiazole/benzothiazolium derivative PBB3 (4). Screening of potential tracers was performed by *in vitro* binding assays in AD brain homogenates and autoradiographies of AD brain sections. [^{18}F]THK5351, [^{18}F]AV-1451, and [^{11}C]PBB3 showed good affinity for tau deposits and no selectivity of amyloid plaques. Accumulating evidence has shown that tau PET using these tracers might not detect pretangles in tauopathy brains (9, 40). Comparative *in vitro* binding assay of [^{18}F]AV-1451 and [^{11}C]PBB3 revealed that the binding of [^{11}C]PBB3 to non-AD-type tau pathology (e.g., tufted astrocytes, astrocytic plaques, and pick bodies) was higher than that of [^{18}F]AV-1451 (9). Another comparative study of [^{3}H]AV-1451 and [^{3}H]THK523 showed a distinct binding affinity for NFTs (41). Potential off-target bindings of [^{18}F]AV-1451 and [^{18}F]THK5351 to monoamine oxidase A (MAO-A) and MAO-B, respectively, were also observed (36, 42, 43). Although binding properties of tau PET tracers have been vigorously investigated for the past decade, the specificity and selectivity of PET signals to tau pathology are still to be fully understood.

TAU PET IMAGING STUDIES OF rTg4510 MICE

Micro-PET imaging of tau pathology in tg mouse models of tauopathy has contributed to the characterization of novel PET tracers. Using [^{18}F]THK523, micro-PET imaging in 6-month-old rTg4510 mice successfully showed significantly higher radiotracer retentions in brains compared with non-tg or PS1/APP mice (44). [^{11}C]PBB3-PET imaging in another tauopathy mouse model, PS19 tg (expressing P301S mutant human tau) (4), and [^{18}F]THK5117-PET imaging in P301S tg and biGT (bigenic GSK-3β × P301L tau) tg mice (45) were reported to show higher tracer uptake in tg than in non-tg mice. On the other hand, there was no significant difference in retention of [^{18}F]AV-1451 between TAPP (bigenic APPswe × P301L tau) tg and non-tg mice (39). Inconsistency of these micro-PET analyses was mostly due to the use of different tg mouse models. Technical limitations also stem from the diversity of pathological characteristics in different mouse models. The distribution of tau deposits and the time course of pathological tau accumulation in tg mice differed from each other. It is very important to compare *in vivo* bindings of different tracers with reproducible mouse models. To initiate the development of a screening platform for tau PET tracers, our group has recently demonstrated longitudinal micro-PET imaging in rTg4510 mice (see text footnote 1). Consistent with neuropathological and biochemical observations, our [^{11}C]PBB3 PET imaging of rTg4510 mice showed an age-dependent increase in [^{11}C]PBB3 signal and that [^{11}C]PBB3 retention was inversely correlated with neocortical volumes. The increasing [^{11}C]PBB3 signal reached a plateau by 7 months of age. The correlation between [^{11}C]PBB3 levels and

TABLE 1 | Reference list for *in vivo* imaging in living rTg4510 mice.

Imaging system	Imaging techniques	Reagents and application for *in vivo* imaging	Reference
Magnetic resonance imaging (MRI)	Volumetric MRI ^{1}H MR spectroscopy		Yang et al. (24) Neuroimage
MRI	Manganese enhanced MRI (MEMRI)	Manganese (intraperitoneal injection)	Perez et al. (25) Mol. Neurodegeneration
MRI	MEMRI	Manganese (nasal lavage)	Majid et al. (28) Neuroimage Clin.
MRI	Diffusion tensor imaging (DTI)		Sahara et al. (29) Neurobiol. Aging
MRI	Volumetric MRI, DTI Arterial spin labeling (ASL), Exchange saturation transfer (CEST), glucose CEST	Glucose (intraperitoneal injection)	Wells et al. (30) Neuroimage
MRI	Volumetric MRI, DTI, ASL, CEST		Holmes et al. (31) Neurobiol. Aging
MRI	MEMRI	Manganese (intraperitoneal injection)	Fontaine et al. (32) Neurobiol. Aging
PET	PET	r^{18}FITHK523	Fodero-Tavoletti et al. (44) Brain
PET MRI	PET volumetric MRI	r^{11}ClPBB3 ^{11}ClAC-5216 (TSPO)	(see text footnote 1)
Two-photon microscopy	Fluorescence imaging	Thioflavin S (intracerebral injection)	Spires-Jones et al. (57) J Neurosci.
Two-photon microscopy	Fluorescence imaging	Thioflavin S (intracerebral injection) X-34 (i.v.)	De Calignon et al. (53) Nature
Two-photon microscopy	Fluorescence imaging	Thioflavin S (intracerebral injection)	Kopeikina et al. (58) PLoS One
Two-photon microscopy	Fluorescence imaging	Thioflavin S (intracerebral injection)	Kuchibhotla et al. (59) PNAS
Two-photon microscopy	Fluorescence imaging	GFP (AAV serotype2) GCaMP6m (AAV 1/2 hybrid serotype)	Jackson et al. (56) Cell Rep.

brain atrophy disappeared in rTg4510 mice over 7 months old. Since, tau pathology is tightly linked to neuronal loss, the disappearance rate of [^{11}C]PBB3-positive neurons may increase at age over 7 months. It should be noted that microglial activation in rTg4510 brains examined using translocator protein (TSPO) (18-kDa TSPO)-PET imaging showed significant correlation with both [^{11}C]PBB3 level and brain atrophy (see text footnote 1). rTg4510 will be a useful model for investigating the mechanisms of tau-induced neuroinflammation. Nevertheless, in combination with tau PET imaging, the imaging of neuroinflammation will offer an additional diagnostic parameter for tauopathy.

IN VIVO FLUORESCENCE IMAGING FOR DETECTING TAU PATHOLOGY

The invention of two-photon excitation laser scanning microscopy has given new impetus to the research field of investigating *in vivo* brain cell dynamics (46). In combination with newly developed fluorescence imaging techniques, cellular and molecular mechanisms underlying brain functions and impairments can be examined using *in vivo* animal models. In theory, the spatial scales of two-photon microscopy are from a micron to a millimeter. The side length of field-of-views can reach a few 100 μm. The imaging depth reached has been up to ~1 mm depending on the properties of the tissue (47). Using this technology, AD mouse models have been investigated with regard to monitoring the time course of disease progression [reviewed in Ref. (48)]. Hyman's group first reported *in vivo* visualization of amyloid plaques in APP tg mouse lines (PDAPP mice and tg2576 mice) (49, 50). Clearance of plaques by anti-Aβ antibody was monitored by two-photon microscopy after Thioflavin S injection into the brain. Fluorescence imaging using Pittsburgh Compound B (PiB), which is used for amyloid PET imaging, was also examined to visualize amyloid plaques in APP tg mouse lines (51). As a result, the multimodality of PiB ligand for both fluorescence and PET imaging was clearly demonstrated. Because the PBB3 ligand was derived from the same tracer family as the PiB ligand, a similar approach was used to visualize the tau pathology in PS19 tg mice (4). Moreover, the current chronic cranial window setting enables the use of long-period two-photon imaging for more than 2 months (52). As for our study, longitudinal monitoring of PBB3-positive neurons has been performed in living rTg4510 mice (Takuwa et al., manuscript in preparation). Our data showed that PBB3-positive inclusions were visualized with two-photon imaging at an age of as early as 4 months, with fluorescence signals then reaching a plateau at 6 months. These data are in agreement

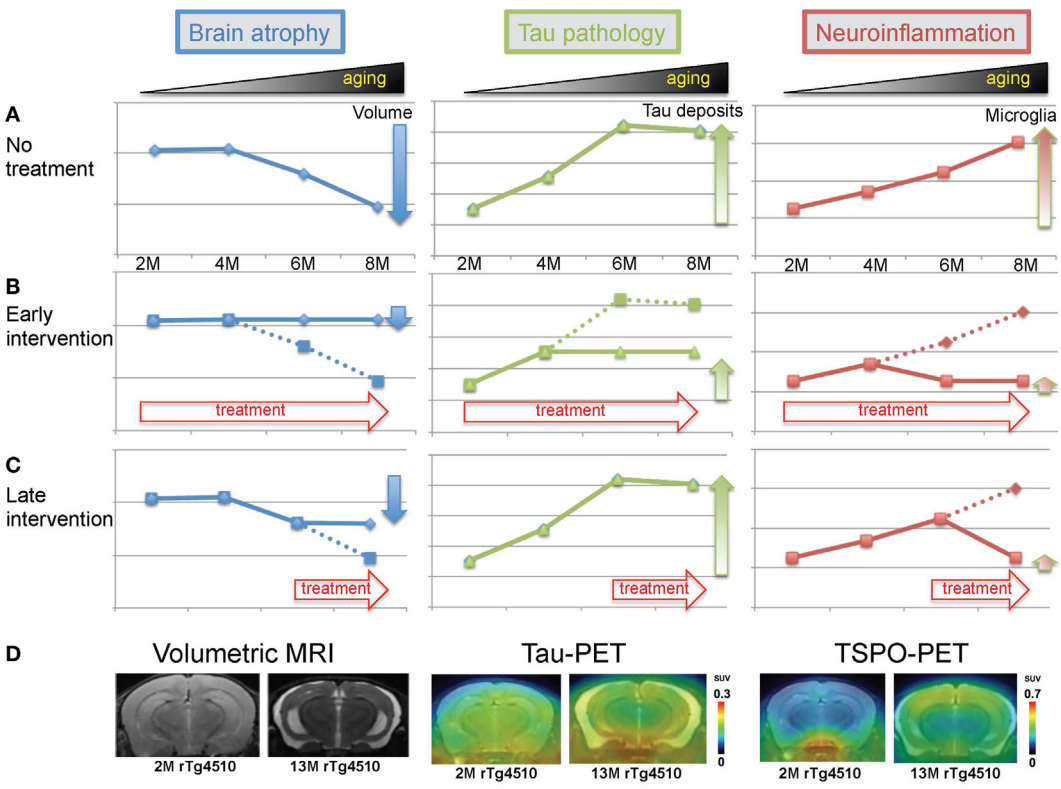

FIGURE 1 | Imaging modalities for investigating tau-induced brain atrophy and neuroinflammation. **(A)** Theoretical processes of volume change, pathological tau accumulation, and microglial activation in rTg4510 mice. **(B)** Effects of early intervention. Treatment was started from 2 months of age. **(C)** Effects of late intervention. Treatment was started from 6 months of age. **(D)** Representative images of volumetric magnetic resonance imaging (MRI), tau-positron emission tomography (PET), and translocator protein-PET in 2- and 13-month-old rTg4510 mice.

with both [^{11}C]PBB3 PET imaging and volumetric MRI, suggesting multimodal imaging utilities of the PBB3 ligand. On the other hand, Hyman's group has investigated the mechanism of neuronal loss in rTg4510 mouse brains using the fluorescence indicator of caspase activation and β-sheet ligand X-34 (a Congo red derivative) (53). Their data indicate that NFT formation has a neuroprotective effect against caspase-mediated neuronal death. Synaptic dysfunction is another key event taking place during the pathogenesis of tauopathy. Previous reports showed decreased dendritic spine and synapse density in cortical slices prepared from 9 to 10-month-old rTg4510 mice (54, 55). Most recently, Jackson et al. demonstrated the visualization of synapses in the somatosensory cortex of rTg4510 mice by two-photon microscopy after the injection of adeno-associated virus that drove neuronal expression of either GFP or GCaMP6m (56). For longitudinal imaging, GFP-expressing axonal and dendritic regions were imaged weekly to investigate the turnover of axonal terminal boutons and dendritic spines. For functional imaging, GCaMP6-expressing neurons were imaged in lightly anesthetized animals to measure neuronal activity in response to whisker stimulation. The authors observed mismatched abnormalities in pre-and post-synaptic turnover coinciding with disrupted neuronal activity at 5 months of age. Their data suggests that synaptic dysfunction precedes tangle-associated neurodegeneration. Although linkage between aggregated tau formation and synaptic dysfunction remains unclear, *in vivo* monitoring of tau pathology at cellular levels provides an advantage for dissecting the mechanisms of tau toxicity.

DESIGN FOR A DIAGNOSTIC PLATFORM OF TAUOPATHY

The rTg4510 mouse is one of the widely used models of tauopathy. As described above, several groups have conducted *in vivo* imaging studies on rTg4510 mice (**Table 1**). Because the time course of tau pathology and forebrain atrophy have been well examined using postmortem materials, experimental designs for drug intervention can be easily designed (**Figure 1**). Since, this mouse model allows the tetracycline-repressible overexpression of human tau, doxycycline treatment for the suppression of tau expression will provide a positive control in an experimental design of the evaluation of therapeutic candidates. Previous study showed that suppression of tau from 5.5 months of age reversed memory deficits, while tangles persisted and continued to accumulate (11). Therefore, early intervention starting at 2 months of age could be more effective to prevent both NFT formation and brain atrophy (**Figure 1B**). Although effects will be limited, late intervention would be worthwhile if aggravation of tau-induced brain atrophy can be slowed down (**Figure 1C**). In our study, we developed a unique diagnostic platform of *in vivo* imaging of volumetric MRI, tau-PET, and TSPO-PET (**Figure 1D**). Brains of living rTg4510 mice can be used to monitor their volume, pathological tau accumulation, and neuroinflammation. Moreover, live cell imaging with two-photon microscopy allows us to capture NFT formation and neuronal death in rTg4510 mice. Using these platforms, we expect to be able to validate several drug candidates in the foreseeable future.

CONCLUSION

For more effective therapies, the pre-clinical evaluation of drugs for tauopathy is needed. The use of animal models that recapitulate the critical features of the disease, such as NFTs, cognitive impairment, brain atrophy, and neuronal loss, is essential. The rTg4510 mouse model of tauopathy fulfills the required features, despite the fact that tau protein was expressed at a non-physiologically higher level over the total life span. *In vivo*, brain imaging offers reliable approaches to validating the pathological status and to determining the efficacy of drugs for exploring disease-modifying therapies.

AUTHOR CONTRIBUTIONS

Authors wrote and proofed the manuscript.

ACKNOWLEDGMENTS

This research was supported in part by grants from Grant-in-Aid for Science Research on Innovation Area ("Brain Protein Aging" 26117001 to NS) and Scientific Research (C) (15K06793 to NS) from the Ministry of Education, Culture, Sports, Science, and Technology, Japan, and from the Strategic Research Program for Brain Sciences from the Japan Agency for Medical Research and Development, AMED. MH holds a patent on compounds including PBB3 (JP 5422782/EP 12 844 742.3).

REFERENCES

1. Alzheimer A, Stelzmann RA, Schnitzlein HN, Murtagh FR. An English translation of Alzheimer's 1907 paper, "Uber eine eigenartige Erkankung der Hirnrinde". *Clin Anat* (1995) 8:429–31. doi:10.1002/ca.980080612
2. Gomez-Isla T, Hollister R, West H, Mui S, Growdon JH, Petersen RC, et al. Neuronal loss correlates with but exceeds neurofibrillary tangles in Alzheimer's disease. *Ann Neurol* (1997) 41:17–24. doi:10.1002/ana.410410106
3. Harada R, Okamura N, Furumoto S, Yoshikawa T, Arai H, Yanai K, et al. Use of a benzimidazole derivative BF-188 in fluorescence multispectral imaging for selective visualization of Tau protein fibrils in the Alzheimer's disease brain. *Mol Imaging Biol* (2014) 16:19–27. doi:10.1007/s11307-013-0667-2
4. Maruyama M, Shimada H, Suhara T, Shinotoh H, Ji B, Maeda J, et al. Imaging of tau pathology in a tauopathy mouse model and in Alzheimer patients compared to normal controls. *Neuron* (2013) 79:1094–108. doi:10.1016/j.neuron.2013.07.037
5. Okamura N, Furumoto S, Harada R, Tago T, Yoshikawa T, Fodero-Tavoletti M, et al. Novel 18F-labeled arylquinoline derivatives for noninvasive imaging of tau pathology in Alzheimer disease. *J Nucl Med* (2013) 54:1420–7. doi:10.2967/jnumed.112.117341
6. Chien DT, Szardenings AK, Bahri S, Walsh JC, Mu F, Xia C, et al. Early clinical PET imaging results with the novel PHF-Tau radioligand [F18]-T808. *J Alzheimers Dis* (2014) 38:171–84. doi:10.3233/JAD-130098
7. Ariza M, Kolb HC, Moechars D, Rombouts F, Andres JI. Tau positron emission tomography (PET) imaging: past, present, and future. *J Med Chem* (2015) 58:4365–82. doi:10.1021/jm5017544

8. Villemagne VL, Fodero-Tavoletti MT, Masters CL, Rowe CC. Tau imaging: early progress and future directions. *Lancet Neurol* (2015) 14:114–24. doi:10.1016/S1474-4422(14)70252-2
9. Ono M, Sahara N, Kumata K, Ji B, Ni R, Koga S, et al. Distinct binding of PET ligands PBB3 and AV-1451 to tau fibril strains in neurodegenerative tauopathies. *Brain* (2017) 140(3):764–80. doi:10.1093/brain/aww339
10. Kimura Y, Ichise M, Ito H, Shimada H, Ikoma Y, Seki C, et al. PET quantification of Tau pathology in human brain with 11C-PBB3. *J Nucl Med* (2015) 56:1359–65. doi:10.2967/jnumed.115.160127
11. Santacruz K, Lewis J, Spires T, Paulson J, Kotilinek L, Ingelsson M, et al. Tau suppression in a neurodegenerative mouse model improves memory function. *Science* (2005) 309:476–81. doi:10.1126/science.1113694
12. Ramsden M, Kotilinek L, Forster C, Paulson J, Mcgowan E, Santacruz K, et al. Age-dependent neurofibrillary tangle formation, neuron loss, and memory impairment in a mouse model of human tauopathy (P301L). *J Neurosci* (2005) 25:10637–47. doi:10.1523/JNEUROSCI.3279-05.2005
13. Dickey C, Kraft C, Jinwal U, Koren J, Johnson A, Anderson L, et al. Aging analysis reveals slowed tau turnover and enhanced stress response in a mouse model of tauopathy. *Am J Pathol* (2009) 174:228–38. doi:10.2353/ajpath.2009.080764
14. Sahara N, Deture M, Ren Y, Ebrahim AS, Kang D, Knight J, et al. Characteristics of TBS-extractable hyperphosphorylated tau species: aggregation intermediates in rTg4510 mouse brain. *J Alzheimers Dis* (2013) 33:249–63. doi:10.3233/JAD-2012-121093
15. Du AT, Schuff N, Amend D, Laakso MP, Hsu YY, Jagust WJ, et al. Magnetic resonance imaging of the entorhinal cortex and hippocampus in mild cognitive impairment and Alzheimer's disease. *J Neurol Neurosurg Psychiatry* (2001) 71:441–7. doi:10.1136/jnnp.71.4.441
16. Apostolova LG, Dutton RA, Dinov ID, Hayashi KM, Toga AW, Cummings JL, et al. Conversion of mild cognitive impairment to Alzheimer disease predicted by hippocampal atrophy maps. *Arch Neurol* (2006) 63:693–9. doi:10.1001/archneur.63.5.693
17. Devanand DP, Pradhaban G, Liu X, Khandji A, De Santi S, Segal S, et al. Hippocampal and entorhinal atrophy in mild cognitive impairment: prediction of Alzheimer disease. *Neurology* (2007) 68:828–36. doi:10.1212/01.wnl.0000256697.20968.d7
18. Fan Y, Batmanghelich N, Clark CM, Davatzikos C, Alzheimer's Disease Neuroimaging Initiative. Spatial patterns of brain atrophy in MCI patients, identified via high-dimensional pattern classification, predict subsequent cognitive decline. *Neuroimage* (2008) 39:1731–43. doi:10.1016/j.neuroimage.2007.10.031
19. Whitwell JL, Shiung MM, Przybelski SA, Weigand SD, Knopman DS, Boeve BF, et al. MRI patterns of atrophy associated with progression to AD in amnestic mild cognitive impairment. *Neurology* (2008) 70:512–20. doi:10.1212/01.wnl.0000280575.77437.a2
20. McDaniel B, Sheng H, Warner DS, Hedlund LW, Benveniste H. Tracking brain volume changes in C57BL/6J and ApoE-deficient mice in a model of neurodegeneration: a 5-week longitudinal micro-MRI study. *Neuroimage* (2001) 14:1244–55. doi:10.1006/nimg.2001.0934
21. Weiss C, Venkatasubramanian PN, Aguado AS, Power JM, Tom BC, Li L, et al. Impaired eyeblink conditioning and decreased hippocampal volume in PDAPP V717F mice. *Neurobiol Dis* (2002) 11:425–33. doi:10.1006/nbdi.2002.0555
22. Lau JC, Lerch JP, Sled JG, Henkelman RM, Evans AC, Bedell BJ. Longitudinal neuroanatomical changes determined by deformation-based morphometry in a mouse model of Alzheimer's disease. *Neuroimage* (2008) 42:19–27. doi:10.1016/j.neuroimage.2008.04.252
23. Maheswaran S, Barjat H, Rueckert D, Bate ST, Howlett DR, Tilling L, et al. Longitudinal regional brain volume changes quantified in normal aging and Alzheimer's APP x PS1 mice using MRI. *Brain Res* (2009) 1270:19–32. doi:10.1016/j.brainres.2009.02.045
24. Yang D, Xie Z, Stephenson D, Morton D, Hicks CD, Brown TM, et al. Volumetric MRI and MRS provide sensitive measures of Alzheimer's disease neuropathology in inducible tau transgenic mice (rTg4510). *Neuroimage* (2011) 54:2652–8. doi:10.1016/j.neuroimage.2010.10.067
25. Perez PD, Hall G, Kimura T, Ren Y, Bailey RM, Lewis J, et al. In vivo functional brain mapping in a conditional mouse model of human tauopathy (taup301l) reveals reduced neural activity in memory formation structures. *Mol Neurodegener* (2013) 8:9. doi:10.1186/1750-1326-8-9
26. Spires TL, Orne JD, Santacruz K, Pitstick R, Carlson GA, Ashe KH, et al. Region-specific dissociation of neuronal loss and neurofibrillary pathology in a mouse model of tauopathy. *Am J Pathol* (2006) 168:1598–607. doi:10.2353/ajpath.2006.050840
27. Yue M, Hanna A, Wilson J, Roder H, Janus C. Sex difference in pathology and memory decline in rTg4510 mouse model of tauopathy. *Neurobiol Aging* (2011) 32:590–603. doi:10.1016/j.neurobiolaging.2009.04.006
28. Majid T, Ali YO, Venkitaramani DV, Jang MK, Lu HC, Pautler RG. In vivo axonal transport deficits in a mouse model of fronto-temporal dementia. *Neuroimage Clin* (2014) 4:711–7. doi:10.1016/j.nicl.2014.02.005
29. Sahara N, Perez PD, Lin WL, Dickson DW, Ren Y, Zeng H, et al. Age-related decline in white matter integrity in a mouse model of tauopathy: an in vivo diffusion tensor magnetic resonance imaging study. *Neurobiol Aging* (2014) 35:1364–74. doi:10.1016/j.neurobiolaging.2013.12.009
30. Wells JA, O'callaghan JM, Holmes HE, Powell NM, Johnson RA, Siow B, et al. In vivo imaging of tau pathology using multi-parametric quantitative MRI. *Neuroimage* (2015) 111:369–78. doi:10.1016/j.neuroimage.2015.02.023
31. Holmes HE, Colgan N, Ismail O, Ma D, Powell NM, O'callaghan JM, et al. Imaging the accumulation and suppression of tau pathology using multiparametric MRI. *Neurobiol Aging* (2016) 39:184–94. doi:10.1016/j.neurobiolaging.2015.12.001
32. Fontaine SN, Ingram A, Cloyd RA, Meier SE, Miller E, Lyons D, et al. Identification of changes in neuronal function as a consequence of aging and tauopathic neurodegeneration using a novel and sensitive magnetic resonance imaging approach. *Neurobiol Aging* (2017) 56:78–86. doi:10.1016/j.neurobiolaging.2017.04.007
33. Pautler RG, Mongeau R, Jacobs RE. In vivo trans-synaptic tract tracing from the murine striatum and amygdala utilizing manganese enhanced MRI (MEMRI). *Magn Reson Med* (2003) 50:33–9. doi:10.1002/mrm.10498
34. Lee JH, Silva AC, Merkle H, Koretsky AP. Manganese-enhanced magnetic resonance imaging of mouse brain after systemic administration of MnCl2: dose-dependent and temporal evolution of T1 contrast. *Magn Reson Med* (2005) 53:640–8. doi:10.1002/mrm.20368
35. Mori S, Zhang J. Principles of diffusion tensor imaging and its applications to basic neuroscience research. *Neuron* (2006) 51:527–39. doi:10.1016/j.neuron.2006.08.012
36. Saint-Aubert L, Lemoine L, Chiotis K, Leuzy A, Rodriguez-Vieitez E, Nordberg A. Tau PET imaging: present and future directions. *Mol Neurodegener* (2017) 12:19. doi:10.1186/s13024-017-0162-3
37. Harada R, Okamura N, Furumoto S, Furukawa K, Ishiki A, Tomita N, et al. 18F-THK5351: a novel PET radiotracer for imaging neurofibrillary pathology in Alzheimer disease. *J Nucl Med* (2016) 57:208–14. doi:10.2967/jnumed.115.164848
38. Zhang W, Arteaga J, Cashion DK, Chen G, Gangadharmath U, Gomez LF, et al. A highly selective and specific PET tracer for imaging of tau pathologies. *J Alzheimers Dis* (2012) 31:601–12. doi:10.3233/JAD-2012-120712
39. Xia CF, Arteaga J, Chen G, Gangadharmath U, Gomez LF, Kasi D, et al. [(18)F] T807, a novel tau positron emission tomography imaging agent for Alzheimer's disease. *Alzheimers Dement* (2013) 9:666–76. doi:10.1016/j.jalz.2012.11.008
40. Harada R, Okamura N, Furumoto S, Tago T, Yanai K, Arai H, et al. Characteristics of Tau and its ligands in PET imaging. *Biomolecules* (2016) 6:7. doi:10.3390/biom6010007
41. Cai L, Qu B, Hurtle BT, Dadiboyena S, Diaz-Arrastia R, Pike VW. Candidate PET radioligand development for neurofibrillary tangles: two distinct radioligand binding sites identified in postmortem Alzheimer's disease brain. *ACS Chem Neurosci* (2016) 7:897–911. doi:10.1021/acschemneuro.6b00051
42. Harada R, Ishiki A, Kai H, Sato N, Furukawa K, Furumoto S, et al. Correlations of 18F-THK5351 PET with post-mortem burden of tau and astrogliosis in Alzheimer's disease. *J Nucl Med* (2017). doi:10.2967/jnumed.117.197426
43. Ng KP, Pascoal TA, Mathotaarachchi S, Therriault J, Kang MS, Shin M, et al. Monoamine oxidase B inhibitor, selegiline, reduces 18F-THK5351 uptake in the human brain. *Alzheimers Res Ther* (2017) 9:25. doi:10.1186/s13195-017-0253-y
44. Fodero-Tavoletti MT, Okamura N, Furumoto S, Mulligan RS, Connor AR, Mclean CA, et al. 18F-THK523: a novel in vivo tau imaging ligand for Alzheimer's disease. *Brain* (2011) 134:1089–100. doi:10.1093/brain/awr038
45. Brendel M, Jaworska A, Probst F, Overhoff F, Korzhova V, Lindner S, et al. Small-animal PET imaging of tau pathology with 18F-THK5117 in 2

transgenic mouse models. *J Nucl Med* (2016) 57:792–8. doi:10.2967/jnumed.115.163493
46. Svoboda K, Yasuda R. Principles of two-photon excitation microscopy and its applications to neuroscience. *Neuron* (2006) 50:823–39. doi:10.1016/j.neuron.2006.05.019
47. Theer P, Denk W. On the fundamental imaging-depth limit in two-photon microscopy. *J Opt Soc Am A Opt Image Sci Vis* (2006) 23:3139–49. doi:10.1364/JOSAA.23.003139
48. Shimojo M, Higuchi M, Suhara T, Sahara N. Imaging multimodalities for dissecting Alzheimer's disease: advanced technologies of positron emission tomography and fluorescence imaging. *Front Neurosci* (2015) 9:482. doi:10.3389/fnins.2015.00482
49. Bacskai BJ, Kajdasz ST, Christie RH, Carter C, Games D, Seubert P, et al. Imaging of amyloid-beta deposits in brains of living mice permits direct observation of clearance of plaques with immunotherapy. *Nat Med* (2001) 7:369–72. doi:10.1038/85525
50. Christie RH, Bacskai BJ, Zipfel WR, Williams RM, Kajdasz ST, Webb WW, et al. Growth arrest of individual senile plaques in a model of Alzheimer's disease observed by in vivo multiphoton microscopy. *J Neurosci* (2001) 21:858–64.
51. Bacskai BJ, Hickey GA, Skoch J, Kajdasz ST, Wang Y, Huang GF, et al. Four-dimensional multiphoton imaging of brain entry, amyloid binding, and clearance of an amyloid-beta ligand in transgenic mice. *Proc Natl Acad Sci U S A* (2003) 100:12462–7. doi:10.1073/pnas.2034101100
52. Tomita Y, Kubis N, Calando Y, Tran Dinh A, Meric P, Seylaz J, et al. Long-term in vivo investigation of mouse cerebral microcirculation by fluorescence confocal microscopy in the area of focal ischemia. *J Cereb Blood Flow Metab* (2005) 25:858–67. doi:10.1038/sj.jcbfm.9600077
53. de Calignon A, Fox LM, Pitstick R, Carlson GA, Bacskai BJ, Spires-Jones TL, et al. Caspase activation precedes and leads to tangles. *Nature* (2010) 464:1201–4. doi:10.1038/nature08890
54. Rocher AB, Crimins JL, Amatrudo JM, Kinson MS, Todd-Brown MA, Lewis J, et al. Structural and functional changes in tau mutant mice neurons are not linked to the presence of NFTs. *Exp Neurol* (2010) 223:385–93. doi:10.1016/j.expneurol.2009.07.029
55. Crimins JL, Rocher AB, Peters A, Shultz P, Lewis J, Luebke JI. Homeostatic responses by surviving cortical pyramidal cells in neurodegenerative tauopathy. *Acta Neuropathol* (2011) 122:551–64. doi:10.1007/s00401-011-0877-0
56. Jackson JS, Witton J, Johnson JD, Ahmed Z, Ward M, Randall AD, et al. Altered synapse stability in the early stages of tauopathy. *Cell Rep* (2017) 18:3063–8. doi:10.1016/j.celrep.2017.03.013
57. Spires-Jones TL, De Calignon A, Matsui T, Zehr C, Pitstick R, Wu HY, et al. In vivo imaging reveals dissociation between caspase activation and acute neuronal death in tangle-bearing neurons. *J Neurosci* (2008) 28:862–7. doi:10.1523/JNEUROSCI.3072-08.2008
58. Kopeikina KJ, Wegmann S, Pitstick R, Carlson GA, Bacskai BJ, Betensky RA, et al. Tau causes synapse loss without disrupting calcium homeostasis in the rTg4510 model of tauopathy. *PLoS One* (2008) 8:e80834. doi:10.1371/journal.pone.0080834
59. Kuchibhotla KV, Wegmann S, Kopeikina KJ, Hawkes J, Rudinskiy N, Andermann ML, et al. Neurofibrillary tangle-bearing neurons are functionally integrated in cortical circuits in vivo. *Proc Natl Acad Sci U S A* (2014) 111:510–4. doi:10.1073/pnas.1318807111

Conflict of Interest Statement: The authors declare that the research was conducted in the absence of any commercial or financial relationships that could be construed as a potential conflict of interest.

frontiers in Neuroscience

REVIEW
published: 20 April 2018
doi: 10.3389/fnins.2018.00259

Phosphorylation of Threonine 175 Tau in the Induction of Tau Pathology in Amyotrophic Lateral Sclerosis—Frontotemporal Spectrum Disorder (ALS-FTSD). A Review

Alexander J. Moszczynski[1†], *Matthew A. Hintermayer*[1†] *and Michael J. Strong*[1,2*]

[1] *Molecular Medicine Research Group, Schulich School of Medicine & Dentistry, Robarts Research Institute, Western University, London, ON, Canada,* [2] *Department of Clinical Neurological Sciences, Schulich School of Medicine & Dentistry, Western University, London, ON, Canada*

OPEN ACCESS

Edited by:
Gen Sobue,
Nagoya University, Japan

Reviewed by:
Jürgen Götz,
The University of Queensland, Australia
Ryuichi Harada,
Tohoku University, Japan

***Correspondence:**
Michael J. Strong
mstrong@uwo.ca

[†]*These authors have contributed equally to this work.*

Specialty section:
This article was submitted to Neurodegeneration, a section of the journal Frontiers in Neuroscience

Received: *14 January 2018*
Accepted: *04 April 2018*
Published: *20 April 2018*

Citation:
Moszczynski AJ, Hintermayer MA and Strong MJ (2018) Phosphorylation of Threonine 175 Tau in the Induction of Tau Pathology in Amyotrophic Lateral Sclerosis—Frontotemporal Spectrum Disorder (ALS-FTSD). A Review. Front. Neurosci. 12:259. doi: 10.3389/fnins.2018.00259

Approximately 50–60% of all patients with amyotrophic lateral sclerosis (ALS) will develop a deficit of frontotemporal function, ranging from frontotemporal dementia (FTD) to one or more deficits of neuropsychological, speech or language function which are collectively known as the frontotemporal spectrum disorders of ALS (ALS-FTSD). While the neuropathology underlying these disorders is most consistent with a widespread alteration in the metabolism of transactive response DNA-binding protein 43 (TDP-43), in both ALS with cognitive impairment (ALSci) and ALS with FTD (ALS-FTD; also known as MND-FTD) there is evidence for alterations in the metabolism of the microtubule associated protein tau. This alteration in tau metabolism is characterized by pathological phosphorylation at residue Thr^{175} ($pThr^{175}$ tau) which *in vitro* is associated with activation of GSK3β ($pTyr^{216}$GSK3β), phosphorylation of Thr^{231}tau, and the formation of cytoplasmic inclusions with increased rates of cell death. This putative pathway of $pThr^{175}$ induction of $pThr^{231}$ and the formation of pathogenic tau inclusions has been recently shown to span a broad range of tauopathies, including chronic traumatic encephalopathy (CTE) and CTE in association with ALS (CTE-ALS). This pathway can be experimentally triggered through a moderate traumatic brain injury, suggesting that it is a primary neuropathological event and not secondary to a more widespread neuronal dysfunction. In this review, we discuss the neuropathological underpinnings of the postulate that ALS is associated with a tauopathy which manifests as a FTSD, and examine possible mechanisms by which phosphorylation at Thr^{175}tau is induced. We hypothesize that this might lead to an unfolding of the hairpin structure of tau, activation of GSK3β and pathological tau fibril formation through the induction of *cis*-Thr^{231} tau conformers. A potential role of TDP-43 acting synergistically with pathological tau metabolism is proposed.

Keywords: amyotrophic lateral sclerosis, chronic traumatic encephalopathy, frontotemporal dementia, TDP-43, microtubule associated tau protein

INTRODUCTION

Amyotrophic lateral sclerosis (ALS, Lou Gehrig's Disease) has classically been considered to be a disorder purely of the descending supraspinal and lower motor neurons, the net result of which is an insidiously progressive degenerative process culminating in death within 3–5 years following symptom onset for the majority of patients (Charcot and Joffroy, 1869; Strong, 2003). However, the concept that ALS is a pure motor disorder has been gradually replaced by one in which it is recognized that between 50 and 60% of all ALS patients will have a concurrent disorder of frontotemporal function (Strong, 2008; Elamin et al., 2011; Phukan et al., 2012; Oh et al., 2014; Montuschi et al., 2015; Strong et al., 2017). Although the literature historically contained a number of individual ALS case reports in whom a concurrent neuropsychological or behavioral disorder had been identified, the recognition that a significant proportion of ALS patients could also have a frank dementia is more recent (Hudson, 1981; Bak and Hodges, 2001). It is now recognized that ALS can include a broad range of neuropsychological, speech, language, or behavioral pathologies that have recently been termed "amyotrophic lateral sclerosis – frontotemporal spectrum disorder (ALS-FTSD)" (Strong et al., 2017). ALS-FTSD includes impairments in cognition (ALSci), behavioral dysfunction (ALSbi), a dysexecutive syndrome (ALScbi), or a frontotemporal dementia (ALS-FTD) meeting the Neary or Hodges criteria (Neary et al., 1998; Hodges and Miller, 2001; Rascovsky et al., 2007).

As our understanding of the clinical phenomenology of ALS-FTSD has evolved, so too has our understanding of its pathobiology. In contemporary nomenclature, the frontotemporal lobar degenerations (FTLD) are categorized into three neuropathological subtypes depending on the pattern of pathological protein deposition that is observed: FTLD-tau for those in which a tauopathy [pathological inclusions consisting of the microtubule associated protein tau (tau)] is clearly evident; FTLD-TDP for those in which transactive response DNA-binding protein of 43 kDa (TDP-43) deposition as neuronal or glial inclusions is the hallmark; and, FTLD-FUS for a small proportion of cases in which the DNA/RNA binding protein, fused in sarcoma (FUS), is deposited. For a minority of cases, none of these markers are evident, but there is evidence of widespread protein ubiquitin conjugation, suggesting a disorder of the ubiquitin-proteasome system (UPS). In this latter subgroup, the terminology FTLD-UPS is applied. Finally, an exceptionally rare subgroup will demonstrate a FTLD in which the molecular pathology (i.e., tau, TDP-43, FUS or ubiquitin) is not known, in which case the terminology of FTLD-NOS (not otherwise specified) is applied (Mackenzie et al., 2011; Irwin et al., 2015).

In its most florid form, ALS-FTSD bears all of the neuropathological features of a FTLD in which there is a strong positive correlation between the degree of cognitive dysfunction and the extent of pathological intraneuronal deposition of TDP-43 (Cykowski et al., 2017). Typically observed as a predominantly nuclear protein, in ALS and under conditions of neuronal stress or injury, TDP-43 undergoes a marked upregulation in its expression and adopts a predominantly cytosolic localization (Arai et al., 2006; Neumann et al., 2006; Mackenzie et al., 2011). This applies to both motor neurons and cortical neurons where the latter forms the basis for characterizing the FTLD of ALS as FTLD-TDP. This has been taken therefore to imply that the frontotemporal dysfunction of ALS cannot be grounded in alterations in the metabolism of tau, or potentially as an overlap syndrome. In this review, we will examine the evidence for alterations in tau metabolism in ALSci, and provide the basis for the consideration of this disorder as a tauopathy that is tightly integrated with the dysmetabolism of TDP-43.

ALS-FTSD: CLINICAL & NEUROIMAGING CHARACTERIZATION

The presence of frontotemporal dysfunction in an ALS patient is a negative prognostic indicator, heralding a significant reduction in survivorship. This is particularly true for those individuals in which the primary manifestation is either a dysexecutive syndrome or behavioral impairment (Olney et al., 2005; Elamin et al., 2011; Hu et al., 2013). While current epidemiological studies consider a range of prognostic factors that can have an impact on survivorship such as age of onset, rate of deterioration as measured by the ALSFRS–R Total Score, diagnostic delay, age at diagnosis, and metabolic markers, it is noteworthy that few account for the presence or absence of neuropsychological, speech or language dysfunction as a significant prognostic variable (Chiò et al., 2009; Lunetta et al., 2015; Couratier et al., 2016). In part, this may represent a bias introduced because of the complexity of detecting neuropsychological, speech, language, or behavioral impairments (Farhan et al., 2017). Because of this, the Strong criteria (2009) have been recently revised to increase the simplicity and applicability of these international consensus criteria (Strong et al., 2009, 2017).

Revision of the Strong criteria was also driven by the need to broaden the definition of frontotemporal spectrum disorder in ALS to include deficits in social cognition, including deficits in Theory of Mind (ToM). ToM refers specifically to the capacity to attribute independent mental states to others, and can be divided into an affective and cognitive component. The affective component of ToM refers to one's ability to make inferences regarding the emotions and feelings of others, whereas the cognitive component refers to the ability to infer others' intentions and beliefs (Shamay-Tsoory et al., 2009; Adenzato et al., 2010; Poletti et al., 2012). Deficits in both social cognition and ToM, localizing to the mesial frontal/anterior cingulate, are present in a significant proportion of ALS patients, even when there is no clear evidence to suggest more widespread higher-order cortical dysfunction (Meier et al., 2010; Girardi et al., 2011; Poletti et al., 2012; Cerami et al., 2014; van der Hulst et al., 2015). This suggests that deficits in social cognition and ToM might be the earliest harbinger of frontotemporal dysfunction in ALS.

The concept of non-motor dysfunction in ALS being reflective of a widespread higher cortical impairment—with a degree of preponderance to the frontal lobes, particularly the mesial frontal cortex—is supported by a broad array of neuroimaging studies

(Abrahams et al., 2004; Lillo et al., 2010; Agosta et al., 2011, 2013; Goldstein et al., 2011; Prudlo et al., 2012; Ambikairajah et al., 2014). Such studies need to be interpreted in the light of underlying genetic traits of the individuals being studied, as it is increasingly clear that ALS is also syndromic with the clinical and molecular phenotype being driven by an ever-increasing array of known genetic variants (Strong, 2001, 2017; Turner and Verstraete, 2015). The contributions of neuroimaging have extended beyond identifying the general degree of cerebral atrophy accompanying frontotemporal syndromes, as visualized with either computed tomography (CT) or magnetic resonance imaging (MRI). Neuroimaging platforms such as single positron emission computerized tomography (SPECT) (Neary et al., 1990), MRI-based measures of functional connectivity (Douaud et al., 2011), and advanced structural MRI sequences that define subcortical frontotemporal white matter tract projection pathology (Agosta et al., 2016) can now provide an evaluation of the extent of loss of functional integrity. Positron emission tomography (PET) has proven invaluable in our understanding of the anatomic and cellular extent of the pathobiology of ALS-FTSD, including the involvement of non-neuronal cells in the disease process (Cistaro et al., 2012, 2014). Increasingly, these neuroimaging modalities are being linked to understanding the molecular pathology of ALS, such as the degree of deeper cortical structures and cerebellar pathology evident in those ALS patients carrying pathological hexanucleotide expansions in *C9orf72*, even in the presymptomatic stages (Mahoney et al., 2012; Bede et al., 2013; Rohrer et al., 2015; Walhout et al., 2015).

Our interest in the pathology of the anterior cingulate gyrus in ALS, and ultimately the importance of alterations in metabolism of the microtubule-associated protein tau, was driven by a broad array of evidence suggesting that alterations in verbal praxis and fluency were key harbingers of higher cortical dysfunction in the disease (Strong et al., 1996). In a prospective study designed to assess the degree of neuronal loss in the anterior cingulate gyrus using ^{1}H-magnetic resonance spectroscopy (^{1}H-MRS), we observed a significant reduction in the NAA/Cr ratio (indicative of neuronal loss) at baseline. This corresponded to early features of cognitive impairment at a time when no changes in the NAA/Cr ratio were observed in the motor cortex in the region of hand representation (Strong et al., 1999). In hindsight, when we returned to these studies to correlate the placement of the STEAM (Stimulated Echo Acquisition Mode) voxel for mesial frontal localization, the localization was predominantly area 24, showing that the region of neuronal loss correlated with those regions described earlier as encoding social cognition and ToM. As will be reviewed below, it was the neuropathological study of these cases that has driven our conceptualization of a tauopathy in association with ALS-FTSD.

ALS-FTSD: NEUROPATHOLOGICAL CHARACTERIZATION

Alterations in RNA Metabolism

Pathological intracellular protein inclusions are amongst the neuropathological hallmarks of ALS and include proteins such as copper/zinc superoxide dismutase 1 (SOD1) (Chou et al., 1996), TDP-43 (Arai et al., 2006; Neumann et al., 2006), fused in sarcoma/translocated in liposarcoma (FUS/TLS) (Kwiatkowski et al., 2009; Vance et al., 2009), TATA-binding protein-associated factor 15 (TAF-15) (Couthouis et al., 2011), Ewing sarcoma breakpoint region 1 (EWSR1) (Couthouis et al., 2011), RNA-binding motif 45 (RBM45) (Collins et al., 2012), Rho guanine nucleotide exchange factor (RGNEF) (Volkening et al., 2010; Keller et al., 2012), intermediate filament proteins (neurofilament Strong et al., 2005 or peripherin Migheli et al., 1993), 14-3-3 proteins (Malaspina et al., 2000; Kawamoto et al., 2004), and abnormal dipeptide repeat (DPR) proteins arising from *C9orf72* G_4C_2 repeat expansions through repeat associated non-AUG (RAN) translation (Ash et al., 2013; Mori et al., 2013).

Amongst these proteins, it is the presence of TDP-43 immunoreactive neuronal cytoplasmic inclusions (NCIs) within degenerating motor neurons that is now recognized as being a ubiquitous neuropathological feature of all variants of ALS, with the exception of cases in which mutations in SOD1 are present. TDP-43 is a dual DNA/RNA binding protein whose metabolism is fundamentally altered in ALS and which forms the core protein of the vast majority of neuronal and glial inclusions in ALS, FTD, and ALS-FTSD (Arai et al., 2006; Neumann et al., 2006). Typically, TDP-43 is predominantly nuclear in its localization, but in response to cellular injury, its expression is markedly upregulated in a process that is accompanied by a nuclear to cytosolic shift in its localization (Moisse et al., 2009a,b). There is a high degree of correlation between the severity of the cognitive deficit that occurs in ALS and the distribution and extent of pathological TDP-43 deposition (Mackenzie, 2008; Mackenzie et al., 2011; Cykowski et al., 2017). Because of this prominence of TDP-43 pathology, and a general lack of deposition of the microtubule associated tau protein, the FTLD of ALS-FTD is currently classified as a "TDP-43 proteinopathy" and not a "tau proteinopathy."

pThr^{175} Tau and Alterations in Tau Metabolism

Notwithstanding this, the evidence in support of alterations in tau metabolism in ALS is robust, including that observed in the hyperendemic focus of ALS in the western Pacific in which the deposition of tau protein is prominent throughout the neuroaxis (Hirano, 1966). The presence of tau pathology has also been described in both sporadic and familial ALS case reports (Orrell et al., 1995; Soma et al., 2012; Dobson-Stone et al., 2013; Nakamura et al., 2014; Takeuchi et al., 2016). Additionally, several more recent studies have reported an elevation in phosphorylated and truncated tau protein in both hippocampal and spinal cord neurons of various ALS populations (Gómez-Pinedo et al., 2016; Vintilescu et al., 2016).

Our interest in the pathological processing of tau protein in ALS was initially aimed at explaining the basis of the superficial linear spongiosus evident in the anterior cingulate gyri of those ALSci patients in whom we observed a loss of neurons in this region through ^{1}H-MRS (Strong et al., 1999; Wilson et al., 2001). Using antibodies against tau protein as

a marker of axonal projections which we postulated would be lost, we instead observed both neuronal and glial cytoplasmic inclusions which were tau immunoreactive throughout the affected anterior cingulate gyrus (Yang et al., 2003). This included a broad range of pathologies, including neurofibrillary tangle-like structures, dystrophic neurites, neuritic granules, and tau-immunoreactive tufted astrocytes. We demonstrated that this was not simply a function of aging as might be expected based on the subsequently described progressive age-related tauopathy (Yang et al., 2005; Crary et al., 2014; Jellinger et al., 2015). Following fractionation of tau protein into sarkosyl-soluble or insoluble fractions from either the cortical or subcortical white matter of the anterior cingulate gyrus of ALSci patients, we observed that in contrast to tau protein isolated from Alzheimer's disease in which the insoluble fraction contained the triplet tau isoforms characteristic of paired helical filaments (PHFs), all six isoforms of tau protein were expressed in both the soluble and insoluble fractions (Strong et al., 2006). We subsequently confirmed this finding independent of the presence or absence of pathological hexanucleotide expansions of C9*orf*72 (Volkening et al., 2017). In the former study, we also observed that sarkosyl-insoluble tau protein from ALSci was resistant to enzymatic dephosphorylation, and, when examined using the Thioflavin S assay, had a significant increase in the tendency to form polymers *ex vivo* (Strong et al., 2006).

Given this suggestion of pathological tau protein phosphorylation in ALSci, we conducted a phospho-epitope analysis and identified a unique tau phosphorylation site at Threonine 175 ($pThr^{175}$ tau) in ALS and ALSci that was not present in either control or AD (both soluble and insoluble tau protein isolates) (Strong et al., 2006). Using a novel polyclonal antibody against $pThr^{175}$ tau, we subsequently confirmed the presence of prominent tau protein glial and neuronal cytoplasmic inclusions in ALSci, and to a lesser degree in ALS without cognitive deficits, in association with an increase in the expression of active GSK3β (Yang et al., 2008; Yang and Strong, 2012) (**Figure 1**). This deposition was accompanied by a diffuse increase in TDP-43 immunoreactivity, suggesting the co-occurrence of these pathological processes (Yang and Strong, 2012). The prominent deposition of tau protein, including $pThr^{175}$ tau, has been subsequently validated in motor neuron disease (MND) and MND in the presence of a behavioral variant of FTD (bvFTD-MND), including the appearance of tau protein deposition in 10% of MND cases that did not conform to traditional morphological criteria (unclassified frontal tau protein) (Behrouzi et al., 2016). While the latter study suggested a morphological appearance reminiscent of AD, as discussed earlier, the characteristic sarkosyl-insoluble tau protein triplet protein molecular signature of AD has not been observed in ALS or ALSci. More recently, we have observed that the pathological phospho-epitope $pThr^{175}$ tau protein is also observed across a broad range of tauopathies, strongly suggesting that its presence in ALSci is not simply incidental, but rather a marker of a fundamental alteration in tau protein processing across a range of tauopathies (Moszczynski et al., 2017).

PATHOGENICITY OF $pTHr^{175}$ TAU

To confirm the pathogenicity of $pThr^{175}$ tau, we transfected either HEK293T or Neuro2a cells with a pseudo-phosphorylated tau protein construct (Thr^{175}Asp-tau), wild type human tau protein (WT-tau) or human tau protein in which phosphorylation at Thr^{175} was irreversibly inhibited (Thr^{175}Ala-tau) (Gohar et al., 2009). We observed a significant induction of pathological tau protein cytoplasmic inclusions and enhanced rates of cell death in the presence of Thr^{175}Asp-tau, regardless of which of the six human tau protein constructs was transfected. Consistent with the observed up-regulation of activated GSK3β ($pTyr^{216}$GSK3β) that co-localized with tau protein pathology in ALSci, we demonstrated a significant increase in $pTyr^{216}$ GSK3β expression in only the Thr^{175}Asp-tau transfected cells (Moszczynski et al., 2015). Inhibition of GSK3β activity, either pharmacologically or by shRNA against GSK3β, abolished inclusion formation. We next demonstrated that the development of pathological inclusions in response to the presence of Thr^{175}Asp-tau was dependent on the unprimed phosphorylation of the Thr^{231} residue of tau protein and that the presence of $pThr^{231}$ was sufficient to induce tau protein inclusions. These observations suggest that a pathway of $pThr^{175}$ induction of GSK3β activation and a consequent phosphorylation of Thr^{231} in tau protein fibril formation is a pathogenic mechanism contributing to neuronal death in ALSci. While investigating evidence for this pathway in human disease, we observed the co-localization of $pThr^{175}$ and $pThr^{231}$ in tau protein NCI-containing hippocampal neurons in ALSci and a broad range of tauopathies including Alzheimer's disease, diffuse Lewy body dementia, and FTLD among others (Moszczynski et al., 2017). What remains to be determined across both sets of experiments however is the ultrastructural characteristics of the cytoplasmic inclusions driven *in vitro* by $pThr^{175}$ tau or as observed *in vivo*.

We then examined the tauopathy associated with chronic traumatic encephalopathy (CTE) and CTE with concurrent ALS (CTE-ALS) (Moszczynski et al., 2018). In both disease states, the neuropathological hallmark is a disseminated tauopathy including not only cortical neuronal and glial cytoplasmic inclusions, but also spinal cord tau protein pathology (McKee et al., 2009, 2010; Mez et al., 2017). Consistent with a role for pathological Thr^{175} tau phosphorylation, we observed $pThr^{175}$, $pThr^{231}$, and T22 immunoreactivity in both hippocampal and spinal motor neurons. Fractionation of the hippocampal tau protein into sarkosyl-soluble and insoluble fractions yielded all six tau protein isoforms partitioning into both fractions, similar to that observed in ALSci. In support of the hypothesis that this pathway is directly related to the induction of tau protein cytoplasmic inclusions, we were able to replicate this pathology following a single cortical impact (moderate brain trauma model) in young adult Sprague Dawley rats (Moszczynski et al., 2018).

While we have suggested that $pThr^{175}$ tau is critical to the induction of a tauopathy, this evidence does not prove it to be sufficient for the development of tauopathy *in vivo*. To test this, we utilized the somatic gene transfer of a pseudophosphorylated human tau protein construct mimicking

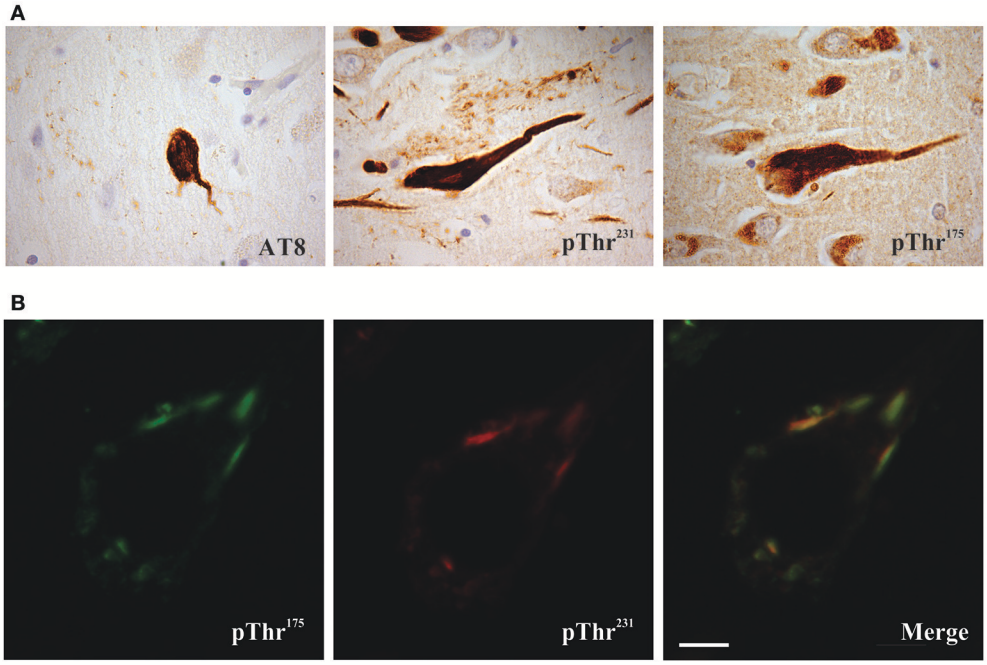

FIGURE 1 | Phosphorylated tau pathology in amyotrophic latera sclerosis with cognitive impairment (ALSci) hippocampal neurons. **(A)** Immunohistochemical probing with AT8 (pSer^{202}, pThr^{205}), pThr^{175}, pThr^{231} all reveal positive inclusions in ALS hippocampal neurons. Images taken with a 100x objective. **(B)** Representative image of pThr^{175} and pThr^{231} co-localization in ALSci hippocampal neuron. Scale bar = 5 μm.

pThr^{175} tau. Young adult Sprague Dawley rats received bilateral stereotactic inoculums of a rAAV9 adenoviral construct containing one of either GFP tagged Thr^{175}Asp-tau (pThr^{175} tau mimic), GFP-tagged WT-tau, GFP-tagged construct alone, or GFP-tagged Thr^{175}Ala-tau (Moszcyznski et al., 2017). At 1 year following inoculation, expression of the viral vector remained prominent as assessed using anti eGFP immunohistochemistry. However, the brains of the Thr^{175}Asp-tau inoculated rats demonstrated prominent neuronal tau protein pathology, including corkscrew neurites, and tau immunoreactive neuronal cytoplasmic inclusions.

POSTULATED PATHOGENIC PATHWAY

In support of the pathogenicity of pThr^{175} tau, phosphorylation at this site is not observed in fetal human tissue (which is normally hyperphosphorylated) (Kenessey and Yen, 1993) or tissue from healthy-aged individuals (Moszczynski et al., 2017). We have shown *in vitro* that a pseudophosphorylated human tau construct (Thr^{175}Asp tau) induces pathological tau protein inclusions accompanied by the activation of GSK3β along with phosphorylation of tau at Thr^{231} (Moszczynski et al., 2015). The *in vivo* observation of co-expression of pThr^{175} tau, pTyr^{216}GSK3β, pThr^{231} tau, and immunoreactivity to a tau protein antibody recognizing oligomeric tau (T22) strongly suggests that this pathway is critical to the induction of pathological tauopathies, including ALSci, CTE and CTE-ALS (Moszczynski et al., 2017, 2018).

The mechanism of Thr^{175} phosphorylation is not known. Candidate kinases include mitogen activated protein kinases (MAPK), GSK3β, p38, and leucine-rich repeat kinase 2 (LRRK2) (Hanger et al., 1998; Reynolds et al., 2000; Atzori et al., 2001) (see also https://docs.google.com/spreadsheets/d/1hGYs1ZcupmTnbB7n6qs1r_WVTXHt1O7NBLyKBN7EOUQ/edit#gid=0). Amongst these, a member of the MAPK family of kinases, c-Jun N-terminal kinase [JNK; also known as stress activated protein kinase (SAPK)], is of specific interest given its increased activity in response to various cellular stresses *in vitro* (Namgung and Xia, 2000) and in the acute phases following traumatic brain injury (TBI) *in vivo* (Tran et al., 2012). Additionally, the inhibition of JNK can reduce pathological tau protein phosphorylation following TBI in a rodent model (Tran et al., 2012).

Although the mechanism(s) by which the phosphorylation of tau at Thr^{175} leads to the activation of GSK3β are not yet known, it is likely that such mechanism(s) will involve altering tau's global hairpin structure given that Thr^{175} lies within the Pro-rich domain/hinge region of the hairpin as it has been shown that the phosphorylation of other residues within this domain can open the hairpin structure (Jeganathan et al., 2006, 2008). There are at least two potential mechanisms of GSK3β activation which may result from tau hairpin structure opening (**Figure 2**). Firstly, opening of the hairpin may expose the N-terminus

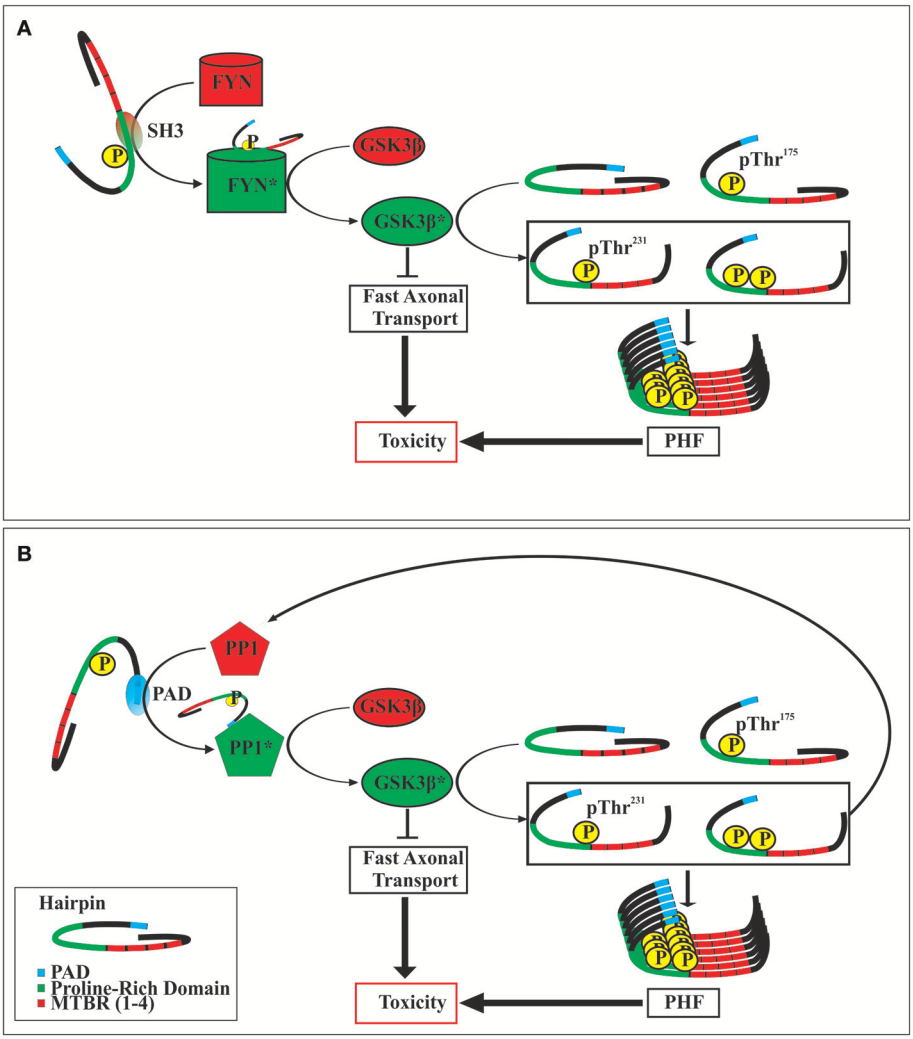

FIGURE 2 | Two postulated mechanisms of toxicity following tau protein phosphorylation at Thr^{175}. Opening of the tau hairpin conformation by phosphorylation at Thr^{175} exposes SH3 homology domains within the proline-rich region **(A)**. This interacts with and activates FYN kinase, which in turn activates GSK3β by phosphorylating at Tyr^{216}. Alternatively, opening of the tau hairpin can expose the N-terminal phosphatase activating domain (PAD) **(B)**, which then activates protein phosphatase 1 (PP1). Activated PP1 dephosphorylates GSK3β at Ser^{9} increasing its activity. The activation of GSK3β may exert toxic effects in the cell by the inhibition of fast axonal transport, and by the phosphorylation of tau protein at Thr^{231}, which promotes the formation of neurofibrillary tangles (paired helical filaments; PHF). Additionally, increased activity of GSK3β can increase the formation of $pThr^{231}$ tau which also contains an exposed PAD, thereby initiating a dysregulated positive feedback loop. Activated enzymes are indicated by an asterisk (*).

proline-rich domain, which has been shown to interact with the SH3 domain of Src-family tyrosine kinase Fyn. In doing so, activated Fyn kinase may then phosphorylate GSK3β at the Tyr^{216} residue thereby enhancing its activity (Lee et al., 1998; Lesort et al., 1999; Klein et al., 2002). Secondly, opening of the hairpin conformation has been shown to expose the N-terminal phosphatase activating domain (PAD), consisting of amino acids 2–18. Exposure of this domain leads to activation of protein phosphatase-1 (PP1) which then dephosphorylates GSK3β at the Ser^{9} residue, enhancing GSK3β activity (Kanaan et al., 2011). In keeping with this mechanism, exposure of the PAD has been suggested to be important in tau protein mediated neuronal toxicity through interference with fast axonal transport, and may be an early event in the development of a number of tauopathies (Kanaan et al., 2011, 2016; Ward et al., 2012; Combs et al., 2016).

In the studies cited above, tau phosphorylation at Thr^{231} is a critical step in the induction of pathological fibrils. Several mechanisms have been proposed by which this may occur, with alterations in tau degradation being key in a process that is dependent on tau conformation. Of note, *cis*-$pThr^{231}$ tau demonstrates specificity in the development of pathology over *trans*-$pThr^{231}$ tau, in which the *cis* conformer is pathological and cannot be degraded, whereas the *trans* conformer is physiological and can be degraded (Nakamura et al., 2012). The isomerase, peptidyl-prolyl *cis-trans* isomerase NIMA-interacting 1 (PIN1), converts the pathologic *cis* conformer to the physiologic *trans*

conformer, allowing for dephosphorylation at this site by protein phosphatase 1 (Lu et al., 1996, 1999). It is of note, therefore, that *cis*-pThr^{231} tau is closely associated with a number of tauopathies including, AD, CTE and experimental CTE (Lu et al., 1996, 1999; Liou et al., 2003; Pastorino et al., 2006; Sultana et al., 2006; Lu and Zhou, 2007; Lim et al., 2008; Lee et al., 2011; Chen et al., 2015; Kondo et al., 2015; Albayram et al., 2017). Given that both *cis*-pThr^{231} tau and pThr^{175} tau are observed exclusively in disease or stressed states, it is attractive to postulate that the phosphorylation of tau protein at Thr^{175} increases the presence of *cis*-pThr^{231}. This may occur through either enhancing the probability of *cis* phosphorylation by GSK3β or by inhibiting the ability of PIN1 to isomerize the epitope from *cis* to *trans*. This is the subject of current studies.

THE POTENTIAL ROLE OF COMORBID PATHOLOGIES

The fact that other cell stressors may induce Thr^{175} tau protein phosphorylation is of great significance to the mechanisms of neurodegenerative disease. Pathologies are rarely, if ever, observed in isolation, and it is common to identify co-morbid pathologies in the same brain (Amador-Ortiz et al., 2007; Josephs et al., 2014a,b; Smith, 2017). While this high incidence of comorbidity has traditionally been attributed to the aging process, it is increasingly evident that multiple pathologies are present even in young cohorts of patients afflicted with neurodegenerative disease. Therefore, there is likely an interplay between pathological processes that drives these co-morbid pathologies (Spires-Jones et al., 2017; Tan et al., 2017). As such, the possibility of synergistic toxicity must be considered when trying to understand the mechanisms that drive neurodegenerative disease, and when attempting to treat such diseases.

As discussed earlier, the FTLD of ALSci is classified as a FTLD-TDP based on the prominence of pathological TDP-43 deposition. The association of TDP-43 pathology with ALS and ALS-FTSD is well described (Arai et al., 2006; Neumann et al., 2006). However, there is also an increasing literature describing comorbid TDP-43 and tau pathologies, such as that observed in AD and CTE (McKee et al., 2010; Josephs et al., 2014a,b). The relationship between tau protein and TDP-43 pathology is strengthened in the observation that the effective elimination of aberrantly phosphorylated tau protein in a rodent model of CTE can also lead to the prevention of TDP-43 pathology (Albayram et al., 2017). It is possible that one pathological process primes the other. In this case, the toxicity of pseudophosphorylated Thr^{175}Asp tau protein expression may be enhanced by the co-expression of TDP-43, serving as a second hit to the CNS. The potential of this synergistic toxicity is the focus of ongoing studies in our lab.

SUMMARY

The presence of pathological tau processing is clearly evident across a broad range of ALS patients—including those found within the hyperendemic foci such as that seen in the western Pacific, a smattering of case reports, and ALSci as well as FTD-MND. This suggests that this is not a simple matter of incidental co-occurrence. Moreover, there is solid evidence to support the pathogenic role of pThr^{175} in the induction of a tauopathy, both *in vitro* and *in vivo*, and the pathological cascade induced by pThr^{175} which culminates in the generation of oligomeric tau has been observed in a broad range of tauopathies. The issue is therefore not whether a tauopathy exists in ALS-FTSD, but rather the extent to which it is the driving pathology—either alone, or in combination with the hallmark pathology of TDP-43—of the clinical and neuropathological phenotype.

Such a proposal however leaves many unanswered questions, including: the mechanism by which the Thr^{175} residue is initially phosphorylated; how pThr^{175} tau leads to the activation of GSK3β; whether pThr^{231} tau is necessary and sufficient to induce neuronal dysfunction and death, or whether additional tau protein pathological phosphorylation is needed; and what (if any) role for the co-existent TDP-43 pathology of ALS-FTSD is also necessary to drive the phenomenological aspects of pThr^{175} tau-mediated tauopathy.

AUTHOR CONTRIBUTIONS

MS conceived and wrote the article. AM conceived and wrote the article. MH wrote the article.

ACKNOWLEDGMENTS

Research funded by the Ontario Neurodegenerative Disorders Research Initiative (ONDRI) and the National Hockey League Players Association (NHLPA) Challenge Fund.

REFERENCES

Abrahams, S., Goldstein, L. H., Simmons, A., Brammer, M., Williams, S. C., Giampietro, V., et al. (2004). Word retrieval in amyotrophic lateral sclerosis: a functional magnetic resonance imaging study. *Brain* 127, 1507–1517. doi: 10.1093/brain/awh170

Adenzato, M., Cavallo, M., and Enrici, I. (2010). Theory of mind ability in the behavioural variant of frontotemporal dementia: an analysis of the neural, cognitive, and social levels. *Neuropsychologia* 48, 2–12. doi: 10.1016/j.neuropsychologia.2009.08.001

Agosta, F., Canu, E., Valsasina, P., Riva, N., Prelle, A., Comi, G., et al. (2013). Divergent brain network connectivity in amyotrophic lateral sclerosis. *Neurobiol. Aging* 34, 419–427. doi: 10.1016/j.neurobiolaging.2012.04.015

Agosta, F., Ferraro, P. M., Riva, N., Spinelli, E. G., Chiò, A., Canu, E., et al. (2016). Structural brain correlates of cognitive and behavioral impairment in MND. *Hum. Brain Mapp.* 37, 1614–1626. doi: 10.1002/hbm.23124

Agosta, F., Valsasina, P., Absinta, M., Riva, N., Sala, S., Prelle, A., et al. (2011). Sensorimotor functional connectivity changes in amyotrophic lateral sclerosis. *Cereb. Cortex* 21, 2291–2298. doi: 10.1093/cercor/bhr002

Albayram, O., Kondo, A., Mannix, R., Smith, C., Tsai, C. Y., Li, C., et al. (2017). Cis P-tau is induced in clinical and preclinical brain injury and contributes to post-injury sequelae. *Nat. Commun.* 8:1000. doi: 10.1038/s41467-017-01068-4

Amador-Ortiz, C., Lin, W. L., Ahmed, Z., Personett, D., Davies, P., Duara, R., et al. (2007). TDP-43 immunoreactivity in hippocampal sclerosis and Alzheimer's disease. *Ann. Neurol.* 61, 435–445. doi: 10.1002/ana.21154

Ambikairajah, A., Devenney, E., Flanagan, E., Yew, B., Mioshi, E., Kiernan, M. C., et al. (2014). A visual MRI atrophy rating scale for the amyotrophic lateral sclerosis-frontotemporal dementia continuum. *Amyotroph. Lateral Scler. Frontotemporal Degener.* 15, 226–234. doi: 10.3109/21678421.2014.880180

Arai, T., Hasegawa, M., Akiyama, H., Ikeda, K., Nonaka, T., Mori, H., et al. (2006). TDP-43 is a component of ubiquitin-positive tau-negative inclusions in frontotemporal lobar degeneration and amyotrophic lateral sclerosis. *Biochem. Biophys. Res. Commun.* 351, 602–611. doi: 10.1016/j.bbrc.2006.10.093

Ash, P. E., Bieniek, K. F., Gendron, T. F., Caulfield, T., Lin, W. L., Dejesus-Hernandez, M., et al. (2013). Unconventional translation of C9ORF72 GGGGCC expansion generates insoluble polypeptides specific to c9FTD/ALS. *Neuron* 77, 639–646. doi: 10.1016/j.neuron.2013.02.004

Atzori, C., Ghetti, B., Piva, R., Srinivasan, A. N., Zolo, P., Delisle, M. B., et al. (2001). Activation of the JNK/p38 pathway occurs in diseases charcterized by tau protein pathology and is related to tau phosphorylation but not to apoptosis. *J. Neuropathol. Exp. Neurol.* 60, 1190–1197. doi: 10.1093/jnen/60.12.1190

Bak, T. H., and Hodges, J. R. (2001). Motor neurone disease, dementia and aphasia; coincidence, co-occurrence or continuum? *J. Neurol.* 248, 260–270. doi: 10.1007/s004150170199

Bede, P., Bokde, A. L., Byrne, S., Elamin, M., McLaughlin, R. L., Kenna, K., et al. (2013). Multiparametric MRI study of ALS stratified for the C9orf72 genotype. *Neurology* 81, 361–369. doi: 10.1212/WNL.0b013e31829c5eee

Behrouzi, R., Liu, X., Wu, D., Robinson, A. C., Tanaguchi-Watanabe, S., Rollinson, S., et al. (2016). Pathological tau deposition in motor neurone disease and frontotemporal lobar degeneration associated with TDP-43 proteinopathy. *Acta Neuropathol. Commun.* 4:33. doi: 10.1186/s40478-016-0301-z

Cerami, C., Dodich, A., Canessa, N., Crespi, C., Iannaccone, S., Corbo, M., et al. (2014). Emotional empathy in amyotrophic lateral sclerosis: a behavioural and voxel-based morphometry study. *Amyotroph. Lateral Scler. Frontotemporal Degener.* 15, 21–29. doi: 10.3109/21678421.2013.785568

Charcot, J. M., and Joffroy, A. (1869). Deux cas d'atrophie musculaire progressive avec lésions de la substance grise et des faisceaux antérolatéraux de la moelle épinière. *Arch. Physiol. Norm. Pathol.* 2, 354–744.

Chen, C. H., Li, W., Sultana, R., You, M. H., Kondo, A., Shahpasand, K., et al. (2015). Pin1 cysteine-113 oxidation inhibits its catalytic activity and cellular function in Alzheimer's disease. *Neurobiol. Dis.* 76, 13–23. doi: 10.1016/j.nbd.2014.12.027

Chiò, A., Logroscino, G., Hardiman, O., Swingler, R., Mitchell, D., Beghi, E., et al. (2009). Prognostic factors in ALS: a critical review. *Amyotroph. Lateral Scler.* 10, 310–323. doi: 10.3109/17482960802566824

Chou, S. M., Wang, H. S., and Komai, K. (1996). Colocalization of NOS and SOD1 in neurofilament accumulation within motor neurons of amyotrophic lateral sclerosis: an immunohistochemical study. *J. Chem. Neuroanat.* 10, 249–258. doi: 10.1016/0891-0618(96)00137-8

Cistaro, A., Cuccurullo, V., Quartuccio, N., Pagani, M., Valentini, M. C., and Mansi, L. (2014). Role of PET and SPECT in the study of amyotrophic lateral sclerosis. *Biomed Res. Int.* 2014:237437. doi: 10.1155/2014/237437

Cistaro, A., Valentini, M. C., Chiò, A., Nobili, F., Calvo, A., Moglia, C., et al. (2012). Brain hypermetabolism in amyotrophic lateral sclerosis: a FDG PET study in ALS of spinal and bulbar onset. *Eur. J. Nucl. Med. Mol. Imaging* 39, 251–259. doi: 10.1007/s00259-011-1979-6

Collins, M., Riascos, D., Kovalik, T., An, J., Krupa, K., Krupa, K., et al. (2012). The RNA-binding motif 45 (RBM45) protein accumulates in inclusion bodies in amyotrophic lateral sclerosis (ALS) and frontotemporal lobar degeneration with TDP-43 inclusions (FTLD-TDP) patients. *Acta Neuropathol.* 124, 717–732. doi: 10.1007/s00401-012-1045-x

Combs, B., Hamel, C., and Kanaan, N. M. (2016). Pathological conformations involving the amino terminus of tau occur early in Alzheimer's disease and are differentially detected by monoclonal antibodies. *Neurobiol. Dis.* 94, 18–31. doi: 10.1016/j.nbd.2016.05.016

Couratier, P., Corcia, P., Lautrette, G., Nicol, M., Preux, P. M., and Marin, B. (2016). Epidemiology of amyotrophic lateral sclerosis: a review of literature. *Rev. Neurol.* 172, 37–45. doi: 10.1016/j.neurol.2015.11.002

Couthouis, J., Hart, M. P., Shorter, J., Dejesus-Hernandez, M., Erion, R., Oristano, R., et al. (2011). A yeast functional screen predicts new candidate ALS disease genes. *Proc. Natl. Acad. Sci. U.S.A.* 108, 20881–20890. doi: 10.1073/pnas.1109434108

Crary, J. F., Trojanowski, J. Q., Schneider, J. A., Abisambra, J. F., Abner, E. L., Alafuzoff, I., et al. (2014). Primary age-related tauopathy (PART): a common pathology associated with human aging. *Acta Neuropathol.* 128, 755–766. doi: 10.1007/s00401-014-1349-0

Cykowski, M. D., Powell, S. Z., Peterson, L. E., Appel, J. W., Rivera, A. L., Takei, H., et al. (2017). Clinical significance of TDP-43 neuropathology in amyotrophic lateral sclerosis. *J. Neuropathol. Exp. Neurol.* 76, 402–413. doi: 10.1093/jnen/nlx025

Dobson-Stone, C., Luty, A. A., Thompson, E. M., Blumbergs, P., Brooks, W. S., Short, C. L., et al. (2013). Frontotemporal dementia-amyotrophic lateral sclerosis syndrome locus on chromosome 16p12.1-q12.2: genetic, clinical and neuropathological analysis. *Acta Neuropathol.* 125, 523–533. doi: 10.1007/s00401-013-1078-9

Douaud, G., Filippini, N., Knight, S., Talbot, K., and Turner, M. R. (2011). Integration of structural and functional magnetic resonance imaging in amyotrophic lateral sclerosis. *Brain* 134, 3470–3479. doi: 10.1093/brain/awr279

Elamin, M., Phukan, J., Bede, P., Jordan, N., Byrne, S., Pender, N., et al. (2011). Executive dysfunction is a negative prognostic indicator in patients with ALS without dementia. *Neurology* 76, 1263–1269. doi: 10.1212/WNL.0b013e318214359f

Farhan, S. M., Bartha, R., Black, S. E., Corbett, D., Finger, E., Freedman, M., et al. (2017). The Ontario Neurodegenerative Disease Research Initiative (ONDRI). *Can. J. Neurol. Sci.* 44, 196–202. doi: 10.1017/cjn.2016.415

Girardi, A., Macpherson, S. E., and Abrahams, S. (2011). Deficits in emotional and social cognition in amyotrophic lateral sclerosis. *Neuropsychology* 25, 53–65. doi: 10.1037/a0020357

Gohar, M., Yang, W., Strong, W. L., Volkening, K., Leystra-Lantz, C., and Strong, M. J. (2009). Tau phosphorylation at ^{175}Thr leads to fibril formation. Implications for the tauopathy of amyotrophic lateral sclerosis. *J. Neurochem.* 108, 634–643. doi: 10.1111/j.1471-4159.2008.05791.x

Goldstein, L. H., Newsom-Davis, I. C., Bryant, V., Brammer, M., Leigh, P. N., and Simmons, A. (2011). Altered patterns of cortical activation in ALS patients during attention and cognitive response inhibition tasks. *J. Neurol.* 258, 2186–2198. doi: 10.1007/s00415-011-6088-8

Gómez-Pinedo, U., Villar-Quiles, R. N., Galán, L., Matías-Guiu, J. A., Benito-Martin, M. S., Guerrero-Sola, A., et al. (2016). Immununochemical markers of the amyloid cascade in the hippocampus in motor neuron diseases. *Front. Neurol.* 7:195. doi: 10.3389/fneur.2016.00195

Hanger, D. P., Betts, J. C., Loviny, T. L. F., Blackstock, W. P., and Anderton, B. H. (1998). New phosphorylation sites identified in hyperphosphorylated tau (paired helical filament tau) from Alzheimer's disease brain using nanoelectrospray mass spectroscopy. *J. Neurochem.* 71, 2465–2476. doi: 10.1046/j.1471-4159.1998.71062465.x

Hirano, A. (1966). "Neuropathology of amyotrophic lateral sclerosis and parkinsonism-dementia complex on Guam," in *Proceedings of the Fifth International Congress of Neuropathology,* eds L. Luthy and A. Bischoff (Amsterdam: Excerpta Medica), 190–194.

Hodges, J. R., and Miller, B. (2001). The classification, genetics and neuropathology of frontotemporal dementia. Introduction to the special topic papers: part 1. *Neurocase* 7, 31–35. doi: 10.1093/neucas/7.1.31

Hu, W. T., Shelnutt, M., Wilson, A., Yarab, N., Kelly, C., Grossman, M., et al. (2013). Behavior matters–cognitive predictors of survival in amyotrophic lateral sclerosis. *PLoS ONE* 8:e57584. doi: 10.1371/journal.pone.0057584

Hudson, A. J. (1981). Amyotrophic lateral sclerosis and its association with dementia, parkinsonism and other neurological disorders: a review. *Brain* 194, 217–247. doi: 10.1093/brain/104.2.217

Irwin, D. J., Cairns, N. J., Grossman, M., McMillan, C. T., Lee, E. B., Van Deerlin, V. M., et al. (2015). Frontotemporal lobar degeneration: defining phenotypic diversity through personalized medicine. *Acta Neuropathol.* 129, 469–491. doi: 10.1007/s00401-014-1380-1

Jeganathan, S., Hascher, A., Chinnathambi, S., Biernat, J., Mandelkow, E. M., and Mandelkow, E. (2008). Proline-directed pseudo-phosphorylation at AT8 and PHF1 epitopes induces a compaction of the paperclip folding of Tau and generates a pathological (MC-1) conformation. *J. Biol. Chem.* 283, 32066–32076. doi: 10.1074/jbc.M805300200

Jeganathan, S., von Bergen, M., Brutlach, H., Steinhoff, H. J., and Mandelkow, E. (2006). Global hairpin folding of tau in solution. *Biochemistry* 45, 2283–2293. doi: 10.1021/bi0521543

Jellinger, K. A., Alafuzoff, I., Attems, J., Beach, T. G., Cairns, N. J., Crary, J. F., et al. (2015). PART, a distinct tauopathy, different from classical sporadic Alzheimer disease. *Acta Neuropathol.* 129, 757–762. doi: 10.1007/s00401-015-1407-2

Josephs, K. A., Murray, M. E., Whitwell, J. L., Parisi, J. E., Petrucelli, L., Jack, C. R., et al. (2014a). Staging TDP-43 pathology in Alzheimer's disease. *Acta Neuropathol.* 127, 441–450. doi: 10.1007/s00401-013-1211-9

Josephs, K. A., Whitwell, J. L., Weigand, S. D., Murray, M. E., Tosakulwong, N., Liesinger, A. M., et al. (2014b). TDP-43 is a key player in the clinical features associated with Alzheimer's disease. *Acta Neuropathol.* 127, 811–824. doi: 10.1007/s00401-014-1269-z

Kanaan, N. M., Cox, K., Alvarez, V. E., Stein, T. D., Poncil, S., and McKee, A. C. (2016). Characterization of early pathological tau conformations and phosphorylation in chronic traumatic encephalopathy. *J. Neuropathol. Exp. Neurol.* 75, 19–34. doi: 10.1093/jnen/nlv001

Kanaan, N. M., Morfini, G. A., LaPointe, N. E., Pigino, G. F., Patterson, K. R., Song, Y., et al. (2011). Pathogenic forms of tau inhibit kinesin-dependent axonal transport through a mechanism involving activation of axonal phosphotransferases. *J. Neurosci.* 31, 9858–9868. doi: 10.1523/JNEUROSCI.0560-11.2011

Kawamoto, Y., Akiguchi, I., Nakamura, A., and Budka, H. (2004). 14-3-3 proteins in Lewy body-like hyaline inclusion in patients with sporadic amyotrophic lateral sclerosis. *Acta Neuropathol.* 108, 531–537. doi: 10.1007/s00401-004-0923-2

Keller, B. A., Volkening, K., Droppelmann, C. A., Ang, L. C., Rademakers, R., and Strong, M. J. (2012). Co-aggregation of RNA binding proteins in ALS spinal motor neurons: evidence of a common pathogenic mechanism. *Acta Neuropathol.* 124, 733–747. doi: 10.1007/s00401-012-1035-z

Kenessey, A., and Yen, S. H. (1993). The extent of phosphorylation of fetal tau is comparable to that of PHF-tau from Alzheimer paired helical filaments. *Brain Res.* 629, 40–46. doi: 10.1016/0006-8993(93)90478-6

Klein, C., Kramer, E. M., Cardine, A. M., Schraven, B., Brandt, R., and Trotter, J. (2002). Process outgrowth of oligodendrocytes is promoted by interaction of fyn kinase with the cytoskeletal protein tau. *J. Neurosci.* 22, 698–707. doi: 10.1523/JNEUROSCI.22-03-00698.2002

Kondo, A., Shahpasand, K., Mannix, R., Qiu, J., Moncaster, J., Chen, C. H., et al. (2015). Antibody against early driver of neurodegeneration cis P-tau blocks brain injury and tauopathy. *Nature* 523, 431–436. doi: 10.1038/nature14658

Kwiatkowski, T. J. Jr., Bosco, D. A., Leclerc, A. L., Tamrazian, E., Vanderburg, C. R., Russ, C., et al. (2009). Mutations in the FUS/TLS gene on chromosome 16 cause familial amyotrophic lateral sclerosis. *Science* 323, 1205–1208. doi: 10.1126/science.1166066

Lee, G., Newman, S. T., Gard, D. L., Band, H., and Panchamoorthy, G. (1998). Tau interacts with src-family non-receptor tyrosine kinases. *J. Cell Sci.* 111 (Pt 21), 3167–3177.

Lee, T. H., Chen, C. H., Suizu, F., Huang, P., Schiene-Fischer, C., Daum, S., et al. (2011). Death-associated protein kinase 1 phosphorylates Pin1 and inhibits its prolyl isomerase activity and cellular function. *Mol. Cell* 42, 147–159. doi: 10.1016/j.molcel.2011.03.005

Lesort, M., Jope, R. S., and Johnson, G. V. (1999). Insulin transiently increases tau phosphorylation: involvement of glycogen synthase kinase-3β and Fyn tyrosine kinase. *J. Neurochem.* 72, 576–584. doi: 10.1046/j.1471-4159.1999.0720576.x

Lillo, P., Garcin, B., Hornberger, M., Bak, T. H., and Hodges, J. R. (2010). Neurobehavioral features in frontotemporal dementia with amyotrophic lateral sclerosis. *Arch. Neurol.* 67, 826–830. doi: 10.1001/archneurol.2010.146

Lim, J., Balastik, M., Lee, T. H., Nakamura, K., Liou, Y. C., Sun, A., et al. (2008). Pin1 has opposite effects on wild-type and P301L tau stability and tauopathy. *J. Clin. Invest.* 118, 1877–1889. doi: 10.1172/JCI34308

Liou, Y. C., Sun, A., Ryo, A., Zhou, X. Z., Yu, Z. X., Huang, H. K., et al. (2003). Role of the prolyl isomerase Pin1 in protecting against age-dependent neurodegeneration. *Nature* 424, 556–561. doi: 10.1038/nature01832

Lu, K. P., Hanes, S. D., and Hunter, T. (1996). A human peptidyl-prolyl isomerase essential for regulation of mitosis. *Nature* 380, 544–547. doi: 10.1038/380544a0

Lu, K. P., and Zhou, X. Z. (2007). The prolyl isomerase PIN1: a pivotal new twist in phosphorylation signalling and disease. *Nat. Rev. Mol. Cell Biol.* 8, 904–916. doi: 10.1038/nrm2261

Lu, P. J., Wulf, G., Zhou, X. Z., Davies, P., and Lu, K. P. (1999). The prolyl isomerase Pin1 restores the function of Alzheimer-associated phosphorylated tau protein. *Nature* 399, 784–788. doi: 10.1038/21650

Lunetta, C., Lizio, A., Melazzini, M. G., Maestri, E., and Sansone, V. A. (2015). Amyotrophic Lateral Sclerosis Survival Score (ALS-SS): a simple scoring system for early prediction of patient survival. *Amyotroph. Lateral Scler. Frontotemporal Degener.* 17, 93–100. doi: 10.3109/21678421.2015.1083585

Mackenzie, I. R. (2008). The neuropathology of FTD associated with ALS. *Alzheimer Dis. Assoc. Disord.* 21, S44–S49. doi: 10.1097/WAD.0b013e31815c3486

Mackenzie, I. R., Neumann, M., Baborie, A., Sampathu, D. M., Du Plessis, D., Jaros, E., et al. (2011). A harmonized classification system for FTLD-TDP pathology. *Acta Neuropathol.* 122, 111–113. doi: 10.1007/s00401-011-0845-8

Mahoney, C. J., Downey, L. E., Ridgway, G. R., Beck, J., Clegg, S., Blair, M., et al. (2012). Longitudinal neuroimaging and neuropsychological profiles of frontotemporal dementia with C9ORF72 expansions. *Alzheimers. Res. Ther.* 4:41. doi: 10.1186/alzrt144

Malaspina, A., Kaushik, N., and de Belleroche, J. (2000). A 14-3-3 mRNA is up-regulated in amyotrophic lateral sclerosis spinal cord. *J. Neurochem.* 75, 2511–2520. doi: 10.1046/j.1471-4159.2000.0752511.x

McKee, A. C., Cantu, R. C., Nowinski, C. J., Hedley-Whyte, E. T., Gavett, B. E., Budson, A. E., et al. (2009). Chronic traumatic encephalopathy in athletes: progressive tauopathy after repetitive head injury. *J. Neuropathol. Exp. Neurol.* 68, 709–735. doi: 10.1097/NEN.0b013e3181a9d503

McKee, A. C., Gavett, B. E., Stern, R. A., Nowinski, C. J., Cantu, R. C., Kowall, N. W., et al. (2010). TDP-43 proteinopathy and motor neuron disease in chronic traumatic encephalopathy. *J. Neuropathol. Exp. Neurol.* 69, 918–929. doi: 10.1097/NEN.0b013e3181ee7d85

Meier, S. L., Charleston, A. J., and Tippett, L. J. (2010). Cognitive and behavioural deficits associated with the orbitomedial prefrontal cortex in amyotrophic lateral sclerosis. *Brain* 133, 3444–3457. doi: 10.1093/brain/awq254

Mez, J., Daneshvar, D. H., Kiernan, P. T., Abdolmohammadi, B., Alvarez, V. E., Huber, B. R., et al. (2017). Clinicopathological evaluation of chronic traumatic encephalopathy in players of American football. *JAMA* 318, 360–370. doi: 10.1001/jama.2017.8334

Migheli, A., Pezzulo, T., Attanasio, A., and Schiffer, D. (1993). Peripherin immunoreactive structures in amyotrophic lateral sclerosis. *Lab. Invest.* 68, 185–191.

Moisse, K., Mepham, J., Volkening, K., Welch, I., Hill, T., and Strong, M. J. (2009a). Cytosolic TDP-43 expression following axotomy is associated with caspase 3 activation in NFL (-/-) mice: support for a role for TDP-43 in the physiological response to neuronal injury. *Brain Res.* 1296, 176–186. doi: 10.1016/j.brainres.2009.07.023

Moisse, K., Volkening, K., Leystra-Lantz, C., Welch, I., Hill, T., and Strong, M. J. (2009b). Divergent patterns of cytosolic TDP-43 and neuronal progranulin expression following axotomy. *Brain Res.* 1249, 202–211. doi: 10.1016/j.brainres.2008.10.021

Montuschi, A., Iazzolino, B., Calvo, A., Moglia, C., Lopiano, L., Restagno, G., et al. (2015). Cognitive correlates in amyotrophic lateral sclerosis: a population-based study in Italy. *J. Neurol. Neurosurg. Psychiatry* 86, 168–173. doi: 10.1136/jnnp-2013-307223

Mori, K., Weng, S. M., Arzberger, T., May, S., Rentzsch, K., Kremmer, E., et al. (2013). The C9orf72 GGGGCC repeat is translated into aggregating dipeptide-repeat proteins in FTLD/ALS. *Science* 339, 1335–1338. doi: 10.1126/science.1232927

Moszcyznski, A., Gopaul, J., McCunn, P., Volkening, K., Harvey, M., Bartha, R., et al. (2017). ALSci associated tau pathological phosphorylation of Thr^{175} induces a tau proteinopathy *in vivo*. *Amyotroph. Lateral Scler. Frontotemporal Degener.* 18:143.

Moszczynski, A. J., Gohar, M., Volkening, K., Leystra-Lantz, C., Strong, W., and Strong, M. J. (2015). Thr175-phosphorylated tau induces pathologic fibril formation via GSK3beta-mediated phosphorylation of Thr231 *in vitro*. *Neurobiol. Aging* 36, 1590–1599. doi: 10.1016/j.neurobiolaging.2014.12.001

Moszczynski, A. J., Strong, W., Xu, K., McKee, A., Brown, A., and Strong, M. J. (2018). Pathological Thr^{175} tau phosphorylationin CTE and CTE with ALS. *Neurology* 90, 1–8. doi: 10.1212/WNL.0000000000004899

Moszczynski, A. J., Yang, W., Hammond, R., Ang, L. C., and Strong, M. J. (2017). Threonine175, a novel pathological phosphorylation site on tau protein linked to multiple tauopathies. *Acta Neuropathol. Commun.* 5:6. doi: 10.1186/s40478-016-0406-4

Nakamura, K., Greenwood, A., Binder, L., Bigio, E. H., Denial, S., Nicholson, L., et al. (2012). Proline isomer-specific antibodies reveal the early pathogenic tau conformation in Alzheimer's disease. *Cell* 149, 232–244. doi: 10.1016/j.cell.2012.02.016

Nakamura, S., Wate, R., Kaneko, S., Ito, H., Oki, M., Tsuge, A., et al. (2014). An autopsy case of sporadic amyotrophic lateral sclerosis associated with the I113T SOD1 mutation. *Neuropathology* 34, 58–63. doi: 10.1111/neup.12049

Namgung, U., and Xia, Z. (2000). Arsenite-induced apoptosis in cortical neurons is mediated by c-Jun N-terminal protein kinase 3 and p38 mitogen-activated protein kinase. *J. Neurosci.* 20, 6442–6451. doi: 10.1523/JNEUROSCI.20-17-06442.2000

Neary, D., Snowden, J. S., Gustafson, L., Passant, U., Stuss, D., Black, S., et al. (1998). Frontotemporal lobar degeneration. A consensus on clinical diagnostic criteria. *Neurology* 51, 1546–1554. doi: 10.1212/WNL.51.6.1546

Neary, D., Snowden, J. S., Mann, D. M., Northern, B., Goulding, P. J., and MacDermott, N. (1990). Frontal lobe dementia and motor neuron disease. *J. Neurol. Neurosurg. Psychiatry* 53, 23–32. doi: 10.1136/jnnp.53.1.23

Neumann, M., Sampathu, D. M., Kwong, L. K., Truax, A. C., Micsenyi, M. C., Chou, T. T., et al. (2006). Ubiquitinated TDP-43 in frontotemporal lobar degeneration and amyotrophic lateral sclerosis. *Science* 314, 130–133. doi: 10.1126/science.1134108

Oh, S. I., Park, A., Kim, H. J., Oh, K. W., Choi, H., Kwon, M. J., et al. (2014). Spectrum of cognitive impairment in Korean ALS patients without known genetic mutations. *PLoS ONE* 9:e87163. doi: 10.1371/journal.pone.0087163

Olney, R. K., Murphy, J., Forshew, D., Garwood, E., Miller, B. L., Langmore, S., et al. (2005). The effects of executive and behavioral dysfunction on the course of ALS. *Neurology* 65, 1774–1777. doi: 10.1212/01.wnl.0000188759.87240.8b

Orrell, R. W., King, A. W., Hilton, D. A., Campbell, M. J., Lane, R. J., and de Belleroche, J. S. (1995). Familial amyotrophic lateral sclerosis with a point mutation of SOD-1: intrafamilial heterogeneity of disease duration associated with neurofibrillary tangles. *J. Neurol. Neurosurg. Psychiatry* 59, 266–270. doi: 10.1136/jnnp.59.3.266

Pastorino, L., Sun, A., Lu, P. J., Zhou, X. Z., Balastik, M., Finn, G., et al. (2006). The prolyl isomerase Pin1 regulates amyloid precursor protein processing and amyloid-beta production. *Nature* 440, 528–534. doi: 10.1038/nature04543

Phukan, J., Elamin, M., Bede, P., Jordan, N., Gallagher, L., Byrne, S., et al. (2012). The syndrome of cognitive impairment in amyotrophic lateral sclerosis: a population-based study. *J. Neurol. Neurosurg. Psychiatry* 83, 102–108. doi: 10.1136/jnnp-2011-300188

Poletti, M., Enrici, I., and Adenzato, M. (2012). Cognitive and affective theory of mind in neurodegenerative diseases: neuropsychological, neuroanatomical and neurochemical levels. *Neurosci. Biobehav. Rev.* 36, 2147–2164. doi: 10.1016/j.neubiorev.2012.07.004

Prudlo, J., Bißbort, C., Glass, A., Grossmann, A., Hauenstein, K., Benecke, R., et al. (2012). White matter pathology in ALS and lower motor neuron ALS variants: a diffusion tensor imaging study using tract-based spatial statistics. *J. Neurol.* 259, 1848–1859. doi: 10.1007/s00415-012-6420-y

Rascovsky, K., Hodges, J. R., Kipps, C. M., Johnson, J. K., Seeley, W. W., Mendez, M. F., et al. (2007). Diagnostic criteria for the behavioral variant of frontotemporal dementia (bvFTD): current limitations and future directions. *Alzheimer Dis. Assoc. Disord.* 21, S14–S18. doi: 10.1097/WAD.0b013e31815c3445

Reynolds, C. H., Betts, J. C., Blackstock, W. P., Nebreda, A. R., and Anderton, B. H. (2000). Phosphorylation sites on tau identified by nanoelectrospray mass spectroscopy: differences *in vitro* between the mitogen-activated protein kinases ERK2, c-Jun N-terminal kinase and P38, and glycogen synthase kinase-3β. *J. Neurochem.* 74, 1587–1595. doi: 10.1046/j.1471-4159.2000.0741587.x

Rohrer, J. D., Nicholas, J. M., Cash, D. M., van Swieten, J., Dopper, E., Jiskoot, L., et al. (2015). Presymptomatic cognitive and neuroanatomical changes in genetic frontotemporal dementia in the Genetic Frontotemporal dementia Initiative (GENFI) study: a cross-sectional analysis. *Lancet Neurol.* 14, 253–262. doi: 10.1016/S1474-4422(14)70324-2

Shamay-Tsoory, S. G., Aharon-Peretz, J., and Perry, D. (2009). Two systems for empathy: a double dissociation between emotional and cognitive empathy in inferior frontal gyrus versus ventromedial prefrontal lesions. *Brain* 132, 617–627. doi: 10.1093/brain/awn279

Smith, E. E. (2017). Clinical presentations and epidemiology of vascular dementia. *Clin. Sci.* 131, 1059–1068. doi: 10.1042/CS20160607

Soma, K., Fu, Y. J., Wakabayashi, K., Onodera, O., Kakita, A., and Takahashi, H. (2012). Co-occurrence of argyrophilic grain disease in sporadic amyotrophic lateral sclerosis. *Neuropathol. Appl. Neurobiol.* 38, 54–60. doi: 10.1111/j.1365-2990.2011.01175.x

Spires-Jones, T. L., Attems, J., and Thal, D. R. (2017). Interactions of pathological proteins in neurodegenerative diseases. *Acta Neuropathol.* 134, 187–205. doi: 10.1007/s00401-017-1709-7

Strong, M. J. (2001). The evidence for ALS as a multisystems disorder of limited phenotypic expression. *Can. J. Neurol. Sci.* 28, 283–298. doi: 10.1017/S0317167100001505

Strong, M. J. (2003). The basic aspects of therapeutics in amyotrophic lateral sclerosis. *Pharmacol. Ther.* 98, 379–414. doi: 10.1016/S0163-7258(03)00040-8

Strong, M. J. (2008). The syndromes of frontotemporal dysfunction in amyotrophic lateral sclerosis. *Amyotroph. Lateral Scler.* 9, 323–338. doi: 10.1080/17482960802372371

Strong, M. J. (2017). Revisiting the concept of amyotrophic lateral sclerosis as a multisystems disorder of limited phenotypic expression. *Curr. Opin. Neurol.* 30, 599–607. doi: 10.1097/WCO.0000000000000488

Strong, M. J., Abrahams, S., Goldstein, L. H., Woolley, S., Mclaughlin, P., Snowden, J., et al. (2017). Amyotrophic lateral sclerosis - frontotemporal spectrum disorder (ALS-FTSD): revised diagnostic criteria. *Amyotroph. Lateral Scler. Frontotemporal Degener.* 18, 153–174. doi: 10.1080/21678421.2016.1267768

Strong, M. J., Grace, G. M., Freedman, M., Lomen-Hoerth, C., Woolley, S., Goldstein, L. H., et al. (2009). Consensus criteria for the diagnosis of frontotemporal cognitive and behavioural syndromes in amyotrophic lateral sclerosis. *Amyotroph. Lateral Scler.* 10, 131–146. doi: 10.1080/17482960802654364

Strong, M. J., Grace, G. M., Orange, J. B., and Leeper, H. A. (1996). Cognition, language and speech in amyotrophic lateral sclerosis: a review. *J. Clin. Exp. Neuropsychol.* 18, 291–303. doi: 10.1080/01688639608408283

Strong, M. J., Grace, G. M., Orange, J. B., Leeper, H. A., Menon, R. S., and Aere, C. (1999). A prospective study of cognitive impairment in ALS. *Neurology* 53, 1665–1670. doi: 10.1212/WNL.53.8.1665

Strong, M. J., Kesavapany, S., and Pant, H. C. (2005). The pathobiology of amyotrophic lateral sclerosis: a proteinopathy? *J. Neuropathol. Exp. Neurol.* 64, 649–664. doi: 10.1097/01.jnen.0000173889.71434.ea

Strong, M. J., Yang, W., Strong, W. L., Leystra-Lantz, C., Jaffe, H., and Pant, H. C. (2006). Tau protein hyperphosphorylation in sporadic ALS with cognitive impairment. *Neurology* 66, 1770–1771. doi: 10.1212/01.wnl.0000218161.15834.db

Sultana, R., Boyd-Kimball, D., Poon, H. F., Cai, J., Pierce, W. M., Klein, J. B., et al. (2006). Oxidative modification and down-regulation of Pin1 in Alzheimer's disease hippocampus: a redox proteomics analysis. *Neurobiol. Aging* 27, 918–925. doi: 10.1016/j.neurobiolaging.2005.05.005

Takeuchi, R., Toyoshima, Y., Tada, M., Tanaka, H., Shimizu, H., Shiga, A., et al. (2016). Globular glial mixed four repeat tau and TDP-43 proteinopathy with motor neuron disease and frontotemporal dementia. *Brain Pathol.* 26, 82–94. doi: 10.1111/bpa.12262

Tan, R. H., Yang, Y., and Halliday, G. M. (2017). Multiple neuronal pathologies are common in young patients with pathologically proven Frontotemporal lobar degeneration. *Neuropathol. Appl. Neurobiol.* doi: 10.1111/nan.12455. [Epub ahead of print].

Tran, H. T., Sanchez, L., and Brody, D. L. (2012). Inhibition of JNK by a peptide inhibitor reduces traumatic brain injury-induced tauopathy in transgenic mice. *J. Neuropathol. Exp. Neurol.* 71, 116–129. doi: 10.1097/NEN.0b013e3182456aed

Turner, M. R., and Verstraete, E. (2015). What does imaging reveal about the pathology of amyotrophic lateral sclerosis? *Curr. Neurol. Neurosci. Rep.* 15:45. doi: 10.1007/s11910-015-0569-6

Vance, C., Rogelj, B., Hortobágyi, T., De Vos, K. J., Nishimura, A. L., Sreedharan, J., et al. (2009). Mutations in FUS, an RNA processing protein, cause familial amyotrophic lateral sclerosis type 6. *Science* 323, 1208–1211. doi: 10.1126/science.1165942

van der Hulst, E. J., Bak, T. H., and Abrahams, S. (2015). Impaired affective and cognitive theory of mind and behavioural change in amyotrophic lateral sclerosis. *J. Neurol. Neurosurg. Psychiatry* 86, 1208–1215. doi: 10.1136/jnnp-2014-309290

Vintilescu, C. R., Afreen, S., Rubino, A. E., and Ferreira, A. (2016). The Neurotoxic TAU45-230 fragment accumulates in upper and lower motor neurons in amyotrophic lateral sclerosis subjects. *Mol. Med.* 22. doi: 10.2119/molmed.2016.00095. [Epub ahead of print].

Volkening, K., Leystra-Lantz, C., and Strong, M. J. (2010). Human low molecular weight neurofilament (NFL) mRNA interacts with a predicted p190RhoGEF homologue (RGNEF). *Amyotroph. Lateral Scler.* 11, 97–103. doi: 10.3109/17482960902995584

Volkening, K., Strong, W. L., Seaton, S., Yang, W., and Strong, M. J. (2017). C9orf72 mutations do not influence the tau signature of amyotrophic lateral sclerosis with cognitive impairment (ALSci). *Amyotroph. Lateral Scler. Frontotemporal. Degener.* 18, 549–554. doi: 10.1080/21678421.2017.1332075

Walhout, R., Schmidt, R., Westeneng, H. J., Verstraete, E., Seelen, M., van Rheenen W., et al. (2015). Brain morphologic changes in asymptomatic C9orf72 repeat expansion carriers. *Neurology* 85, 1780–1788. doi: 10.1212/WNL.0000000000002135

Ward, S. M., Himmelstein, D. S., Lancia, J. K., and Binder, L. I. (2012). Tau oligomers and tau toxicity in neurodegenerative disease. *Biochem. Soc. Trans.* 40, 667–671. doi: 10.1042/BST20120134

Wilson, C. M., Grace, G. M., Munoz, D. G., He, B. P., and Strong, M. J. (2001). Cognitive impairment in sporadic ALS. A pathological continuum underlying a multisystem disorder. *Neurology* 57, 651–657. doi: 10.1212/WNL.57.4.651

Yang, W., Ang, L. C., and Strong, M. J. (2005). Tau protein aggregation in the frontal and entorhinal cortices as a function of aging. *Dev. Brain Res.* 156, 127–138. doi: 10.1016/j.devbrainres.2005.02.004

Yang, W., Leystra-Lantz, C., and Strong, M. J. (2008). Upregulation of GSK3β expression in frontal and temporal cortex of ALS with cognitive impairment (ALSci). *Brain Res.* 1196, 131–139. doi: 10.1016/j.brainres.2007.12.031

Yang, W., Sopper, M. M., Leystra-Lantz, C., and Strong, M. J. (2003). Microtubule-associated tau protein positive neuronal and glial inclusions in amyotrophic lateral sclerosis. *Neurology* 61, 1766–1773. doi: 10.1212/01.WNL.0000099372.75786.F8

Yang, W., and Strong, M. J. (2012). Widespread neuronal and glial hyperphosphorylated tau deposition in ALS with cognitive impairment. *Amyotroph. Lateral Scler.* 13, 178–193. doi: 10.3109/17482968.2011.622405

Conflict of Interest Statement: The authors declare that the research was conducted in the absence of any commercial or financial relationships that could be construed as a potential conflict of interest.

frontiers in Neuroscience

REVIEW
published: 22 May 2018
doi: 10.3389/fnins.2018.00255

Association Between Autophagy and Neurodegenerative Diseases

*Nobuhiro Fujikake, Minkyoung Shin and Shigeomi Shimizu**

Department of Pathological Cell Biology, Medical Research Institute, Tokyo Medical and Dental University, Tokyo, Japan

Autophagy is a phylogenetically conserved mechanism that controls the degradation of subcellular constituents, including misfolded proteins, and damaged organelles. The progression of many neurodegenerative diseases is thought to be driven by the aggregation of misfolded proteins; therefore, autophagic activity is thought to affect disease severity to some extent. In some neurodegenerative diseases, the suppression of autophagic activity accelerates disease progression. Given that the induction of autophagy can potentially mitigate disease severity, various autophagy-inducing compounds have been developed and their efficacy has been evaluated in several rodent models of neurodegenerative diseases.

Keywords: autophagy, neurodegenerative disease, Alzheimer disease, tauopathy, Parkinson disease, amyotrophic lateral sclerosis, polyglutamine disease

OPEN ACCESS

Edited by:
Naruhiko Sahara,
National Institute of Radiological Sciences (NIRS), Japan

Reviewed by:
Gen Matsumoto,
Nagasaki University, Japan
Patrícia Maciel,
Escola de Medicina da Universidade do Minho, Portugal
Sabine Gilch,
University of Calgary, Canada

****Correspondence:***
Shigeomi Shimizu
shimizu.pcb@mri.tmd.ac.jp

Specialty section:
This article was submitted to Neurodegeneration, a section of the journal Frontiers in Neuroscience

Received: *04 December 2017*
Accepted: *03 April 2018*
Published: *22 May 2018*

Citation:
Fujikake N, Shin M and Shimizu S (2018) Association Between Autophagy and Neurodegenerative Diseases. Front. Neurosci. 12:255. doi: 10.3389/fnins.2018.00255

INTRODUCTION

A common pathology shared by several neurodegenerative diseases, including Alzheimer disease (AD), Parkinson disease (PD), amyotrophic lateral sclerosis (ALS), and the polyglutamine (polyQ) diseases is the accumulation of misfolded proteins. Because autophagy is a cellular function that degrades abnormal proteins, including those that are misfolded, the onset and progression of these diseases are affected by autophagic activity within neurons. In this review, we first summarize the molecular mechanism and physiological relevance of autophagy. Next, we review how autophagy is involved in the pathology of several neurodegenerative diseases. We also summarize the therapeutic effects of autophagy-modulating compounds on these neurodegenerative diseases.

MOLECULAR MECHANISMS OF AUTOPHAGY

Autophagy is a catabolic process in which cellular contents, including proteins, lipids, and entire organelles, are degraded by lysosomal lytic enzymes. Autophagy constitutively functions at low levels but is highly induced by a variety of cellular stressors, such as nutrient starvation, growth factor withdrawal, DNA damage, the accumulation of abnormal proteins, and organelle damage. In many physiological and pathological contexts, autophagy protects cells by facilitating the degradation of superfluous or damaged cellular constituents, for the subsequent recycling of amino acids, lipids, nutrients, and metabolites.

There are at least three distinct autophagic mechanisms, namely, macroautophagy, microautophagy, and chaperone-mediated autophagy. Macroautophagy is believed to be the core pathway for degrading cytoplasmic proteins and organelles (Nakatogawa et al., 2009). In this process, cytoplasmic components and organelles are incorporated into double-membrane structures called autophagosomes. Subsequently, the outer membrane of the cellular constituents are broken down by acid hydrolases (Mizushima et al., 2002). The term "autophagy" is usually used synonymously with macroautophagy (hereafter referred to simply as "autophagy" unless

otherwise indicated). The second type of autophagy is microautophagy, which occurs via direct invagination of the lysosomal membrane to engulf cellular constituents, followed by closure of the membrane pocket and degradation of the constituents within the lysososomal lumen (Li et al., 2012). Microautophagy can deliver entire organelles, such as peroxisomes, directly into lysosomes. The third type of autophagy is chaperone-mediated autophagy. During chaperone-mediated autophagy, cytoplasmic proteins with a targeting motif interact with the cytosolic heat shock cognate 70 chaperone, which delivers the proteins to the lysosomal membranes (Kaushik and Cuervo, 2012). Substrate proteins are subsequently recognized by the lysosomal receptor and are unfolded to penetrate the lysosomal membrane through a multimeric complex. After substrate translocation, rapid degradation of substrate proteins occurs in the lysosomal lumen. Thus, chaperone-mediated autophagy enables targeted protein degradation as opposed to the nonspecific or "bulk" protein degradation that occurs during macroautophagy.

Analysis of the molecular mechanisms involved in autophagy began with a genetic approach using autophagy-defective mutant yeast strains (Nakatogawa et al., 2009). Subsequently, many mammalian homologs of yeast autophagy proteins and their biochemical functions have been identified (**Figure 1**). It is now accepted that autophagy is driven by more than 30 autophagy-related proteins (Atgs) (Mizushima and Komatsu, 2011). Atg1 was the first such protein identified and shown to have intrinsic serine/threonine kinase activity, which is essential for the initiation of autophagy (Kabeya et al., 2005). Autophagy is regulated by phosphatidylinositol 3-kinase (PI3K) type I and type III. PI3K type I is activated by growth factors, and suppresses autophagy through the regulation of mammalian target of rapamycin (mTOR). Conversely, PI3K type III, which exists in a multiprotein complex including Atg6 (also called Beclin 1), facilitates the generation of the omegasomes, which is the initial membrane component of the isolation membrane (Axe et al., 2008). Isolation membranes subsequently expand, curve and close by two conjugation pathways, namely, the Atg5–Atg12 pathway and the microtubule-associated protein 1 light chain 3 (LC3) pathway (Mizushima and Komatsu, 2011). The ubiquitin-like conjugation of phosphatidylethanolamine (PE) to LC3 couples with the translocation of LC3 from the soluble fraction to autophagic membranes. Therefore, the localization of LC3-PE in autophagic membranes is a reliable marker of autophagy. The following lines of evidence indicate that the Atg5–Atg12 pathway is essential for the initiation of autophagy: (1) yeast Atg5 is crucial for autophagy, (2) autophagy is suppressed in some cell types from Atg5-deficient mice, and (3) LC3-PE formation has never been detected in Atg5-deficient cells. However, Atg5-deficient mouse embryos develop normally until the perinatal period (Kuma et al., 2004; Komatsu et al., 2005), suggesting that an alternative autophagic pathway may exist that compensates for the lack of Atg5-dependent autophagy in embryonic mutant mice.

In fact, we found that treatment with etoposide, a topoisomerase inhibitor that induces DNA strand breaks in mitotic cells, causes the formation of autophagic structures even in Atg5-deficient mouse embryonic fibroblasts (MEFs). The numbers and sizes of these autophagic vacuoles were equivalent in wild-type and Atg5-deficient MEFs, and the morphology of these etoposide-induced autophagic structures was indistinguishable from the autophagic vacuoles observed during starvation-induced autophagy (Nishida et al., 2009). Therefore, MEFs appear to perform two distinct types of autophagy, an Atg5-dependent conventional type and an Atg5-independent alternative type, which show similar morphological characteristics (**Figure 1**). Unlike Atg5-dependent autophagy, the molecules required for and the physiological roles of alternative autophagy have not yet been elucidated.

THE ULK1 COMPLEX

Molecular mechanisms of conventional autophagy have been extensively studied using nutrient-starved cells, by referring to the information obtained from starved yeast cells, in which functional complexes containing Atg proteins drive for the formation of autophagic vacuoles. Starvation-induced autophagy begins from modifications in mTor and AMK-activated protein kinase (AMPK), which are well-established cellular nutritional sensors. mTor is a member of the serine/threonine protein kinase family and serves as a core component of two distinct protein complexes, mTor complex 1 (mTorc1) and mTorc2, which regulate different cellular processes. In healthy cells, mTorc1 suppresses autophagy by phosphorylating and inactivating Unc-51-like kinase 1 (Ulk1), a homolog of yeast Atg1 and an initiator of mammalian autophagy. AMPK is another kinase that plays a role in cellular energy homeostasis, and also suppresses autophagy by phosphorylating different amino acid residues of Ulk1. Upon nutrient starvation, Ulk1 is dephosphorylated by protein phosphatase 2A (PP2A) and translocates to limited membranes together with Fip200, Atg13, and Atg101. The membrane-associated ULK1 complex then phosphorylates multiple substrates, leading to the induction of conventional autophagy.

The Ulk1 protein is also crucial for alternative autophagy. Addition of etoposide induced the accumulation and autophosphorylation of Ulk1 in Atg5-deficient MEFs. Furthermore, no autophagic membranes were observed within Ulk1-silenced Atg5-deficient MEFs in response to etoposide. Similar results were also observed when Fip200, another component of the Ulk1 complex, was silenced. Thus, Ulk1 functions in the initiation of both conventional and alternative autophagy (**Figure 1**) (Nishida et al., 2009). The mechanism involved in the specific activation of each pathway by different stressors remains unclear. These two forms of autophagy may be selectively activated by the phosphorylation and activation of different Ulk1 substrates.

THE PI3K COMPLEX

The class III PI3 kinase Vps34 phosphorylates PI at the 3′-hydroxyl position to produce PI3P, an abundant component of

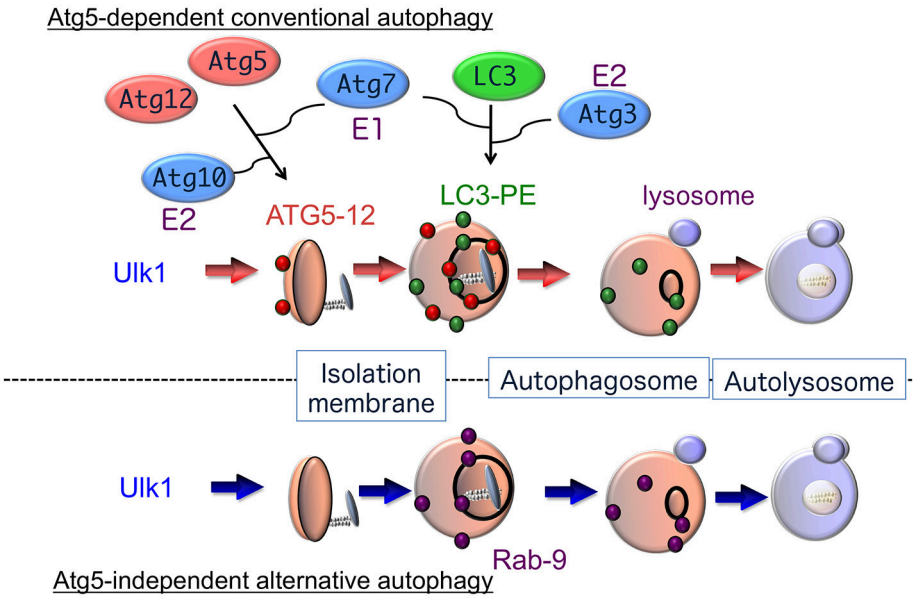

FIGURE 1 | Hypothetical model of autophagy. There are at least two modes of macroautophagy, i.e., conventional and alternative autophagy. Conventional autophagy requires Atg5 and Atg7, is associated with LC3 modification, and is thought to originate from the ER membrane. After Ulk1 stimulation, Atg5-12 complexes (red circles) attach to isolation membranes, and then LC3-PE puncta (green circles) are incorporated into autophagosomal membranes. In contrast, alternative autophagy occurs independently of Atg5 and Atg7, as well as LC3 modification. The generation of autophagic vacuoles in alternative autophagy is mediated by the fusion of isolation membranes with vesicles derived from the *trans*-Golgi as well as late endosomes, in a Rab9-dependent manner. After Ulk1 stimulation, Rab9 puncta (purple circles) attach to autophagic membranes.

autophagosomal membranes that is essential for autophagosome formation (Kihara et al., 2001). An autophagosome formation-specific PI3 kinase complex composed of Atg14L, Beclin 1, Vps15, and Vps34 was identified (Itakura et al., 2008). Two additional Vps34 complexes, Vps34-Vps15-Beclin 1-UVRAG and Vps34-Vps15-Beclin 1-UVRAG-Rubicon, function in the endocytic pathway and in the regulation of autophagosome/lysosome fusion, respectively (Matsunaga et al., 2009) (Zhong et al., 2009). Beclin 1 is also regulated by B-cell leukemia/lymphoma-2 (Bcl-2) family proteins, such as Bcl-2, Bcl-x_L, and Bim (Levine et al., 2008). The protein double FYVE domain-containing protein 1 has been identified as a downstream effector of PI3P and it is concentrated within membrane domains of the endoplasmic reticulum (ER) that are sites of isolation membrane creation (Axe et al., 2008). The ULK1 complex was also reported to associate with the autophagosome formation-specific PI3K complex to generate isolation membranes. This PI3K complex is also crucial for alternative autophagy, as silencing Vps34 and Beclin 1 inhibited the alternative pathway (Nishida et al., 2009).

ATG5-ATG12 AND LC3 PATHWAYS

Two unique ubiquitin-like conjugation systems, the Atg5–Atg12 pathway and the LC3 pathway, are believed to be essential for the induction of conventional autophagy (**Figure 1**). The Atg5–Atg12 pathway is initiated when Atg12 is conjugated to Atg5 by Atg7 (E1 enzyme) and Atg10 (E2 enzyme) (Mizushima and Komatsu, 2011), and the Atg5–Atg12 conjugate further binds with Atg16 to generate an Atg5–Atg12/Atg16 complex. The second protein conjugation system is controlled by the Atg8 homolog LC3, gamma-aminobutyric acid receptor-associated protein (GABARAP), and Golgi-associated ATPase enhancer of 16 kD (GATE-16). During autophagy, these proteins are cleaved by the cysteine protease Atg4, resulting in the exposure of a glycine residue, which is then catalyzed by Atg7 (E1 enzyme), Atg3 (E2 enzyme), and the Atg5–Atg12/Atg16 complex (E3 enzyme). PE then binds to the exposed glycine residue and acts to localize these proteins to isolation membranes and autophagosome membranes. The PE-conjugated forms of LC3, GABARAP, and GATE-16 (termed LC3-II, type II GABARAP, and type II GATE16) are reliable markers of conventional autophagy (Kabeya et al., 2000).

Although Ulk1 and PI3K complexes participate in both conventional and alternative autophagy, neither the Atg5–Atg12 nor the LC3 conjugation pathway is required for alternative autophagy. Furthermore, the conversion of LC3-I to PE-conjugated LC3-II does not occur in alternative autophagy (Nishida et al., 2009). Thus, it is unknown as to how extension and closure of autophagic membranes are accomplished during alternative autophagy without these two ubiquitin-like systems. Detailed morphological analysis has, however, provided some clues. We demonstrated that elongation and closure of isolation membranes, presumably derived from trans-Golgi membranes are generated by fusion with endosomal vesicular membranes (Nishida et al., 2009). The involvement

of trans-Golgi/endosomal fusion in the extension and closure of isolation membranes was confirmed by the colocalization of mannose-6-phosphate receptors (a trans-Golgi/late endosomal marker) and syntaxin 7 (a late endosomal marker) with Lamp2-positive vacuoles in etoposide-treated Atg5-deficient MEFs (Nishida et al., 2009). The formation of isolation membranes by trans-Golgi/endosomal fusion is also supported by studies showing a requirement for Rab9, a GTPase required for the trafficking of proteins from late endosomes to trans-Golgi membranes (Kabeya et al., 2000). First, GFP-Rab9 was colocalized with autolysosomes in etoposide-treated Atg5-deficient MEFs, and this colocalization was increased by the expression of GFP-Rab9^{Q66L}, a constitutively active Rab9 mutant, and reduced by the expression of GFP-Rab9^{S21N}, a guanosine diphosphate (GDP)-preferring dominant-negative Rab9 mutant (Nishida et al., 2009). Moreover, Rab9 silencing by a targeted siRNA reduced the number of autophagic vacuoles but induced the accumulation of isolation membranes. Numerous isolation membranes are normally generated by etoposide exposure, so siRab9 did not merely slow down the progression of autophagy but rather inhibited autophagosome maturation. The role of Rab9 in the extension and closure of isolation membranes in the alternative autophagy pathway is thought to replace the role of Atg5/Atg7/LC3 in conventional autophagy (**Figure 1**).

PHYSIOLOGICAL ROLE OF AUTOPHAGY IN NEURODEGENERATION

Autophagy can be classified into constitutive and inducible types according to the mechanism of induction (**Table 1**). Whereas constitutive autophagy continuously degrades abnormal proteins to maintain cellular homeostasis, inducible autophagy occurs on a larger scale to suppress cellular injury against various stressors. Autophagy can also be classified into bulk and selective types based on the cargo that is degraded. Autophagy was originally considered to degrade subcellular constituents in a nonselective manner, i.e., bulk autophagy. However, specific molecules and organelles are also digested by selective autophagy during which cargo molecules are recognized by cargo receptors and subsequently enclosed by autophagic structures. According to these classification criteria, the well-studied starvation-induced type of autophagy is considered as inducible and bulk autophagy. Many phenotypes observed in systemic and tissue-specific *Atg* knockout mice, such as defects in preimplantation fetal development (Kuma et al., 2004), are due to the failure of constitutive and selective autophagy. As *Atg7*-deficient mice lack conventional autophagy, they demonstrate neurological defects, including the abnormal limb-clasping reflexes, because of the severe damage to cortical and cerebellar neurons (Komatsu et al., 2006). Furthermore, there was reactive gliosis was observed in association with neuronal loss. Importantly, ubiquitin-positive aggregates were found in neurons. These findings illustrate that conventional autophagy prevents neuronal damage by constitutively eliminating ubiquitin-positive aggregates.

TABLE 1 | Classification of autophagy from the view of inducers and substrates.

Inducer \ Substrate	Bulk autophagy (non-specific degradation)	Selective autophagy (specific degradation)
Constitutive autophagy (maintain homeostasis)	**Cellular metabolism** Replace old proteins/organelles with new ones	**Cell protection** Degrade unfavorable, damaged proteins, and organelles
Inducible autophagy (response to various stimuli)	**Nutrient supply** Starvation-induced Rapamycin-activated	**Cellular adaptation** Cellular stress (DNA damage, etc.) Differentiation

NEURODEGENERATIVE DISEASES AND AUTOPHAGY IN HUMANS

Consistent with the findings observed in autophagy-deficient mice showing neurodegenerative defects, an impairment of autophagy is often associated with human neurodegenerative diseases. In some cases, autophagy failure is considered as the primary underlying disease pathology. In most neurodegenerative diseases, including ALS, PD, AD, and the polyQ diseases, the accumulation of misfolded proteins is a common pathological hallmark. These misfolded proteins damage neurons, eventually causing their death. Because the reduction of autophagic activity directly affects the accumulation of misfolded proteins, autophagy is a key target pathway for the treatment of neurodegenerative diseases (**Figure 2**). In this section, we briefly describe the relationship between conventional autophagy and several major neurodegenerative diseases.

ALS/ TDP-43 PROTEINOPATHIES

ALS, a fatal neurodegenerative disorder, is primarily a sporadic disease; however, approximately 5–10% of the cases are familial. In particular, mutations in several genes including superoxide dismutase 1 (*SOD1*), TAR DNA-binding protein-43 (*TDP-43*), fused in sarcoma/translocated in liposarcoma (*FUS/TLC*), and/or *C9orf72*, are thought to contribute to the progressive degeneration of motor neurons. A mutation in *SOD1* was the first genetic mutation that was shown to be associated with ALS, and more than 170 *SOD1* mutations have been identified to date. TDP-43, a nuclear factor that controls the fate of cellular RNAs, is found in an aggregated form in neurons of ALS patients, and genetic mutations in *TDP-43* were recently identified in some ALS patients. These mutants commonly fail to fold properly, leading to the accumulation of misfolded proteins in neurons of ALS patients. Numerous studies suggest that autophagy might be a significant regulator of pathological aggregate formation in ALS. For example, the overexpression of transcription factor EB (TFEB), a master regulator of the transcription of autophagy-related genes, led to increases in the expression of Beclin 1 and LC3 and suppressed the cellular toxicity induced by the expression of these mutant proteins (Chen Y. et al., 2015).

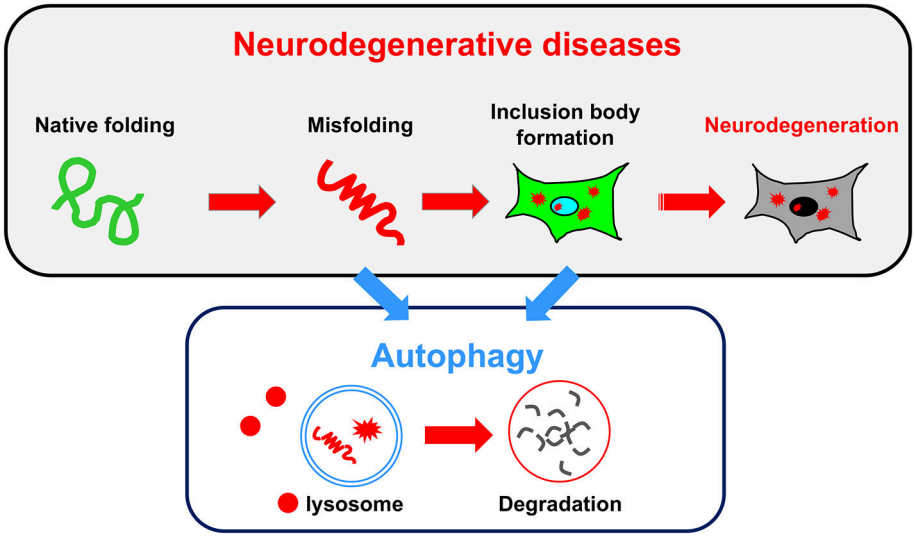

FIGURE 2 | Relationship between neurodegenerative diseases and autophagy. A common pathology shared by several neurodegenerative diseases is the accumulation of misfolded proteins and inclusion bodies. Autophagy may be useful for degrading both misfolded proteins and inclusion bodies.

Recently, receptors for selective autophagy, such as sequestosome-1 (SQSTM1)/p62 and optineurin (OPTN), as well as TANK-binding kinase 1 (TBK1) were shown to be involved in the degeneration of motor neurons (Maruyama et al., 2010; Teyssou et al., 2013; Freischmidt et al., 2015). Insoluble protein aggregates of these proteins were found to accumulate in motor neurons and surrounding glial cells. Intriguingly, these inclusions were found in the brainstem, spinal cord, cerebellum, hippocampus, and frontal and temporal lobes of ALS patients. SQSTM1 interacts with and sequesters autophagy substrates to isolation membranes via its interaction with LC3, and ALS-causing *SQSTM1* mutants increase the expression levels of TDP-43 (Teyssou et al., 2013). Consistently, mutations in the *SQSTM1* were shown to suppress the recruitment of mutant SOD1 into autophagosomes (Gal et al., 2017). OPTN also plays a role in sequestering cargo to nascent autophagic vacuoles via its interaction with LC3 (Wild et al., 2011). In addition, OPTN interacts with myosin VI for the proper trafficking of autophagosomes (Sahlender et al., 2005). Interestingly, most of the ALS-causing mutations in *OPTN* are located in the myosin VI-binding domain (Sundaramoorthy et al., 2015). These mutants do not interact with myosin VI and are unable to eliminate mutant SOD1 and TDP-43. Finally, TBK1 promotes autophagy by phosphorylating both SQSTM1 and OPTN, and ALS-associated mutations in *TBK1* reduce its binding affinity with OPTN and decrease the clearance of dysfunctional mitochondria (Richter et al., 2016).

Mutations in *C9orf72*, the most common cause of ALS, have been proposed to downregulate autophagy (Ji et al., 2017). C9orf72 is a core component of GDP/ GTP exchange factor (GEF) for Rab8 and Rab39, which is crucial for autophagosome maturation. This molecule also interacts with Ulk1 and advances the autophagy machinery; as such, ALS-associated mutations of *C9orf72* do not interact with Rab proteins, and autophagy fails to proceed (Tang, 2016; Corbier and Sellier, 2017). These findings indicate that selective autophagy, which degrades SOD1 and TDP-43 mutants and requires SQSTM1, OPTN, and TBK1, is crucial for protection from ALS.

Autophagy facilitates the reduction of unfolded proteins. For example, progesterone and lithium were shown to activate autophagic flux, thereby decreasing SOD1 aggregates and improving motor dysfunction in SOD1-mutant mice (Motoi et al., 2014). Consistently, trehalose, a disaccharide that induces mTor-independent autophagy, was demonstrated to inhibit TDP-43 aggregate formation (Wang et al., 2010), whereas the activation of mTor-dependent autophagy by rapamycin also rescued motor dysfunction in TDP-43 transgenic mice (Wang et al., 2012). Not only misfolded protein aggregation but also mitophagy failure contributes to ALS pathology. Disease-associated mutants of OPTN, a key molecule in mitophagy, results in the failure to remove damaged mitochondria, as well as misfolded protein aggregates, and contribute to the neurodegeneration in ALS (Wong and Holzbaur, 2014). Despite the widespread evidence regarding the therapeutic outcomes of autophagy induction in diseased neurons, the role of autophagy is more complex, because n-butylidenephthalide (n-BP), an extract from *Angelica sinensis*, inhibits neuronal autophagy by activating the Akt/mTOR signaling but attenuates neuronal loss and improves motor function (Hsueh et al., 2016). Therefore, autophagy activators do not always show positive effects on ALS progression. The manner in which autophagy is induced is key to its protective or destructive effects in ALS. Studies to further our understanding of the autophagy pathway and

its utility as a promising therapeutic strategy for ALS are important.

POLYGLUTAMINE DISEASES

PolyQ diseases, including Huntington disease (HD), spinal and bulbar muscular atrophy, dentatorubral-pallidoluysian atrophy, spinocerebellar ataxia (SCA) types 1, 2, 3, 6, 7, and 17, and HD-like 2 are inherited progressive neurodegenerative diseases elicited by expansions of CAG triplet repeats within specific genes. PolyQ tracts in mutant proteins, i.e., mutant Huntingtin (Htt) in HD, encoded by the CAG repeat, are responsible for the formation of toxic oligomers and aggregates. The length of the polyQ tract is crucial, because longer tracts are more prone to form aggregates. These mutant proteins accumulate and form intracellular inclusions, and previous studies showed that autophagy degrades not only these inclusions but also soluble mutant proteins. Importantly, the degradation of mutant proteins was shown to decrease neuronal damage and improve neurodegenerative deficits in mouse models of the polyQ diseases.

Recent studies have increasingly focused on the perturbation of autophagy in the polyQ diseases, such as that observed in striatal neurons in HD mouse models and lymphocytes in HD patients. In HD cells, cargo recognition was shown to be significantly impaired due to the failure of p62 interaction with mutant Htt, which leads to the inefficient selective degradation of mutant Htt (Fu et al., 2017). Moreover, because the accumulated mutant Htt can potentially trap and inactivate Beclin 1 (Shibata et al., 2006), autophagy is significantly suppressed at the autophagosome-lysosome fusion stage. Mutant Htt also interacts with and inactivates Ras homolog enriched in striatum (Rhes), an autophagy regulator (Mealer et al., 2014). Rhes accelerates autophagy by inhibition of the interaction of Beclin 1 with Bcl-2. The inhibition of autophagy leads to the further accumulation of mutant Htt and neuronal injury. Consistently, in SCA7-mutant patients and mice, the accumulation of p62 and ubiquitin were observed, indicating the impairement of autophagic activity (Alves et al., 2014). Furthermore, the androgen receptor with an expanded polyQ repeat was shown to interact and attenuate the function of TFEB (Song et al., 2013; Cortes et al., 2014). Although studies suggesting that autophagic activity is altered in mouse models of polyQ disease are controversial, an impairment of autophagy is expected to occur in many of the neurons with polyQ accumulation.

PolyQ disease pathogenesis is strongly affected by neuronal autophagic activity. Therefore, the activation of autophagy can potentially prevent the accumulation of aggregate-prone proteins, thus inhibiting or slowing the progression of neurodegeneration. Upregulating autophagy with rapamycin reduced the formation of aggregates and cytotoxicity in cells *in vitro* and in a fly model of HD *in vivo* (Ravikumar et al., 2002, 2004). CCI-779, a rapamycin analog, also improved behavioral and motor performance in mouse models of HD and SCA3 (Ravikumar et al., 2004). Other autophagy inducers, such as berberine, metformin, rilmenidine, and trehalose also activate autophagy, decrease polyQ aggregation, and improve behavioral performance in polyQ disease mouse models (Tanaka et al., 2004; Ma et al., 2007; Rose et al., 2010; Chen Z. Z. et al., 2015; Jiang et al., 2015). Metformin is an antidiabetic drug that activates AMPK-dependent autophagy (Poels et al., 2009), and rilmenidine is used for hypertension and activates mTor-independent autophagy (Rose et al., 2010). Both drugs are already used clinically in humans. In contrast, in a mouse model of SCA3, the combination of CCI-779 with LiCl showed no beneficial effects, but rather toxic effects (Duarte-Silva et al., 2016). Clinical trials have been performed to assess their utility in neurodegenerative diseases.

ALZHEIMER DISEASE

AD is a chronic neurodegenerative disease that causes memory and cognitive deficits. AD is characterized by the accumulation of neurotoxic extracellular beta-amyloid (Aβ) plaques and hyperphosphorylated tau in intracellular neurofibrillary tangles (NFTs) in the brain. Aβ is generated from amyloid precursor protein (APP) by two cleavage events. Aβ homeostasis in the brain is believed to play a key role in the progression of neurodegeneration, and several studies demonstrated that various clearance mechanisms play pivotal roles in the development of AD. However, the role of autophagy in AD pathogenesis remains controversial. Numerous studies have reported the degradation of Aβ and APP by autophagy and the reduction of Aβ expression by the upregulation of autophagy, similar to that observed with other proteins associated with neurodegenerative diseases. However, some studies have reported the requirement of autophagy in AD pathogenesis. These contradictory findings stem from studies showing that Aβ generation was suppressed following the inhibition of autophagy by 3-methyl adenine (Zheng et al., 2011). Furthermore, this idea is supported by the presence of APP and Aβ in purified autophagic vacuoles from brains of AD patients. In these vacuoles, presenilin-1 (PS-1), an enzyme that cleaves APP, is highly enriched. Autophagy was also shown to contribute to Aβ secretion, a crucial event in AD pathogenesis. Delivery of Aβ to the extracellular space and plaque formation were significantly reduced due to the lack of Atg7 in APP transgenic mice, and restoration of autophagy restored Aβ secretion to normal levels (Nilsson et al., 2013).

The downregulation of autophagy was morphologically and genetically demonstrated in AD brains. Morphologically, numerous immature autophagic vacuoles were observed in dystrophic neurites of AD patients, suggesting the impairment of trafficking of autophagic vacuoles or autophagosome-lysosome fusion (Nixon et al., 2005). Genetically, Beclin 1, a major player in autophagy, was identified as a causative molecule in AD pathology. AD brains were reported to have decreased expression levels of Beclin 1 early in the disease process (Pickford et al., 2008). A reduction in Beclin 1 levels was shown to attenuate autophagic activity, which likely facilitates the proteolytic cleavage of APP. Another factor that was shown to be associated with AD is phosphatidylinositol-binding clathrin

assembly protein (PICALM), which plays a role in autophagy (Tian et al., 2013) by the trafficking of soluble NSF attachment protein receptors. PICALM was also reported to play a role as an autophagy receptor that sequesters APP to LC3-positive autophagosomes (Tian et al., 2014). Genetic studies showing a reduction in PICALM indicate that not only bulk autophagy but also selective autophagy for APP might be suppressed in AD brains. Mutations in PS-1 cause familial AD via the alteration of APP processing. However, recently, another pathological role for mutant PS-1 was proposed, which includes inhibition of the maturation of the lysosomal v-ATPase that leads to an increase in lysosomal pH and a consequent reduction in autophagic cargo elimination (Lee et al., 2010). This process might be mediated by the failure of the ER chaperone function of PS-1, which facilitates the proper assembly of the V_0a1 subunit of the v-ATPase.

Whereas the role of autophagy in Aβ generation remains controversial, various autophagy-related compounds were tested for potential therapeutic utility. Lithium and berberine, which are both autophagy inducers targeting the Ulk1-pathway, were demonstrated to induce autophagy and exert neuroprotective effects through the regulation of APP processing and a reduction in Aβ levels in the CRND8 transgenic mouse model of AD (Fiorentini et al., 2010; Durairajan et al., 2012). Both trehalose and carbamazepine were shown to exert protective effects on AD mice via mTor-independent autophagy (Du et al., 2013; Li et al., 2013). Carbamazepine was shown to significantly enhance autophagic flux in the APP(swe)/PS-1(deltaE9) AD mouse model and reduce the cerebral amyloid plaque burden and Aβ 1–42 levels (Li et al., 2013). Latrepirdine stimulates Atg5-dependent autophagy and reduces the accumulation of toxic Aß aggregates in AD mice (Steele et al., 2013). Rapamycin and SMER28, a small-molecule rapamycin enhancer, both activate autophagy and decrease the expression levels of Aß 1–42 (Spilman et al., 2010; Tian et al., 2011), which is the most amyloidogenic form of Aß, in PD-APP transgenic mice, one of the earliest mouse models of AD. Taken together, these findings suggest that, although the exact pathological role of autophagy in AD remains to be elucidated, autophagy inducers might provide a new effective therapeutic strategy by degrading aggregates in the early stages of AD. In contrast, the activation of autophagy might enhance disease severity during the late stages of AD, by accelerating Aβ production.

TAUOPATHIES

Tau is a microtubule-binding protein that attaches to and stabilizes microtubules. Tauopathies are a constellation of neurodegeneration diseases, including AD, frontotemporal lobar degeneration (FTLD), progressive supranuclear palsy (PSP), and corticobasal degeneration (CBD), in which hyperphosphorylated tau accumulates in intracellular tangles and extracellular Aβ deposits. The phosphorylation of tau by glycogen synthase kinase 3β facilitates its accumulation within the cytosol (Sperber et al., 1995). Similar to that observed with other proteins implicated in neurodegenerative diseases, the inhibition of autophagy, such as that activated by chloroquine, causes a delay in tau clearance and aggregation (Hamano et al., 2008). Furthermore, phosphorylated tau accumulation is higher in brain-specific *Atg7* knockout mice than control mice (Inoue et al., 2012), indicating that phosphorylated tau is a substrate of conventional autophagy. Consistently, phosphorylated tau colocalizes with LC3 and p62 proteins in postmortem brain specimens from patients with AD, PSP, and CBD, likely because these proteins are engulfed into autophagosomes but are not degraded by autolysosomes (Piras et al., 2016). These studies suggest that an impairment of autophagy plays a crucial role in the progression of tauopathies, and that autophagy facilitates the degradation of phosphorylated tau to maintain it at low levels.

Based on these findings, the induction of autolysosome formation appears to be a good therapeutic strategy for the tauopathies. Indeed, the activation of autophagy using rapamycin or temsirolimus, an analog of rapamycin, was shown to alleviate tau phosphorylation in neurons and to improve the progression of tau pathology in P301S mutant human tau transgenic mice (Ozcelik et al., 2013; Jiang et al., 2014). Furthermore, trehalose, and methylthioninium chloride were shown to reduce tau aggregates and improve neuronal survival in several mouse models of the tauopathies (Congdon et al., 2012; Schaeffer et al., 2012). Finally, metformin, which inhibits tau hyperphosphorylation via the inhibition of TORC1, is currently being tested for its utility against AD in several clinical trials (Kickstein et al., 2010).

PARKINSON DISEASE

PD is the second most common neurodegenerative disease following AD. The main underlying pathology of PD is functional failure and subsequent death of dopaminergic neurons in the substantia nigra, which leads to muscle rigidity, bradykinesia, resting tremor, and even neurocognitive impairment. Many of the dopaminergic neurons in PD patients contain round, cytoplasmic inclusions called Lewy bodies that are comprised of α-synuclein and ubiquitin-positive proteins. Most PD cases are sporadic, and 5–10% are familial, due to mutations in various PD-associated genes that encode for PD-associated proteins (PARK).

One subtype of familial PD arises from the A53T mutation in α-synuclein, which is encoded by *PARK1*. The level of α-synuclein in neurons is a key to neurotoxicity in PD; therefore, efficient α-synuclein degradation is a crucial determinant of PD severity. Findings from recent studies indicate that deubiquitinated α-synuclein is the main target of autophagy (Rott et al., 2011), and that degradation of stress-increased, rather than basal α-synuclein was crucial in a transgenic mouse model (Wu et al., 2016). In contrast, inclusions containing α-synuclein were shown to reduce autophagic activity during the maturation of autophagosomes and their fusion with lysosomes (Button et al., 2017). Furthermore, α-synuclein itself was also reported to suppress autophagy by the induction of Atg9 mislocalization, which was observed in α-synuclein transgenic mice (Winslow

et al., 2010). Interestingly, similar Atg9 mislocalization was observed in patients with the D620N mutation of vacuolar protein sorting-associated protein 35 (Vps35; PARK17) (Zavodszky et al., 2014). Atg9 is a Golgi-localizing protein, whereas Vps35 regulates various Golgi proteins by affecting the retromer complex. Therefore, the Vps35 mutant fails to appropriately localize Atg9 and leads to impaired autophagy.

Leucine-rich repeat serine-threonine protein kinase-2 (*LRRK2*; *PARK8*) is another PD-causing gene. LRRK2 colocalizes with Lewy bodies in some PD patient brains. LRRK2 is a large protein containing a Ras-like small GTPase domain and a MAPKKK-like kinase domain. Loss of LRRK2 causes the accumulation of α-synuclein phosphorylated on Ser129 and the impairment of protein degradation pathways, leading to apoptotic cell death in aged mice (Tong et al., 2010). The G2019S LRRK2 mutation is found not only in familial PD patients but also in 1–2% of patients with sporadic PD (Goldwurm et al., 2005). LRRK2 was suggested to suppress autophagy, because silencing of *LRRK2* or inhibition of its kinase activity was shown to increase autophagic flux (Alegre-Abarrategui et al., 2009).

Loss-of-function mutations in the P-type ATPase ATP13A2 (PARK9) causes early-onset PD (Ramirez et al., 2006). Because lysosomal ATPase is essential for the maintenance of lysosomal pH and autophagosome-lysosome fusion, mutations in ATP13A2 impair these processes, resulting in the accumulation of autophagosomes. A defect in autophagy accelerates the accumulation of α-synuclein, thereby worsening the disease.

As described above, autophagy contributes to the suppression of various neurodegenerative processes by degrading unfolded proteins. In addition, autophagy functions to inhibit certain PD types by degrading damaged mitochondria. Among the genes associated with familial PD, Parkin (*PARK2*) and Pink1 (*PARK6*) eliminate damaged mitochondria by autophagy (Clark et al., 2006; Park et al., 2006). This mechanism, termed mitophagy, starts with the accumulation of Pink1 on the outer mitochondrial membrane from the cytosol following mitochondrial depolarization. Next, Parkin, a cytosolic E3-like ligase, associates with Pink1 on the outer mitochondrial membrane, which leads to ubiquitination of depolarized mitochondria by the ubiquitin ligase activity of Parkin and recruitment of several autophagy components, including p62 (Geisler et al., 2010). Finally, ubiquitinated mitochondria are recognized by autophagic molecules and are digested by autophagy. Thus, genetic mutations in Parkin and Pink1, which cause early-onset familial and sporadic PD, fail to eliminate damaged mitochondria, which culminates in the degeneration of dopaminergic neurons. Importantly, Parkin-mediated mitophagy is significantly suppressed by the lack of Atg5 (Huang et al., 2011).

Based on these data, reduction of α-synuclein aggregation and the induction of mitophagy by autophagy might be useful therapeutic approaches against PD. In cell-based assays, several polyphenols, including resveratrol demonstrated autophagy-inducing activity and might be useful as therapeutic agents for PD. Kaempferol and celastrol also prevent rotenone-induced SH-SY5Y cell loss via autophagy activation (Filomeni et al., 2012; Deng et al., 2013). Furthermore, microencapsulated rapamycin improved motor function in mice overexpressing α-synuclein (Bai et al., 2015). Oral administration of trehalose also activated autophagy and suppressed insoluble α-synuclein accumulation (Tanji et al., 2015), whereas nilotinib, a receptor tyrosine kinase inhibitor approved for chronic myelogenous leukemia, was also shown to inhibit the protein phosphatase PP2A and induce AMPK phosphorylation and autophagy, resulting in modulation of the neuroimmune response to α-synuclein expression in mice (Yu et al., 2013).

CLOSING REMARK

In this review, we described two distinct autophagic pathways, namely, conventional and alternative autophagy, and compared their characteristics. We also described the involvement of conventional autophagy in the progression of many neurodegenerative diseases. However, the association between alternative autophagy and neurodegenerative diseases has not been fully clarified to date. In this review, we also summarized the potential uses of conventional autophagy for the treatment of various neurodegenerative diseases. Given that the induction of autophagy can potentially mitigate disease severity, various autophagy-inducing compounds have been developed and evaluated in various rodent models of the neurodegenerative diseases. However, most compounds have multiple functions, and hence it is difficult to confirm that their therapeutic effects are a result of autophagy. Detailed analysis using rodent models are expected to clarify the effect of autophagy-inducing therapies on neurodegenerative diseases.

AUTHOR CONTRIBUTIONS

NF, MS contributed to the design of this review. SS described the manuscript.

FUNDING

This study was supported in part by a Grant-in-Aid for Grant-in-Aid for Scientific Research (A) (17H01533 and 17H06414), Grant-in-Aid for challenging Exploratory Research (16K15230), Grant-in-Aid for Scientific Research on Innovative Areas (17H05691), Grant-in-Aid for Scientific Research (C) (16K09668) from the MEXT of Japan, by the Project for Cancer Research and Therapeutic Evolution (P-CREATE) and by the Project for Psychiatric and Neurological Disorders from the Japan Agency for Medical Research and Development, AMED. This study was also supported by the Joint Usage/Research Program of Medical Research Institute, Tokyo Medical and Dental University.

REFERENCES

Alegre-Abarrategui, J., Christian, H., Lufino, M. M., Mutihac, R., Venda, L. L., Ansorge, O., et al. (2009). LRRK2 regulates autophagic activity and localizes to specific membrane microdomains in a novel human genomic reporter cellular model. *Hum. Mol. Genet.* 18, 4022–4034. doi: 10.1093/hmg/ddp346

Alves, S., Cormier-Dequaire, F., Marinello, M., Marais, T., Muriel, M. P., Beaumatin, F., et al. (2014). The autophagy/lysosome pathway is impaired in SCA7 patients and SCA7 knock-in mice. *Acta Neuropathol.* 128, 705–722. doi: 10.1007/s00401-014-1289-8

Axe, E. L., Walker, S. A., Manifava, M., Chandra, P., Roderick, H. L., Habermann, A., et al. (2008). Autophagosome formation from membrane compartments enriched in phosphatidylinositol 3-phosphate and dynamically connected to the endoplasmic reticulum. *J. Cell Biol.* 182, 685–701. doi: 10.1083/jcb.200803137

Bai, X., Wey, M. C., Fernandez, E., Hart, M. J., Gelfond, J., Bokov, A. F., et al. (2015). Rapamycin improves motor function, reduces 4-hydroxynonenal adducted protein in brain, and attenuates synaptic injury in a mouse model of synucleinopathy. *Pathobiol. Aging Age Relat. Dis.* 5:28743. doi: 10.3402/pba.v5.28743

Button, R. W., Roberts, S. L., Willis, T. L., Hanemann, C. O., and Luo, S. (2017). Accumulation of autophagosomes confers cytotoxicity. *J. Biol. Chem.* 292, 13599–13614. doi: 10.1074/jbc.M117.782276

Chen, Y., Liu, H., Guan, Y., Wang, Q., Zhou, F., Jie, L., et al. (2015). The altered autophagy mediated by TFEB in animal and cell models of amyotrophic lateral sclerosis. *Am. J. Transl. Res.* 7, 1574–1587.

Chen, Z. Z., Wang, C. M., Lee, G. C., Hsu, H. C., Wu, T. L., Lin, C. W., et al. (2015), Trehalose attenuates the gait ataxia and gliosis of spinocerebellar ataxia type 17 mice. *Neurochem. Res.* 40, 800–810. doi: 10.1007/s11064-015-1530-4

Clark, I. E., Dodson, M. W., Jiang, C., Cao, J. H., Huh, J. R., Seol, J. H., et al. (2006). *Drosophila pink1* is required for mitochondrial function and interacts genetically with *parkin*. *Nature* 441, 1162–1166. doi: 10.1038/nature04779

Congdon, E. E., Wu, J. W., Myeku, N., Figueroa, Y. H., Herman, M., Marinec, P. S., et al. (2012). Methylthioninium chloride (methylene blue) induces autophagy and attenuates tauopathy *in vitro* and *in vivo*. *Autophagy* 8, 609–622. doi: 10.4161/auto.19048

Corbier, C., and Sellier, C. (2017). C9ORF72 is a GDP/GTP exchange factor for Rab8 and Rab39 and regulates autophagy. *Small GTPases* 8, 181–186. doi: 10.1080/21541248.2016.1212688

Cortes, C. J., Miranda, H. C., Frankowski, H., Batlevi, Y., Young, J. E., Le, A., et al. (2014). Polyglutamine-expanded androgen receptor interferes with TFEB to elicit autophagy defects in SBMA. *Nat. Neurosci.* 17, 1180–1189. doi: 10.1038/nn.3787

Deng, Y. N., Shi, J., Liu, J., and Qu, Q. M. (2013). Celastrol protects human neuroblastoma SH-SY5Y cells from rotenone-induced injury through induction of autophagy. *Neurochem. Int.* 63, 1–9. doi: 10.1016/j.neuint.2013.04.005

Du, J., Liang, Y., Xu, F., Sun, B., and Wang, Z. (2013). Trehalose rescues Alzheimer's disease phenotypes in APP/PS1 transgenic mice. *J. Pharm. Pharmacol.* 65, 1753–1756. doi: 10.1111/jphp.12108

Duarte-Silva, S., Silva-Fernandes, A., Neves-Carvalho, A., Soares-Cunha, C., Teixeira-Castro, A., and Maciel, P. (2016). Combined therapy with m-TOR-dependent and -independent autophagy inducers causes neurotoxicity in a mouse model of Machado-Joseph disease. *Neuroscience* 313, 162–173. doi: 10.1016/j.neuroscience.2015.11.030

Durairajan, S. S., Liu, L. F., Lu, J. H., Chen, L. L., Yuan, Q., Chung, S. K., et al. (2012). Berberine ameliorates β-amyloid pathology, gliosis, and cognitive impairment in an Alzheimer's disease transgenic mouse model. *Neurobiol. Aging* 33, 2903–2919. doi: 10.1016/j.neurobiolaging.2012.02.016

Filomeni, G., Graziani, I., De Zio, D., Dini, L., Centonze, D., and Ciriolo, M. R. (2012). Neuroprotection of kaempferol by autophagy in models of rotenone-mediated acute toxicity: possible implications for Parkinson's disease. *Neurobiol. Aging* 33, 767–785. doi: 10.1016/j.neurobiolaging.2010.05.021

Fiorentini, A., Rosi, M. C., Grossi, C., Luccarini, I., and Casamenti, F. (2010). Lithium improves hippocampal neurogenesis, neuropathology and cognitive functions in APP mutant mice. *PLoS ONE* 5:e14382. doi: 10.1371/journal.pone.0014382

Freischmidt, A., Wieland, T., Richter, B., Ruf, W., Schaeffer, V., Müller, K., et al. (2015). Haploinsufficiency of *TBK1* causes familial ALS and fronto-temporal dementia *Nat. Neurosci.* 18, 631–636. doi: 10.1038/nn.4000

Fu, Y., Wu, P., Pan, Y., Sun, X., Yang, H., Difiglia, M., et al. (2017). A toxic mutant huntingtin species is resistant to selective autophagy. *Nat. Chem. Biol.* 13, 1152–1154. doi: 10.1038/nchembio.2461

Gal, J., Ström, A. L., Kilty, R., Zhang, F., and Zhu, H. (2017). p62 accumulates and enhances aggregate formation in model systems of familial amyotrophic lateral sclerosis. *J. Biol. Chem.* 282, 11068–11077. doi: 10.1074/jbc.M608787200

Geisler, S., Holmström, K. M., Skujat, D., Fiesel, F. C., Rothfuss, O. C., Kahle, P. J., et al. (2010). PINK1/Parkin-mediated mitophagy is dependent on VDAC1 and p62/SQSTM1. *Nat. Cell Biol.* 12, 119–131. doi: 10.1038/ncb2012

Goldwurm, S., Di, Fonzo, A., Simons, E. J., Rohé, C. F., and Zini, M. (2005). The G6055A (G2019S) mutation in LRRK2 is frequent in both early and late onset Parkinson's disease and originates from a common ancestor. *J. Med. Genet.* 42, e65. doi: 10.1136/jmg.2005.035568

Hamano, T., Gendron, T. F., Causevic, E., Yen, S. H., Lin, W. L., Isidoro, C., et al. (2008). Autophagic-lysosomal perturbation enhances tau aggregation in transfectants with induced wild-type tau expression. *Eur. J. Neurosci.* 27, 1119–1130. doi: 10.1111/j.1460-9568.2008.06084.x

Hsueh, K. W., Chiou, T. W., Chiang, S. F., Yamashita, T., Abe, K., Borlongan, C. V., et al. (2016). Autophagic down-regulation in motor neurons remarkably prolongs the survival of ALS mice. *Neuropharmacology* 108, 152–160. doi: 10.1016/j.neuropharm.2016.03.035

Huang, C., Andres, A. M., Ratliff, E. P., Hernandez, G., Lee, P., and Gottlieb, R. A. (2011). Preconditioning involves selective mitophagy mediated by Parkin and p62/SQSTM1. *PLoS ONE* 6:e20975. doi: 10.1371/journal.pone.0020975

Inoue, K., Rispoli, J., Kaphzan, H., Klann, E., Chen, E. I., Kim, J., et al. (2012). Macroautophagy deficiency mediates age-dependent neurodegeneration through a phospho-tau pathway. *Mol. Neurodegener.* 7, 48. doi: 10.1186/1750-1326-7-48

Itakura, E., Kishi, C., Inoue, K., and Mizushima, N. (2008). Beclin 1 forms two distinct phosphatidylinositol 3-kinase complexes with mammalian Atg14 and UVRAG. *Mol. Biol. Cell* 19, 5360–5372. doi: 10.1091/mbc.E08-01-0080

Ji, Y. J., Ugolino, J., Brady, N. R., Hamacher-Brady, A., and Wang, J. (2017). Systemic deregulation of autophagy upon loss of ALS- and FTD-linked C9orf72. *Autophagy* 13, 1254–1255. doi: 10.1080/15548627.2017.1299312

Jiang, T., Yu, J. T., Zhu, X. C., Zhang, Q. Q., Cao, L., Wang, H. F., et al. (2014). Temsirolimus attenuates tauopathy *in vitro* and *in vivo* by targeting tau hyperphosphorylation and autophagic clearance. *Neuropharmacology* 85, 121–130. doi: 10.1016/j.neuropharm.2014.05.032

Jiang, W., Wei, W., Gaertig, M. A., Li, S., and Li, X. J. (2015). Therapeutic effect of berberine on Huntington's disease transgenic mouse model. *PLoS ONE* 10:e0134142. doi: 10.1371/journal.pone.0134142

Kabeya, Y., Kamada, Y., Baba, M., Takikawa, H., Sasaki, M., and Ohsumi, Y. (2005). Atg17 functions in cooperation with Atg1 and Atg13 in yeast autophagy. *Mol. Biol. Cell* 16, 2544–2553. doi: 10.1091/mbc.E04-08-0669

Kabeya, Y., Mizushima, N., Ueno, T., Yamamoto, A., Kirisako, T., Noda, T., et al. (2000). LC3, a mammalian homologue of yeast Apg8p, is localized in autophagosome membranes after processing. *EMBO J.* 19, 5720–5728. doi: 10.1093/emboj/19.21.5720

Kaushik, S., and Cuervo, A. M. (2012). Chaperone-mediated autophagy: a unique way to enter the lysosome world. *Trends Cell Biol.* 22, 407–417. doi: 10.1016/j.tcb.2012.05.006

Kickstein, E., Krauss, S., Thornhill, P., Rutschow, D., Zeller, R., Sharkey, J., et al. (2010). Biguanide metformin acts on tau phosphorylation via mTOR/protein phosphatase 2A (PP2A) signaling. *Proc. Natl. Acad. Sci. U.S.A.* 107, 21830–21835. doi: 10.1073/pnas.0912793107

Kihara, A., Kabeya, Y., Ohsumi, Y., and Yoshimori, T. (2001). Beclin-phosphatidylinositol 3-kinase complex functions at the trans-Golgi network. *EMBO Rep.* 2, 330–335. doi: 10.1093/embo-reports/kve061

Komatsu, M., Waguri, S., Chiba, T., Murata, S., Iwata, J., Tanida, I., et al. (2006). Loss of autophagy in the central nervous system causes neurodegeneration in mice. *Nature* 441, 880–884. doi: 10.1038/nature04723

Komatsu, M., Waguri, S., Ueno, T., Iwata, J., Murata, S., Tanida, I., et al. (2005). Impairment of starvation-induced and constitutive autophagy in Atg7-deficient mice. *J. Cell Biol.* 169, 425–434. doi: 10.1083/jcb.200412022

Kuma, A., Hatano, M., Matsui, M., Yamamoto, A., Nakaya, H., Yoshimori, T., et al. (2004). The role of autophagy during the early neonatal starvation period. *Nature* 432, 1032–1036. doi: 10.1038/nature03029

Lee, J. H., Yu, W. H., Kumar, A., Lee, S., Mohan, P. S., Peterhoff, C. M., et al. (2010). Lysosomal proteolysis and autophagy require presenilin 1 and are disrupted by Alzheimer-related PS1 mutations. *Cell* 141, 1146–1158. doi: 10.1016/j.cell.2010.05.008

Levine, B., Sinha, S., and Kroemer, G. (2008). Bcl-2 family members: dual regulators of apoptosis and autophagy. *Autophagy* 4, 600–606. doi: 10.4161/auto.6260

Li, L., Zhang, S., Zhang, X., Li, T., Tang, Y., Liu, H., et al. (2013). Autophagy enhancer carbamazepine alleviates memory deficits and cerebral amyloid-beta pathology in a mouse model of Alzheimer's disease. *Curr. Alzheimer Res.* 10, 433–441. doi: 10.2174/1567205011310040008

Li, W. W., Li, J., and Bao, J. K. (2012). Microautophagy: lesser-known self-eating. *Cell. Mol. Life Sci.* 69, 1125–1136. doi: 10.1007/s00018-011-0865-5

Ma, T. C., Buescher, J. L., Oatis, B., Funk, J. A., Nash, A. J., Carrier, R. L., et al. (2007). Metformin therapy in a transgenic mouse model of Huntington's disease. *Neurosci. Lett.* 411, 98–103. doi: 10.1016/j.neulet.2006.10.039

Maruyama, H., Morino, H., Ito, H., Izumi, Y., Kato, H., Watanabe, Y., et al. (2010). Mutations of optineurin in amyotrophic lateral sclerosis. *Nature* 465, 223–226. doi: 10.1038/nature08971

Matsunaga, K., Saitoh, T., Tabata, K., Omori, H., Satoh, T., Kurotori, N., et al. (2009). Two Beclin 1-binding proteins, Atg14L and Rubicon, reciprocally regulate autophagy at different stages. *Nat. Cell Biol.* 11, 385–396. doi: 10.1038/ncb1846

Mealer, R. G., Murray, A. J., Shahani, N., Subramaniam, S., and Snyder, S. H. (2014). Rhes, a striatal-selective protein implicated in Huntington disease, binds beclin-1 and activates autophagy. *J. Biol. Chem.* 289, 3547–3554. doi: 10.1074/jbc.M113.536912

Mizushima, N., and Komatsu, M. (2011). Autophagy: renovation of cells and tissues. *Cell* 147, 728–741. doi: 10.1016/j.cell.2011.10.026

Mizushima, N., Ohsumi, Y., and Yoshimori, T. (2002). Autophagosome formation in mammalian cells. *Cell Struct. Funct.* 27, 421–429. doi: 10.1247/csf.27.421

Motoi, Y., Shimada, K., Ishiguro, K., and Hattori, N. (2014). Lithium and autophagy. *ACS Chem. Neurosci.* 5, 434–442. doi: 10.1021/cn500056q

Nakatogawa, H., Suzuki, K., Kamada, Y., and Ohsumi, Y. (2009). Dynamics and diversity in autophagy mechanisms: lessons from yeast. *Nat. Rev. Mol. Cell Biol.* 10, 458–467. doi: 10.1038/nrm2708

Nilsson, P., Loganathan, K., Sekiguchi, M., Matsuba, Y., Hui, K., Tsubuki, S., et al. (2013). Abeta secretion and plaque formation depend on autophagy. *Cell Rep.* 5, 61–69. doi: 10.1016/j.celrep.2013.08.042

Nishida, Y., Arakawa, S., Fujitani, K., Yamaguchi, H., Mizuta, T., Kanaseki, T., et al. (2009). Discovery of Atg5/Atg7-independent alternative macroautophagy. *Nature* 461, 654–658. doi: 10.1038/nature08455

Nixon, R. A., Wegiel, J., Kumar, A., Yu, W. H., Peterhoff, C., Cataldo, A., et al. (2005). Extensive involvement of autophagy in Alzheimer disease: an immuno-electron microscopy study. *J. Neuropathol. Exp. Neurol.* 64, 113–122. doi: 10.1093/jnen/64.2.113

Ozcelik, S., Fraser, G., Castets, P., Schaeffer, V., Skachokova, Z., Breu, K., et al. (2013). Rapamycin attenuates the progression of tau pathology in P301S tau transgenic mice. *PLoS ONE* 8:e62459. doi: 10.1371/journal.pone.0062459

Park, J., Lee, S. B., Lee, S., Kim, Y., Song, S., Kim, S., et al. (2006). Mitochondrial dysfunction in *Drosophila PINK1* mutants is complemented by *parkin*. *Nature* 441, 1157–1161. doi: 10.1038/nature04788

Pickford, F., Masliah, E., Britschgi, M., Lucin, K., Narasimhan, R., Jaeger, P. A., et al. (2008). The autophagy-related protein beclin 1 shows reduced expression in early Alzheimer disease and regulates amyloid beta accumulation in mice. *J. Clin. Invest.* 118, 2190–2199. doi: 10.1172/jci33585

Piras, A., Collin, L., Grüninger, F., Graff, C., and Rönnbäck, A. (2016). Autophagic and lysosomal defects in human tauopathies: analysis of post-mortem brain from patients with familial Alzheimer disease, corticobasal degeneration and progressive supranuclear palsy. *Acta Neuropathol. Commun.* 4, 22. doi: 10.1186/s40478-016-0292-9

Poels, J., Spasić, M. R., Callaerts, P., and Norga, K. K. (2009). Expanding roles for AMP-activated protein kinase in neuronal survival and autophagy. *Bioessays* 31, 944–952. doi: 10.1002/bies.200900003

Ramirez, A., Heimbach, A., Gründemann, J., Stiller, B., Hampshire, D., Cid, L. P., et al. (2006). Hereditary parkinsonism with dementia is caused by mutations in *ATP13A2*, encoding a lysosomal type 5 P-type ATPase. *Nat. Genet.* 38, 1184–1191. doi: 10.1038/ng1884

Ravikumar, B., Duden, R., and Rubinsztein, D. C. (2002). Aggregate-prone proteins with polyglutamine and polyalanine expansions are degraded by autophagy. *Hum. Mol. Genet.* 11, 1107–1117. doi: 10.1093/hmg/11.9.1107

Ravikumar, B., Vacher, C., Berger, Z., Davies, J. E., Luo, S., Oroz, L. G., et al. (2004). Inhibition of mTOR induces autophagy and reduces toxicity of polyglutamine expansions in fly and mouse models of Huntington disease. *Nat. Genet.* 36, 585–595. doi: 10.1038/ng1362

Richter, B., Sliter, D. A., Herhaus, L., Stolz, A., Wang, C., Beli, P., et al. (2016). Phosphorylation of OPTN by TBK1 enhances its binding to Ub chains and promotes selective autophagy of damaged mitochondria. *Proc. Natl. Acad. Sci. U.S.A.* 113, 4039–4044. doi: 10.1073/pnas.1523926113

Rose, C., Menzies, F. M., Renna, M., Acevedo-Arozena, A., Corrochano, S., Sadiq, O., et al. (2010). Rilmenidine attenuates toxicity of polyglutamine expansions in a mouse model of Huntington's disease. *Hum. Mol. Genet.* 19, 2144–2153. doi: 10.1093/hmg/ddq093

Rott, R., Szargel, R., Haskin, J., Bandopadhyay, R., Lees, A. J., Shani, V., et al. (2011). alpha-Synuclein fate is determined by USP9X-regulated monoubiquitination. *Proc. Natl. Acad. Sci. U.S.A.* 108, 18666–18671. doi: 10.1073/pnas.1105725108

Sahlender, D. A., Roberts, R. C., Arden, S. D., Spudich, G., Taylor, M. J., Luzio, J. P., et al. (2005). Optineurin links myosin VI to the Golgi complex and is involved in Golgi organization and exocytosis. *J. Cell Biol.* 169, 285–295. doi: 10.1083/jcb.200501162

Schaeffer, V., Lavenir, I., Ozcelik, S., Tolnay, M., Winkler, D. T., and Goedert, M. (2012). Stimulation of autophagy reduces neurodegeneration in a mouse model of human tauopathy. *Brain* 135, 2169–2177. doi: 10.1093/brain/aws143

Shibata, M., Lu, T., Furuya, T., Degterev, A., Mizushima, N., Yoshimori, T., et al. (2006). Regulation of intracellular accumulation of mutant Huntingtin by Beclin 1. *J. Biol. Chem.* 281, 14474–14485. doi: 10.1074/jbc.M600364200

Song, W., Wang, F., Savini, M., Ake, A., Di Ronza, A., Sardiello, M., et al. (2013). TFEB regulates lysosomal proteostasis. *Hum. Mol. Genet.* 22, 1994–2009. doi: 10.1093/hmg/ddt052

Sperber, B. R., Leight, S., Goedert, M., and Lee, V. M. (1995). Glycogen synthase kinase-3 beta phosphorylates tau protein at multiple sites in intact cells. *Neurosci. Lett.* 197, 149–153. doi: 10.1016/0304-3940(95)11902-9

Spilman, P., Podlutskaya, N., Hart, M. J., Debnath, J., Gorostiza, O., Bredesen, D., et al. (2010). Inhibition of mTOR by rapamycin abolishes cognitive deficits and reduces amyloid-beta levels in a mouse model of Alzheimer's disease. *PLoS ONE* 5:e9979. doi: 10.1371/journal.pone.0009979

Steele, J. W., Lachenmayer, M. L., Ju, S., Stock, A., Liken, J., Kim, S. H., et al. (2013). Latrepirdine improves cognition and arrests progression of neuropathology in an Alzheimer's mouse model. *Mol. Psychiatry* 18, 889–897. doi: 10.1038/mp.2012.106

Sundaramoorthy, V., Walker, A. K., Tan, V., Fifita, J. A., Mccann, E. P., Williams, K. L., et al. (2015). Defects in optineurin- and myosin VI-mediated cellular trafficking in amyotrophic lateral sclerosis. *Hum. Mol. Genet.* 24, 3830–3846. doi: 10.1093/hmg/ddv126

Tanaka, M., Machida, Y., Niu, S., Ikeda, T., Jana, N. R., Doi, H., et al. (2004). Trehalose alleviates polyglutamine-mediated pathology in a mouse model of Huntington disease. *Nat. Med.* 10, 148–154 doi: 10.1038/nm985

Tang, B. L. (2016). C9orf72's interaction with Rab GTPases-modulation of membrane traffic and autophagy. *Front. Cell. Neurosci.* 10:228. doi: 10.3389/fncel.2016.00228

Tanji, K., Miki, Y., Maruyama, A., Mimura, J., Matsumiya, T., Mori, F., et al. (2015). Trehalose intake induces chaperone molecules along with autophagy in a mouse model of Lewy body disease. *Biochem. Biophys. Res. Commun.* 465, 746–752. doi: 10.1016/j.bbrc.2015.08.076

Teyssou, E., Takeda, T., Lebon, V., Boillée, S., Doukour,é B., Bataillon, G., et al. (2013). Mutations in SQSTM1 encoding p62 in amyotrophic lateral sclerosis: genetics and neuropathology. *Acta Neuropathol.* 125, 511–522. doi: 10.1007/s00401-013-1090-0

Tian, Y., Bustos, V., Flajolet, M., and Greengard, P. (2011). A small-molecule enhancer of autophagy decreases levels of Abeta and APP-CTF via Atg5-dependent autophagy pathway. *FASEB J.* 25, 1934–1942. doi: 10.1096/fj.10-175158

Tian, Y., Chang, J. C., Fan, E. Y., Flajolet, M., and Greengard, P. (2013). Adaptor complex AP2/PICALM, through interaction with LC3, targets Alzheimer's APP-CTF for terminal degradation via autophagy. *Proc. Natl. Acad. Sci. U.S.A.* 110, 17071–17076. doi: 10.1073/pnas.1315110110

Tian, Y., Chang, J. C., Greengard, P., and Flajolet, M. (2014). The convergence of endosomal and autophagosomal pathways: implications for APP-CTF degradation. *Autophagy* 10, 694–696. doi: 10.4161/auto.27802

Tong, Y., Yamaguchi, H., Giaime, E., Boyle, S., Kopan, R., Kelleher, R. J. III., et al. (2010). Loss of leucine-rich repeat kinase 2 causes impairment of protein degradation pathways, accumulation of alpha-synuclein, and apoptotic cell death in aged mice. *Proc. Natl. Acad. Sci. U.S.A.* 107, 9879–9884. doi: 10.1073/pnas.1004676107

Wang, I. F., Guo, B. S., Liu, Y. C., Wu, C. C., Yang, C. H., Tsai, K. J., et al. (2012). Autophagy activators rescue and alleviate pathogenesis of a mouse model with proteinopathies of the TAR DNA-binding protein 43. *Proc. Natl. Acad. Sci. U.S.A.* 109, 15024–15029. doi: 10.1073/pnas.1206362109

Wang, X., Fan, H., Ying, Z., Li, B., Wang, H., and Wang, G. (2010). Degradation of TDP-43 and its pathogenic form by autophagy and the ubiquitin-proteasome system. *Neurosci. Lett.* 469, 112–116. doi: 10.1016/j.neulet.2009.11.055

Wild, P., Farhan, H., Mcewan, D. G., Wagner, S., Rogov, V. V., Brady, N. R., et al. (2011). Phosphorylation of the autophagy receptor optineurin restricts Salmonella growth. *Science* 333, 228–233. doi: 10.1126/science.1205405

Winslow, A. R., Chen, C. W., Corrochano, S., Acevedo-Arozena, A., Gordon, D. E., Peden, A. A., et al. (2010). alpha-Synuclein impairs macroautophagy: implications for Parkinson's disease. *J. Cell Biol.* 190, 1023–1037. doi: 10.1083/jcb.201003122

Wong, Y. C., and Holzbaur, E. L. (2014). Optineurin is an autophagy receptor for damaged mitochondria in parkin-mediated mitophagy that is disrupted by an ALS-linked mutation. *Proc. Natl. Acad. Sci. U.S.A.* 111, E4439–E4448. doi: 10.1073/pnas.1405752111

Wu, Q., Yang, X., Zhang, Y., Zhang, L., and Feng, L. (2016). Chronic mild stress accelerates the progression of Parkinson's disease in A53T α-synuclein transgenic mice. *Exp. Neurol.* 285(Pt A), 61–71. doi: 10.1016/j.expneurol.2016.09.004

Yu, H. C., Lin, C. S., Tai, W. T., Liu, C. Y., Shiau, C. W., and Chen, K. F. (2013). Nilotinib induces autophagy in hepatocellular carcinoma through AMPK activation. *J. Biol. Chem.* 288, 18249–18259. doi: 10.1074/jbc.M112.446385

Zavodszky, E., Seaman, M. N., Moreau, K., Jimenez-Sanchez, M., Breusegem, S. Y., Harbour, M. E., et al. (2014). Mutation in VPS35 associated with Parkinson's disease impairs WASH complex association and inhibits autophagy. *Nat. Commun.* 5, 3828. doi: 10.1038/ncomms4828

Zheng, L., Terman, A., Hallbeck, M., Dehvari, N., Cowburn, R. F., Benedikz, E., et al. (2011). Macroautophagy-generated increase of lysosomal amyloid β-protein mediates oxidant-induced apoptosis of cultured neuroblastoma cells. *Autophagy* 7, 1528–1545. doi: 10.4161/auto.7.12.18051

Zhong, Y., Wang, Q. J., Li, X., Yan, Y., Backer, J. M., Chait, B. T., et al. (2009). Distinct regulation of autophagic activity by Atg14L and Rubicon associated with Beclin 1-phosphatidylinositol-3-kinase complex. *Nat. Cell Biol.* 11, 468–476. doi: 10.1038/ncb1854

Conflict of Interest Statement: The authors declare that the research was conducted in the absence of any commercial or financial relationships that could be construed as a potential conflict of interest.

frontiers in Neuroscience

REVIEW
published: 10 January 2018
doi: 10.3389/fnins.2017.00743

DnaJ/Hsp40 Family and Parkinson's Disease

Takafumi Hasegawa, Shun Yoshida, Naoto Sugeno, Junpei Kobayashi and Masashi Aoki*

Division of Neurology, Department of Neuroscience and Sensory Organs, Tohoku University Graduate School of Medicine, Sendai, Japan

Parkinson's disease (PD) is the second most common devastating neurodegenerative disorder after Alzheimer's disease. The precise molecular and cellular basis underlying PD still remains uncertain; however, accumulating evidence suggests that neuronal cell death is caused by a combination of environmental and genetic factors. Over the previous two decades, more than 20 genes have been identified as the cause of and/or risk for PD. Because sporadic and familial forms of PD have many similarities in clinical and neuropathological features, common molecular pathways, such as aberrant mitochondrial and protein homeostasis, are likely to exist in both conditions. Of the various genes and proteins involved in PD, the versatile DnaJ/Hsp40 co-chaperones have attracted particular attention since several genes encoding this protein family have been successively identified as the cause of the familial forms of PD/Parkinsonism. In this review, we will introduce the current knowledge regarding the integratory and modulatory effect of DnaJ/Hsp40 in various cellular functions and argue how the failure of these proteins may initiate and/or facilitate of the disease.

Keywords: DnaJ protein, Hsp40, co-chaperones, Parkinson's disease, neurodegeneration

OPEN ACCESS

Edited by:
Naruhiko Sahara, National Institute of Radiological Sciences (NIRS), Japan

Reviewed by:
Takashi Nonaka, Tokyo Metropolitan Institute of Medical Science, Japan
Chiara Zurzolo, Institut Pasteur, France

****Correspondence:***
Takafumi Hasegawa
thasegawa@med.tohoku.ac.jp

Specialty section:
This article was submitted to Neurodegeneration, a section of the journal Frontiers in Neuroscience

Received: *21 October 2017*
Accepted: *20 December 2017*
Published: *10 January 2018*

Citation:
Hasegawa T, Yoshida S, Sugeno N, Kobayashi J and Aoki M (2018) DnaJ/Hsp40 Family and Parkinson's Disease. Front. Neurosci. 11:743. doi: 10.3389/fnins.2017.00743

INTRODUCTION

Newly synthesized proteins are transported to the destination site where they exert distinct functions; however, some proteins fail to properly fold, and misfolded proteins tend to form aggregates that may be potentially harmful to cells. To combat these perpetual threats, cells have evolved dexterous quality control mechanisms that facilitate degradation by the ubiquitin-proteasome system and autophagy-lysosome pathway or refolding of misfolded proteins to normal tertiary structures by molecular chaperones (Oshima et al., 2016; Ciechanover and Kwon, 2017). The most well-known molecular chaperones are heat shock proteins (HSPs), which were named after the phenomenon of puffing in larval salivary gland chromosomes of *Drosophila* following heat exposure (Pauli et al., 1992). Heat shock and numerous noxious stimuli, including UV, oxidative stress, hypoxia, osmotic stress, and heavy metals, induce the expression of HSPs, which is considered as a fundamental biological defense mechanism (Piano et al., 2004). The family of HSPs are evolutionarily conserved proteins across species and are classified based on their molecular weights; different HSPs have distinct yet partially overlapping functions. For example, Hsp90, which is known to be one of the most abundantly expressed proteins (1–2% of total soluble proteins in an unstressed condition) in the cytosol, forms a complex with its client proteins, such as cell surface receptors, transcription factors, and protein kinases, to modulate their functions (Schopf et al., 2017). Thus, Hsp90 plays pivotal roles in various cellular processes, such as proliferation, differentiation, carcinogenesis, and neurodegeneration. Several Hsp90 inhibitors, including the geldanamycin and its analogs demonstrate anti-tumor effects in various cellular and animal models

(Soga et al., 2013). The Hsp70 family is the eukaryotic homolog of the bacterial molecular chaperone DnaK and is widely expressed in various tissues and organs. The members of the Hsp70 family are characterized by their expression levels, activities, and subcellular distribution (Zuiderweg et al., 2017). Under physiological conditions, Hsp70 mainly resides in the cytoplasmic space, whereas in response to stress, it is upregulated and relocates from the cytosol to the nucleus and nucleoli. The heat shock cognate 70 (Hsc70) is, on the other hand, defined by its constitutive expression and cytoplasmic localization. Another Hsp70 member, BiP (also referred to as a 78-kDa of glucose-regulated protein: GRP78), expresses in the endoplasmic reticulum (ER) and acts as a chaperone for secreted or membrane proteins (Dudek et al., 2009). Hsp70 binds and shields the hydrophobic peptides of client proteins in an ATP-dependent manner, thus preventing protein aggregation and proper folding (Zuiderweg et al., 2017). Hsc70 chaperone mediates the lysosomal targeting of substrates with a KFERQ-like sequence (i.e., chaperone-mediated autophagy; Cai et al., 2015). Furthermore, Hsp70 is involved in the intracellular traffic of membranes, including the involvement in regulation of endocytosis and exocytosis mechanisms (Goldfarb et al., 2006).

The complex and multifaceted functions of Hsp70 members are achieved by the assistance of their Hsp40/DnaJ co-chaperones (Qiu et al., 2006; Gorenberg and Chandra, 2017). Hsp40 family proteins were originally identified as mammalian homologs of bacterial DnaJ proteins and are subdivided into three distinct groups, i.e., DnaJA, DnaJB, and DnaJC. Structurally, DnaJ proteins consist of 4 functional domains, namely, an evolutionarily conserved J domain with a stretch of 70 amino acid residues, a glycine/phenylalanine-rich domain (G/F-rich domain), a zinc finger domain that contains CXXCXGXG motifs, and a cysteine-rich region (Qiu et al., 2006). In DnaJA and DnaJB proteins, the J domain is always located at the N-terminus which is followed by the G/F-rich domain. The DnaJC family usually lacks the G/F domain and the cysteine-rich region, and the J domain may be located at any location in the entire sequence. Through the intermediary of the J domain, Hsp40 binds to Hsp70 and promotes its ATPase activity, thus generating the ADP-bound Hsp70, which stably interacts with client proteins (**Figure 1**; Greene et al., 1998). Both the G/F-rich domain and c-terminal region of Hsp40/DnaJ proteins are likely to be important in their substrate recognition (Perales-Calvo et al., 2010). Although the Hsp40/DnaJ families are ubiquitously expressed, widespread distribution is also present in the central and peripheral nervous systems (Gorenberg and Chandra, 2017). Furthermore, recent genetic and biological studies suggest that Hsp40/DnaJ family genes/proteins directly or cooperatively influence on the initiation of familial Parkinson's disease (PD) and other inherited forms of parkinsonism (**Figure 2** and **Table 1**; Gorenberg and Chandra, 2017; Hasegawa et al., 2017; Puschmann, 2017). It remains obscure how the different mutated genes could result in the progressive loss of striatal dopaminergic innervation as well as the death of nigral neurons. Nevertheless, some relationships, involving the perturbation of cellular systems, now appear to be apparent. The affected systems include synaptic transmission, endosomal trafficking, protein-quality control, and/or mitochondrial systems. In this review, we will summarize the current understandings regarding the functional roles of Hsp40/DnaJ co-chaperones in the familial forms of PD/parkinsonism and discuss how these molecules may influence on the pathological consequence of this disease.

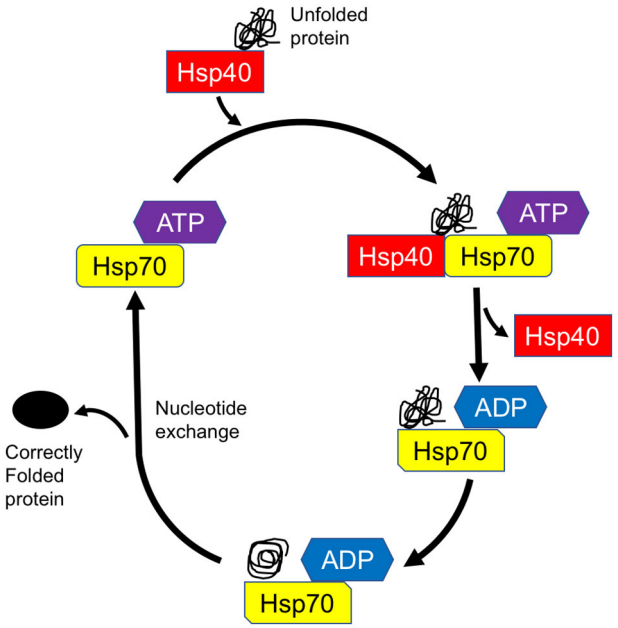

FIGURE 1 | Model of chaperone-assisted protein folding by Hsp70-DnaJ/Hsp40 complex. DnaJ/Hsp40 transiently associates with unfolded protein (substrate) for delivery of the substrate to Hsp70. Through the intermediary of the J domain, Hsp40 binds to Hsp70 and promotes its ATPase activity, thus generating the ADP-bound Hsp70, which stably interacts with client protein. After nucleotide exchange, the substrate is released from Hsp70 and leaves the cycle as a correctly folded protein.

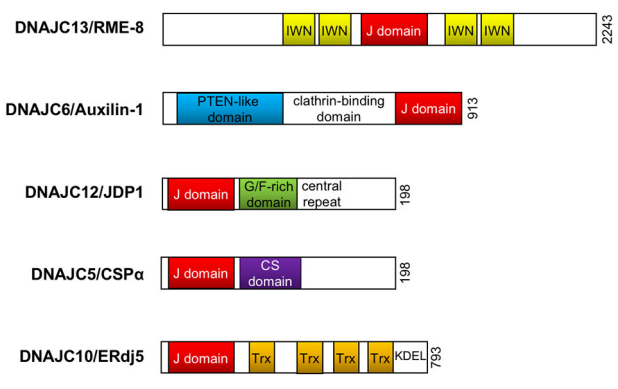

FIGURE 2 | DnaJ/Hsp40 proteins implicated in Parkinson's disease. Schematic illustration of the functional domain organization of DnaJ proteins (DNAJC8/RME-8, DNAJC6/Auxilin-1, DNAJC12/JDP1, DNAJC5/CSPα, and DNAJC10/ERdj5) reviewed in this article. The illustration does not represent the actual molecular size. PTEN, phosphoinositide phosphatase; G/F, glycine/phenylalanine; CS, cysteine-string; Trx, thioredoxin; KDEL, KDEL (Lys-Asp-Glu-Leu) targeting sequence to the ER.

TABLE 1 | Clinicopathological features of DnaJ/Hsp40-linked PD/Parkinsonism.

Gene	Transcript	Inheritance	Age at onset	Clinical symptoms	Neuroimaging findings	Response to L-dopa	LB pathology	Reference
DNAJC13	RME-8	AD	57–76	Classic Parkinsonism, sometimes accompanied by dementia, some case clinically manifested PSP or essential tremor	Rostrocaudal striatal deficits in dopaminergic PET imaging	+	+	Appel-Cresswell et al., 2014; Vilariño-Güell et al., 2014; Lorenzo-Betancor et al., 2015; Rajput et al., 2015
DNAJC6	Auxilin-1	AR	7–42	Early-onset parkinsonism, occasionally accompanied by pyramidal tract sign, epilepsy, mild mental retardation and visual hallucination	Unremarkable MRI scans except for one case showing diffuse brain atrophy, abnormalities in ^{18}F-DOPA-PET imaging	+/−	n.a.	Edvardson et al., 2012; Koroglu et al., 2013; Elsayed et al., 2016; Olgiati et al., 2016
DNAJC12	JDP1	AR	0–51	Dystonia, mental retardation, axial hypotonia, limb hypertonia, nystagmus and non-progressive parkinsonism in any combination	Unremarkable Brain MRI scans, abnormalities on ^{8}F-DOPA-PET imaging was noted in one case	+	LB-negative nigral degeneration with AD pathology	Anikster et al., 2017; Straniero et al., 2017; van Spronsen et al., 2017
DNAJC5	CSPα	AD	26–43	Myoclonic and tonic-clonic seizure, ataxia and myoclonus, dementia with depression, premature death, sometimes accompanied by parkinsonism and pyramidal tract sign	Mild to moderate cerebro-cerebellar atrophy	n.a.	n.a.	Burneo et al., 2003; Noskova et al., 2011; Velinov et al., 2012; Cadieux-Dion et al., 2013
DNAJC10	ERdj5	Risk	54–70	Classic parkinsonism	n.a.	n.a.	n.a.	Yuan et al., 2016

RME-8, receptor-mediated endocytosis-8; JDP1, J domain-containing protein; CSPα, cysteine string protein α; AD, autosomal dominant; AR, autosomal recessive; PSP, progressive supranuclear palsy; PET, positron emission tomography; MRI, magnetic resonance imaging; LB, Lewy body; n.a., not available.

DNAJC13/RME-8

DNAJC13 is a human homolog of *receptor-mediated endocytosis 8* (*RME-8*), which was originally identified in a genetic screening for mutants defective in the endocytic uptake of yolk protein in nematodes (Zhang et al., 2001). Recently, a p.N855S missense mutation of *DNAJC13* was reported in a large Canadian Mennonite PD pedigree with Dutch-German-Russian ancestry (Appel-Cresswell et al., 2014; Vilariño-Güell et al., 2014). The pathogenicity of the N855S mutant is supported by segregation with disease, lack of healthy controls with mutation, and the high level of sequence conservation across species; however, genetic screening in a Caucasian series consisting of 1,938 patients with clinically diagnosed PD and 838 pathologically proven Lewy Body Disease failed to detect any coding variant in exon 24 containing Asn855 in *DNAJC13* gene, indicating that mutations in this exon are not a common cause of PD or LBD among Caucasian populations (Lorenzo-Betancor et al., 2015). Subsequent genotyping in a Canadian cohort indicated that missense mutations, such as p.P336A, p.V722L, p.R1266Q, and P.T1895M, are only identified in affected members, and p.E1740Q, and p.L2170W may be associated with the risk variants for PD (Gustavsson et al., 2015). Clinically, DNAJC-linked PD (subsequently designated as PARK21) manifests as slowly progressive, late-onset, dopa-responsive typical parkinsonism with an autosomal dominant inheritance (Vilariño-Güell et al., 2014). Of note, the N855S mutation in *DNAJC13* gene has also been observed in patients with essential tremor, a monosymptomatic disorder characterized exclusively by postural- or action-type tremor, suggesting heterogeneity in the clinical manifestation with this mutation (Rajput et al., 2015). Neuropathological examination in three N855S mutation carriers indicated a brainstem or transitional type of Lewy body pathology (Vilariño-Güell et al., 2014). DNAJC13/RME-8 is a large protein with a high molecular mass of 254 kDa; it is widely expressed and is abundant in

nervous tissue. Structurally, it consists of four conserved IWN repeats, which are characterized by seven invariant residues, including isoleucine, tryptophan and asparagine, and a J domain in the center region (Fujibayashi et al., 2008). An *in vitro* pull-down assay demonstrated that the J domain of RME-8 binds to Hsc70 in the presence of ADP (Chang et al., 2004). Cell biological studies have demonstrated that DNAJC13 resides in the endosomal membrane and interacts with a family with sequence similarity 21 (FAM21) tail in the Wiskott–Aldrich syndrome protein and Scar homolog (WASH) complex and sorting nexin 1 (SNX1), thereby controlling the formation of the tubular structure on the endosome surface where retromer-mediated cargo transport occurs (Freeman et al., 2014). From a functional point of view, DNAJC13 plays important roles in the cell surface recycling and lysosomal degradation of transferrin and EGFR, as well as the retrograde transport of cation-independent mannose phosphate receptor (CI-MPR; Girard et al., 2005; Popoff et al., 2009; Shi et al., 2009; **Figure 3**). The over-expression of p.N855S mutant, but not wild-type, in cultured cells leads to aberrant retention of transferrin in endosomes (Vilariño-Güell et al., 2014), which indicates that a PD-linked DNAJC13 mutation may confer a toxic gain-of-function and hampers endosomal cargo trafficking. Intriguingly, immunofluorescence and co-immunoprecipitation studies demonstrate that vacuolar protein sorting 35 (VPS35), a vital element of retromer that is established as a causal gene for PARK17 PD, is co-localized with DNAJC13 in a primary cortical neuron culture obtained from mice (Vilariño-Güell et al., 2014). Further studies using appropriate animal models are required to better understand the precise molecular mechanisms by which *DNAJC13* mutation leads to the dopaminergic degeneration with Lewy body pathology. In an independent study, Deng et al. identified loss-of-function mutations in *TMEM230* gene in the same Canadian Mennonite group that Vilariño-Güell and his colleagues previously identified mutations in DNAJC13 (Deng et al., 2016). The *TMEM230* transcript localizes to the secretory and recycling vesicle in the neuron and may be involved in synaptic vesicle trafficking and recycling. Another study has shown that TMEM230 is required for Rab8a-mediated transport of secretory vesicles and retromer-mediated cargo trafficking (Kim et al., 2017). Further discussion and reassessment are needed to understand this complex situation.

DNAJC6/AUXILIN-1

In 2012, deleterious (c.801-2 A>G) and truncating (p.Q734X) mutations in the *DNAJC6* gene were discovered in two consanguineous families with Palestinian and Turkish origins, respectively (Edvardson et al., 2012; Koroglu et al., 2013). The clinical phenotypes of DNAJC6-linked familial parkinsonism (termed PARK19) are characterized by a juvenile-onset, progressive parkinsonism, which includes bradykinesia, muscle

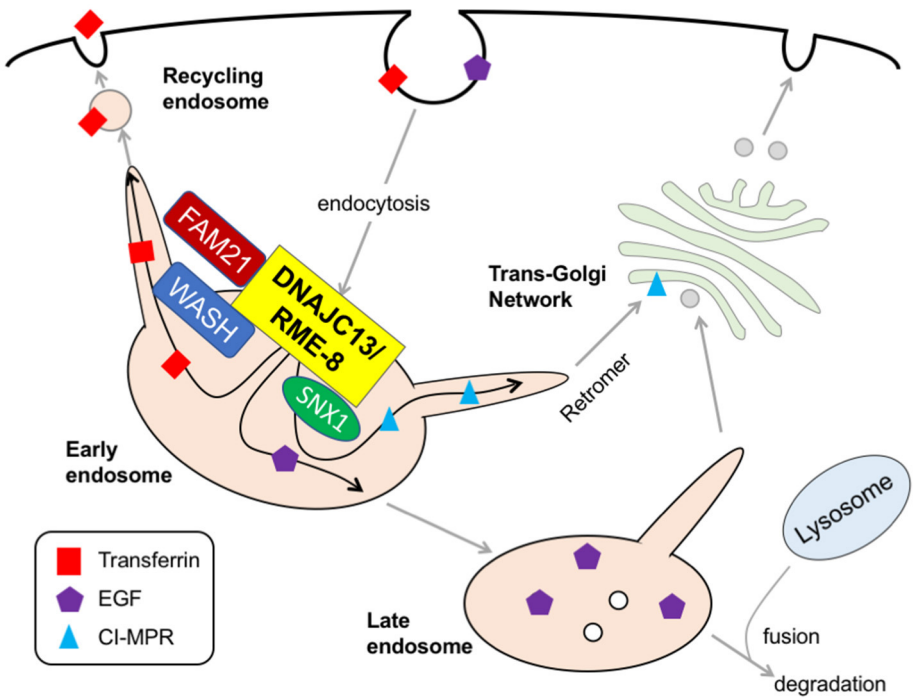

FIGURE 3 | DNAJC13/RME-8. At the surface of early endosome, DNAJC13 interacts with FAM21 tail in the WASH complex and SNX1, thereby controlling the formation of tubular structure on endosome surface where a retromer-mediated cargo transport (e.g., CI-MPR) occurs. DNAJC13 also play important roles in the recycling and the degradation of transferrin and EGFR, respectively. RME-8, receptor-mediated endocytosis-8; FAM21, family with sequence similarity 21; WASH, Wiskott–Aldrich syndrome protein and Scar homolog; SNX1, sorting nexin 1; EGF, epidermal growth factor; CI-MPR, cation-independent mannose 6-phosphate receptor.

rigidity, resting tremor, hypomimia, and postural instability. In addition to extrapyramidal signs, four members of the Turkish family exhibited hypomentia, pyramidal tract signs and/or seizures (Koroglu et al., 2013). Patients in the Palestinian family had dopa-refractory parkinsonism, whereas affected members in the Turkish family showed a favorable response to levodopa replenishment therapy. Subsequent genetic studies identified 2 different homozygous mutations in the *DNAJC6* gene, i.e., a missense mutation (p.R927G) and a putative splice site mutation (c.2223A-T; Olgiati et al., 2016). These families accounted for 2 (2.2%) of 92 probands (mean age at onset: 54.65; range 19–84) with autosomal recessive PD who underwent *DNAJC6* genetic screening. These patients showed milder phenotype compared to the patients with truncating mutations probably due to some residual activity of DNAJC6. Another novel non-sense mutation (exon 16, p.Q789*) has also been reported in a consanguineous family with juvenile-onset PD (Elsayed et al., 2016). Of interest, a patient in this family manifested rigid-akinetic form of parkinsonism with visual hallucinations, which are frequently observed non-motor symptom in sporadic PD and dementia with Lewy bodies (Shoji et al., 2014). Because there is variation in the responsiveness of dopamine-replacement therapy, the term "parkinsonism" rather than PD would be suitable in *DNAJC6*-linked movement disorder. The *DNAJC6* encodes the neuron-specific isoform of the co-chaperone auxilin-1, which has a crucial role in the detachment of the clathrin-coat after clathrin-mediated endocytosis (CME, **Figure 4**). Auxilin-1 is a 100 kDa protein and structurally consists of 3 distinct domains: the N-terminal phosphoinositide phosphatase (PTEN) like domain (residue 40–421), which is required for the recruitment to a clathrin-coated pit, the central clathrin-binding domain, and a C-terminal J domain, which enables its interaction with Hsc70 (Lee et al., 2006). The c.801-2 A>G homozygous splice-site mutation in *DNAJC6* yields two misspliced abnormal transcripts that lack either a significant part of the J domain or the PTEN-like domain, which indicates that this pathological mutation results in the defect of functionally active auxilin-1 (Edvardson et al., 2012). The homozygous mutation p.Q734X deletes the 180 amino acid residues of Auxilin-1 at the C-terminus, which are considered important for supporting Hsc70 function in clathrin dissociation from coated vesicles (Koroglu et al., 2013). Moreover, an *in silico* structural analysis predicted that that the p.R927G missense mutation in the J domain reduces the positive charge on the protein surface, which would be involved in the molecular interaction of auxilin-1 with Hsc70 or other partners (Olgiati et al., 2016). Interestingly, common variants in *cyclin-G-associated kinase* (*GAK*), which encodes auxilin-2/DNAJC26, a ubiquitously expressed paralog of auxilin, are also considered a risk factor for idiopathic PD (Pankratz et al., 2009). Auxilin-null mice exhibited a high mortality rate in early life; however, they did not exhibit no obvious neuropathological alterations in the midbrain (Yim et al., 2010). These mice showed higher GAK levels in the brain; however, this compensation appeared to be insufficient for the lack of auxilin in clathrin uncoating since they exhibited an aberrant retention of clathrin-coated vesicles and empty clathrin cages at the synaptic terminals, which may be attributed to the parkinsonian phenotypes. Further investigation using genetically modified animal models is warranted to better understand the role of DNAJC6 in synaptic dopamine function.

DNAJC12/JDP1

DNAJC12, a member of the Hsp70/Hsc70 co-chaperone proteins, has the J domain and a highly conserved C terminus; however, it lacks other canonical domains present in DnaJ family proteins. This protein is a mammalian ortholog of the J domain-containing protein (JDP) originally identified in *Drosophila* and is thus termed JDP1 (Hahn et al., 1999). In mammals, two transcript variants of DNAJC12/JDP1 have been identified: the primary isoform is 1.2 kb and encodes 198 amino acids, and the other isoform is 0.7 kb and is composed of 107 amino acids. Northern blot analysis showed that the major transcript of mouse JDP1 is ubiquitously expressed in various organs, including the brain (Hahn et al., 1999). Recently, biallelic mutations [del. 6943 (c.298-968_503-2603del) and p.R72P] of the *DNAJC12* gene have been identified as causes for phenylketonuria (PKU), the most frequent inherited metabolic disorder (Anikster et al., 2017). Segregation analysis confirmed autosomal-recessive inheritance in all families. Furthermore, a subsequent study of the genotype-phenotype correlation in *DNAJC12* mutations demonstrated that several homozygous null variants (c.187A>T and c.79-2A>G) in *DNAJC12* present young-onset, dopa-responsive non-progressive parkinsonism as the cardinal symptom and mild cognitive decline without apparent dystonia (Straniero et al., 2017). The autopsy studies of the proband's brain showed depigmentation in the substantia nigra, and no α-synuclein-positive Lewy pathology was observed. Thus, the PKU with the *DNAJC12* mutation should be considered as a differential diagnosis of early-onset parkinsonism, since a strict diet therapy with low phenylalanine may prevent the progression of the disease. Most patients with PKU have mutations in a gene that encodes phenylalanine hydroxylase (PAH), a rate-limiting enzyme of the metabolic pathway that degrades excess phenylalanine to tyrosine (Blau, 2016). Patients with PKU do not show any abnormalities at birth; however, if left untreated, the accumulation of phenylalanine and the insufficient level of tyrosine insidiously lead to psychomotor retardation, microcephaly, epilepsy, generalized dystonia, and hypopigmentation in the skin and hair (Al Hafid and Christodoulou, 2015). A limited number (up to 2%) of PKU cases are caused by a deficiency of tetrahydrobiopterin (BH_4), a co-factor of PAH and other members of aromatic amino acid hydroxylases (AAAHs), such as tyrosine hydroxylase (TH) and tryptophan hydroxylase (TPH), which are required for the biosynthesis of dopamine and serotonin, respectively (Blau, 2016). Affinity capture-mass spectrometry (AC-MS) and co-immunoprecipitation demonstrated that DNAJC12 interacts with AAAHs including PAH, TH, and peripheral and neuronal isoforms of TPH (Huttlin et al., 2015; Anikster et al., 2017). A molecular interaction between PAH and JDP, the ortholog of DNAJC12 in fruit fly, was also detected in the two-hybrid-based protein-interaction datasets of *Drosophila* (the Biological General Repository for Interaction Datasets, BioGRID; Giot et al.,

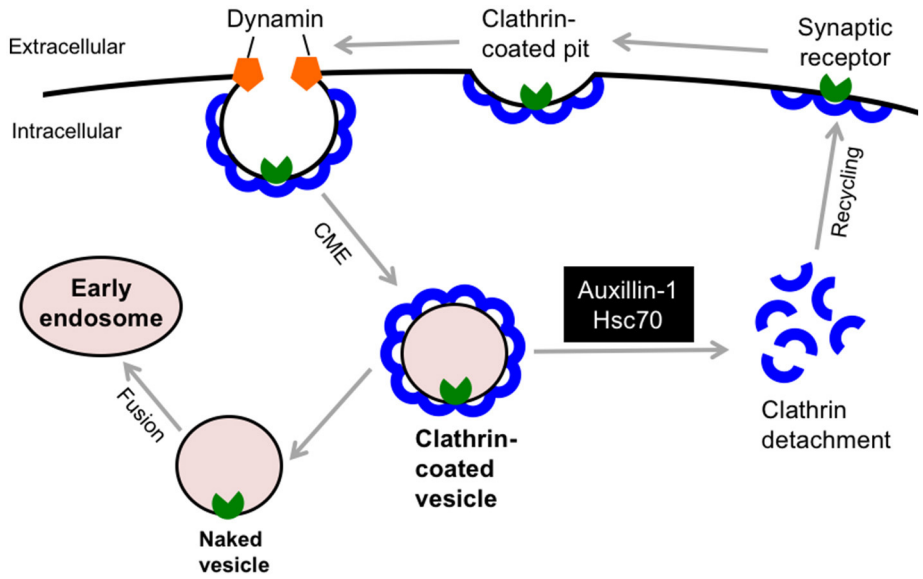

FIGURE 4 | DNAJC6/Auxilin-1 regulates the clathrin-mediated endocytosis. DNAJC6/Auxilin-1 is highly expressed in nerve terminals and plays a crucial role in clathrin uncoating during synaptic receptor endocytosis. CME, clathrin-mediated endocytosis; Hsc70, heat shock cognate 70.

2003). Furthermore, analysis of cerebrospinal fluid from affected individuals showed deficiencies of several catecholamines and their metabolites, including dopamine, serotonin, HVA, and 5-HIAA (van Spronsen et al., 2017). These findings suggest the importance of DNAJC12 for proper function of enzymes involved in catecholamine biosynthesis. The c.158-2A>T splice variant and entire deletion in exon 4 (del. 6943) are considered to be null mutants as the DNAJC12 protein was below the detection level in the fibroblasts obtained from individuals carrying these mutations (Anikster et al., 2017). Moreover, the p.R72P missense variant located in the J domain appears to affect the stability of DNAJC12 as the Arg72 residue is well-conserved across species and is indispensable for maintaining the 3D structure of the J domain through the interactions with the Ser25 residue (Anikster et al., 2017).

DNAJC5/CSPα

DNAJC5, also referred to as cysteine string protein α (CSPα), is a 34 kDa protein and synaptic co-chaperone of the DnaJ/Hsp40 family (Burgoyne and Morgan, 2015). The name originates from the existence of a cysteine string domain that consists of 13–15 heavily palmitoylated cysteine residues within 25 amino acids. Structurally, DNAJC5/CSPα is divided into the following domains: a phosphorylation site for protein kinase A at an N-terminus, a conserved J domain, an adjacent linker region, the cysteine string domain, and a less conserved C-terminal domain (Burgoyne and Morgan, 2015). Mutations (p.L116del and p.L115R) in the cysteine string domain of *DNAJC5* have previously been identified as causes for an autosomal-dominant, adult-onset neuronal ceroid lipofuscinosis (ANCL, also referred to as Kufs disease), a neurodegenerative disorder characterized by abnormal accumulation of fluorogenic lipids, granular substances not only in the neuronal cells in the brain but also in some other tissues (Noskova et al., 2011; Velinov et al., 2012; Cadieux-Dion et al., 2013). Sanger sequencing revealed that p.L116del mutation was the only indel completely co-segregating with the phenotype in the pedigree. The clinical picture of individuals who carry pathogenic *DNAJC5* mutations consists of tonic-clonic and myoclonic epileptic seizure, ataxia, and dementia with premature death. In some cases, patients subsequently began to manifest parkinsonism (Burneo et al., 2003; Cadieux-Dion et al., 2013). The over-expression of EGFP-tagged DNAJC5 in the subclone of murine Cath.a differentiated neuronal cell line (CAD5) demonstrated cell surface localization of wild-type DNAJC5, whereas the p.L116del and p.L115R mutant proteins showed diffuse cytoplasmic localization in addition to aberrant accumulation in the ER and Golgi apparatus (Noskova et al., 2011). As expected, these mutants were less palmitoylated than wild-type DNAJC5, which may lead to impaired membrane tethering of DNAJC5/CSPα and a reduced protein level of DNAJC5/CSPα in the brains of affected individuals. Furthermore, p.L116del and p.L115R mutations in the cysteine-string domain cause DNAJC5/CSPα to form high molecular weight SDS-resistant aggregates, which are also present in post-mortem brain tissue from patients, suggesting a cluster of palmitoylated cysteines are essential for aggregation of CSPα (Diez-Ardanuy et al., 2017). In agreement with this, transgenic zebrafish model expressing the human mutant *DNAJC5* gene under the control of a zebrafish neuron-specific promoter demonstrated mutant DNAJC5 protein aggregates in the affected neurons (Yao et al., 2017). However, the precise molecular mechanisms by which the mutant DNAJC5 leads

to neurodegeneration accompanied by abnormal accumulation of autofluorescence materials in neuronal tissues still remain obscure. Accumulating evidence suggests that the DNAJC5/CSPα behaves as a critical regulator of synaptic proteostasis. Together with a small glutamine-rich tetratricopeptide repeat domain protein (SGT), DNAJC5/CSPα forms an enzymatically active chaperone complex and binds misfolded client proteins on synaptic vesicles, thereby preventing the buildup of misfolded proteins in the nerve terminal (Donnelier and Braun, 2014). For example, the DNAJC5-Hsc70-SGT chaperone complex stabilizes synaptosomal-associated protein 25 (SNAP-25) and facilitates its ability to assemble into the soluble NSF attachment protein receptor (SNARE) complex (Sharma et al., 2011). Intriguingly, the over-expression of α-synuclein, a culprit protein in PD, protects DNAJC5/CSPα-deficient mice from neurodegeneration (Chandra et al., 2005), which suggests that α-synuclein may compensate for the loss of DNAJC5/CSPα in the nervous system. This finding has been corroborated by a recent study showing that DNAJC5/CSPα removes neurodegeneration-related toxic proteins (e.g., abnormally expanded huntingtin and mutant superoxide dismutase 1) from neurons via extracellular vesicles (Deng et al., 2017).

DNAJC10/ERDJ5

A recent comprehensive analysis of genetic variants in a well-characterized Han-Chinese cohort with sporadic PD demonstrated that the *DNAJC10* gene variant rs13414223 decreased the risk of PD (Yuan et al., 2016). The statistical differences in genotypic and allelic frequencies between the PD and the controls were $p = 0.004$ and 0.002 (odds ratio = 0.652), respectively. The gene of *DNAJC10* encodes the 90 kDa ER-resident co-chaperone ERdj5, which is a component of ER-associated degradation (ERAD), a quality-control machinery by which unfolded/misfolded proteins are degraded in eukaryotic cells (Ushioda et al., 2008). The ERdj family comprises five members, and each member contains a conserved N-terminal J domain; ERdj5 is the only member that has thioredoxin (Trx)-like domains with catalytic active CXXC motifs (Cunnea et al., 2003). A KDEL tetrapeptide sequence is present at the C terminus of DNAJC10/ERdj5, possibly mediating the targeting to the ER (Stornaiuolo et al., 2003). Via its reductase activity, DNAJC10/ERdj5 cleaves the disulfide bonds of misfolded proteins and thereby accelerates ERAD through the associations with EDEM (ER degradation-enhancing alpha-mannosidase-like protein) and the ER chaperone BiP/GRP78 (Ushioda et al., 2008). DNAJC10/ERdj5 is ubiquitously expressed across brain areas, including the cerebral cortex, striatum, hippocampus, hypothalamus, cerebellar cortex, and brainstem (Cunnea et al., 2003), which are the anatomical regions of neuronal cell loss and Lewy body formation in PD (Braak and Braak, 2000). Intriguingly, *C. elegans* DJ-27, an ortholog of mammalian ERdj5, showed a protective effect against aggregate formation, behavior abnormalities, and mitochondrial fragmentation in worm models of human Alzheimer, Parkinson, and Huntington diseases (Munoz-Lobato et al., 2014); these findings suggest that DNAJC5 may counteract protein misfolding/aggregation toxicity in neuronal cells. Studies in higher model organisms, such as vertebrates, would be useful and advantageous to figure out how the DNAJC10/ERdj5 mutation can be involved in the pathogenesis of PD.

CONCLUDING REMARKS

Although more than 90% of PD cases occur sporadically, both familial and sporadic PD share common pathological features, such as cytoplasmic inclusions and dopaminergic cell loss (Hasegawa et al., 2004; Takeda et al., 2006). Evidence from recent genetic studies in rare familial forms of PD indicates that DnaJ/Hsp40 molecular chaperones are profoundly involved in the pathogenesis of PD. The diverse functions of the DnaJ/Hsp40 family in protein folding/unfolding, membrane trafficking, synaptic modulation and mitochondrial function are considered to not only affect the dopaminergic neurotransmission but also concomitantly influence on the PD-related neuropathological changes, such as nigral cell loss and Lewy body formation. HSPs are known to be localized with noxious proteinaceous aggregates in various neurodegenerative diseases including PD, Alzheimer's disease and prion disease (Matsuzaki et al., 2004; San Gil et al., 2017). Interestingly, several studies have shown that selective upregulation of HSPs such as DnaJ/Hsp40 and Hsp70 prevents clinicopathological progression in a variety of cellular and animal models (Popiel et al., 2012; Gao et al., 2015; Takeuchi et al., 2015). Thus, genetic as well as pharmacological manipulation of specific DnaJ/Hsp40 function may provide beneficial effects on protein and cellular homeostasis in neurodegenerative conditions. Deciphering the precise modes of DnaJ/Hsp40 functions in the pathological cascades in PD will shed light on the pathogenic mechanisms involved and may provide important clues regarding the disease-modifying strategies for this devastating neurodegenerative disease.

AUTHOR CONTRIBUTIONS

All authors (TH, SY, NS, JK, and MA) participated in the discussion of the paper. TH and SY mainly wrote the manuscript.

FUNDING

This work was supported in part by a Grant-in-Aid for Scientific Research on Innovative Areas (Brain Protein Aging and Dementia Control) [grant number 17H05683] and a Grant-in-Aid for Scientific Research (C) [grant number 17K09744] from the Ministry of Education, Culture, Sports, Science and Technology, MEXT; the Strategic Research Program for Brain Sciences from the Japan Agency for Medical Research and Development, AMED; Novartis Pharma Research Grants.

REFERENCES

Al Hafid, N., and Christodoulou, J. (2015). Phenylketonuria: a review of current and future treatments. *Transl. Pediatr.* 4, 304–317. doi: 10.3978/j.issn.2224-4336.2015.10.07

Anikster, Y., Haack, T. B., Vilboux, T., Pode-Shakked, B., Thony, B., Shen, N., et al. (2017). Biallelic mutations in DNAJC12 cause hyperphenylalaninemia, dystonia, and intellectual disability. *Am. J. Hum. Genet.* 100, 257–266. doi: 10.1016/j.ajhg.2017.01.002

Appel-Cresswell, S., Rajput, A. H., Sossi, V., Thompson, C., Silva, V., McKenzie, J., et al. (2014). Clinical, positron emission tomography, and pathological studies of DNAJC13 p.N855S Parkinsonism. *Mov. Disord.* 29, 1684–1687. doi: 10.1002/mds.26019

Blau, N. (2016). Genetics of phenylketonuria: then and now. *Hum. Mutat.* 37, 508–515. doi: 10.1002/humu.22980

Braak, H., and Braak, E. (2000). Pathoanatomy of Parkinson's disease. *J. Neurol.* 247(Suppl. 2), II3–II10. doi: 10.1007/PL00007758

Burgoyne, R. D., and Morgan, A. (2015). Cysteine string protein (CSP) and its role in preventing neurodegeneration. *Semin. Cell Dev. Biol.* 40, 153–159. doi: 10.1016/j.semcdb.2015.03.008

Burneo, J. G., Arnold, T., Palmer, C. A., Kuzniecky, R. I., Oh, S. J., and Faught, E. (2003). Adult-onset neuronal ceroid lipofuscinosis (Kufs disease) with autosomal dominant inheritance in Alabama. *Epilepsia* 44, 841–846. doi: 10.1046/j.1528-1157.2003.39802.x

Cadieux-Dion, M., Andermann, E., Lachance-Touchette, P., Ansorge, O., Meloche, C., Barnabe, A., et al. (2013). Recurrent mutations in DNAJC5 cause autosomal dominant Kufs disease. *Clin. Genet.* 83, 571–575. doi: 10.1111/cge.12020

Cai, Z., Zeng, W., Tao, K., E, Z., Wang, B., and Yang, Q. (2015). Chaperone-mediated autophagy: roles in neuroprotection. *Neurosci. Bull.* 31, 452–458. doi: 10.1007/s12264-015-1540-x

Chandra, S., Gallardo, G., Fernandez-Chacon, R., Schluter, O. M., and Sudhof, T. C. (2005). Alpha-synuclein cooperates with CSPalpha in preventing neurodegeneration. *Cell* 123, 383–396. doi: 10.1016/j.cell.2005.09.028

Chang, H. C., Hull, M., and Mellman, I. (2004). The J-domain protein Rme-8 interacts with Hsc70 to control clathrin-dependent endocytosis in Drosophila. *J. Cell Biol.* 164, 1055–1064. doi: 10.1083/jcb.200311084

Ciechanover, A., and Kwon, Y. T. (2017). Protein quality control by molecular chaperones in neurodegeneration. *Front. Neurosci.* 11:185. doi: 10.3389/fnins.2017.00185

Cunnea, P. M., Miranda-Vizuete, A., Bertoli, G., Simmen, T., Damdimopoulos, A. E., Hermann, S., et al. (2003). ERdj5, an endoplasmic reticulum (ER)-resident protein containing DnaJ and thioredoxin domains, is expressed in secretory cells or following ER stress. *J. Biol. Chem.* 278, 1059–1066. doi: 10.1074/jbc.M206995200

Deng, H. X., Shi, Y., Yang, Y., Ahmeti, K. B., Miller, N., Huang, C., et al. (2016). Identification of TMEM230 mutations in familial Parkinson's disease. *Nat. Genet.* 48, 733–739. doi: 10.1038/ng.3589

Deng, J., Koutras, C., Donnelier, J., Alshehri, M., Fotouhi, M., Girard, M., et al. (2017). Neurons export extracellular vesicles enriched in cysteine string protein and misfolded protein cargo. *Sci. Rep.* 7:956. doi: 10.1038/s41598-017-01115-6

Diez-Ardanuy, C., Greaves, J., Munro, K. R., Tomkinson, N. C., and Chamberlain, L. H. (2017). A cluster of palmitoylated cysteines are essential for aggregation of cysteine-string protein mutants that cause neuronal ceroid lipofuscinosis. *Sci. Rep.* 7:10. doi: 10.1038/s41598-017-00036-8

Donnelier, J., and Braun, J. E. (2014). CSPα-chaperoning presynaptic proteins. *Front. Cell Neurosci.* 8:116. doi: 10.3389/fncel.2014.00116

Dudek, J., Benedix, J., Cappel, S., Greiner, M., Jalal, C., Muller, L., et al. (2009). Functions and pathologies of BiP and its interaction partners. *Cell Mol. Life Sci.* 66, 1556–1569. doi: 10.1007/s00018-009-8745-y

Edvardson, S., Cinnamon, Y., Ta-Shma, A., Shaag, A., Yim, Y. I., Zenvirt, S., et al. (2012). A deleterious mutation in DNAJC6 encoding the neuronal-specific clathrin-uncoating co-chaperone auxilin, is associated with juvenile parkinsonism. *PLoS ONE* 7:e36458. doi: 10.1371/journal.pone.0036458

Elsayed, L. E., Drouet, V., Usenko, T., Mohammed, I. N., Hamed, A. A., Elseed, M. A., et al. (2016). A novel nonsense mutation in DNAJC6 expands the phenotype of autosomal-recessive juvenile-onset Parkinson's disease. *Ann. Neurol.* 79, 335–337. doi: 10.1002/ana.24591

Freeman, C. L., Hesketh, G., and Seaman, M. N. (2014). RME-8 coordinates the activity of the WASH complex with the function of the retromer SNX dimer to control endosomal tubulation. *J. Cell Sci.* 127, 2053–2070. doi: 10.1242/jcs.144659

Fujibayashi, A., Taguchi, T., Misaki, R., Ohtani, M., Dohmae, N., Takio, K., et al. (2008). Human RME-8 is involved in membrane trafficking through early endosomes. *Cell Struct. Funct.* 33, 35–50. doi: 10.1247/csf.07045

Gao, X., Carroni, M., Nussbaum-Krammer, C., Mogk, A., Nillegoda, N. B., Szlachcic, A., et al. (2015). Human Hsp70 disaggregase reverses Parkinson's-linked alpha-synuclein amyloid fibrils. *Mol. Cell* 59, 781–793. doi: 10.1016/j.molcel.2015.07.012

Giot, L., Bader, J. S., Brouwer, C., Chaudhuri, A., Kuang, B., Li, Y., et al. (2003). A protein interaction map of *Drosophila melanogaster*. *Science* 302, 1727–1736. doi: 10.1126/science.1090289

Girard, M., Poupon, V., Blondeau, F., and McPherson, P. S. (2005). The DnaJ-domain protein RME-8 functions in endosomal trafficking. *J. Biol. Chem.* 280, 40135–40143. doi: 10.1074/jbc.M505036200

Goldfarb, S. B., Kashlan, O. B., Watkins, J. N., Suaud, L., Yan, W., Kleyman, T. R., et al. (2006). Differential effects of Hsc70 and Hsp70 on the intracellular trafficking and functional expression of epithelial sodium channels. *Proc. Natl. Acad. Sci. U.S.A.* 103, 5817–5822. doi: 10.1073/pnas.0507903103

Gorenberg, E. L., and Chandra, S. S. (2017). The role of co-chaperones in synaptic proteostasis and neurodegenerative disease. *Front. Neurosci.* 11:248. doi: 10.3389/fnins.2017.00248

Greene, M. K., Maskos, K., and Landry, S. J. (1998). Role of the J-domain in the cooperation of Hsp40 with Hsp70. *Proc. Natl. Acad. Sci. U.S.A.* 95, 6108–6113. doi: 10.1073/pnas.95.11.6108

Gustavsson, E. K., Trinh, J., Guella, I., Vilarino-Guell, C., Appel-Cresswell, S., Stoessl, A. J., et al. (2015). DNAJC13 genetic variants in parkinsonism. *Mov. Disord.* 30, 273–278. doi: 10.1002/mds.26064

Hahn, Y., Lee, J., Seong, C., Yoon, J., and Chung, J. H. (1999). Structural analysis of phylogenetically conserved J domain protein gene. *Biochim. Biophys. Acta* 1447, 325–333. doi: 10.1016/S0167-4781(99)00162-1

Hasegawa, T., Matsuzaki, M., Takeda, A., Kikuchi, A., Akita, H., Perry, G., et al. (2004). Accelerated alpha-synuclein aggregation after differentiation of SH-SY5Y neuroblastoma cells. *Brain Res.* 1013, 51–59. doi: 10.1016/j.brainres.2004.04.018

Hasegawa, T., Sugeno, N., Kikuchi, A., Baba, T., and Aoki, M. (2017). Membrane trafficking illuminates a path to Parkinson's disease. *Tohoku J. Exp. Med.* 242, 63–76. doi: 10.1620/tjem.242.63

Huttlin, E. L., Ting, L., Bruckner, R. J., Gebreab, F., Gygi, M. P., Szpyt, J., et al. (2015). The BioPlex network: a systematic exploration of the human interactome. *Cell* 162, 425–440. doi: 10.1016/j.cell.2015.06.043

Kim, M. J., Deng, H. X., Wong, Y. C., Siddique, T., and Krainc, D. (2017). The Parkinson's disease-linked protein TMEM230 is required for Rab8a-mediated secretory vesicle trafficking and retromer trafficking. *Hum. Mol. Genet.* 26, 729–741. doi: 10.1093/hmg/ddw413

Koroglu, C., Baysal, L., Cetinkaya, M., Karasoy, H., and Tolun, A. (2013). DNAJC6 is responsible for juvenile parkinsonism with phenotypic variability. *Parkinson. Relat. Disord.* 19, 320–324. doi: 10.1016/j.parkreldis.2012.11.006

Lee, D. W., Wu, X., Eisenberg, E., and Greene, L. E. (2006). Recruitment dynamics of GAK and auxilin to clathrin-coated pits during endocytosis. *J. Cell Sci.* 119, 3502–3512. doi: 10.1242/jcs.03092

Lorenzo-Betancor, O., Ogaki, K., Soto-Ortolaza, A. I., Labbe, C., Walton, R. L., Strongosky, A. J., et al. (2015). DNAJC13 p.Asn855Ser mutation screening in Parkinson's disease and pathologically confirmed Lewy body disease patients. *Eur. J. Neurol.* 22, 1323–1325. doi: 10.1111/ene.12770

Matsuzaki, M., Hasegawa, T., Takeda, A., Kikuchi, A., Furukawa, K., Kato, Y., et al. (2004). Histochemical features of stress-induced aggregates in alpha-synuclein overexpressing cells. *Brain Res.* 1004, 83–90. doi: 10.1016/j.brainres.2004.01.017

Munoz-Lobato, F., Rodriguez-Palero, M. J., Naranjo-Galindo, F. J., Shephard, F., Gaffney, C. J., Szewczyk, N. J., et al. (2014). Protective role of DNJ-27/ERdj5 in *Caenorhabditis elegans* models of human neurodegenerative diseases. *Antioxid. Redox Signal.* 20, 217–235. doi: 10.1089/ars.2012.5051

Noskova, L., Stranecky, V., Hartmannova, H., Pristoupilova, A., Baresova, V., Ivanek, R., et al. (2011). Mutations in DNAJC5, encoding cysteine-string protein alpha, cause autosomal-dominant adult-onset neuronal ceroid lipofuscinosis. *Am. J. Hum. Genet.* 89, 241–252. doi: 10.1016/j.ajhg.2011.07.003

Olgiati, S., Quadri, M., Fang, M., Rood, J. P., Saute, J. A., Chien, H. F., et al. (2016). DNAJC6 mutations associated with early-onset Parkinson's disease. *Ann. Neurol.* 79, 244–256. doi: 10.1002/ana.24553

Oshima, R., Hasegawa, T., Tamai, K., Sugeno, N., Yoshida, S., Kobayashi, J., et al. (2016). ESCRT-0 dysfunction compromises autophagic degradation of protein aggregates and facilitates ER stress-mediated neurodegeneration via apoptotic and necroptotic pathways. *Sci. Rep.* 6:24997. doi: 10.1038/srep24997

Pankratz, N., Wilk, J. B., Latourelle, J. C., Destefano, A. L., Halter, C., Pugh, E. W., et al. (2009). Genomewide association study for susceptibility genes contributing to familial Parkinson disease. *Hum. Genet.* 124, 593–605. doi: 10.1007/s00439-008-0582-9

Pauli, D., Arrigo, A. P., and Tissieres, A. (1992). Heat shock response in Drosophila. *Experientia* 48, 623–629. doi: 10.1007/BF02118306

Perales-Calvo, J., Muga, A., and Moro, F. (2010). Role of DnaJ G/F-rich domain in conformational recognition and binding of protein substrates. *J. Biol. Chem.* 285, 34231–34239. doi: 10.1074/jbc.M110.144642

Piano, A., Valbonesi, P., and Fabbri, E. (2004). Expression of cytoprotective proteins, heat shock protein 70 and metallothioneins, in tissues of *Ostrea edulis* exposed to heat and heavy metals. *Cell Stress Chaperones* 9, 134–142. doi: 10.1379/483.1

Popiel, H. A., Takeuchi, T., Fujita, H., Yamamoto, K., Ito, C., Yamane, H., et al. (2012). Hsp40 gene therapy exerts therapeutic effects on polyglutamine disease mice via a non-cell autonomous mechanism. *PLoS ONE* 7:e51069. doi: 10.1371/journal.pone.0051069

Popoff, V., Mardones, G. A., Bai, S. K., Chambon, V., Tenza, D., Burgos, P. V., et al. (2009). Analysis of articulation between clathrin and retromer in retrograde sorting on early endosomes. *Traffic* 10, 1868–1880. doi: 10.1111/j.1600-0854.2009.00993.x

Puschmann, A. (2017). New genes causing hereditary Parkinson's disease or Parkinsonism. *Curr. Neurol. Neurosci. Rep.* 17:66. doi: 10.1007/s11910-017-0780-8

Qiu, X. B., Shao, Y. M., Miao, S., and Wang, L. (2006). The diversity of the DnaJ/Hsp40 family, the crucial partners for Hsp70 chaperones. *Cell Mol. Life Sci.* 63, 2560–2570. doi: 10.1007/s00018-006-6192-6

Rajput, A., Ross, J. P., Bernales, C. Q., Rayaprolu, S., Soto-Ortolaza, A. I., Ross, O. A., et al. (2015). VPS35 and DNAJC13 disease-causing variants in essential tremor. *Eur. J. Hum. Genet.* 23, 887–888. doi: 10.1038/ejhg.2014.164

San Gil, R., Ooi, L., Yerbury, J. J., and Ecroyd, H. (2017). The heat shock response in neurons and astroglia and its role in neurodegenerative diseases. *Mol. Neurodegener.* 12:65. doi: 10.1186/s13024-017-0208-6

Schopf, F. H., Biebl, M. M., and Buchner, J. (2017). The HSP90 chaperone machinery. *Nat. Rev. Mol. Cell Biol.* 18, 345–360. doi: 10.1038/nrm.2017.20

Sharma, M., Burre, J., and Sudhof, T. C. (2011). CSPα promotes SNARE-complex assembly by chaperoning SNAP-25 during synaptic activity. *Nat. Cell Biol.* 13, 30–39. doi: 10.1038/ncb2131

Shi, A., Sun, L., Banerjee, R., Tobin, M., Zhang, Y., and Grant, B. D. (2009). Regulation of endosomal clathrin and retromer-mediated endosome to Golgi retrograde transport by the J-domain protein RME-8. *EMBO J.* 28, 3290–3302. doi: 10.1038/emboj.2009.272

Shoji, Y., Nishio, Y., Baba, T., Uchiyama, M., Yokoi, K., Ishioka, T., et al. (2014). Neural substrates of cognitive subtypes in Parkinson's disease: a 3-year longitudinal study. *PLoS ONE* 9:e110547. doi: 10.1371/journal.pone.0110547

Soga, S., Akinaga, S., and Shiotsu, Y. (2013). Hsp90 inhibitors as anti-cancer agents, from basic discoveries to clinical development. *Curr. Pharm. Des.* 19, 366–376. doi: 10.2174/138161213804143617

Stornaiuolo, M., Lotti, L. V., Borgese, N., Torrisi, M. R., Mottola, G., Martire, G., et al. (2003). KDEL and KKXX retrieval signals appended to the same reporter protein determine different trafficking between endoplasmic reticulum, intermediate compartment, and Golgi complex. *Mol. Biol. Cell* 14, 889–902. doi: 10.1091/mbc.E02-08-0468

Straniero, L., Guella, I., Cilia, R., Parkkinen, L., Rimoldi, V., Young, A., et al. (2017). DNAJC12 and dopa-responsive nonprogressive parkinsonism. *Ann. Neurol.* 82, 640–646. doi: 10.1002/ana.25048

Takeda, A., Hasegawa, T., Matsuzaki-Kobayashi, M., Sugeno, N., Kikuchi, A., Itoyama, Y., et al. (2006). Mechanisms of neuronal death in synucleinopathy. *J. Biomed. Biotechnol.* 2006:19365. doi: 10.1155/JBB/2006/19365

Takeuchi, T., Suzuki, M., Fujikake, N., Popiel, H. A., Kikuchi, H., Futaki, S., et al. (2015). Intercellular chaperone transmission via exosomes contributes to maintenance of protein homeostasis at the organismal level. *Proc. Natl. Acad. Sci. U.S.A.* 112, E2497–E2506. doi: 10.1073/pnas.1412651112

Ushioda, R., Hoseki, J., Araki, K., Jansen, G., Thomas, D. Y., and Nagata, K. (2008). ERdj5 is required as a disulfide reductase for degradation of misfolded proteins in the ER. *Science* 321, 569–572. doi: 10.1126/science.1159293

van Spronsen, F. J., Himmelreich, N., Rüfenacht, V., Shen, N., Vliet, D. V., Al-Owain, M., et al. (2017). Heterogeneous clinical spectrum of DNAJC12-deficient hyperphenylalaninemia: from attention deficit to severe dystonia and intellectual disability. *J. Med. Genet.* doi: 10.1136/jmedgenet-2017-104875. [Epub ahead of print].

Velinov, M., Dolzhanskaya, N., Gonzalez, M., Powell, E., Konidari, I., Hulme, W., et al. (2012). Mutations in the gene DNAJC5 cause autosomal dominant Kufs disease in a proportion of cases: study of the Parry family and 8 other families. *PLoS ONE* 7:e29729. doi: 10.1371/annotation/26d7eb64-ccd2-41db-b1aa-7cdc8c1eff95

Vilariño-Güell, C., Rajput, A., Milnerwood, A. J., Shah, B., Szu-Tu, C., Trinh, J., et al. (2014). DNAJC13 mutations in Parkinson disease. *Hum. Mol. Genet.* 23, 1794–1801. doi: 10.1093/hmg/ddt570

Yao, X., Liu, X., Zhang, Y., Li, Y., Zhao, C., Yao, S., et al. (2017). Gene therapy of adult neuronal ceroid lipofuscinoses with CRISPR/Cas9 in Zebrafish. *Hum. Gene Ther.* 28, 588–597. doi: 10.1089/hum.2016.190

Yim, Y. I., Sun, T., Wu, L. G., Raimondi, A., De Camilli, P., Eisenberg, E., et al. (2010). Endocytosis and clathrin-uncoating defects at synapses of auxilin knockout mice. *Proc. Natl. Acad. Sci. U.S.A.* 107, 4412–4417. doi: 10.1073/pnas.1000738107

Yuan, L., Song, Z., Deng, X., Zheng, W., Guo, Y., Yang, Z., et al. (2016). Systematic analysis of genetic variants in Han Chinese patients with sporadic Parkinson's disease. *Sci. Rep.* 6:33850. doi: 10.1038/srep33850

Zhang, Y., Grant, B., and Hirsh, D. (2001). RME-8, a conserved J-domain protein, is required for endocytosis in *Caenorhabditis elegans*. *Mol. Biol. Cell* 12, 2011–2021. doi: 10.1091/mbc.12.7.2011

Zuiderweg, E. R., Hightower, L. E., and Gestwicki, J. E. (2017). The remarkable multivalency of the Hsp70 chaperones. *Cell Stress Chaperones* 22, 173–189. doi: 10.1007/s12192-017-0776-y

Conflict of Interest Statement: The authors declare that the research was conducted in the absence of any commercial or financial relationships that could be construed as a potential conflict of interest.

frontiers in Neuroscience

REVIEW
published: 20 February 2018
doi: 10.3389/fnins.2018.00091

ER Dynamics and Derangement in Neurological Diseases

Tomoyuki Yamanaka and Nobuyuki Nukina*

Laboratory of Structural Neuropathology, Graduate School of Brain Science, Doshisha University, Kyoto, Japan

The endoplasmic reticulum (ER) is a morphologically dynamic organelle containing different membrane subdomains with distinct cellular functions. Numerous observations have revealed that ER stress response induced by disturbed ER homeostasis is linked to various neurological/neurodegenerative disorders. In contrast, recent findings unveil that ER structural derangements are linked to the progression of several neurological diseases. The derangements involve two distinct, and likely opposing pathways. One is dysfunction of ER dynamics machinery, leading to disruption of ER network organization. Another one is facilitation of pre-existing machinery, leading to generation of markedly-ordered *de novo* membranous structure. Restoring the ER network can be the effective way toward the cure of ER-deranged neurological disorders.

Keywords: endoplasmic reticulum, ER architecture, ER dynamics, neurological disease, neurodegeneration, NF-Y

OPEN ACCESS

Edited by:
Gen Sobue,
Nagoya University, Japan

Reviewed by:
Corinne Lasmezas,
Scripps Florida, United States
Smitha Karunakaran,
Indian Institute of Science, India

****Correspondence:***
Tomoyuki Yamanaka
toyamana@mail.doshisha.ac.jp

Specialty section:
This article was submitted to Neurodegeneration, a section of the journal Frontiers in Neuroscience

Received: *26 September 2017*
Accepted: *05 February 2018*
Published: *20 February 2018*

Citation:
Yamanaka T and Nukina N (2018) ER Dynamics and Derangement in Neurological Diseases. Front. Neurosci. 12:91. doi: 10.3389/fnins.2018.00091

INTRODUCTION

Endoplasmic reticulum (ER) is a continuous membrane organelle dispersing throughout the cells. It consist of two differentially shaped membranous domains; the nuclear envelope, a highly regulated membrane barrier that separates the nucleus from the cytoplasm, and the peripheral ERs including ribosome-studded rough ER (RER) and ribosome-free smooth ER (SER) (**Figure 1**). The RER plays a key role in synthesis and transport of secretary/membrane proteins. The SER is critical for synthesis of lipids / sterols, storage and regulated release of calcium, and metabolism and detoxification. These peripheral ERs are highly dynamic and change their shapes and volumes on the demand of cellular needs (Federovitch et al., 2005; Park and Blackstone, 2010; Westrate et al., 2015).

ER dysfunction causes deleterious effects on the cells and is associated with many diseases including various neurological/neurodegenerative disorders. The major pathway involved in this is ER stress responses induced by disturbance of ER homeostasis due to protein misfolding and aggregation (Matus et al., 2011; Remondelli and Renna, 2017). In contrast, recent findings highlight another ER abnormalities associated with ER morphological alteration in neurological diseases. These are mainly caused by dysregulations of ER-resident membrane proteins. In this review, we discussed the ER dynamics and its derangement in neuropathogenesis.

Peripheral ER Organization and Dynamics

The peripheral ERs are morphologically subdivided into two domains, ER sheets and tubules (**Figure 1**). The sheets mainly located in perinuclear region and tend to be studded with ribosomes (RER), whereas tubules form cytoplasmic network and are largely devoid of ribosomes (SER). Different sets of proteins are involved in the organization of these distinct ER membrane domains (**Figure 2**; Park and Blackstone, 2010; Chen et al., 2013; Westrate et al., 2015). In the sheets, one of the key regulators is stubbed ribosome, which is elegantly shown by the experiment using two

translation inhibitors, puromycin or cycloheximide; the ER sheets are disrupted by puromycin that quickly dissociates polysomes from ER membranes, but not by cycloheximide that stabilizes ribosomal association with translocons, in cultured cells (Puhka et al., 2007). Two transmembrane protein Climp63 and TMEM170A are also shown to be important regulators for RER sheet formation; knockdown of each one decreased ER sheets whereas its overexpression increased them (Shibata et al., 2010; Christodoulou et al., 2016). As for TMEM170A, its localization to nuclear envelopes and regulation of nuclear morphology are also reported (Christodoulou et al., 2016). Thus, the ER sheets are organized by different types of proteins (**Figure 2**).

On the contrary, the ER tubules are generated by a set of specific membrane proteins that contain one or two "hairpin" transmembrane domains. This domain is inserted into outer leaflet of the membrane bilayer and suggested to generate curvature to bend the membrane (**Figure 2**; Park and Blackstone, 2010; Chen et al., 2013; Westrate et al., 2015). The membrane proteins include Reticulons (Rtn1-4), DP1 (deleted in polyposis locus 1; also known as REEP5), other REEPs (receptor expression-enhancing proteins; REEP1-4 and 6), Atlastin-1, M1-Spastin and Lunapark. Among them, Reticulons, DP1 and Atlastin-1 are extensively analyzed and shown to be required for formation of ER tubular network *in vitro* (Hu et al., 2008; Wang et al., 2016; Powers et al., 2017) and in cultured cells (Voeltz et al., 2006; Hu et al., 2009). These three proteins interact with each other (Hu et al., 2009), and form immobile oligomer complex in the tubules (Shibata et al., 2008; Orso et al., 2009). Complex formation of REEP1 with Atlastin-1 and M1-Spastin and its contribution of ER tubule formation are also reported (Evans et al., 2006; Park et al., 2010). Thus, interconnected interactions of these membrane-inserting proteins mediate the ER tubule formation. Atlastin-1 and Lunapark also induce homotypic ER fusion to generate branched tubules (Orso et al., 2009; Chen et al., 2012, 2015). Binding to microtubule cytoskeleton through REEP1-4 and M1-spastin is further involved in establishment and maintenance of complicated tubular network (Park and Blackstone, 2010; Westrate et al., 2015).

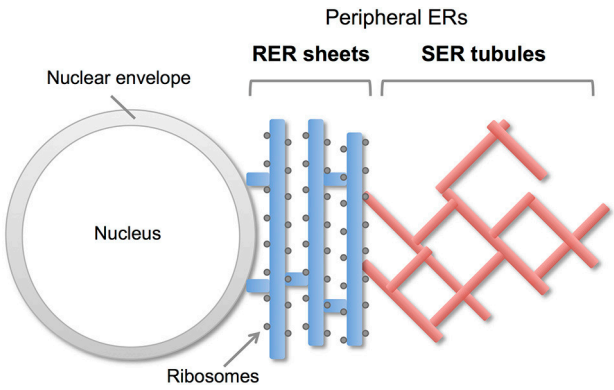

FIGURE 1 | Morphology of peripheral ERs in mammalian cells. The peripheral ERs are composed of two different subdomains; a ribosome-studded rough ER (RER) and a ribosome-free smooth ER (SER). The RERs form sheets in perinuclear region and play a role in protein synthesis and transport. The SERs form tubule networks in cytoplasm and are involved in lipids synthesis, calcium storage and detoxification.

Disruption of ER Dynamics in Neurological Diseases

Notably, some of the ER tubule proteins have been shown to be mutated in hereditary spastic paraplegia (HSP), a group of genetic disorders caused by a length-dependent, distal axonopathy of corticospinal motor neurons, leading to lower limb spasticity and weakness. Currently, over 40 different genetic loci (SPG1–45) are reported (Blackstone et al., 2011; Lo Giudice et al., 2014). Despite the large number of loci, about 60% of HSP patients harbor pathogenic mutations in one of three proteins: Spastin (SPG4), Atlastin-1 (SPG3A), or REEP1 (SPG31), all of which are the regulators of ER tubule formation as described

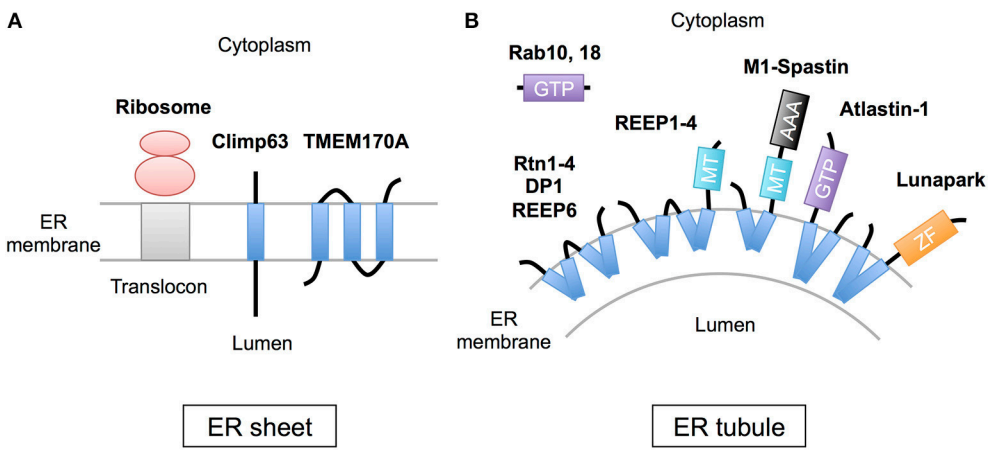

FIGURE 2 | Scheme of the proteins regulating ER morphology. **(A)** The ER sheet formation is regulated by membrane-attaching ribosomes and two transmembrane proteins, Climp63 and TMEM170A. **(B)** The ER tubule formation is regulated by a set of hairpin transmembrane domain-containing proteins, including Reticulons (Rtn1-4), DP1 (REEP5), REEP1-4, REEP6, Atlastin-1, M1-Spastin and Lunapark, those generate curvature to bend the membrane. Rab GTPases (10 and 18) are also involved in this process. MT; microtubule binding region, GTP, GTPase domain; ZF, zinc finger motif.

above. In addition, another ER tubule protein Rtn2 is also mutated in SPG12 patients. Thus, these SPG proteins are critical for motor neuron integrity *in vivo*. Indeed, knockdown of Spastin or Atlastin-1 in zebrafish induces axonal degeneration in motor neurons and locomotion defects (Butler et al., 2010; Fassier et al., 2010; Patten et al., 2014). In mice, mutation in Spastin or REEP1 causes progressive axonal degeneration of corticospinal motor neurons and motor defects (Tarrade et al., 2006; Beetz et al., 2013; Renvoise et al., 2016). Furthermore, peripheral ER complexity decreases in primary motor neurons of REEP1 mutant mice (Beetz et al., 2013). These observations suggest that these SPG proteins are necessary for axonal development and/or maintenance probably by modulating ER architecture in motor neurons. Because Spastin, Atlastin-1, and REEP1 are co-enriched in axonal growth cones in cultured neurons (Park et al., 2010), they may regulate axonal growth by modulating ER tubule network dynamics.

The other factors involved in the ER tubule formation are Rab GTPases, central regulators of vesicle budding, motility, and fusion (**Figure 2**). Two Rab GTPases, Rab10, and Rab18, are shown to localize to ER tubules and its dysfunction results in ER tubule disorganization in cultured cells (English and Voeltz, 2013; Gerondopoulos et al., 2014). Notably, loss-of-function mutations of Rab18 or its regulator RabGAP cause Warburg Micro Syndrome, a rare autosomal recessive genetic disorder characterized by severe eye and brain abnormalities (Bem et al., 2011). Knockdown of Rab18 in zebrafish causes developmental abnormalities including microphthalmia and microcephaly (Bem et al., 2011). In addition, knockdown of Rab10 or Rab18 induces defects in neuronal differentiation in mouse brain cortex (Wang et al., 2011; Wu et al., 2016). These observations reveal critical roles of these Rab GTPases in neuronal development *in vivo*.

An ER membrane protein FAM134B is also linked to a neurological disease named hereditary sensory and autonomic neuropathy (HSAN) (Kurth et al., 2009). Interestingly, this protein is shown to be an autophagy receptor to mediate degradation of ER through autophagic system. This phenomenon is called ER-phagy, which is considered to be involved in ER homeostasis (Khaminets et al., 2015). Being its localization mainly to ER sheets, FAM134B is thought to be an ER sheet-specific autophagy receptor. Recently, an ER tubule protein Rtn3 is identified as another ER-phagy receptor, which induce fragmentation and autophagic degradation of ER tubules independently of FAM134B (Grumati et al., 2017). Thus, FAM134B and Rtn3 may regulate different ER membranes to regulate overall ER homeostasis.

The ER Tubule Network and Neurodegenerative Diseases

The ER tubules are interacting with other membranous organelles such as mitochondria, plasma membrane, peroxisomes and lysosomes. The mitochondria-associated ER membrane (MAM) mediates several fundamental cellular processes including calcium exchange, phospholipid exchange, intracellular trafficking and autophagy. The ER–mitochondria associations through MAM are shown to be disrupted in several neurodegenerative diseases such as Alzheimer's disease (AD), Parkinson's disease and amyotrophic lateral sclerosis with associated frontotemporal dementia (ALS/FTD), resulting in alteration in cellular functions regulated by MAM (Paillusson et al., 2016).

Direct implications of ER tubule proteins in disease pathogenesis have been reported. In superoxide dismutase 1 (SOD1) G93A transgenic mouse, a model for ALS, depletion of Rtn4 accelerates disease onset and progression possibly by disrupting normal distribution of protein disulfide isomerase (PDI), suggesting protective role of Reticulon in motor neuron degeneration (Yang et al., 2009). As for AD, Rtn3 binds to and colocalizes with BACE1, a beta-secretase involved in amyloid precursor protein (APP) cleavage and amyloid beta production. Interestingly, overexpression of Rtn3 reduces the production of amyloid beta while its knockdown enhances it in cultured cells. Furthermore, Rtn3 blocks BACE1 interactions with APP, suggesting that the Reticulon negatively modulates BACE1 activity and amyloid beta production (He et al., 2004). In addition, enhanced expression of Rtn3 suppresses amyloid plaque formation in transgenic mice expressing mutants for APP and presenilin-1 (Shi et al., 2009). In contrast to these beneficial effects, Rtn3 is found to be aggregated and accumulated in dystrophic neurites, named as Rtn3 immunoreactive dystrophic neurites (RIDNs) in brains of AD cases and mice brains expressing mutant APP. Furthermore, Rtn3 transgenic expression impairs spatial learning and memory as well as synaptic plasticity in mice, implying that RIDNs potentially contribute to AD cognitive dysfunction (Hu et al., 2007). Thus, Rtn3 may bidirectionally regulate AD pathogenesis *in vivo*.

Biogenesis of Highly-Ordered ERs, the Stacked SERs

In addition to the tubular architecture as described above, the SER is known to form highly-organized membranous structures where cisternae are stacked with ordered arrays (Federovitch et al., 2005; Borgese et al., 2006). This "stacked SER" is observed in the cells highly demanding SER-related functions such as lipid biosynthesis and drug metabolism. These include adrenal cells that produce large amount of sterol lipids, and liver cells of animal treated with phenobarbital (Feldman et al., 1981; Federovitch et al., 2005). Treatment of statins (cholesterol synthesis inhibitors) also leads to stacked SER formation by induced expression of an ER-resident enzyme, hydroxy-methylglutaryl (HMG)-CoA reductase (Singer et al., 1988; Borgese et al., 2006). Interestingly, overexpression of ER resident membrane proteins such as cytochrome b(5), P450, aldehyde dehydrogenase, Sec61 and Calnexin in cultured cells is shown to be sufficient for stacked SER formation (Yamamoto et al., 1996; Snapp et al., 2003; Korkhov and Zuber, 2009). Thus, load of ER-resident membrane proteins is one of the factors for stacked SER biogenesis.

As for the molecular mechanism, selective activation of ATF6 and following lipid synthesis are suggested to be involved in stacked SER generation upon cytochrome b(5)

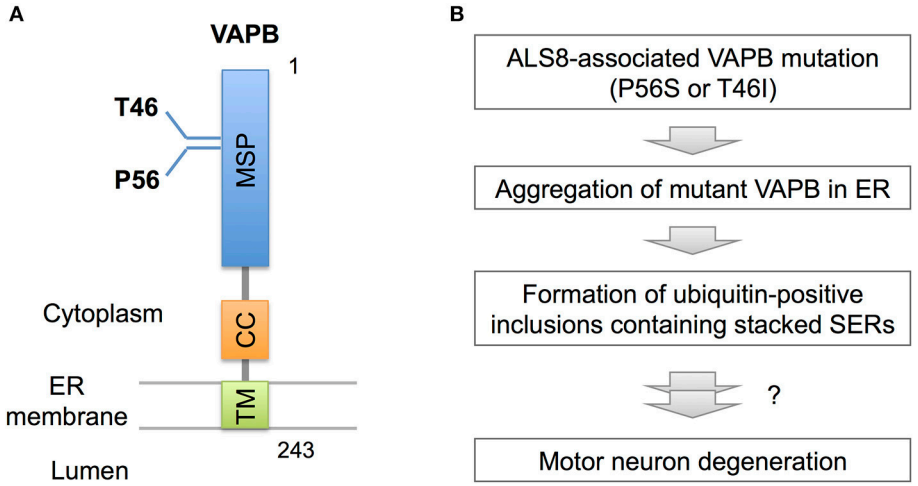

FIGURE 3 | VAPB mutations and SER pathology. **(A)** Domain structure of VAPB. VAPB is composed of the 125-residue major sperm protein (MSP), coiled coil (CC), and transmembrane (TM) domains. The residues Thr46 and Pro56 are mutated to Ile and Ser, respectively, in familial ALS (ALS8). **(B)** A model for VAPB-pathology in ALS8. The mutant VAPB proteins are insolubilized and aggregated in ER, leading to formation of ubiquitin-positive inclusions containing stacked SER. The direct link of ER pathology to motor neuron degeneration is still uncertain, however.

expression (Maiuolo et al., 2011). Because of no inductions of ER chaperone expression, XBP1 splicing or eIF2-alpha phosphorylation, the usual unfolded protein response (UPR) pathway may not be involved in ATF6-dependent pathway. Knockdown of Syntaxin 18, a SNARE component involved in ER-Golgi transport and ER-network organization, also induces stacked SER formation (Iinuma et al., 2009). Furthermore, knockdown of a membrane protein Yip1A, which cycles between ER and early Golgi, induces formation of stacked SER (Dykstra et al., 2010). A compound phenyl-2-decanoyl-amino-3-morpholino-1-propanol-hydrocholride (PDMP) that blocks membrane transport from ER to Golgi also induces generation of this type of ER (Sprocati et al., 2006). Experiments using several compounds further suggested that altering ionic homeostasis in ER is also an inducer of stacked SER formation independently of known UPR pathways (Varadarajan et al., 2012, 2013). Notably, the stacked SER formation often accompanies Golgi fragmentation and delay of ER export (Iinuma et al., 2009; Dykstra et al., 2010; Varadarajan et al., 2012). These observations suggest close relationship of ER-Golgi transport machineries, rather than canonical UPR pathways, to stacked SER biogenesis.

Despite the drastic alterations of ER and Golgi architectures, there is no report describing distinct reduction of cell viability. Importantly, the ER structure is reversible because depletion of the compounds such as PDMP leads to disappearance of stacked SER (Sprocati et al., 2006; Varadarajan et al., 2012). Thus, the stacked SER formation may not be the toxic inducer for cells but is suggested to be a novel stress response to cope with overload of ER membrane proteins independently of usual UPR pathways.

Stacked SER Pathologies in Neurological Diseases

Recent observations, however, indicate pathogenic significance of stacked SER in neurological diseases. In familial ALS (ALS8), an ER-resident membrane protein, vesicle-associated membrane protein-associated protein B (VAPB) is mutated (**Figure 3**; Nishimura et al., 2004). Overexpressed mutant VAPB protein in cultured cells is insolubilized and aggregated in ER, leading to formation of ubiquitin-positive inclusions containing stacked SERs (**Figure 3**; Teuling et al., 2007; Fasana et al., 2010). In cultured neurons, the mutant VAPB overexpression induces Golgi fragmentation and cell death (Teuling et al., 2007). Furthermore, in VAPB mutant-transgenic mice ubiquitin-positive inclusions associated with stacked SER are developed in motor neurons (Tudor et al., 2010; Aliaga et al., 2013; Kuijpers et al., 2013; Qiu et al., 2013), and furthermore progressive loss of corticospinal motor neurons is observed in some of mice lines (Aliaga et al., 2013). Although the neurotoxic effect of mutant VAPB is still controversial because other transgenic mice lines do not show neuronal loss or motor phenotypes (Tudor et al., 2010; Kuijpers et al., 2013; Qiu et al., 2013), VAPB mutant knock-in mice are shown to display slow progression of motor behavior defects (Larroquette et al., 2015), suggesting a certain involvement of VAPB mutation on motor neuron dysfunction.

Torsion dystonia-1 (DYT1) is the most common inherited dystonia characterized by involuntary muscle contractions and abnormal postures, which is caused by mutation in TorsinA, an ER glycoprotein belonging to AAA family of proteins (Ozelius et al., 1997). The mutant TorsinA forms cytoplasmic inclusions containing stacked SER in cultured neuronal cells (Hewett et al., 2000; Gonzalez-Alegre and Paulson, 2004). In peripheral nervous system, mutation in peripheral myelin protein 22 (PMP22) is linked to Charcot-Marie-Tooth disease, a sensorineural peripheral polyneuropathy. PMP22 is expressed in Schwann cells and its mutation induces formation of cytoplasmic inclusion containing mutant protein in association with stacked SER formation (Dickson et al., 2002). These observations further provide the pathological significance of cytoplasmic inclusions containing stacked SER in neurological diseases.

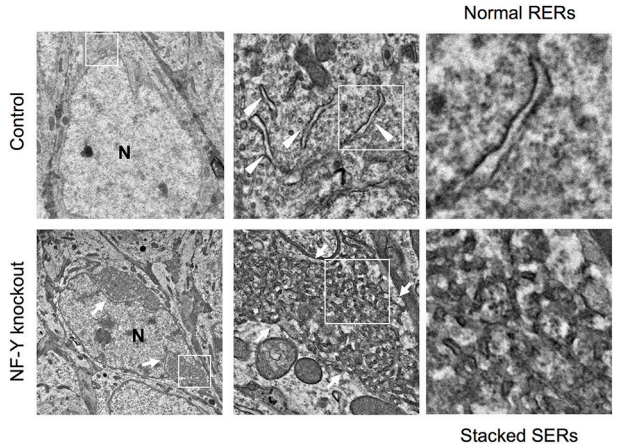

FIGURE 4 | SER pathology in NF-Y knockout neurons. Electron microgram of hippocampal CA1 neurons in control and NF-Y knockout mouse. Boxed areas are enlarged in the next panels. The neurons of NF-Y knockout mouse contain stacked SERs at perinuclear regions (arrows in lower panels) whereas control mouse neurons contain normal RERs (arrowheads in upper panels). N indicates nucleus. The data are reproduced from our previous paper (Yamanaka et al., 2014) with slight modifications.

A novel mouse model for stacked SER pathology in brain neurons was recently established (Yamanaka et al., 2014, 2016). Importantly, it does not involve disease-associated gene mutation but just caused by inactivation of CCAAT-binding factor NF-Y, a ubiquitous transcription factor shown to be affected in polyglutamine diseases (Yamanaka et al., 2008; Katsuno et al., 2010; Huang et al., 2011). The neuron-specific knockdown of NF-Y induces insolubilization of various membrane proteins including Calnexin, Reticulon, Atlastin-1, APP and Carboxypeptidase E together with ubiquitin and p62/Sqstm1, all of which are accumulated on ER (Yamanaka et al., 2014, 2016). It also accompanies perinuclear accumulation of ribosome-free SERs and Golgi disassembly (**Figure 4**). Chromatin immunoprecipitation identifies several genes involved in protein folding in ER and ER-associated degradation (ERAD) as targets of NF-Y, suggesting a critical role of NF-Y in ER protein homeostasis to maintain normal ER architecture in brain neurons.

CONCLUSIONS

Among the peripheral ERs, SERs appear to be deranged in several neurological diseases through at least two pathways. One is disturbance of peripheral ER network in the diseases such as HSPs, which is caused by mutations of genes required for SER tubule organization. The SER network disruption may also be involved in Alzheimer's disease and ALS pathogenesis. Another one is development of highly-ordered stacked SER in the diseases such as ALS8, which is caused by overload of misfolded and insolubilized proteins on ER membranes. NF-Y-mediated gene regulatory pathway can be involved in this atypical ER pathogenesis. Finding the way to restore SER networks is a future challenging issue toward the cure of these ER-related neurological disorders.

AUTHOR CONTRIBUTIONS

All authors listed have made a substantial, direct and intellectual contribution to the work, and approved it for publication.

ACKNOWLEDGMENTS

This work was supported by Grant-in-Aid for Scientific Research on Innovative Areas (Brain Protein Aging and Dementia Control) (15H01567) from Ministry of Education, Culture, Sports, Science and Technology (MEXT), and Grant-in-Aids from MEXT/The Japan Society for the Promotion of Science (JSPS). (17H01564, 16H01345, 17KT0131, 15K06762), Takeda Science Foundation, and Center for Baby Science in Doshisha University (Joint Usage/Research Center accredited by MEXT). This work is partially supported by the Strategic Research Program for Brain Sciences from Japan Agency for Medical Research and Development, AMED.

REFERENCES

Aliaga, L., Lai, C., Yu, J., Chub, N., Shim, H., Sun, L., et al. (2013). Amyotrophic lateral sclerosis-related VAPB P56S mutation differentially affects the function and survival of corticospinal and spinal motor neurons. *Hum. Mol. Genet.* 22, 4293–4305. doi: 10.1093/hmg/ddt279

Beetz, C., Koch, N., Khundadze, M., Zimmer, G., Nietzsche, S., Hertel, N., et al. (2013). A spastic paraplegia mouse model reveals REEP1-dependent ER shaping. *J. Clin. Invest.* 123, 4273–4282. doi: 10.1172/JCI65665

Bem, D., Yoshimura, S., Nunes-Bastos, R., Bond, F. C., Kurian, M. A., Rahman, F., et al. (2011). Loss-of-function mutations in RAB18 cause Warburg micro syndrome. *Am. J. Hum. Genet.* 88, 499–507. doi: 10.1016/j.ajhg.2011.03.012

Blackstone, C., O'kane, C. J., and Reid, E. (2011). Hereditary spastic paraplegias: membrane traffic and the motor pathway. *Nat. Rev. Neurosci.* 12, 31–42. doi: 10.1038/nrn2946

Borgese, N., Francolini, M., and Snapp, E. (2006). Endoplasmic reticulum architecture: structures in flux. *Curr. Opin. Cell Biol.* 18, 358–364. doi: 10.1016/j.ceb.2006.06.008

Butler, R., Wood, J. D., Landers, J. A., and Cunliffe, V. T. (2010). Genetic and chemical modulation of spastin-dependent axon outgrowth in zebrafish embryos indicates a role for impaired microtubule dynamics in hereditary spastic paraplegia. *Dis. Model. Mech.* 3, 743–751. doi: 10.1242/dmm.004002

Chen, S., Desai, T., McNew, J. A., Gerard, P., Novick, P. J., and Ferro-Novick, S. (2015). Lunapark stabilizes nascent three-way junctions in the endoplasmic reticulum. *Proc. Natl. Acad. Sci. U.S.A.* 112, 418–423. doi: 10.1073/pnas.1423026112

Chen, S., Novick, P., and Ferro-Novick, S. (2012). ER network formation requires a balance of the dynamin-like GTPase Sey1p and the Lunapark family member Lnp1p. *Nat. Cell Biol.* 14, 707–716. doi: 10.1038/ncb2523

Chen, S., Novick, P., and Ferro-Novick, S. (2013). ER structure and function. *Curr. Opin. Cell Biol.* 25, 428–433. doi: 10.1016/j.ceb.2013.02.006

Christodoulou, A., Santarella-Mellwig, R., Santama, N., and Mattaj, I. W. (2016). Transmembrane protein TMEM170A is a newly discovered regulator of ER and nuclear envelope morphogenesis in human cells. *J. Cell Sci.* 129, 1552–1565. doi: 10.1242/jcs.175273

Dickson, K. M., Bergeron, J. J., Shames, I., Colby, J., Nguyen, D. T., Chevet, E., et al. (2002). Association of calnexin with mutant peripheral myelin protein-22 *ex vivo*: a basis for "gain-of-function" ER diseases. *Proc. Natl. Acad. Sci. U.S.A.* 99, 9852–9857. doi: 10.1073/pnas.152621799

Dykstra, K. M., Pokusa, J. E., Suhan, J., and Lee, T. H. (2010). Yip1A structures the mammalian endoplasmic reticulum. *Mol. Biol. Cell* 21, 1556–1568. doi: 10.1091/mbc.E09-12-1002

English, A. R., and Voeltz, G. K. (2013). Rab10 GTPase regulates ER dynamics and morphology. *Nat. Cell Biol.* 15, 169–178. doi: 10.1038/ncb2647

Evans, K., Keller, C., Pavur, K., Glasgow, K., Conn, B., and Lauring, B. (2006). Interaction of two hereditary spastic paraplegia gene products, spastin and atlastin, suggests a common pathway for axonal maintenance. *Proc. Natl. Acad. Sci. U.S.A.* 103, 10666–10671. doi: 10.1073/pnas.0510863103

Fasana, E., Fossati, M., Ruggiano, A., Brambillasca, S., Hoogenraad, C. C., Navone, F., et al. (2010). A VAPB mutant linked to amyotrophic lateral sclerosis generates a novel form of organized smooth endoplasmic reticulum. *FASEB J.* 24, 1419–1430. doi: 10.1096/fj.09-147850

Fassier, C., Hutt, J. A., Scholpp, S., Lumsden, A., Giros, B., Nothias, F., et al. (2010). Zebrafish atlastin controls motility and spinal motor axon architecture via inhibition of the BMP pathway. *Nat. Neurosci.* 13, 1380–1387. doi: 10.1038/nn.2662

Federovitch, C. M., Ron, D., and Hampton, R. Y. (2005). The dynamic ER: experimental approaches and current questions. *Curr. Opin. Cell Biol.* 17, 409–414. doi: 10.1016/j.ceb.2005.06.010

Feldman, D., Swarm, R. L., and Becker, J. (1981). Ultrastructural study of rat liver and liver neoplasms after long-term treatment with phenobarbital. *Cancer Res.* 41, 2151–2162.

Gerondopoulos, A., Bastos, R. N., Yoshimura, S., Anderson, R., Carpanini, S., Aligianis, I., et al. (2014). Rab18 and a Rab18 GEF complex are required for normal ER structure. *J. Cell Biol.* 205, 707–720. doi: 10.1083/jcb.201403026

Gonzalez-Alegre, P., and Paulson, H. L. (2004). Aberrant cellular behavior of mutant torsinA implicates nuclear envelope dysfunction in DYT1 dystonia. *J. Neurosci.* 24, 2593–2601. doi: 10.1523/JNEUROSCI.4461-03.2004

Grumati, P., Morozzi, G., Holper, S., Mari, M., Harwardt, M. I., Yan, R., et al. (2017). Full length RTN3 regulates turnover of tubular endoplasmic reticulum via selective autophagy. *Elife* 6:e25555 doi: 10.7554/eLife.25555

He, W., Lu, Y., Qahwash, I., Hu, X. Y., Chang, A., and Yan, R. (2004). Reticulon family members modulate BACE1 activity and amyloid-beta peptide generation. *Nat. Med.* 10, 959–965. doi: 10.1038/nm1088

Hewett, J., Gonzalez-Agosti, C., Slater, D., Ziefer, P., Li, S., Bergeron, D., et al. (2000). Mutant torsinA, responsible for early-onset torsion dystonia, forms membrane inclusions in cultured neural cells. *Hum. Mol. Genet.* 9, 1403–1413. doi: 10.1093/hmg/9.9.1403

Hu, J., Shibata, Y., Voss, C., Shemesh, T., Li, Z., Coughlin, M., et al. (2008). Membrane proteins of the endoplasmic reticulum induce high-curvature tubules. *Science* 319, 1247–1250. doi: 10.1126/science.1153634

Hu, J., Shibata, Y., Zhu, P. P., Voss, C., Rismanchi, N., Prinz, W. A., et al. (2009). A class of dynamin-like GTPases involved in the generation of the tubular ER network. *Cell* 138, 549–561. doi: 10.1016/j.cell.2009.05.025

Hu, X., Shi, Q., Zhou, X., He, W., Yi, H., Yin, X., et al. (2007). Transgenic mice overexpressing reticulon 3 develop neuritic abnormalities. *EMBO J.* 26, 2755–2767. doi: 10.1038/sj.emboj.7601707

Huang, S., Ling, J. J., Yang, S., Li, X. J., and Li, S. (2011). Neuronal expression of TATA box-binding protein containing expanded polyglutamine in knock-in mice reduces chaperone protein response by impairing the function of nuclear factor-Y transcription factor. *Brain* 134, 1943–1958. doi: 10.1093/brain/awr146

Iinuma, T., Aoki, T., Arasaki, K., Hirose, H., Yamamoto, A., Samata, R., et al. (2009). Role of syntaxin 18 in the organization of endoplasmic reticulum subdomains. *J. Cell Sci.* 122, 1680–1690. doi: 10.1242/jcs.036103

Katsuno, M., Adachi, H., Minamiyama, M., Waza, M., Doi, H., Kondo, N., et al. (2010). Disrupted transforming growth factor-beta signaling in spinal and bulbar muscular atrophy. *J. Neurosci.* 30, 5702–5712. doi: 10.1523/JNEUROSCI.0388-10.2010

Khaminets, A., Heinrich, T., Mari, M., Grumati, P., Huebner, A. K., Akutsu, M., et al. (2015). Regulation of endoplasmic reticulum turnover by selective autophagy. *Nature* 522, 354–358. doi: 10.1038/nature14498

Korkhov, V. M., and Zuber, B. (2009). Direct observation of molecular arrays in the organized smooth endoplasmic reticulum. *BMC Cell Biol.* 10:59. doi: 10.1186/1471-2121-10-59

Kuijpers, M., Van Dis, V., Haasdijk, E. D., Harterink, M., Vocking, K., Post, J. A., et al. (2013). Amyotrophic lateral sclerosis (ALS)-associated VAPB-P56S inclusions represent an ER quality control compartment. *Acta Neuropathol. Commun.* 1:24. doi: 10.1186/2051-5960-1-24

Kurth, I., Pamminger, T., Hennings, J. C., Soehendra, D., Huebner, A. K., Rotthier, A., et al. (2009). Mutations in FAM134B, encoding a newly identified Golgi protein, cause severe sensory and autonomic neuropathy. *Nat. Genet.* 41, 1179–1181. doi: 10.1038/ng.464

Larroquette, F., Seto, L., Gaub, P. L., Kamal, B., Wallis, D., Lariviere, R., et al. (2015). Vapb/Amyotrophic lateral sclerosis 8 knock-in mice display slowly progressive motor behavior defects accompanying ER stress and autophagic response. *Hum. Mol. Genet.* 24, 6515–6529. doi: 10.1093/hmg/ddv360

Lo Giudice, T., Lombardi, F., Santorelli, F. M., Kawarai, T., and Orlacchio, A. (2014). Hereditary spastic paraplegia: clinical-genetic characteristics and evolving molecular mechanisms. *Exp. Neurol.* 261, 518–539. doi: 10.1016/j.expneurol.2014.06.011

Maiuolo, J., Bulotta, S., Verderio, C., Benfante, R., and Borgese, N. (2011). Selective activation of the transcription factor ATF6 mediates endoplasmic reticulum proliferation triggered by a membrane protein. *Proc. Natl. Acad. Sci. U.S.A.* 108, 7832–7837. doi: 10.1073/pnas.1101379108

Matus, S., Glimcher, L. H., and Hetz, C. (2011). Protein folding stress in neurodegenerative diseases: a glimpse into the ER. *Curr. Opin. Cell Biol.* 23, 239–252. doi: 10.1016/j.ceb.2011.01.003

Nishimura, A. L., Mitne-Neto, M., Silva, H. C., Richieri-Costa, A., Middleton, S., Cascio, D., et al. (2004). A mutation in the vesicle-trafficking protein VAPB causes late-onset spinal muscular atrophy and amyotrophic lateral sclerosis. *Am. J. Hum. Genet.* 75, 822–831. doi: 10.1086/425287

Orso, G., Pendin, D., Liu, S., Tosetto, J., Moss, T. J., Faust, J. E., et al. (2009). Homotypic fusion of ER membranes requires the dynamin-like GTPase atlastin. *Nature* 460, 978–983. doi: 10.1038/nature08280

Ozelius, L. J., Hewett, J. W., Page, C. E., Bressman, S. B., Kramer, P. L., Shalish, C., et al. (1997). The early-onset torsion dystonia gene (DYT1) encodes an ATP-binding protein. *Nat. Genet.* 17, 40–48. doi: 10.1038/ng0997-40

Paillusson, S., Stoica, R., Gomez-Suaga, P., Lau, D. H., Mueller, S., Miller, T., et al. (2016). There's something wrong with my MAM; the ER-Mitochondria axis and neurodegenerative diseases. *Trends Neurosci.* 39, 146–157. doi: 10.1016/j.tins.2016.01.008

Park, S. H., and Blackstone, C. (2010). Further assembly required: construction and dynamics of the endoplasmic reticulum network. *EMBO Rep.* 11, 515–521. doi: 10.1038/embor.2010.92

Park, S. H., Zhu, P. P., Parker, R. L., and Blackstone, C. (2010). Hereditary spastic paraplegia proteins REEP1, spastin, and atlastin-1 coordinate microtubule interactions with the tubular ER network. *J. Clin. Invest.* 120, 1097–1110. doi: 10.1172/JCI40979

Patten, S. A., Armstrong, G. A., Lissouba, A., Kabashi, E., Parker, J. A., and Drapeau, P. (2014). Fishing for causes and cures of motor neuron disorders. *Dis. Model. Mech.* 7, 799–809. doi: 10.1242/dmm.015719

Powers, R. E., Wang, S., Liu, T. Y., and Rapoport, T. A. (2017). Reconstitution of the tubular endoplasmic reticulum network with purified components. *Nature* 543, 257–260. doi: 10.1038/nature21387

Puhka, M., Vihinen, H., Joensuu, M., and Jokitalo, E. (2007). Endoplasmic reticulum remains continuous and undergoes sheet-to-tubule transformation during cell division in mammalian cells. *J. Cell Biol.* 179, 895–909. doi: 10.1083/jcb.200705112

Qiu, L., Qiao, T., Beers, M., Tan, W., Wang, H., Yang, B., et al. (2013). Widespread aggregation of mutant VAPB associated with ALS does not cause motor neuron degeneration or modulate mutant SOD1 aggregation and toxicity in mice. *Mol. Neurodegener.* 8:1. doi: 10.1186/1750-1326-8-1

Remondelli, P., and Renna, M. (2017). The Endoplasmic Reticulum unfolded protein response in neurodegenerative disorders and its potential therapeutic significance. *Front. Mol. Neurosci.* 10:187. doi: 10.3389/fnmol.2017.00187

Renvoise, B., Malone, B., Falgairolle, M., Munasinghe, J., Stadler, J., Sibilla, C., et al. (2016). Reep1 null mice reveal a converging role for hereditary spastic paraplegia proteins in lipid droplet regulation. *Hum. Mol. Genet.* 25, 5111–5125. doi: 10.1093/hmg/ddw315.

Shi, Q., Prior, M., He, W., Tang, X., Hu, X., and Yan, R. (2009). Reduced amyloid deposition in mice overexpressing RTN3 is adversely affected by preformed dystrophic neurites. *J. Neurosci.* 29, 9163–9173. doi: 10.1523/JNEUROSCI.5741-08.2009

Shibata, Y., Shemesh, T., Prinz, W. A., Palazzo, A. F., Kozlov, M. M., and Rapoport, T. A. (2010). Mechanisms determining the morphology of the peripheral ER. *Cell* 143, 774–788. doi: 10.1016/j.cell.2010.11.007

Shibata, Y., Voss, C., Rist, J. M., Hu, J., Rapoport, T. A., Prinz, W. A., et al. (2008). The reticulon and DP1/Yop1p proteins form immobile oligomers in the tubular endoplasmic reticulum. *J. Biol. Chem.* 283, 18892–18904. doi: 10.1074/jbc.M800986200

Singer, I.i, Scott, S., Kazazis, D. M., and Huff, J. W. (1988). Lovastatin, an inhibitor of cholesterol synthesis, induces hydroxymethylglutaryl-coenzyme a reductase directly on membranes of expanded smooth endoplasmic reticulum in rat hepatocytes. *Proc. Natl. Acad. Sci. U.S.A.* 85, 5264–5268. doi: 10.1073/pnas.85.14.5264

Snapp, E. L., Hegde, R. S., Francolini, M., Lombardo, F., Colombo, S., Pedrazzini, E., et al. (2003). Formation of stacked ER cisternae by low affinity protein interactions. *J. Cell Biol.* 163, 257–269. doi: 10.1083/jcb.200306020

Sprocati, T., Ronchi, P., Raimondi, A., Francolini, M., and Borgese, N. (2006). Dynamic and reversible restructuring of the ER induced by PDMP in cultured cells. *J. Cell Sci.* 119, 3249–3260. doi: 10.1242/jcs.03058

Tarrade, A., Fassier, C., Courageot, S., Charvin, D., Vitte, J., Peris, L., et al. (2006). A mutation of spastin is responsible for swellings and impairment of transport in a region of axon characterized by changes in microtubule composition. *Hum. Mol. Genet.* 15, 3544–3558. doi: 10.1093/hmg/ddl431

Teuling, E., Ahmed, S., Haasdijk, E., Demmers, J., Steinmetz, M. O., Akhmanova, A., et al. (2007). Motor neuron disease-associated mutant vesicle-associated membrane protein-associated protein (VAP) B recruits wild-type VAPs into endoplasmic reticulum-derived tubular aggregates. *J. Neurosci.* 27, 9801–9815. doi: 10.1523/JNEUROSCI.2661-07.2007

Tudor, E. L., Galtrey, C. M., Perkinton, M. S., Lau, K. F., De Vos, K. J., Mitchell, J. C., et al. (2010). Amyotrophic lateral sclerosis mutant vesicle-associated membrane protein-associated protein-B transgenic mice develop TAR-DNA-binding protein-43 pathology. *Neuroscience* 167, 774–785. doi: 10.1016/j.neuroscience.2010.02.035

Varadarajan, S., Bampton, E. T., Smalley, J. L., Tanaka, K., Caves, R. E., Butterworth, M., et al. (2012). A novel cellular stress response characterised by a rapid reorganisation of membranes of the endoplasmic reticulum. *Cell Death Differ.* 19, 1896–1907. doi: 10.1038/cdd.2012.108

Varadarajan, S., Tanaka, K., Smalley, J. L., Bampton, E. T., Pellecchia, M., Dinsdale, D., et al. (2013). Endoplasmic reticulum membrane reorganization is regulated by ionic homeostasis. *PLoS ONE* 8:e56603. doi: 10.1371/journal.pone.0056603

Voeltz, G. K., Prinz, W. A., Shibata, Y., Rist, J. M., and Rapoport, T. A. (2006). A class of membrane proteins shaping the tubular endoplasmic reticulum. *Cell* 124, 573–586. doi: 10.1016/j.cell.2005.11.047

Wang, S., Tukachinsky, H., Romano, F. B., and Rapoport, T. A. (2016). Cooperation of the ER-shaping proteins atlastin, lunapark, and reticulons to generate a tubular membrane network. *Elife* 5:e18605 doi: 10.7554/eLife.18605

Wang, T., Liu, Y., Xu, X. H., Deng, C. Y., Wu, K. Y., Zhu, J., et al. (2011). Lgl1 activation of rab10 promotes axonal membrane trafficking underlying neuronal polarization. *Dev. Cell* 21, 431–444. doi: 10.1016/j.devcel.2011.07.007

Westrate, L. M., Lee, J. E., Prinz, W. A., and Voeltz, G. K. (2015). Form follows function: the importance of endoplasmic reticulum shape. *Annu. Rev. Biochem.* 84, 791–811. doi: 10.1146/annurev-biochem-072711-163501

Wu, Q., Sun, X., Yue, W., Lu, T., Ruan, Y., Chen, T., et al. (2016). RAB18, a protein associated with Warburg Micro syndrome, controls neuronal migration in the developing cerebral cortex. *Mol. Brain* 9:19. doi: 10.1186/s13041-016-0198-2

Yamamoto, A., Masaki, R., and Tashiro, Y. (1996). Formation of crystalloid endoplasmic reticulum in COS cells upon overexpression of microsomal aldehyde dehydrogenase by cDNA transfection. *J. Cell Sci.* 109(Pt 7), 1727–1738.

Yamanaka, T., Miyazaki, H., Oyama, F., Kurosawa, M., Washizu, C., Doi, H., et al. (2008). Mutant Huntingtin reduces HSP70 expression through the sequestration of NF-Y transcription factor. *EMBO J.* 27, 827–839. doi: 10.1038/emboj.2008.23

Yamanaka, T., Tosaki, A., Kurosawa, M., Matsumoto, G., Koike, M., Uchiyama, Y., et al. (2014). NF-Y inactivation causes atypical neurodegeneration characterized by ubiquitin and p62 accumulation and endoplasmic reticulum disorganization. *Nat. Commun.* 5:3354. doi: 10.1038/ncomms4354

Yamanaka, T., Tosaki, A., Miyazaki, H., Kurosawa, M., Koike, M., Uchiyama, Y., et al. (2016). Differential roles of NF-Y transcription factor in ER chaperone expression and neuronal maintenance in the CNS. *Sci. Rep.* 6:34575. doi: 10.1038/srep34575

Yang, Y. S., Harel, N. Y., and Strittmatter, S. M. (2009). Reticulon-4A (Nogo-A) redistributes protein disulfide isomerase to protect mice from SOD1-dependent amyotrophic lateral sclerosis. *J. Neurosci.* 29, 13850–13859. doi: 10.1523/JNEUROSCI.2312-09.2009

Conflict of Interest Statement: The authors declare that the research was conducted in the absence of any commercial or financial relationships that could be construed as a potential conflict of interest.

frontiers in Neuroscience

ORIGINAL RESEARCH
published: 20 June 2018
doi: 10.3389/fnins.2018.00415

Imbalanced Expression of Tau and Tubulin Induces Neuronal Dysfunction in *C. elegans* Models of Tauopathy

Tomohiro Miyasaka[1], Yuki Shinzaki[1], Satomi Yoshimura[1], Sawako Yoshina[2], Eriko Kage-Nakadai[2,3], Shohei Mitani[2] and Yasuo Ihara[1]*

[1] Department of Neuropathology, Faculty of Life and Medical Sciences, Doshisha University, Kyoto, Japan, [2] Department of Physiology, School of Medicine, Tokyo Women's Medical University, Tokyo, Japan, [3] Graduate School of Human Life Science, Osaka City University, Osaka, Japan

Tauopathy is a type of dementia defined by the accumulation of filamentous tau inclusions in neural cells. Most types of dementia in the elderly, including Alzheimer's disease, are tauopathies. Although it is believed that tau protein abnormalities and/or the loss of its functions results in neurodegeneration and dementia, the mechanism of tauopathy remains obscure. Loss of microtubules and/or tubulin is a known consequence of tau accumulating in neurons in Alzheimer's disease. In other words, there is an excess level of tau relative to tubulin in tauopathy neurons. To test whether this imbalance of tau and tubulin expression results in the neurotoxicity of tau, we developed several transgenic *C. elegans* lines that express human tau at various levels in pan-neurons. These worms showed behavioral abnormalities in a tau expression-dependent manner. The knockdown of a tubulin-specific chaperon, or a subset of tubulin, led to enhanced tau toxicity even in low-expressing tau-transgenic worms that showed no abnormal behaviors. In addition, the suppression of tau expression in tubulin knockdown worms rescued neuronal dysfunction. Thus, not only the overexpression of tau but also a reduction in tubulin can trigger the neurotoxicity of tau. Tau expressed in worms was also highly phosphorylated and largely bound to tubulin dimers rather than microtubules. Relative amount of tubulin-unbound tau was increased in high-expressing tau-transgenic worms showing tau toxicity. We further demonstrated that tau aggregation was inhibited by co-incubation of purified tubulin *in vitro*, meaning sufficient amounts of tubulin can protect against the formation of tau inclusions. These results suggest that the expression ratio of tau to tubulin may be a determinant of the tauopathy cascade.

Keywords: tau, tauopathy, microtubule, tubulin, neurodegeneration, *C. elegans*, Alzheimer's disease

OPEN ACCESS

Edited by:
Naruhiko Sahara, National Institute of Radiological Sciences (NIRS), Japan

Reviewed by:
Emmanuel Planel, Laval University, Canada
Kentaro Tanemura, Tohoku University, Japan

****Correspondence:***
Tomohiro Miyasaka
tomiyasa@mail.doshisha.ac.jp

Specialty section:
This article was submitted to Neurodegeneration, a section of the journal Frontiers in Neuroscience

Received: *27 February 2018*
Accepted: *31 May 2018*
Published: *20 June 2018*

Citation:
Miyasaka T, Shinzaki Y, Yoshimura S, Yoshina S, Kage-Nakadai E, Mitani S and Ihara Y (2018) Imbalanced Expression of Tau and Tubulin Induces Neuronal Dysfunction in C. elegans Models of Tauopathy Front. Neurosci. 12:415. doi: 10.3389/fnins.2018.00415

INTRODUCTION

In certain types of neurodegenerative diseases, affected neurons or glial cells have filamentous tau inclusions called neurofibrillary tangles, neuropil threads, and glial fibrillary tangles (Serrano-Pozo et al., 2011; Spillantini and Goedert, 2013). These disorders, which constitute the majority of age-dependent dementia, are called tauopathies and include Alzheimer's disease (AD), frontotemporal

dementia, progressive supranuclear palsy, and corticobasal degeneration. The severity of dementia in tauopathies has been shown to correlate with the abundance of tau inclusions and the extent of neuronal loss (Gomez-Isla et al., 1997; Delacourte et al., 1999). Furthermore, the pathogenic mutations in the tau gene have been identified from genetic studies of familial tauopathy, FTDP-17 (Iqbal et al., 2016). These findings indicate that changes in tau and its function lead to neurodegeneration and dementia.

Numerous studies revealed that pathological tau inclusions are composed of insoluble filaments, paired helical filaments (PHF) and straight filaments (Grundke-Iqbal et al., 1986; Greenberg and Davies, 1990; Lee et al., 1991; Fitzpatrick et al., 2017). This pathologically deposited tau is abnormally phosphorylated to a greater extent than physiological tau (Khatoon et al., 1992; Hanger et al., 2009). Since this abnormal phosphorylation disrupts the ability of tau to promote microtubule (MT) assembly (Yoshida and Ihara, 1993), it has been considered a key element of the pathology that underlies tauopathies. However, the pathological significance of the phosphorylation on individual sites of tau remains unclear. Other abnormal modifications, such as ubiquitination, acetylation, glycation, isomerization, and truncation, do not occur as often in physiological tau but were also identified (Miyasaka et al., 2005b; Iqbal et al., 2016). In contrast to the huge filamentous inclusions, it is currently assumed that the small soluble aggregates called oligomers are an essential part of the tau toxicity or substance that propagates tau pathology (Goedert et al., 2017; Shafiei et al., 2017). However, it is also suggested that unaggregated tau can affect neuronal function (Miyasaka et al., 2016; Xie and Miyasaka, 2016). Thus, the definitive trigger of tau, as well as which type of tau is toxic, is currently unknown.

Loss of MTs and/or tubulin is an invariable feature of tau-accumulating neurons in AD (Terry et al., 1964; Cash et al., 2003; Zhang et al., 2015). This inverse relationship is reproduced in the affected neurons of tauopathy animal models (Tatebayashi et al., 2002; Miyasaka et al., 2005a, 2016). Because the physiological function of tau is known to promote the assembly of tubulin or to stabilize MTs by binding to them, it is believed that the hyper-phosphorylation of tau may lead to MT loss (Bodea et al., 2016; Wang and Mandelkow, 2016). However, the finding that tau-knockout mice did not show obvious developmental abnormalities or brain function abnormalities, suggests that MT loss cannot simply be explained by a lack of tau (Harada et al., 1994; Kimura et al., 2014). Recently, we showed that the hyper-phosphorylation of tau in hypothermic brains did not directly detach tau from MTs and that forced MT destruction induced simultaneous tau liberation and phosphorylation in cultured cells (Planel et al., 2008; Miyasaka et al., 2010). Furthermore, a reduction of MTs was found in the neurons of AD brains regardless of neurofibrillary tangle formation (Cash et al., 2003). These findings suggest that MT loss (or tubulin reduction) is not a passive event and is involved in the early pathogenesis of tauopathy.

We speculated that the amount of the tubulin in neural cells determines tau toxicity and that excess tau relative to tubulin triggers the tauopathy cascade. To confirm that the imbalanced expression of tau and tubulin can induce tauopathy, we developed several lines of transgenic *C. elegans* that express various levels of human tau pan-neuronally, and then, we assessed the effects of tubulin knockdown.

MATERIALS AND METHODS

Development and Maintenance of Worm Strain

Development and maintenance of integrant worm lines were performed as previously described (Xie et al., 2014; Miyasaka et al., 2016). Briefly, human tau or DsRed cDNA was subcloned into the site downstream of "pan-neuronal" *unc-119* promoter (punc-119) of pFXneo-punc119 vector (Maduro and Pilgrim, 1995). The transgenes were injected into N2 together with a marker, pFXneo-Pges-1::EGFP. Germline transformation and generation of extrachromosomal arrays in C. elegans strains were performed according to the standard protocol (Mitani, 1995). Stable tau-transgenic (Tg)-lines, generated by UV irradiation, were backcrossed to N2 five times before analysis. Tg-strains used here were as follows: Mock-Tg (tmIs388), WT4R(L)-Tg (tmIs389), WT4R(H)-Tg (tmIs390), WT4R(ExH1)-Tg (tmIs763), and WT4R(ExH2)-Tg (tmIs765). For RNAi, tau-Tg worms were crossbred with *rrf-3* mutant lines (Mock-Tg/rrf-3 and WT4R(L)/rrf-3). For *mec-7* or *mec-12* knockout, mec-7 (e1506) or mec-12 (tm5083) mutant lines were used. All *C. elegans* strains were maintained on a nematode growth medium (NGM) plate spread with E. coli OP50 under standard conditions (Miyasaka et al., 2016).

Feeding RNAi

The RNA interference of C. elegans by feeding with dsRNA-expressing *E. coli.* was performed as previously described, with minor modifications (Kage-Nakadai et al., 2016). Complementary DNA fragments encoding human tau (748–1326 bp; corresponding to 2N4R isoform tau cDNA), *K07H8.1* (*tbce-1*; 1066–1298 bp), and *mec-12* (619–1058 bp) were subcloned into the multiple cloning site of the L4440 vector and transformed to the HT115 (DE3) *E. coli.* strain. The desired double-stranded RNA (dsRNA) was produced by bi-directional expression induced by 1 mM IPTG. The bacteria expressing dsRNA were spread on NGM media supplemented with ampicillin and IPTG. Synchronously cultured worms were grown on these RNAi plates for 4 days and subjected to behavioral and biochemical analyses. To ensure efficient knockdown in neuronal cells, the worm lines crossbred with *rrf-3* were used for all RNAi experiments (Simmer et al., 2002).

Behavioral Analyses

A touch assay was performed as previously described (Miyasaka et al., 2005a). Briefly, on the forth day after hatching the worms were isolated onto new 3.5-cm plates, and their escape reactions were assessed in response to gentle touch with an eyelash under a stereoscopic microscope. The number of responses to 10 touch trials, five for the anterior plus five for the posterior, were counted. Uncoordinated movements (Unc) were also assessed

under a microscope. The severity of Unc was scored as follows: normal, wide bending with fast movement (2 point); Unc, slow movement (1 point); severe Unc, negligible movement (0 point). Twenty worms were used in each assay for each experiment, and the experiment was performed three to four times. Thus, 60–80 worms were assessed for each line. For the abnormality in *tbce-1* knockdown, the severities of Unc of all worms grown on knockdown plates were scored as follows: normal, wide bending with fast movement (2 point); Unc, slow movement (1 point); severe Unc, negligible movement and burst (0 point).

Biochemical Analyses

For biochemical analysis, worms were grown on NGM plates at large rectangular plates (No. 2 square schale, Eiken chemical co ltd., Tokyo, Japan). Synchronized worms were harvested in M9 buffer and pelleted by brief centrifugation. After washing twice with M9 buffer (22 mM KH_2PO_4, 42 mM Na_2HPO_4, 85 mM NaCl, and 1 mM $MgSO_4$), the worm pellets were weighed and stored at −80°C. Total worm lysates were prepared as previously described (Miyasaka et al., 2016). The worm pellets were sonicated in sodium dodecyl sulfate (SDS) sample buffer (80-mM Tris-HCl, 2% SDS, 10% glycerol, 1% 2-mercaptoethanol, pH 6.8) and cleared by ultracentrifugation at 150,000 × *g* for 10 min at 20°C. The protein concentration for each sample was verified by Coomassie Brilliant Blue (Wako Pure Chemical Industries, Ltd., Osaka, Japan) staining on SDS-poly acrylamide gel electrophoresis (PAGE). Soluble fractions were subjected to SDS-PAGE followed by Western blotting. The MT-binding of expressed tau was analyzed as previously described (Miyasaka et al., 2016). Freshly harvested worms were homogenized in MS buffer (0.1 M MES, 1 mM EGTA, 1 mM $MgSO_4$, 2 mM DTT, and 0.5% Triton X-100, pH 6.8) containing 20 μM Taxol, 2 mM guanosine triphosphate (GTP), and protease inhibitors (cOmplete®, Sigma-Aldrich, St. Louis, MO, United States) and phosphatase inhibitors (1 mM Na3VO4, 1 mM NaF, 1 mM okadaic acid, and 1 mM b-glycerophosphate) at room temperature and then immediately chilled. After brief centrifugation, soluble fractions were centrifuged at 100,000 × *g* for 15 min at 2°C to obtain the soluble free tubulin and insoluble MT fractions. MT-unbound tau in free tubulin fraction was immunoprecipitated with H-150 anti-tau antibody bound on ProteinG-conjugated Dynabeads (Thermo Fisher Scientific Inc., Waltham, MA, United States) at 4°C for 3 h. After washing with MS buffer, bound proteins on the beads were solubilized in SDS-sample buffer. The amount of tau and tubulin were analyzed by Western blotting.

Purification and Dephosphorylation of Tau Expressed in Worms and MT-Binding Assay

Purification and dephosphorylation of tau and an MT-binding assay were performed as previously described with minor modifications (Xie et al., 2014). Four-day-old WT4R-Tg worm pellets were homogenized in ×10 volume of Tris-saline buffer (TS; 50 mM Tris, 150 mM NaCl, pH 7.6) containing protease and phosphoatase inhibitors described above. After ultra-centrifugation at 120,000 × *g* for 15 min at 2°C, the soluble fractions were adjusted in 0.5 M NaCl and 2% 2-mercaptoethanol and heated at 100°C for 5 min. After the precipitates were removed by brief centrifugation, the soluble (heat-stable) fractions were precipitated by 50% ammonium sulfate. After

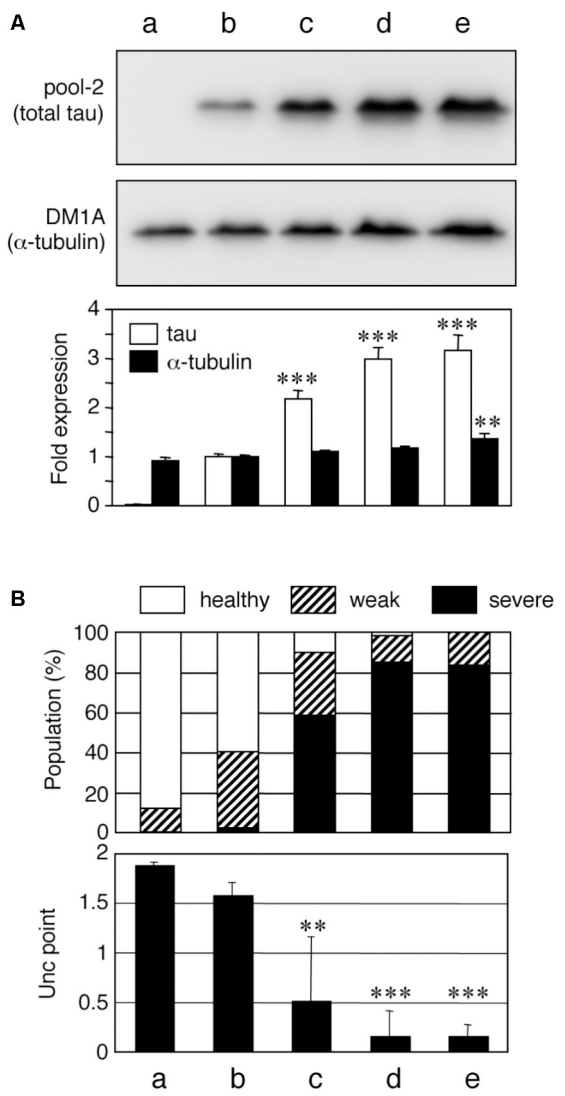

FIGURE 1 | Tau level-dependent neuronal dysfunction in WT4R-tau-Tg worms. Mock-Tg **(a)**, WT4R(L)-Tg **(b)**, WT4R(H)-Tg **(c)**, WT4R(ExH1)-Tg **(d)**, and WT4R(ExH2)-Tg **(e)** worms were grown on NGM plates and subjected to **(A)** Western blotting of tau (pool-2) and tubulin (DM1A) in the total lysate. Expression levels were quantified and shown against WT4R(L)-Tg (Lower panel). Average of four independent experiments are shown (means ± SEM, $n = 4$). Statistical significance was analyzed by Tukey's *post hoc* test (**$p < 0.01$, ***$p < 0.001$, *vs. WT4R(L)-Tg*). **(B)** The behavioral analysis of uncoordinated movement in each worm line was analyzed. Upper panel shows the population of healthy (open), weak Unc (hatched), and severe Unc (closed) worms ($n = 60$) in each line. Lower panel shows that the severity of Unc as described in Materials and Methods section. Average scores of three independent experiments are shown (means ± SEM, $n = 3$). Statistical significance was analyzed by Tukey's *post hoc* test (*$p < 0.05$, **$p < 0.01$, ***$p < 0.001$, *vs. Mock-Tg*).

centrifugation at 20,000 × *g* for 15 min at 2°C, the resultant pellets were re-solubilized and incubated with or without Lambda protein phosphatase (New England BioLabs, Inc., Ipswich, MA, United States) for 30 min at 30°C. Dephosphorylated and non-dephosphorylated tau were purified by using both heat and ammonium sulfate precipitation as described above. For the preparation of worm MT, fresh Mock-Tg worms were homogenized in ×5 volume of MS buffer containing protease and phosphatase inhibitors and centrifuged at 120,000 × *g* for 15 min at 2°C. Then, the soluble fraction was incubated with 20 μM Taxol and 2 mM GTP for 30 min at 25°C. After the addition of 0.5 M NaCl to remove the endogenous MAPs, polymerized MTs were collected by ultra-centrifugation and re-suspended into MS buffer containing Taxol and GTP. After the re-binding of purified tau on MTs at 25°C for 20 min, MT-unbound and MT-bound fractions were separated by ultra-centrifugation.

Morphological Analyses

Immunocytochemical analyses were performed by using the freeze-cracking method (Miyasaka et al., 2005a). Cracked worms put on PDL (poly-d-lysine)-coated glass slides were immersed in pre-cooled MeOH followed by hydration and permeabilization with 0.1% Triton X-100 in TS. After the worms were soaked with 10% goat serum in TS, the specimens were incubated with 1% BSA in TS containing primary antibodies. Bound antibodies were visualized using Alexa-conjugated secondary antibodies (Molecular Probes, Inc., Eugene, OR), and observed under an LSM700 microscope (Carl Zeiss Inc., Jena, Germany).

Drug Treatment

Trimethylamine-N-oxide (TMAO) was dissolved in H_2O and stored in −20°C. For treatment, the compound was diluted with M9 buffer and directly added onto NGM plate. Worms were synchronized and grown on drug-containing plates for 3 days and subjected to biochemical analyses.

In Vitro Tau Aggregation Assay

Purification of recombinant tau corresponding to the 0N4R isoform and *in vitro* tau aggregation assays, were performed as previously described (Xie et al., 2014, 2015). Briefly, the recombinant tau 0N4R isoform expressed in *E. coli* [BL21(DE3)] was solubilized in homogenization buffer (50 mM PIPES, 1 mM EGTA, 1 mM DTT, and pH 6.8) with protease inhibitors and charged onto a phosphocellulose column (P11, Whatman). Tau protein fraction eluted in 0.1–0.3 M NaCl was precipitated by ammonium sulfate precipitation. The resultant pellet was re-solubilized by homogenization buffer containing 0.5 M NaCl and 1% 2-mercaptoethanol and fractionated by heat stability. The heat-stable fraction was further purified using reverse-phase HPLC (Cosmosyl protein-R, Nacalai tesque, Kyoto, Japan).

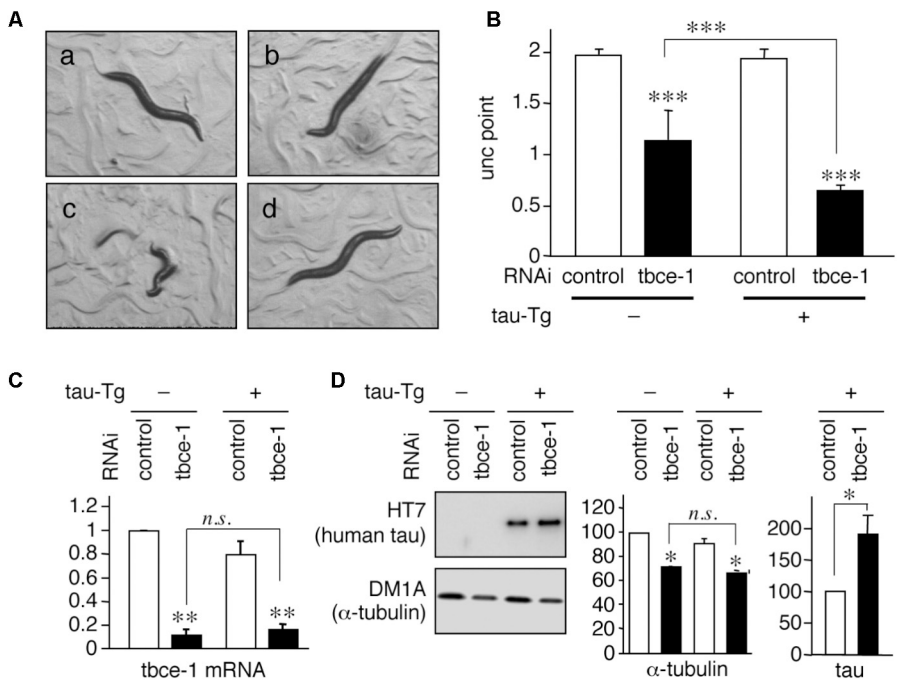

FIGURE 2 | Tau expression enhances uncoordinated movement induced by *tbce-1* gene knock down. **(A)** WT4R(L)-Tg/rrf-3 **(a–c)** and Mock-Tg/rrf-3 worms **(d)** were grown on L4440::T (a; control) or L4440:: *tbce-1* (**b–d**; *tbce-1*) RNAi plates from embryo to 3 days after hatch. Rrf-3 background worms grown on *tbce-1* RNAi plates showed Unc **(b)** or a frequent burst phenotype **(c)**. **(B)** The severity of Unc was assessed as described in Materials and Methods section. Average scores of three independent experiments are shown (means ± SEM, *n* = 3). WT4R(L)-Tg/rrf-3 worms showed a significantly higher sensitivity to tubulin chaperon knockdown. **(C)** The levels of *tbce-1* mRNA were quantified by quantitative real time RT-PCR (means ± SEM, *n* = 3). *tbce-1* mRNA is suppressed to less than 25% compared to controls, regardless of tau expression. **(D)** The levels of tau and α-tubulin were analyzed by Western blotting. The percent expression of control worms is shown (means ± SEM, *n* = 3). Statistical significance was analyzed by Tukey's *post hoc* test (**p* < *0.05*, ***p* < *0.01*, and ****p* < *0.001*) or Student's *t*-test (**p* < *0.05*).

Purified porcine tubulin was purchased from Cytoskeleton Inc. (Denver, CO, United States). Purity and protein amount were analyzed by SDS-PAGE followed by Coomassie brilliant blue staining. For *in vitro* aggregation, 60 mg/ml of heparin was mixed with 10 mM purified tau, 100 mM NaCl, 10 mM thioflavine-T (Th-T), 10 mM HEPES (pH 7.4), and with/without tubulin. The time-dependent changes in Th-T fluorescence were measured at 465–635 nm (excitation) and 535–625 nm (emission) for 3 days. After incubation, the mixtures were centrifuged at 100,000 × *g* for 15 min before or after 1% Sarkosyl, treatment. The fractions were analyzed by SDS-PAGE followed by CBB staining and Western blotting.

Antibodies and Compounds

The antibodies used here were as follows: pool-2 (anti-pan-tau, a generous gift of Dr. H. Mori), HT7 (anti-pan-tau, Innogenetics), H-150 (anti-human-tau, Santa Cruz Biotechnology, Dallas, TX, United States), AT8 (anti-phospho-tau, Thermo Fisher Scientific Inc.), tau-1 (anti-dephospho-tau, Merck Millipore, Billerica, MA, United States), PHF-1 (anti-phospho-tau, a generous gift of Dr. P Davies), pS262 (anti-phospho-tau, Sigma-Aldrich, St. Louis, MO, United States), DM1A (anti-α-tubulin, Sigma-Aldrich), KMX-1 (anti-β-tubulin, Merck Millipore), anti-mec-12 (6-11B1, Sigma-Aldrich), 1A4 (anti-α-actin, Sigma), and 6C5 (anti-GAPDH, Abcam). Taxol and trimethylamine-N-oxide were purchased from Sigma-Aldrich. Other materials were purchased from Nachalai tesque unless otherwise specified (Kyoto, Japan).

Statistical Analysis

All statistical analyses were performed using IBM SPSS statistics 25 (IBM, Armonk, NY, United States). Analysis of variance (ANOVA) was used for comparisons made between three or more groups, followed by Tukey's *post hoc* test. All data were presented as the means ± SEM. In all cases, *P* values lower than 0.05 were considered as significant.

RESULTS

To date, a number of Tg mouse lines have been developed (Noble et al., 2010), with varying neurological phenotypes. Although some of the unique phenotypes may be caused by

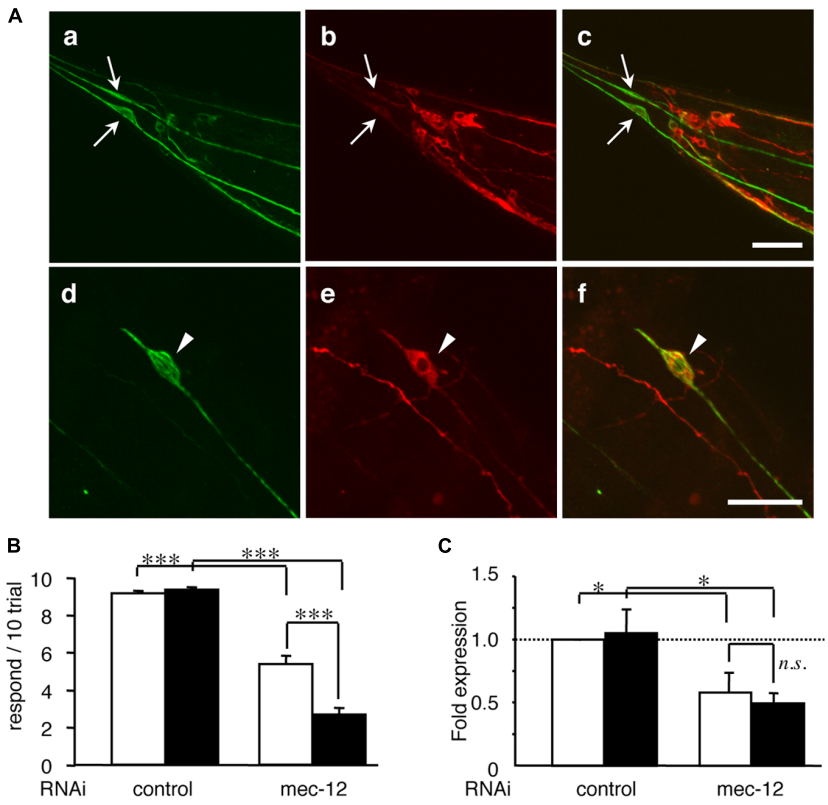

FIGURE 3 | Tau expression in mechanosensory neurons exacerbates touch sense abnormality induced by tubulin knockdown. **(A)** WT4R(L)-Tg/rrf-3 **(a–c)** and Mock-Tg/rrf-3 **(d–f)** worms were subjected to immunolabeling using 6-11B1 (anti-mec-12; **a** and **d**), and pool-2 (anti-tau; **b** and **e**). Merged views are also shown **(c** and **f)**. Human tau was expressed in as pan-neuronal pattern (**b** and **e**) including PLMs (arrows in **a–c**) in lumber ganglia and ALMs (arrowheads in **d–f**) in the abdomen. Scale bars = 30 μm. **(B)** Mock-Tg/rrf-3 (open) and WT4R(L)-Tg/rrf-3 (solid) worms were grown on L4440::T (control) or L4440::mec-12 RNAi plates from embryo to 4 days after hatch. Touch sensitivity was analyzed as described in the Materials and Methods section (means ± SEM, $n = 60$). **(C)** The expression of *mec-12* mRNA in the indicated worms was quantified by quantitative real time RT-PCR (means ± SEM, $n = 3$). Statistical significance was analyzed by Tukey's *post hoc* test (*$p < 0.05$, ***$p < 0.001$).

the promoter used for exogenous tau expression in particular lines, it is generally understood that the expression level of tau correlates with the severity of the pathology in Tg mice. To probe whether the amount of tau expression affects its neuronal phenotype, we developed several lines of tau-expressing worms using the pan-neuronal punc-119 promoter (Xie et al., 2014; Miyasaka et al., 2016). Integration of extrachromosomal arrays in the worm genome allows for the introduction of various numbers of transgene copies (Mitani, 1995). We isolated four independent integrant human wild-type 0N4R-tau-Tg lines with different expression levels (**Figure 1A**). WT4R(H)-Tg, WT4R(ExH1)-Tg, and WT4R(ExH2)-Tg lines express tau at 2.17 ± 0.17, 2.98 ± 0.24, and 3.16 ± 0.31 fold than WT4R(L)-Tg respectively. We also found the amount of α-tubulin expression was slightly but significantly higher in WT4R(Ex2)-Tg line. As shown in **Figure 1**, WT4R(L)-Tg worms showed minimal Unc but the WT4R(H)-Tg worms expressing three times more tau had a more severe Unc phenotype as previously described (Miyasaka et al., 2016). Furthermore, most of the lines with extremely high tau expression levels, WT4R(ExH1)-Tg and WT4R(ExH2)-Tg, suffered from severe Unc and were immobile (**Figure 1B**). Therefore, in these lines, the severity of Unc seemed to be correlated with the expression levels of exogenous tau.

When tau expression levels were greater than that of in WT4R(H)-Tg, neurotoxicity was present. Pathological studies indicated that the amount of MTs and/or tubulin is inversely correlated with tau-accumulating neurons (Terry et al., 1964; Cash et al., 2003; Zhang et al., 2015). Therefore, we hypothesize that the amount of tubulins may determine a threshold of neurotoxicity induced by tau. To test whether the expression level of tubulin affects tau toxicity, we sought to reduce tubulin expression in tau expressing worms. Because there are nine α-tubulin genes and six β-tubulin genes in C. elegans (Gogonea et al., 1999), a direct knockdown of a single tubulin isotype may not be sufficient to reduce the level of total tubulin in neurons. Therefore, we chose the *tbce-1* gene, a homologue of human tubulin-folding cofactor E (*tbce*), a tubulin chaperon needed for *de novo* synthesis of α-tubulin (Tian and Cowan, 2013; Nithianantham et al., 2015). A missense mutation of the Tbce gene is identified in the spontaneous mouse model of progressive motor neuronopathy (Bommel et al., 2002; Martin et al., 2002), indicating that the functional decline of TBCE can induce MT abnormality in neurons. In C. elegans model, target genes can be knocked down easily by feeding E. coli expressing sence/antisense RNA *in vivo*. As shown in **Figure 2**, *tbce-1* knockdown by feeding-RNAi resulted in the reduction of α-tubulin and induced abnormal Unc behavior. In severe cases, the worms showed complete immobility and burst (**Figure 2A**). The severity of unc was significantly increased in human-tau expression (**Figure 2B**). *tbce-1* knockdown showed reduced expression of α-tubulin (**Figures 2C,D**). Intriguingly, *tbce-1* knockdown increased tau expression (**Figure 2D**). Thus, the low expression of tau can affect neuronal functions when the expression of tubulin is reduced.

To address whether tubulin knockdown directly enhances tau-induced neuronal dysfunction, we reduced the expression of *mec-12*, an isotype of α-tubulin specifically expressed in touch neurons (Fukushige et al., 1999), in WT4R(L)-Tg/rrf-3 worms, which express human-tau (**Figure 3A**). This is probably the only *in vivo* experimental model in which the relationship between specific tubulin isotype and neural function is strictly corresponded. Knocking-down *mec-12* in wild-type worms showed touch sense abnormality (**Figures 3B,C**), a phenotype of *mec-12* mutant worms. When the *mec-12* RNAi was applied to Mock-Tg and WT4R(L)-Tg worms in the *rrf-3* background, we found that the touch sense abnormality was significantly exacerbated in the WT4R(L)-Tg line (**Figures 3B,C**).

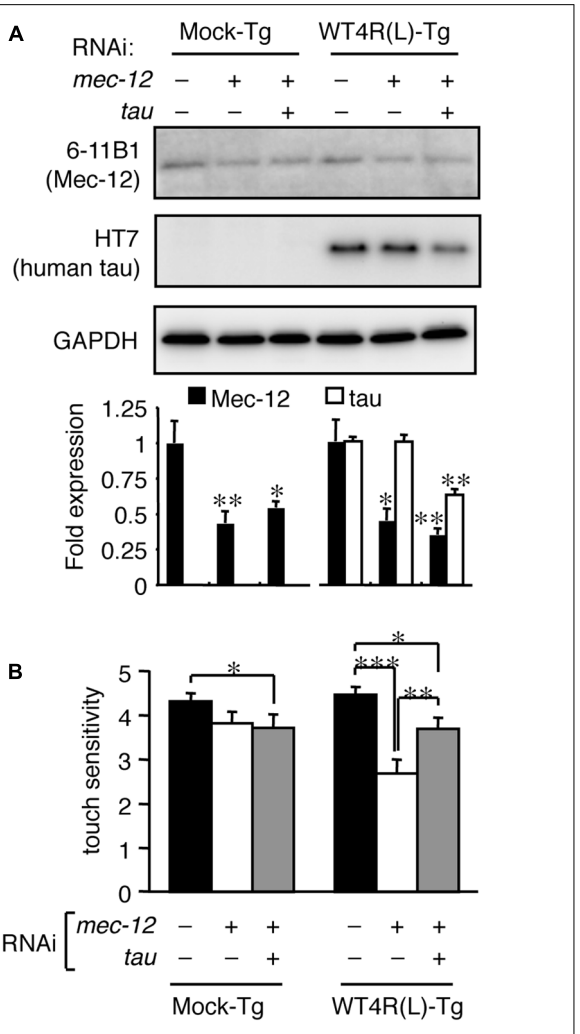

FIGURE 4 | Tau reduction rescues the neuronal dysfunction induced by tubulin knockdown. Mock-Tg/rrf-3 and WT4R(L)-Tg/rrf-3 worms were grown on L4440::T, L4440::mec-12 + L4440::T, or L4440::mec-12 + L4440::tau RNAi plates from embryo to 4 days after hatch. **(A)** Expression levels of MEC-12, tau and GAPDH were quantified by Western blotting. Lower panel showed the relative expression of Mec-12 and tau against naive worms (means ± SEM, $n = 4$). **(B)** The average number of responses per 5 trials of anterior touch are shown (means ± SEM, $n = 80$). The touch-sense abnormality of WT4R(L)-Tg/rrf-3 induced by *mec-12* RNAi was significantly reduced by co-administering tau RNAi. Statistical significance was analyzed by Tukey's *post hoc* test (*$p < 0.05$, **$p < 0.01$, and ***$p < 0.001$).

Control RNAi (**Figures 3B,C**) on WT4R(L)-Tg/rrf-3 worms did not cause any tactile abnormalities. Thus, α-tubulin downregulation alone can cause abnormalities in touch neurons, which are enhanced by the expression of human-tau. We addressed whether these exacerbations were specific to tau and found that the toxicity of tubulin knockdowns or tubulin chaperon knockdowns was not enhanced by DsRed expression by the same *Unc-119* promoter (data not shown). Furthermore, the knockdown of genes unrelated to tubulin or MTs, including *gfp*, *far-3*, *mtl-1*, and *col-149*, did not show any abnormalities in tau-Tg worms (data not shown).

These data indicate that the relative levels of tau and tubulin are important regulators of tau toxicity. We next tested whether the abnormalities of *mec-12* RNAi worms can be rescued by reducing tau expression. Reduced expression of tau by simultaneous RNAi knockdown significantly rescued touch sense abnormalities induced by *mec-12* RNAi in WT4R(L)-Tg/rrf-3 worms (**Figure 4**). Thus, excessive expression of tau against tubulin is critical for tau-induced neurotoxicity.

How does the imbalance of tau and tubulin (or MTs) cause neurotoxicity? We first analyzed the properties of the MT-binding of tau expressed in the transgenic worms. MT-bound tau and free MT-unbound tau were fractionated

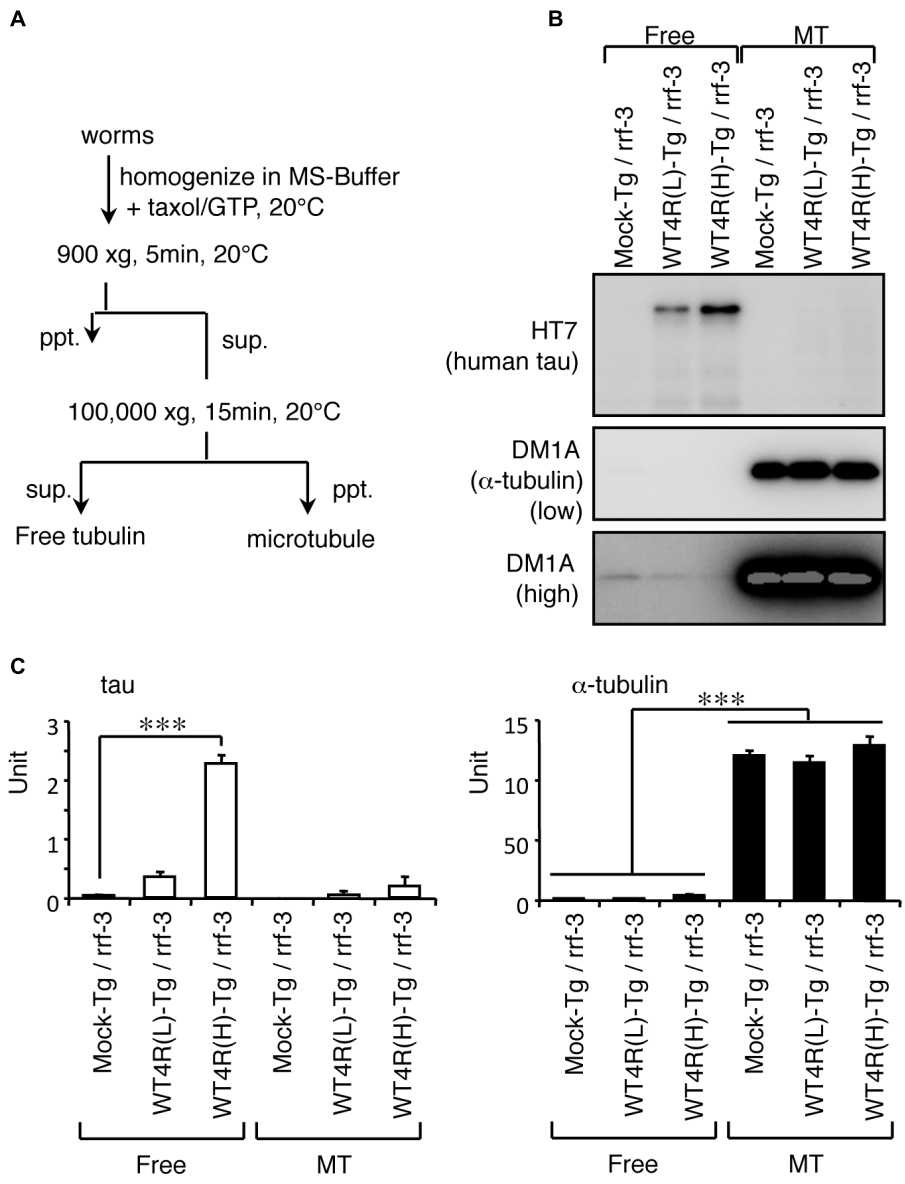

FIGURE 5 | Human-tau in punc-119::tau worms are not bound to MTs. **(A)** Flowchart of fractionation of MT and free tubulin fractions from worms are shown. **(B)** Western blotting of free tubulin (Free) and MT fractions from indicated worms using anti-tau (HT7) and anti-α-tubulin (DM1A) antibodies. **(C)** The amounts of tau and α-tubulin in Free and MT fractions were quantified (means ± SEM, $n = 5$). Statistical significance was analyzed by Tukey's *post hoc* test (***$p < 0.001$).

after stabilizing MTs by Taxol. We found that human-tau, even in WT4R(L)-Tg worms, was almost completely recovered in the MT-unbound fraction (**Figure 5**). Because tau in transgenic worms is phosphorylated to a higher extent similar to PHF-tau (Miyasaka et al., 2016), we suspected that this may be caused by the abnormal phosphorylation. To investigate this, we purified human-tau from tau-Tg worms and tested their MT-binding after dephosphorylation. As shown in **Figure 6**, dephosphorylation by lambda protein phosphatase induced a large electrophoretic mobility shift and resulted in the loss of immunoreactivity for phosphorylation-dependent antibodies. Interestingly, dephosphorylation also resulted in the increased binding of tau to MTs (**Figure 6**). This suggests that the MT itself or MT-binding of tau is not a plausible explanation for how the imbalance of tau and tubulin causes neurotoxicity.

Recently, it has been suggested that tau also interacts with tubulin dimer(s) (Li et al., 2015; Li and Rhoades, 2017). To test whether MT-unbound tau is associated with tubulin dimers, we immunoprecipitated tau from tau-Tg worms and performed Western blotting As shown in **Figure 7**, both α- and β-tubulin were co-immunoprecipitated with soluble tau (**Figure 7**), despite tau being unbound to MTs (**Figure 5**), indicating that tau binds to tubulin dimers. Quantitative analyses showed that the higher amount of tau was recovered from WT4R(H)-Tg than WT4R(L)-Tg. However, the relative amount of co-purified α- and β-tubulins were significantly lower in WT4R(H)-Tg than that of tau. This finding indicatets that free-tau, which does not bind to either MTs or tubulin, may increase when the expression levels of tau are high. Approximately equal proportion of α- and β-tubulins were recovered in tau-bound fraction, suggesting that the α/β-tubulin dimers are associated with soluble tau (**Figure 7D**). The binding between tubulin dimers and MT-unbound tau is also confirmed in the mouse brain (data not shown).

The abundance of free-tau in neurons is a possible cause of tau toxicity. If so, it is conceivable that enhanced binding of tau to MT or tubulin may rescue tau neurotoxicity. TMAO is a chemical osmolyte that can stabilize protein conformations and is known to restore the MT-binding ability of phosphorylated tau *in vitro* (Tseng et al., 1999; Smith et al., 2000). WT4R(H)-Tg worms were grown on media containing TMAO and subjected to behavioral and biochemical analyses. As shown in **Figure 8**, the number of Tg worms having the Unc phenotype was significantly reduced by TMAO in a dose-dependent manner (**Figure 8A**). TMAO did not affect the expression of tau. However, high-dose of TMAO slightly enhanced the expression of tubulin (**Figures 8B,C**). Thus, the optimization of protein conformations

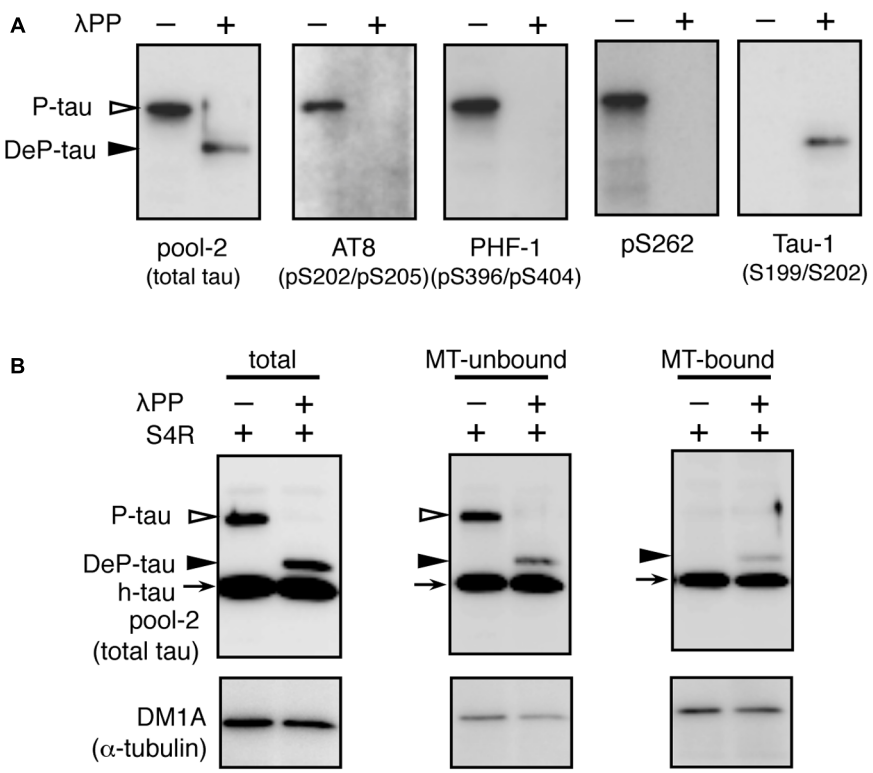

FIGURE 6 | *In vitro* dephosphorylation restores the MT-binding activity of human-tau in tau-Tg worms. **(A)** l-phosphatase dephosphorylation of tau in worms was assessed by Western blotting using the indicated antibodies. **(B)** Purified tau from WT4R(H)-Tg worms were remixed with recombinant human 0N4R tau isoform (h-tau, positive control) and MTs from naive worms (total). MT-unbound and MT-bound fractions were prepared from this mixture as described in the Materials and Methods section. Bands corresponding to phosphorylated tau (P-tau, open arrowheads), dephosphorylated tau (DeP-tau, closed arrowheads), and recombinant tau (h-tau, arrows) are indicated. Note that a portion of dephosphorylated tau, but not phosphorylated tau, was recovered in the MT-bound fraction like recombinant tau.

and/or protein-protein interactions can ameliorate the neuronal dysfunction of WT4R(H)-Tg worms.

We further addressed whether tubulin directly attenuates tau aggregation, a typical abnormality identified in tauopathy neurons. As shown in **Figure 9**, recombinant tau formed Th-T-positive insoluble aggregates following co-incubation with heparin (**Figure 9A**). When similar amounts of purified tubulin and tau were added to the mixture, the Th-T values immediately increased. Because MT formations can occur under these conditions, the transient increase in Th-T fluorescence may be caused by MT-formation (Ackmann et al., 2000), but not tau aggregation. However, after 24 h, the Th-T fluorescence decreased and by 48 h, and the fluorescence was significantly lower than control values (**Figure 9A**). After 72 h of incubation, Sarkosyl-insoluble tau, corresponding to the aggregated tau, was verified. **Figure 9B** indicates that the Sarkosyl-insoluble tau emerged only in the presence of heparin. Co-incubation of equivalent tubulin with tau reduced the amount of tau fractionated into the Sarkosyl-insoluble fraction (**Figure 9B**). Although the lower (one-fifth) amount of tubulin did not showed a transient Th-T increase, a weak but significant Th-T reduction was observed at 72 h. Taken together with the TMAO results, these data indicate that enhancing the binding of tau to tubulins may help reduce tau pathology through the reduction of neuronal dysfunction and tau aggregation.

DISCUSSION

Here, we demonstrated that not only an overexpression of tau but also a reduction of tubulins enhances tau-related pathology in worm models of tauopathy. Neuronal function was consistently rescued by either the suppression of tau expression or the pharmacological stabilization of tau/tubulin-binding. Furthermore, tubulin inhibited tau aggregation promoted by

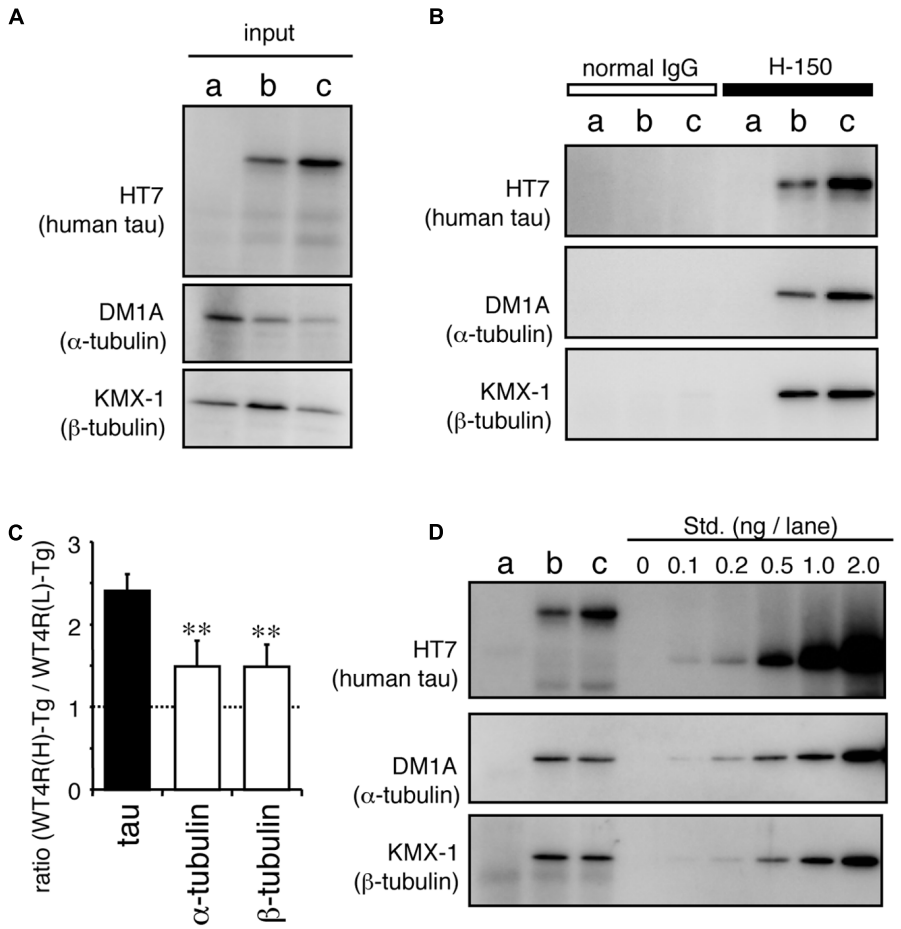

FIGURE 7 | MT-unbound tau in tau-Tg worms interacts with α/β-tubulin dimers in the soluble fraction. MT-unbound soluble fractions were prepared from Mock-Tg **(a)**, WT4R(L)-Tg **(b)**, and WT4R(H)-Tg **(c)** worms and subjected to the immunoprecipitation using anti-tau IgG (H-150). **(A)** Expression of tau, α-tubulin, and α-actin in the total lysate (input) are shown. **(B)** Immunoprecipitated proteins were analyzed using anti-tau (HT7), anti-α-tubulin (DM1A), and anti-β-tubulin (KMX-1) antibodies. **(C)** Relative amount of tau and α/β-tubulin in the co-immunoprecipitaed fraction from tau-Tg worms were quantified (mean ± SEM, $n = 6$). **(D)** Quantitative analysis of each protein indicates that the nearly equal amount of α- and β-tubulin were co-immunoprecipitated with tau. Std. indicates the purified recombinant tau (for HT7) or porcine tubulins (for DM1A and KMX-1). Statistical significance was analyzed by Tukey's *post hoc* test (**$p < 0.01$).

heparin *in vitro*. These data indicate that an imbalanced expression of tau compared to tubulin, specifically an excess of tau, is detrimental.

A loss of MTs and tubulin have been reported in the neurons of AD brains (Terry et al., 1964; Cash et al., 2003; Zhang et al., 2015). Interestingly, MT loss was found in neurons without neurofibrillary tangle formations, suggesting that the MT loss occurs independent of or ahead of the tangle formation. It is well known that tubulins are vulnerable proteins and need energy or co-factors to function properly (Arai et al., 1975). Thus, it is reasonable that the chronic decrease in metabolism, or the increased impairment of the MT protection and/or repair systems, will read the fray of cytoskeleton in the long-lived neurons.

Age is considered as a strong risk factor in neurodegenerative diseases such as AD. Various age-related abnormalities in cellular systems are considered in neurons (Baker and Petersen, 2018), and it is plausible that one or some of them are involved in triggering of tauopathy. Although further analysis is needed, dysregulation of the neuronal cytoskeletal proteins can also be defined as one character of brain protein aging, which may leads to the onset of neurodegenerative diseases. In the natural course of aging, the destruction of MTs has not been identified in nematodes or mice. Considering the lifetime of them, it is reasonable to assume that it takes longer time for this phenomenon to occur. In that sense, we cannot deny the possibility that the age-dependent tubulin/MT loss is a phenomenon unique to the neurons in the human brain that can live for decades.

In physiological condition, a much higher amount of tubulin compared to tau is present in brains. Our preliminary study indicated that there is roughly a 60-fold higher concentration of tubulin than tau in adult mice brains (data not shown). Although, it is difficult to estimate the local concentration of tau and tubulin in each cell type (ex. neuron, glia) or in each subcellular compartment (ex. cell body, axon, and dendrite), the above estimate indicates that slight changes of tau expression or tubulin reduction may not immediately tip their balance. This is consistent with the finding that it takes 8 months to develop pathology even in the PS19 line expressing P301S-tau at a five-fold higher level than endogenous tau (Yoshiyama et al., 2007). Interestingly, in the R406W-tau Tg mice, which have a lower level of tau and show mild pathology only after 18 months of age (Tatebayashi et al., 2002), tau aggregates were sparsely observed in neurons exhibiting tubulin-loss. Therefore, we speculate that tau pathology could result from not only aberrant expression of tau but also tubulin loss in aged neurons. It is also possible that once the aggregation of tau is initiated,

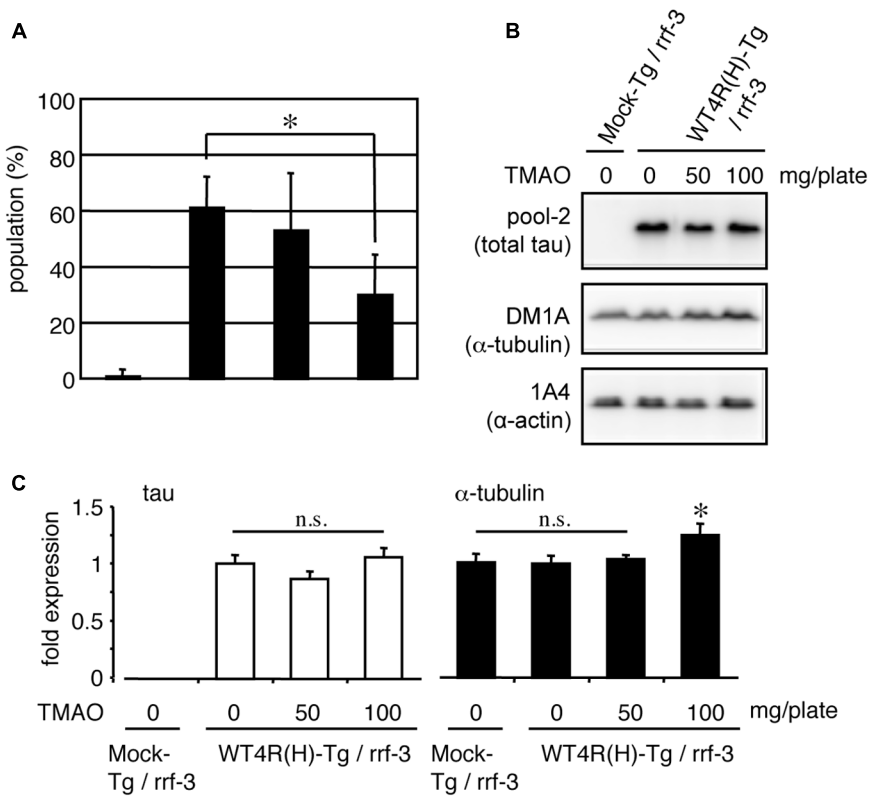

FIGURE 8 | TMAO improves behavioral phenotypes of tau-expressing worms. **(A)** Mock-Tg or WT4R(H)-Tg worms were treated with TMAO for 4 days and evaluated for Unc. The data indicate the populations of severely affected worms (means ± SEM, $n = 5$). **(B)** Total lysates from TMAO treated worms were analyzed by Western blotting using antibodies indicated. **(C)** The amounts of tau and α-tubulin were quantified (means ± SEM, $n = 7$). Statistical significance was analyzed by Tukey's *post hoc* test (*$p < 0.05$).

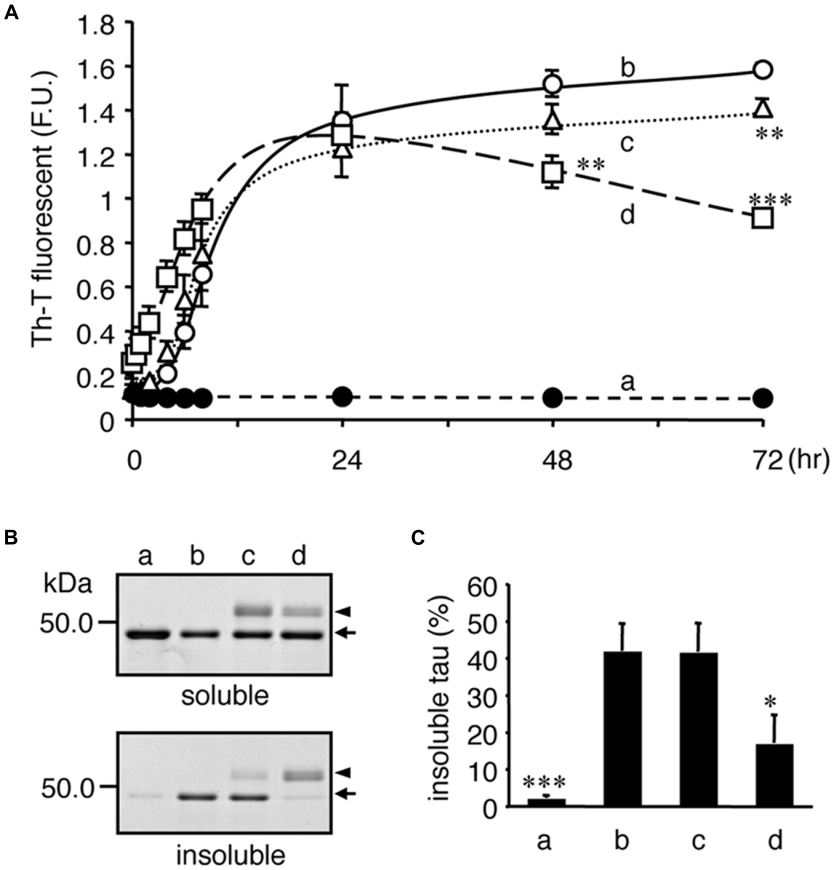

FIGURE 9 | Tubulin inhibits heparin-induced aggregation of tau. Recombinant tau **(a–d)** and tubulin (0.2 mg/ml; **c**, 1.0 mg/ml; **d**) were incubated without (closed: **a**) or with (open: **b–d**) heparin at indicated periods. **(A)** Time courses of Th-T fluorescence change are shown (means ± SEM, $n = 4$). The statistical significance compared to controls (+heparin, 0 mg/mL tubulin) was analyzed by Tukey's *post hoc* test (*$p < 0.05$, **$p < 0.01$, and ***$p < 0.001$). **(B)** After 72 hincubation, the proteins were subjected to the Sarkosyl-solubility assay as described in the Materials and Methods section. Gel images of CBB staining of total, Sarkosyl-soluble, and Sarkosyl-insoluble fractions are shown. Arrows and arrowheads indicate tau and tubulin, respectively. Note that the Sarkosyl-insoluble tau was reduced in the presence of tubulin (the arrow in lowest panel). **(C)** The amounts of Sarkosyl-insoluble tau were quantified (means ± SEM, $n = 4$). Statistical significance was analyzed by Tukey's *post hoc* test (*$p < 0.05$, ***$p < 0.001$).

MT-degeneration is stimulated (Alonso et al., 1997). Thus, tau aggregation and tubulin degeneration may be developed cooperatively.

Here, we showed an interaction between tau and tubulin dimers in the MT-unbound fraction prepared from worms. This is reproduced in mouse brains (data not shown). Recently, it has been demonstrated that tau can bind to tubulin dimers and form multiple oligomers *in vitro* (Elbaum-Garfinkle et al., 2014; Li et al., 2015; Li and Rhoades, 2017). Because tau binds to the C-terminal region of tubulin at sub-micromolar Kd, it is reasonable that virtually all tau molecules are bound to MT or soluble tubulin dimers in healthy neurons (Fauquant et al., 2011; Lefevre et al., 2011). We could not distinguish by ultracentrifugation if the complex consisted of simple trimers of tau and α/β-tubulin dimers, or multiple complexes like small soluble MTs. However, it is likely that the MT-unbound tau does not behave alone despite its tau/MTs binding ability. Therefore, the regulatory mechanism for tau-MT binding by phosphorylation could be more complicated than has ever been considered (Bodea et al., 2016; Wang and Mandelkow, 2016).

Both of the responsible regions for MT/tubulin-binding and tau-tau binding (for aggregate formation) are located in the C-terminal region of tau containing MT-binding repeats (Gustke et al., 1994; Perez et al., 1996; Goode et al., 1997; Kadavath et al., 2015; Fitzpatrick et al., 2017; Lathuiliere et al., 2017). We also showed that the C-terminal fragment, including the MT-binding repeats, is responsible for the neurotoxicity of tau (Xie et al., 2014). Simply, it is conceivable that the interaction of an unknown factor(s), or tau-itself on a naked MT-binding domain, is crucial for exerting tau toxicity. Thus, as shown here, the binding of tubulin (or MT) on an MT-binding domain of tau, interferes with the undesirable interaction with other factors, including tau-itself. Because the affinity of tau-tau binding is about 20 times higher than that of the tau/tubulin interaction, a sufficient amount of tubulin may be necessary to suppress the neurotoxicity of tau (Lai et al., 2016). If the level of tubulins

declines due to aging or metabolic impairment, neurons may become prone to have higher levels of free tau and eventually tau aggregates.

In summary, our data suggested that the imbalanced expression of tau vs. tubulin might be a key step in the pathogenesis of tauopathy, and "free-tau" may be a toxic species of tauopathy. Thus, we propose the following hypothesis. Tau has the potential to be cytotoxic due to its MT-binding repeats. However, in healthy neurons MTs or tubulin dimers bind on the MT-binding repeats, thereby masking the toxicity. However, in some aged neurons in the elderly, a decline of tubulin and/or ectopic expression of tau occur by energy failure, oxidative stress, or amyloid depositions, which need to be experimentally identified. This will result in genuine "free-tau" that has free, exposed MT-binding repeats, which behave as either a toxic factor by itself, or promotes the self-aggregation of tau.

AUTHOR CONTRIBUTIONS

TM and YI designed the experiments. TM, YS, and SatY performed the behavioral and biochemical analyses. SawY, EK-N, and SM developed the *C. elegans* models. TM wrote the manuscript.

FUNDING

This work was supported in part by the Grant-in-Aid for Scientific Research on Innovative Areas "Brain Protein Aging and Dementia Control" (TM 26117004), the "Integrated research on neuropsychiatric disorder", which was carried out under the Strategic Research Program for Brain Sciences (TM and YI), and the JSPS KAKENHI Grant Numbers 20700324 (TM) and 22650074 (TM).

REFERENCES

Ackmann, M., Wiech, H., and Mandelkow, E. (2000). Nonsaturable binding indicates clustering of tau on the microtubule surface in a paired helical filament-like conformation. *J. Biol. Chem.* 275, 30335–30343. doi: 10.1074/jbc.M002590200

Alonso, A. D., Grundke-Iqbal, I., Barra, H. S., and Iqbal, K. (1997). Abnormal phosphorylation of tau and the mechanism of Alzheimer neurofibrillary degeneration: sequestration of microtubule-associated proteins 1 and 2 and the disassembly of microtubules by the abnormal tau. *Proc. Natl. Acad. Sci. U.S.A.* 94, 298–303. doi: 10.1073/pnas.94.1.298

Arai, T., Ihara, Y., Arai, K., and Kaziro, Y. (1975). Purification of tubulin from bovine brain and its interaction with guanine nucleotides. *J. Biochem.* 77, 647–658. doi: 10.1093/oxfordjournals.jbchem.a130767

Baker, D. J., and Petersen, R. C. (2018). Cellular senescence in brain aging and neurodegenerative diseases: evidence and perspectives. *J. Clin. Invest.* 128, 1208–1216. doi: 10.1172/JCI95145

Bodea, L. G., Eckert, A., Ittner, L. M., Piguet, O., and Gotz, J. (2016). Tau physiology and pathomechanisms in frontotemporal lobar degeneration. *J. Neurochem.* 138(Suppl. 1), 71–94. doi: 10.1111/jnc.13600

Bommel, H., Xie, G., Rossoll, W., Wiese, S., Jablonka, S., Boehm, T., et al. (2002). Missense mutation in the tubulin-specific chaperone E (Tbce) gene in the mouse mutant progressive motor neuronopathy, a model of human motoneuron disease. *J. Cell Biol.* 159, 563–569. doi: 10.1083/jcb.200208001

Cash, A. D., Aliev, G., Siedlak, S. L., Nunomura, A., Fujioka, H., Zhu, X., et al. (2003). Microtubule reduction in Alzheimer's disease and aging is independent of tau filament formation. *Am. J. Pathol.* 162, 1623–1627. doi: 10.1016/S0002-9440(10)64296-4

Delacourte, A., David, J. P., Sergeant, N., Buee, L., Wattez, A., Vermersch, P., et al. (1999). The biochemical pathway of neurofibrillary degeneration in aging and Alzheimer's disease. *Neurology* 52, 1158–1165. doi: 10.1212/WNL.52.6.1158

Elbaum-Garfinkle, S., Cobb, G., Compton, J. T., Li, X. H., and Rhoades, E. (2014). Tau mutants bind tubulin heterodimers with enhanced affinity. *Proc. Natl. Acad. Sci. U.S.A.* 111, 6311–6316. doi: 10.1073/pnas.1315983111

Fauquant, C., Redeker, V., Landrieu, I., Wieruszeski, J. M., Verdegem, D., Laprevote, O., et al. (2011). Systematic identification of tubulin-interacting fragments of the microtubule-associated protein Tau leads to a highly efficient promoter of microtubule assembly. *J. Biol. Chem.* 286, 33358–33368. doi: 10.1074/jbc.M111.223545

Fitzpatrick, A. W. P., Falcon, B., He, S., Murzin, A. G., Murshudov, G., Garringer, H. J., et al. (2017). Cryo-EM structures of tau filaments from Alzheimer's disease. *Nature* 547, 185–190. doi: 10.1038/nature23002

Fukushige, T., Siddiqui, Z. K., Chou, M., Culotti, J. G., Gogonea, C. B., Siddiqui, S. S., et al. (1999). MEC-12, an alpha-tubulin required for touch sensitivity in *C. elegans*. *J. Cell Sci.* 112(Pt 3), 395–403.

Goedert, M., Eisenberg, D. S., and Crowther, R. A. (2017). Propagation of tau aggregates and neurodegeneration. *Annu. Rev. Neurosci.* 40, 189–210. doi: 10.1146/annurev-neuro-072116-031153

Gogonea, C. B., Gogonea, V., Ali, Y. M., Merz, K. M. Jr., and Siddiqui, S. S. (1999). Computational prediction of the three-dimensional structures for the *Caenorhabditis elegans* tubulin family. *J. Mol. Graph. Model.* 17, 126–130. doi: 10.1016/S1093-3263(99)00025-X

Gomez-Isla, T., Hollister, R., West, H., Mui, S., Growdon, J. H., Petersen, R. C., et al. (1997). Neuronal loss correlates with but exceeds neurofibrillary tangles in Alzheimer's disease. *Ann. Neurol.* 41, 17–24. doi: 10.1002/ana.410410106

Goode, B. L., Denis, P. E., Panda, D., Radeke, M. J., Miller, H. P., Wilson, L., et al. (1997). Functional interactions between the proline-rich and repeat regions of tau enhance microtubule binding and assembly. *Mol. Biol. Cell* 8, 353–365. doi: 10.1091/mbc.8.2.353

Greenberg, S. G., and Davies, P. (1990). A preparation of Alzheimer paired helical filaments that displays distinct tau proteins by polyacrylamide gel electrophoresis. *Proc. Natl. Acad. Sci. U.S.A.* 87, 5827–5831. doi: 10.1073/pnas.87.15.5827

Grundke-Iqbal, I., Iqbal, K., Quinlan, M., Tung, Y. C., Zaidi, M. S., and Wisniewski, H. M. (1986). Microtubule-associated protein tau. A component of Alzheimer paired helical filaments. *J. Biol. Chem.* 261, 6084–6089.

Gustke, N., Trinczek, B., Biernat, J., Mandelkow, E. M., and Mandelkow, E. (1994). Domains of tau protein and interactions with microtubules. *Biochemistry* 33, 9511–9522. doi: 10.1021/bi00198a017

Hanger, D. P., Anderton, B. H., and Noble, W. (2009). Tau phosphorylation: the therapeutic challenge for neurodegenerative disease. *Trends Mol. Med.* 15, 112–119. doi: 10.1016/j.molmed.2009.01.003

Harada, A., Oguchi, K., Okabe, S., Kuno, J., Terada, S., Ohshima, T., et al. (1994). Altered microtubule organization in small-calibre axons of mice lacking tau protein. *Nature* 369, 488–491. doi: 10.1038/369488a0

Iqbal, K., Liu, F., and Gong, C. X. (2016). Tau and neurodegenerative disease: the story so far. *Nat. Rev. Neurol.* 12, 15–27. doi: 10.1038/nrneurol.2015.225

Kadavath, H., Hofele, R. V., Biernat, J., Kumar, S., Tepper, K., Urlaub, H., et al. (2015). Tau stabilizes microtubules by binding at the interface between tubulin heterodimers. *Proc. Natl. Acad. Sci. U.S.A.* 112, 7501–7506. doi: 10.1073/pnas.1504081112

Kage-Nakadai, E., Ohta, A., Ujisawa, T., Sun, S., Nishikawa, Y., Kuhara, A., et al. (2016). *Caenorhabditis elegans* homologue of Prox1/Prospero is expressed in the glia and is required for sensory behavior and cold tolerance. *Genes Cells* 21, 936–948. doi: 10.1111/gtc.12394

Khatoon, S., Grundke-Iqbal, I., and Iqbal, K. (1992). Brain levels of microtubule-associated protein tau are elevated in Alzheimer's disease: a radioimmuno-slot-blot assay for nanograms of the protein. *J. Neurochem.* 59, 750–753. doi: 10.1111/j.1471-4159.1992.tb09432.x

Kimura, T., Whitcomb, D. J., Jo, J., Regan, P., Piers, T., Heo, S., et al. (2014). Microtubule-associated protein tau is essential for long-term depression in

the hippocampus. *Philos. Trans. R. Soc. Lond. B Biol. Sci.* 369, 20130144. doi: 10.1098/rstb.2013.0144

Lai, R. Y., Harrington, C. R., and Wischik, C. M. (2016). Absence of a role for phosphorylation in the tau pathology of Alzheimer's disease. *Biomolecules* 6:E19. doi: 10.3390/biom6020019

Lathuiliere, A., Valdes, P., Papin, S., Cacquevel, M., Maclachlan, C., Knott, G. W., et al. (2017). Motifs in the tau protein that control binding to microtubules and aggregation determine pathological effects. *Sci. Rep.* 7:13556. doi: 10.1038/s41598-017-13786-2

Lee, V. M., Balin, B. J., Otvos, L. Jr., and Trojanowski, J. Q. (1991). A68: a major subunit of paired helical filaments and derivatized forms of normal Tau. *Science* 251, 675–678. doi: 10.1126/science.1899488

Lefevre, J., Chernov, K. G., Joshi, V., Delga, S., Toma, F., Pastre, D., et al. (2011). The C terminus of tubulin, a versatile partner for cationic molecules: binding of Tau, polyamines, and calcium. *J. Biol. Chem.* 286, 3065–3078. doi: 10.1074/jbc.M110.144089

Li, X. H., Culver, J. A., and Rhoades, E. (2015). Tau binds to multiple tubulin dimers with helical structure. *J. Am. Chem. Soc.* 137, 9218–9221. doi: 10.1021/jacs.5b04561

Li, X. H., and Rhoades, E. (2017). Heterogeneous tau-tubulin complexes accelerate microtubule polymerization. *Biophys. J.* 112, 2567–2574. doi: 10.1016/j.bpj.2017.05.006

Maduro, M., and Pilgrim, D. (1995). Identification and cloning of unc-119, a gene expressed in the *Caenorhabditis elegans* nervous system. *Genetics* 141, 977–988.

Martin, N., Jaubert, J., Gounon, P., Salido, E., Haase, G., Szatanik, M., et al. (2002). A missense mutation in Tbce causes progressive motor neuronopathy in mice. *Nat. Genet.* 32, 443–447. doi: 10.1038/ng1016

Mitani, S. (1995). Genetic regulation of mec-3 gene expression implicated in the specification of the mechanosensory neuron cell types in *Caenorhabditis elegans*. *Dev. Growth Diff.* 37, 551–557. doi: 10.1046/j.1440-169X.1995.t01-4-00010.x

Miyasaka, T., Sato, S., Tatebayashi, Y., and Takashima, A. (2010). Microtubule destruction induces tau liberation and its subsequent phosphorylation. *FEBS Lett.* 584, 3227–3232. doi: 10.1016/j.febslet.2010.06.014

Miyasaka, T., Ding, Z., Gengyo-Ando, K., Oue, M., Yamaguchi, H., Mitani, S., et al. (2005a). Progressive neurodegeneration in *C. elegans* model of tauopathy. *Neurobiol. Dis.* 20, 372–383.

Miyasaka, T., Watanabe, A., Saito, Y., Murayama, S., Mann, D. M., Yamazaki, M., et al. (2005b). Visualization of newly deposited tau in neurofibrillary tangles and neuropil threads. *J. Neuropathol. Exp. Neurol.* 64, 665–674.

Miyasaka, T., Xie, C., Yoshimura, S., Shinzaki, Y., Yoshina, S., Kage-Nakadai, E., et al. (2016). Curcumin improves tau-induced neuronal dysfunction of nematodes. *Neurobiol. Aging* 39, 69–81. doi: 10.1016/j.neurobiolaging.2015.11.004

Nithianantham, S., Le, S., Seto, E., Jia, W., Leary, J., Corbett, K. D., et al. (2015). Tubulin cofactors and Arl2 are cage-like chaperones that regulate the soluble alphabeta-tubulin pool for microtubule dynamics. *eLife* 4:e08811. doi: 10.7554/eLife.08811

Noble, W., Hanger, D. P., and Gallo, J. M. (2010). Transgenic mouse models of tauopathy in drug discovery. *CNS Neurol. Disord. Drug Targets* 9, 403–428. doi: 10.2174/187152710791556131

Perez, M., Valpuesta, J. M., Medina, M., Montejo de Garcini, E., and Avila, J. (1996). Polymerization of tau into filaments in the presence of heparin: the minimal sequence required for tau-tau interaction. *J. Neurochem.* 67, 1183–1190. doi: 10.1046/j.1471-4159.1996.67031183.x

Planel, E., Krishnamurthy, P., Miyasaka, T., Liu, L., Herman, M., Kumar, A., et al. (2008). Anesthesia-induced hyperphosphorylation detaches 3-repeat tau from microtubules without affecting their stability in vivo. *J. Neurosci* 28, 12798–12807. doi: 10.1523/JNEUROSCI.4101-08.2008

Serrano-Pozo, A., Frosch, M. P., Masliah, E., and Hyman, B. T. (2011). Neuropathological alterations in Alzheimer disease. *Cold Spring Harb. Perspect. Med.* 1:a006189. doi: 10.1101/cshperspect.a006189

Shafiei, S. S., Guerrero-Munoz, M. J., and Castillo-Carranza, D. L. (2017). Tau oligomers: cytotoxicity, propagation, and mitochondrial damage. *Front. Aging Neurosci.* 9:83. doi: 10.3389/fnagi.2017.00083

Simmer, F., Tijsterman, M., Parrish, S., Koushika, S. P., Nonet, M. L., Fire, A., et al. (2002). Loss of the putative RNA-directed RNA polymerase RRF-3 makes *C. elegans* hypersensitive to RNAi. *Curr. Biol.* 12, 1317–1319. doi: 10.1016/S0960-9822(02)01041-2

Smith, M. J., Crowther, R. A., and Goedert, M. (2000). The natural osmolyte trimethylamine N-oxide (TMAO) restores the ability of mutant tau to promote microtubule assembly. *FEBS Lett.* 484, 265–270. doi: 10.1016/S0014-5793(00)02169-4

Spillantini, M. G., and Goedert, M. (2013). Tau pathology and neurodegeneration. *Lancet Neurol.* 12, 609–622. doi: 10.1016/S1474-4422(13)70090-5

Tatebayashi, Y., Miyasaka, T., Chui, D. H., Akagi, T., Mishima, K., Iwasaki, K., et al. (2002). Tau filament formation and associative memory deficit in aged mice expressing mutant (R406W) human tau. *Proc. Natl. Acad. Sci. U.S.A.* 99, 13896–13901. doi: 10.1073/pnas.202205599

Terry, R. D., Gonatas, N. K., and Weiss, M. (1964). Ultrastructural studies in Alzheimer's presenile dementia. *Am. J. Pathol.* 44, 269–297.

Tian, G., and Cowan, N. J. (2013). Tubulin-specific chaperones: components of a molecular machine that assembles the alpha/beta heterodimer. *Methods Cell Biol.* 115, 155–171. doi: 10.1016/B978-0-12-407757-7.00011-6

Tseng, H. C., Lu, Q., Henderson, E., and Graves, D. J. (1999). Phosphorylated tau can promote tubulin assembly. *Proc. Natl. Acad. Sci. U.S.A.* 96, 9503–9508. doi: 10.1073/pnas.96.17.9503

Wang, Y., and Mandelkow, E. (2016). Tau in physiology and pathology. *Nat. Rev. Neurosci.* 17, 5–21. doi: 10.1038/nrn.2015.1

Xie, C., and Miyasaka, T. (2016). The role of the carboxyl-terminal sequence of tau and MAP2 in the pathogenesis of dementia. *Front. Mol. Neurosci.* 9:158. doi: 10.3389/fnmol.2016.00158

Xie, C., Miyasaka, T., Yoshimura, S., Hatsuta, H., Yoshina, S., Kage-Nakadai, E., et al. (2014). The homologous carboxyl-terminal domains of microtubule-associated protein 2 and TAU induce neuronal dysfunction and have differential fates in the evolution of neurofibrillary tangles. *PLoS One* 9:e89796. doi: 10.1371/journal.pone.0089796

Xie, C., Soeda, Y., Shinzaki, Y., In, Y., Tomoo, K., Ihara, Y., et al. (2015). Identification of key amino acids responsible for the distinct aggregation properties of microtubule-associated protein 2 and tau. *J. Neurochem.* 135, 19–26. doi: 10.1111/jnc.13228

Yoshida, H., and Ihara, Y. (1993). Tau in paired helical filaments is functionally distinct from fetal tau: assembly incompetence of paired helical filament-tau. *J. Neurochem.* 61, 1183–1186. doi: 10.1111/j.1471-4159.1993.tb03642.x

Yoshiyama, Y., Higuchi, M., Zhang, B., Huang, S. M., Iwata, N., Saido, T. C., et al. (2007). Synapse loss and microglial activation precede tangles in a P301S tauopathy mouse model. *Neuron* 53, 337–351. doi: 10.1016/j.neuron.2007.01.010

Zhang, F., Su, B., Wang, C., Siedlak, S. L., Mondragon-Rodriguez, S., Lee, H. G., et al. (2015). Posttranslational modifications of alpha-tubulin in alzheimer disease. *Transl. Neurodegener.* 4:9. doi: 10.1186/s40035-015-0030-4

Conflict of Interest Statement: The authors declare that the research was conducted in the absence of any commercial or financial relationships that could be construed as a potential conflict of interest.

frontiers in Neuroscience

REVIEW
published: 29 November 2017
doi: 10.3389/fnins.2017.00667

Extracellular Tau and Its Potential Role in the Propagation of Tau Pathology

*Kaoru Yamada**

Department of Neuropathology, Graduate School of Medicine, The University of Tokyo, Tokyo, Japan

The pathological aggregation of tau protein is a hallmark of a set of neurodegenerative diseases collectively referred to as tauopathies. Tau aggregates independently in each neuron, but this aggregation can also occur in a non-cell autonomous manner in which aggregated tau is transmitted from one cell to another. Such trans-cellular propagation is initiated by the uptake of extracellular tau, which then seeds soluble tau in the recipient cells to spread the tau pathology. Accumulating evidence has demonstrated that tau is not only present in the cytoplasm of neurons but also actively released into the extracellular space. This finding has led to the idea that extracellular tau could be a novel therapeutic target to halt the propagation of tau pathology. From this perspective, the present review article focuses on recent advances in understanding the mechanisms regulating the levels of extracellular tau and discusses the role of such mechanisms in the propagation of tau pathology.

Keywords: propagation, extracellular tau, tauopathies, Alzheimer's disease, unconventional protein secretion

OPEN ACCESS

Edited by:
Naruhiko Sahara,
National Institute of Radiological Sciences (NIRS), Japan

Reviewed by:
Roland Brandt,
University of Osnabrück, Germany
Shuko Takeda,
Osaka University, Japan

***Correspondence:**
Kaoru Yamada
yamadaka@m.u-tokyo.ac.jp

Specialty section:
This article was submitted to Neurodegeneration, a section of the journal Frontiers in Neuroscience

Received: *30 September 2017*
Accepted: *16 November 2017*
Published: *29 November 2017*

Citation:
Yamada K (2017) Extracellular Tau and Its Potential Role in the Propagation of Tau Pathology. Front. Neurosci. 11:667. doi: 10.3389/fnins.2017.00667

INTRODUCTION

The abnormal accumulation of tau protein as neurofibrillary tangles is the common pathological hallmark of a set of neurodegenerative diseases, including Alzheimer's disease (AD), that are collectively referred to as tauopathies. The deposition of neurofibrillary tangles highly correlates with cognitive decline in AD, suggesting that tau plays a critical role in neurodegeneration (Gómez-Isla et al., 1997). Tau is intrinsically highly soluble; however, in tauopathies, it self-assembles into fibrillar aggregates. This process involves a nucleation and elongation mechanism where tau first forms small intermediate oligomers that convert normally folded tau into misfolded aggregates by acting as aggregation nuclei or seeds (hereinafter referred to as "seed-competent tau"). Such nucleation-dependent aggregation was thought to occur only in a cell-autonomous manner, but compelling evidence now suggests that non-cell autonomous aggregation can also occur via seed-competent tau transmission from neurons to neurons via the extracellular space. The present review article discusses recent knowledge about the roles of extracellular tau including trans-cellular propagation, the possible mechanisms that regulate its extracellular levels, and the pathological implications of those mechanisms in tauopathies.

EXTRACELLULAR TAU AND ITS PHYSIOLOGICAL/PATHOLOGICAL ROLES

Tau is well-recognized for its role in assembling/stabilizing microtubules although tau single knockout mice do not show major phenotypic changes in neuronal microtubule stability because of a putative functional redundancy (Takei et al., 2000). Due to this interaction with microtubules, its localization has been long assumed to be restricted to the cytoplasm of neurons. However, accumulating evidence now demonstrates that tau is also physiologically present in the extracellular fluid. Tau is present in full-length (Karch et al., 2013) or truncated forms (Bright et al., 2015; Kanmert et al., 2015) not only in the culture media of cells over-expressing human tau (Chai et al., 2012), primary neurons (Karch et al., 2012), and iPSC derived neurons (Chai et al., 2012; Bright et al., 2015) but also in the brain interstitial fluid (ISF) and cerebrospinal fluid (CSF) of mice (Yamada et al., 2011) and human (Magnoni et al., 2012).

Although the physiological function of extracellular tau still remains unclear, extracellular tau currently receives considerable attention due to its role in trans-cellular propagation. Tau propagation was initially described in cell culture models where the extracellular application of tau fibrils enters the cells and robustly seeds aggregation of the soluble tau expressed in cells (Frost et al., 2009). Such a seeding effect was not observed when soluble monomeric tau was applied. Subsequent studies have shown that injecting tau fibrils into the brain also induces trans-neuronal propagation *in vivo* (Clavaguera et al., 2009; Iba et al., 2013). In cell culture studies, the transfer of conditioned media from cells with aggregates was sufficient to induce aggregation in the recipient cells (Kfoury et al., 2012; Wu et al., 2016), suggesting that seed-competent tau is released into the culture media. It remains uncertain that trans-cellular propagation also contributes to the progression of tau pathology in human (Walsh and Selkoe, 2016): nonetheless, seeding activity detected in human CSF using sensitive assays such as real-time quaking-induced conversion (RT-QuIC) analysis (Saijo et al., 2017) or tau biosensor cells (Holmes et al., 2014; Takeda et al., 2016) supports this tau spreading hypothesis.

In addition to being trans-cellularly propagated, tau may have specific functions in the extracellular space. For example, the application of extracellular tau increases the electrical activity of iPSC-derived or primary cortical neurons (Bright et al., 2015). Moreover, extracellular tau may elicit cellular toxicity under certain conditions. The addition of tau into the cell culture media binds to muscarinic acetylcholine receptors and increases intracellular calcium, eventually leading to cell death (Gómez-Ramos et al., 2006, 2008). Furthermore, extracellular oligomeric tau impairs memory and long-term potentiation (LTP) in mice (Fá et al., 2016; Puzzo et al., 2017). However, in some experimental models, the amount of tau needed to elicit impairment is far more than the circulating levels of tau; thus, further investigation is needed to determine whether aforementioned effects indeed reflect the pathophysiological function of extracellular tau.

POSSIBLE MECHANISMS OF TAU RELEASE

The amount of soluble monomeric tau released from cells is altered by the various types of external stimuli. For example, starvation or lysosomal dysfunction increases tau release (Mohamed et al., 2014). In addition, stimulating neuronal activity in either cultured neurons or *in vivo* also enhances tau release (Pooler et al., 2013; Yamada et al., 2014; Fá et al., 2016). Given that extracellular tau influences neuronal activity (Bright et al., 2015), this observation suggests that the activity-dependent release of tau participates in a positive feedback loop on neuronal activity.

Differences in tau species or isoforms also impact its release. For example, extracellular tau levels are differentially altered by the presence of mutations in *MAPT,* an amino-terminal insertion sequence, or a repeat domain (Karch et al., 2012). Moreover, hyperphosphorylation-mimicking mutant tau is preferentially released while extracellular tau is rather less phosphorylated compared to intracellular tau (Plouffe et al., 2012; Bright et al., 2015). Furthermore, caspase-3 cleavage at D421 increases tau release (Plouffe et al., 2012). These observations of variable tau release suggest the presence of active cellular mechanisms regulating its release.

Tau does not contain an apparent signal peptide sequence to regulate its trans-location to the endoplasmic reticulum (ER) for conventional secretory pathway, thus, it remains to be elucidated how tau reaches the extracellular space. In addition to tau, an increasing number of proteins without a signal peptide sequence are being recognized for their unexpected release into the extracellular space. Such secretion is termed unconventional protein secretion and occurs via vesicular or non-vesicular pathways.

One of the best-characterized mechanisms for unconventional vesicular secretion is the exosome-dependent pathway. Exosomes are the extracellular vesicles that are released upon fusion of the multivesicular bodies with the plasma membrane. Tau from the CSF (Saman et al., 2012) and blood of patients with AD (Fiandaca et al., 2015) is associated with exosomes. N2a cells over-expressing tau (Wang et al., 2017) and microglia also release tau in an exosome-dependent manner (Asai et al., 2015). However, other studies show that the majority of extracellular tau is membrane-free (Chai et al., 2012; Karch et al., 2012) and not associated with extracellular vesicles such as exosomes or ectosomes (i.e., plasma-membrane originating vesicles) (Dujardin et al., 2014). Therefore, the exosome-dependent mechanism may only explain a small fraction of the total tau that is released into the extracellular space.

Current understanding of exosome-independent tau release mechanisms is limited, however, chaperones and proteins responsible for intracellular vesicle trafficking have been implicated. For example, DnaJ/Hsc70 chaperone complexes control the release of tau and knockdown of SNAP23, a SNARE protein involved in vesicle-mediated exocytosis, blocks tau release (Fontaine et al., 2016). Interestingly, a significant portion of endogenous tau in neurons is associated with membrane fractions and membrane-associated tau is largely

dephosphorylated, like extracellular tau (Pooler et al., 2012). Although the identity of membrane-associated tau remains to be clarified, it is tempting to speculate that tau is translocated into intracellular vesicles prior to its release.

Rab GTPase regulates various steps of intracellular vesicle trafficking and membrane fusion. Rab7a (Rodriguez et al., 2017) and Rab1a (Mohamed et al., 2017) have been recently implicated in tau release, further suggesting that tau release involves vesicle transport. Elucidating the precise molecular mechanism involving these proteins will uncover release pathway in more detail.

Some substrates such as fibroblast growth factor 2 are secreted via the unconventional secretion pathway by direct translocation across the plasma membrane (La Venuta et al., 2015). Tau also interacts with plasma membrane via amino terminal projection domain (Brandt et al., 1995), which is influenced by a tauopathy-associated mutation (Gauthier-Kemper et al., 2011). Nevertheless, there is no evidence to date that tau is also released through such a non-vesicular secretion pathway.

The majority of tau binds to microtubules (Weissmann et al., 2009), thus one might speculate that detachment of tau from microtubules increase releasable pool of tau. However, the relationship between tau release and interaction with microtubules is not understood well. To date, there is no clear demonstration that microtubule binding properties directly influence tau release. The stabilization or destabilization of microtubules with paclitaxel or pseudolaric acid B both increased tau release (Karch et al., 2012). This may be the consequence of altered homeostasis of tau by perturbation of microtubule binding. How the release of tau is related to its dynamic kiss-and-hop interaction with microtubules needs further investigation.

Finally, the majority of current literature only describes the release of soluble monomeric tau and there is little definitive evidence of whether and how seed-competent tau is released into the extracellular space. Soluble monomeric tau and seed-competent tau may exit cells via distinct pathways. Because tau aggregates that leak from dying or degenerating neurons also likely mediate transcellular propagation, further studies are needed to investigate whether there are active release mechanisms for seed-competent tau from living cells.

CLEARANCE OF TAU FROM THE EXTRACELLULAR SPACE

Extracellular tau levels are maintained based on a balance between cellular release and clearance; thus, changes in clearance will also affect extracellular tau levels. A study of regulatable tau transgenic mice found a relatively low turnover rate of ISF tau (the expected half-life was ∼11–17 days) (Yamada et al., 2015); nonetheless, the molecular mechanism for clearing extracellular tau remains largely uninvestigated.

The paravascular clearance pathway, also termed the "glymphatic system," has been recently recognized for its critical role in eliminating extracellular molecules from the brain via perivascular tunnels (Iliff et al., 2012). This pathway may participate in tau clearance, as tau accumulates along the veins upon injection into the brain (Iliff et al., 2014).

Uptake and degradation of seed-competent tau by glial cells may inhibit propagation by blocking neuronal uptake. Anti-tau antibodies facilitate microglial uptake of tau aggregates (Funk et al., 2015; Luo et al., 2015; Yanamandra et al., 2015). In addition to microglia-mediated degradation, a brain-to-blood clearance pathway may play a role. A study has shown that tau injected into the CSF appeared in plasma and underwent degradation (Yanamandra et al., 2017). Although the precise mechanism remains to be elucidated, these data suggest the presence of pathway that eliminates extracellular tau from the CNS to the peripheral bloodstream.

CONCLUSION

Accumulating evidence suggests that tau is physiologically released into the extracellular space independently of cell death or neurodegeneration. This evidence suggests the novel possibility that tau may play pivotal extracellular roles. Given that tau propagation is mediated by extracellular seed-competent tau, a possible therapeutic intervention strategy is to reduce such pathological tau levels in the extracellular space. However, such a strategy may interfere with the yet-to-be-identified physiological functions of normal extracellular tau.

Elevated CSF tau is a diagnostic biomarker in AD patients (Tapiola et al., 2009). The physiological presence of extracellular tau may challenge the view that this elevation merely reflects the degree of neurodegeneration. Notably, CSF tau levels begin to increase during the period when a significant neuronal loss would not be expected (Bateman et al., 2012). Consistent with this observation, CSF tau in *APP* transgenic mice is increased in an age-dependent manner without a global neuronal loss (Maia et al., 2013).

Elucidating the precise mechanisms regulating extracellular tau levels, especially mechanisms involving prior to neurodegeneration, will lead to important new insights to better understand the physiological/pathological roles of tau in the brain and improve the diagnosis and treatment of tauopathies.

AUTHOR CONTRIBUTIONS

The author confirms being the sole contributor of this work and approved it for publication.

FUNDING

This work was supported by Grant-in-Aid for Scientific Research on Innovative Areas (Brain Protein Aging and Dementia Control) (15H01552) from MEXT.

REFERENCES

Asai, H., Ikezu, S., Tsunoda, S., Medalla, M., Luebke, J., Haydar, T., et al. (2015). Depletion of microglia and inhibition of exosome synthesis halt tau propagation. *Nat. Neurosci.* 18, 1584–1593. doi: 10.1038/nn.4132

Bateman, R. J., Xiong, C., Benzinger, T. L., Fagan, A. M., Goate, A., Fox, N. C., et al. (2012). Clinical and biomarker changes in dominantly inherited Alzheimer's disease. *N. Engl. J. Med*. 367, 795–804. doi: 10.1056/NEJMoa1202753

Brandt, R., Léger, J., and Lee, G. (1995). Interaction of tau with the neural plasma membrane mediated by tau's amino-terminal projection domain. *J. Cell Biol.* 131, 1327–1340. doi: 10.1083/jcb.131.5.1327

Bright, J., Hussain, S., Dang, V., Wright, S., Cooper, B., Byun, T., et al. (2015). Human secreted tau increases amyloid-beta production. *Neurobiol. Aging* 36, 693–709. doi: 10.1016/j.neurobiolaging.2014.09.007

Chai, X., Dage, J. L., and Citron, M. (2012). Constitutive secretion of tau protein by an unconventional mechanism. *Neurobiol. Dis.* 48, 356–366. doi: 10.1016/j.nbd.2012.05.021

Clavaguera, F., Bolmont, T., Crowther, R. A., Abramowski, D., Frank, S., Probst, A., et al. (2009). Transmission and spreading of tauopathy in transgenic mouse brain. *Nat. Cell Biol*. 11, 909–913. doi: 10.1038/ncb1901

Dujardin, S., Bégard, S., Caillierez, R., Lachaud, C., Delattre, L., Carrier, S., et al. (2014). Ectosomes: a new mechanism for non-exosomal secretion of Tau protein. *PLoS ONE* 9:100760. doi: 10.1371/journal.pone.0100760

Fá, M., Puzzo, D., Piacentini, R., Staniszewski, A., Zhang, H., Baltrons, M. A., et al. (2016). Extracellular tau oligomers produce an immediate impairment of LTP and Memory. *Sci. Rep.* 6:19393. doi: 10.1038/srep19393

Fiandaca, M. S., Kapogiannis, D., Mapstone, M., Boxer, A., Eitan, E., Schwartz, J. B., et al. (2015). Identification of preclinical Alzheimer's disease by a profile of pathogenic proteins in neurally derived blood exosomes: a case-control study. *Alzheimer's Dement*. 11, 600–607.e1. doi: 10.1016/j.jalz.2014.06.008

Fontaine, S. N., Zheng, D., Sabbagh, J. J., Martin, M. D., Chaput, D., Darling, A., et al. (2016). DnaJ/Hsc70 chaperone complexes control the extracellular release of neurodegenerative-associated proteins. *EMBO J.* 35, 1537–1549. doi: 10.15252/embj.201593489

Frost, B., Jacks, R. L., and Diamond, M. I. (2009). Propagation of Tau misfolding from the outside to the inside of a cell. *J. Biol. Chem.* 284, 12845–12852. doi: 10.1074/jbc.M808759200

Funk, K. E., Mirbaha, H., Jiang, H., Holtzman, D. M., and Diamond, M. I. (2015). Distinct therapeutic mechanisms of Tau antibodies: promoting microglial clearance versus blocking neuronal uptake. *J. Biol. Chem*. 290, 21652–21662. doi: 10.1074/jbc.M115.657924

Gauthier-Kemper, A., Weissmann, C., Golovyashkina, N., Sebö-Lemke, Z., Drewes, G., Gerke, V., et al. (2011). The frontotemporal dementia mutation R406W blocks tau's interaction with the membrane in an annexin A2–dependent manner. *J. Cell Biol.* 192, 647–661. doi: 10.1083/jcb.201007161

Gómez-Isla, T., Hollister, R., West, H., Mui, S., Growdon, J. H., Petersen, R. C., et al. (1997). Neuronal loss correlates with but exceeds neurofibrillary tangles in Alzheimer's disease. *Ann. Neurol.* 41, 17–24. doi: 10.1002/ana.410410106

Gómez-Ramos, A., Díaz-Hernández, M., Cuadros, R., Hernández, F., and Avila, J. (2006). Extracellular tau is toxic to neuronal cells. *FEBS Lett*. 580, 4842–4850. doi: 10.1016/j.febslet.2006.07.078

Gómez-Ramos, A., Díaz-Hernández, M., Rubio, A., Miras-Portugal, M. T., and Avila, J. (2008). Extracellular tau promotes intracellular calcium increase through M1 and M3 muscarinic receptors in neuronal cells. *Mol. Cell. Neurosci.* 37, 673–681. doi: 10.1016/j.mcn.2007.12.010

Holmes, B. B., Furman, J. L., Mahan, T. E., Yamasaki, T. R., Mirbaha, H., Eades, W. C., et al. (2014). Proteopathic tau seeding predicts tauopathy *in vivo*. *Proc. Natl. Acad. Sci. U.S.A.* 111, E4376–E4385. doi: 10.1073/pnas.1411649111

Iba, M., Guo, J. L., McBride, J. D., Zhang, B., Trojanowski, J. Q., and Lee, V. M. (2013). Synthetic tau fibrils mediate transmission of neurofibrillary tangles in a transgenic mouse model of Alzheimer's-like tauopathy. *J. Neurosci.* 33, 1024–1037. doi: 10.1523/JNEUROSCI.2642-12.2013

Iliff, J. J., Chen, M. J., Plog, B. A., Zeppenfeld, D. M., Soltero, M., Yang, L., et al. (2014). Impairment of glymphatic pathway function promotes tau pathology after traumatic brain injury. *J. Neurosci.* 34, 16180–16193. doi: 10.1523/JNEUROSCI.3020-14.2014

Iliff, J. J., Wang, M., Liao, Y., Plogg, B. A., Peng, W., Gundersen, G. A., et al. (2012). A paravascular pathway facilitates CSF flow through the brain parenchyma and the clearance of interstitial solutes, including amyloid. *Sci. Transl. Med.* 4:147ra111. doi: 10.1126/scitranslmed.3003748

Kanmert, D., Cantlon, A., Muratore, C. R., Jin, M., O'Malley, T. T., Lee, G., et al. (2015). C-terminally truncated forms of tau, but not full-length tau or its C-terminal fragments, are released from neurons independently of cell death. *J. Neurosci.* 35, 10851–10865. doi: 10.1523/JNEUROSCI.0387-15.2015

Karch, C. M., Jeng, A. T., and Goate, A. M. (2012). Extracellular tau levels are influenced by variability in tau that is associated with tauopathies. *J. Biol. Chem.* 287, 42751–42762. doi: 10.1074/jbc.M112.380642

Karch, C. M., Jeng, A. T., and Goate, A. M. (2013). Calcium phosphatase calcineurin influences tau metabolism. *Neurobiol. Aging* 34, 374–386. doi: 10.1016/j.neurobiolaging.2012.05.003

Kfoury, N., Holmes, B. B., Jiang, H., Holtzman, D. M., and Diamond, M. I. (2012). Trans-cellular propagation of Tau aggregation by *fibrillar* species. *J. Biol. Chem.* 287, 19440–19451. doi: 10.1074/jbc.M112.346072

La Venuta, G., Zeitler, M., Steringer, J. P., Müller, H.-M., and Nickel, W. (2015). The startling properties of fibroblast growth factor 2: how to exit mammalian cells without a signal peptide at hand. *J. Biol. Chem.* 290, 27015–27020. doi: 10.1074/jbc.R115.689257

Luo, W., Liu, W., Hu, X., Hanna, M., Caravaca, A., and Paul, S. M. (2015). Microglial internalization and degradation of pathological tau is enhanced by an anti-tau monoclonal antibody. *Sci. Rep.* 5:11161. doi: 10.1038/srep11161

Magnoni, S., Esparza, T. J., Conte, V., Carbonara, M., Carrabba, G., Holtzman, D. M., et al. (2012). Tau elevations in the brain extracellular space correlate with reduced amyloid-β levels and predict adverse clinical outcomes after severe traumatic brain injury. *Brain* 135, 1268–1280. doi: 10.1093/brain/awr286

Maia, L. F., Kaeser, S. A., Reichwald, J., Hruscha, M., Martus, P., Staufenbiel, M., et al. (2013). Changes in amyloid-β and tau in the cerebrospinal fluid of transgenic mice overexpressing amyloid precursor protein. *Sci. Transl. Med.* 5:194re2. doi: 10.1126/scitranslmed.3006446

Mohamed, N. V., Desjardins, A., and Leclerc, N. (2017). Tau secretion is correlated to an increase of Golgi dynamics. *PLoS ONE* 12:178288. doi: 10.1371/journal.pone.0178288

Mohamed, N.-V., Plouffe, V., Rémillard-Labrosse, G., Planel, E., and Leclerc, N. (2014). Starvation and inhibition of lysosomal function increased tau secretion by primary cortical neurons. *Sci. Rep*. 4:5715. doi:10.1038/srep05715

Plouffe, V., Mohamed, N.-V., Rivest-McGraw, J., Bertrand, J., Lauzon, M., and Leclerc, N. (2012). Hyperphosphorylation and Cleavage at D421 enhance tau secretion. *PLoS ONE* 7:e36873. doi: 10.1371/journal.pone.0036873

Pooler, A. M., Phillips, E. C., Lau, D. H., Noble, W., and Hanger, D. P. (2013). Physiological release of endogenous tau is stimulated by neuronal activity. *EMBO Rep*. 14, 389–394. doi: 10.1038/embor.2013.15

Pooler, A. M., Usardi, A., Evans, C. J., Philpott, K. L., Noble, W., and Hanger, D. P. (2012). Dynamic association of tau with neuronal membranes is regulated by phosphorylation. *Neurobiol. Aging* 33, 431.e27–431.e38. doi: 10.1016/j.neurobiolaging.2011.01.005

Puzzo, D., Piacentini, R., Fá, M., Gulisano, W., Li Puma, D. D., Staniszewski, A., et al. (2017). LTP and memory impairment caused by extracellular Aβ and Tau oligomers is APP-dependent. *Elife* 6:e26991. doi: 10.7554/eLife.26991

Rodriguez, L., Mohamed, N. V., Desjardins, A., Lippé, R., Fon, E. A., and Leclerc, N. (2017). Rab7A regulates tau secretion. *J. Neurochem*. 141, 592–605. doi: 10.1111/jnc.13994

Saijo, E., Ghetti, B., Zanusso, G., Oblak, A., Furman, J. L., Diamond, M. I., et al. (2017). Ultrasensitive and selective detection of 3-repeat tau seeding activity in Pick disease brain and cerebrospinal fluid. *Acta Neuropathol*. 133, 751–765. doi: 10.1007/s00401-017-1692-z

Saman, S., Kim, W., Raya, M., Visnick, Y., Miro, S., Saman, S., et al. (2012). Exosome-associated tau is secreted in tauopathy models and is selectively phosphorylated in cerebrospinal fluid in early Alzheimer disease. *J. Biol. Chem.* 287, 3842–3849. doi: 10.1074/jbc.M111.277061

Takeda, S., Commins, C., DeVos, S. L., Nobuhara, C. K., Wegmann, S., Roe, A. D., et al. (2016). Seed-competent high-molecular-weight tau species accumulates in the cerebrospinal fluid of Alzheimer's disease mouse model and human patients. *Ann. Neurol.* 80, 355–367. doi: 10.1002/ana.24716

Takei, Y., Teng, J., Harada, A., and Hirokawa, N. (2000). Defects in axonal elongation and neuronal migration in mice with disrupted tau and map1b genes. *J. Cell Biol.* 150, 989–1000. doi: 10.1083/jcb.150.5.989

Tapiola, T., Alafuzoff, I., Herukka, S.-K., Parkkinen, L., Hartikainen, P., Soininen, H., et al. (2009). Cerebrospinal fluid β-amyloid 42 and tau proteins as biomarkers of Alzheimer-type pathologic changes in the brain. *Arch. Neurol.* 66, 382–389. doi: 10.1001/archneurol.2008.596

Walsh, D. M., and Selkoe, D. J. (2016). A critical appraisal of the pathogenic protein spread hypothesis of neurodegeneration. *Nat. Rev. Neurosci.* 17, 251–260. doi: 10.1038/nrn.2016.13

Wang, Y., Balaji, V., Kaniyappan, S., Krüger, L., Irsen, S., Tepper, K., et al. (2017). The release and trans-synaptic transmission of Tau via exosomes. *Mol. Neurodegener.* 12, 5. doi: 10.1186/s13024-016-0143-y

Weissmann, C., Reyher, H. J., Gauthier, A., Steinhoff, H. J., Junge, W., and Brandt, R. (2009). Microtubule binding and trapping at the tip of neurites regulate tau motion in living neurons. *Traffic* 10, 1655–1668. doi: 10.1111/j.1600-0854.2009.00977.x

Wu, J. W., Hussaini, S. A., Bastille, I. M., Rodriguez, G. A., Mrejeru, A., Rilett, K., et al. (2016). Neuronal activity enhances tau propagation and tau pathology *in vivo*. *Nat. Neurosci.* 19, 1085–1092. doi: 10.1038/nn.4328

Yamada, K., Cirrito, J. R., Stewart, F. R., Jiang, H., Finn, M. B., Holmes, B. B., et al. (2011). *In vivo* microdialysis reveals age-dependent decrease of brain interstitial fluid tau levels in P301S human tau transgenic mice. *J. Neurosci.* 31, 13110–13117. doi: 10.1523/JNEUROSCI.2569-11.2011

Yamada, K., Holth, J. K., Liao, F., Stewart, F. R., Mahan, T. E., Jiang, H., et al. (2014). Neuronal activity regulates extracellular tau *in vivo*. *J. Exp. Med.* 211, 387–393. doi: 10.1084/jem.20131685

Yamada, K., Patel, T. K., Hochgräfe, K., Mahan, T. E., Jiang, H., Stewart, F. R., et al. (2015). Analysis of *in vivo* turnover of tau in a mouse model of tauopathy. *Mol. Neurodegener.* 10, 55. doi: 10.1186/s13024-015-0052-5

Yanamandra, K., Jiang, H., Mahan, T. E., Maloney, S. E., Wozniak, D. F., Diamond, M. I., et al. (2015). Anti-tau antibody reduces insoluble tau and decreases brain atrophy. *Ann. Clin. Transl. Neurol.* 2, 278–288. doi: 10.1002/acn3.176

Yanamandra, K., Patel, T. K., Jiang, H., Schindler, S., Ulrich, J. D., Boxer, A. L., et al. (2017). Anti-tau antibody administration increases plasma tau in transgenic mice and patients with tauopathy. *Sci. Transl. Med.* 9:eaal2029. doi: 10.1126/scitranslmed.aal2029

Conflict of Interest Statement: The author declares that the research was conducted in the absence of any commercial or financial relationships that could be construed as a potential conflict of interest.

frontiers in Neuroscience

REVIEW
published: 06 February 2018
doi: 10.3389/fnins.2018.00044

Phospho-Tau Bar Code: Analysis of Phosphoisotypes of Tau and Its Application to Tauopathy

Taeko Kimura[1†], *Govinda Sharma*[1], *Koichi Ishiguro*[2] *and Shin-ichi Hisanaga*[1*]

[1] *Laboratory of Molecular Neuroscience, Department of Biological Sciences, Tokyo Metropolitan University, Hachioji, Japan,*
[2] *Department of Neurology, Graduate School of Medicine, Juntendo University, Bunkyo, Japan*

Tau is a microtubule-associated protein which regulates the assembly and stability of microtubules in the axons of neurons. Tau is also a major component of neurofibrillary tangles (NFTs), a pathological hallmark in Alzheimer's disease (AD). A characteristic of AD tau is hyperphosphorylation with more than 40 phosphorylation sites. Aggregates of hyperphosphorylated tau are also found in other neurodegenerative diseases which are collectively called tauopathies. Although a large number of studies have been performed on the phosphorylation of AD tau, it is not known if there is disease-specific phosphorylation among tauopathies. This is due to the lack of a proper method for analyzing tau phosphorylation *in vivo*. Most previous phosphorylation studies were conducted using a range of phosphorylation site-specific antibodies. These studies describe relative changes of different phosphorylation sites, however, it is hard to estimate total, absolute and collective changes in phosphorylation. To overcome these problems, we have recently applied the Phos-Tag technique to the analysis of tau phosphorylation *in vitro* and *in vivo*. This method separates tau into many bands during SDS-PAGE depending on its phosphorylation states, creating a bar code appearance. We propose calling this banding pattern of tau the "phospho-tau bar code." In this review article, we describe what is newly discovered regarding tau phosphorylation through the use of the Phos-Tag. We would like to propose its use for the postmortem diagnosis of tauopathy which is presently done by immunostaining diseased brains with anti-phospho-antibodies. While Phos-tag SDS-PAGE, like other biochemical assays, will lose morphological information, it could provide other types of valuable information such as disease-specific phosphorylation.

Keywords: phos-tag, tau, phosphorylation, Alzheimer' disease, tauopathy, Cdk5, phospho-tau bar code, GSK3β

OPEN ACCESS

Edited by:
Gen Sobue,
Nagoya University, Japan

Reviewed by:
Laura J Blair,
University of South Florida, United States
Cheng-Xin Gong,
Institute for Basic Research in Developmental Disabilities (IBR), United States

***Correspondence:**
Shin-ichi Hisanaga
hisanaga-shinichi@tmu.ac.jp

†Present Address:
Taeko Kimura,
Department of Functional Brain Imaging Research, National Institute of Radiological Sciences, Chiba, Japan

Specialty section:
This article was submitted to Neurodegeneration, a section of the journal Frontiers in Neuroscience

Received: *09 November 2017*
Accepted: *18 January 2018*
Published: *06 February 2018*

Citation:
Kimura T, Sharma G, Ishiguro K and Hisanaga S (2018) Phospho-Tau Bar Code: Analysis of Phosphoisotypes of Tau and Its Application to Tauopathy. Front. Neurosci. 12:44. doi: 10.3389/fnins.2018.00044

INTRODUCTION

Tau is a microtubule (MT)-associated protein (MAP) predominantly expressed in the axons of neurons (Dehmelt and Halpain, 2005; Iqbal et al., 2016; Wang and Mandelkow, 2016). Tau is a phosphoprotein that is targeted by a number of protein kinases. The phosphorylation of tau regulates its functions, namely the assembly and stabilization of MTs (Lindwall and Cole, 1984; Iqbal et al., 2016; Wang and Mandelkow, 2016). Additionally, it is well known that hyperphosphorylated tau is a major component of neurofibrillary tangles (NFTs) in Alzheimer's

disease (AD) (Ballatore et al., 2007; Spillantini and Goedert, 2013; Wang et al., 2013; Arendt et al., 2016). There are many other neurodegenerative diseases in which deposits of hyperphosphorylated tau are found. These diseases are collectively called tauopathies (Lee et al., 2001). The fact that Frontotemporal dementia with Parkinsonism linked to Chromosome 17 (FTDP-17), a tauopathy, is caused by the mutation of the tau gene *MAPT* indicates that tau may be a causative factor for other tauopathies in addition to FTDP-17 (Hutton et al., 1998; Poorkaj et al., 1998; Spillantini et al., 1998). It is not known how tau gains neuronal toxicity, however, several possibilities such as oligomerization, aggregation, or hyperphosphorylation have been proposed. It is unclear whether or not the hyperphosphorylation is a cause or result of disease, however, the immunostaining of postmortem brains with anti-phospho-tau antibodies such as AT8, AT180, and PHF1 is usually used as a definitive diagnosis of AD and tauopathy. Therefore, extensive efforts have been made to identify phosphorylation sites and the hyperphosphorylation mechanism. Nevertheless, it is not yet known how this phosphorylation is regulated not only under disease conditions but also in normal brains.

Comprehensive analysis of tau phosphorylation by mass spectroscopy has revealed more than 40 phosphorylation sites in AD pathological tau (Morishima-Kawashima et al., 1995; Hanger et al., 2007). Since antibodies against many of these phosphorylation sites are now commercially available, phosphorylation of tau is currently analyzed using those phosphorylation-site specific antibodies in both physiological and pathological studies. While their use is relatively easy and they are sensitive enough to detect slight changes in phosphorylation levels, there are several unavoidable limitations (described later in detail). When proteins have many phosphorylation sites it is hard to estimate the absolute degree of *in vivo* phosphorylation and discern any combinations of these phosphorylation sites. To answer these difficult but important questions we applied the Phos-Tag SDS-PAGE method to the analysis of tau phosphorylation *in vitro* and *in vivo* (Kimura et al., 2016a,b). We found that tau consists of many bands, resembling a bar code, which indicates heterogeneous phosphorylation in cells and brains. Further, the banding patterns were different depending on phosphorylation states. We call this phosphorylation-dependent banding pattern of tau the "phospho-tau bar code." We think that the phosphorylation profile would be very useful to identify and diagnose different tauopathies if their phosphorylation is distinctive. Here, we introduce the use of the Phos-tag method in the analysis of tau phosphorylation in physiology and pathology.

Abbreviations: 3R, 3 repeats; 4R, 4 repeats; AD, Alzheimer's disease; CBD, corticobasal degeneration; Cdk5, cyclin-dependent kinase 5; GSK3β, glycogen synthase kinase 3beta; MAP, microtubule-associated protein; MT, microtubule; MTB, microtubule-binding repeats; MAPK, mitogen-activated kinase; NFT, neurofibrillary tangle; PDPK, proline-directed protein kinase; FTDP-17, frontotemporal dementia and parkinsonism linked to chromosome 17; NF-H, Neurofilament heavy chain; PKA, protein kinase A; PKC, protein kinase C; CaMKII, calcium-calmodulin-dependent protein kinase II; SDS-PAGE, sodium dodecyl sulfate polyacrylamide gel electrophoresis.

COMPLICATED PHOSPHORYLATION OF TAU IN CELLS AND BRAINS

Tau may be one of the most complicatedly phosphorylated proteins. Tau has 45 serine, 35 threonine and 5 tyrosine residues, resulting in a total of 85 possible phosphorylation sites in the longest human tau isoform composed of 441 amino acids (Goedert et al., 1989). Among them, more than 40 sites are reported to be phosphorylated (**Figure 1**; Chauhan et al., 2005; Hanger et al., 2007; Wang et al., 2013; Iqbal et al., 2016), and most reside in the Pro-rich region and C-terminal tail region flanking the MT-binding repeats (MTBs). The high density of phosphorylation could be, at least partly, due to an unfolded and extended structure of tau enabling protein kinases to easily access their target sites in consensus phosphorylation sequences. The total number of phosphorylation sites were compiled from data reported in a large number of publications. While it is not likely that a single tau molecule is phosphorylated at all of these sites, it is also unlikely that phosphorylation at all of these sites is completely independent (Hernández et al., 2003). If they were phosphorylated independently, the number of tau phosphorylation combinations would be $\sim 10^{12}$ ($= 2^{40}$) (**Figure 1**), an astronomical figure. It is important to understand which sites are phosphorylated in which occasions. A number of phosphorylation sites have been found to regulate MT-binding and -assembly activity of tau and to be involved in development, morphogenesis, and the maintenance of axons in neurons (Lindwall and Cole, 1984; Dehmelt and Halpain, 2005; Wang and Mandelkow, 2016). While those sites are suggested to be in the Pro-rich region and MTB repeats domain, their site-specific functions are not completely understood. Other sites are abnormally phosphorylated in aggregates in AD brains. However, it is not clear which sites contribute to the aggregate formation or are just phosphorylated within the aggregates.

Phosphorylation is the balance of protein kinase and protein phosphatase activity. Several tau kinases such as PKA, CaMKII, PKC, and MAPKs are transiently activated by external or internal stimuli, and their target sites should also be phosphorylated only transiently in healthy neurons and brains. In contrast, several Ser/Thr-Pro {(S/T)P} phosphorylation sites in tau are constitutively phosphorylated which suggests that they are phosphorylated by house-keeping kinase–protein kinases that are active in resting cells (Kimura et al., 2014). However, it is still unclear which sites are phosphorylated, and to what extent and in what context they are phosphorylated. Therefore, the tau phosphorylation is often mentioned as just "phosphorylation" without considering context-dependency.

Tau phosphorylation has several other characteristics that make its phosphorylation complex. A lot of sites are phosphorylated by multiple protein kinases (Chauhan et al., 2005; Hanger et al., 2009; Wang et al., 2013). For example, Ser262 in KXGS motifs in the repeat domain is phosphorylated by MARK, PKA and CaMKII with different activation mechanisms (Drewes et al., 1995; Sironi et al., 1998; Ando et al., 2016). There are 16 (S/T)P sequences in tau, many of which are known as abnormal phosphorylation sites in AD brains

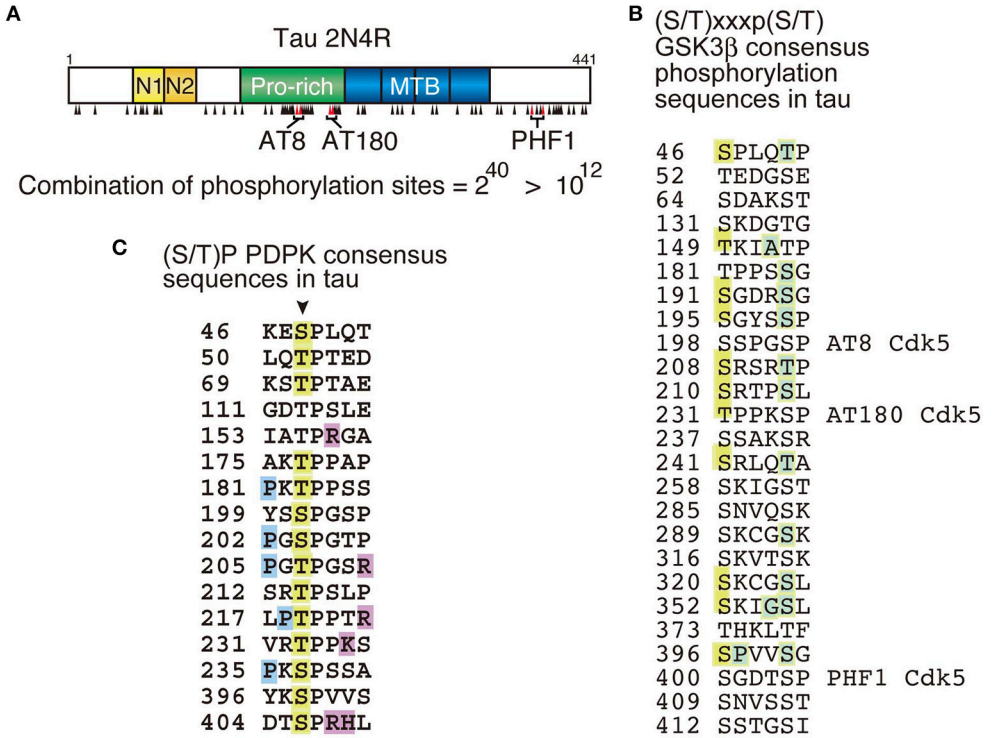

FIGURE 1 | Phosphorylation sites in tau molecule. **(A)** The longest human tau isoform is composed of 441 amino acids with four microtubule-binding (MTB) repeats in the C-terminal half. Phosphorylation sites are indicated by black arrowheads. AT8 (Ser202 and Thr205), AT180 (Thr231 and Ser235) and PHF1 (Ser396 and Ser404) are phosphospecific antibodies frequently used for the postmortem diagnosis of tauopathy and their epitopes are indicated. The number of phosphorylation combination, if all sites are phosphorylated independently, is indicated below. **(B)** Amino acid sequences conforming to the GSK3β consensus sequences, (S/T)xx(x)p(S/T), in tau. There are 25 such sequences and 12 sites are reported to be phosphorylated (orange). The site in the C-terminal sides known to be phosphorylated are indicated by green. **(C)** Ser/Thr-Pro {(S/T)P} sequences in tau targeted by proline-directed protein kinases (PDPK). Arrow indicates Ser or Thr in (S/T)P sequences. Orange is the reported phosphorylation sites, blue is proline (P) conforming to the consensus sequence {Px(S/T)P or P(S/T)P} for MAPK, and magenta is basic amino acids at the C-terminal site which makes Ser or Thr phosphorylation sites favorable for Cdk5.

(**Figure 1C**; Kimura et al., 2014). Those (S/T)P sites are targeted by proline-directed protein kinases (PDPKs) such as MAPK (ERK, JNK, and p38 SAPK), GSK3β, Cdk5-p35/p25, and Dyrk1A (Chauhan et al., 2005; Ryoo et al., 2007; Hanger et al., 2009). Since these PDPKs display different substrate preferences; ERK prefers Px(S/T)P or P(S/T)P sequence, Cdk5-p35/p25's consensus is (S/T)Px(K/R/H), and GSK3β phosphorylates (S/T)XXXp(S/T) sequence in addition to (S/T)P sites; their phosphorylation profiles of tau should be different. In fact, some differences are shown by 2D-phospho-peptide mapping–the method which displays the whole phosphorylation profile at once (Illenberger et al., 1998; Sakaue et al., 2005). However, because this method requires isotope labeling of proteins, it is almost impossible to apply to *in vivo* phosphorylation studies. Further with respect to phosphorylation by a single kinase, there are major and minor phosphorylation sites. It has been recently reported that the phosphorylation at Thr205 specifically inhibits amyloid beta (Aβ) toxicity; (Ittner et al., 2016). In that paper, authors examine phosphorylation of tau by p38γ *in vitro* and in cell and in mouse brains using phospho-specific antibodies and Mass spectrometry. They showed four major sites at Ser199, Thr205, Ser396, and Ser404 with 14 minor sites in an *in vitro* kinase assay, but Thr205 alone is strongly phosphorylated in cells and brains overexpressing p38γ. This kind of comprehensive analysis is not always done in every laboratory. More often the phosphorylation sites are discussed without considering quantitative aspects. About 8–11 sites in tau are reported to be Cdk5-p35/p25 phosphorylation sites (Chauhan et al., 2005; Hanger et al., 2009). However, if phosphorylation sites are examined by biochemical methods, it turns out that there are only 3 or 4 major sites located at Ser202 or Thr205, Ser235, and Ser404 (Wada et al., 1998; Sakaue et al., 2005; Kimura et al., 2014). Other sites might be detected with anti-phospho-antibodies which are sensitive enough to detect small levels of phosphorylation, but not distinguish between major and minor phosphorylation sites. Interestingly, these major sites are phosphorylated in consecutive order from the C-terminal site: Ser404, Ser235, and then Thr205 (Kimura et al., 2016b). This kind of information can be determined if the total phosphorylation profile is seen.

The second complicating factor in tau phosphorylation is the ordered phosphorylation, or phosphorylation affected by prior phosphorylation. It is well known that GSK3β is a hierarchical kinase acting on a target site which has prior

phosphorylation at +4 (or +3) site, (S/T)xx(x)p(S/T), by a priming kinase. There are 25 such sequences in tau, and 12 sites are indeed phosphorylated, even though not all of them have the primary phosphorylation (**Figure 1B**). This disagreement between the consensus and real phosphorylation sites may arise from an incomplete analysis with anti-phospho-antibodies. Pathological phosphorylation sites at AT8, AT180 and PHF1 by GSK3β are primed by Cdk5-p35/25 (Li et al., 2006; Kimura et al., 2014). Therefore, tau phosphorylation by GSK3β in cultured cells is dependent on the coexpression of Cdk5-p35. In other words, neurons expressing endogenous Cdk5-p35 or in the case of non-neuronal cells, coexpression with Cdk5-p35 is required for tau phosphorylation by GSK3β. More complicatedly, phosphorylation of tau at the AT-8 (and/or PHF-1) site by GSK3β is primed by PKA phosphorylation at Ser214 even though their phosphorylation sites are separated (Liu et al., 2002, 2004), while GSK3β phosphorylation at Thr212 enhances phosphorylation at Ser214 by PKA (Zheng-Fischhöfer et al., 1998). Phosphorylation by Cdk5 is also influenced, but negatively, by prior phosphorylation. For example, it has been shown that Cdk5-p35/p25 phosphorylates Ser202 and Thr205 at the AT8 site (Shahpasand et al., 2012), but they are not phosphorylated at the same time by Cdk5-p35/p25. In *in vitro* phosphorylation of tau by Cdk5, Cdk5-p35/p25 phosphorylates Thr205 faster than Ser202, and when Thr205 is phosphorylated once, Ser202 phosphorylation by Cdk5 is suppressed (Kimura et al., 2016b). In contrast, in cultured cells where there is endogenous protein kinase(s) phosphorylating Ser202 strongly, Cdk5 can no longer target the Thr205 of tau with Ser202 phosphorylation (Kimura et al., 2016b). However, if tau binds to microtubules, these two sites can be phosphorylated simultaneously by Cdk5 (Wada et al., 1998).

The third complication in tau phosphorylation is problems in the specificity or reactivity of anti-phospho-specific antibodies. Some phospho-specific antibodies are generated against a phosphopeptide with a single phosphorylation at a site of interest. However, several phosphorylation sites in tau are located very close together and, in extreme cases, are right next to each other. The reactivity of the phospho-specific antibody would be affected by any other phosphorylated sites nearby. We recently encountered such a case where the reactivity of anti-pSer202 varied depending of phosphorylation at Thr205 (Kimura et al., 2016b). We therefore found it difficult to assess the *in vivo* phosphorylation of tau at Ser202 properly with that antibody.

THE ROLE OF PHOSPHORYLATION ON CELLULAR LOCALIZATION AND STRUCTURE OF TAU

Tau is mainly localized to axons of neurons in association with microtubules. The axonal tau is detected with Tau-1 antibody which recognizes nonphosphorylation at Ser199 and Ser202 (Binder et al., 1985), and displays a gradient distribution such that dephosphorylated tau is more abundant at the distal region of the axon (Mandell and Banker, 1996). However, it has recently been shown that a small amount of tau is present in dendrites and dendritic spines (Ittner et al., 2010). Dendritic or dendritic spine tau is phosphorylated at AT8 sites, whose phosphorylation is increased by a brief and nontoxic treatment of neurons with glutamate (Kobayashi et al., 2017). Abnormal accumulation of tau in the cell body and dendrites is the result of mislocalization, which is considered an early event in tau pathology. For example, the treatment of neurons with Aβ oligomers induces the transfer of tau to dendrites with enhanced phosphorylation at 12E8 sites (Ser262 and Ser356), which are mediated by MARK, SAD or p70S6K localized in dendrites and spines (Zempel et al., 2010). A fraction (10 ∼ 20%) of tau binds to plasma membrane (Brandt et al., 1995; Arrasate et al., 2000; Gauthier-Kemper et al., 2011; Pooler et al., 2012). This tau is not phosphorylated, at least at AD sites such as AT8, PHF-1, and AT-180 (Maas et al., 2000; Pooler et al., 2012). The interaction with membranes is increased by inhibiting casein kinase I or GSK3β or by a phosphorylation-mimicking mutation at the N-terminal residues (Pooler et al., 2012). Tau is also found in the nucleus where it exists mainly in a dephosphorylated state (Loomis et al., 1990; Greenwood and Johnson, 1995; Sultan et al., 2011). Thus, phosphorylation regulates cellular localization of tau but the mechanism is not completely understood.

Phosphorylation also controls the conformation of tau. Tau is a naturally unfolded protein. Nevertheless, tau adopts a "paperclip-like shape" conformation where the N-terminal and C-terminal domains fold to approach the repeat domain (Jeganathan et al., 2006). Phosphorylation at AT8 and PHF sites open the structure to move the N-terminal and C-terminal away respectively (Jeganathan et al., 2008). AT8 site phosphorylation extends the N-terminal region, resulting in the increase of the inter-microtubule distance in neurites (Shahpasand et al., 2012). Phosphorylation at the proline-directed (S/T)P motifs regulates the *trans*-to-*cis* isomerization (Lu et al., 1999). Peptidyl-prolyl cis-trans isomerase Pin1 binds to phosphorylated (S/T)P sequences to convert *cis* to a *trans* conformation, which can be dephosphorylated by protein phosphatase 2A (Zhou et al., 2000: Kimura et al., 2013). In particular, the cis conformation at phosphorylated Thr231 has a toxic activity, leading to tau-dependent neurodegeneration (Kondo et al., 2015). AD tau is highly phosphorylated and aggregated (Ballatore et al., 2007; Spillantini and Goedert, 2013; Wang et al., 2013; Arendt et al., 2016). A role for the HSP90-CHIP complex is suggested in pathology of tauopathies via its recognition and selective degradation of phosphorylated tau (Dickey et al., 2007). Tyr phosphorylation of tau also correlates with the formation of tau aggregates (Vega et al., 2005).

PHOS-TAG SDS-PAGE; A POWERFUL TECHNIQUE FOR ANALYSIS OF OVERALL, QUANTITATIVE AND COMBINATORY PHOSPHORYLATION

Phosphorylation often reduces the electrophoretic mobility of proteins in Laemmli's SDS-PAGE. These shifts have been considered as evidence of phosphorylation. Neurofilament

proteins NF-M and NF-H are typical examples of phosphorylated, shifted proteins. NF-H which is phosphorylated at the KSP sequences in the C-terminal tail region–as many as ∼50 sites in the axons of neurons–moves to a position of 200 kDa on Laemmli's SDS-PAGE (Julien and Mushynski, 1998; Pant et al., 2000). Dephosphorylation of NF-H decreases its apparent molecular size to 140 kDa (Julien and Mushynski, 1982; Hisanaga and Hirokawa, 1989). While the up-shift and down-shift can be used as an indication of phosphorylation and dephosphorylation, they do not, however, provide further information on phosphorylation. Moreover, a shift does not always occur in every protein. Larger numbers of proteins, particularly those with a few phosphorylation sites, have an overall unaffected electrophoretic mobility upon phosphorylation.

Phos-tag SDS-PAGE is a phosphoaffinity electrophoresis method which was developed by Kinoshita et al. (2006). The procedure of Phos-tag SDS-PAGE is simple, similar to that of Laemmli's SDS-PAGE except for the use of Phos-tag acrylamide (commercially available from Wako Chemical) as a separating gel. The Phos-tag is a chemical structure capable of capturing the phosphate on proteins. Therefore, migration of phosphorylated proteins are extraordinarily delayed during electrophoresis due to their binding to the Phos-tag moiety conjugated to acrylamide. Importantly, the degree of the delay, that is the upward shift, is dependent on the number and site of phosphorylation so that phosphorylated proteins are separated into distinct bands depending on their phosphorylation states (**Figure 2**). Species of proteins with different combinations of phosphorylated sites are designated as "phosphoisotypes" (Kinoshita et al., 2009; Hosokawa et al., 2010). After blotting on a nitrocellulose or PVDF membrane, all phosphoisotyes would be detected with a phosphorylation-independent antibody of a protein of interest (see Kinoshita et al., 2009 more in detail).

There are the following advantages in the use of the Phos-tag method. (1) The total phosphorylation profile of the particular protein is seen at a glance (see **Figure 4** for an example). This is because all phosphoisotypes of the protein including the nonphosphorylated one, can be detected on a single blot membrane with a single antibody. It is easy to know whether your protein of interest is phosphorylated *in vivo* or not without prior labeling of proteins or the use of phospho-specific antibodies. The only thing to be cautious of is dephosphorylation and the proteolytic cleavage of proteins during sample preparation. (2) If it is known that the protein is phosphorylated, then a phosphorylation site(s) can be readily determined by the loss of the upward shift with a nonphosphorylation Ala mutant at candidate sites. We have newly identified the phosphorylation sites of several proteins, ataxin 2, drebrin and GRAB, by applying this method (Asada et al., 2014; Tanabe et al., 2014; Furusawa et al., 2017). (3) Once you have determined the phosphorylation states of each band, you may determine the combination of phosphorylated sites even *in vivo* by comparing with the standard profile of phosphoisotypes. (4) The relative ratio of each phosphoisotype can be measured as a percent ratio of the total by densitometric scanning of the blots. We have determined the ratio of phosphoisotypes of p35 Cdk5 activator *in vivo* and found it changes with brain development (Hosokawa et al., 2010; Krishnankutty et al., 2017). It was difficult to obtain this kind of information through the use of previous methods. We think this method would be useful to reveal the age-dependent changes of tau phosphorylation.

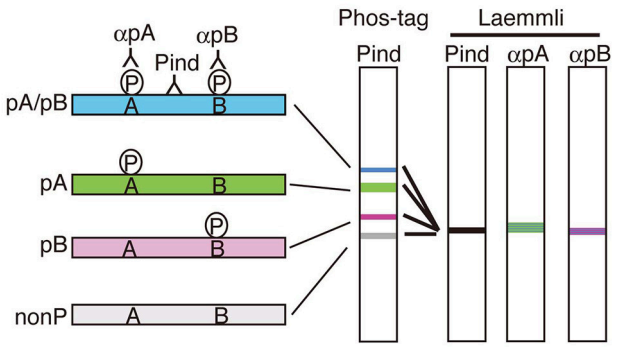

FIGURE 2 | Separation of phosphoisotypes of a protein on Phos-tag SDS-PAGE. If there are two phosphorylation sites, A and B, in a protein, there would be 4 phosphoisotypes, doubly phosphorylated (blue), two single site-phosphorylated (green and red) and nonphosphorylated (left). These four phosphoisotypes can be separated into four bands on Phos-tag SDS-PAGE by shifting upward differently depending on the number and site of phosphorylation (Phos-tag). Phospho-specific antibodies, αpA and αpB, are required to detect the respective phosphorylation in Laemmli's SDS-PAGE, in contrast, the separation in Phos-tag indicates not only phosphorylation but also the degree of phosphorylation detected with a phosphorylation-independent antibody alone (Pind).

Another favorable feature of this technique is its easy and simple implementation. Every laboratory, where immunoblotting is routinely carried out, can employ it immediately without any extra equipment. Further, the method does not require the preparation of phosphospecific antibodies, although it is preferable to use them if possible. Moreover, the samples already prepared for Laemmli's SDS-PAGE can be used for Phos-tag SDS-PAGE as well. In contrast, a weakness of Phos-tag SDS-PAGE is the analysis of phosphoproteins composed of multiple isoforms with different molecular weights such as tau. Because the method depends on the upward mobility shift of phosphorylated isoforms, it would be difficult to distinguish the phosphorylated bands from the larger isoforms. Further, when the number of phosphorylation sites is increased, the banding pattern would become more complicated. This method may be most powerful on single isoform proteins with 2∼3 phosphorylation sites such as a p35 Cdk5 activator or GSK3β we have reported (Hosokawa et al., 2010; Krishnankutty et al., 2017). Therefore, it is somewhat challenging to analyze tau by this method. So far we have employed one-dimensional Phos-tag SDS-PAGE, where we have identified most of the phosphorylation sites of a single tau isoform expressed in cultured cells and not *in vivo* tau in mouse brains. However, by increasing resolution, for example, using 2-dimentional SDS-PAGE composed of Laemmli's and Phos-tag, it would become possible to analyze each isoform separately. Otherwise, by developing the isolation method

of a single isoform, for example, by immunoprecipitation, we may determine the isoform-specific phosphorylation sites.

PHOSPHO-TAU BAR CODE

While the identification of tau phosphorylation was initially determined comprehensively by the methods of amino acid sequence and Mass analysis (Watanabe et al., 1993; Morishima-Kawashima et al., 1995), recently most studies use anti-phospho-antibodies to detect and confirm them. The use of anti-phospho-antibodies describe phosphorylation states of corresponding epitope sites, but as described above, however, the heterogeneous and complicated phosphorylation of tau make the interpretation of total and quantitative phosphorylation difficult. It is as difficult to conceive of the total complete picture of tau phosphorylation as a whole, as it is for the blind men touching just part of an elephant to describe the whole animal (**Figure 3A**). It is desirable to ascertain the total phosphorylation of a protein easily and simply (**Figure 3B**). In order to reveal the overall phosphorylation profiles of tau, we have applied the Phos-tag method to tau phosphorylation *in vitro*, in cells, and in mouse and human brains (Kimura et al., 2016a,b). In *in vitro* experiments using Cdk5-p25 as a protein kinase, we found that tau was phosphorylated mainly at Thr205, Ser235, and Ser404 sequentially from the C-terminal to N-terminal sites. When expressed in COS-7 cells, tau was separated into as many as 12 bands using Phos-tag SDS-PAGE. Their respective phosphorylation sites were determined and it was found that tau was phosphorylated at 0–5 sites in different combinations (**Figure 4A**; Kimura et al., 2016b). Coexpression of Cdk5-p35 shifted up each tau bands by phosphorylating Ser404. Through quantification, it was determined that Thr231 was easily phosphorylated in about 50% of total tau molecules expressed

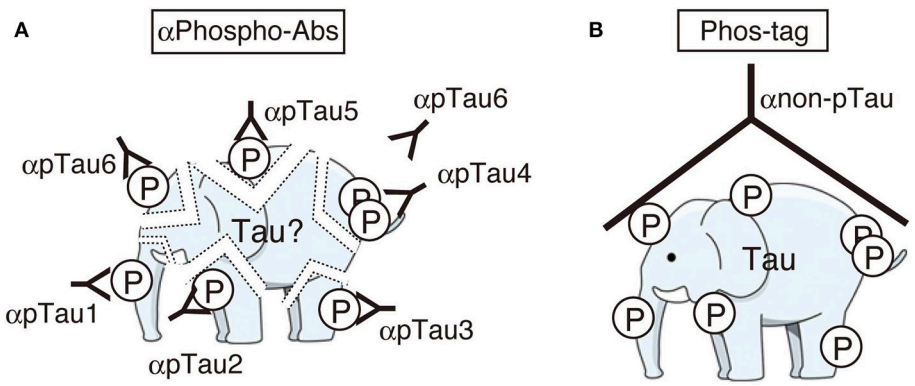

FIGURE 3 | Cartoons representing the images of immunoblotting with many phospho-specific antibodies **(A)** and a phosphorylation-independent single antibody after Phos-tag SDS-PAGE **(B)**. Phosphospecific antibodies detect only part of phosphorylation at each site and some sites can be masked by another phosphorylated site nearby (here the site for αpTau6 is masked by a phosphorylated site which reacts with αpTau4). Phos-tag shows the whole phosphorylation profile at once. An illustration of an elephant was downloaded from the free illustration site at: http://illpop.com/png_animalhtm/elephant_a04.htm.

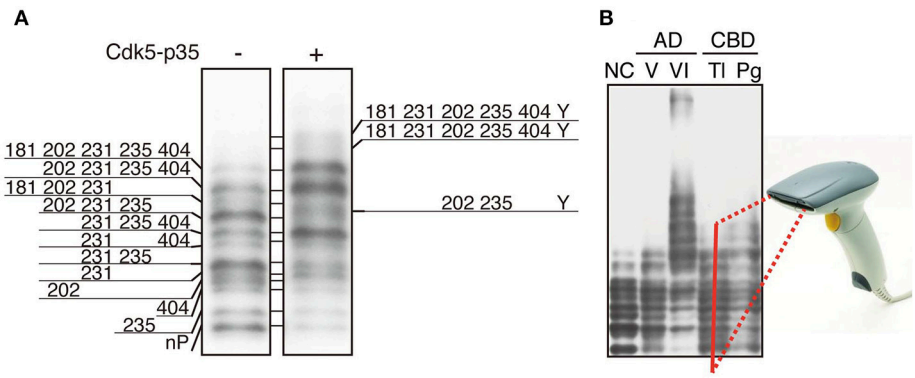

FIGURE 4 | Phosphoisotypes of tau on Phos-tag SDS-PAGE. **(A)** Immunoblotting of tau expressed in COS-7 cells with tau5 in the presence (+) or absence (–) of Cdk5-p35 after Phos-tag-SDS-PAGE, and the phosphorylation sites in each band are indicated by the amino acid number according to the human longest isoform of tau. Y is an unknown phosphorylation site. **(B)** Immunoblotting of tau in human brains after Phos-tag SDS-PAGE. NC, normal control; AD V and VI, Braak stage V and VI of Alzheimer's disease (AD); CBD TI and Pg, temporal lobe (TI) and prefrontal gyrus (Pg) of corticobasal degeneration (CBD). We propose that the banding pattern created using Phos-tag SDS-PAGE could be read by a bar code reader and result in a simple method for diagnosing tauopathy. **(A,B)** are reproduced and modified from figures reported previously by Kimura et al. (2016a,b), respectively.

in COS-7 cells. Tau in mouse brains was also composed of a number of different phosphoisotypes and this pattern changed with brain development (Kimura et al., 2016a). To us the banding patterns resemble a bar code, thus we call it "Phospho-tau bar code."

APPLYING THE PHOSPHO-TAU BAR CODE TO PATHOLOGICAL PHOSPHORYLATION IN TAUOPATHY BRAINS

Tau is highly phosphorylated in aggregates in AD brains and possibly in other tauopathy brains. In fact, postmortem diagnosis of tauopathies, including AD, is done by immunohistochemical staining of patients' brains with anti-tau phospho-specific antibodies such as AT8 (Ser202 and Thr205), AT180 (Thr231 and Ser235) and PHF1 (Ser396 and Ser404) (**Figure 1A**). Since each tauopathy differs in the affected regions and aggregated structures (Ballatore et al., 2007; Spillantini and Goedert, 2013; Wang et al., 2013; Arendt et al., 2016), the immunohistochemistry involving morphological information can serve as diagnosis. In contrast, although it is known by the immunoblotting that isoforms forming aggregates are different depending on tauopathies; both 3R and 4R in AD, 4R in CBD and PSP, and 3R in Pick's disease, it is not used for diagnosis because the procedure is relatively burdensome and the isoform differences may not be sufficient for distinguishing between many tauopathies. However, it has recently been proposed that there are tau strains with distinct structural conformations which could underlie the heterogeneity of tauopahites (Sanders et al., 2014). While the strain specific for each tauopathy has not been established yet, there is a possibility that respective strains might differ in their phosphorylation. We have compared phosphorylation profiles of tau in AD and corticobasal degeneration (CBD) with that of normal control using Phs-tag SDS-PAGE (Kimura et al., 2016a). The expression of 6 tau isoforms with slightly different molecular sizes in human adult brains made analysis extremely difficult, although the use of 3R (tau isoforms with three MTB) or 4R (tau isoforms with four MTB) specific antibodies or phospho-specific antibodies reduced the number of bands to some extent. Even though tau in Sarkosyl-insoluble aggregates prepared from AD patient brains displayed a smeared banding pattern on the immunoblots after Laemmli's SDS-PAGE, their separation on Phos-tag suggests that several phosphorylated tau bands show similar mobility to hyperphosphorylated tau species in brains of perinatal mice or hypothermia mice. This suggests some similarity in phosphorylation between AD and embryonic/perinatal brains, as was previously reported (Morishima-Kawashima et al., 1995). When tau in the brain extracts was analyzed by Phos-tag, tau at Braak stage V of AD contained slightly shifted up bands compared to normal control (**Figure 4B**), and tau in brains of corticobasal degeneration (CBD) patients displayed a slightly different banding pattern. This different banding patterns of tau between AD and CBD may suggest different phosphorylation states among tauopathies. If distinct phosphorylation profiles will be found among tauopathies, the method can be applied to their diagnosis. Even if this method alone is not enough to make the diagnosis, the obtained information would assist the diagnosis by immunohistochemistry and also be useful for better understanding tau pathology. Further, if the sensitivity of detection will be increased, this method may be applied to diagnosis using cerebrospinal fluids. Moreover, phosphorylation profiles would be used for the development of therapeutic drugs. Several protein kinase inhibitors are in Phase II trials for AD in 2017 (Cummings et al., 2017). Despite considerable efforts, however, success so far is insufficient. If the involvement of a specific kinase in particular processes of different tauopathies is clarified, the more specific strategy could become possible. In addition to the development of small chemical molecules, it would be possible to develop the drug based on the activation or inhibition mechanism of respective protein kinases. One such kinase inhibitor is TFP5, the peptide derived from the amino acid sequence of p35 Cdk5 activator, which inhibits hyperactive Cdk5-p25 specifically *in vivo* (Shukla et al., 2017).

CONCLUSION

Tauopathy neurodegenerative disorders including AD are characterized by intracellular inclusions composed of hyperphosphorylated tau. Immunocytochemical detection of tau inclusions with phospho-specific tau antibodies is usually used as a postmortem diagnosis of diseases. The different staining patterns depending on disease type suggest disease-specific phosphorylation but it is not yet clear. It is desirable to use a method which examines the total phosphorylation profiles of tau simply. We recently applied the Phos-tag technique to analyze tau phosphorylation in mouse and human brains, and found that tau is separated into many bands, resembling a bar code of many different phosphoisotypes. Here, we name such a banding pattern of tau on Phos-tag SDS-PAGE the "phospho-tau bar code" and propose its use for the diagnosis of tauopathies.

AUTHOR CONTRIBUTIONS

TK and SH wrote the whole manuscript. GS and KI made figures and edited the manuscript.

ACKNOWLEDGMENTS

We thank Ms. Elizabeth Stone at The Ohio State University for reading the manuscript. This work was supported in part by Grants-in-Aid #16K07060 to SH and #17K07113 to TK, and those for Scientific Research on Innovation Area (Brain Protein Aging and Dementia control) from MEXT in Japan.

REFERENCES

Ando, K., Maruko-Otake, A., Ohtake, Y., Hayashishita, M., Sekiya, M., and Iijima, K. M. (2016). Stabilization of Microtubule-Unbound Tau via Tau Phosphorylation at Ser262/356 by Par-1/MARK Contributes to Augmentation of AD-Related Phosphorylation and Aβ42-Induced Tau Toxicity. *PLoS Genet.* 2:e1005917. doi: 10.1371/journal.pgen.1005917

Arendt, T., Stieler, J. T., and Holzer, M. (2016). Tau and tauopathies. *Brain Res. Bull.* 126, 238–292. doi: 10.1016/j.brainresbull.2016.08.018

Arrasate, M., Pérez, M., and Avila, J. (2000). Tau dephosphorylation at tau-1 site correlates with its association to cell membrane. *Neurochem. Res.* 25, 43–50. doi: 10.1023/A:1007583214722

Asada, A., Yamazaki, R., Kino, Y., Saito, T., Kimura, T., Miyake, M., et al. (2014). Cyclin-dependent kinase 5 phosphorylates and induces the degradation of ataxin-2. *Neurosci. Lett.* 563, 112–117. doi: 10.1016/j.neulet.2014.01.046

Ballatore, C., Lee, V. M., and Trojanowski, J. Q. (2007). Tau-mediated neurodegeneration in Alzheimer's disease and related disorders. *Nat. Rev. Neurosci.* 8, 663–672. doi: 10.1038/nrn2194

Binder, L. I., Frankfurter, A., and Rebhun, L. I. (1985). The distribution of tau in the mammalian central nervous system. *J. Cell Biol.* 101, 1371–1378. doi: 10.1083/jcb.101.4.1371

Brandt, R., Léger, J., and Lee, G. (1995). Interaction of tau with the neural plasma membrane mediated by tau's amino-terminal projection domain. *J. Cell Biol.* 131, 1327–1340. doi: 10.1083/jcb.131.5.1327

Chauhan, N. B., Siegel, G. J., and Feinstein, D. L. (2005). Propentofylline attenuates tau hyperphosphorylation in Alzheimer's Swedish mutant model Tg2576. *Neuropharmacology* 48, 93–104. doi: 10.1016/j.neuropharm.2004.09.014

Cummings, J., Lee, G., Mortsdorf, T., Ritter, A., and Zhong, K. (2017). Alzheimer's disease drug development pipeline: 2017. *Alzheimers Dement (N. Y)* 3, 367–384. doi: 10.1016/j.trci.2017.05.002

Dehmelt, L., and Halpain, S. (2005). The MAP2/Tau family of microtubule-associated proteins. *Genome Biol.* 6:204. doi: 10.1186/gb-2004-6-1-204

Dickey, C. A., Kamal, A., Lundgren, K., Klosak, N., Bailey, R. M., Dunmore, J., et al. (2007). The high-affinity HSP90-CHIP complex recognizes and selectively degrades phosphorylated tau client proteins. *J. Clin. Invest.* 117, 648–658. doi: 10.1172/JCI29715

Drewes, G., Trinczek, B., Illenberger, S., Biernat, J., Schmitt-Ulms, G., Meyer, H. E., et al. (1995). Microtubule-associated protein/microtubule affinity-regulating kinase (p110mark) a novel protein kinase that regulates tau-microtubule interactions and dynamic instability by phosphorylation at the Alzheimer-specific site serine 262. *J. Biol. Chem.* 270, 7679–7688. doi: 10.1074/jbc.270.13.7679

Furusawa, K., Asada, A., Saito, T., Fukuda, M., and Hisanaga, S. (2017). Cdk5 regulates Rab8-dependent axonal outgrowth via phosphorylation of Rab8 guanine-exchange factor Grab. *J. Neurosci.* 37, 790–806. doi: 10.1523/JNEUROSCI.2197-16.2016

Gauthier-Kemper, A., Weissmann, C., Golovyashkina, N., Sebö-Lemke, Z., Drewes, G., Gerke, V., et al. (2011). The frontotemporal dementia mutation R406W blocks tau's interaction with the membrane in an annexin A2–dependent manner. *J. Cell Biol.* 192, 647–661. doi: 10.1083/jcb.201007161

Goedert, M., Spillantini, M. G., Jakes, R., Rutherford, D., and Crowther, R. A. (1989). Multiple isoforms of human microtubule-associated protein tau: sequences and localization in neurofibrillary tangles of Alzheimer's disease. *Neuron* 3, 519–526. doi: 10.1016/0896-6273(89)90210-9

Greenwood, J. A., and Johnson, G. V. (1995). Localization and in situ phosphorylation state of nuclear tau. *Exp. Cell Res.* 220, 332–337. doi: 10.1006/excr.1995.1323

Hanger, D. P., Anderton, B. H., and Noble, W. (2009). Tau phosphorylation: the therapeutic challenge for neurodegenerative disease. *Trends Mol. Med.* 15, 112–119. doi: 10.1016/j.molmed.2009.01.003

Hanger, D. P., Byers, H. L., Wray, S., Leung, K. Y., Saxton, M. J., Seereeram, A., et al. (2007). Novel phosphorylation sites in tau from Alzheimer brain support a role for casein kinase 1 in disease pathogenesis. *J. Biol. Chem.* 282, 23645–23654. doi: 10.1074/jbc.M703269200

Hernández, F., Lucas, J. J., Cuadros, R., and Avila, J. (2003). GSK-3 dependent phosphoepitopes recognized by PHF-1 and AT-8 antibodies are present in different tau isoforms. *Neurobiol. Aging* 24, 1087–1094.

Hisanaga, S., and Hirokawa, N. (1989). The effects of dephosphorylation on the structure of the projections of neurofilament. *J. Neurosci.* 9, 959–966.

Hosokawa, T., Saito, T., Asada, A., Fukunaga, K., and Hisanaga, S. (2010). Quantitative measurement of *in vivo* phosphorylation states of Cdk5 activator p35 by Phos-tag SDS-PAGE. *Mol. Cell Proteom* 9, 1133–1143. doi: 10.1074/mcp.M900578-MCP200

Hutton, M., Lendon, C. L., Rizzu, P., Baker, M., Froelich, S., Houlden, H., et al. (1998). Association of missense and 5'-splice-site mutations in tau with the inherited dementia FTDP-17. *Nature* 393, 702–705. doi: 10.1038/31508

Illenberger, S., Zheng-Fischhöfer, Q., Preuss, U., Stamer, K., Baumann, K., Trinczek, B., et al. (1998). The endogenous and cell cycle-dependent phosphorylation of tau protein in living cells: implications for Alzheimer's disease. *Mol. Biol. Cell* 9, 1495–1512. doi: 10.1091/mbc.9.6.1495

Iqbal, K., Liu, F., and Gong, C. X. (2016). Tau and neurodegenerative disease: the story so far. *Nat. Rev. Neurol.* 12, 15–27. doi: 10.1038/nrneurol.2015.225

Ittner, A., Chua, S. W., Bertz, J., Volkerling, A., van der Hoven, J., Gladbach, A., et al. (2016). Site-specific phosphorylation of tau inhibits amyloid-β toxicity in Alzheimer's mice. *Science* 354, 904–908. doi: 10.1126/science.aah6205

Ittner, L. M., Ke, Y. D., Delerue, F., Bi, M., Gladbach, A., van Eersel, J., et al. (2010). Dendritic function of tau mediates amyloid-β toxicity in Alzheimer's disease mouse models. *Cell* 142, 387–397. doi: 10.1016/j.cell.2010.06.036

Jeganathan, S., Hascher, A., Chinnathambi, S., Biernat, J., Mandelkow, E. M., and Mandelkow, E. (2008). Proline-directed pseudo-phosphorylation at AT8 and PHF1 epitopes induces a compaction of the paperclip folding of Tau and generates a pathological (MC-1) conformation. *J. Biol. Chem.* 283, 32066–32076. doi: 10.1074/jbc.M805300200

Jeganathan, S., von Bergen, M., Brutlach, H., Steinhoff, H. J., and Mandelkow, E. (2006). Global hairpin folding of tau in solution. *Biochemistry* 45, 2283–2293. doi: 10.1021/bi0521543

Julien, J. P., and Mushynski, W. E. (1982). Multiple phosphorylation sites in mammalian neurofilament polypeptides. *J. Biol. Chem.* 257, 10467–10470.

Julien, J. P., and Mushynski, W. E. (1998). Neurofilaments in health and disease. *Prog. Nucleic Acid Res. Mol. Biol.* 61, 1–23. doi: 10.1016/S0079-6603(08)60823-5

Kimura, T., Hatsuta, H., Masuda-Suzukake, M., Hosokawa, M., Ishiguro, K., Akiyama, H., et al. (2016a). The abundance of nonphosphorylated tau in mouse and human tauopathy brains revealed by the use of phos-tag method. *Am. J. Pathol.* 186, 398–409. doi: 10.1016/j.ajpath.2015.10.009

Kimura, T., Hosokawa, T., Taoka, M., Tsutsumi, K., Ando, K., Ishiguro, K., et al. (2016b). Quantitative and combinatory determination of in situ phosphorylation of tau and its FTDP-17 mutants. *Sci. Rep.* 6:33479. doi: 10.1038/srep33479

Kimura, T., Ishiguro, K., and Hisanaga, S. (2014). Physiological and pathological phosphorylation of tau by Cdk5. *Front. Mol. Neurosci.* 7:65. doi: 10.3389/fnmol.2014.00065

Kimura, T., Tsutsumi, K., Taoka, M., Saito, T., Masuda-Suzukake, M., Ishiguro, K., et al. (2013). Isomerase Pin1 stimulates dephosphorylation of tau protein at cyclin-dependent kinase (Cdk5)-dependent Alzheimer phosphorylation sites. *J. Biol. Chem.* 288, 7968–7977. doi: 10.1074/jbc.M112.433326

Kinoshita, E., Kinoshita-Kikuta, E., and Koike, T. (2009). Separation and detection of large phosphoproteins using Phos-tag SDS-PAGE. *Nat. Protocol.* 4:1513. doi: 10.1038/nprot.2009.154

Kinoshita, E., Kinoshita-Kikuta, E., Takiyama, K., and Koike, T. (2006). Phosphate-binding tag, a new tool to visualize phosphorylated proteins. *Mol. Cell Proteomics* 5, 749–757. doi: 10.1074/mcp.T500024-MCP200

Kobayashi, S., Tanaka, T., Soeda, Y., Almeida, O. F. X., and Takashima, A. (2017). Local somatodendritic translation and hyperphosphorylation of tau protein triggered by AMPA and NMDA receptor stimulation. *EBioMedicine* 20, 120–126. doi: 10.1016/j.ebiom.2017.05.012

Kondo, A., Shahpasand, K., Mannix, R., Qiu, J., Moncaster, J., Chen, C. H., et al. (2015). Antibody against early driver of neurodegeneration cis P-tau blocks brain injury and tauopathy. *Nature* 523, 431–436. doi: 10.1038/nature14658

Krishnankutty, A., Kimura, T., Saito, T., Aoyagi, K., Asada, A., Takahashi, S. I., et al. (2017). *In vivo* regulation of glycogen synthase kinase 3β activity in neurons and brains. *Sci. Rep.* 7:8602. doi: 10.1038/s41598-017-09239-5

Lee, V. M., Goedert, M., and Trojanowski, J. Q. (2001). Neurodegenerative tauopathies. *Ann. Rev. Neurosci.* 24, 1121–1159. doi: 10.1146/annurev.neuro.24.1.1121

Li, T., Hawkes, C., Qureshi, H. Y., Kar, S., and Paudel, H. K. (2006). Cyclin-dependent protein kinase 5 primes microtubule-associated protein tau site-specifically for glycogen synthase kinase 3β. *Biochemistry* 45, 3134–3145. doi: 10.1021/bi051635j

Lindwall, G., and Cole, R. D. (1984). Phosphorylation affects the ability of tau protein to promote microtubule assembly. *J. Biol. Chem.* 259, 5301–5305.

Liu, F., Iqbal, K., Grundke-Iqbal, I., and Gong, C. X. (2002). Involvement of aberrant glycosylation in phosphorylation of tau by cdk5 and GSK-3β. *FEBS Lett.* 530, 209–214. doi: 10.1016/S0014-5793(02)03487-7

Liu, S. J., Zhang, J. Y., Li, H. L., Fang, Z. Y., Wang, Q., Deng, H. M., et al. (2004). Tau becomes a more favorable substrate for GSK-3 when it is prephosphorylated by PKA in rat brain. *J. Biol. Chem.* 279, 50078–50088. doi: 10.1074/jbc.M406109200

Loomis, P. A., Howard, T. H., Castleberry, R. P., and Binder, L. I. (1990). Identification of nuclear tau isoforms in human neuroblastoma cells. *Proc. Natl. Acad. Sci. U.S.A.* 87, 8422–8426. doi: 10.1073/pnas.87.21.8422

Lu, P.-J., Wulf, G., Zhou, X. Z., Davies, P., and Lu, K. P. (1999). The prolyl isomerase Pin1 restores the function of Alzheimer-associated phosphorylated tau protein. *Nature* 399, 784–788. doi: 10.1038/21650

Maas, T., Eidenmüller, J., and Brandt, R. (2000). Interaction of tau with the neural membrane cortex is regulated by phosphorylation at sites that are modified in paired helical filaments. *J. Biol. Chem.* 275, 15733–15740. doi: 10.1074/jbc.M000389200

Mandell, J. W., and Banker, G. A. (1996). A spatial gradient of tau protein phosphorylation in nascent axons. *J. Neurosci.* 16, 5727–5740.

Morishima-Kawashima, M., Hasegawa, M., Takio, K., Suzuki, M., Yoshida, H., Titani, K., et al. (1995). Proline-directed and non-proline-directed phosphorylation of PHF-tau. *J. Biol. Chem.* 270, 823–829. doi: 10.1074/jbc.270.2.823

Pant, H. C., Veeranna, and Grant, P. (2000). Regulation of axonal neurofilament phosphorylation. *Curr. Top. Cell. Regul.* 36, 133–150. doi: 10.1016/S0070-2137(01)80006-6

Pooler, A. M., Usardi, A., Evans, C. J., Philpott, K. L., Noble, W., and Hanger, D. P. (2012). Dynamic association of tau with neuronal membranes is regulated by phosphorylation. *Neurobiol. Aging* 33, 431.e427–431.e38. doi: 10.1016/j.neurobiolaging.2011.01.005

Poorkaj, P., Bird, T. D., Wijsman, E., Nemens, E., Garruto, R. M., Anderson, L., et al. (1998). Tau is a candidate gene for chromosome 17 frontotemporal dementia. *Ann. Neurol.* 43, 815–825. doi: 10.1002/ana.410430617

Ryoo, S. R., Jeong, H. K., Radnaabazar, C., Yoo, J. J., Cho, H. J., Lee, H. W., et al. (2007). DYRK1A-mediated hyperphosphorylation of Tau A functional link between Down syndrome and Alzheimer disease. *J. Biol. Chem.* 282, 34850–34857. doi: 10.1074/jbc.M707358200

Sakaue, F., Saito, T., Sato, Y., Asada, A., Ishiguro, K., Hasegawa, M., et al. (2005). Phosphorylation of FTDP-17 mutant tau by cyclin-dependent kinase 5 complexed with p35, p25, or p39. *J. Biol. Chem.* 280, 31522–31529. doi: 10.1074/jbc.M504792200

Sanders, D. W., Kaufman, S. K., DeVos, S. L., Sharma, A. M., Mirbaha, H., Li, A., et al. (2014). Distinct tau prion strains propagate in cells and mice and define different tauopathies. *Neuron* 82, 1271–1288. doi: 10.1016/j.neuron.2014.04.047

Shahpasand, K., Uemura, I., Saito, T., Asano, T., Hata, K., Shibata, K., et al. (2012). Regulation of mitochondrial transport and inter-microtubule spacing by tau phosphorylation at the sites hyperphosphorylated in Alzheimer's disease. *J. Neurosci.* 32, 2430–2441. doi: 10.1523/JNEUROSCI.5927-11.2012

Shukla, V., Seo, J., Binukumar, B., Amin, N. D., Reddy, P., Grant, P., et al. (2017). TFP5, a peptide inhibitor of aberrant and hyperactive Cdk5/p25, attenuates pathological phenotypes and restores synaptic function in CK-p25Tg mice. *J. Alzheimers Dis.* 56, 335–349. doi: 10.3233/JAD-160916

Sironi, J. J., Yen, S.-H., Gondal, J. A., Wu, Q., Grundke-Iqbal, I., and Iqbal, K. (1998). Ser-262 in human recombinant tau protein is a markedly more favorable site for phosphorylation by CaMKII than PKA or PhK. *FEBS Lett.* 436, 471–475. doi: 10.1016/S0014-5793(98)01185-5

Spillantini, M. G., and Goedert, M. (2013). Tau pathology and neurodegeneration. *Lancet Neurol.* 12, 609–622. doi: 10.1016/S1474-4422(13)70090-5

Spillantini, M. G., Murrell, J. R., Goedert, M., Farlow, M. R., Klug, A., and Ghetti, B. (1998). Mutation in the tau gene in familial multiple system tauopathy with presenile dementia. *Proc. Natl. Acad. Sci. U.S.A.* 95, 7737–7741. doi: 10.1073/pnas.95.13.7737

Sultan, A., Nesslany, F., Violet, M., Bégard, S., Loyens, A., Talahari, S., et al. (2011). Nuclear tau, a key player in neuronal DNA protection. *J. Biol. Chem.* 286, 4566–4575. doi: 10.1074/jbc.M110.199976

Tanabe, K., Yamazaki, H., Inaguma, Y., Asada, A., Kimura, T., Takahashi, J., et al. (2014). Phosphorylation of drebrin by cyclin-dependent kinase 5 and its role in neuronal migration. *PLoS ONE* 9:e92291. doi: 10.1371/journal.pone.0092291

Vega, I. E., Cui, L., Propst, J. A., Hutton, M. L., Lee, G., and Yen, S.-H. (2005). Increase in tau tyrosine phosphorylation correlates with the formation of tau aggregates. *Mol. Brain Res.* 138, 135–144. doi: 10.1016/j.molbrainres.2005.04.015

Wada, Y., Ishiguro, K., Itoh, T. J., Uchida, T., Hotani, H., Saito, T., et al. (1998). Microtubule-stimulated phosphorylation of tau at Ser202 and Thr205 by cdk5 decreases its microtubule nucleation activity. *J. Biochem.* 124, 738–746. doi: 10.1093/oxfordjournals.jbchem.a022174

Wang, J. Z., Xia, Y. Y., Grundke-Iqbal, I., and Iqbal, K. (2013). Abnormal hyperphosphorylation of tau: sites, regulation, and molecular mechanism of neurofibrillary degeneration. *J. Alzheimers Dis.* 33, S123–S139. doi: 10.3233/JAD-2012-129031

Wang, Y., and Mandelkow, E. (2016). Tau in physiology and pathology. *Nat. Rev. Neurosci.* 17, 5–21. doi: 10.1038/nrn.2015.1

Watanabe, A., Hasegawa, M., Suzuki, M., Takio, K., Morishima-Kawashima, M., Titani, K., et al. (1993). *In vivo* phosphorylation sites in fetal and adult rat tau. *J. Biol. Chem.* 268, 25712–25717.

Zempel, H., Thies, E., Mandelkow, E., and Mandelkow, E. M. (2010). Aβ oligomers cause localized Ca^{2+} elevation, missorting of endogenous Tau into dendrites, Tau phosphorylation, and destruction of microtubules and spines. *J. Neurosci.* 30, 11938–11950. doi: 10.1523/JNEUROSCI.2357-10.2010

Zheng-Fischhöfer, Q., Biernat, J., Mandelkow, E. M., Illenberger, S., Godemann, R., et al. (1998). Sequential phosphorylation of Tau by glycogen synthase kinase-3β and protein kinase A at Thr212 and Ser214 generates the Alzheimer-specific epitope of antibody AT100 and requires a paired-helical-filament-like conformation. *FEBS J.* 252, 542–552.

Zhou, X. Z., Kops, O., Werner, A., Lu, P. J., Shen, M., Stoller, G., et al. (2000). Pin1-dependent prolyl isomerization regulates dephosphorylation of Cdc25C and tau proteins. *Mol. Cell* 6, 873–883. doi: 10.1016/S1097-2765(05)00083-3

Conflict of Interest Statement: The authors declare that the research was conducted in the absence of any commercial or financial relationships that could be construed as a potential conflict of interest.

frontiers in Neuroscience

MINI REVIEW
published: 15 May 2018
doi: 10.3389/fnins.2018.00326

Linking hnRNP Function to ALS and FTD Pathology

Maria D. Purice[1] *and J. Paul Taylor*[1,2]*

[1] Department of Cell and Molecular Biology, St. Jude Children's Research Hospital, Memphis, TN, United States, [2] Howard Hughes Medical Institute, Chevy Chase, MD, United States

Following years of rapid progress identifying the genetic underpinnings of amyotrophic lateral sclerosis (ALS) and related diseases such as frontotemporal dementia (FTD), remarkable consistencies have emerged pointing to perturbed biology of heterogeneous nuclear ribonucleoproteins (hnRNPs) as a central driver of pathobiology. To varying extents these RNA-binding proteins are deposited in pathological inclusions in affected tissues in ALS and FTD. Moreover, mutations in hnRNPs account for a significant number of familial cases of ALS and FTD. Here we review the normal function and potential pathogenic contribution of TDP-43, FUS, hnRNP A1, hnRNP A2B1, MATR3, and TIA1 to disease. We highlight recent evidence linking the low complexity sequence domains (LCDs) of these hnRNPs to the formation of membraneless organelles and discuss how alterations in the dynamics of these organelles could contribute to disease. In particular, we discuss the various roles of disease-associated hnRNPs in stress granule assembly and disassembly, and examine the emerging hypothesis that disease-causing mutations in these proteins lead to accumulation of persistent stress granules.

Keywords: amyotrophic lateral sclerosis, frontotemporal dementia, stress granules, hnRNPs, membraneless organelles

OPEN ACCESS

Edited by:
Gen Sobue,
Nagoya University, Japan

Reviewed by:
Luke McAlary,
University of British Columbia, Canada
Osamu Onodera,
Niigata University, Japan

***Correspondence:**
J. Paul Taylor
jpaul.taylor@stjude.org

Specialty section:
This article was submitted to Neurodegeneration, a section of the journal Frontiers in Neuroscience

Received: *15 January 2018*
Accepted: *26 April 2018*
Published: *15 May 2018*

Citation:
Purice MD and Taylor JP (2018) Linking hnRNP Function to ALS and FTD Pathology. Front. Neurosci. 12:326. doi: 10.3389/fnins.2018.00326

INTRODUCTION

RNA-binding proteins (RBPs) are a large class of proteins that assemble with RNA to form ribonucleoproteins (RNPs). These proteins largely govern the function and fate of client RNAs, controlling their metabolism at all stages from RNA synthesis (transcription) to degradation (decay). RBPs are among the most abundant proteins in cells, localizing to both the nucleus and cytoplasm, and most are expressed ubiquitously. Heterogeneous nuclear ribonucleoproteins (hnRNPs) are a major subclass of evolutionarily conserved RNPs that are primarily concentrated in the nucleus, although many hnRNPs [e.g., hnRNP A1 and TAR DNA-binding protein 43 (TDP-43)] shuttle between the nucleus and the cytoplasm. The hnRNP family initially consisted of 24 proteins, termed hnRNP A1 through hnRNP U; however, the hnRNP family has grown as well-studied proteins have been later identified as hnRNPs. hnRNPs coat nascent pre-mRNAs to form messenger RNPs (mRNPs), which operate as the functional center of diverse biological processes, including mRNA splicing, polyadenylation, nuclear export, localization, and translation, providing many potential avenues by which hnRNP dysfunction could lead to pathogenesis.

Over the last decade, disturbances in the function of hnRNPs have become closely linked to neurodegenerative diseases, most prominently amyotrophic lateral sclerosis (ALS) and frontotemporal dementia (FTD), two diseases with significant genetic and pathological overlap (Taylor et al., 2016). ALS is a progressive and uniformly fatal neurodegenerative disease characterized by loss of motor neurons in the brain and spinal cord. FTD is a lethal syndrome

that results in progressive changes in personality, behavior, and language due to progressive loss of neurons in the frontal and temporal lobes of the brain. Importantly, ALS shows clinical overlap with several other adult-onset degenerative disorders, most frequently FTD, but also inclusion body myopathy (IBM) and Paget's disease of bone (PDB). When manifestations of these conditions (i.e., ALS, FTD, IBM, and/or PDB) are found together, they constitute a clinical syndrome termed multisystem proteinopathy (MSP) (Taylor, 2015).

The first link between hnRNPs and neurodegeneration arose from a 2006 study which recognized that ALS and FTD share a pathological signature defined by prominent deposition of ubiquitin-positive cytoplasmic inclusions that contain TDP-43 (Neumann et al., 2006). Indeed, it is now appreciated that redistribution of TDP-43 from the nucleus to cytoplasmic inclusions is observed in the vast majority (∼97%) of sporadic and familial ALS cases, perhaps only absent in those cases involving mutations in *FUS* (fused in sarcoma) or *SOD1* (Cu–Zn superoxide dismutase). TDP-43 pathology is also a prominent feature of virtually all cases of tau-negative FTD (accounting for roughly 50% of FTD cases) (Irwin et al., 2015). In 2007, similar TDP-43 pathology was found also to be a prominent feature of nearly all cases of sporadic and familial IBM (Weihl et al., 2008; Salajegheh et al., 2009). Several years after the appreciation of TDP-43 pathology in ALS, FTD, and IBM, the importance of this feature was underscored by the identification of ALS-causing mutations in the gene encoding this RBP (Gitcho et al., 2008; Kabashi et al., 2008; Kuhnlein et al., 2008; Rutherford et al., 2008; Sreedharan et al., 2008; Van Deerlin et al., 2008; Yokoseki et al., 2008; Pamphlett et al., 2009). Since then, mutations impacting additional RBPs, including FUS, hnRNP A1, hnRNP A2B1, matrin-3 (MATR3), and TIA1, were identified that are causative of ALS, FTD, and/or IBM (Kwiatkowski et al., 2009; Vance et al., 2009; Kim et al., 2013; Liu et al., 2013; Johnson et al., 2014; Mackenzie et al., 2017). Moreover, in these diseases many of these RBPs have been reported to become depleted from the nucleus and deposited in cytoplasmic inclusions.

These findings suggest that perturbed RBP function and associated alteration in RNA metabolism are important drivers of the progression and pathology of sporadic ALS and FTD and could therefore link inherited and spontaneous forms of the disease. However, critical gaps exist in our understanding of the links between neuronal function, dysfunctional RNA metabolism, and other cellular events underlying the pathogenesis of ALS and FTD. Although a growing list of mutations responsible for ALS and FTD impinge on many aspects of RNA metabolism and protein homeostasis (recently reviewed in Taylor et al., 2016; Webster et al., 2017), in this mini-review, we focus on the subset of disease-causing RBPs that are hnRNPs, namely TDP-43, FUS, hnRNP A1, hnRNP A2B1, MATR3, and TIA1.

COMMON CHARACTERISTICS OF DISEASE-CAUSING hnRNPS

Structurally, all hnRNPs contain one or more RNA-binding domains, the most common of which is designated as an RNA recognition motif (RRM) (**Figure 1**). While all hnRNPs discussed in this review include an RRM, they each contain at least one additional type of RNA-binding domain, defined as a K-homology (KH) domain or a zinc finger motif, both of which facilitate binding to specific RNA sequences, and/or one or more RGG (Arg-Gly-Gly) boxes, which provide strong RNA interaction without a great deal of specificity (**Figure 1**).

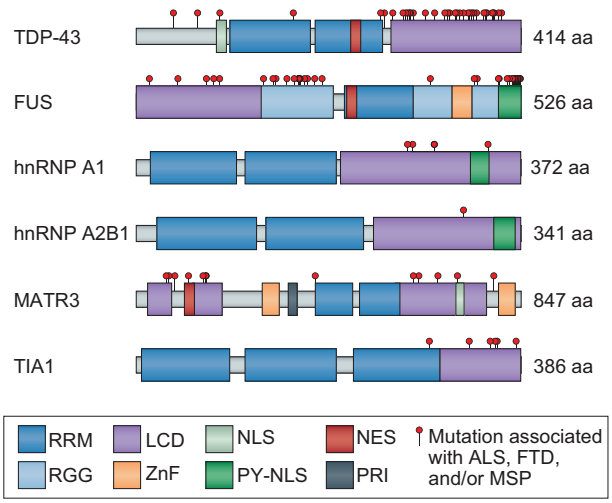

FIGURE 1 | Mutations that cause ALS and FTD cluster in the LCD of hnRNPs and/or disrupt nuclear localization. TDP-43, FUS, hnRNP A1, hnRNP A2B1, MATR3, and TIA1 are ubiquitously expressed hnRNPs that are similar in domain structure and function, each containing at least one RRM and LCD. The LCD region of all hnRNPs is well established with the exception of MATR3, for which PONDR score analysis (http://www.pondr.com/) was used to identify the disordered LCD regions. Mutations identified in patients with ALS, FTD, and/or MSP are depicted as red circles. Mutations in TDP-43, FUS, hnRNP A1, hnRNP A2B1, and TIA1 primarily cluster in the LCD region, whereas mutations in MATR3 are less concentrated in a single region. Several mutations are also found in the NLS of FUS and one in the NLS of TDP-43, causing them to mislocalize to the cytoplasm. MATR3 contains mutations in both the NES and NLS, although further studies are necessary to confirm their effects on MATR3 localization. RRM, RNA recognition motif; LCD, low-complexity domain; NLS, nuclear localization signal; NES, nuclear export signal; RGG, Arg-Gly-Gly box; ZnF, zinc finger; PY-NLS, proline-tyrosine NLS; PRI, polypyrimidine tract binding (PTB)-RRM interaction domain.

TDP-43, FUS, hnRNP A1, hnRNP A2B1, MATR3, and TIA1 are all ubiquitously expressed and carry out varying functions depending on whether they are localized to the nucleus or the cytoplasm. Such localization is facilitated by both nuclear export sequences and nuclear localization sequences (NLSs), allowing nucleocytoplasmic shuttling (**Figure 1**). TDP-43 and MATR3 each contain a classic bipartite NLS, and MATR3 also includes a membrane retention signal that can anchor chromosomes to the nuclear matrix (Hibino et al., 1992, 2006; Coelho et al., 2015). In contrast, FUS, hnRNP A1, and hnRNP A2B1 each contain a single proline-tyrosine NLS (PY-NLS), a specialized type of NLS that confers dependence on a single receptor (KapB2 or transportin) (Lee et al., 2006; Dormann et al., 2012; Twyffels et al., 2014; **Figure 1**). Although detailed analysis of TIA1 has not revealed sequence determinants related

to classically understood nuclear localization, the localization of TIA1 is transcription-dependent and its nuclear import and export are mediated by its RRM2/3 domains (Zhang et al., 2005).

Each of the disease-associated hnRNPs discussed in this review also contains at least one low complexity sequence domain (LCD), such as glycine-, proline-, or acid-rich domains: TDP-43 has a C-terminal glycine-rich LCD that mediates interactions with other hnRNPs, including hnRNP A1, hnRNP A2B1, hnRNP A3, and FUS (Buratti et al., 2005; Kitamura et al., 2016); FUS contains an N-terminal SYGQ-rich (serine-, tyrosine-, glycine-, glutamine-rich) LCD that functions in transcriptional activation; hnRNP A1 and hnRNP A2B1 each contain a C-terminal glycine-rich LCD that contains an RGG motif required for stress granule localization; MATR3 has several predicted LCDs; and TIA1 contains a glutamine-rich C-terminal LCD that promotes stress granule assembly (Kedersha et al., 2000; Gilks et al., 2004; Panas et al., 2016). Although historically considered to be protein-protein interaction domains, LCDs contain motifs that can be recognized by other proteins or nucleic acids, resulting in multivalent interactions. This ability to interact with multiple partners is essential for the liquid-liquid phase separation property exhibited by hnRNPs, a biophysical phenomenon that promotes higher order intracellular assemblies, most notably membraneless organelles. These types of organelles are highly relevant to RNA metabolism, as several types of RNP-based membraneless organelles, including nuclear speckles, processing bodies (P bodies), RNA transport granules, and stress granules, have recently emerged as complexes that can regulate RNA metabolism (e.g., RNA splicing, translation, and decay). These structures are of particular interest in the context of highly polarized neurons, some of which have axons 10,000 times longer than their cell bodies, and in which local translation in distinct (and distant) subcellular compartments is necessary for rapid responses to local stimuli. In these neurons, as in many other cell types, nascent mRNA transcripts are sequestered with associated RBPs (e.g., TDP-43, hnRNP A1, and FUS) into RNA granules that inhibit mRNA translation and decay until the granules are delivered to specific sites within the cell (Kanai et al., 2004; Belly et al., 2005; Elvira et al., 2006; Sephton and Yu, 2015). Moreover, TDP-43, FUS, hnRNP A1, hnRNP A2B1, and TIA1 are required for the dynamic assembly, disassembly, and function of stress granules, while MATR3 is important for the formation of P bodies (Rajgor et al., 2016). RNA granules, stress granules, and P bodies are highly dynamic structures that behave like liquid droplets in cells, similar to how oil droplets act when mixed with water. Stress granules can be targeted for degradation by autophagy in a process termed granulophagy. However, as described below, ALS- and FTD-causing mutations in hnRNPs and other RBPs are thought to foster a less dynamic (and typically less soluble) state within stress granules and/or other membraneless organelles, possibly promoting fibrillization of aggregation-prone proteins and likely also adversely affecting RNA metabolism by disturbing their normal functions (**Figure 2**).

TDP-43

Structure and Function

A central player in the pathogenesis of ALS/FTD, TDP-43 is a 414-amino acid protein implicated in a wide variety of cellular functions (**Figure 1**). The amino terminus is composed of a 77-amino acid domain that mediates homodimerization and tetramer formation, an assemblage that appears to be important to its function in pre-mRNA splicing (Jiang et al., 2017). TDP-43 also harbors two tandem RRMs that preferentially bind UG-rich RNA or TG-rich DNA with high affinity (Buratti and Baralle, 2001; Kuo et al., 2014). Biochemical cross-linking studies suggest that TDP-43 may bind to thousands of RNA targets (Polymenidou et al., 2011; Tollervey et al., 2011), indicating that this protein has the potential to impact RNA metabolism on a broad scale. Indeed, early proteomic studies found that TDP-43 strongly interacts with proteins involved in RNA splicing and translation machinery (Freibaum et al., 2010). Since then, evidence has accumulated implicating TDP-43 as influencing RNA metabolism at every stage of the RNA life cycle, including transcription, splicing, mRNA processing, microRNA processing, regulation of coding and long non-coding RNA expression, mRNA transport, mRNA stability, and the formation of cytoplasmic RNA granules (recently summarized in Ratti and Buratti, 2016). As may be expected for a protein that plays a central role in RNA metabolism, levels of TDP-43 are tightly regulated (Ayala et al., 2011; Polymenidou et al., 2011) and, in fact, TDP-43 regulates its own expression by binding to its own 3′ untranslated region (Ayala et al., 2011; Polymenidou et al., 2011; Avendano-Vazquez et al., 2012). Additional RNA-related functions have been revealed by characterization of mouse embryonic stem cells in which TDP-43 has been knocked out, including the notable finding that a lack of TDP-43 leads to retention of cryptic exons that in some cases disrupts translation or promotes nonsense-mediated decay, revealing a role for TDP-43 as a guardian of the transcriptome through repression of cryptic exons (Ling et al., 2015). TDP-43 has also been found to physically associate with the Drosha microprocessor complex, suggesting a role in miRNA biogenesis (Gregory et al., 2004; Ling et al., 2010; Kawahara and Mieda-Sato, 2012). Consistent with this suggestion, a defect in microRNA biogenesis has been reported in neurons derived from patients with TDP-43 mutations (Zhang et al., 2013). Studies of the localization and dynamics of TDP-43 in neurons have reported that cytoplasmic TDP-43 redistributes to axons and dendrites in response to activity and influences neurite outgrowth (Wang et al., 2008; Fallini et al., 2012). Subsequently, TDP-43 was recognized as a constituent of RNA granules that traffic mRNAs to distal compartments for local translation (Wang et al., 2008).

Role in Disease

In both neurons and glia of patients with ALS and/or FTD, TDP-43 is mislocalized from the nucleus to the cytoplasm, where it is heavily post-translationally modified via cleavage, phosphorylation, acetylation, and ubiquitination, and forms granular pathology that evolves to one or a few large inclusions.

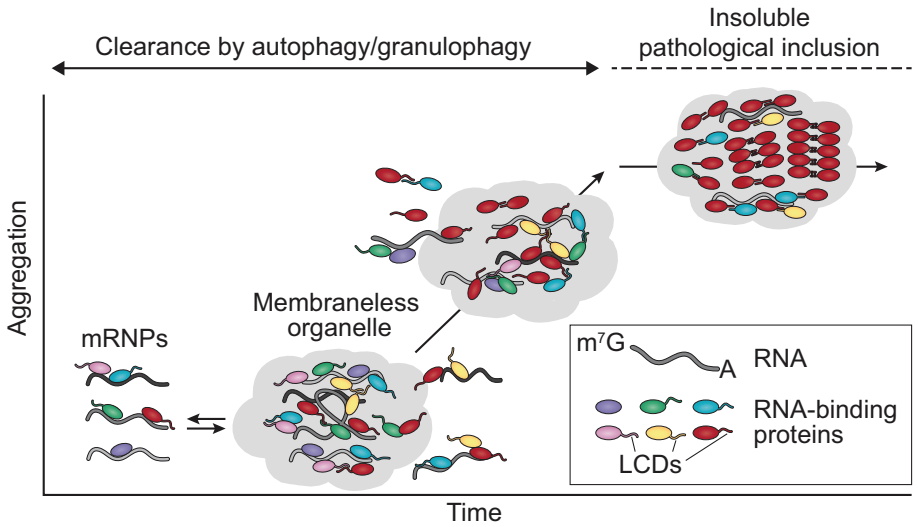

FIGURE 2 | ALS mutations alter the dynamics and function of membraneless organelles. RNA-binding proteins associate with mRNA, forming mRNPs that are transported to the cytosol. The hnRNPs discussed in this review contain LCDs that mediate phase separation, contributing to the assembly/disassembly, dynamics, and liquid properties of membraneless organelles such as stress granules. Stress granules that begin forming aggregates and are no longer capable of being disassembled by liquid-liquid phase separation mechanisms are cleared by autophagy/granulophagy. Disease-causing mutations can trigger the assembly of aberrant or persistent membraneless organelles in which the high concentration and close interactions of the LCDs over time may promote the transition of aggregation-prone proteins (e.g., TDP-43, FUS) to pathogenic amyloid fibrils. mRNP, messenger ribonucleoprotein particle; LCDs, low complexity domains.

Because this subcellular redistribution leads to nuclear depletion of TDP-43, the pathogenic mechanism may involve loss of nuclear function, gain of cytoplasmic function, or, most likely, a contribution from both. Currently, more than 40 familial and sporadic mutations in TDP-43 are known to lead to ALS and/or FTD, accounting for an estimated 5% of familial ALS cases and <1% of sporadic cases (Gendron et al., 2013; Taylor et al., 2016). Interestingly, nearly all of the disease-causing mutations are clustered in the LCD region. The LCD of TDP-43 is required for the recruitment of TDP-43 to stress granules and is thought to mediate the assembly of translation-stalling cytoplasmic granules and their liquid properties; furthermore, it influences the solubility and cellular localization of TDP-43 (Ayala et al., 2008; Dewey et al., 2011; Ramaswami et al., 2013). Two disease-causing mutations are located in the RRM and are predicted to generate a more stable protein that is cleaved more efficiently, thereby increasing the amount of cytoplasmic C-terminal fragments of TDP-43 (Austin et al., 2014; Chiang et al., 2016).

Recent *in vitro* studies have demonstrated that within the LCD of TDP-43, a balance between hydrophobic and electrostatic forces results in a conserved α-helical structure that is required for induction of liquid-liquid phase separation; interestingly, ALS mutations within this region significantly disrupt phase separation and promote the conversion to aggregates (Conicella et al., 2016; Li et al., 2018). Consistent with these observations linking the mutation-rich LCD to the biophysical behavior of TDP-43, several recent investigations of disease-causing TDP-43 mutations have yielded important insights into RNP granule dynamics in primary neurons. In these studies, RNP granules consisting of wild-type TDP-43 exhibited distinct biophysical properties depending on their axonal location, suggesting that the properties of TDP-43 granules are dependent on subcellular context and can change over time (Gopal et al., 2017). In contrast, granules formed by ALS-linked mutant TDP-43 are more viscous and show disrupted axonal transport dynamics, suggesting that the increased viscosity observed in TDP-43 mutant granules may lead to a toxic gain of function, possibly enhancing its propensity for aggregation (Alami et al., 2014; Gopal et al., 2017). Disruption in trafficking of RNA granules due to mutant expression of TDP-43 or lack of expression of wild-type TDP-43 also has detrimental consequences for neurons, since local protein synthesis is highly dependent on mRNP granule transport and TDP-43 binds to mRNAs that encode genes related to synaptic development and function (Wang et al., 2008; Godena et al., 2011; Narayanan et al., 2013; Alami et al., 2014; Coyne et al., 2014).

FUS

Structure and Function

FUS or FUS/TLS (fused in sarcoma/translocated in liposarcoma) is a 526-amino acid protein that shares its classic domain architecture (SYGD domain, three RGGs, one RRM, one zinc finger domain, and a PY-NLS) with EWS and TAF15 proteins, which together with FUS form the FET family of proteins (**Figure 1**). FUS is primarily localized to the nucleus, although super-resolution imaging of mouse hippocampal neurons has detected FUS in dendritic post-synaptic compartments and within axonal terminals in close proximity to presynaptic proteins and vesicles (Schoen et al., 2015). FUS is involved in diverse cellular processes including cell proliferation (Bertrand et al., 1999), DNA damage repair (Baechtold et al., 1999; Bertrand et al., 1999; reviewed in Sama et al., 2014), and almost every aspect of RNA metabolism, including transcription and stress granule

function (Yang et al., 1998; Bentmann et al., 2013). Most recently, FUS has been shown to control back-splicing reactions leading to production of circular RNA (RNA in which the 3′ and 5′ ends have been joined together) in rodent stem cell-derived motor neurons, further adding to the complexity of FUS-dependent functions (Errichelli et al., 2017). Interestingly, FUS has also been found to associate with the Drosha microprocessor (Gregory et al., 2004; Ling et al., 2010; Kawahara and Mieda-Sato, 2012) as well as Dicer complexes (Freibaum et al., 2010; Kawahara and Mieda-Sato, 2012), suggesting a role for FUS (along with TDP-43, which also associates with Drosha) in miRNA biogenesis.

Role in Disease

Three years after the discovery of TDP-43 as the major component of inclusions in the central nervous system of nearly all ALS patients, FUS was identified as the primary component of TDP-43-negative cytoplasmic inclusions in rare patients with ALS, all of whom had causative genetic mutations in *FUS* (Vance et al., 2009; Suzuki et al., 2010; Tateishi et al., 2010). Mutations in *FUS* have been estimated to account for up to 4% and 1% of total familial and sporadic ALS cases respectively (Lagier-Tourenne et al., 2010). FUS pathology is also observed in approximately 10% of FTD cases, although there are no reported cases of FUS-related mutations that lead to FTD (Nolan et al., 2016). The majority of pathogenic FUS mutations are located in the C-terminal PY-NLS or completely delete the NLS sequence, thereby impairing nuclear import of FUS (Dormann et al., 2010), leading to accumulation of FUS in the cytosol and giving rise to an apparent toxic gain of function (Scekic-Zahirovic et al., 2016; Sharma et al., 2016). Mutations in the NLS correlate with both severity of disease and age of onset, such that increased mislocalization to the cytoplasm is associated with earlier onset and more aggressive disease (Dormann et al., 2012; Kuang et al., 2017).

Similar to mutated TDP-43, mislocalized mutant FUS protein expressed in mammalian cell lines or in primary rodent neurons is recruited to stress granules (Bosco et al., 2010; Dormann et al., 2010; Ito et al., 2011; Bentmann et al., 2012; Baron et al., 2013; Lenzi et al., 2015; Kuang et al., 2017). Moreover, biophysical studies have demonstrated that FUS, at physiological concentrations, forms liquid-like droplets that can convert into a solid state, a process of phase conversion that is exacerbated by disease-causing mutations in the LCD (Han et al., 2012; Patel et al., 2015). Taken together, these findings suggest a model in which disease-associated LCD mutations or nuclear import defects cause increased cytoplasmic concentration of FUS and augment its recruitment to stress granules, which over time develop into pathological inclusions, potentially due to increased FUS self-interactions or misfolding (Bentmann et al., 2013; Lin Y. et al., 2015; Molliex et al., 2015; Patel et al., 2015).

hnRNP A1 AND hnRNP A2B1

Structure and Function

Two of the most abundantly expressed proteins in cells, hnRNP A1 is a 372-amino acid protein encoded by *HNRNPA1* and hnRNP A2B1 is a 341-amino acid protein (identical to its isoform hnRNP B1 but lacking 12 amino acids) encoded by *HNRNPA2B1* (Jean-Philippe et al., 2013). hnRNP A1 and hnRNP A2B1 share similar domain architecture and are primarily localized to the nucleus (Nakielny and Dreyfuss, 1999; Jean-Philippe et al., 2013; Kim et al., 2013; Thandapani et al., 2013; Wall and Lewis, 2017; **Figure 1**). Because the LCDs of both proteins contain steric-zipper motifs, which are two self-complementary beta sheets that can give rise to the spine of an amyloid fibril, these domains are predicted to have high fibrillization propensity (Goldschmidt et al., 2010). Although the two proteins do have some distinct roles in transcriptional control, hnRNP A1 and hnRNP A2B1 have many overlapping functions, including processing of heterogeneous nuclear RNAs into mature mRNAs, splicing, translation, stabilization of mRNA, transcriptional elongation, and regulation of DNA metabolism associated with telomeres (Beriault et al., 2004; Zhao et al., 2009; Flynn et al., 2011; Guo et al., 2013; Jean-Philippe et al., 2013; Lemieux et al., 2015). Notably, hnRNP A1 and hnRNP A2B1 are components of RNA transport granules in neurons (Elvira et al., 2006). In addition, hnRNP A1 and hnRNP A2B1 translocate to the cytoplasm in response to stress and are recruited to stress granules (Guil et al., 2006; McDonald et al., 2011).

Role in Disease

Mutations in the aggregation-prone LCDs of hnRNP A1 and hnRNP A2B1 account for <1% of familial and sporadic forms of ALS and are more frequently associated with the broader spectrum disorder MSP (Kim et al., 2013; Taylor, 2015). Interestingly, muscle biopsies of MSP patients have revealed concurrent cytoplasmic mislocalization/nuclear clearing and partial colocalization of TDP-43 and hnRNP A1 or TDP-43 and hnRNP A2B1 (Kim et al., 2013). Disease-causing mutations are predicted to strengthen the steric zippers of hnRNP A1 and hnRNP A2B1, altering the dynamics of stress granule assembly and accelerating nucleation and fibrillization *in vitro* (Kim et al., 2013). Consistent with these predictions, *in vitro* synthetic studies have shown that both wild-type hnRNP A1 and hnRNP A2B1 form fibrils and that disease mutations greatly enhance this fibrillization. Furthermore, mutated hnRNP A1 and hnRNP A2B1 form fibrils that are self-seeding and can recruit wild-type protein, suggesting that these proteins have prion-like properties (Kim et al., 2013). In a more detailed study of hnRNP A1, the LCD was demonstrated to drive the phase separation that mediates the assembly of stress granules and their liquid properties. In these experiments, RNA binding contributed to phase separation and enhanced fibrillization in protein-rich droplets (Molliex et al., 2015). These findings suggest that hnRNP A1 acts in a concentration-dependent manner and interacts with RNA to mediate phase transition and drive the formation of membraneless organelles. Furthermore, since disease-causing mutations in hnRNP A1 promote fibrillization *in vitro*, mutations that alter the dynamics of membraneless organelles could result in accelerated fibrillization and the formation of aggregates that can accumulate within the cell (Molliex et al., 2015).

MATR3

Structure and Function

MATR3 is an 847-amino acid protein encoded by the *MATR3* gene and consists of two RRMs flanked by two zinc finger domains and a conserved polypyrimidine tract binding-RRM interaction (PTB-RRM; PRI) domain (**Figure 1**). MATR3 is predicted to have extensive LCDs, and PONDR (Predictor Of Naturally Disordered Regions) score analysis identifies three disordered LCD regions of 50 or more amino acids in length (Romero and Dunker, 1997; Garner et al., 1998, 1999; Coelho et al., 2015; **Figure 1**). Although MATR3 is primarily localized to the inner nuclear matrix and nucleoplasm, it has also been detected in the cytoplasm at low levels (Hibino et al., 2006). MATR3 has several functions, including roles in transcription (Skowronska-Krawczyk and Rosenfeld, 2015) and early stages of the DNA damage response (Salton et al., 2010). MATR3 also functions in RNA metabolism, including mRNA stabilization (Salton et al., 2011), the coupling of transcription to splicing via interaction with RNA polymerase II (Das et al., 2007), nuclear retention of hyperedited RNAs to prevent their translation (Zhang and Carmichael, 2001), and splicing (Coelho et al., 2015). In addition, MATR3 interacts via RNA with other hnRNPs, including TDP-43 and hnRNP K, potentially to regulate several RNA processes including transcription and splicing (Salton et al., 2011; Johnson et al., 2014).

Role in Disease

Mutations in *MATR3* account for approximately 1% of total cases of ALS (Johnson et al., 2014; Lin K. P. et al., 2015; Origone et al., 2015; Leblond et al., 2016; Xu et al., 2016; Marangi et al., 2017) and are also causative of autosomal dominant late-onset distal myopathy (Muller et al., 2014). In both sporadic and familial cases, MATR3 binds directly to TDP-43, and at least some disease-causing mutations alter this binding in a mutation-selective and RNA-dependent manner (Johnson et al., 2014). In healthy human tissue, MATR3 is found in a granular pattern in the nuclei of motor neurons and surrounding glial cells. In patients with disease-causing ALS mutations, MATR3 is largely localized to the nucleus, with occasional immunostaining in the cytoplasm (Johnson et al., 2014). These findings parallel a cellular model that showed that ALS/myopathy-associated MATR3 mutations do not produce profound changes in the localization of MATR3 (Gallego-Iradi et al., 2015). However, recently evidence has demonstrated that MATR3 is a component of neuronal cytoplasmic inclusions in motor neurons in cases of sporadic ALS (Tada et al., 2017). Surprisingly, unlike the other hnRNPs discussed in this review, stressed cells overexpressing wild-type or mutant MATR3 do not recruit MATR3 to stress granules or change the nuclear localization of MATR3, and do not induce the formation of inclusion-like structures in either the cytoplasm or nucleus (Gallego-Iradi et al., 2015). Although the mechanisms by which MATR3 might lead to ALS pathology remain to be elucidated, it appears that alterations in expression levels of MATR3 in the muscle and spinal cord might be critical for neuromuscular function and that dysregulation of its expression may underlie some aspects of neuromuscular dysfunction (Moloney et al., 2016; Rayaprolu et al., 2016). In addition, recent data suggest that expression of disease-causing MATR3 mutations leads to defects in nuclear export of global mRNA and more specifically mRNA encoding TDP-43 and FUS, potentially contributing to pathogenesis (Boehringer et al., 2017).

TIA1

Structure and Function

TIA1 is a 386-amino acid protein that is structurally very similar to TDP-43 (**Figure 1**). Notably, each of its three RRMs has a distinct RNA-binding profile (Dember et al., 1996; Forch et al., 2002; Kim et al., 2007; Bauer et al., 2012; Wang et al., 2014). RRM1 binds AU-rich pre-mRNA sequences and interacts with the LCD to recruit and stabilize the U1 small nuclear ribonucleoprotein-associated protein U1C, a splicing regulator (Forch et al., 2002). RRM2 is necessary and sufficient for TIA1 to bind RNA and exhibits the highest binding affinity to U-rich pre-mRNA sequences, and RNA binding is further enhanced when RRM3 is present (Bauer et al., 2012). TIA1 is largely localized to the nucleus and has been associated with several functions related to RNA metabolism, including alternative splicing, translational repression, and mRNA silencing (Lopez de Silanes et al., 2005; Carrascoso et al., 2014; Waris et al., 2014). In response to cellular stress, TIA1 translocates to the cytoplasm, suppresses mRNA translation by binding to specific mRNA transcripts marked by AU-rich elements, and nucleates stress granule formation through self-association of its LCD (Gilks et al., 2004; Lopez de Silanes et al., 2005; Wang et al., 2014; Waris et al., 2014).

Role in Disease

One of the most recent genes associated with ALS, *TIA1* harbors several ALS- and ALS/FTD-associated mutations in its LCD (Mackenzie et al., 2017). Notably, the LCD of TIA1 is also the site of a mutation that causes Welander distal myopathy, a myopathy characterized by TDP-43-positive inclusions (Klar et al., 2013). These disease mutations alter the biophysical properties of TIA1 by significantly increasing its propensity toward phase separation, delaying stress granule disassembly following removal of stressful stimuli, and promoting the accumulation of non-dynamic stress granules that sequester TDP-43 (Mackenzie et al., 2017). Furthermore, TDP-43 recruited to these stress granules becomes immobile and insoluble. Interestingly, although TIA1 is similar in structure and function to TDP-43, examination of patient pathology has revealed inclusions that are immunoreactive for TDP-43 but not TIA1 (Mackenzie et al., 2017). These findings reinforce the importance of disturbed RNA metabolism in neurodegenerative disorders and place dysfunctional membraneless organelle dynamics at the center of disease progression and pathogenesis.

RBP-MEDIATED PATHOGENIC MECHANISMS IN ALS AND FTD

Disease-causing mutations in TDP-43, FUS, hnRNP A1, hnRNP A2B1, MATR3, and TIA1 point to disturbed biology of RBPs, especially hnRNPs, as playing a central pathogenic role in ALS

and FTD. This view is further supported by evidence that alleles of the RBP ataxin-2 (ATXN2) with intermediate repeat expansion increase the risk of ALS-FTD, as well as evidence that variants in RBPs not discussed in this review (e.g., ANG, EWS, TAF15) may contribute to the burden of ALS-FTD. All of these RBPs have related domain architecture that includes multiple RNA-binding domains and sizeable LCDs that are predicted to be intrinsically disordered (**Figure 1**). Notably, for most of these proteins there is a tendency for disease-causing mutations to impact the composition of the LCD, which is a domain that strongly promotes liquid-liquid phase separation to drive the assembly of membraneless organelles such as stress granules (**Figure 1**). It is important to point out, however, that these RBPs engage in a variety of additional assemblies that arise through phase separation, for example the nucleolus (Berry et al., 2015), P granules (Elbaum-Garfinkle et al., 2015), nuclear speckles (Hennig et al., 2015), and others, and that disease-causing mutations that disturb phase transitions are likely to have a broad impact on cellular physiology that stretches beyond alterations to stress granule dynamics.

Recent findings related to mutations in chromosome 9 open reading frame 72 (*C9ORF72*) have reinforced the importance of phase separation in disease (DeJesus-Hernandez et al., 2011; Renton et al., 2011; Majounie et al., 2012). The leading cause of sporadic and familial ALS, mutations in C9ORF72 lead to disease when an intronic GGGGCC hexanucleotide repeat is massively expanded. In patients with these mutations, the expanded GGGGCC repeats are translated into five different species of dipeptide repeat proteins (DPRs). Two species of these repeats (polyGR and polyPR) feature alternating arginine residues, which are charged, highly polar, and carry a dipole moment. Arginine residues frequently engage in charge-charge interactions with basic residues or Pi-cation interactions with aromatic residues, two interaction types that are thought to contribute significantly to intermolecular adhesion between LCDs to permit phase separation. Notably, the arginine-containing DPRs (polyGR and polyPR) insinuate into and disturb the properties of membraneless organelles, including stress granules, Cajal bodies, nuclear speckles, and the nucleolus—all organelles that are active liquids and are mediated by phase separation (Lee et al., 2016; Boeynaems et al., 2017). Not surprisingly, the arginine-containing DPRs are consistently reported to be the most toxic in living cells (Kwon et al., 2014; Mizielinska et al., 2014; Wen et al., 2014; Freibaum et al., 2015; Lee et al., 2016). Further evidence suggesting a role for arginine-containing DPRs comes from a recent report revealing correlation between the regions of polyGR deposition and neurodegeneration in the brains of patients with C9ORF72-related ALS-FTD (Saberi et al., 2017).

Additional evidence that disturbance in the dynamics of membraneless organelles, especially stress granules, are a unifying mechanism between the many disease-causing RBPs and ALS and/or FTD pathogenesis can be found in the study of disease genes not traditionally linked to RBP biology. For example, mutations in valosin-containing protein (VCP) cause both ALS and FTD. VCP has emerged as an essential factor in the autophagic degradation of stress granules and, indeed, ALS-FTD-causing mutations lead to accumulation of poorly dynamic, TDP-43-positive stress granules (Buchan et al., 2013). Moreover, an enhancer/suppressor screen in *Drosophila* VCP mutants identified three RBPs (TDP-43, hnRNP A1, hnRNP A2B1) that suppressed the mutant VCP-associated phenotype when knocked down (Ritson et al., 2010). As discussed above, all three of these proteins lead to ALS when mutated, all three contain LCDs, and all three are associated with stress granules. In a separate screen of DPR toxicity, proteomic analysis of DPRs identified several DPR interactors, including TDP-43 and ATXN2, another ALS-related RBP that contains an LCD and is recruited to stress granules. TDP-43 and ATXN2 were found to interact genetically with DPRs, as knockdown of these genes suppressed the DPR-associated viability phenotype in flies (Lee et al., 2016). The observations that knockdown of disease-causing LCD-containing RBPs (i.e., TDP-43, ATXN2, hnRNP A1, hnRNP A2B1) suppresses the toxicity caused by other disease-associated proteins (i.e., VCP and DPRs) demonstrates that although disease-causing RBPs have separate functions, they are constituents of stress granules and normally maintain the material properties (i.e., assembly/disassembly rates, mobility, and viscosity) of stress granules, further strengthening the hypothesis that stress granules are dysregulated in ALS and FTD.

Taken together, an emerging refrain of these studies suggests that the consequence of disease-causing mutations in RBPs is a perturbation in the material properties of RNA granules due to increased adhesive forces between constituent proteins, thus increasing the viscosity of these liquid assemblies. This disturbance is expected to have two potentially adverse consequences. First, increased viscosity results in impaired dynamics of RNA granules (i.e., the ability to exchange components with the surrounding cytoplasm or to unpack their RNA cargo at the appropriate time and place) and impaired normal function. Consistent with this hypothesis, mutations in hnRNP A1, hnRNP A2B1, and TIA1 increase the adhesive forces that drive higher order assembly (Kim et al., 2013; Mackenzie et al., 2017), alter the material properties and dynamics of RNA granules composed of these proteins (Mackenzie et al., 2017), and produce poorly dynamic RNA granules (Kim et al., 2013; Mackenzie et al., 2017). Second, the accumulation of poorly dynamic RNA granules is likely to promote longer length-scale (and thus more stable) assemblies of fibrillization-prone proteins such as TDP-43 and FUS. According to this view, persistent, poorly dynamic RNA granules may evolve over time into pathological inclusions that are appreciated in end-stage disease, thus accounting for the frequent association of RNA granule components with ALS-FTD pathology (**Figure 2**)—a hypothesis that remains to be tested.

FUTURE QUESTIONS

Although immense progress has been made toward defining the genetic and biological basis of ALS and FTD, it remains challenging to define the molecular mechanisms that link specific disease-causing mutations to stress granule dysfunction and the accumulation of pathological inclusions. Given the

converging evidence described here, one of the most compelling hypotheses is founded on the notion that impairment of the material properties of stress granules leads to impairment of the functions supported by these organelles (**Figure 2**). At the same time, the residence time of aggregation-prone proteins in the highly concentrated environment is prolonged, increasing the opportunity for nucleating the assembly of stable, amyloid structures and also promoting their growth and maturation (**Figure 2**). Perhaps the most stable of these is TDP-43, which may be prone to form stable assemblies and become toxic within poorly dynamic stress granules. Going forward, there are four pressing enigmas to resolve that relate to how assemblies built from hnRNPs (such as stress granules) contribute to disease. First, we must define precisely how disease mutations impair the material properties of membraneless organelles. Second, we must identify which function(s) of membraneless organelles are impaired in a manner that contributes to ALS and FTD pathology. Third, in a related question, we need to determine which membraneless organelles are important in this process, including delineating whether stress granules are indeed the key target. Finally, we must define whether impaired membraneless organelles (e.g., stress granules) are the source of TDP-43 pathology, and if so, whether this contributes to driving the pathogenic process. Answering these questions will advance our understanding of the key molecular processes that drive ALS and FTD with the long-term goal of identifying potential targets or processes for therapeutic intervention.

AUTHOR CONTRIBUTIONS

All authors listed have made a substantial, direct and intellectual contribution to the work, and approved it for publication.

FUNDING

This work was supported by an ALSA Milton Safenowitz Fellowship (MP), a Hartwell Foundation Fellowship (MP), National Institutes of Health R35 NS097974 (JT), and the Howard Hughes Medical Institute (JT).

ACKNOWLEDGMENTS

We thank Natalia Nedelsky for editorial assistance.

REFERENCES

Alami, N. H., Smith, R. B., Carrasco, M. A., Williams, L. A., Winborn, C. S., Han, S. S. W., et al. (2014). Axonal transport of TDP-43 mRNA granules is impaired by ALS-causing mutations. *Neuron* 81, 536–543. doi: 10.1016/j.neuron.2013.12.018

Austin, J. A., Wright, G. S., Watanabe, S., Grossmann, J. G., Antonyuk, S. V., Yamanaka, K., et al. (2014). Disease causing mutants of TDP-43 nucleic acid binding domains are resistant to aggregation and have increased stability and half-life. *Proc. Natl. Acad. Sci. U.S.A.* 111, 4309–4314. doi: 10.1073/pnas.1317317111

Avendano-Vazquez, S. E., Dhir, A., Bembich, S., Buratti, E., Proudfoot, N., and Baralle, F. E. (2012). Autoregulation of TDP-43 mRNA levels involves interplay between transcription, splicing, and alternative polyA site selection. *Genes Dev.* 26, 1679–1684. doi: 10.1101/gad.194829.112

Ayala, Y. M., De Conti, L., Avendano-Vazquez, S. E., Dhir, A., Romano, M., D'ambrogio, A., et al. (2011). TDP-43 regulates its mRNA levels through a negative feedback loop. *EMBO J.* 30, 277–288. doi: 10.1038/emboj.2010.310

Ayala, Y. M., Zago, P., D'ambrogio, A., Xu, Y. F., Petrucelli, L., Buratti, E., et al. (2008). Structural determinants of the cellular localization and shuttling of TDP-43. *J. Cell Sci.* 121, 3778–3785. doi: 10.1242/jcs.038950

Baechtold, H., Kuroda, M., Sok, J., Ron, D., Lopez, B. S., and Akhmedov, A. T. (1999). Human 75-kDa DNA-pairing protein is identical to the pro-oncoprotein TLS/FUS and is able to promote D-loop formation. *J. Biol. Chem.* 274, 34337–34342. doi: 10.1074/jbc.274.48.34337

Baron, D. M., Kaushansky, L. J., Ward, C. L., Sama, R. R., Chian, R. J., Boggio, K. J., et al. (2013). Amyotrophic lateral sclerosis-linked FUS/TLS alters stress granule assembly and dynamics. *Mol. Neurodegener.* 8:30. doi: 10.1186/1750-1326-8-30

Bauer, W. J., Heath, J., Jenkins, J. L., and Kielkopf, C. L. (2012). Three RNA recognition motifs participate in RNA recognition and structural organization by the pro-apoptotic factor TIA-1. *J. Mol. Biol.* 415, 727–740. doi: 10.1016/j.jmb.2011.11.040

Belly, A., Moreau-Gachelin, F., Sadoul, R., and Goldberg, Y. (2005). Delocalization of the multifunctional RNA splicing factor TLS/FUS in hippocampal neurones: exclusion from the nucleus and accumulation in dendritic granules and spine heads. *Neurosci. Lett.* 379, 152–157. doi: 10.1016/j.neulet.2004.12.071

Bentmann, E., Haass, C., and Dormann, D. (2013). Stress granules in neurodegeneration–lessons learnt from TAR DNA binding protein of 43 kDa and fused in sarcoma. *FEBS J.* 280, 4348–4370. doi: 10.1111/febs.12287

Bentmann, E., Neumann, M., Tahirovic, S., Rodde, R., Dormann, D., and Haass, C. (2012). Requirements for stress granule recruitment of fused in sarcoma (FUS) and TAR DNA-binding protein of 43 kDa (TDP-43). *J. Biol. Chem.* 287, 23079–23094. doi: 10.1074/jbc.M111.328757

Beriault, V., Clement, J. F., Levesque, K., Lebel, C., Yong, X., Chabot, B., et al. (2004). A late role for the association of hnRNP A2 with the HIV-1 hnRNP A2 response elements in genomic RNA, Gag, and Vpr localization. *J. Biol. Chem.* 279, 44141–44153. doi: 10.1074/jbc.M404691200

Berry, J., Weber, S. C., Vaidya, N., Haataja, M., and Brangwynne, C. P. (2015). RNA transcription modulates phase transition-driven nuclear body assembly. *Proc. Natl. Acad. Sci. U.S.A.* 112, E5237–E5245. doi: 10.1073/pnas.1509317112

Bertrand, P., Akhmedov, A. T., Delacote, F., Durrbach, A., and Lopez, B. S. (1999). Human POMp75 is identified as the pro-oncoprotein TLS/FUS: both POMp75 and POMp100 DNA homologous pairing activities are associated to cell proliferation. *Oncogene* 18, 4515–4521. doi: 10.1038/sj.onc.1203048

Boehringer, A., Garcia-Mansfield, K., Singh, G., Bakkar, N., Pirrotte, P., and Bowser, R. (2017). ALS associated mutations in matrin 3 alter protein-protein interactions and impede mRNA nuclear export. *Sci. Rep.* 7:14529. doi: 10.1038/s41598-017-14924-6

Boeynaems, S., Bogaert, E., Kovacs, D., Konijnenberg, A., Timmerman, E., Volkov, A., et al. (2017). Phase separation of C9orf72 dipeptide repeats perturbs stress granule dynamics. *Mol. Cell* 65, 1044 e1045–1055 e1045. doi: 10.1016/j.molcel.2017.02.013

Bosco, D. A., Lemay, N., Ko, H. K., Zhou, H., Burke, C., Kwiatkowski, T. J. Jr., et al. (2010). Mutant FUS proteins that cause amyotrophic lateral sclerosis incorporate into stress granules. *Hum. Mol. Genet.* 19, 4160–4175. doi: 10.1093/hmg/ddq335

Buchan, J. R., Kolaitis, R. M., Taylor, J. P., and Parker, R. (2013). Eukaryotic stress granules are cleared by autophagy and Cdc48/VCP function. *Cell* 153, 1461–1474. doi: 10.1016/j.cell.2013.05.037

Buratti, E., and Baralle, F. E. (2001). Characterization and functional implications of the RNA binding properties of nuclear factor TDP-43, a novel splicing regulator of CFTR exon 9. *J. Biol. Chem.* 276, 36337–36343. doi: 10.1074/jbc.M104236200

Buratti, E., Brindisi, A., Giombi, M., Tisminetzky, S., Ayala, Y. M., and Baralle, F. E. (2005). TDP-43 binds heterogeneous nuclear ribonucleoprotein A/B through its C-terminal tail: an important region for the inhibition of cystic fibrosis transmembrane conductance regulator exon 9 splicing. *J. Biol. Chem.* 280, 37572–37584. doi: 10.1074/jbc.M505557200

Carrascoso, I., Sanchez-Jimenez, C., and Izquierdo, J. M. (2014). Genome-wide profiling reveals a role for T-cell intracellular antigens TIA1 and TIAR in the control of translational specificity in HeLa cells. *Biochem. J.* 461, 43–50. doi: 10.1042/BJ20140227

Chiang, C. H., Grauffel, C., Wu, L. S., Kuo, P. H., Doudeva, L. G., Lim, C., et al. (2016). Structural analysis of disease-related TDP-43 D169G mutation: linking enhanced stability and caspase cleavage efficiency to protein accumulation. *Sci. Rep.* 6:21581. doi: 10.1038/srep21581

Coelho, M. B., Attig, J., Bellora, N., Konig, J., Hallegger, M., Kayikci, M., et al. (2015). Nuclear matrix protein Matrin3 regulates alternative splicing and forms overlapping regulatory networks with PTB. *EMBO J.* 34, 653–668. doi: 10.15252/embj.201489852

Conicella, A. E., Zerze, G. H., Mittal, J., and Fawzi, N. L. (2016). ALS mutations disrupt phase separation mediated by alpha-helical structure in the TDP-43 low-complexity C-terminal domain. *Structure* 24, 1537–1549. doi: 10.1016/j.str.2016.07.007

Coyne, A. N., Siddegowda, B. B., Estes, P. S., Johannesmeyer, J., Kovalik, T., Daniel, S. G., et al. (2014). Futsch/MAP1B mRNA is a translational target of TDP-43 and is neuroprotective in a Drosophila model of amyotrophic lateral sclerosis. *J. Neurosci.* 34, 15962–15974. doi: 10.1523/JNEUROSCI.2526-14.2014

Das, R., Yu, J., Zhang, Z., Gygi, M. P., Krainer, A. R., Gygi, S. P., et al. (2007). SR proteins function in coupling RNAP II transcription to pre-mRNA splicing. *Mol. Cell* 26, 867–881. doi: 10.1016/j.molcel.2007.05.036

DeJesus-Hernandez, M., Mackenzie, I. R., Boeve, B. F., Boxer, A. L., Baker, M., Rutherford, N. J., et al. (2011). Expanded GGGGCC hexanucleotide repeat in noncoding region of C9ORF72 causes chromosome 9p-linked FTD and ALS. *Neuron* 72, 245–256. doi: 10.1016/j.neuron.2011.09.011

Dember, L. M., Kim, N. D., Liu, K. Q., and Anderson, P. (1996). Individual RNA recognition motifs of TIA-1 and TIAR have different RNA binding specificities. *J. Biol. Chem.* 271, 2783–2788. doi: 10.1074/jbc.271.5.2783

Dewey, C. M., Cenik, B., Sephton, C. F., Dries, D. R., Mayer, P. III, Good, S. K., et al. (2011). TDP-43 is directed to stress granules by sorbitol, a novel physiological osmotic and oxidative stressor. *Mol. Cell. Biol.* 31, 1098–1108. doi: 10.1128/MCB.01279-10

Dormann, D., Madl, T., Valori, C. F., Bentmann, E., Tahirovic, S., Abou-Ajram, C., et al. (2012). Arginine methylation next to the PY-NLS modulates Transportin binding and nuclear import of FUS. *EMBO J.* 31, 4258–4275. doi: 10.1038/emboj.2012.261

Dormann, D., Rodde, R., Edbauer, D., Bentmann, E., Fischer, I., Hruscha, A., et al. (2010). ALS-associated fused in sarcoma (FUS) mutations disrupt Transportin-mediated nuclear import. *EMBO J.* 29, 2841–2857. doi: 10.1038/emboj.2010.143

Elbaum-Garfinkle, S., Kim, Y., Szczepaniak, K., Chen, C. C., Eckmann, C. R., Myong, S., et al. (2015). The disordered P granule protein LAF-1 drives phase separation into droplets with tunable viscosity and dynamics. *Proc. Natl. Acad. Sci. U.S.A.* 112, 7189–7194. doi: 10.1073/pnas.1504822112

Elvira, G., Wasiak, S., Blandford, V., Tong, X. K., Serrano, A., Fan, X., et al. (2006). Characterization of an RNA granule from developing brain. *Mol. Cell. Proteomics* 5, 635–651. doi: 10.1074/mcp.M500255-MCP200

Errichelli, L., Dini Modigliani, S., Laneve, P., Colantoni, A., Legnini, I., Capauto, D., et al. (2017). FUS affects circular RNA expression in murine embryonic stem cell-derived motor neurons. *Nat. Commun.* 8:14741. doi: 10.1038/ncomms14741

Fallini, C., Bassell, G. J., and Rossoll, W. (2012). The ALS disease protein TDP-43 is actively transported in motor neuron axons and regulates axon outgrowth. *Hum. Mol. Genet.* 21, 3703–3718. doi: 10.1093/hmg/dds205

Flynn, R. L., Centore, R. C., O'sullivan, R. J., Rai, R., Tse, A., Songyang, Z., et al. (2011). TERRA and hnRNPA1 orchestrate an RPA-to-POT1 switch on telomeric single-stranded DNA. *Nature* 471, 532–536. doi: 10.1038/nature09772

Forch, P., Puig, O., Martinez, C., Seraphin, B., and Valcarcel, J. (2002). The splicing regulator TIA-1 interacts with U1-C to promote U1 snRNP recruitment to 5' splice sites. *EMBO J.* 21, 6882–6892. doi: 10.1093/emboj/cdf668

Freibaum, B. D., Chitta, R. K., High, A. A., and Taylor, J. P. (2010). Global analysis of TDP-43 interacting proteins reveals strong association with RNA splicing and translation machinery. *J. Proteome Res.* 9, 1104–1120. doi: 10.1021/pr901076y

Freibaum, B. D., Lu, Y., Lopez-Gonzalez, R., Kim, N. C., Almeida, S., Lee, K. H., et al. (2015). GGGGCC repeat expansion in C9orf72 compromises nucleocytoplasmic transport. *Nature* 525, 129–133. doi: 10.1038/nature14974

Gallego-Iradi, M. C., Clare, A. M., Brown, H. H., Janus, C., Lewis, J., and Borchelt, D. R. (2015). Subcellular localization of matrin 3 containing mutations associated with ALS and distal myopathy. *PLoS ONE* 10:e0142144. doi: 10.1371/journal.pone.0142144

Garner, E., Cannon, P., Romero, P., Obradovic, Z., and Dunker, A. K. (1998). Predicting disordered regions from amino acid sequence: common themes despite differing structural characterization. *Genome Inform. Ser. Workshop Genome Inform.* 9, 201–213.

Garner, E., Romero, P., Dunker, A. K., Brown, C., and Obradovic, Z. (1999). Predicting binding regions within disordered proteins. *Genome Inform. Ser. Workshop Genome Inform.* 10, 41–50.

Gendron, T. F., Bieniek, K. F., Zhang, Y. J., Jansen-West, K., Ash, P. E., Caulfield, T., et al. (2013). Antisense transcripts of the expanded C9ORF72 hexanucleotide repeat form nuclear RNA foci and undergo repeat-associated non-ATG translation in c9FTD/ALS. *Acta Neuropathol.* 126, 829–844. doi: 10.1007/s00401-013-1192-8

Gilks, N., Kedersha, N., Ayodele, M., Shen, L., Stoecklin, G., Dember, L. M., et al. (2004). Stress granule assembly is mediated by prion-like aggregation of TIA-1. *Mol. Biol. Cell* 15, 5383–5398. doi: 10.1091/mbc.E04-08-0715

Gitcho, M. A., Baloh, R. H., Chakraverty, S., Mayo, K., Norton, J. B., Levitch, D., et al. (2008). TDP-43 A315T mutation in familial motor neuron disease. *Ann. Neurol.* 63, 535–538. doi: 10.1002/ana.21344

Godena, V. K., Romano, G., Romano, M., Appocher, C., Klima, R., Buratti, E., et al. (2011). TDP-43 regulates Drosophila neuromuscular junctions growth by modulating Futsch/MAP1B levels and synaptic microtubules organization. *PLoS ONE* 6:e17808. doi: 10.1371/journal.pone.0017808

Goldschmidt, L., Teng, P. K., Riek, R., and Eisenberg, D. (2010). Identifying the amylome, proteins capable of forming amyloid-like fibrils. *Proc. Natl. Acad. Sci. U.S.A.* 107, 3487–3492. doi: 10.1073/pnas.0915166107

Gopal, P. P., Nirschl, J. J., Klinman, E., and Holzbaur, E. L. (2017). Amyotrophic lateral sclerosis-linked mutations increase the viscosity of liquid-like TDP-43 RNP granules in neurons. *Proc. Natl. Acad. Sci. U.S.A.* 114, E2466–E2475. doi: 10.1073/pnas.1614462114

Gregory, R. I., Yan, K. P., Amuthan, G., Chendrimada, T., Doratotaj, B., Cooch, N., et al. (2004). The Microprocessor complex mediates the genesis of microRNAs. *Nature* 432, 235–240. doi: 10.1038/nature03120

Guil, S., Long, J. C., and Caceres, J. F. (2006). hnRNP A1 relocalization to the stress granules reflects a role in the stress response. *Mol. Cell. Biol.* 26, 5744–5758. doi: 10.1128/MCB.00224-06

Guo, R., Li, Y., Ning, J., Sun, D., Lin, L., and Liu, X. (2013). HnRNP A1/A2 and SF2/ASF regulate alternative splicing of interferon regulatory factor-3 and affect immunomodulatory functions in human non-small cell lung cancer cells. *PLoS ONE* 8:e62729. doi: 10.1371/journal.pone.0062729

Han, T. W., Kato, M., Xie, S., Wu, L. C., Mirzaei, H., Pei, J., et al. (2012). Cell-free formation of RNA granules: bound RNAs identify features and components of cellular assemblies. *Cell* 149, 768–779. doi: 10.1016/j.cell.2012.04.016

Hennig, S., Kong, G., Mannen, T., Sadowska, A., Kobelke, S., Blythe, A., et al. (2015). Prion-like domains in RNA binding proteins are essential for building subnuclear paraspeckles. *J. Cell Biol.* 210, 529–539. doi: 10.1083/jcb.201504117

Hibino, Y., Nakamura, K., Asano, S., and Sugano, N. (1992). Affinity of a highly repetitive bent DNA for nuclear scaffold proteins from rat liver. *Biochem. Biophys. Res. Commun.* 184, 853–858. doi: 10.1016/0006-291X(92)90668-B

Hibino, Y., Usui, T., Morita, Y., Hirose, N., Okazaki, M., Sugano, N., et al. (2006). Molecular properties and intracellular localization of rat liver nuclear scaffold protein P130. *Biochim. Biophys. Acta* 1759, 195–207. doi: 10.1016/j.bbaexp.2006.04.010

Irwin, D. J., Cairns, N. J., Grossman, M., Mcmillan, C. T., Lee, E. B., Van Deerlin, V. M., et al. (2015). Frontotemporal lobar degeneration: defining phenotypic diversity through personalized medicine. *Acta Neuropathol.* 129, 469–491. doi: 10.1007/s00401-014-1380-1

Ito, D., Seki, M., Tsunoda, Y., Uchiyama, H., and Suzuki, N. (2011). Nuclear transport impairment of amyotrophic lateral sclerosis-linked mutations in FUS/TLS. *Ann. Neurol.* 69, 152–162. doi: 10.1002/ana.22246

Jean-Philippe, J., Paz, S., and Caputi, M. (2013). hnRNP A1: the Swiss army knife of gene expression. *Int. J. Mol. Sci.* 14, 18999–19024. doi: 10.3390/ijms140918999

Jiang, L. L., Xue, W., Hong, J. Y., Zhang, J. T., Li, M. J., Yu, S. N., et al. (2017). The N-terminal dimerization is required for TDP-43 splicing activity. *Sci. Rep.* 7:6196. doi: 10.1038/s41598-017-06263-3

Johnson, J. O., Pioro, E. P., Boehringer, A., Chia, R., Feit, H., Renton, A. E., et al. (2014). Mutations in the Matrin 3 gene cause familial amyotrophic lateral sclerosis. *Nat. Neurosci.* 17, 664–666. doi: 10.1038/nn.3688

Kabashi, E., Valdmanis, P. N., Dion, P., Spiegelman, D., Mcconkey, B. J., Vande Velde, C., et al. (2008). TARDBP mutations in individuals with sporadic and familial amyotrophic lateral sclerosis. *Nat. Genet.* 40, 572–574. doi: 10.1038/ng.132

Kanai, Y., Dohmae, N., and Hirokawa, N. (2004). Kinesin transports RNA: isolation and characterization of an RNA-transporting granule. *Neuron* 43, 513–525. doi: 10.1016/j.neuron.2004.07.022

Kawahara, Y., and Mieda-Sato, A. (2012). TDP-43 promotes microRNA biogenesis as a component of the Drosha and Dicer complexes. *Proc. Natl. Acad. Sci. U.S.A.* 109, 3347–3352. doi: 10.1073/pnas.1112427109

Kedersha, N., Cho, M. R., Li, W., Yacono, P. W., Chen, S., Gilks, N., et al. (2000). Dynamic shuttling of TIA-1 accompanies the recruitment of mRNA to mammalian stress granules. *J. Cell Biol.* 151, 1257–1268. doi: 10.1083/jcb.151.6.1257

Kim, H. J., Kim, N. C., Wang, Y. D., Scarborough, E. A., Moore, J., Diaz, Z., et al. (2013). Mutations in prion-like domains in hnRNPA2B1 and hnRNPA1 cause multisystem proteinopathy and ALS. *Nature* 495, 467–473. doi: 10.1038/nature11922

Kim, H. S., Kuwano, Y., Zhan, M., Pullmann, R. Jr., Mazan-Mamczarz, K., Li, H., et al. (2007). Elucidation of a C-rich signature motif in target mRNAs of RNA-binding protein TIAR. *Mol. Cell. Biol.* 27, 6806–6817. doi: 10.1128/MCB.01036-07

Kitamura, A., Nakayama, Y., Shibasaki, A., Taki, A., Yuno, S., Takeda, K., et al. (2016). Interaction of RNA with a C-terminal fragment of the amyotrophic lateral sclerosis-associated TDP43 reduces cytotoxicity. *Sci. Rep.* 6:19230. doi: 10.1038/srep19230

Klar, J., Sobol, M., Melberg, A., Mabert, K., Ameur, A., Johansson, A. C., et al. (2013). Welander distal myopathy caused by an ancient founder mutation in TIA1 associated with perturbed splicing. *Hum. Mutat.* 34, 572–577. doi: 10.1002/humu.22282

Kuang, L., Kamelgarn, M., Arenas, A., Gal, J., Taylor, D., Gong, W., et al. (2017). Clinical and experimental studies of a novel P525R FUS mutation in amyotrophic lateral sclerosis. *Neurol. Genet.* 3:e172. doi: 10.1212/NXG.0000000000000172

Kuhnlein, P., Sperfeld, A. D., Vanmassenhove, B., Van Deerlin, V., Lee, V. M., Trojanowski, J. Q., et al. (2008). Two German kindreds with familial amyotrophic lateral sclerosis due to TARDBP mutations. *Arch. Neurol.* 65, 1185–1189. doi: 10.1001/archneur.65.9.1185

Kuo, P. H., Chiang, C. H., Wang, Y. T., Doudeva, L. G., and Yuan, H. S. (2014). The crystal structure of TDP-43 RRM1-DNA complex reveals the specific recognition for UG- and TG-rich nucleic acids. *Nucleic Acids Res.* 42, 4712–4722. doi: 10.1093/nar/gkt1407

Kwiatkowski, T. J. Jr., Bosco, D. A., Leclerc, A. L., Tamrazian, E., Vanderburg, C. R., Russ, C., et al. (2009). Mutations in the FUS/TLS gene on chromosome 16 cause familial amyotrophic lateral sclerosis. *Science* 323, 1205–1208. doi: 10.1126/science.1166066

Kwon, I., Xiang, S., Kato, M., Wu, L., Theodoropoulos, P., Wang, T., et al. (2014). Poly-dipeptides encoded by the C9orf72 repeats bind nucleoli, impede RNA biogenesis, and kill cells. *Science* 345, 1139–1145. doi: 10.1126/science.1254917

Lagier-Tourenne, C., Polymenidou, M., and Cleveland, D. W. (2010). TDP-43 and FUS/TLS: emerging roles in RNA processing and neurodegeneration. *Hum. Mol. Genet.* 19, R46–R64. doi: 10.1093/hmg/ddq137

Leblond, C. S., Gan-Or, Z., Spiegelman, D., Laurent, S. B., Szuto, A., Hodgkinson, A., et al. (2016). Replication study of MATR3 in familial and sporadic amyotrophic lateral sclerosis. *Neurobiol. Aging 37*, 209 e217–209 e221. doi: 10.1016/j.neurobiolaging.2015.09.013

Lee, B. J., Cansizoglu, A. E., Suel, K. E., Louis, T. H., Zhang, Z., and Chook, Y. M. (2006). Rules for nuclear localization sequence recognition by karyopherin beta 2. *Cell* 126, 543–558. doi: 10.1016/j.cell.2006.05.049

Lee, K. H., Zhang, P., Kim, H. J., Mitrea, D. M., Sarkar, M., Freibaum, B. D., et al. (2016). C9orf72 dipeptide repeats impair the assembly, dynamics, and function of membrane-less organelles. *Cell* 167, 774–788.e17. doi: 10.1016/j.cell.2016.10.002

Lemieux, B., Blanchette, M., Monette, A., Mouland, A. J., Wellinger, R. J., and Chabot, B. (2015). A function for the hnRNP A1/A2 proteins in transcription elongation. *PLoS ONE* 10:e0126654. doi: 10.1371/journal.pone.0126654

Lenzi, J., De Santis, R., De Turris, V., Morlando, M., Laneve, P., Calvo, A., et al. (2015). ALS mutant FUS proteins are recruited into stress granules in induced pluripotent stem cell-derived motoneurons. *Dis. Model. Mech.* 8, 755–766. doi: 10.1242/dmm.020099

Li, H. R., Chen, T. C., Hsiao, C. L., Shi, L., Chou, C. Y., and Huang, J. R. (2018). The physical forces mediating self-association and phase-separation in the C-terminal domain of TDP-43. *Biochim. Biophys. Acta* 1866, 214–223. doi: 10.1016/j.bbapap.2017.10.001

Lin, K. P., Tsai, P. C., Liao, Y. C., Chen, W. T., Tsai, C. P., Soong, B. W., et al. (2015). Mutational analysis of MATR3 in Taiwanese patients with amyotrophic lateral sclerosis. *Neurobiol. Aging* 36, 2005.e1–2005.e14. doi: 10.1016/j.molcel.2015.08.018

Lin, Y., Protter, D. S., Rosen, M. K., and Parker, R. (2015). Formation and maturation of phase-separated liquid droplets by RNA-binding proteins. *Mol. Cell* 60, 208–219. doi: 10.1016/j.neurobiolaging.2015.02.008

Ling, J. P., Pletnikova, O., Troncoso, J. C., and Wong, P. C. (2015). TDP-43 repression of nonconserved cryptic exons is compromised in ALS-FTD. *Science* 349, 650–655. doi: 10.1126/science.aab0983

Ling, S. C., Albuquerque, C. P., Han, J. S., Lagier-Tourenne, C., Tokunaga, S., Zhou, H., et al. (2010). ALS-associated mutations in TDP-43 increase its stability and promote TDP-43 complexes with FUS/TLS. *Proc. Natl. Acad. Sci. U.S.A.* 107, 13318–13323. doi: 10.1073/pnas.1008227107

Liu, Y. C., Chiang, P. M., and Tsai, K. J. (2013). Disease animal models of TDP-43 proteinopathy and their pre-clinical applications. *Int. J. Mol. Sci.* 14, 20079–20111. doi: 10.3390/ijms141020079

Lopez de Silanes, I., Galban, S., Martindale, J. L., Yang, X., Mazan-Mamczarz, K., Indig, F. E., et al. (2005). Identification and functional outcome of mRNAs associated with RNA-binding protein TIA-1. *Mol. Cell. Biol.* 25, 9520–9531. doi: 10.1128/MCB.25.21.9520-9531.2005

Mackenzie, I. R., Nicholson, A. M., Sarkar, M., Messing, J., Purice, M. D., Pottier, C., et al. (2017). TIA1 mutations in amyotrophic lateral sclerosis and frontotemporal dementia promote phase separation and alter stress granule dynamics. *Neuron* 95, 808 e809–816 e809. doi: 10.1016/j.neuron.2017.07.025

Majounie, E., Renton, A. E., Mok, K., Dopper, E. G., Waite, A., Rollinson, S., et al. (2012). Frequency of the C9orf72 hexanucleotide repeat expansion in patients with amyotrophic lateral sclerosis and frontotemporal dementia: a cross-sectional study. *Lancet Neurol.* 11, 323–330. doi: 10.1016/S1474-4422(12)70043-1

Marangi, G., Lattante, S., Doronzio, P. N., Conte, A., Tasca, G., Monforte, M., et al. (2017). Matrin 3 variants are frequent in Italian ALS patients. *Neurobiol Aging* 49, 218 e1–218 e7. doi: 10.1016/j.neurobiolaging.2016.09.023

McDonald, K. K., Aulas, A., Destroismaisons, L., Pickles, S., Beleac, E., Camu, W., et al. (2011). TAR DNA-binding protein 43 (TDP-43) regulates stress granule dynamics via differential regulation of G3BP and TIA-1. *Hum. Mol. Genet.* 20, 1400–1410. doi: 10.1093/hmg/ddr021

Mizielinska, S., Gronke, S., Niccoli, T., Ridler, C. E., Clayton, E. L., Devoy, A., et al. (2014). C9orf72 repeat expansions cause neurodegeneration in Drosophila through arginine-rich proteins. *Science* 345, 1192–1194. doi: 10.1126/science.1256800

Molliex, A., Temirov, J., Lee, J., Coughlin, M., Kanagaraj, A. P., Kim, H. J., et al. (2015). Phase separation by low complexity domains promotes stress granule assembly and drives pathological fibrillization. *Cell* 163, 123–133. doi: 10.1016/j.cell.2015.09.015

Moloney, C., Rayaprolu, S., Howard, J., Fromholt, S., Brown, H., Collins, M., et al. (2016). Transgenic mice overexpressing the ALS-linked protein Matrin 3 develop a profound muscle phenotype. *Acta Neuropathol. Commun.* 4:122. doi: 10.1186/s40478-016-0393-5

Muller, T. J., Kraya, T., Stoltenburg-Didinger, G., Hanisch, F., Kornhuber, M., Stoevesandt, D., et al. (2014). Phenotype of matrin-3-related distal myopathy in 16 German patients. *Ann. Neurol.* 76, 669–680. doi: 10.1002/ana.24255

Nakielny, S., and Dreyfuss, G. (1999). Transport of proteins and RNAs in and out of the nucleus. *Cell* 99, 677–690. doi: 10.1016/S0092-8674(00)81666-9

Narayanan, R. K., Mangelsdorf, M., Panwar, A., Butler, T. J., Noakes, P. G., and Wallace, R. H. (2013). Identification of RNA bound to the TDP-43 ribonucleoprotein complex in the adult mouse brain. *Amyotroph. Lateral Scler. Frontotemporal Degener.* 14, 252–260. doi: 10.3109/21678421.2012.734520

Neumann, M., Sampathu, D. M., Kwong, L. K., Truax, A. C., Micsenyi, M. C., Chou, T. T., et al. (2006). Ubiquitinated TDP-43 in frontotemporal lobar degeneration and amyotrophic lateral sclerosis. *Science* 314, 130–133. doi: 10.1126/science.1134108

Nolan, M., Talbot, K., and Ansorge, O. (2016). Pathogenesis of FUS-associated ALS and FTD: insights from rodent models. *Acta Neuropathol. Commun.* 4:99. doi: 10.1186/s40478-016-0358-8

Origone, P., Verdiani, S., Bandettini Di Poggio, M., Zuccarino, R., Vignolo, M., Caponnetto, C., et al. (2015). A novel Arg147Trp MATR3 missense mutation in a slowly progressive ALS Italian patient. *Amyotroph. Lateral Scler. Frontotemporal Degener.* 16, 530–531. doi: 10.3109/21678421.2015.1058397

Pamphlett, R., Luquin, N., Mclean, C., Jew, S. K., and Adams, L. (2009). TDP-43 neuropathology is similar in sporadic amyotrophic lateral sclerosis with or without TDP-43 mutations. *Neuropathol. Appl. Neurobiol.* 35, 222–225. doi: 10.1111/j.1365-2990.2008.00982.x

Panas, M. D., Ivanov, P., and Anderson, P. (2016). Mechanistic insights into mammalian stress granule dynamics. *J. Cell Biol.* 215, 313–323. doi: 10.1083/jcb.201609081

Patel, A., Lee, H. O., Jawerth, L., Maharana, S., Jahnel, M., Hein, M. Y., et al. (2015). A liquid-to-solid phase transition of the ALS protein FUS accelerated by disease mutation. *Cell* 162, 1066–1077. doi: 10.1016/j.cell.2015.07.047

Polymenidou, M., Lagier-Tourenne, C., Hutt, K. R., Huelga, S. C., Moran, J., Liang, T. Y., et al. (2011). Long pre-mRNA depletion and RNA missplicing contribute to neuronal vulnerability from loss of TDP-43. *Nat. Neurosci.* 14, 459–468. doi: 10.1038/nn.2779

Rajgor, D., Hanley, J. G., and Shanahan, C. M. (2016). Identification of novel nesprin-1 binding partners and cytoplasmic matrin-3 in processing bodies. *Mol. Biol. Cell* 27, 3894–3902. doi: 10.1091/mbc.E16-06-0346

Ramaswami, M., Taylor, J. P., and Parker, R. (2013). Altered ribostasis: RNA-protein granules in degenerative disorders. *Cell* 154, 727–736. doi: 10.1016/j.cell.2013.07.038

Ratti, A., and Buratti, E. (2016). Physiological functions and pathobiology of TDP-43 and FUS/TLS proteins. *J. Neurochem.* 138(Suppl. 1), 95–111. doi: 10.1111/jnc.13625

Rayaprolu, S., D'alton, S., Crosby, K., Moloney, C., Howard, J., Duffy, C., et al. (2016). Heterogeneity of Matrin 3 in the developing and aging murine central nervous system. *J. Comp. Neurol.* 524, 2740–2752. doi: 10.1002/cne.23986

Renton, A. E., Majounie, E., Waite, A., Simon-Sanchez, J., Rollinson, S., Gibbs, J. R., et al. (2011). A hexanucleotide repeat expansion in C9ORF72 is the cause of chromosome 9p21-linked ALS-FTD. *Neuron* 72, 257–268. doi: 10.1016/j.neuron.2011.09.010

Ritson, G. P., Custer, S. K., Freibaum, B. D., Guinto, J. B., Geffel, D., Moore, J., et al. (2010). TDP-43 mediates degeneration in a novel Drosophila model of disease caused by mutations in VCP/p97. *J. Neurosci.* 30, 7729–7739. doi: 10.1523/JNEUROSCI.5894-09.2010

Romero, O., and Dunker, K. (1997). Sequence data analysis for long disordered regions prediction in the calcineurin family. *Genome Inform. Ser. Workshop Genome Inform.* 8, 110–124.

Rutherford, N. J., Zhang, Y. J., Baker, M., Gass, J. M., Finch, N. A., Xu, Y. F., et al. (2008). Novel mutations in TARDBP (TDP-43) in patients with familial amyotrophic lateral sclerosis. *PLoS Genet.* 4:e1000193. doi: 10.1371/journal.pgen.1000193

Saberi, S., Stauffer, J. E., Jiang, J., Garcia, S. D., Taylor, A. E., Schulte, D., et al. (2017). Sense-encoded poly-GR dipeptide repeat proteins correlate to neurodegeneration and uniquely co-localize with TDP-43 in dendrites of repeat-expanded C9orf72 amyotrophic lateral sclerosis. *Acta Neuropathol.* 135, 459–474. doi: 10.1007/s00401-017-1793-8

Salajegheh, M., Pinkus, J. L., Taylor, J. P., Amato, A. A., Nazareno, R., Baloh, R. H., et al. (2009). Sarcoplasmic redistribution of nuclear TDP-43 in inclusion body myositis. *Muscle Nerve* 40, 19–31. doi: 10.1002/mus.21386

Salton, M., Elkon, R., Borodina, T., Davydov, A., Yaspo, M. L., Halperin, E., et al. (2011). Matrin 3 binds and stabilizes mRNA. *PLoS ONE* 6:e23882. doi: 10.1371/journal.pone.0023882

Salton, M., Lerenthal, Y., Wang, S. Y., Chen, D. J., and Shiloh, Y. (2010). Involvement of Matrin 3 and SFPQ/NONO in the DNA damage response. *Cell Cycle* 9, 1568–1576. doi: 10.4161/cc.9.8.11298

Sama, R. R., Ward, C. L., and Bosco, D. A. (2014). Functions of FUS/TLS from DNA repair to stress response: implications for ALS. *ASN Neuro* 6:1759091414544472. doi: 10.1177/1759091414544472

Scekic-Zahirovic, J., Sendscheid, O., El Oussini, H., Jambeau, M., Sun, Y., Mersmann, S., et al. (2016). Toxic gain of function from mutant FUS protein is crucial to trigger cell autonomous motor neuron loss. *EMBO J.* 35, 1077–1097. doi: 10.15252/embj.201592559

Schoen, M., Reichel, J. M., Demestre, M., Putz, S., Deshpande, D., Proepper, C., et al. (2015). Super-resolution microscopy reveals presynaptic localization of the ALS/FTD related protein FUS in hippocampal neurons. *Front. Cell. Neurosci.* 9:496. doi: 10.3389/fncel.2015.00496

Sephton, C. F., and Yu, G. (2015). The function of RNA-binding proteins at the synapse: implications for neurodegeneration. *Cell. Mol. Life Sci.* 72, 3621–3635. doi: 10.1007/s00018-015-1943-x

Sharma, A., Lyashchenko, A. K., Lu, L., Nasrabady, S. E., Elmaleh, M., Mendelsohn, M., et al. (2016). ALS-associated mutant FUS induces selective motor neuron degeneration through toxic gain of function. *Nat. Commun.* 7:10465. doi: 10.1038/ncomms10465

Skowronska-Krawczyk, D., and Rosenfeld, M. G. (2015). Nuclear matrix revisited? *Cell Cycle* 14, 1487–1488. doi: 10.1080/15384101.2015.1032643

Sreedharan, J., Blair, I. P., Tripathi, V. B., Hu, X., Vance, C., Rogelj, B., et al. (2008). TDP-43 mutations in familial and sporadic amyotrophic lateral sclerosis. *Science* 319, 1668–1672. doi: 10.1126/science.1154584

Suzuki, N., Aoki, M., Warita, H., Kato, M., Mizuno, H., Shimakura, N., et al. (2010). FALS with FUS mutation in Japan, with early onset, rapid progress and basophilic inclusion. *J. Hum. Genet.* 55, 252–254. doi: 10.1038/jhg.2010.16

Tada, M., Doi, H., Koyano, S., Kubota, S., Fukai, R., Hashiguchi, S., et al. (2017). Matrin 3 Is a Component of Neuronal Cytoplasmic Inclusions of Motor Neurons in Sporadic Amyotrophic Lateral Sclerosis. *Am. J. Pathol.* 188, 507–514. doi: 10.1016/j.ajpath.2017.10.007.

Tateishi, T., Hokonohara, T., Yamasaki, R., Miura, S., Kikuchi, H., Iwaki, A., et al. (2010). Multiple system degeneration with basophilic inclusions in Japanese ALS patients with FUS mutation. *Acta Neuropathol.* 119, 355–364. doi: 10.1007/s00401-009-0621-1

Taylor, J. P. (2015). Multisystem proteinopathy: intersecting genetics in muscle, bone, and brain degeneration. *Neurology* 85, 658–660. doi: 10.1212/WNL.0000000000001862

Taylor, J. P., Brown, R. H. Jr., and Cleveland, D. W. (2016). Decoding ALS: from genes to mechanism. *Nature* 539, 197–206. doi: 10.1038/nature20413

Thandapani, P., O'connor, T. R., Bailey, T. L., and Richard, S. (2013). Defining the RGG/RG motif. *Mol. Cell* 50, 613–623. doi: 10.1016/j.molcel.2013.05.021

Tollervey, J. R., Curk, T., Rogelj, B., Briese, M., Cereda, M., Kayikci, M., et al. (2011). Characterizing the RNA targets and position-dependent splicing regulation by TDP-43. *Nat. Neurosci.* 14, 452–458. doi: 10.1038/nn.2778

Twyffels, L., Gueydan, C., and Kruys, V. (2014). Transportin-1 and Transportin-2: protein nuclear import and beyond. *FEBS Lett.* 588, 1857–1868. doi: 10.1016/j.febslet.2014.04.023

Van Deerlin, V. M., Leverenz, J. B., Bekris, L. M., Bird, T. D., Yuan, W., Elman, L. B., et al. (2008). TARDBP mutations in amyotrophic lateral sclerosis with TDP-43 neuropathology: a genetic and histopathological analysis. *Lancet Neurol.* 7, 409–416. doi: 10.1016/S1474-4422(08)70071-1

Vance, C., Rogelj, B., Hortobagyi, T., De Vos, K. J., Nishimura, A. L., Sreedharan, J., et al. (2009). Mutations in FUS, an RNA processing protein, cause familial amyotrophic lateral sclerosis type 6. *Science* 323, 1208–1211. doi: 10.1126/science.1165942

Wall, M. L., and Lewis, S. M. (2017). Methylarginines within the RGG-motif region of hnRNP A1 affect Its IRES trans-acting factor activity and are required for hnRNP A1 stress granule localization and formation. *J. Mol. Biol.* 429, 295–307. doi: 10.1016/j.jmb.2016.12.011

Wang, I. F., Wu, L. S., Chang, H. Y., and Shen, C. K. (2008). TDP-43, the signature protein of FTLD-U, is a neuronal activity-responsive factor. *J. Neurochem.* 105, 797–806. doi: 10.1111/j.1471-4159.2007.05190.x

Wang, I., Hennig, J., Jagtap, P. K., Sonntag, M., Valcarcel, J., and Sattler, M. (2014). Structure, dynamics and RNA binding of the multi-domain

splicing factor TIA-1. *Nucleic Acids Res.* 42, 5949–5966. doi: 10.1093/nar/gku193

Waris, S., Wilce, M. C., and Wilce, J. A. (2014). RNA recognition and stress granule formation by TIA proteins. *Int. J. Mol. Sci.* 15, 23377–23388. doi: 10.3390/ijms151223377

Webster, C. P., Smith, E. F., Shaw, P. J., and De Vos, K. J. (2017). Protein homeostasis in amyotrophic lateral sclerosis: therapeutic opportunities? *Front. Mol. Neurosci.* 10:123. doi: 10.3389/fnmol.2017.00123

Weihl, C. C., Temiz, P., Miller, S. E., Watts, G., Smith, C., Forman, M., et al. (2008). TDP-43 accumulation in inclusion body myopathy muscle suggests a common pathogenic mechanism with frontotemporal dementia. *J. Neurol. Neurosurg. Psychiatr.* 79, 1186–1189. doi: 10.1136/jnnp.2007.131334

Wen, X., Tan, W., Westergard, T., Krishnamurthy, K., Markandaiah, S. S., Shi, Y., et al. (2014). Antisense proline-arginine RAN dipeptides linked to C9ORF72-ALS/FTD form toxic nuclear aggregates that initiate *in vitro* and *in vivo* neuronal death. *Neuron* 84, 1213–1225. doi: 10.1016/j.neuron.2014.12.010

Xu, L., Li, J., Tang, L., Zhang, N., and Fan, D. (2016). MATR3 mutation analysis in a Chinese cohort with sporadic amyotrophic lateral sclerosis. *Neurobiol Aging* 38, 218.e3–218.e4. doi: 10.1016/j.neurobiolaging.2015.11.023

Yang, L., Embree, L. J., Tsai, S., and Hickstein, D. D. (1998). Oncoprotein TLS interacts with serine-arginine proteins involved in RNA splicing. *J. Biol. Chem.* 273, 27761–27764. doi: 10.1074/jbc.273.43.27761

Yokoseki, A., Shiga, A., Tan, C. F., Tagawa, A., Kaneko, H., Koyama, A., et al. (2008). TDP-43 mutation in familial amyotrophic lateral sclerosis. *Ann. Neurol.* 63, 538–542. doi: 10.1002/ana.21392

Zhang, T., Delestienne, N., Huez, G., Kruys, V., and Gueydan, C. (2005). Identification of the sequence determinants mediating the nucleo-cytoplasmic shuttling of TIAR and TIA-1 RNA-binding proteins. *J. Cell Sci.* 118, 5453–5463. doi: 10.1242/jcs.02669

Zhang, Z., Almeida, S., Lu, Y., Nishimura, A. L., Peng, L., Sun, D., et al. (2013). Downregulation of microRNA-9 in iPSC-derived neurons of FTD/ALS patients with TDP-43 mutations. *PLoS ONE* 8:e76055. doi: 10.1371/journal.pone.0076055

Zhang, Z., and Carmichael, G. G. (2001). The fate of dsRNA in the nucleus: a p54(nrb)-containing complex mediates the nuclear retention of promiscuously A-to-I edited RNAs. *Cell* 106, 465–475. doi: 10.1016/S0092-8674(01)00466-4

Zhao, T. T., Graber, T. E., Jordan, L. E., Cloutier, M., Lewis, S. M., Goulet, I., et al. (2009). hnRNP A1 regulates UV-induced NF-kappaB signalling through destabilization of cIAP1 mRNA. *Cell Death Differ.* 16, 244–252. doi: 10.1038/cdd.2008.146

Conflict of Interest Statement: The authors declare that the research was conducted in the absence of any commercial or financial relationships that could be construed as a potential conflict of interest.

frontiers in Neuroscience

REVIEW
published: 05 July 2018
doi: 10.3389/fnins.2018.00464

An Overview of the Role of Lipofuscin in Age-Related Neurodegeneration

Alexandra Moreno-García[1†], *Alejandra Kun*[2,3†], *Olga Calero*[1,4†], *Miguel Medina*[4,5*] and *Miguel Calero*[1,4,5*]

[1] Chronic Disease Programme-CROSADIS, Instituto de Salud Carlos III, Madrid, Spain, [2] Biochemistry Section, Science School, Universidad de la República, Montevideo, Uruguay, [3] Protein and Nucleic Acids Department, Instituto de Investigaciones Biológicas Clemente Estable, Montevideo, Uruguay, [4] Centro de Investigación Biomédica en Red sobre Enfermedades Neurodegenerativas, Madrid, Spain, [5] Alzheimer Disease Research Unit, CIEN Foundation, Queen Sofia Foundation Alzheimer Center, Madrid, Spain

Despite aging being by far the greatest risk factor for highly prevalent neurodegenerative disorders, the molecular underpinnings of age-related brain changes are still not well understood, particularly the transition from normal healthy brain aging to neuropathological aging. Aging is an extremely complex, multifactorial process involving the simultaneous interplay of several processes operating at many levels of the functional organization. The buildup of potentially toxic protein aggregates and their spreading through various brain regions has been identified as a major contributor to these pathologies. One of the most striking morphologic changes in neurons during normal aging is the accumulation of lipofuscin (LF) aggregates, as well as, neuromelanin pigments. LF is an autofluorescent lipopigment formed by lipids, metals and misfolded proteins, which is especially abundant in nerve cells, cardiac muscle cells and skin. Within the Central Nervous System (CNS), LF accumulates as aggregates, delineating a specific senescence pattern in both physiological and pathological states, altering neuronal cytoskeleton and cellular trafficking and metabolism, and being associated with neuronal loss, and glial proliferation and activation. Traditionally, the accumulation of LF in the CNS has been considered a secondary consequence of the aging process, being a mere bystander of the pathological buildup associated with different neurodegenerative disorders. Here, we discuss recent evidence suggesting the possibility that LF aggregates may have an active role in neurodegeneration. We argue that LF is a relevant effector of aging that represents a risk factor or driver for neurodegenerative disorders.

Keywords: aging, amyloid, autofluorescence, lipofuscin, neurodegeneration, oxidative stress, protein deposits

OPEN ACCESS

Edited by:
Naruhiko Sahara,
National Institute of Radiological Sciences (NIRS), Japan

Reviewed by:
Tomohiro Miyasaka,
Doshisha University, Japan
Sandra Tenreiro,
CEDOC-Chronic Diseases Research Center, NMS-UNL, Portugal

***Correspondence:**
Miguel Medina
mmedina@ciberned.es
Miguel Calero
mcalero@isciii.es

[†] *These authors have contributed equally to this work.*

Specialty section:
This article was submitted to Neurodegeneration, a section of the journal Frontiers in Neuroscience

Received: *18 January 2018*
Accepted: *18 June 2018*
Published: *05 July 2018*

Citation:
Moreno-García A, Kun A, Calero O, Medina M and Calero M (2018) An Overview of the Role of Lipofuscin in Age-Related Neurodegeneration. Front. Neurosci. 12:464. doi: 10.3389/fnins.2018.00464

INTRODUCTION

Despite aging being by far the greatest risk factor for highly prevalent neurodegenerative disorders, the molecular underpinning of age-related brain changes is still not well understood (Kukull et al., 2002). Physiological changes associated with aging are inherent to all animals, representing an extremely complex and multifactorial process involving the simultaneous interplay of several processes operating at many levels of the functional organization.

Recently, it has been proposed a classification of the main cellular and molecular events affected by aging, and particularly by brain aging (López-Otín et al., 2013). For any factor to be considered a hallmark of aging, it should meet the following criteria: (I) it should be present during normal aging; (II) its exacerbation should trigger an accelerated aging; and (III) its amelioration should prevent the normal aging course, even extending lifespan. Accordingly, one of the most relevant features of aging is related to the increasingly dysfunctional mechanisms of renewal of cellular constituents that precludes the clearance of damaged biomolecules and organelles and its replacement by new functional structures. This sustained inefficient recycling mechanism leads to the accumulation of unfit molecules that further interfere with cellular functions, preferentially within long-lived post-mitotic cells such as neurons (Hung et al., 2010; López-Otín et al., 2013). Among the main components of this biological "garbage," we could find indigestible protein aggregates, defective mitochondria and lipofuscin (LF) (Terman, 2001).

LF is a post-mitotic pigment traditionally associated with aging ("age pigment") (Terman and Brunk, 1998). In this review, we discuss recent evidence that suggests the possibility that rather than being a mere bystander of the aging process, LF may have an active role in neurodegenerative disorders such as Alzheimer's disease (AD), Parkinson's disease (PD), age-related macular degeneration (AMD).

LIPOFUSCIN COMPOSITION AND DISTRIBUTION

LF is a fluorescent complex mixture composed of highly oxidized cross-linked macromolecules (proteins, lipids, and sugars) with multiple metabolic origins (Höhn et al., 2010; König et al., 2017; Rodolfo et al., 2018). The nature and structure of LF complexes seem to vary among tissues and show temporal heterogeneity in composition of oxidized proteins (30–70%), lipids (20–50%), metals cations (Fe^{3+}, Fe^{2+}, Cu^{2+}, Zn^{2+}, Al^{3+}, Mn^{2+}, Ca^{2+}) (2%), and sugar residues (Benavides et al., 2002; Double et al., 2008).

Because of its polymeric and highly cross-linked nature, LF cannot be degraded, nor cleared by exocytosis, thus being accumulated within the lysosomes and cell cytoplasm of long-lived post-mitotic and senescent animal cells. Opposite, proliferative cells efficiently dilute LF aggregates during cell division, showing low or no accumulation of the pigment (Brunk and Terman, 2002; Porta, 2002; Terman and Brunk, 2005; Rodgers et al., 2009; Firlag et al., 2013). For this reason, LF deposits are especially abundant in nerve cells, cardiac muscle cells, and skin.

LF fluorescence shows a large heterogeneity in the emission spectra, which reveals differences in its chemical composition, as a result of its ripening in specific metabolic pathways (Schwartsburd, 1995). In general, the LF fluorescence emission presents a very wide spectra ranging from 400 to 700 nm, with a maximum around of 578 nm for excitation at 364 nm (Warburton et al., 2007). Due to its elevated levels within brain tissue, LF fluorescence interferes with different analytical techniques such as immunoconfocal microscopy. Thus, different experimental protocols have been used to block LF autofluorescence in tissue samples, such as Sudan Black, copper sulfate or picric acid treatments. However, these methods do not allow the study of LF concurrently with neurodegeneration markers, thus impeding the analysis of LF contribution to pathology.

Additionally, as LF plays a clear role in cellular senescence, and increasing interest is focused on the study of its potential pathophysiological role, several methods have been developed to quantify LF in brain tissue. Based on its high lipid content, classical methods of isolation and quantitation of LF employed organic solvent extraction or density gradient ultracentrifugation protocols (Siakotos, 1974; Taubold et al., 1975; Ottis et al., 2012). However, due to its fluorescent properties, most recent methods for LF detection and quantification are based on the use of fluorescence microscopy (Moore et al., 1995; Jung et al., 2010; Zheng et al., 2010; Jensen et al., 2016). Provided that LF presents a very broad fluorescence spectrum, fluorescence images of tissue preparations can be acquired over a broad range of wavelengths. Depending on the need to colocalized LF autofluorescence with other cellular structures, non-overlapping anti-antibodies or probes should be selected (Jung et al., 2010). For example, DNA probes emitting in the far-red range can be combined with the detection of LF in both green and red channels (Zheng et al., 2010). Recently, we have developed a method based on channel filtering of confocal microscopy to identify and discriminate LF autofluorescence signals from the specific ones, such as amyloid plaques in the AD brain (see **Figure 1**) (Kun et al., 2018).

MECHANISMS OF LIPOFUSCIN ACCUMULATION

Altered Cellular Proteostasis

Three main mechanisms actively maintain cellular proteostasis: (i) degradation by the ubiquitin-proteasome system (UPS); (ii) re-folding and suppression of aggregates by heat shock proteins; and (iii) clearing of abnormal cell contents by lysosome-mediated autophagy (macroautophagy) (Mizushima et al., 2004; Mizushima, 2007). Both under normal and pathological conditions, the combination of these pathways are also possible (Fortun et al., 2003, 2005; Hara et al., 2006), including chaperone-mediated autophagy (Kaushik and Cuervo, 2012) and the ubiquitin-mediated autophagy required for the UPS system (Opalach et al., 2010).

With aging, cellular proteostasis becomes less effective, hampering degradation of misfolded proteins, which in turn expose their hydrophobic domains and tend to form high-order complexes with other perinuclear/centrosomal-proximal proteins that are prone to aggregate into aggresomes (Kettern et al., 2011; Richter-Landsberg and Leyk, 2013; Seiberlich et al., 2013; Popovic et al., 2014; An and Statsyuk, 2015; Rodolfo et al., 2018). Then, upon lysosomal uptake of these aggregates via macroautophagy, highly cross-linked materials such as LF accumulate within the lysosomes (Höhn and Grune, 2013). Thus,

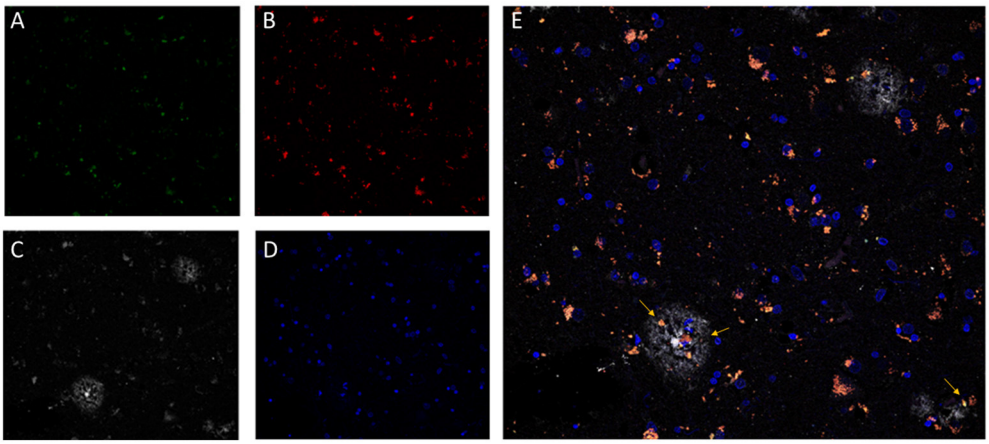

FIGURE 1 | Confocal fluorescence microscopy analysis of AD brain tissue. The characteristic perinuclear lipofuscin deposits can be clearly identified in brain tissue by autofluorescent emission at 510–530 nm (**A**, green) and at 570–600 nm (**B**, red), with excitation at 488 nm and 561 nm, respectively. Additionally, amyloid beta plaques (**C**, white) were immunostained by the specific monoclonal antibody 4G8 (Covance) followed by an anti-antibody conjugated to a fluorophore excitable to 633 nm and emitting light from 670 to 700 nm (Invitrogen GAM-A-21052). DNA in nuclear domains was identified by DAPI probe (**D**, blue). In the merged image **(E)**, lipofuscin aggregates (pink-orange) appears widely distributed throughout the tissue with incidental colocalization within the amyloid beta plaques. Images represent a single confocal plane of cryosections of prefrontal cortex from an AD patient treated with 70% formic acid for 10 s. The yellow arrows indicate LF aggregates that are located within senile plaques. Adapted with permission from chapter 31 "Characterization of Amyloid-β Plaques and Autofluorescent Lipofuscin Aggregates in Alzheimer's Disease Brain: A Confocal Microscopy Approach" in Amyloid Proteins. Methods and Protocols, Volume 1179 in Methods Molecular Biology Series (ISBN: 978-1-4939-7815-1); Series Ed.: Walker, John M. Humana Press-Springer.

although most of intracellular LF is located in the lysosomes, after inhibition of the macroautophagy pathway, LF can accumulate also in the cytosol (Höhn and Grune, 2013).

These authors propose a mechanism by which the presence of high amounts of LF inhibit the proteasome, preventing the degradation of oxidized proteins and increasing the formation of free radicals, leading to cytotoxicity (Sitte et al., 2000; Ryhänen et al., 2009; Höhn et al., 2011). Then, oxidized proteins further accumulate and tend to aggregate (Höhn and Grune, 2013; Reeg and Grune, 2015). Hence, the 20S proteasome binds to the surface of LF aggregates at patches rich in unfolded oxidized proteins, but it remains attached, unable to degrade the LF due to its cross-linked nature (Reeg and Grune, 2015). In turn, lysosomal LF appears to impair autophagy and lysosomal degradation, resulting in increased reactive oxygen species (ROS) generation, protein oxidation, further aggregation, and further LF formation (Terman and Brunk, 2004). Moreover, cytosolic LF deposits produce ROS, decreasing cellular viability by defective cytosolic protein degradation (Grune et al., 2001; Höhn and Grune, 2013; Lei et al., 2017).

In healthy conditions, the functional cost of proteostasis is high, but essential (Rangaraju et al., 2009; König et al., 2017). A consequence of the inhibition of the proteasome system is the decreased degradation of pro-apoptotic proteins (including c-jun, Bax, and p27), triggering the initiation of the apoptotic cascade (Powell et al., 2005), as well as the blockage of NFkB nuclear translocation and signal transduction (Powell et al., 2005; Reeg and Grune, 2015). Thus, cells overloaded with cytosolic and lysosomal LF may become dysfunctional and undergo apoptotic proteostasis-mediated cell death (Powell et al., 2005; Höhn et al., 2011).

Additionally, LF ability to incorporate different metals contributes to reactive oxygen species (ROS) generation through the Fenton reaction and further protein oxidation and LF formation (Jolly et al., 1995; Tokutake et al., 1995; Reeg and Grune, 2015). For example, in Mn^{2+}-exposed wild-type mice, it was observed an increased number of LF granules associated with neurodegenerating spiral ganglion neurons (Ohgami et al., 2016). Similarly, in ferritin light chain gene transgenic mice, it was shown the accumulation of LF granules within iron deposits, particularly at degenerating regions of the cerebellum and striatum (Maccarinelli et al., 2015).

Mitochondrial Involvement in Lipofuscinogenesis

The oxidative stress and the accumulated mitochondrial DNA mutations during lifetime lead to impairment metabolism of mitochondria, which in turn yields further oxidative stress by ROS production through oxidative phosphorylation. Cellular quality control mechanisms activate mitophagy to eliminate non-functional mitochondria by the lysosomal system (Atkins et al., 2016; Rodolfo et al., 2018), and then, the lysosomes accumulate non-degraded molecules, such as the mitochondrial small hydrophobic ATP-synthase subunit-c, which appears to be the main component of LF in neuronal ceroid lipofuscinosis diseases (Ezaki et al., 1995; Vidal-Donet et al., 2013). During aging, mitochondrial repair systems are further compromised by a general reduction of macroautophagy and downregulation of specific mitochondrial proteases, which are responsible for the degradation of oxidatively modified proteins (Ngo and Davies, 2007; Davies, 2014; König et al., 2017).

These findings underscore an important crosstalk between mitochondria and lysosomes during aging that directly involves LF and other macromolecular aggregates (Terman et al., 2010). Accumulation of LF within the lysosomes leads to reduced autophagy and lower turnover of effective mitochondria. In turn, functionally deficient mitochondria generate increased ROS levels that further intensifies lipofuscinogenesis in a feedback loop of dysfunctional mitochondria and lysosomes, resulting in enhanced oxidative stress, lower energy production and dysfunction of the catabolic pathways (Brunk and Terman, 2002; Terman et al., 2010).

Lipid Metabolism

As lipids are one of the main components of LF, a dysfunction of lipid metabolism has been suggested for the synthesis and accumulation of LF. Thus, Hebbar and collaborators have proposed that the buildup of LF deposits is a direct consequence of an imbalance in brain ceramides and sphingosines at early stages of neurodegeneration (Hebbar et al., 2017). Zhao and collaborators also demonstrated that defective ceramide biosynthesis causes neurodegeneration, suggesting a novel mechanism for LF formation (Zhao et al., 2011). Similarly, Pan and collaborators demonstrated in an *in vivo* knock-out mouse model that neuraminidases 3 and 4 play a key role in the central nervous system (CNS) function through the catabolism of gangliosides, and the prevention of their conversion into LF aggregates (Pan et al., 2017). Additionally, Horie and collaborators demonstrated that LF is also constituted by glycation products which interact through Schiff base reactions with protein-lipid complexes (Horie et al., 1997).

The various mechanisms of production and accumulation of LF discussed within this section depict a complex panorama in which the lysosomes play a central role in lipofuscinogenesis. Thus, the increasing amount of LF deposits during aging in certain post-mitotic tissues, and the massive buildup of LF in disorders associated with lysosomal dysfunction, such as *Neuronal Ceroid Lipofuscinosis* (see next sections), are arguably some of the best established findings about the pathophysiological accumulation of LF. However, due to its diverse origin, amalgamated composition, cross-linked nature, autofluorescent properties, and its age-related ubiquitous distribution within the CNS, the role of LF in neurodegeneration is still yet to be elucidated. Moreover, the analysis of a potential pathophysiological role of LF has been hampered by the absence of adequate animal models and their corresponding controls; thus, underscoring the need for simpler system study models.

IN VITRO LIPOFUSCIN SYNTHESIS FOR NEURODEGENERATIVE STUDIES

In order to explore the physicochemical properties, interactions, and functions of LF, it is essential to have a reliable system to produce it, either *in vitro* or in *in vivo* models. Numerous authors have described different approaches to obtain LF from diverse biological sources. For example, several methods have been established to produce N-retinylidene-N-retinylethanolamine (A2E), which is one of the principal fluorescent components of LF from retinal pigmented epithelial cells (Parish et al., 1998).

Other authors, considering that LF is the final product of a peroxidation reaction between lipids and proteinaceous components within the cell, have used the process of photo-oxidation of subcellular fractions to obtain high quantities of "synthetic" LF through UV irradiation (Nilsson and Yin, 1997; Höhn et al., 2010; Frolova et al., 2015). Interestingly, these studies demonstrate that mitochondria can produce LF granules without oxidative factors (oxygen saturation or pro-oxidants) and that the presence of lipids is not an absolute requirement for LF formation (Frolova et al., 2015). These methods allow the synthesis of LF similar to that found in post-mitotic cells with analogous composition and properties. However, for some experimental setups, naturally produced LF may be more suitable and relevant. Arguably, LF fractions purified from the retinal pigment epithelium (RPE) or derived from cell culture models through organic solvent extractions are the most widely used procedures (Folch et al., 1957; Lamb and Simon, 2004; Boulton, 2014; Feldman et al., 2015).

LIPOFUSCIN IN NEURODEGENERATION

As mentioned above, LF is considered a hallmark of cellular aging. In fact, the accumulation with time of LF pigments within post-mitotic cells is so constant that it is used to calculate the age of crustacean (Pearse, 1985; Maxwell et al., 2007). In normal aged mammal brains, LF distributes delineating a specific senescence pattern that correlates with altered neuronal cytoskeleton and cellular trafficking. Thus, as we age, the brain of the human adult becomes heavily laden with intraneuronal deposits of LF and neuromelanin pigment (Braak et al., 1999). However, in neurodegenerative disorders, LF aggregates appear to increase not only with age but also with pathological processes such as neuronal loss, proliferation, and activation of glial cells, and a repertoire of cellular alterations, including oxidative stress, proteasome, lysosomal, and mitochondrial dysfunction (González-Scarano and Baltuch, 1999; Grune et al., 2004; Keller et al., 2004; Riga et al., 2006a; Hebbar et al., 2017; Wellings et al., 2017).

Neuronal Ceroid Lipofuscinosis

Arguably, the most relevant group of disorders clearly related with LF deposits are the neuronal ceroid lipofuscinoses (NCLs). NCLs are a group of rare neurodegenerative disorders characterized by intracellular (and at a minor extent extracellular) accumulation of a fluorescent lipopigment called "ceroid lipofuscin" (Kohan et al., 2011). Clinically, NCLs are associated with variable, progressive symptoms, including dementia, visual loss, seizures, and cerebral atrophy (Grubman et al., 2014). Genetically, NCLs are a homogeneous group associated with mutations in at least 14 affected genes termed as from *CLN1* to *CLN14* generally with autosomal recessive inheritance (for an updated list of mutation check http://www.ucl.ac.uk/ncl/mutation.shtml). Mutations in these genes are associated with several distinct NCL disorders, which share several common features, including inflammation, lysosomal

LF deposits, and lipid abnormalities, but have different age at onset, clinical phenotypes, and progression rates (Grubman et al., 2014). In general, NCLs are considered lysosomal storage diseases; although, they also exhibit characteristics that set them apart from typical lysosomal storage diseases (Mink et al., 2013; Nita et al., 2016). One prototypical example of these disorders is NCL2. The NCL2 disease is one type of inherited infantile neuronal ceroid lipofuscinoses caused by the deficiency of the lysosomal enzyme tripeptidyl peptidase 1, which affects the brain and the retina and is characterized by the lysosomal accumulation of ceroid LF (Williams et al., 2017). Interestingly, related to the presence of "normal" LF aggregates in tissue, the diagnosis of adult forms of NCL is challenging due to the misinterpretation of age-related LF deposits as abnormal storage material, with more than one-third of cases misdiagnosed; therefore, stressing the need of analysis of known causative genes and the identification of newly associated genes (Berkovic et al., 2016).

Outside this group, several other disorders show resemblance with the NCLs as they progress with ceroid LF deposition. Among them, we highlight disorders that are associated with mutations in the *CLC-3* (a member of the CLC chloride channel family) gene (Yoshikawa et al., 2002), the *ClC-7* (chloride channel of late endosomes and lysosomes) gene (Kasper et al., 2005; Weinert et al., 2010), the *cathepsin D* (a major lysosomal protease) gene (Koike et al., 2000), as well as neuronopathic osteopetrosis associated to defects in the genes *TCIRG1* or *ClC-7* (Steward, 2003). In these disorders, far from being a consequence of the neurodegenerative process, LF appears to have an important role in the etiology of clinical symptoms.

Age-Related Macular Degeneration

Age-related macular degeneration (AMD) is a degenerative disorder of the RPE of the central retina, which represents the most important cause of vision loss in the elderly. It has a multifactorial etiopathology and is characterized by the presence of deposits of lysosomal origin, such as LF, melanolipofuscin, and melanosomes (Rodríguez-Muela et al., 2013; Pollreisz et al., 2018). It is generally accepted that LF can contribute to the pathogenesis of AMD. Due to its nature as a fluorochrome, exposure of the spherical microparticles of LF at the RPE to blue light produces a phototoxic and proinflammatory effect, mediated by reactive oxygen intermediates (ROI), which contributes to atrophy in AMD patients (Brunk and Terman, 2002; Pollreisz et al., 2018). Interestingly, A2E, a major LF fluorophore that accumulates during AMD progression, appears to be directly involved in the photo-induced oxidative stress, and the disruption of membrane integrity at the RPE (Lamb and Simon, 2004). Similarly, the levels of A2E in the retina of an AMD mouse model [Ccl2(-/-)/Cx3cr1(-/-) mice] were significantly higher when compared to wild-type retina (Tuo et al., 2007).

In addition, Stargardt disease, the most common form of inherited juvenile macular degeneration which is associated with progressive vision loss caused by the death of photoreceptor cells in the macula of the retina, presents significant LF accumulation in the lysosomal compartment of the retinal pigment epithelium of the eye (Adler et al., 2015).

Furthermore, LF particles have been recently detected in the aged human optic nerve from controls, and glaucoma or AMD donors (de Castro et al., 2013). Although similar amounts of LF were observed among the different groups, the authors found that optic nerves derived from donors with glaucoma contain larger LF particles compared to those observed in the age-matched control and AMD groups. Moreover, they observed that optic nerves from glaucoma donors display a smaller diameter and higher concentration of LF relative to age-matched controls, suggesting that the increased LF levels may have an active role in inducing pro-inflammatory phenotypes in microglia and astrocytes, thus exacerbating optic nerve damage (de Castro et al., 2013).

Frontotemporal Degeneration

Heterozygous loss-of-function mutations in the progranulin gene (*GRN*) are associated with frontotemporal degeneration with TDP-43-positive inclusions (FTD-TDP). FTD is highly heterogeneous in its clinical presentation, age at onset and duration of the disease even within the same families, suggesting the mediation of additional modifying genes. Strikingly, while the deletion c.813_816del (rs63749877) in the *GRN* gene in heterozygosis is also associated with FTD, the same mutation when presented in homozygosis causes adult-onset NCL, revealing a remarkable link between neurodegeneration and lipofuscinogenesis (Smith et al., 2012). More recently, Ward and collaborators have demonstrated that heterozygous *GRN* mutation carriers also present preclinical retinal lipofuscinosis, as well as increased lipofuscinosis and intracellular NCL-like deposits in the cerebral cortex (Ward et al., 2017).

In animal models, progranulin deficiency partially recapitulates FTD behavioral abnormalities and neuropathological changes, including altered dendritic morphology and synaptic deficits in the hippocampus (Petkau et al., 2016). Aged progranulin-deficiency mice also show increased lipofuscinosis, microgliosis, and astrogliosis, as well as mild regional specific cell loss. However, conditional loss of progranulin in neurons is not sufficient to cause neuronal ceroid lipofuscinosis-like neuropathology in mice, as progranulin expressed by the microglia appears to compensate the neuronal deficit of progranulin (Petkau et al., 2017). Interestingly, although neurodegeneration and LF accumulation clearly correlate in most animal models, in this progranulin deficiency mouse model, it has been shown that deletion of the *TMEM106B* (Transmembrane protein 106B) gene normalizes lysosomal activity and rescues FTD-related behavioral abnormalities and retinal degeneration, without showing a decrease in LF accumulation (Klein et al., 2017); therefore, suggesting that neurodegeneration and lipofuscinogenesis are independent processes. As recent evidence suggests that progranulin is a key player for the appropriate maintenance of lysosomal function during aging (Zhou et al., 2017), these data point out to a common role of endolysosomal dysfunction for FTD neurodegeneration and NCL pathology. Further studies should

be aimed at elucidating the specific pathological role LF in FTD neurodegeneration.

Parkinson's Disease

In PD, LF granular aggregates and upregulation of α-synuclein (α-syn) appear to be directly involved in the selective degeneration of dopaminergic neurons in the SNC (Lv et al., 2011). Additionally, increased expression of divalent metal transporter 1 and decreased expression of ferroportin 1 seem to associate with elevated levels of iron at the SNC; therefore, suggesting that increased iron levels are involved in the selective degeneration of dopaminergic neurons (Lv et al., 2011). Interestingly, Braak and collaborators found that only those neuronal types containing LF or neuromelanin show an increased susceptibility to develop pathological changes including cytoskeletal changes and α-syn Lewy body deposits (Braak et al., 2001). Moreover, α-syn appears to be a constituent of the lipofuscin deposits present in the neurons of the *substantia nigra* of PD patients and in nigral neurons of MPTP-treated mice, suggesting that LF deposits may have a role in the selective nigral degeneration (Braak et al., 2001; Meredith et al., 2002).

Similarly, in Deiters' neurons, which express the cytostructural non-phosphorylated neurofilament protein (NPNFP), Wellings and collaborators found a strong inverse correlation between NPNFP intensity and LF autofluorescence, suggesting that these changes contribute to degeneration of postural reflexes observed in PD (Wellings et al., 2017). According to the authors, LF accumulation may lead to cytoskeletal abnormalities, including decreased NPNFP levels and disrupting Deiters' neurons functions, even in neuropathological normal controls (Wellings et al., 2017). Interestingly, non-dopaminergic areas as the medullary nuclei that are early affected during PD progression (Braak et al., 2001) present concomitant accumulation of Lewy bodies and LF granules (Wellings et al., 2017). Similarly, Braak and collaborators described that Lewy bodies are normally found within the LF deposits of medullary neurons (Braak et al., 2003). Opposite, Drach and collaborators found reduced intraneuronal LF content in patients with Lewy body dementia (LBD) compared to AD and controls, arguing that these findings are related to either a reduced metabolic rate in LBD or to an uneven use of neuroleptics among groups (Drach et al., 1998).

Alzheimer's Disease

In AD, at initial stages of neurodegeneration, affected pyramidal neurons in prefrontal cortex and hippocampus increasingly accumulate lysosomes at the basal pole and then extensively in the perikarya and proximal dendrites (Cataldo et al., 1994). Lysosomes become filled with LF aggregates as a result of initial autophagocytosis and lysosomal system activation. At more advanced stages of neurodegeneration, surviving neurons show a great cytoplasmic accumulation of large LF deposits. Interestingly, following neuronal death, LF aggregates are found in the extracellular space, usually associated with senile β-amyloid plaques (Cataldo et al., 1994). Tokutake and collaborators suggested that LF granules associated to the senile plaques are the responsible for binding aluminum, providing an argument to explain the divergent reports on the presence of this metal in AD plaques (Tokutake et al., 1995).

LF is formed when products of lipid peroxidation (reactive aldehydes and lipid radicals) attack lipids, proteins and other susceptible groups, either locally or far from their origin, because they are diffusible and can migrate and act at a distance. Consequently, lipid peroxidation end-products (also called LF-like pigments), are produced and their distribution could be either restricted to a specific tissue or tissue domains or be systemically distributed. For instance, in brains from AD patients, the lipid peroxidation product malondialdehyde, an important component of the phospholipid bilayer membranes of neurons, is significantly increased (Dalle-Donne et al., 2006); thus, promoting free radical damage, protein cross-linking and decreased membrane fluidity (Goldstein and McDonagh, 1976; Chmátalová et al., 2016). Thus, the reactive compounds from brain tissue can act like a messenger, diffusing through the bloodstream and attacking polyunsaturated fatty acids in membranes of erythrocytes or soluble plasma proteins leading to the formation of LF. In AD patients, it was found that erythrocyte-bound LF levels were significantly higher than those observed in controls (Goldstein and McDonagh, 1976; Skoumalová and Hort, 2012).

In the same line, in the cerebral cortex of aged control and AD brains, a subset of neurons covered by perineuronal nets (PNs) are less frequently affected by LF accumulation. The polyanionic character of PNs appears to contribute to reducing local oxidative potential in the neuronal microenvironment by scavenging and binding redox-active iron (Morawski et al., 2004). Braak and Braak previously observed a similar effect related to cortical myelination. They found a clear inverse correlation between the average myelin content and the density of intraneuronal LF deposits, as well as with the appearance of the neurofibrillary changes associated with neurodegeneration, suggesting that the LF-laden neurons with a long, thin, and sparsely myelinated axon are prone to develop AD-related changes (Braak and Braak, 1998). Interestingly, LF deposits are also found to colocalize with β-amyloid plaques (Riga et al., 2006a; Moreira et al., 2010; Firlag et al., 2013). Altogether, these facts have set the basis for the hypothesis that the release of LF into the extracellular space following the death of neurons may substantially contribute to the formation of AD senile plaques and neurodegeneration (Giaccone et al., 2011).

Huntington Disease

Huntington's disease (HD) is an inherited disorder caused by an autosomal dominant mutation in the Huntingtin gene (*htt*), related to the expansion of CAG triplet repeats, resulting in an extended polyglutamine stretch (polyQ) within the huntingtin protein, which becomes unstable, gradually damaging neuronal cells (Ross et al., 2014).

Increased LF has been observed in the brain of people suffering from HD (Tellez-Nagel et al., 1974; Goebel et al., 1978; Braak and Braak, 1992; Vonsattel and Difiglia, 1998). Thus, in HD brains, Braak and Braak found that the loss of neurons at the subiculum was marked by the presence of extraneuronal deposits of LF within layers of pyramidal neurons (Braak and

Braak, 1992). Later, Vonsattel and Difiglia described that neurons from HD cases "contain more lipofuscin and may be smaller than usually expected" (Vonsattel and Difiglia, 1998).

Similarly, a transgenic mouse model for HD has shown that the formation of huntingtin neuronal intranuclear inclusions is accompanied by the appearance of accumulations of LF within the cytoplasm of neurons even in juvenile mice from 12 weeks old (Davies et al., 1997, 1999). Interestingly, Zheng and collaborators have demonstrated that the expression of full-length htt lacking its polyglutamine stretch (ΔQ-htt) in a mouse model of HD was able to rescue the HD phenotype, reducing huntingtin aggregates and LF levels, motor and behavioral deficits and extending life span (Zheng et al., 2010). The authors also found that ΔQ-htt expression increases autophagosome synthesis, arguing that this autophagy upregulation may be beneficial in diseases caused by toxic intracellular aggregate-prone proteins (Zheng et al., 2010), as it is the case of most neurodegenerative disorders. As we discussed previously, the observed normalization of LF levels may be directly correlated with autophagosome function restoration.

Diabetic Encephalopathy

Diabetic encephalopathy refers to a pathology that courses with brain damage associated with diabetes type 1 or type 2, caused by either acute hypoglycemia or severe hyperglycemia. In type 2 diabetes, diabetic encephalopathy increases the risk of developing AD and other forms of dementia, while in type 1 diabetic encephalopathy is less likely to develop into dementia as the patients are younger, but type 1 diabetics with encephalopathy are more likely to develop learning disabilities and deficits in memory retrieval. In a mouse model of type 1 diabetes induced by treatment with streptozotocin, Sugaya and collaborators found that diabetes onset caused accelerated accumulation of LF granules in trigeminal neurons (Sugaya et al., 2004). Later, Alvarez and collaborators demonstrated that in the same streptozotocin model, the animals showed a phenotype similar to diabetic encephalopathy with mild neurodegeneration in the dentate gyrus and a strong decrease in hippocampal proliferation. Interestingly, the authors found a marked enhancement of intracellular LF deposits, characteristic of increased oxidative stress and aging in both, the hilus and the subgranular zone and granular cell layer (Alvarez et al., 2009). In a different model of diabetes, induced by administration of alloxan, the animals also showed signs of diabetic encephalopathy with rapidly progressing neuronal and glial losses in the primary somatosensory cortex and hippocampus, accompanied by accumulation of LF in neocortical neurons (Volchegorskii et al., 2013). These findings with different mouse models of diabetes underscore the exquisite sensitivity of neuronal tissues to LF buildup, suggesting an active neurotoxic role of these aggregates.

Other Conditions

Aggregates of lipofuscin or ceroid LF are found in various metabolic disorders associated with mutations in several genes. Thus, in familial spastic paraplegia cases associated with neurodegeneration and gliosis, a marked presence of LF deposits in surviving neurons has been observed (Wakabayashi et al., 2001).

In rat cerebral cortex, cathepsin D (but no cathepsin B) has been found to colocalize with LF aggregates in the extracellular space (Jung et al., 1999) that in turn activates the p38 MAP kinase cascade through the increased intracellular generation of ROS, and promote the expression of iNOS and CAT-2, thereby inducing NO overproduction (Yamasaki et al., 2007). Cathepsin F-deficient mice (cat F-/-) display CNS neurons with large accumulations of lysosomal LF (Tang et al., 2006). Also in a murine model, it was observed that chronic sleep disruption resulted in frequent activation of wake-activated neurons (WAN), which promotes mitochondrial metabolic stress and increased LF accumulation in a subgroup of WAN (Zhu et al., 2015). On the other hand, chronic alcohol consumption induces increasing LF deposition in rat hippocampal neurons (Borges et al., 1986) and Purkinje (Lewandowska et al., 1994; Wenisch et al., 1997; Dlugos, 2015). Mice lacking the expression of glycerophosphodiester phosphodiesterase 2 (a six-transmembrane protein that cleaves glycosylphosphatidylinositol anchors) show early neurodegeneration with vacuolization, microgliosis, cytoskeletal accumulation, and LF deposition followed by astrogliosis and cell death (Cave et al., 2017).

As a whole, these data from human disorders and mouse models point to a common dyshomeostasis of the endolysosomal pathway not necessarily associated with oxidative stress and mitochondrial dysfunction, but in which LF is always present, likely acting as a pathology booster.

THERAPEUTIC APPROACHES

As LF and other lipopigments, such as ceroids, represent a marker of post-mitotic normal and pathologic aging, and they have been causally associated with neuropathological changes, LF elimination has been suggested as a suitable target in anti-aging therapies (Riga et al., 2006b). Recently, a clinical trial (ClinicalTrials.gov identifier NCT00028262) for the treatment of patients with infantile NCL associated with mutations in the *CLN1* gene encoding for palmitoyl-protein thioesterase-1 has been carried out by orally administering the nucleophilic small molecules cysteamine bitartrate and N-acetylcysteine, aiming at the reduction of ceroid lipofuscin and granular osmiophilic deposits (GROD) (Levin et al., 2014). The results of the trial indicated that the patients presented a significant decrease of GROD in peripheral leukocytes, together with improved functional and behavioral parameters and fewer seizures. However, the results of these trials did not support the idea that the removal of the storage deposits correlates with a clinical benefit or halt neurodegeneration (Levin et al., 2014; Neverman et al., 2015).

There are also several approaches in the field of AMD targeting LF or its precursors. Thus, two visual cycle inhibitors, namely Fenretinide and Emixustat, have been used trying to prevent the phototoxicity and proinflammatory effects of LF. A phase II clinical trial with Fenretinide (NCT00429936) did not show efficacy to halt the growth rate of geographic atrophy

(GA) in AMD, but patients seemed to tolerate it well. A phase IIa clinical trial with Emixustat (NCT01002950) showed a biological effect in GA in AMD patients. A Phase II/III study (NCT01802866) has been completed, but no results are yet available (Bandello et al., 2017) (information checked in May 2018).

A study with rats showed that treatment with melatonin or coenzyme Q10 for 4 weeks reduced the LF content of the hippocampus and carbonyl level (Abd El Mohsen et al., 2005). In fish, analysis of age-dependent mortality revealed that dietary restriction prevented the accumulation of LF in the liver and the neurodegeneration marker FluoroJade B in the brain (Terzibasi et al., 2009).

Regenerative neuroactive factors have been also suggested to enhance antioxidative defense, stimulate brain anabolism and potentiate lysosomal system, while decreasing LF levels. By acting also on glial cells, the mechanism of clearance of LF deposits and other residues appear to be also improved (Riga et al., 2006b).

Interestingly, the presence of LF appears to have a positive effect for certain therapies with antitumor drugs that produce free radicals, whose action is inhibitory or deadly for tumor cells (Schwarzburd and Aslanidi, 1991). Under the oxidative stress provoked by the drugs, it appears that normal cells respond with an increase in the amount of LF in their lysosomes and cytoplasm hampering further damage. Opposite, cancer cells, unable to accumulate LF particles are more susceptible to the action of the drug. In this sense, Schwartsburd in 1995 put forward the idea that lipofuscinogenesis is an adaptative cell response to oxidative stress that improves cell survival under harsh conditions (Schwartsburd, 1995). In *Drosophila melanogaster*, a similar protective effect of LF is suggested by *spin* gene mutants that presented degeneration of adult neural cells, while surviving neurons were atrophied with heavy LF deposition (Nakano et al., 2001). However, once a certain threshold of LF level is trespassed, and the system is overload, this mechanism appears to produce the opposite effect, by multiplying the effects of oxidative stress.

CONCLUDING REMARKS

As we grow older, LF gets accumulated in post-mitotic cells due to its highly complex cross-linked structure that is not amenable to degradation, as a marker of partially dysfunctional metabolism. Thus, LF has been traditionally considered a consequence of "normal" aging that gets increasingly deposited as cellular garbage, starting early in life.

Similarly, pathognomonic protein deposits such as amyloid beta plaques, tau neurofibrillary tangles or alpha-synuclein Lewy bodies are present even in normal individuals, and their accumulation appears to be the result of a protective cellular response to handle an excess of misfolded proteins (Ross and Poirier, 2005). Thus, the process of LF formation may represent a protective neuronal mechanism by which molecules that are highly toxic in soluble form are sequestered in a more stable, less-toxic state as aggregates (Zhao et al., 2011). However, recent findings indicate that LF is not an inert byproduct of cells, but it rather actively alters cellular metabolism at different levels by inhibiting the proteasome, impairing autophagy and lysosomal degradation, and serving as a reservoir of metal ions leading to ROS generation and apoptotic cell death (reviewed in Reeg and Grune, 2015) (see also **Figure 2**). Additionally, the dispersed nature of the deposits, which are distributed throughout the tissue, may argue for a mechanism of LF diffusion and seeding for new LF aggregates.

The presence of LF as a pathognomonic marker in both infantile-juvenile and adult neuronal ceroid lipofuscinoses, as well as its role as ROS amplifier mediated by UV-exposure in age-related macular degeneration, underscore the pathological role of LF in these groups of neurodegenerative disorders. However, the direct involvement of LF in other neurodegenerative disorders such as AD or PD is still a matter of debate.

In order to discuss whether LF is a subproduct of defective cellular homeostasis associated with aging or it has a pathological role of its own in neurodegeneration, it is relevant to compare the temporal profile of accumulation of LF aggregates with pathognomonic protein deposits associated with diverse neurodegenerative disorders. Interestingly, the temporal pattern of accumulation is similar to the one observed for protein deposits in different neurodegenerative disorders (Braak et al., 2011; Ferrer et al., 2011; Del Tredici and Braak, 2016). According to the study by Braak and coworkers, in the case of AD, both β-amyloid and neurofibrillar pathological features are present very early in life (even in the first decade), and also as in the case of LF, their presence increases with age (Braak et al., 2011). However, these pathology markers are not associated with overt disease until they reach a certain threshold that varies with age. Thus, lipofuscinogenesis and neuropathogenesis of the main CNS degenerative conditions seem to share an equivalent temporal kinetics: early pathological changes and slow relentless development with late sensorial, motor and cognitive deterioration.

Moreover, LF may also exert a neuropathological role by the dysregulation of protein homeostasis through its ability to sequester functional molecules and proteins (Hashemzadeh-Bonehi et al., 2006). Provided the hydrophobic nature of LF aggregates, a similar role sequestering other functional molecules and later release of diffusible molecules that are more neurotoxic cannot be ruled out. Additionally, the interaction with pathognomonic aggregation-prone proteins, such as Aβ, α-syn, or tau needs further research, but the presence of LF aggregates within neurodegeneration-specific protein deposits such as the AD senile plaques suggests an involvement of LF in pathogenesis (Cataldo et al., 1994; Giaccone et al., 2011) (see also **Figure 1**).

Taken together, all these data suggest a neuropathological role of LF by impairing the same mechanisms and acting like other protein aggregates (e.g., amyloid beta, tau, alpha-synuclein) of different neurodegenerative diseases. Thus, we argue that LF plays a transversal function on both cellular senescence and across neurodegeneration. Provided that LF increasingly accumulates with age, and assuming the hypothesis that LF is a risk factor for different neurodegenerative disorders, one may expect higher incidences of neurodegenerative disorders with the increased levels of the risk factor (in this case LF). However, although age is also one of the strongest risk factors for late-onset

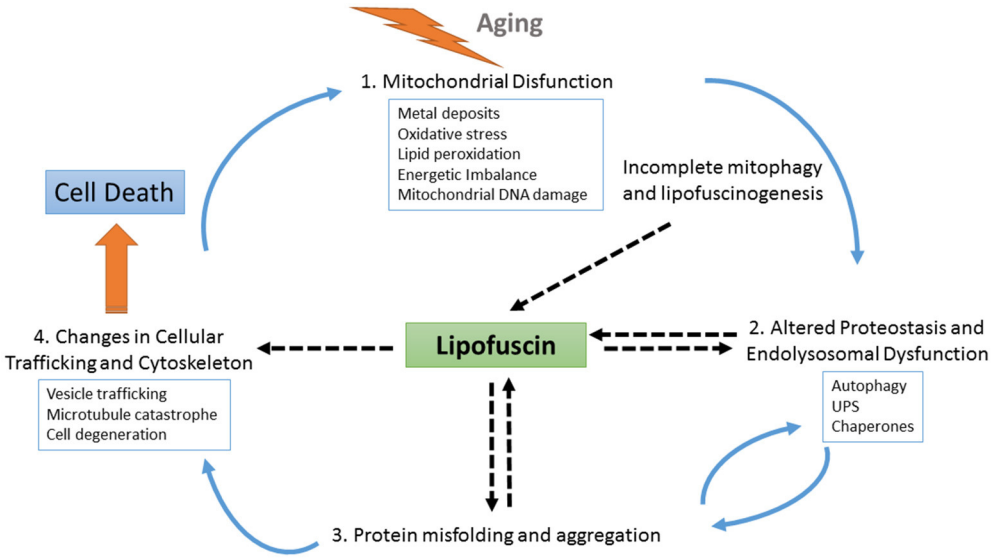

FIGURE 2 | Schematic representation of the role of LF at different points of cellular physiology. With aging, the levels of oxidative stress increase, causing the impairment of several interconnected cellular homeostatic pathways such as the endolysosomal and mitochondrial systems and leading to defective proteostasis, incomplete mitophagy and the activation of lipofuscinogenesis. On the one hand, lipofuscin accumulation harms the proteostasis pathway, further promoting oxidative stress, energetic imbalance, and increased lipofuscinogenesis. On the other hand, altered proteostasis together with endolysosomal dysfunction also obstruct the clearance of misfolded proteins, which may accumulate as seeds for protein aggregation contributing to neurodegeneration. As protein aggregates deposits within the brain tissue, LF formation also increases, hindering both vesicle trafficking and cellular physiology. Finally, as the cell is unable to deal with the cascade of damaging events it degenerates. Upon cell death, LF content is released to the parenchyma, where it can be found associated with pathognomonic protein deposits, such as amyloid beta plaques. These LF deposits recruit cellular debris and metals ions, provoking more oxidative stress, and microglial activation, which triggers neuroinflammation and proinflammatory interleukin production, thus contributing to expanding the neurodegeneration.

neurodegenerative disorders, the normalized incidence of each entity (perhaps with the exception of AD) peaks at certain age range, from which it starts to decay. This apparent disagreement between a continuously increasing buildup of LF deposits as a risk factor and the variable age-specific peak incidence of diverse neurodegenerative disorders (de Pedro-Cuesta et al., 2015) is similar to other pathognomonic protein deposits. This could be explained either by a subclinical expression of LF deposits (vs. the clinical definition of incidence counts) or by more complex phenomena associated with a ceiling effect, above which the LF levels are already irrelevant.

In line with the work from Giaccone and collaborators that discussed the potential pathogenic role of LF in AD (Giaccone et al., 2011), we propose that LF is one relevant effector of aging that represents a risk factor (or more properly, a risk modifier) for neurodegenerative disorders. In the context of our previous works, LF fits well with the concept of *driver* (defined as "neither protein/gene nor entity-specific features identifiable in the clinical and general epidemiology of neurodegenerative diseases as potential footprints of templating/spread/transfer mechanisms") (de Pedro-Cuesta et al., 2016a). This transversal approach provides a unified view of LF pathological role in neurodegeneration for genetic (neuronal ceroid lipofuscinosis, and others) and sporadic neurodegenerative disorders with specific age-at-onset related patterns (de Pedro-Cuesta et al., 2016b). In conclusion, the relentless accumulation of LF is clearly associated to aging, but as we have reviewed herein, increasing evidence suggest that LF formation leads to neuropathology exacerbation by different mechanisms (see **Figure 2**). Further studies to determine whether LF accumulation itself, both within the neuronal cell and in the brain parenchyma, is contributing to neuronal loss and disease are needed. Proof-of-concept studies in mouse models aiming at specifically clearing existing LF deposits in NCLs may help to elucidate the role of LF and guide new therapeutic approaches for neurodegenerative disorders.

AUTHOR CONTRIBUTIONS

All authors participated in the conception and aims of the review. AM-G, AK, and OC participated in the literature search, and analysis of references, participated in the experimental acquisition of images for **Figure 1**, wrote sections of the manuscript. MM performed the critical revision of the article. MC wrote the first draft of the manuscript. All authors contributed to manuscript revision, read and approved the submitted version.

FUNDING

This work was supported by grant SA1F2016-78603-R from Spanish Ministry of Economy, Industry and Competitiveness (MINECO) to MM and MC, the *National Programme for the Promotion of Talent and its Employability* from MINECO (AM-G), and the Spanish CIBERNED network (OC, MM, MC).

REFERENCES

Abd El Mohsen, M. M., Iravani, M. M., Spencer, J. P. E., Rose, S., Fahim, A. T., Motawi, T. M. K., et al. (2005). Age-associated changes in protein oxidation and proteasome activities in rat brain: modulation by antioxidants. *Biochem. Biophys. Res. Commun.* 336, 386–391. doi: 10.1016/j.bbrc.2005.07.201

Adler, L., Boyer, N. P., Chen, C., Ablonczy, Z., Crouch, R. K., and Koutalos, Y. (2015). The 11-cis retinal origins of lipofuscin in the retina. *Prog. Mol. Biol. Transl. Sci.* 134, e1–e12. doi: 10.1016/bs.pmbts.2015.07.022

Alvarez, E. O., Beauquis, J., Revsin, Y., Banzan, A. M., Roig, P., De Nicola, A. F., et al. (2009). Cognitive dysfunction and hippocampal changes in experimental type 1 diabetes. *Behav. Brain Res.* 198, 224–230. doi: 10.1016/j.bbr.2008.11.001

An, H., and Statsyuk, A. V. (2015). An inhibitor of ubiquitin conjugation and aggresome formation. *Chem. Sci.* 6, 5235–5245. doi: 10.1039/c5sc01351h

Atkins, K., Dasgupta, A., Chen, K.-H., Mewburn, J., and Archer, S. L. (2016). The role of Drp1 adaptor proteins MiD49 and MiD51 in mitochondrial fission: implications for human disease. *Clin. Sci.* 130, 1861–1874. doi: 10.1042/CS20160030

Bandello, F., Sacconi, R., Querques, L., Corbelli, E., Cicinelli, M. V., and Querques, G. (2017). Recent advances in the management of dry age-related macular degeneration: a review. *F1000Research* 6:245. doi: 10.12688/f1000research.10664.1

Benavides, S. H., Monserrat, A. J., Fariña, S., and Porta, E. A. (2002). Sequential histochemical studies of neuronal lipofuscin in human cerebral cortex from the first to the ninth decade of life. *Arch. Gerontol. Geriatr.* 34, 219–231. doi: 10.1016/S0167-4943(01)00223-0

Berkovic, S. F., Staropoli, J. F., Carpenter, S., Oliver, K. L., Kmoch, S., Anderson, G. W., et al. (2016). Diagnosis and misdiagnosis of adult neuronal ceroid lipofuscinosis (Kufs disease). *Neurology* 87, 579–584. doi: 10.1212/WNL.0000000000002943

Borges, M. M., Paula-Barbosa, M. M., and Volk, B. (1986). Chronic alcohol consumption induces lipofuscin deposition in the rat hippocampus. *Neurobiol. Aging* 7, 347–355. doi: 10.1016/0197-4580(86)90161-2

Boulton, M. E. (2014). Studying melanin and lipofuscin in RPE cell culture models. *Exp. Eye Res.* 126, 61–67. doi: 10.1016/j.exer.2014.01.016

Braak, E., Griffing, K., Arai, K., Bohl, J., Bratzke, H., and Braak, H. (1999). Neuropathology of Alzheimer's disease: what is new since A. Alzheimer? *Eur. Arch. Psychiatry Clin. Neurosci.* 249(Suppl. 3), 14–22.

Braak, E., Sandmann-Keil, D., Rüb, U., Gai, W. P., de Vos, R. A., Steur, E. N., et al. (2001). Alpha-synuclein immunopositive Parkinson's disease-related inclusion bodies in lower brain stem nuclei. *Acta Neuropathol.* 101, 195–201. doi: 10.1007/s004010000247

Braak, H., and Braak, E. (1992). Allocortical involvement in Huntington's disease. *Neuropathol. Appl. Neurobiol.* 18, 539–547.

Braak, H., and Braak, E. (1998). Evolution of neuronal changes in the course of Alzheimer's disease. *J. Neural Transm. Suppl.* 53, 127–140.

Braak, H., Del Tredici, K., Rüb, U., de Vos, R. A. I., Jansen Steur, E. N. H., and Braak, E. (2003). Staging of brain pathology related to sporadic Parkinson's disease. *Neurobiol. Aging* 24, 197–211. doi: 10.1016/S0197-4580(02)00065-9

Braak, H., Thal, D. R., Ghebremedhin, E., and Del Tredici, K. (2011). Stages of the pathologic process in Alzheimer disease: age categories from 1 to 100 years. *J. Neuropathol. Exp. Neurol.* 70, 960–969. doi: 10.1097/NEN.0b013e318232a379

Brunk, U. T., and Terman, A. (2002). Lipofuscin: mechanisms of age-related accumulation and influence on cell function. *Free Radic. Biol. Med.* 33, 611–619. doi: 10.1016/S0891-5849(02)00959-0

Cataldo, A. M., Hamilton, D. J., and Nixon, R. A. (1994). Lysosomal abnormalities in degenerating neurons link neuronal compromise to senile plaque development in Alzheimer disease. *Brain Res.* 640, 68–80. doi: 10.1016/0006-8993(94)91858-9

Cave, C., Park, S., Rodriguez, M., Nakamura, M., Hoke, A., Pletnikov, M., et al. (2017). GDE2 is essential for neuronal survival in the postnatal mammalian spinal cord. *Mol. Neurodegener.* 12:8. doi: 10.1186/s13024-017-0148-1

Chmátalová, Z., Vyhnálek, M., Laczó, J., Hort, J., and Skoumalová, A. (2016). Analysis of lipophilic fluorescent products in blood of Alzheimer's disease patients. *J. Cell. Mol. Med.* 20, 1367–1372. doi: 10.1111/jcmm.12824

Dalle-Donne, I., Rossi, R., Colombo, R., Giustarini, D., and Milzani, A. (2006). Biomarkers of oxidative damage in human disease. *Clin. Chem.* 52, 601–623. doi: 10.1373/clinchem.2005.061408

Davies, K. J. A. (2014). What goes wrong with Lon in ageing? *Free Radic. Biol. Med.* 75(Suppl. 1):S6. doi: 10.1016/j.freeradbiomed.2014.10.840

Davies, S. W., Turmaine, M., Cozens, B. A., DiFiglia, M., Sharp, A. H., Ross, C. A., et al. (1997). Formation of neuronal intranuclear inclusions underlies the neurological dysfunction in mice transgenic for the HD mutation. *Cell* 90, 537–548. doi: 10.1016/S0092-8674(00)80513-9

Drach, L. M., Bohl, J., Wach, S., Schlote, W., and Goebel, H. H. (1998). Reduced intraneurona lipofuscin content in dementia with Lewy bodies compared with Alzheimer's disease and controls. *Dement. Geriatr. Cogn. Disord.* 9, 1–5. doi: 10.1159/000017013

Davies, S. W., Turmaine, M., Cozens, B. A., Raza, A. S., Mahal, A., Mangiarini, L., et al. (1999). From neuronal inclusions to neurodegeneration: neuropathological investigation of a transgenic mouse model of Huntington's disease. *Philos. Trans. R. Soc. B Biol. Sci.* 354, 981–989.

de Castro, J. P. F., Mullins, R. F., Manea, A. M., Hernandez, J., Wallen, T., and Kuehn, M. H. (2013). Lipofuscin in human glaucomatous optic nerves. *Exp. Eye Res.* 111, 61–66. doi: 10.1016/j.exer.2013.03.019

Del Tredici, K., and Braak, H. (2016). Review: sporadic Parkinson's disease: development and distribution of α-synuclein pathology. *Neuropathol. Appl. Neurobiol.* 42, 33–50. doi: 10.1111/nan.12298

de Pedro-Cuesta, J., Martínez-Martín, P., Rábano, A., Alcalde-Cabero, E., José García López, F., Almazán-Isla, J., et al. (2016a). Drivers: a biologically contextualized, cross-inferential view of the epidemiology of neurodegenerative disorders. *J. Alzheimers. Dis.* 51, 1003–1022. doi: 10.3233/JAD-150884

de Pedro-Cuesta, J., Martínez-Martín, P., Rábano, A., Ruiz-Tovar, M., Alcalde-Cabero, E., and Calero, M. (2016b). Etiologic framework for the study of neurodegenerative disorders as well as vascular and metabolic comorbidities on the grounds of shared epidemiologic and biologic features. *Front. Aging Neurosci.* 8:138. doi: 10.3389/fnagi.2016.00138

de Pedro-Cuesta, J., Rábano, A., Martínez-Martín, P., Ruiz-Tovar, M., Alcalde-Cabero, E., Almazán-Isla, J., et al. (2015). Comparative incidence of conformational, neurodegenerative disorders. *PLoS ONE* 10:e0137342. doi: 10.1371/journal.pone.0137342

Dlugos, C. A. (2015). Ethanol-induced alterations in purkinje neuron dendrites in adult and aging rats: a review. *Cerebellum Lond. Engl.* 14, 466–473. doi: 10.1007/s12311-014-0636-6

Double, K. L., Dedov, V. N., Fedorow, H., Kettle, E., Halliday, G. M., Garner, B., et al. (2008). The comparative biology of neuromelanin and lipofuscin in the human brain. *Cell. Mol. Life Sci.* 65, 1669–1682. doi: 10.1007/s00018-008-7581-9

Ezaki, J., Wolfe, L. S., and Kominami, E. (1995). Defect of proteolysis of mitochondrial ATP synthase subunit C in neuronal ceroid lipofuscinosis. *Gerontology* 41(Suppl. 2), 259–269. doi: 10.1159/000213748

Feldman, T. B., Yakovleva, M. A., Arbukhanova, P. M., Borzenok, S. A., Kononikhin, A. S., Popov, I. A., et al. (2015). Changes in spectral properties and composition of lipofuscin fluorophores from human-retinal-pigment epithelium with age and pathology. *Anal. Bioanal. Chem.* 407, 1075–1088. doi: 10.1007/s00216-014-8353-z

Ferrer, I., Martinez, A., Blanco, R., Dalfó, E., and Carmona, M. (2011). Neuropathology of sporadic Parkinson disease before the appearance of parkinsonism: preclinical Parkinson disease. *J. Neural Transm.* 118, 821–839. doi: 10.1007/s00702-010-0482-8

Firlag, M., Kamaszewski, M., Gaca, K., and Bałasinska, B. (2013). Age-related changes in the central nervous system in selected domestic mammals and primates. *Postepy Hig. Med. Doswiadczalnej Online* 67, 269–275. doi: 10.5604/17322693.1044490

Folch, J., Lees, M., and Stanley, G. H. S. (1957). A simple method for the isolation and purification of total lipides from animal tissues. *J. Biol. Chem.* 226, 497–509.

Fortun, J., Dunn, W. A., Joy, S., Li, J., and Notterpek, L. (2003). Emerging role for autophagy in the removal of aggresomes in schwann cells. *J. Neurosci.* 23, 10672–10680. doi: 10.1523/JNEUROSCI.23-33-10672.2003

Fortun, J., Li, J., Go, J., Fenstermaker, A., Fletcher, B. S., and Notterpek, L. (2005). Impaired proteasome activity and accumulation of ubiquitinated substrates in a hereditary neuropathy model. *J. Neurochem.* 92, 1531–1541. doi: 10.1111/j.1471-4159.2004.02987.x

Frolova, M. S., Surin, A. M., Braslavski, A. V., and Vekshin, N. L. (2015). Degradation of mitochondria to lipofuscin upon heating and illumination. *Biophysics* 60, 934–939. doi: 10.1134/S0006350915060081

Giaccone, G., Orsi, L., Cupidi, C., and Tagliavini, F. (2011). Lipofuscin hypothesis of Alzheimer's disease. *Dement. Geriatr. Cogn. Disord. Extra* 1, 292–296. doi: 10.1159/000329544

Goebel, H. H., Heipertz, R., Scholz, W., Iqbal, K., and Tellez-Nagel, I. (1978). Juvenile Huntington chorea: clinical, ultrastructural, and biochemical studies. *Neurology* 28, 23–31. doi: 10.1212/WNL.28.1.23

Goldstein, B. D., and McDonagh, E. M. (1976). Spectrofluorescent detection of *in vivo* red cell lipid peroxidation in patients treated with diaminodiphenylsulfone. *J. Clin. Invest.* 57, 1302–1307. doi: 10.1172/JCI108398

González-Scarano, F., and Baltuch, G. (1999). Microglia as mediators of inflammatory and degenerative diseases. *Annu. Rev. Neurosci.* 22, 219–240. doi: 10.1146/annurev.neuro.22.1.219

Grubman, A., Pollari, E., Duncan, C., Caragounis, A., Blom, T., Volitakis, I., et al. (2014). Deregulation of biometal homeostasis: the missing link for neuronal ceroid lipofuscinoses? *Met. Integr. Biometal Sci.* 6, 932–943. doi: 10.1039/C4MT00032C

Grune, T., Jung, T., Merker, K., and Davies, K. J. (2004). Decreased proteolysis caused by protein aggregates, inclusion bodies, plaques, lipofuscin, ceroid, and "aggresomes" during oxidative stress, aging, and disease. *Int. J. Biochem. Cell Biol.* 36, 2519–2530. doi: 10.1016/j.biocel.2004.04.020

Grune, T., Shringarpure, R., Sitte, N., and Davies, K. (2001). Age-related changes in protein oxidation and proteolysis in mammalian cells. *J. Gerontol. A Biol. Sci. Med. Sci.* 56, B459–B467. doi: 10.1093/gerona/56.11.B459

Hara, T., Nakamura, K., Matsui, M., Yamamoto, A., Nakahara, Y., Suzuki-Migishima, R., et al. (2006). Suppression of basal autophagy in neural cells causes neurodegenerative disease in mice. *Nature* 441, 885–889. doi: 10.1038/nature04724

Hashemzadeh-Bonehi, L., Phillips, R. G., Cairns, N. J., Mosaheb, S., and Thorpe, J. R. (2006). Pin1 protein associates with neuronal lipofuscin: potential consequences in age-related neurodegeneration. *Exp. Neurol.* 199, 328–338. doi: 10.1016/j.expneurol.2005.12.030

Hebbar, S., Khandelwal, A., Jayashree, R., Hindle, S. J., Chiang, Y. N., Yew, J. Y., et al. (2017). Lipid metabolic perturbation is an early-onset phenotype in adult spinster mutants: a Drosophila model for lysosomal storage disorders. *Mol. Biol. Cell* 28, 3728–3740. doi: 10.1091/mbc.e16-09-0674

Höhn, A., and Grune, T. (2013). Lipofuscin: formation, effects and role of macroautophagy. *Redox Biol.* 1, 140–144. doi: 10.1016/j.redox.2013.01.006

Höhn, A., Jung, T., Grimm, S., Catalgol, B., Weber, D., and Grune, T. (2011). Lipofuscin inhibits the proteasome by binding to surface motifs. *Free Radic. Biol. Med.* 50, 585–591. doi: 10.1016/j.freeradbiomed.2010.12.011

Höhn, A., Jung, T., Grimm, S., and Grune, T. (2010). Lipofuscin-bound iron is a major intracellular source of oxidants: role in senescent cells. *Free Radic. Biol. Med.* 48, 1100–1108. doi: 10.1016/j.freeradbiomed.2010.01.030

Horie, K., Miyata, T., Yasuda, T., Takeda, A., Yasuda, Y., Maeda, K., et al. (1997). Immunohistochemical localization of advanced glycation end products, pentosidine, and carboxymethyllysine in lipofuscin pigments of Alzheimer's disease and aged neurons. *Biochem. Biophys. Res. Commun.* 236, 327–332.

Hung, C.-W., Chen, Y.-C., Hsieh, W.-L., Chiou, S.-H., and Kao, C.-L. (2010). Ageing and neurodegenerative diseases. *Ageing Res. Rev.* 9(Suppl), S36–S46. doi: 10.1016/j.arr.2010.08.006

Jensen, T., Holten-Rossing, H., Svendsen, I. H., Jacobsen, C., and Vainer, B. (2016). Quantitative analysis of myocardial tissue with digital autofluorescence microscopy. *J. Pathol. Inform.* 7:15. doi: 10.4103/2153-3539.179908

Jolly, R. D., Douglas, B. V., Davey, P. M., and Roiri, J. E. (1995). Lipofuscin in bovine muscle and brain: a model for studying age pigment. *Gerontology* 41(Suppl. 2), 283–295. doi: 10.1159/000213750

Jung, H., Lee, E. Y., and Lee, S. I. (1999). Age-related changes in ultrastructural features of cathepsin B- and D-containing neurons in rat cerebral cortex. *Brain Res.* 844, 43–54. doi: 10.1016/S0006-8993(99)01888-0

Jung, T., Höhn, A., and Grune, T. (2010). "Lipofuscin: detection and quantification by microscopic techniques," in *Advanced Protocols in Oxidative Stress II*, ed D. Armstrong (Totowa, NJ: Humana Press), 173–193.

Kasper, D., Planells-Cases, R., Fuhrmann, J. C., Scheel, O., Zeitz, O., Ruether, K., et al. (2005). Loss of the chloride channel ClC-7 leads to lysosomal storage disease and neurodegeneration. *EMBO J.* 24, 1079–1091. doi: 10.1038/sj.emboj.7600576

Kaushik, S., and Cuervo, A. M. (2012). Chaperone-mediated autophagy: a unique way to enter the lysosome world. *Trends Cell Biol.* 22, 407–417. doi: 10.1016/j.tcb.2012.05.006

Keller, J. N., Dimayuga, E., Chen, Q., Thorpe, J., Gee, J., and Ding, Q. (2004). Autophagy, proteasomes, lipofuscin, and oxidative stress in the aging brain. *Int. J. Biochem. Cell Biol.* 36, 2376–2391. doi: 10.1016/j.biocel.2004.05.003

Kettern, N., Rogon, C., Limmer, A., Schild, H., and Höhfeld, J. (2011). The Hsc/Hsp70 co-chaperone network controls antigen aggregation and presentation during maturation of professional antigen presenting cells. *PLoS ONE* 6:e16398. doi: 10.1371/journal.pone.0016398

Klein, Z. A., Takahashi, H., Ma, M., Stagi, M., Zhou, M., Lam, T. T., et al. (2017). Loss of TMEM106B ameliorates lysosomal and frontotemporal dementia-related phenotypes in progranulin-deficient mice. *Neuron* 95, 281.e6–296.e6. doi: 10.1016/j.neuron.2017.06.026

Kohan, R., Cismondi, I. A., Oller-Ramirez, A. M., Guelbert, N., Anzolini, V. T., Alonso, G., et al. (2011). Therapeutic approaches to the challenge of neuronal ceroid lipofuscinoses. *Curr. Pharm. Biotechnol.* 12, 867–883. doi: 10.2174/138920111795542633

Koike, M., Nakanishi, H., Saftig, P., Ezaki, J., Isahara, K., Ohsawa, Y., et al. (2000). Cathepsin D deficiency induces lysosomal storage with ceroid lipofuscin in mouse CNS neurons. *J. Neurosci. Off. J. Soc. Neurosci.* 20, 6898–6906. doi: 10.1523/JNEUROSCI.20-18-06898.2000

König, J., Ott, C., Hugo, M., Jung, T., Bulteau, A. L., Grune, T., et al. (2017). Mitochondrial contribution to lipofuscin formation. *Redox Biol.* 11, 673–681. doi: 10.1016/j.redox.2017.01.017

Kukull, W. A., Higdon, R., Bowen, J. D., McCormick, W. C., Teri, L., Schellenberg, G. D., et al. (2002). Dementia and Alzheimer disease incidence: a prospective cohort study. *Arch. Neurol.* 59, 1737–1746. doi: 10.1001/archneur.59.11.1737

Kun, A., González-Camacho, F., Hernández, S., Moreno-García, A., Calero, O., and Calero, M. (2018). "Characterization of Amyloid-β Plaques and Autofluorescent Lipofuscin Aggregates in Alzheimer's Disease Brain: A Confocal Microscopy Approach," in *Amyloid Proteins*, eds. E. M. Sigurdsson, M. Calero, and M. Gasset (New York, NY: Springer New York), 497–512. doi: 10.1007/978-1-4939-7816-8_31

Lamb, L. E., and Simon, J. D. (2004). A2E: a component of ocular lipofuscin. *Photochem. Photobiol.* 79, 127–136. doi: 10.1111/j.1751-1097.2004.tb00002.x

Lei, L., Tzekov, R., Li, H., McDowell, J. H., Gao, G., Smith, W. C., et al. (2017). Inhibition or stimulation of autophagy affects early formation of lipofuscin-like autofluorescence in the retinal pigment epithelium cell. *Int. J. Mol. Sci.* 18:728. doi: 10.3390/ijms18040728

Levin, S. W., Baker, E. H., Zein, W. M., Zhang, Z., Quezado, Z. M. N., Miao, N., et al. (2014). Oral Cysteamine bitartrate and N-acetylcysteine combination for patients with infantile neuronal ceroid lipofuscinosis:a pilot study. *Lancet Neurol.* 13, 777–787. doi: 10.1016/S1474-4422(14)70142-5

Lewandowska, E., Kujawa, M., and Jedrzejewska, A. (1994). Ethanol-induced changes in Purkinje cells of rat cerebellum. II. The ultrastructural changes after chronic ethanol intoxication. (Morphometric evaluation). *Folia Neuropathol.* 32, 61–64.

López-Otín, C., Blasco, M. A., Partridge, L., Serrano, M., and Kroemer, G. (2013). The hallmarks of aging. *Cell* 153, 1194–1217. doi: 10.1016/j.cell.2013.05.039

Lv, Z., Jiang, H., Xu, H., Song, N., and Xie, J. (2011). Increased iron levels correlate with the selective nigral dopaminergic neuron degeneration in Parkinson's disease. *J. Neural Transm.* 118, 361–369. doi: 10.1007/s00702-010-0434-3

Maccarinelli, F., Pagani, A., Cozzi, A., Codazzi, F., Di Giacomo, G., Capoccia, S., et al. (2015). A novel neuroferritinopathy mouse model (FTL 498InsTC) shows progressive brain iron dysregulation, morphological signs of early neurodegeneration and motor coordination deficits. *Neurobiol. Dis.* 81, 119–133. doi: 10.1016/j.nbd.2014.10.023

Maxwell, K. E., Matthews, T. R., Sheehy, M. R., Bertelsen, R. D., and Derby, C. D. (2007). Neurolipofuscin is a measure of age in *Panulirus argus*, the Caribbean spiny lobster, in Florida. *Biol. Bull.* 213, 55–66. doi: 10.2307/25066618

Meredith, G. E., Totterdell, S., Petroske, E., Santa Cruz, K., Callison, R. C., and Lau, Y.-S. (2002). Lysosomal malfunction accompanies alpha-synuclein aggregation in a progressive mouse model of Parkinson's disease. *Brain Res.* 956, 156–165. doi: 10.1016/S0006-8993(02)03514-X

Mink, J. W., Augustine, E. F., Adams, H. R., Marshall, F. J., and Kwon, J. M. (2013). Classification and natural history of the neuronal ceroid lipofuscinoses. *J. Child Neurol.* 28, 1101–1105. doi: 10.1177/0883073813494268

Mizushima, N. (2007). Autophagy: process and function. *Genes Dev.* 21, 2861–2873. doi: 10.1101/gad.1599207

Mizushima, N., Yamamoto, A., Matsui, M., Yoshimori, T., and Ohsumi, Y. (2004). *In vivo* analysis of autophagy in response to nutrient starvation using transgenic mice expressing a fluorescent autophagosome marker. *Mol. Biol. Cell* 15, 1101–1111. doi: 10.1091/mbc.e03-09-0704

Moore, W. A., Davey, V. A., Weindruch, R., Walford, R., and Ivy, G. O. (1995). The effect of caloric restriction on lipofuscin accumulation in mouse brain with age. *Gerontology* 41, 173–186. doi: 10.1159/000213741

Morawski, M., Brückner, M. K., Riederer, P., Brückner, G., and Arendt, T. (2004). Perineuronal nets potentially protect against oxidative stress. *Exp. Neurol.* 188, 309–315. doi: 10.1016/j.expneurol.2004.04.017

Moreira, P. I., Carvalho, C., Zhu, X., Smith, M. A., and Perry, G. (2010). Mitochondrial dysfunction is a trigger of Alzheimer's disease pathophysiology. *Biochim. Biophys. Acta* 1802, 2–10. doi: 10.1016/j.bbadis.2009.10.006

Nakano, Y., Fujitani, K., Kurihara, J., Ragan, J., Usui-Aoki, K., Shimoda, L., et al. (2001). Mutations in the novel membrane protein spinster interfere with programmed cell death and cause neural degeneration in *Drosophila melanogaster*. *Mol. Cell. Biol.* 21, 3775–3788. doi: 10.1128/MCB.21.11.3775-3788.2001

Neverman, N. J., Best, H. L., Hofmann, S. L., and Hughes, S. M. (2015). Experimental therapies in the neuronal ceroid lipofuscinoses. *Biochim. Biophys. Acta* 1852, 2292–2300. doi: 10.1016/j.bbadis.2015.04.026

Ngo, J. K., and Davies, K. J. (2007). Importance of the lon protease in mitochondrial maintenance and the significance of declining lon in aging. *Ann. N. Y. Acad. Sci.* 1119, 78–87. doi: 10.1196/annals.1404.015

Nilsson, E., and Yin, D. (1997). Preparation of artificial ceroid/lipofuscin by UV-oxidation of subcellular organelles. *Mech. Ageing Dev.* 99, 61–78. doi: 10.1016/S0047-6374(97)00091-2

Nita, D. A., Mole, S. E., and Minassian, B. A. (2016). Neuronal ceroid lipofuscinoses. *Epileptic Disord.* 18, 73–88. doi: 10.1684/epd.2016.0844

Ohgami, N., Yajima, I., Iida, M., Li, X., Oshino, R., Kumasaka, M. Y., et al. (2016). Manganese-mediated acceleration of age-related hearing loss in mice. *Sci. Rep.* 6:36306. doi: 10.1038/srep36306

Opalach, K., Rangaraju, S., Madorsky, I., Leeuwenburgh, C., and Notterpek, L. (2010). Lifelong calorie restriction alleviates age-related oxidative damage in peripheral nerves. *Rejuvenation Res.* 13, 65–74. doi: 10.1089/rej.2009.0892

Ottis, P., Koppe, K., Onisko, B., Dynin, I., Arzberger, T., Kretzschmar, H., et al. (2012). Human and rat brain lipofuscin proteome. *Proteomics* 12, 2445–2454. doi: 10.1002/pmic.201100668

Pan, X., De Aragão, C. B. P., Velasco-Martin, J. P., Priestman, D. A., Wu, H. Y., Takahashi, K., et al. (2017). Neuraminidases 3 and 4 regulate neuronal function by catabolizing brain gangliosides. *FASEB J.* 31, 3467–3483. doi: 10.1096/fj.201601299R

Parish, C. A., Hashimoto, M., Nakanishi, K., Dillon, J., and Sparrow, J. (1998). Isolation and one-step preparation of A2E and iso-A2E, fluorophores from human retinal pigment epithelium. *Proc. Natl. Acad. Sci. U.S.A.* 95, 14609–14613. doi: 10.1073/pnas.95.25.14609

Pearse, A. G. E. (1985). *Histochemistry. Theoretical and Applied. Analytical Technology, 4th Edn*. London: Churchill Livingstone.

Petkau, T. L., Blanco, J., and Leavitt, B. R. (2017). Conditional loss of progranulin in neurons is not sufficient to cause neuronal ceroid lipofuscinosis-like neuropathology in mice. *Neurobiol. Dis.* 106, 14–22. doi: 10.1016/j.nbd.2017.06.012

Petkau, T. L., Hill, A., and Leavitt, B. R. (2016). Core neuropathological abnormalities in progranulin-deficient mice are penetrant on multiple genetic backgrounds. *Neuroscience* 315, 175–195. doi: 10.1016/j.neuroscience.2015.12.006

Pollreisz, A., Messinger, J. D., Sloan, K. R., Mittermueller, T. J., Weinhandl, A. S., Benson, E. K., et al. (2018). Visualizing melanosomes, lipofuscin, and melanolipofuscin in human retinal pigment epithelium using serial block face scanning electron microscopy. *Exp. Eye Res.* 166, 131–139. doi: 10.1016/j.exer.2017.10.018

Popovic, D., Vucic, D., and Dikic, I. (2014). Ubiquitination in disease pathogenesis and treatment. *Nat. Med.* 20, 1242–1253. doi: 10.1038/nm.3739

Porta, E. A. (2002). Pigments in aging: an overview. *Ann. N. Y. Acad. Sci.* 959, 57–65. doi: 10.1111/j.1749-6632.2002.tb02083.x

Powell, S. R., Wang, P., Divald, A., Teichberg, S., Haridas, V., McCloskey, T. W., et al. (2005). Aggregates of oxidized proteins (lipofuscin) induce apoptosis through proteasome inhibition and dysregulation of proapoptotic proteins. *Free Radic. Biol. Med.* 38, 1093–1101. doi: 10.1016/j.freeradbiomed.2005.01.003

Rangaraju, S., Hankins, D., Madorsky, I., Madorsky, E., Lee, W. H., Carter, C. S., et al. (2009). The molecular architecture of myelinated peripheral nerves is supported by calorie restriction with aging. *Aging Cell* 8, 178–191. doi: 10.1111/j.1474-9726.2009.00460.x

Reeg, S., and Grune, T. (2015). Protein oxidation in aging: does it play a role in aging progression? *Antioxid. Redox Signal.* 23, 239–255. doi: 10.1089/ars.2014.6062

Richter-Landsberg, C., and Leyk, J. (2013). Inclusion body formation, macroautophagy, and the role of HDAC6 in neurodegeneration. *Acta Neuropathol.* 126, 793–807. doi: 10.1007/s00401-013-1158-x

Riga, D., Riga, S., Halalau, F., and Schneider, F. (2006a). Brain lipopigment accumulation in normal and pathological aging. *Ann. N. Y. Acad. Sci.* 1067, 158–163. doi: 10.1196/annals.1354.019

Riga, S., Riga, D., Schneider, F., and Halalau, F. (2006b). Processing, lysis, and elimination of brain lipopigments in rejuvenation therapies. *Ann. N. Y. Acad. Sci.* 1067, 383–387. doi: 10.1196/annals.1354.054

Rodgers, K. J., Ford, J. L., and Brunk, U. T. (2009). Heat shock proteins: keys to healthy ageing? *Redox Rep.* 14, 147–153. doi: 10.1179/135100009X392593

Rodolfo, C., Campello, S., and Cecconi, F. (2018). Mitophagy in neurodegenerative diseases. *Neurochem. Int.* 117, 156–166. doi: 10.1016/j.neuint.2017.08.004

Rodríguez-Muela, N., Koga, H., García-Ledo, L., de la Villa, P., de la Rosa, E. J., Cuervo, A. M., et al. (2013). Balance between autophagic pathways preserves retinal homeostasis. *Aging Cell* 12, 478–488. doi: 10.1111/acel.12072

Ross, C. A., Aylward, E. H., Wild, E. J., Langbehn, D. R., Long, J. D., Warner, J. H., et al. (2014). Huntington disease: natural history, biomarkers and prospects for therapeutics. *Nat. Rev. Neurol.* 10, 204–216. doi: 10.1038/nrneurol.2014.24

Ross, C. A., and Poirier, M. A. (2005). Opinion: what is the role of protein aggregation in neurodegeneration? *Nat. Rev. Mol. Cell Biol.* 6, 891–898. doi: 10.1038/nrm1742

Ryhänen, T., Hyttinen, J. M. T., Kopitz, J., Rilla, K., Kuusisto, E., Mannermaa, E., et al. (2009). Crosstalk between Hsp70 molecular chaperone, lysosomes and proteasomes in autophagy-mediated proteolysis in human retinal pigment epithelial cells. *J. Cell. Mol. Med.* 13, 3616–3631. doi: 10.1111/j.1582-4934.2008.00577.x

Schwartsburd, P. M. (1995). On the origin of heterogeneity of lipofuscin fluorophores and their possible interrelations. *Gerontology* 41(Suppl. 2), 29–37. doi: 10.1159/000213723

Schwarzburd, P. M., and Aslanidi, K. B. (1991). Resistance of single tumor cells and their intracellular compartments to lipid peroxidation. *Med. Oncol. Tumor Pharmacother.* 8, 57–61.

Seiberlich, V., Borchert, J., Zhukareva, V., and Richter-Landsberg, C. (2013). Inhibition of protein deubiquitination by PR-619 activates the autophagic pathway in OLN-t40 oligodendroglial cells. *Cell Biochem. Biophys.* 67, 149–160. doi: 10.1007/s12013-013-9622-8

Siakotos, A. N. (1974). Procedures for the isolation of brain lipopigments: ceroid and lipofuscin. *Meth. Enzymol.* 31, 478–485. doi: 10.1016/0076-6879(74)31053-1

Sitte, N., Huber, M., Grune, T., Ladhoff, A., Doecke, W. D., Zglinicki, T. V., et al. (2000). Proteasome inhibition by lipofuscin/ceroid during postmitotic aging of fibroblasts. *FASEB J.* 14, 1490–1498. doi: 10.1096/fj.99-0843com

Skoumalová, A., and Hort, J. (2012). Blood markers of oxidative stress in Alzheimer's disease. *J. Cell. Mol. Med.* 16, 2291–2300. doi: 10.1111/j.1582-4934.2012.01585.x

Smith, K. R., Damiano, J., Franceschetti, S., Carpenter, S., Canafoglia, L., Morbin, M., et al. (2012). Strikingly different clinicopathological phenotypes determined by progranulin-mutation dosage. *Am. J. Hum. Genet.* 90, 1102–1107. doi: 10.1016/j.ajhg.2012.04.021

Steward, C. G. (2003). Neurological aspects of osteopetrosis. *Neuropathol. Appl. Neurobiol.* 29, 87–97. doi: 10.1046/j.1365-2990.2003.00474.x

Sugaya, A., Sugimioto, H., Mogi, N., Tsujigami, H., and Deguchi, S. (2004). Experimental diabetes accelerates accumulation of fluorescent pigments in rat trigeminal neurons. *Brain Res.* 999, 132–134. doi: 10.1016/j.brainres.2003.11.033

Tang, C. H., Lee, J. W., Galvez, M. G., Robillard, L., Mole, S. E., and Chapman, H. A. (2006). Murine cathepsin F deficiency causes neuronal lipofuscinosis and late-onset neurological disease. *Mol. Cell. Biol.* 26, 2309–2316. doi: 10.1128/MCB.26.6.2309-2316.2006

Taubold, R. D., Siakotos, A. N., and Perkins, E. G. (1975). Studies on chemical nature of lipofuscin (age pigment) isolated from normal human brain. *Lipids* 10, 383–390. doi: 10.1007/BF02532441

Tellez-Nagel, I., Johnson, A. B., and Terry, R. D. (1974). Studies on brain biopsies of patients with Huntington's chorea. *J. Neuropathol. Exp. Neurol.* 33, 308–332.

Terman, A. (2001). Garbage catastrophe theory of aging: imperfect removal of oxidative damage? *Redox Rep. Commun. Free Radic. Res.* 6, 15–26. doi: 10.1179/135100001101535996

Terman, A., and Brunk, U. T. (1998). Lipofuscin: Mechanisms of formation and increase with age. *APMIS* 106, 265–276. doi: 10.1111/j.1699-0463.1998.tb01346.x

Terman, A., and Brunk, U. T. (2004). Lipofuscin. *Int. J. Biochem. Cell Biol.* 36, 1400–1404. doi: 10.1016/j.biocel.2003.08.009

Terman, A., and Brunk, U. T. (2005). The aging myocardium: roles of mitochondrial damage and lysosomal degradation. *Heart Lung Circ.* 14, 107–114. doi: 10.1016/j.hlc.2004.12.023

Terman, A., Kurz, T., Navratil, M., Arriaga, E. A., and Brunk, U. T. (2010). Mitochondrial turnover and aging of long-lived postmitotic cells: the mitochondrial–lysosomal axis theory of aging. *Antioxid. Redox Signal.* 12, 503–535. doi: 10.1089/ars.2009.2598

Terzibasi, E., Lefrançois, C., Domenici, P., Hartmann, N., Graf, M., and Cellerino, A. (2009). Effects of dietary restriction on mortality and age-related phenotypes in the short-lived fish Nothobranchius furzeri. *Aging Cell* 8, 88–99. doi: 10.1111/j.1474-9726.2009.00455.x

Tokutake, S., Nagase, H., Morisaki, S., and Oyanagi, S. (1995). Aluminium detected in senile plaques and neurofibrillary tangles is contained in lipofuscin granules with silicon, probably as aluminosilicate. *Neurosci. Lett.* 185, 99–102. doi: 10.1016/0304-3940(94)11234-A

Tuo, J., Bojanowski, C. M., Zhou, M., Shen, D., Ross, R. J., Rosenberg, K. I., et al. (2007). Murine Ccl2/Cx3cr1 deficiency results in retinal lesions mimicking human age-related macular degeneration. *Invest. Ophthalmol. Vis. Sci.* 48, 3827–3836. doi: 10.1167/iovs.07-0051

Vidal-Donet, J. M., Cárcel-Trullols, J., Casanova, B., Aguado, C., and Knecht, E. (2013). Alterations in ROS activity and lysosomal pH account for distinct patterns of macroautophagy in LINCL and JNCL fibroblasts. *PLoS ONE* 8:e55526. doi: 10.1371/journal.pone.0055526

Volchegorskii, I. A., Rassokhina, L. M., and Miroshnichenko, I. Y. (2013). Dynamics of lipid peroxidation-antioxidant defense system during alloxan diabetes in rats. *Bull. Exp. Biol. Med.* 155, 26–29. doi: 10.1007/s10517-013-2071-y

Vonsattel, J. P. G., and Difiglia, M. (1998). Huntington Disease. *J. Neuropathol. Exp. Neurol.* 57, 369–384. doi: 10.1097/00005072-199805000-00001

Wakabayashi, K., Kobayashi, H., Kawasaki, S., Kondo, H., and Takahashi, H. (2001). Autosomal recessive spastic paraplegia with hypoplastic corpus callosum, multisystem degeneration and ubiquitinated eosinophilic granules. *Acta Neuropathol.* 101, 69–73. doi: 10.1007/s004010000255

Warburton, S., Davis, W. E., Southwick, K., Xin, H., Woolley, A. T., Burton, G. F., et al. (2007). Proteomic and phototoxic characterization of melanolipofuscin: correlation to disease and model for its origin. *Mol. Vis.* 13, 318–329. doi: 10.1007/0-387-32442-9_11

Ward, M. E., Chen, R., Huang, H. Y., Ludwig, C., Telpoukhovskaia, M., Taubes, A., et al. (2017). Individuals with progranulin haploinsufficiency exhibit features of neuronal ceroid lipofuscinosis. *Sci. Transl. Med.* 9:eaah5642. doi: 10.1126/scitranslmed.aah5642

Weinert, S., Jabs, S., Supanchart, C., Schweizer, M., Gimber, N., Richter, M., et al. (2010). Lysosomal pathology and osteopetrosis upon loss of H+-driven lysosomal Cl- accumulation. *Science* 328, 1401–1403. doi: 10.1126/science.1188072

Wellings, T. P., Brichta, A. M., and Lim, R. (2017). Altered neurofilament protein expression in the lateral vestibular nucleus in Parkinson's disease. *Exp. Brain Res.* 235, 3695–3708. doi: 10.1007/s00221-017-5092-3

Wenisch, S., Hild, A., Bitsch, I., Leiser, R., and Hummel, G. (1997). Ultrastructure of rat Purkinje neurons after chronic ethanol consumption and prolonged abstinence. *Anat. Histol. Embryol.* 26, 93–98. doi: 10.1111/j.1439-0264.1997.tb00106.x

Williams, R. E., Adams, H. R., Blohm, M., Cohen-Pfeffer, J. L., Reyes, E. de los, Denecke, J., et al. (2017). Management Strategies for CLN2 Disease. *Pediatr. Neurol.* 69, 102–112. doi: 10.1016/j.pediatrneurol.2017.01.034

Yamasaki, R., Zhang, J., Koshiishi, I., Sastradipura Suniarti, D. F., Wu, Z., Peters, C., et al. (2007). Involvement of lysosomal storage-induced p38 MAP kinase activation in the overproduction of nitric oxide by microglia in cathepsin D-deficient mice. *Mol. Cell. Neurosci.* 35, 573–584. doi: 10.1016/j.mcn.2007.05.002

Yoshikawa, M., Uchida, S., Ezaki, J., Rai, T., Hayama, A., Kobayashi, K., et al. (2002). CLC-3 deficiency leads to phenotypes similar to human neuronal ceroid lipofuscinosis. *Genes Cells Devoted Mol. Cell. Mech.* 7, 597–605. doi: 10.1046/j.1365-2443.2002.00539.x

Zhao, L., Spassieva, S. D., Jucius, T. J., Shultz, L. D., Shick, H. E., Macklin, W. B., et al. (2011). A deficiency of ceramide biosynthesis causes cerebellar purkinje cell neurodegeneration and lipofuscin accumulation. *PLoS Genet.* 7:e1002063. doi: 10.1371/journal.pgen.1002063

Zheng, S., Clabough, E. B. D., Sarkar, S., Futter, M., Rubinsztein, D. C., and Zeitlin, S. O. (2010). Deletion of the Huntingtin polyglutamine stretch enhances neuronal autophagy and longevity in mice. *PLoS Genet.* 6:e1000838. doi: 10.1371/journal.pgen.1000838

Zhou, X., Sun, L., Brady, O. A., Murphy, K. A., and Hu, F. (2017). Elevated TMEM106B levels exaggerate lipofuscin accumulation and lysosomal dysfunction in aged mice with progranulin deficiency. *Acta Neuropathol. Commun.* 5:9. doi: 10.1186/s40478-017-0412-1

Zhu, Y., Fenik, P., Zhan, G., Xin, R., and Veasey, S. C. (2015). Degeneration in arousal neurons in chronic sleep disruption modeling sleep apnea. *Front. Neurol.* 6:109. doi: 10.3389/fneur.2015.00109

Conflict of Interest Statement: The authors declare that the research was conducted in the absence of any commercial or financial relationships that could be construed as a potential conflict of interest.

frontiers in Neuroscience

ORIGINAL RESEARCH
published: 07 February 2018
doi: 10.3389/fnins.2018.00055

Safety and Efficacy of Scanning Ultrasound Treatment of Aged APP23 Mice

*Gerhard Leinenga and Jürgen Götz**

Clem Jones Centre for Ageing Dementia Research, Queensland Brain Institute, University of Queensland, Brisbane, QLD, Australia

Deposition of amyloid-β (Aβ) peptide leads to amyloid plaques that together with tau deposits characterize the brains of patients with Alzheimer's disease (AD). In modeling this pathology, transgenic animals such as the APP23 strain, that expresses a mutant form of the amyloid precursor protein found in familial cases of AD, have been instrumental. In previous studies, we have shown that repeated treatments with ultrasound in a scanning mode (termed scanning ultrasound or SUS) were effective in removing Aβ and restoring memory functions, without the need for a therapeutic agent such as an Aβ antibody. Considering that age is the most important risk factor for AD, we extended this study in which the mice were only 12 months old at the time of treatment by assessing a cohort of 2 year-old mice. Interestingly, at this age, APP23 mice are characterized by cerebral amyloid angiopathy (CAA) and the presence of occasional microbleeds. We found that SUS in aged mice that have been exposed to four SUS sessions that were spread out over 8 weeks and analyzed 4 weeks later did not show evidence of increased CAA or microbleeds. Furthermore, amyloid was reduced as assessed by methoxy-XO4 fluorescence. In addition, plaque-associated microglia were more numerous in SUS treated mice. Together this adds to the notion that SUS may be a treatment modality for human neurodegenerative diseases.

Keywords: Alzheimer's disease, microbleeds, scanning ultrasound, amyloid-β, microglia, therapy

OPEN ACCESS

Edited by:
Naruhiko Sahara, National Institute of Radiological Sciences (NIRS), Japan

Reviewed by:
Emmanuel Planel, Laval University, Canada
Takami Tomiyama, Osaka City University, Japan

***Correspondence:**
Jürgen Götz
j.goetz@uq.edu.au

Specialty section:
This article was submitted to Neurodegeneration, a section of the journal Frontiers in Neuroscience

Received: *14 November 2017*
Accepted: *23 January 2018*
Published: *07 February 2018*

Citation:
Leinenga G and Götz J (2018) Safety and Efficacy of Scanning Ultrasound Treatment of Aged APP23 Mice. Front. Neurosci. 12:55. doi: 10.3389/fnins.2018.00055

INTRODUCTION

Life expectancy has increased dramatically in the past decades, owing to general lifestyle improvements and better medication; however, the ensuing dramatic demographic shift in age distribution is associated with an increased prevalence of diseases such as cerebrovascular disease, cancer and dementia (Leinenga et al., 2017). In contrast to cerebrovascular disease and cancer, where non-pharmacological therapies play important roles, the focus in neurological disease research has been on drug discovery, despite the fact that delivery of drugs to the brain presents a particular challenge due to the presence of the blood-brain barrier (BBB). This barrier not only prevents any exchange between the blood and nervous tissue, thereby protecting the brain parenchyma from circulating factors, and restricting access of pathogens and immune cells to the brain (Wong et al., 2013); it also allows only a small subset of small-molecule drugs to enter the brain via lipid-mediated free diffusion, posing a major problem for drug delivery (Pardridge, 2012).

Whether the BBB in neurodegenerative diseases (different from stroke and glioma) is leaky remains a matter of debate (Leinenga et al., 2016). The notion that the BBB becomes leaky in

neurological disease disregards the fact that the brain is not completely sealed off from the periphery when healthy. Active exchange between the blood and the brain under normal physiological conditions is indicated by the fact that, for example, steady-state brain levels of peripherally administered antibodies are approximately 0.1% of those in the plasma (Levites et al., 2006). Such evidence does not mean that the BBB is not compromised under certain pathological conditions, but rather that the precise nature of the damage is incompletely understood (Gilad et al., 2012; Krueger et al., 2013; Knowland et al., 2014). Although cellular senescence can impair BBB function (Murugesan et al., 2012; Lucke-Wold et al., 2014), several lines of evidence from studies of Alzheimer's disease (AD) show that disruption of the BBB in neurodegenerative disease should not be assumed, with a study published in 2015 reporting a lack of widespread BBB disruption in several mouse models of Alzheimer's disease, and a similar occurrence of infarcts (one indication of BBB breakdown) in patients with AD and age-matched healthy controls (Bien-Ly et al., 2015).

In order to manipulate the opening of the BBB for targeted drug or gene delivery, non-thermal ultrasound can be used to capitalize on the interaction between ultrasound and microscopic bubbles of gas (microbubbles) in tissue or fluids (Sirsi and Borden, 2009). Injection of preformed, commercially available microbubbles is used to ensure biological effects even at low acoustic pressures (Konofagou, 2012). These microbubbles are routinely used for contrast-enhanced ultrasound imaging. They are biologically inert and have a gas core encapsulated by a thin shell of lipid or polymer, and a diameter $<10\,\mu m$. Ultrasound causes them to cavitate, i.e., expand and contract, resulting in vessel wall displacement (McDannold et al., 2006; Caskey et al., 2007; Raymond et al., 2007). Displacement causes transient opening of tight junctions because of the disintegration of the associated junction complexes. This transiently facilitates transport across the BBB (Sheikov et al., 2008).

The two key molecules implicated in AD are Aβ and tau (Li and Götz, 2017b). Aβ is a small peptide derived by proteolytic cleavage from the larger amyloid precursor protein (APP) that aggregates and forms histological lesions known as amyloid plaques. While AD is characterized by the intraparenchymal deposition of amyloid-β in plaques, a majority of AD patients also exhibit deposition of amyloid in blood vessel walls, mainly small arteries, a pathology called cerebral amyloid angiopathy abbreviated CAA (Attems et al., 2005). CAA increases the risk of intracerebral hemorrhage by making amyloid-laden blood vessels more susceptible to damage (Banerjee et al., 2017). Tau is a microtubule-associated protein that forms neurofibrillary tangles. Tau pathology is found not only in AD but also in many diseases collectively termed tauopathies which includes a major subset of FTLD termed FTLD-Tau. Tau is required for Aβ toxicity (Ittner et al., 2010), and Aβ initiates the *de novo* protein synthesis of tau in the somatodendritic domain (Li and Götz, 2017a).

We and others have previously shown that microbubble-mediated BBB opening without any therapeutic agent reduces an Aβ pathology in APP mutant mice (Jordão et al., 2013; Leinenga and Götz, 2015). By weekly treatments of 12 month-old APP23 mice between 5 and 8 times using ultrasound in a scanning mode (SUS for scanning ultrasound), Aβ species ranging from monomers to oligomers to high molecular weight species could be cleared effectively, plaques were partially cleared, and memory functions were restored in three complementary tests (Leinenga and Götz, 2015). As an underlying clearance mechanism we had identified the internalization of Aβ by brain-resident dormant microglial cells that became activated by unidentified blood-borne factors that entered the brain as a consequence of the transient opening of the BBB. Interestingly, we found that tau pathology (being mostly intraneuronal) could also be partially cleared with this approach as shown in the pR5 transgenic mouse model of tauopathy which accumulates hyperphosphorylated tau in neurons (Nisbet et al., 2017). Long-term safety has been demonstrated in wild-type mice (Hatch et al., 2016), and an application to proteinopathies more generally can be envisaged (Leinenga et al., 2017; Li and Götz, 2017b). Here, we aimed to determine whether the cerebral amyloid angiopathy (CAA) and microbleeds that characterize aged APP23 mice (Calhoun et al., 1999) would be features that are augmented by a SUS treatment, and also, whether there would be a reduction in amyloid in mice with advanced amyloid pathology.

MATERIALS AND METHODS

Animal Models and Ethics

APP23 mice express hAPP751 together with the Swedish double mutation under control of the neuron-specific mThy1.2 promoter (Sturchler-Pierrat et al., 1997). APP23 mice are characterized by amyloid plaque formation mainly in the cortex, as well as associated memory deficits, and cerebral amyloid angiopathy as they age (Calhoun et al., 1999; Winkler et al., 2001). They also display a premature lethality that comes to a hold when they reach a few months of age (Ittner et al., 2010). Animal experimentation was approved by the Animal Ethics Committee of the University of Queensland (approval number QBI/412/14/NHMRC).

SUS Equipment

An integrated focused ultrasound system was used (Therapy Imaging Probe System, TIPS, Philips Research) (Seip et al., 2010). The system consisted of an annular array transducer with a natural focus of 80 mm, a radius of curvature of 80 mm, a spherical shell of 80 mm with a central opening of 31 mm diameter, a 3D positioning system, and a programmable motorized system to move the ultrasound focus in the x and y planes to cover the entire brain. A coupler mounted to the transducer was filled with degassed water and placed on the head of the mouse with ultrasound gel for coupling, to ensure propagation of the ultrasound to the brain (**Figure 1A**). The focal zone of the array was an ellipse of approximately 1.5 × 1.5 × 12 mm.

Production of Microbubbles

In-house prepared microbubbles comprising a phospholipid shell and octafluoropropane gas core were used. 1,2-distearoyl-*sn*-glycero-3-phosphocholine (DSPC) and 1,2-distearoyl-sn -glycero-3-phosphoethanolamine-N-[amino(polyethylene

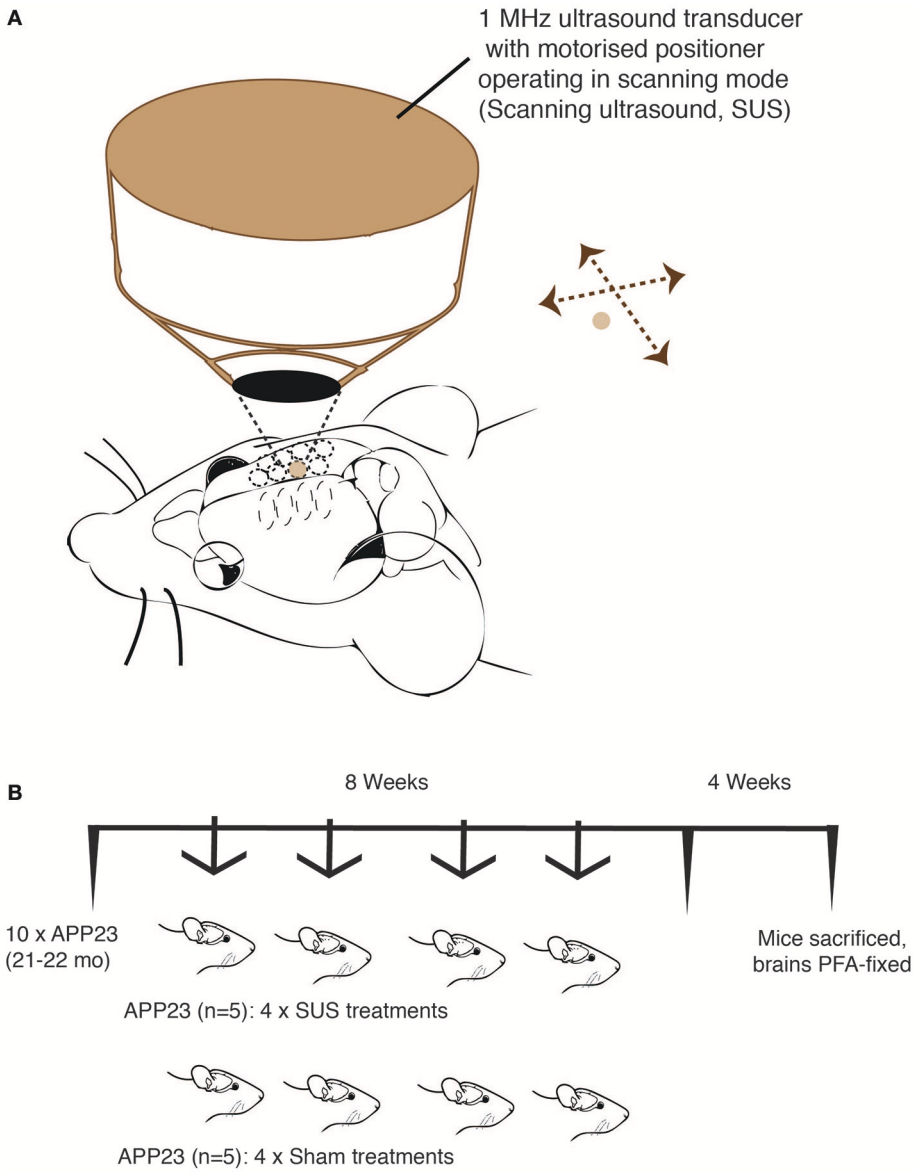

FIGURE 1 | Treatment scheme for of aged APP23 mice. Scanning ultrasound (SUS) approach using the TIPS system (Philips Research) that consists of an annular 1 MHz transducer operating on a motorized stage to allow the sequential treatment of multiple foci until a total coverage of the mouse forebrain is achieved. **(A)** Treatment scheme of 21–22 month-old APP23 mice (mixed gender) divided into two matching groups ($n = 5$ per group). **(B)** One group received 4 SUS treatments spread out over an 8 week period, whereas the other group received 4 sham treatments (anesthetics and microbubbles only) over the same period. Four weeks after the final treatment, the mice were sacrificed and their forebrains fixed in 4% PFA for histology.

glycol)-2000] (DSPE-PEG2000) (Avanti Polar Lipids) were mixed at a 9:1 molar ratio dissolved in chloroform (Sigma) and the chloroform solvent was evaporated under vacuum. The dried phospholipid cake was then dissolved in PBS with 10% glycerol to a concentration of 1 mg lipid/ml and heated to 55°C in a sonicating water bath. The solution was placed in 1.5 ml glass HPLC vials and the air in the vial was replaced with octafluoropropane (Arcadophta). Microbubbles were generated on the day of the experiment by agitation in a dental amalgamator at 4,000 rpm for 40 s. Microbubbles were observed under a microscope to be polydispersed and under 10 μm in size at a concentration of $1–5 \times 10^8$ microbubbles/ml.

SUS Application

Mice were anesthetized with ketamine (100 mg/kg) and xylazine (10 mg/kg) and the hair on the head was shaved and depilated. Mice were injected intravenous retro-orbitally with 1 μl/g body weight of microbubble solution and then placed under the ultrasound transducer with the head immobilized. We have previously found that retro-orbital injections give identical

results as tail vein injections and are technically easier to perform. Parameters for the ultrasound delivery were 0.7 MPa peak rarefactional pressure, 10 Hz pulse repetition frequency, 10% duty cycle, and a 6 s sonication time per spot. The focus of the transducer had dimensions of 1.5 × 12 mm in the transverse and axial planes, respectively. The motorized positioning system moved the focus of the transducer array in a grid with 1.5 mm spacing between individual sites of sonication so that ultrasound was delivered sequentially to the entire brain as described (Nisbet et al., 2017). Mice typically received a total of 24 spots of sonication in a 6 × 4 raster grid pattern. For sham treatment, mice received all injections and were placed under the ultrasound transducer, but no ultrasound was emitted.

Tissue Processing

Mice were deeply anesthetized with pentobarbitone before being perfused with 30 ml of phosphate-buffered saline (PBS), followed by 30 ml of 4% wt/vol paraformaldehyde. They were postfixed for 24 h, cryoprotected in 30% sucrose and sectioned sagitally at 30 μm thickness on a freezing-sliding microtome. A one-in-six series of sections was stored in PBS with 0.02% sodium azide at 4°C until staining.

Assessment of Bleeds

Two methods were used to assess cerebral microbleeds, staining adjacent sections with hematoxylin & eosin (H&E) and Perl's Prussian blue. H&E staining was performed according to a standard procedure using Meyer's Hematoxylin and was also used to detect any other damage to the tissue. Prussian blue staining was performed using freshly prepared 5% potassium hexacyanoferratetrihydrate and 5% hydrochloric acid for 10 min. Sections were rinsed in water and counterstained with nuclear fast red, dehydrated, and mounted with Depex. Cerebral microbleeds were identified at a 20× magnification as cherry-red colored erythrocytes using H&E staining, and as blue deposits using Prussian blue staining. For each of these stainings, four mid-sagittal sections per mouse were analyzed blinded, with no identification of treatment group until after the data were obtained.

Assessment of Amyloid Plaque Load

For staining plaques with methoxy-X04 (Burgold et al., 2011; Burgess et al., 2014), sections were washed with PBS, incubated with 10 μM methoxy-XO4 (Tocris Bioscience) in 50% DMSO/50% NaCl 0.9%, pH 12 for 10 min and washed twice with PBS. A Metafer fluorescent VSlide Scanner by MetaSystems using a Zeiss Axio Imager Z2 acquired images with a 20x objective. The analysis was performed with ImageJ (National Institutes of Health). Four mid-sagittal sections from each mouse brain were analyzed blinded, with no identification of treatment group until after measurements were obtained. Data were obtained for total plaque number, individual plaque sizes, forebrain plaque-positive area fraction, and mean gray value per section as well as the mean gray value per thresholded plaque area were calculated. Automatic thresholding of plaques was performed by the following procedure: The average fluorescence in the cerebral peduncle of the cerebellum was defined as non-specific fluorescence, due to lack of plaques in this brain region, and subtracted from the image. The MaxEntropy function was used to identify the plaques and convert the image to a binary image. Watershed and fill hole functions were applied. From this the number of plaques, plaque area, plaque size, and mean gray values were calculated using the "analyze particles" plugin. A minimum size of 10 μm in diameter and 0.1 circularity was used to ensure specificity of plaque detection. The Aβ area fraction was determined by dividing the total plaque area by the area of the forebrain. CAA length was determined manually by a blinded observer, using ImageJ.

Microglial Assessment

Microglia were immunostained with anti-Iba1 antibody (Wako, JP 1:1,000) followed by incubation with an anti-rabbit secondary antibody AlexaFluor 568 conjugate (Invitrogen). Sections were then co-stained with 10 μM methoxy-XO4 (Tocris Bioscience) in PBS with 20% Ethanol before coverslipping. Images were obtained with a spinning disk confocal microscope (Nikon Diskovery) with a 20x objective acquiring z-stacks through the entire depth of the section. An experimenter blinded to experimental groups then manually outlined plaque areas and manually counted the number of microglia cell bodies within 20 μm of the perimeter of a plaque using Nikon NIS software. The total number of plaques analyzed was 179 total, 82 for the sham condition and 97 for the SUS condition. Three-four randomly chosen fields of view were captured from 2 to 4 sections from each mouse, resulting in a total number of between 14 and 23 plaques analyzed from each mouse.

Statistics

Statistical analyses were conducted with Prism 7 software (GraphPad Software, USA). Values are always reported as mean ± SEM. Two-tailed *t*-tests with Welch's correction were used for all analyses except for the microglia analysis where a Deming multiple linear regression was performed.

RESULTS

Study Design to Address the Effects of SUS in Aged APP23 Mice

Using a previously established protocol (Leinenga and Götz, 2015), 10 21–22 month-old male APP23 mice were used. At this advanced age, APP23 mice have a massive plaque burden and also extensive CAA (Calhoun et al., 1999). Over a period of 8 weeks, 5 mice received 4 SUS treatment, and 5 mice received 4 sham treatments (with "sham" meaning an injection of microbubbles and anesthesia, but without applying ultrasound) (**Figure 1B**). After the last treatment, we waited for 4 weeks and then sacrificed the mice by perfusion fixation and analyzed them histologically. Mice were 23–24 months old at sacrifice.

Safety of Sonication in Aged APP23 Mice and Effects on Cerebral Amyloid Angiopathy (CAA)

Cerebral microbleeds are increasingly being recognized as a critical factor in the cognitive impairment in AD (Cacciottolo et al., 2016). In addition, anti-Aβ vaccines that are currently in

clinical trials may pose the risk of microbleeds, so-called ARIA-H on magnetic resonance imaging (Sevigny et al., 2016). Therefore, we carried out a histopathological study to determine whether SUS causes microbleeds or hemorrhage in the APP23 mouse model with significant cerebrovascular amyloid and occurrence of cerebral microbleeds (Reuter et al., 2016). However, upon dissection, all brains were unremarkable without the appearance of surface bleeds. To detect microbleeds, sagittal sections were stained with H&E that detects newly formed bleeds with intact erythrocytes and with Prussian blue that can detect leftover brain iron from previously occurring bleeds (old lesions). While there were Prussian blue-reactive iron deposits in aged APP23 mice, there was no difference between treatment groups (**Figure 2A**). H&E staining did again not reveal differences between the treatment groups, as microbleeds that are also known as petechiae (<50 μm diameter) were found in one of the five sham-treated mice and in one of the five SUS-treated mouse for the sections analyzed. Erythrocyte clusters were detected by H&E staining that were around 100 μm in diameter and were confined to the cortex and thalamus in one sham-treated APP23 mouse and in the hippocampus of one SUS-treated APP23 mouse (**Figure 2B**). The risk of microbleeds is related to CAA, and therefore, the length of CAA was quantified on sections manually by a blinded observer. Again, no difference was found between the SUS- and sham-treated groups (**Figure 2C**).

SUS Treatment of 2 Year-Old APP23 Mice Does Not Reduce the Total Plaque Area, but Reduces the Fraction of Larger Plaques

Methoxy-X04 is a derivative of Congo red and Chrysamine-G that contains no acid groups and is therefore smaller and much more lipophilic than Congo red or Chrysamine-G. Methoxy-X04 is fluorescent and stains amyloid plaques, tangles (that do not develop in APP23 mice), and CAA in postmortem sections of AD brain with good specificity (Klunk et al., 2002). We performed methoxy-XO4 staining for plaques in SUS- and sham-treated APP23 mice (**Figure 3A**). In these very old APP23 mice, after only four treatments, there was neither a reduction in

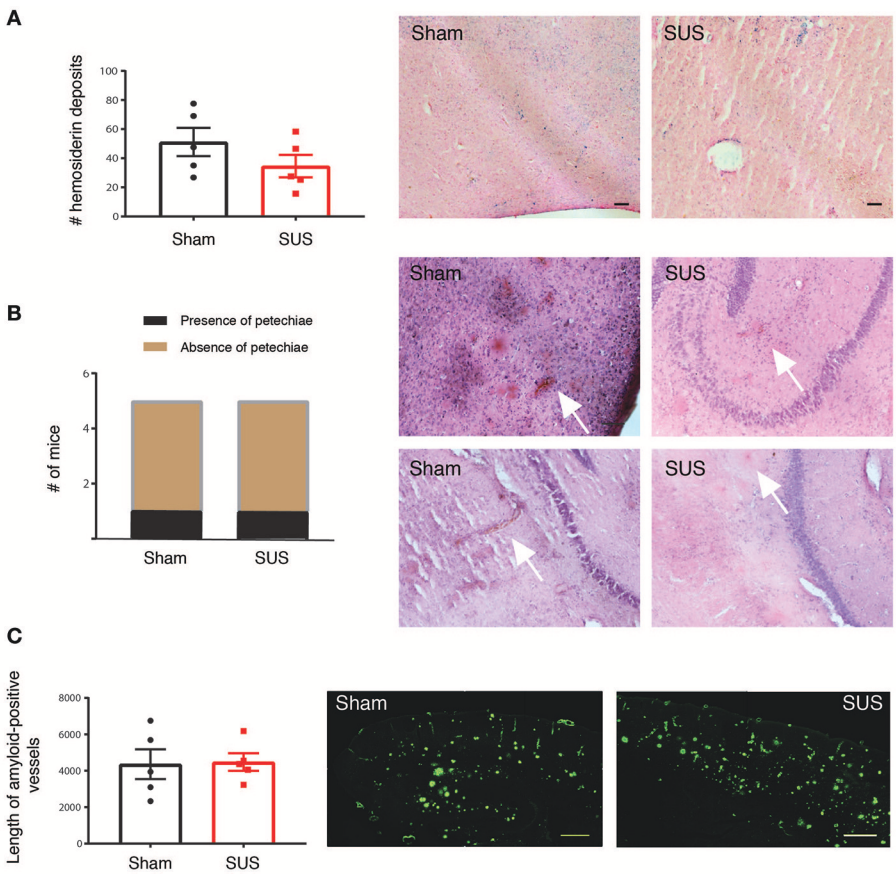

FIGURE 2 | SUS in aged APP23 mice does not augment microbleeds and cerebral amyloid angiopathy (CAA). **(A)** Perl's Prussian blue staining detecting hemosiderin deposits reveals significant iron deposition in brains of aged APP23 mice, with no difference in numbers between sham- and SUS-treated mice. Blue spots label iron deposits from previous microbleeds. **(B)** Hematoxylin and eosin (H&E) staining reveals small acute cerebral microbleeds known as petechiae only in one sham- and one SUS-treated mouse in the sections analyzed. **(C)** Prominent amyloid-laden vessels (pathology known as CAA) are found in aged APP23 mice, with their length not differing between sham- and SUS-treated mice as determined with methoxy-XO4. Scale bars: 100 μm, data shown as mean ± SEM. White arrows indicate microbleeds.

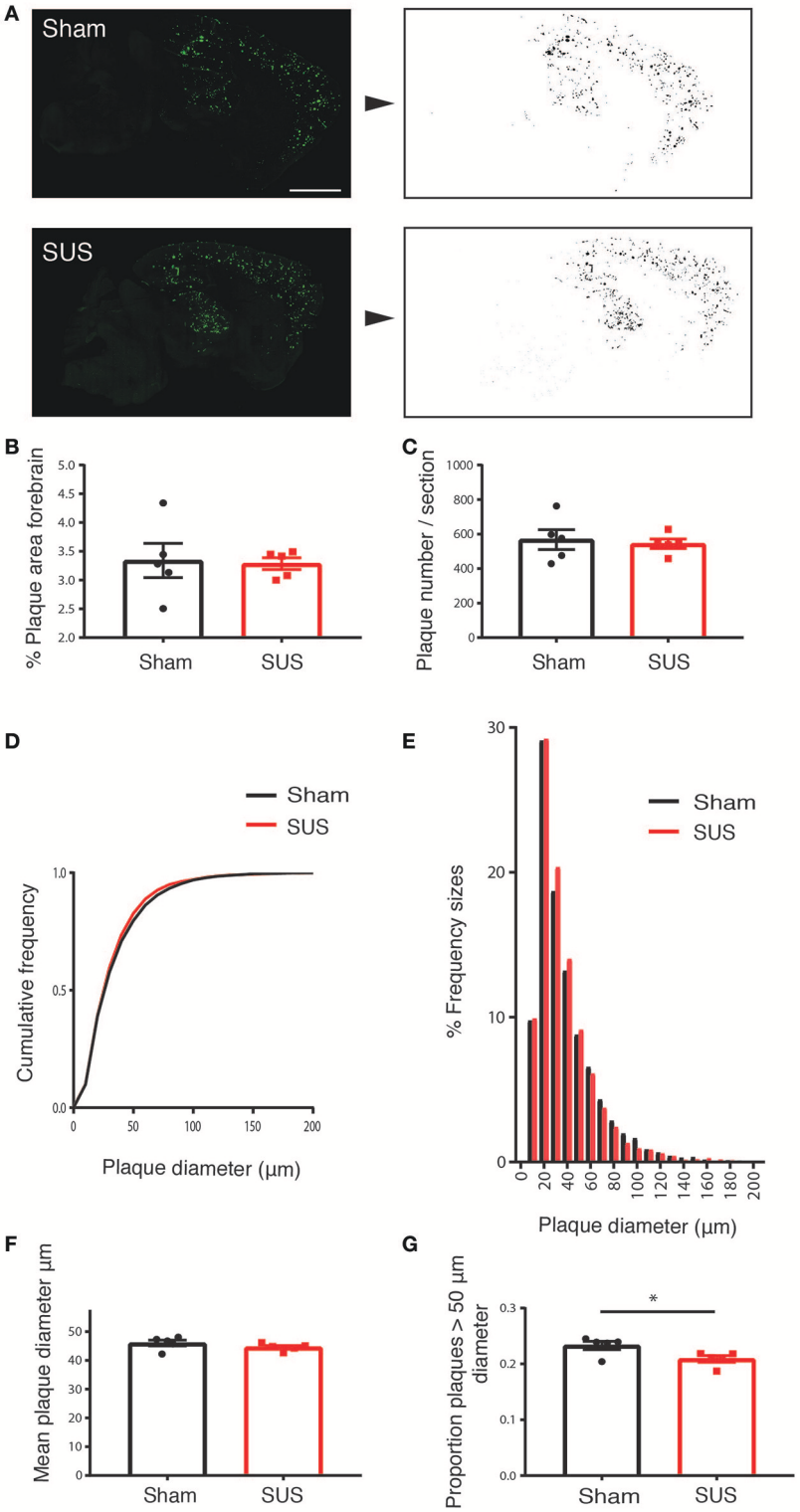

FIGURE 3 | SUS treatment of aged APP23 mice does not reduce total plaque numbers, but the fraction of larger plaques. Methoxy-XO4 staining was used to visualize plaques (**A**, left). An automated threshold was applied and a binary image of plaques produced to obtain the size and number of plaques (**A**, right). This reveals no difference in the total amyloid-positive area **(B)**, and the number of plaques per section **(C)**. SUS shifts the cumulative frequency of plaque sizes toward smaller plaques **(D,E)**, without reducing the mean plaque size **(F)**. The proportion of large plaques is reduced, with large plaques being defined as having a diameter larger than 50 µm (accounting for about the largest 30% of plaques) **(G)**. Scale bar: 500 µm, mean ± SEM. $^*p < 0.05$.

the percentage plaque area in the forebrain nor the number of plaques per section (**Figures 3B,C**). However, we observed an effect on plaque size such that in the SUS-treated group, the cumulative frequency distribution of plaque sizes was shifted toward smaller plaques (**Figures 3D,E**), without affecting the mean plaque size (**Figure 3F**). When comparing the proportion of plaques that were larger than 50 μm^2 (representing about the largest third of plaques), SUS reduced the proportion of these large plaques ($p < 0.05$; **Figure 3G**).

SUS Treatment Reduces Fibrillar Amyloid

We next quantified the fluorescent staining of the amyloid plaques in the SUS- compared to the sham-treated mice because visual inspection revealed an obvious reduction in methoxy-XO4 fluorescence intensity on the sections from SUS-treated mice (**Figure 4A**). When a color is assigned to the mean gray value based on intensity, there was a visible 58% reduction in the SUS-treated group ($p < 0.001$) (**Figure 4B**).

Together, this indicates a reduction in amyloid in APP23 mice even at a very high age and after only four SUS sessions, and also, that SUS treatment does not elicit damage as shown by the absence of increased microbleeds and CAA pathology, underscoring the potential safety of a therapeutic ultrasound treatment targeting the amyloid pathology.

SUS Treatment Increases the Number of Plaque-Associated Microglia

To investigate possible mechanistic explanations for the reduced amyloid in SUS-treated mice, we determined the number of amyloid-associated microglia in the two groups as we have previously shown that SUS leads to microglia activation and increased phagocytosis of amyloid (Leinenga and Götz, 2015). To do this we performed co-staining for plaques and microglia with methoxy-XO4 and an anti-Iba1 antibody, respectively. This revealed an increased association of microglia with plaques in SUS-treated mice (**Figure 5A**). Plaque-associated microglia surrounding a total of 187 plaques of various sizes were analyzed. The number of plaque-associated microglia per plaque and plaque area was plotted as a scatter plot (**Figure 5B**). Plotting best-fit Deming regression lines for each group, it was found that there was a significant correlation between plaque area and the number of microglia in close proximity to plaques for both sham [$F_{(1, 80)} = 113.9$, $p < 0.0001$] and SUS [$F_{(1, 95)} = 92.94$, $p < 0.0001$] groups. The overall slopes were significantly different, indicating an interaction effect of the experimental group [$F_{(1, 175)} = 6.227$, $p = 0.014$]. These results show that plaques in the SUS-treated group have more plaque-associated microglia, and that in SUS-treated mice the the number of microglia per plaque is substantially increased for larger plaques. This conclusion was also supported by an analysis where normalizing for plaque size (microglia /1000 μm^2 plaque) and averaging all plaques into one value per mouse revealed a significant increase in microglia per plaque in the SUS group compared to sham (Unpaired t-test with Welch's correction, $p = 0.028$; **Figure 5C**).

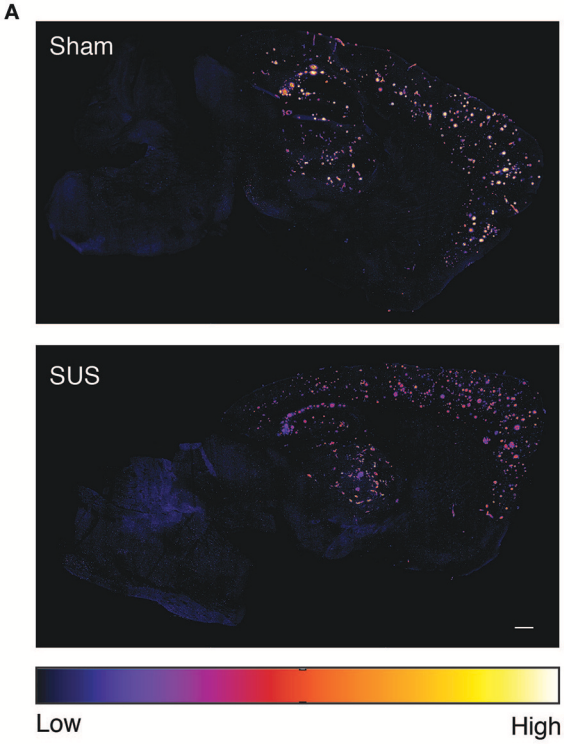

FIGURE 4 | SUS treatment reduces fibrillar amyloid. **(A)** Sections treated with methoxy-XO4 render plaques fluorescent, followed by colorizing based on intensity reveals a reduction in fluorescence intensity in SUS-treated sections. **(B)** Scale bar: 500 μm, mean ± SEM. ***$p < 0.001$.

DISCUSSION

Therapeutic ultrasound is a novel potential treatment modality for human neurodegenerative diseases that may only employ an ultrasound sonication facilitated by biologically inert microbubbles or may be used in combination with a therapeutic agent (Leinenga et al., 2016). Several studies in mice have shown that the interaction of ultrasound with microbubbles transiently opens the BBB, allowing unidentified blood-borne factors and exogenously added antibodies or antibody fragments to enter the brain where they ameliorate the two defining pathologies of AD, Aβ and tau deposition, by an incompletely understood

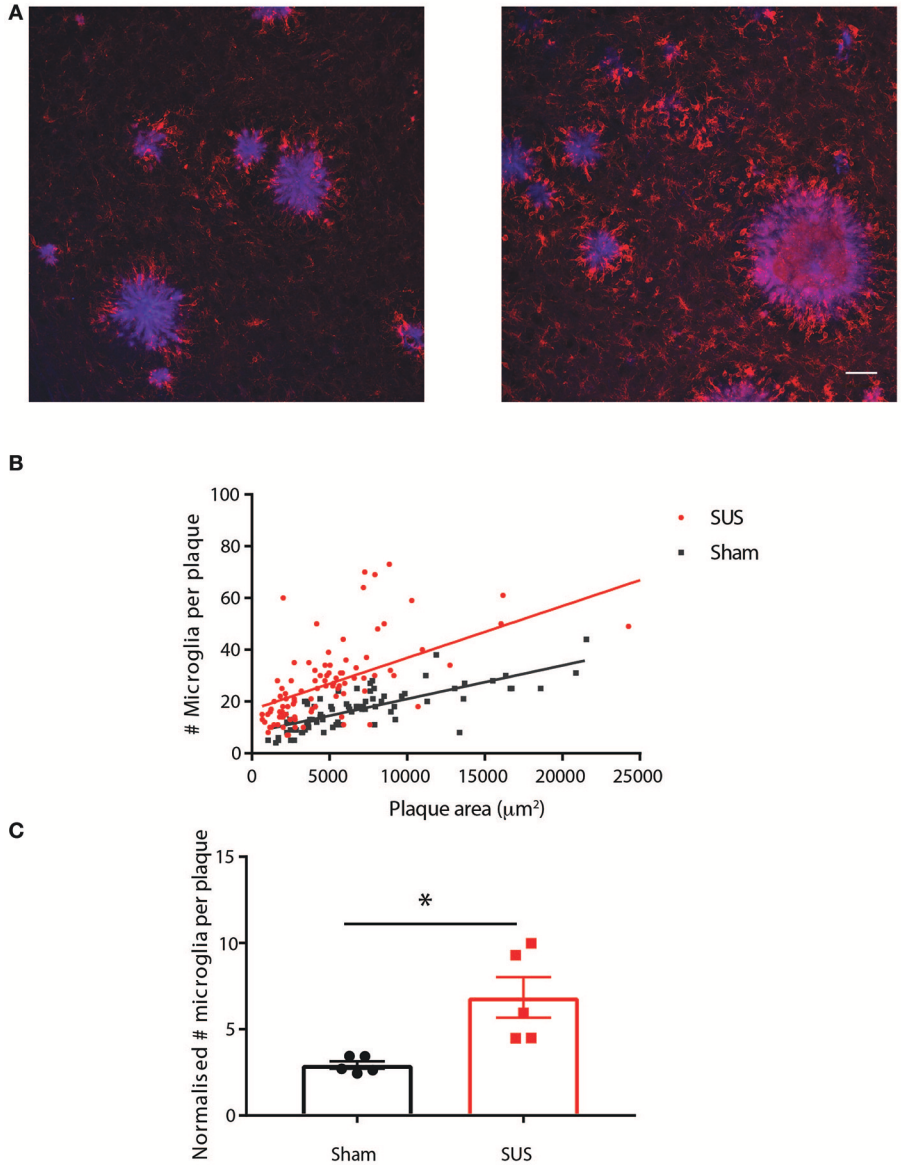

FIGURE 5 | SUS treatment increases the number of plaque-associated microglia. **(A)** Co-labeling plaques (blue) and microglia (red) reveals an increase in plaque-associated microglia in SUS-treated mice. **(B)** A scatter plot of the data with Deming best fit regression lines reveals significant correlation between plaque size and number of microglia in plaque proximity, which is more pronounced for plaques in the SUS-treated mice. **(C)** Normalizing microglia number to plaque area and averaging per mouse reveals that more microglia per plaque in the SUS-treated mice. Scale bar: 50 μm, mean ± SEM. *$p < 0.05$.

mechanism that involves microglia (Jordão et al., 2010, 2013; Leinenga and Götz, 2015). These studies have been done in mice that in the case of tau were quite young, and in the case of Aβ middle-aged, yet old enough to display an amyloid pathology, but not old enough to develop microbleeds and CAA. Here, we addressed the question whether SUS treatments in 2 year-old APP23 mice that are characterized by CAA and occasional microbleeds would augment these two pathologies. To detect microbleeds we used two complementary methods, one for acute bleeds (H&E staining) and the other for visualizing older, pre-existing lesions by detecting left-over hemosiderin from bleeds (Prussian blue). Interestingly, Prussian blue staining revealed iron deposits in all mice analyzed, irrespective of whether they were sham- or SUS-treated (Marinescu et al., 2017). Fresher lesions as determined by H&E staining were only found in one mouse each. Together this reveals that SUS treatment with the ultrasound parameters established used by us did not augment this pre-existing pathology. We had also analyzed CAA, finding neither an increase in vascular amyloid nor its clearance. This was not surprising as we had shown in APP23 mice that clearance of Aβ is mediated by microglia which are brain-resident and CAA mainly affects arterioles which are

ensheathed in smooth muscle tissue (Calhoun et al., 1999) to which microglia would have limited access.

We further assessed the potential effect of SUS on amyloid load in the aged APP23 mice. As we had taken total brains for histological analysis, our study precluded a biochemical analysis. By histology, we made the intriguing observation that the cumulative frequency distribution of plaque sizes was shifted toward smaller plaques, but because the percentage plaque area was not reduced this may imply that upon SUS treatment the larger plaques are broken down into smaller plaques as the microglia perform their role of taking up Aβ. We performed stainings for microglia and plaques and found an increased interaction of microglia with plaques in SUS-treated mice, which is especially pronounced for large plaques which combined with our finding of reductions in larger plaques in SUS-treated mice suggests that microglia encircle and degrade large plaques in aged APP23 mice. These data suggests that activated microglia englobe and degrade large plaques based on the increased number of plaque-associated microglia in the SUS-treated group and the significant interaction effect when performing multiple linear regression of microglia number and plaque size which shows a more dramatic increase in the number of microglia for larger plaque sizes in the SUS-treated group compared to the sham condition.

When we visually inspected the methoxy-XO4-labeled plaques, this suggested a significant reduction in the fluorescent signal. Indeed, when a thresholding was performed this indicated a 58% reduction in the signal intensity indicative of a corresponding reduction of fibrillar Aβ in the SUS-treated mice.

In this study we compared SUS-treated mice which have openings of their BBB performed through the application of ultrasound concomitant with microbubble injection, and sham-treated mice which receive microbubbles but ultrasound is not turned on. Sham treated mice do not have openings of their BBB, and we believe are most similar to a placebo in clinical trial. It would have been interesting to test the effect of ultrasound without an injection of microbubbles; however, we aimed to model the treatment groups based on our earlier study that had used younger APP23 mice (Leinenga and Götz, 2015). It should be considered that previously, we had used a protocol with either 5 or 8 weekly treatments, followed by sacrifice (and analysis) either 3 or 1 day after the last sonication, respectively (Leinenga and Götz, 2015), whereas in the current study, we had spaced out the sonications much more, with four treatments over the course of 8 weeks, followed by sacrifice 4 weeks later. Considering this delay and the lower number of treatments in the context of a much more pronounced amyloid pathology our findings suggest that SUS causes reductions in amyloid pathology, even at an advanced stage. The number of plaque-associated microglia was higher in SUS-treated mice even 4 weeks following the last SUS treatment and even in these very old mice. It would be interesting to determine how Aβ that has dissociated from plaques might be cleared from the brain into the periphery. Of note, in a previous study in middle-aged APP23 mice we did not detect increases in plasma concentrations of Aβ immediately following SUS, which we believe to be due to microglia internalizing Aβ and degrading it (Leinenga and Götz, 2015).

It would have been interesting to determine if the reductions in pathology seen were sufficient to lead to increased performance of the mice in behavioral tests, or if too much damage has accumulated in 24 month old mice to see improvements following treatment. We did not perform behavioral tests because APP23 mice have an increased mortality (Ittner et al., 2010) making it impossible to obtain enough 24 month-old APP23 mice for sufficiently powered testing. More importantly, already wild-type mice at this age are significantly impaired in memory tests and we are currently addressing the effect of SUS in aged wild-type mice with memory impairment.

In regards to a possible application of the SUS technique in a clinical setting, one would envisage a treatment at an early MCI (mild cognitive impairment) stage when an amyloid pathology can be detected by either a PET (positron electron tomography) scan or a blood- or cerebrospinal fluid-based biomarker and before a point of no return has been reached. Therapeutic ultrasound targeting AD has already entered clinical safety trials (NCT02986932 and NCT03119961) and it remains to be seen whether this technology will stand up to its promises.

AUTHOR CONTRIBUTIONS

GL and JG: Designed and monitored the experiments; GL: Performed the experiments and data analysis; JG and GL: wrote the manuscript.

FUNDING

We acknowledge support by the Estate of Dr. Clem Jones AO, the Australian Research Council [DP160103812], the National Health and Medical Research Council of Australia [GNT1037746, GNT1127999], and the State Government of Queensland (DSITI, Department of Science, Information Technology and Innovation) to JG.

ACKNOWLEDGMENTS

We thank David Brici and Tishila Palliyaguru for help with histology, Alan Ho for statistical advice, Linda Cumner for monitoring the animal colony, and Rowan Tweedale for critically reading the manuscript.

REFERENCES

Attems, J., Jellinger, K. A., and Lintner, F. (2005). Alzheimer's disease pathology influences severity and topographical distribution of cerebral amyloid angiopathy. *Acta Neuropathol.* 110, 222–231. doi: 10.1007/s00401-005-1064-y

Banerjee, G., Carare, R., Cordonnier, C., Greenberg, S. M., Schneider, J. A., Smith, E. E., et al. (2017). The increasing impact of cerebral amyloid angiopathy: 446 essential new insights 447 for clinical practice. *J. Neurol. Neurosurg. Psychiatr.* 88, 982–994. doi: 10.1136/jnnp-2016-314697

Bien-Ly, N., Boswell, C. A., Jeet, S., Beach, T. G., Hoyte, K., Luk, W., et al. (2015). Lack of widespread BBB disruption in Alzheimer's disease models: focus on therapeutic antibodies. *Neuron* 88, 289–297. doi: 10.1016/j.neuron.2015.09.036

Burgess, A., Nhan, T., Moffatt, C., Klibanov, A. L., and Hynynen, K. (2014). Analysis of focused ultrasound-induced blood-brain barrier permeability in a mouse model of Alzheimer's disease using two-photon microscopy. *J. Control. Release* 192, 243–248. doi: 10.1016/j.jconrel.2014.07.051

Burgold, S., Bittner, T., Dorostkar, M. M., Kieser, D., Fuhrmann, M., Mitteregger, G., et al. (2011). *In vivo* multiphoton imaging reveals gradual growth of newborn amyloid plaques over weeks. *Acta Neuropathol.* 121, 327–335. doi: 10.1007/s00401-010-0787-6

Cacciottolo, M., Morgan, T. E., and Finch, C. E. (2016). Rust on the brain from microbleeds and its relevance to Alzheimer studies: invited commentary on Cacciottolo neurobiology of aging, 2016. *J. Alzheimers. Dis. Parkinsonism* 6:287. doi: 10.4172/2161-0460.1000287

Calhoun, M. E., Burgermeister, P., Phinney, A. L., Stalder, M., Tolnay, M., Wiederhold, K. H., et al. (1999). Neuronal overexpression of mutant amyloid precursor protein results in prominent deposition of cerebrovascular amyloid. *Proc. Natl. Acad. Sci. U.S.A.* 96, 14088–14093. doi: 10.1073/pnas.96.24.14088

Caskey, C. F., Stieger, S. M., Qin, S., Dayton, P. A., and Ferrara, K. W. (2007). Direct observations of ultrasound microbubble contrast agent interaction with the microvessel wall. *J. Acoust. Soc. Am.* 122, 1191–1200. doi: 10.1121/1.2747204

Gilad, R., Lampl, Y., Eilam, A., Boaz, M., and Loyberboim, M. (2012). SPECT-DTPA as a tool for evaluating the blood-brain barrier in post-stroke seizures. *J. Neurol.* 259, 2041–2044. doi: 10.1007/s00415-012-6445-2

Hatch, R. J., Leinenga, G., and Götz, J. (2016). Scanning ultrasound (SUS) causes no changes to neuronal excitability and prevents age-related reductions in hippocampal CA1 dendritic structure in wild-type mice. *PLoS ONE* 11:e0164278. doi: 10.1371/journal.pone.0164278

Ittner, L. M., Ke, Y. D., Delerue, F., Bi, M., Gladbach, A., van Eersel, J., et al. (2010). Dendritic function of tau mediates amyloid-beta toxicity in Alzheimer's disease mouse models. *Cell* 142, 387–397. doi: 10.1016/j.cell.2010.06.036

Jordão, J. F., Ayala-Grosso, C. A., Markham, K., Huang, Y., Chopra, R., McLaurin, J., et al. (2010). Antibodies targeted to the brain with image-guided focused ultrasound reduces amyloid-beta plaque load in the TgCRND8 mouse model of Alzheimer's disease. *PLoS ONE* 5:e10549. doi: 10.1371/journal.pone.0010549

Jordão, J. F., Thévenot, E., Markham-Coultes, K., Scarcelli, T., Weng, Y. Q., Xhima, K., et al. (2013). Amyloid-beta plaque reduction, endogenous antibody delivery and glial activation by brain-targeted, transcranial focused ultrasound. *Exp. Neurol.* 248, 16–29. doi: 10.1016/j.expneurol.2013.05.008

Klunk, W. E., Bacskai, B. J., Mathis, C. A., Kajdasz, S. T., McLellan, M. E., Frosch, M. P., et al. (2002). Imaging abeta plaques in living transgenic mice with multiphoton microscopy and methoxy-X04, a systemically administered Congo red derivative. *J. Neuropathol. Exp. Neurol.* 61, 797–805. doi: 10.1093/jnen/61.9.797

Knowland, D., Arac, A., Sekiguchi, K. J., Hsu, M., Lutz, S. E., Perrino, J., et al. (2014). Stepwise recruitment of transcellular and paracellular pathways underlies blood-brain barrier breakdown in stroke. *Neuron* 82, 603–617. doi: 10.1016/j.neuron.2014.03.003

Konofagou, E. E. (2012). Optimization of the ultrasound-induced blood-brain barrier opening. *Theranostics* 2, 1223–1237. doi: 10.7150/thno.5576

Krueger, M., Härtig, W., Reichenbach, A., Bechmann, I., and Michalski, D. (2013). Blood-brain barrier breakdown after embolic stroke in rats occurs without ultrastructural evidence for disrupting tight junctions. *PLoS ONE* 8:e56419. doi: 10.1371/journal.pone.0056419

Leinenga, G., and Götz, J. (2015). Scanning ultrasound removes amyloid-beta and restores memory in an Alzheimer's disease mouse model. *Sci. Transl. Med.* 7:278ra233. doi: 10.1126/scitranslmed.aaa2512

Leinenga, G., Langton, C., Nisbet, R., and Götz, J. (2016). Ultrasound treatment of neurological diseases - current and emerging applications. *Nat. Rev. Neurol.* 12, 161–174. doi: 10.1038/nrneurol.2016.13

Leinenga, G., Nisbet, R. M., and Götz, J. (2017). Ultrasound as a treatment modality for neurological diseases. *Med. J. Aust.* 206, 470–471. doi: 10.5694/mja16.01013

Levites, Y., Smithson, L. A., Price, R. W., Dakin, R. S., Yuan, B., Sierks, M. R., et al. (2006). Insights into the mechanisms of action of anti-Abeta antibodies in Alzheimer's disease mouse models. *FASEB J.* 20, 2576–2578. doi: 10.1096/fj.06-6463fje

Li, C., and Götz, J. (2017a). Somatodendritic accumulation of Tau in Alzheimer's disease is promoted by Fyn-mediated local protein translation. *EMBO J.* 36, 3120–3138. doi: 10.15252/embj.201797724

Li, C., and Götz, J. (2017b). Tau-based therapies in neurodegeneration – opportunities and challenges. *Nat. Rev. Drug Discov.* 16, 863–883. doi: 10.1038/nrd.2017.155

Lucke-Wold, B. P., Logsdon, A. F., Turner, R. C., Rosen, C. L., and Huber, J. D. (2014). Aging, the metabolic syndrome, and ischemic stroke: redefining the approach for studying the blood-brain barrier in a complex neurological disease. *Adv. Pharmacol.* 71, 411–449. doi: 10.1016/bs.apha.2014.07.001

Marinescu, M., Sun, L., Fatar, M., Neubauer, A., Schad, L., van Ryn, J., et al. (2017). Cerebral microbleeds in murine amyloid angiopathy: natural course and anticoagulant effects. *Stroke* 48, 2248–2254. doi: 10.1161/STROKEAHA.117.017994

McDannold, N., Vykhodtseva, N., and Hynynen, K. (2006). Targeted disruption of the blood-brain barrier with focused ultrasound: association with cavitation activity. *Phys. Med. Biol.* 51, 793–807. doi: 10.1088/0031-9155/51/4/003

Murugesan, N., Demarest, T. G., Madri, J. A., and Pachter, J. S. (2012). Brain regional angiogenic potential at the neurovascular unit during normal aging. *Neurobiol. Aging* 33, 1004.e1–1004.e16. doi: 10.1016/j.neurobiolaging.2011.09.022

Nisbet, R. M., van der Jeugd, A., Leinenga, G., Evans, H. T., Janowicz, P. W., and Götz, J. (2017). Combined effects of scanning ultrasound and a tau-specific single chain antibody in a tau transgenic mouse model. *Brain* 140, 1220–1230. doi: 10.1093/brain/awx052

Pardridge, W. M. (2012). Drug transport across the blood-brain barrier. *J. Cereb. Blood Flow Metab.* 32, 1959–1972. doi: 10.1038/jcbfm.2012.126

Raymond, S. B., Skoch, J., Hynynen, K., and Bacskai, B. J. (2007). Multiphoton imaging of ultrasound/Optison mediated cerebrovascular effects *in vivo*. *J. Cereb. Blood Flow Metab.* 27, 393–403. doi: 10.1038/sj.jcbfm.9600336

Reuter, B., Venus, A., Heiler, P., Schad, L., Ebert, A., Hennerici, M. G., et al. (2016). Development of cerebral microbleeds in the APP23-transgenic mouse model of cerebral amyloid angiopathy-A 9.4 Tesla MRI study. *Front. Aging Neurosci.* 8:170. doi: 10.3389/fnagi.2016.00170

Seip, R., Chin, C. T., Hall, C. S., Raju, B. I., Ghanem, A., and Tiemann, K. (2010). Targeted ultrasound-mediated delivery of nanoparticles: on the development of a new HIFU-based therapy and imaging device. *IEEE Trans. Biomed. Eng.* 57, 61–70. doi: 10.1109/TBME.2009.2028874

Sevigny, J., Chiao, P., Bussière, T., Weinreb, P. H., Williams, L., Maier, M., et al. (2016). The antibody aducanumab reduces Abeta plaques in Alzheimer's disease. *Nature* 537, 50–56. doi: 10.1038/nature19323

Sheikov, N., McDannold, N., Sharma, S., and Hynynen, K. (2008). Effect of focused ultrasound applied with an ultrasound contrast agent on the tight junctional integrity of the brain microvascular endothelium. *Ultrasound Med. Biol.* 34, 1093–1104. doi: 10.1016/j.ultrasmedbio.2007.12.015

Sirsi, S., and Borden, M. (2009). Microbubble compositions, properties and biomedical applications. *Bubble Sci. Eng. Technol.* 1, 3–17. doi: 10.1179/175889709X446507

Sturchler-Pierrat, C., Abramowski, D., Duke, M., Wiederhold, K. H., Mistl, C., Rothacher, S., et al. (1997). Two amyloid precursor protein transgenic mouse models with Alzheimer disease-like pathology. *Proc. Natl. Acad. Sci. U.S.A.* 94, 13287–13292. doi: 10.1073/pnas.94.24.13287

Winkler, D. T., Bondolfi, L., Herzig, M. C., Jann, L., Calhoun, M. E., Wiederhold, K. H., et al. (2001). Spontaneous hemorrhagic stroke in a mouse model of cerebral amyloid angiopathy. *J. Neurosci.* 21, 1619–1627.

Wong, A. D., Ye, M., Levy, A. F., Rothstein, J. D., Bergles, D. E., and Searson, P. C. (2013). The blood-brain barrier: an engineering perspective. *Front. Neuroeng.* 6:7. doi: 10.3389/fneng.2013.00007

Conflict of Interest Statement: The authors declare that the research was conducted in the absence of any commercial or financial relationships that could be construed as a potential conflict of interest.

frontiers in Neuroscience

ORIGINAL RESEARCH
published: 04 January 2018
doi: 10.3389/fnins.2017.00723

Imaging of Neuronal Activity in Awake Mice by Measurements of Flavoprotein Autofluorescence Corrected for Cerebral Blood Flow

Manami Takahashi[1†], Takuya Urushihata[1,2†], Hiroyuki Takuwa[1], Kazumi Sakata[2], Yuhei Takado[1], Eiji Shimizu[3], Tetsuya Suhara[1], Makoto Higuchi[1] and Hiroshi Ito[1,4]*

[1] Department of Functional Brain Imaging Research, National Institutes for Quantum and Radiological Science and Technology, Chiba, Japan, [2] Division of Thermo-Biosystem Relations, United Graduate School of Agricultural Science, Iwate University, Morioka, Japan, [3] Department of Cognitive Behavioral Physiology, Graduate School of Medicine, Cognitive Behavioral Therapy Center Research Center for Child Mental Development, Chiba University, Chiba, Japan, [4] Advanced Clinical Research Center, Fukushima Global Medical Science Center, Fukushima Medical University, Fukushima, Japan

OPEN ACCESS

Edited by:
Gen Sobue,
Nagoya University, Japan

Reviewed by:
M. Heather West Greenlee,
Iowa State University, United States
Keisuke Matsubara,
Research Institute for Brain and Blood Vessels-Akita, Japan

***Correspondence:**
Hiroyuki Takuwa
takuwa.hiroyuki@qst.go.jp

[†] These authors have contributed equally to this work.

Specialty section:
This article was submitted to Neurodegeneration, a section of the journal Frontiers in Neuroscience

Received: 19 October 2017
Accepted: 11 December 2017
Published: 04 January 2018

Citation:
Takahashi M, Urushihata T, Takuwa H, Sakata K, Takado Y, Shimizu E, Suhara T, Higuchi M and Ito H (2018) Imaging of Neuronal Activity in Awake Mice by Measurements of Flavoprotein Autofluorescence Corrected for Cerebral Blood Flow. Front. Neurosci. 11:723. doi: 10.3389/fnins.2017.00723

Green fluorescence imaging (e.g., flavoprotein autofluorescence imaging, FAI) can be used to measure neuronal activity and oxygen metabolism in living brains without expressing fluorescence proteins. It is useful for understanding the mechanism of various brain functions and their abnormalities in age-related brain diseases. However, hemoglobin in cerebral blood vessels absorbs green fluorescence, hampering accurate assessments of brain function in animal models with cerebral blood vessel dysfunctions and subsequent cerebral blood flow (CBF) alterations. In the present study, we developed a new method to correct FAI signals for hemoglobin-dependent green fluorescence reductions by simultaneous measurements of green fluorescence and intrinsic optical signals. Intrinsic optical imaging enabled evaluations of light absorption and scatters by hemoglobin, which could then be applied to corrections of green fluorescence intensities. Using this method, enhanced flavoprotein autofluorescence by sensory stimuli was successfully detected in the brains of awake mice, despite increases of CBF, and hemoglobin interference. Moreover, flavoprotein autofluorescence could be properly quantified in a resting state and during sensory stimulation by a CO_2 inhalation challenge, which modified vascular responses without overtly affecting neuronal activities. The flavoprotein autofluorescence signal data obtained here were in good agreement with the previous findings from a condition with drug-induced blockade of cerebral vasodilation, justifying the current assaying methodology. Application of this technology to studies on animal models of brain diseases with possible changes of CBF, including age-related neurological disorders, would provide better understanding of the mechanisms of neurovascular coupling in pathological circumstances.

Keywords: flavoprotein autofluorescence imaging, intrinsic optical signal imaging, cerebral blood flow, oxygen metabolism, image correction method for green fluorescent imaging

INTRODUCTION

To better understand the mechanisms of brain function during resting and stimulation states, green fluorescence imaging (e.g., GCaMP calcium indicator and flavoprotein autofluorescence imaging, FAI) has been used in many biological and medical studies (Nakai et al., 2001; Shibuki et al., 2003). In particular, using *in vivo* animal models, green fluorescence imaging allows us to estimate acute and longitudinal neural and astroglial activity. Intrinsic optical signal imaging (IOSI) and voltage-sensitive dye imaging (VSDI) are also used to evaluate brain function. However, IOSI measurement mainly indicates cerebral blood volume (CBV) (Martin et al., 2006; Ma et al., 2013), and cannot be used to estimate neural activation directly. VSDI is not sensitive enough to accurately observe activated brain regions in small animals, and it is not suitable for longitudinal measurement because an invasive dye-injection process is required during each experiment.

Flavoprotein autofluorescence imaging (FAI) has recently been utilized to capture the changes in mitochondrial oxidative metabolism in the brain (Husson et al., 2007; L'Heureux et al., 2009; Sirotin and Das, 2010). Since neuronal activity is closely related to aerobic energy metabolism and oxygen consumption (Shibuki, 1989; Malonek and Grinvald, 1996), examining oxygen metabolism in the brain is useful for understanding the mechanism of brain functions.

Hemoglobin in cerebral blood vessels absorbs green fluorescence during brain functional imaging. In particular, the cerebral blood flow (CBF) response to neural activity increases the absorption of flavoprotein autofluorescence with a wavelength of 525 ± 25 nm (Vazquez et al., 2012). The possibility exists that the CBF response could greatly affect the signals of green fluorescence obtained from the neuronal and astroglial activation. However, because the onset of an increase in CBF, evoked by neural activation, is generally later than that in FAI, we can obtain the original FAI signal at an earlier time point after neural activation. Thus, the signal change of FAI would be consistent with changes of neuronal activation in the healthy mouse brain (Shibuki et al., 2003). In addition, CBF response-evoked neural activity generally shows both short- and long-term high reproducibility in healthy mice (Takuwa et al., 2011). Therefore, we hypothesized that the interference by CBF due to fluorescence absorption during green fluorescence imaging can be ignored for the estimation of brain function in normal animals.

On the other hand, previous studies have indicated that animal models of stroke and dementia have an attenuated CBF response to neural activation (Iadecola, 2004; Tajima et al., 2014). As a result of the reduction of absorption of fluorescence in cerebrovascular diseases, there is a possibility that the change in signals of green fluorescence during neural activation will be overestimated. Thus, in the case of animal models of brain disease, it may be difficult to accurately estimate brain function using green fluorescence imaging. For this reason, in the present study, we developed a correction method for green fluorescence imaging to remove the effects of light absorption on the signal during neural activation. The basic concept of the compensation method is as follows. IOSI generally represents the reduction rate of reflection light with the light absorption effects of CBF. Therefore, if we simultaneously measure FAI and IOSI in animal brain, the light absorption effects of CBF on FAI signals may be corrected with IOSI signals. Finally, we successfully demonstrated accurate estimation of brain function regardless of the hemodynamics, indicating that this method is useful for estimating brain function in animal models of stroke and dementia.

MATERIALS AND METHODS

Animal Preparation

A total of 15 male C57BL/6J mice (20–30 g, 7–11 weeks; Japan SLC, Inc., Hamamatsu) were used for simultaneous measurements of FAI and IOSI. These mice were housed with *ad libitum* food and water in their cages at 25°C in a 12-h light/dark cycle. All experiments were performed in accordance with the institutional guidelines on humane care and use of laboratory animals and were approved by the Institutional Committee for Animal Experimentation of National Institutes for Quantum and Radiological Science and Technology.

The animals were anesthetized using a mixture of air, oxygen, and isoflurane (3–5% for induction and 2% for surgery) via a facemask, and a thinned-skull window (5 mm in diameter) was attached over the left somatosensory cortex (including the somatosensory barrel cortex). The previously reported thinned-skull window creation method (Takuwa et al., 2011) was improved and implemented. A midline incision (10 mm) was made to expose the skull over the left somatosensory cortex. The skull (3 by 3 mm centered at 1.8 mm caudal and 2.5 mm lateral from the bregma) was thinned to translucency using a dental drill. The thinned skull was coated with a layer of cyanoacrylate glue and then covered with a cover glass (5 mm in diameter). Dental cement was applied around the edges of the coverslip to stabilize the cover glass to the skull (Shih et al., 2012). A custom metal plate was affixed to the skull through a 7-mm-diameter hole centered over the cranial window. After completion of the surgery, the animals were allowed to recover from anesthesia and housed for at least 1week before initiation of the experiments.

Experimental Protocol

The experimental protocol for measurements using awake mice was reported previously (Takuwa et al., 2011, 2012, 2013a,b). Briefly, the metal plate on the animal's head was screwed to a custom-made stereotactic apparatus. The animal was then placed on a styrofoam ball that was floated using a stream of air. This allowed the animal to exercise freely on the ball while its head was fixed to the apparatus. Under this condition, FAI and IOSI measurements in the somatosensory cortex were performed.

Simultaneous measurements of FAI and IOSI were performed under three separate measurement conditions: (1), sensory stimulation, (2) 5% CO_2 inhalation, (3) sensory stimulation 10 s after CO_2 inhalation. To validate our correction method we compared the corrected FAI signals measured under different stimulation and CO_2 inhalation condition. Although the increase in CBF under hypercapnia greatly reduces the FAI signal, it is

expected that the corrected FAI time activity curve will be the same with or without hypercapnia because the level of nerved activity does not change (Matsuura et al., 2000).

Simultaneous Measurement of FAI and IOSI

Takuwa et al. (2014) previously described a custom setup for the simultaneous measurement of FAI and IOSI (**Figure 1**). FAI and IOSI were simultaneously performed using two CCD cameras (MiCAM02, Brainvision, Tokyo, Japan) (**Figure 1A**). Temporal resolution and spatial resolution were 10 Hz for 25 s (250 frames/trial) and 192 × 128 pixels (each pixel size was 15 × 15 μm). A total of 25 trials were successively performed with an inter-trial interval of 30 s, and the image was averaged over the trials to improve the signal-to-noise ratio. The exposed cortical surface in the cranial window was simultaneously illuminated with light from two halogen lamps passing through two types of band pass filters (wavelength: 470 and 570 nm). For IOSI measurements, a reduction rate of reflection at 570 nm, which is an isosbestic wavelength of hemoglobin, can allow the measurement of total hemoglobin and is closely correlated to CBV if hematocrit remains constant and proportional to CBF (Martin et al., 2006; Zhao et al., 2009; Ma et al., 2013). In FAI measurements, the autofluorescence emitted from brain cells was collected with an objective lens. Autofluorescence, filtered by a longpass filter (>490 nm) and reflected by a dichroic mirror (<560 nm), was introduced to a MiCAM02 CCD camera through a band-pass filter (535 nm) (**Figure 1**). Since the flavoprotein fluorescence is at 535 nm, which is also an isosbestic wavelength of hemoglobin, the measured FAI is mainly the sum of autofluorescence and the absorption of light with hemoglobin (**Figure 2**).

Compensational Method for FAI using IOSI Data

An uncorrected FAI signal contains not only the flavoprotein autofluorescence but also the absorption and scattering effects with CBF. The purpose of this method was to remove these effects of CBF on FAI and accurately estimate the original flavoprotein autofluorescence caused by neuronal activity (**Figure 2**). At first, a scatter plot was created from the values of FAI and IOSI signals at each time point during the resting state; we calculated an approximate straight line, confidence interval and prediction interval from a scatter plot using the Curve Fitting Toolbox of MatLab (MathWorks, MA, USA) (**Figures 3A,B**).

The corrected FAI is expressed as follows:

Corrected FAI = FAI − α × IOSI, where α is the slope of the approximate line equation, and FAI and IOSI data are simultaneously obtained during resting state. We calculated the corrected FAI in all frames (250) and pixels (192 × 128) for each experiment.

Sensory Stimulation and Hypercapnia

In sensory stimulation experiments, the hemodynamic response to neuronal activation was induced by sensory stimulation. An air puff was delivered to all of the right whiskers of the mice at a pressure of ∼15 psi using a compressed-air bottle. Rectangular pulse stimulation (50-ms pulse width and 100-ms onset-to-onset interval, i.e., 10 Hz frequency) generated with a Master-8 (A.M.P.I., Jerusalem, Israel) was induced for a 2-s duration (Takuwa et al., 2011).

In hypercapnia experiments, the hemodynamic response to hypercapnia was induced by 5% CO_2 inhalation. A hypercapnic gas mixture of 5% CO_2, 21% O_2, and residual N_2 was inhaled by awake-behaving mice via a facemask (300 ml/min). At all

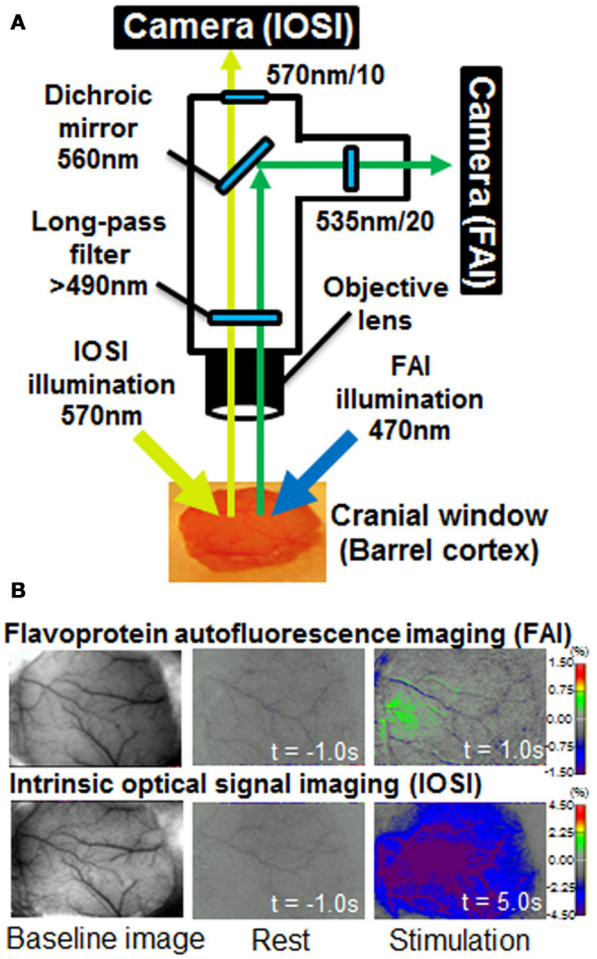

FIGURE 1 | (A) Diagram of the experimental apparatus used for simultaneous flavoprotein autofluorescence imaging (FAI) and intrinsic optical signal imaging (IOSI). The exposed cortical surface in the cranial window was simultaneously illuminated with light from two halogen sources passing through two types of band pass filter (wavelength: 470 and 570 nm). For IOSI measurements, reflected light from the cortical surface was reflected to a camera via a 560-nm dichroic mirror. A 570 ± 10 nm filter was placed in front of the camera. For FAI measurements, autofluorescence, filtered by a longpass filter (>490 nm) and reflected by a dichroic mirror (<560 nm), was introduced to a charged couple device (CCD) camera through a band-pass filter (535 nm). FAI and IOSI signals were simultaneously captured using two MiCAM02 CCD cameras. **(B)** Typical images of FAI and IOSI measurements. Each image shows baseline, rest ($t = -1$ s) and stimulation ($t = 1$ or 5 s) from the left. The rest and stimulation images indicate the rate of change relative to the mean value at resting state (10 s).

times except during the CO_2 inhalation, the mice inhaled room air (300 ml/min). CO_2 gas was given to the mice using the same time schedule as in the sensory stimulation (experiment 1), i.e., 10-s pre-inhalation, 2-s CO_2 inhalation, and 30-s post-inhalation periods, using the Master-8 (**Figure 1**). CO_2 inhalation was repeated 25 times at 60-s intervals after post-stimulus periods, and all trials of the FAI and IOSI signals were averaged offline.

Data Analysis

The magnitudes of increases in the measurements of FAI and IOSI during whisker stimulation were calculated as the mean percentage change from baseline over a 10-s resting state period. A circle with a diameter of 1 mm around the peak of the signal change was chosen as the region of interest (ROI), and the time–response curves of FAI and IOSI were recorded from the mean in the ROI. Statistical analyses were performed with a paired *t*-test and Pearson product-moment correlation coefficient.

RESULTS

Simultaneous Measurements of FAI and IOSI

Figure 1 shows a schematic diagram of the experimental apparatus for simultaneous FAI and IOSI, and representative data from before (resting condition) and after whisker stimulation. The increase in FAI was observed within 1 s after whisker stimulation. The reduction of a signal in IOSI appeared 5 s after the stimulation, a result of the increasing light absorption associated with the CBF response to neural activation. The activated regions of IOSI (5 s) and FAI (1 s) were observed in almost the same brain area, although the size of the active region in IOSI was larger than that in FAI.

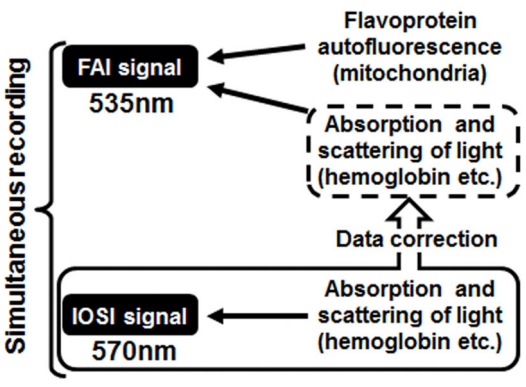

FIGURE 2 | Schematic diagram of the correction method. The absorption and scattering effects of cerebral blood flow contained in the flavoprotein autofluorescence imaging (FAI) signal were removed using a converted value calculated from intrinsic optical signal imaging, which was measured at the same time as FAI.

Comparison between Signals of FAI and IOSI during Resting State

The waveforms of FAI and IOSI during resting state are shown in **Figure 3A**. To evaluate the relationship between these parameters, we investigated the correlation between FAI and IOSI during resting state. A linear relationship between the percentage changes in FAI and IOSI during resting state was revealed (**Figure 3B**). The FAI signal showed a positive correlation with the IOSI signal during resting state (**Table 1**).

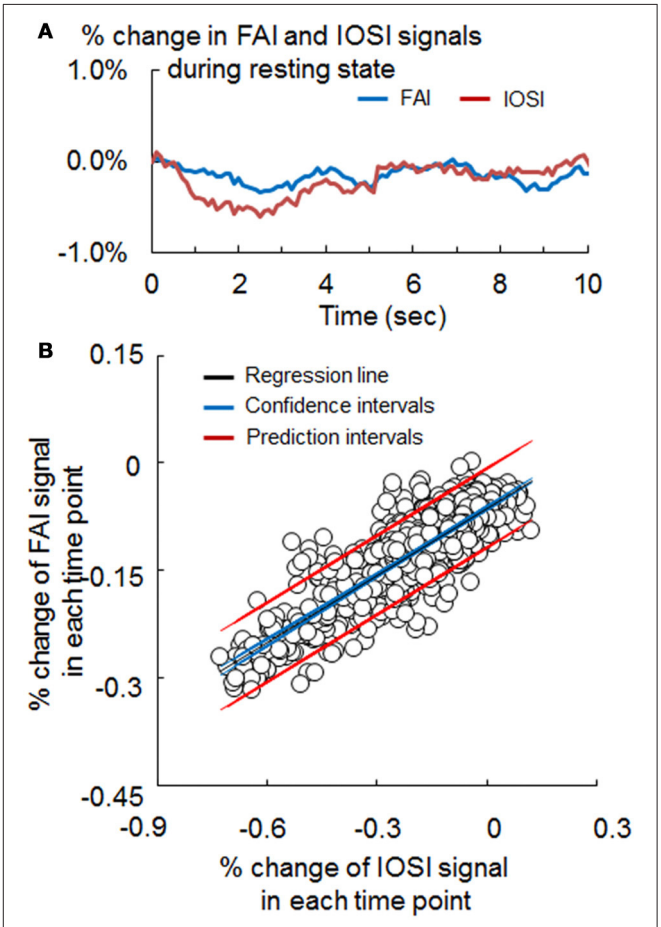

FIGURE 3 | (A) Signal change of flavoprotein autofluorescence imaging (FAI; blue) and intrinsic optical signal imaging (IOSI; red) in the resting state, obtained by simultaneous measurement. **(B)** Scatter plot of the FAI and IOSI signals during resting state. The coefficient (α) used for the correction method was obtained from the slope of the approximation straight line (black). Confidence intervals (blue) and prediction intervals (red) are also drawn on the graph.

TABLE 1 | Relationship between FAI and IOSI signals in each pixel at resting state.

Animal no.	Regression line	Correlation coefficient
Animal 1	$y = 0.60x + 0.36$	$r = 0.82$
Animal 2	$y = 0.45x + 0.51$	$r = 0.83$
Animal 3	$y = 0.91x + 0.29$	$r = 0.78$
Animal 4	$y = 0.76x + 0.35$	$r = 0.74$

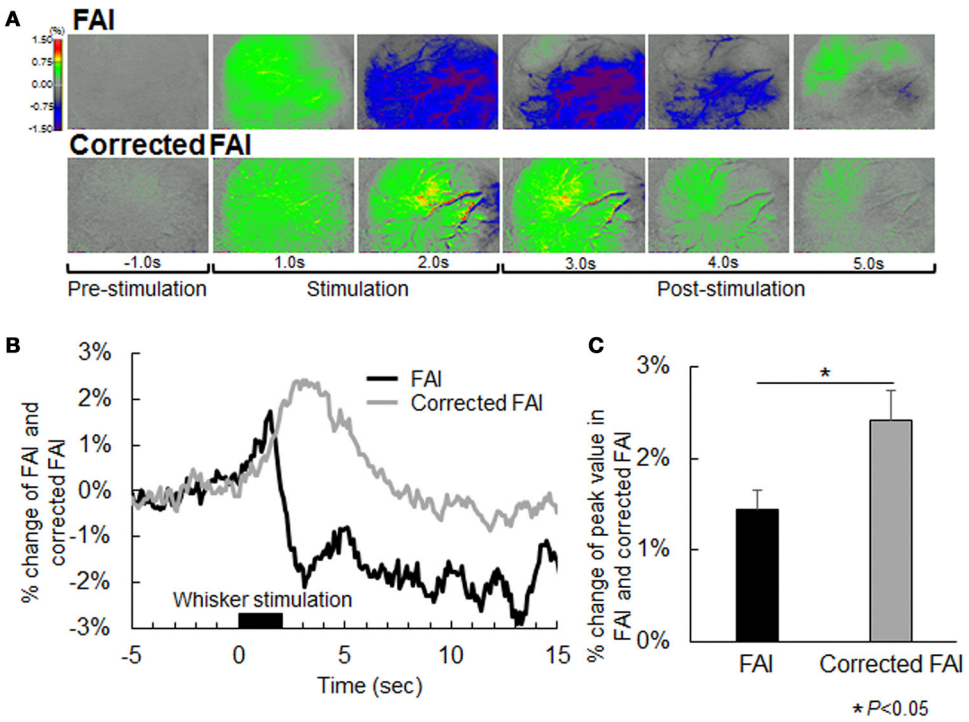

FIGURE 4 | (A) Flavoprotein autofluorescence imaging (FAI; top) and corrected FAI images (bottom) from one representative animal. Nerves of each animal were activated by air stimulation to the whiskers. Each image is indicated as pre-stimulation (−1.0 s), stimulation period (1.0 s and 2.0 s), and post-stimulation (3.0, 4.0, and 5.0 s) from the left. The decrease in signal observed by uncorrected FAI was not confirmed by corrected FAI. **(B)** Averaged time-response curves of FAI and corrected FAI from all animals. Black bar indicates duration of whisker stimulation. **(C)** Average of peak value of signal change rate of FAI (black) and corrected FAI (gray) from all animals. Peak value of the corrected FAI signal was significantly higher than that of FAI ($P < 0.05$).

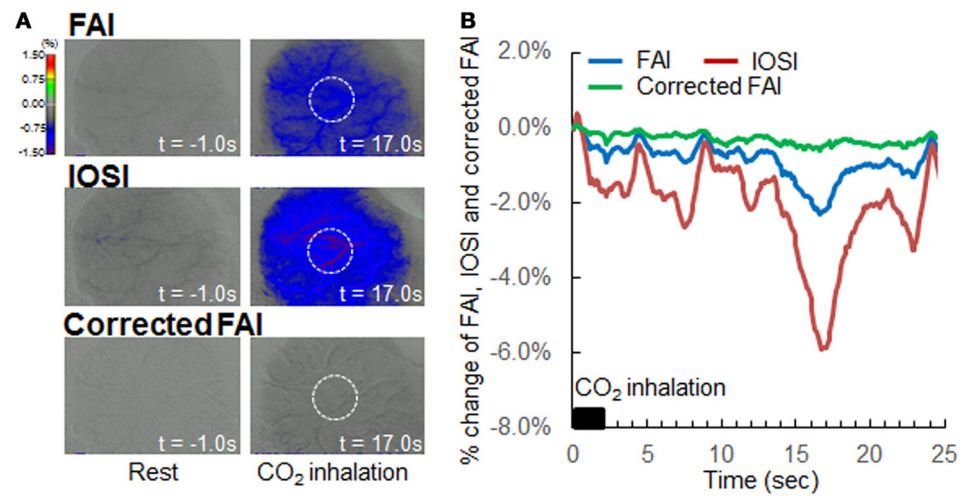

FIGURE 5 | Verification of correction method by hypercapnia during resting state. **(A)** Flavoprotein autofluorescence imaging (FAI; top), intrinsic optical signal imaging (IOSI; middle), corrected FAI (bottom) images from one representative animal. Resting state (left) and hypercapnia state as a result of 5% CO_2 inhalation (right) are indicated. Circles drawn with white dotted lines indicate regions of interest. **(B)** Averaged time-response curves of FAI (blue), IOSI (red), and corrected FAI (green) signals from all animals. Black bar indicates duration of CO_2 inhalation. Corrected FAI showed no signal reduction by hypercapnia, and the signal plateaued for the duration of the experiment.

Using a scatter plot of FAI and IOSI data, corrected FAI was calculated.

Comparison between FAI and Corrected FAI during Neural Activation

The representative FAI and corrected FAI before (resting state) and after sensory stimulation are shown in **Figure 4A**. Although the area of increase in FAI appeared 1 s after stimulation, the active area in FAI disappeared, declining from the baseline level 2 s after stimulation (**Figure 4A**). On the other hand, in the case of corrected FAI, the area of increase in FAI was maintained during sensory stimulation (**Figure 4A**). The time–response curve of FAI exhibited an initial peak at an earlier time point than that of corrected FAI (**Figure 4B**). The peak value of FAI was significantly lower than that of corrected FAI (**Figure 4C**).

Validation of Our Correction Method (Hypercapnia during Resting State)

In previous reports, hypercapnia condition by 5% CO_2 inhalation resulted in an increase in CBF but did not change neural activation (Matsuura et al., 2000). If there are no effects of light absorption with CBF on FAI, the time-response curve of FAI will show a plateau during and after hypercapnia condition. However, light absorption with CBF decreased the FAI signal in this study. Using our correction method, the FAI signal plateaued for the entire measurement period (**Figure 5**).

Validation of Our Correction Method (Hypercapnia during Neural Activation)

In this experiment, mice were subjected to both 5% CO_2 inhalation and whisker stimulation to validate our correlation method. As presented in **Figure 6A**, an increase in CBF with hypercapnia suppressed the increase in FAI during neural activation, and the active area of FAI after stimulation disappeared. On the other hand, using our method, the time response curve of corrected FAI with hypercapnia was consistent with that of corrected FAI without hypercapnia (**Figure 6B**). There were no significant differences in the change of peak value between the corrected FAI with and without hypercapnia (**Figure 6C**).

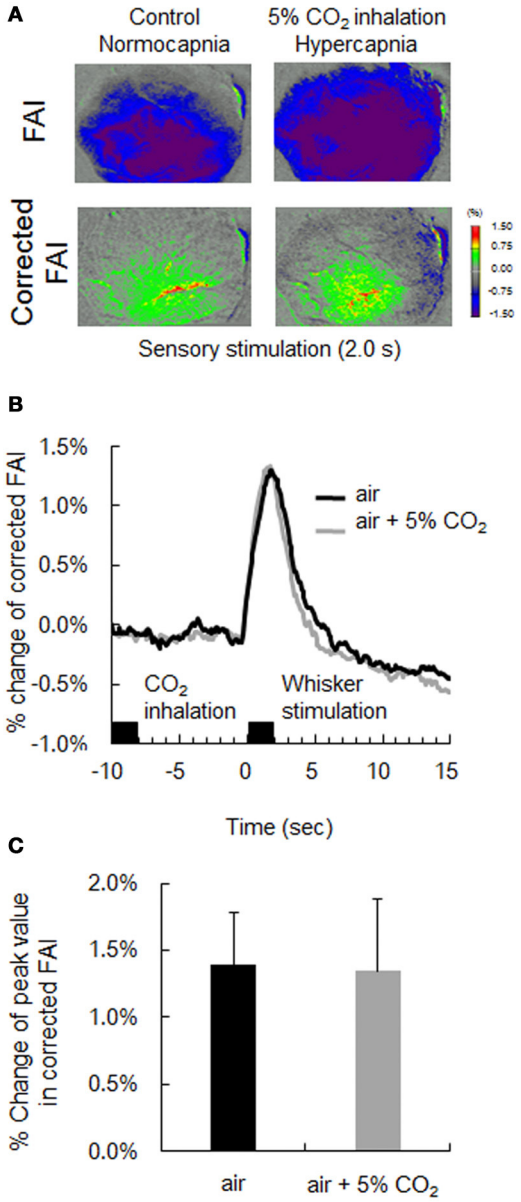

FIGURE 6 | Verification of correction method by hypercapnia during neural activation. **(A)** Flavoprotein autofluorescence imaging (FAI; top) and corrected FAI (bottom) images during sensory stimulation (2.0 s) from one representative animal. Animals were given only sensory stimulation (left) or both sensory stimulation and CO_2 inhalation (right). **(B)** Averaged time-response curves of corrected FAI signal from all animals. Black bar indicates duration of CO_2 inhalation and whisker stimulation. **(C)** Average peak value of signal change rate of only air puff (black) and both air puff and 5% CO_2 inhalation (gray) of all animals. There were no significant differences.

DISCUSSION

We newly developed a correction method for FAI in an animal study. Our correction method could cancel out the light absorption effects on change in FAI with an increase in CBF during neural activation. To the best of our knowledge, this is the first method to obtained original time activity curve of FAI during neural activity under normal physiological condition in awake mouse brain. Increase in CBF during neural activity is caused by the neurovascular unit in the brain (Attwell et al., 2010). Thus, cerebrovascular dysfunction leads directly to a decrease in light absorption by CBF, resulting in an inaccurate assessment of brain function by green fluorescence imaging. The correction method developed in the present study provides a way of solving the technical problem of the attenuating effects of CBF on green fluorescence imaging during neural activation.

Our results, as presented in **Figure 1B**, showed that signal changes of FAI and IOSI were observed in almost the same brain region. As a result, the peak amplitude of uncorrected FAI was smaller than that of corrected FAI during neural activation,

suggesting that the amount of oxygen metabolism or neural activation is underestimated in uncorrected FAI. This result indicated that, in the case of healthy animals, our correction method is necessary for accurate measurement of brain function.

Comparison of neural function before and after the onset of disease is important for more clearly understanding the mechanism of brain disorders in animal models. For example, we previously showed that the CBF response to sensory stimulation was attenuated 1 week after chronic hypoperfusion caused by unilateral common carotid artery occlusion (CCAO) (Nishino et al., 2016). Our future studies will focus on the measurement of neural activation in animal models of stroke and dementia. However, as a result of a decrease in CBF response after CCAO, uncorrected FAI will overestimate the neural activation after occlusion. We hypothesized that the same technical problem will exist in green fluorescence imaging in several animal models of brain disease. Vazquez et al. (2012) previously demonstrated that inhibition of additional cerebral vasodilation from the baseline level using drug administration (vasodilatory agent sodium nitroprusside) allows us to obtain the original time activity curve of FAI during neural activity. The previous study indicated that increase in FAI signal continuously maintained within sensory stimulation after inhibition of CBF response with drug administration. The time activity curve of FAI obtained with our correction method in this study was in good agreement with the results of drug administration by Vazquez et al. (2012). On the other hand, a condition without drug administration is preferable for accurate measurement of brain function. Our results indicated that, although the increase in CBF under hypercapnia greatly attenuated the signal of FAI during both resting state and sensory stimulation, the time activity curve of corrected FAI was the same with and without hypercapnia. These results indicated that, if animal models of cerebrovascular disease are used, our correction method is essential for the accurate measurement of brain function using green fluorescence imaging.

Although light scattering and absorption mainly contributed to the reduction of FAI, their causes are still unclear. The structure of the brain is too complex to allow a complete identification of all elements causing a change in fluorescence with the current technology. One of the important advantages of our method is that we corrected FAI using the actual measurement value (IOSI) as an index of light scattering and absorption. Therefore, although we could not identify all elements of light scattering and absorption, we could calculate the corrected FAI. In addition, there is no need to consider the abundance ratio of oxygenated and reduced-type hemoglobin in this correction method, because both wavelengths of FAI and IOSI are isosbestic points of hemoglobin. However, spontaneous neuronal activation during the resting state may cause fluctuations in the FAI signal.

It is well known that two-photon imaging using a GCaMP calcium indicator can detect neural activation at a single-cell level. Unfortunately, our correction method is not suitable for high spatial-resolution microscopy because two-photon microscopy separates and detects nerve cells and blood vessels independently. However, the field of view in two-photon imaging is too small to compare the activities of multiple brain regions. To perform wide-field functional *in vivo* imaging, single-photon imaging with a charge-coupled device (CCD) or a complementary metal-oxide semiconductor camera is still being used in animal studies (Vanni and Murphy, 2014). We think that our correction method will be useful for not only FAI, but also wide-field functional *in vivo* imaging using a fluorescence microscope with a CCD camera and a GCaMP indicator.

In conclusion, we developed a new correction method for green fluorescence imaging using the simultaneous measurement system of FAI and IOSI. Our correction method can remove the attenuation effects of CBF on FAI during neural activation. We conclude that the application of our correction method to brain disease-model animals could provide a better understanding of the mechanisms of neurovascular coupling and age-related brain disorders including stroke and dementia.

AUTHOR CONTRIBUTIONS

HT and HI designed the research; MT, TU, and HT performed the research; MT, TU, KS, and HT analyzed the data; YT, ES, MH, and TS helped with the data interpretation and discussion; MT, TU, HT, MH, and HI wrote the paper.

ACKNOWLEDGMENTS

The assistance of members of the National Institute of Radiological Sciences in performing all the experiments is gratefully acknowledged. This work was partially supported by a Grant-in-Aid for Scientific Research to HT from the Japan Society for the Promotion of Science.

REFERENCES

Attwell, D., Buchan, A. M., Charpak, S., Lauritzen, M., Macvicar, B. A., and Newman, E. A. (2010). Glial and neuronal control of brain blood flow. *Nature* 468, 232–243. doi: 10.1038/nature09613

Husson, T. R., Mallik, A. K., Zhang, J. X., and Issa, N. P. (2007). Functional imaging of primary visual cortex using flavoprotein autofluorescence. *J. Neurosci.* 27, 8665–8675. doi: 10.1523/JNEUROSCI.2156-07.2007

Iadecola, C. (2004). Neurovascular regulation in the normal brain and in Alzheimer's disease. *Nat. Rev. Neurosci.* 5, 347–360. doi: 10.1038/nrn1387

L'Heureux, B., Gurden, H., and Pain, F. (2009). Autofluorescence imaging of NADH and flavoproteins in the rat brain: insights from monte carlo simulations. *Opt. Express* 17, 9477–9490. doi: 10.1364/OE.17.009477

Ma, H., Zhao, M., and Schwartz, T. H. (2013). Dynamic neurovascular coupling and uncoupling during ictal onset, propagation, and termination revealed by simultaneous *in vivo* optical imaging of neural activity and local blood volume. *Cereb. Cortex* 23, 885–899. doi: 10.1093/cercor/bhs079

Malonek, D., and Grinvald, A. (1996). Interactions between electrical activity and cortical microcirculation revealed by imaging spectroscopy: implications for functional brain mapping. *Science* 272, 551–554. doi: 10.1126/science.272.5261.551

Martin, C., Martindale, J., Berwick, J., and Mayhew, J. (2006). Investigating neural-hemodynamic coupling and the hemodynamic response function in the awake rat. *Neuroimage* 32, 33–48. doi: 10.1016/j.neuroimage.2006.02.021

Matsuura, T., Fujita, H., Kashikura, K., and Kanno, I. (2000). Evoked local cerebral blood flow induced by somatosensory stimulation is proportional to the baseline flow. *Neurosci. Res.* 38, 341–348. doi: 10.1016/S0168-0102(00)00175-9

Nakai, J., Ohkura, M., and Imoto, K. (2001). A high signal-to-noise Ca2+ probe composed of a single green fluorescent protein. *Nat. Biotechnol.* 19, 137–141. doi: 10.1038/84397

Nishino, A., Tajima, Y., Takuwa, H., Masamoto, K., Taniguchi, J., Wakizaka, H., et al. (2016). Long-term effects of cerebral hypoperfusion on neural density and function using misery perfusion animal model. *Sci. Rep.* 6:25072. doi: 10.1038/srep25072

Shibuki, K. (1989). Calcium-dependent and ouabain-resistant oxygen consumption in the rat neurohypophysis. *Brain Res.* 487, 96–104. doi: 10.1016/0006-8993(89)90944-X

Shibuki, K., Hishida, R., Murakami, H., Kudoh, M., Kawaguchi, T., Watanabe, M., et al. (2003). Dynamic imaging of somatosensory cortical activity in the rat visualized by flavoprotein autofluorescence. *J. Physiol.* 15, 919–927. doi: 10.1113/jphysiol.2003.040709

Shih, A. Y., Mateo, C., Drew, P. J., Tsai, P. S., and Kleinfeld, D. (2012). A polished and reinforced thinned-skull window for long-term imaging of the mouse brain. *J. Vis. Exp.* 61:3742. doi: 10.3791/3742

Sirotin, Y. B., and Das, A. (2010). Spatial relationship between flavoprotein fluorescence and the hemodynamic response in the primary visual cortex of alert macaque monkeys. *Front. Neuroenergetics* 2:6. doi: 10.3389/fnene.2010.00006

Tajima, Y., Takuwa, H., Kokuryo, D., Kawaguchi, H., Seki, C., Masamoto, K., et al. (2014). Changes in cortical microvasculature during misery perfusion measured by two-photon laser scanning microscopy. *J. Cereb. Blood Flow Metab.* 34, 1363–1372. doi: 10.1038/jcbfm.2014.91

Takuwa, H., Autio, J., Nakayama, H., Matsuura, T., Obata, T., Okada, E., et al. (2011). Reproducibility and variance of a stimulation-induced hemodynamic response in barrel cortex of awake behaving mice. *Brain Res.* 1369, 103–111. doi: 10.1016/j.brainres.2010.11.007

Takuwa, H., Masamoto, K., Yamazaki, K., Kawaguchi, H., Ikoma, Y., Tajima, Y., et al. (2013a). Long-term adaptation of cerebral hemodynamic response to somatosensory stimulation during chronic hypoxia in awake mice. *J. Cereb. Blood Flow Metab.* 33, 774–779. doi: 10.1038/jcbfm.2013.16

Takuwa, H., Matsuura, T., Nishino, A., Sakata, K., Tajima, Y., and Ito, H. (2014). Development of new optical imaging systems of oxygen metabolism and simultaneous measurement in hemodynamic changes using awake mice. *J. Neurosci. Methods* 237, 9–15. doi: 10.1016/j.jneumeth.2014.08.022

Takuwa, H., Matsuura, T., Obata, T., Kawaguchi, H., Kanno, I., and Ito, H. (2012). Hemodynamic changes during somatosensory stimulation in awake and isoflurane-anesthetized mice measured by laser-doppler flowmetry. *Brain Res.* 1472, 107–112. doi: 10.1016/j.brainres.2012.06.049

Takuwa, H., Tajima, Y., Kokuryo, D., Matsuura, T., Kawaguchi, H., Masamoto, K., et al. (2013b). Hemodynamic changes during neural deactivation in awake mice: a measurement by laser-doppler flowmetry in crossed cerebellar diaschisis. *Brain Res.* 6, 350–355. doi: 10.1016/j.brainres.2013.09.023

Vanni, M. P., and Murphy, T. H. (2014). Mesoscale transcranial spontaneous activity mapping in GCaMP3 transgenic mice reveals extensive reciprocal connections between areas of somatomotor cortex. *J. Neurosci.* 34, 15931–15946. doi: 10.1523/JNEUROSCI.1818-14.2014

Vazquez, A. L., Fukuda, M., and Kim, S. G. (2012). Evolution of the dynamic changes in functional cerebral oxidative metabolism from tissue mitochondria to blood oxygen. *J. Cereb. Blood Flow Metab.* 32, 745–758. doi: 10.1038/jcbfm.2011.198

Zhao, M., Ma, H., Suh, M., and Schwartz, T. H. (2009). Spatiotemporal dynamics of perfusion and oximetry during ictal discharges in the rat neocortex. *J. Neurosci.* 29, 2814–2823. doi: 10.1523/JNEUROSCI.4667-08.2009

Conflict of Interest Statement: The authors declare that the research was conducted in the absence of any commercial or financial relationships that could be construed as a potential conflict of interest.

frontiers in Neuroscience

REVIEW
published: 12 December 2017
doi: 10.3389/fnins.2017.00680

Alzheimer's Disease: The Role of Microglia in Brain Homeostasis and Proteopathy

Kevin A. Clayton[1], *Alicia A. Van Enoo*[1] *and Tsuneya Ikezu*[1,2*]

[1] Department of Pharmacology and Experimental Therapeutics, Medical School, Boston University, Boston, MA, United States, [2] Department of Neurology, Medical School, Boston University, Boston, MA, United States

Brain aging is central to late-onset Alzheimer's disease (LOAD), although the mechanisms by which it occurs at protein or cellular levels are not fully understood. Alzheimer's disease is the most common proteopathy and is characterized by two unique pathologies: senile plaques and neurofibrillary tangles, the former accumulating earlier than the latter. Aging alters the proteostasis of amyloid-β peptides and microtubule-associated protein tau, which are regulated in both autonomous and non-autonomous manners. Microglia, the resident phagocytes of the central nervous system, play a major role in the non-autonomous clearance of protein aggregates. Their function is significantly altered by aging and neurodegeneration. This is genetically supported by the association of microglia-specific genes, *TREM2* and *CD33,* and late onset Alzheimer's disease. Here, we propose that the functional characterization of microglia, and their contribution to proteopathy, will lead to a new therapeutic direction in Alzheimer's disease research.

Keywords: Alzheimer's disease, microglia, neurodegeneration, amyloid-beta peptide, tau protein, neuroinflammation, proteopathy

OPEN ACCESS

Edited by:
Naruhiko Sahara,
National Institute of Radiological Sciences (NIRS), Japan

Reviewed by:
Takahisa Kanekiyo,
Mayo Clinic Florida, United States
Aurel Popa-Wagner,
University of Rostock, Germany

***Correspondence:**
Tsuneya Ikezu
tikezu@bu.edu

Specialty section:
This article was submitted to Neurodegeneration, a section of the journal Frontiers in Neuroscience

Received: *01 October 2017*
Accepted: *21 November 2017*
Published: *12 December 2017*

Citation:
Clayton KA, Van Enoo AA and Ikezu T (2017) Alzheimer's Disease: The Role of Microglia in Brain Homeostasis and Proteopathy. Front. Neurosci. 11:680. doi: 10.3389/fnins.2017.00680

INTRODUCTION

Aging results in a loss of proteostasis that is characteristic of many neurodegenerative disorders. During aging, the mechanisms responsible for protein synthesis, post-translational modifications, and clearance, cumulatively known as "proteostasis," become dysregulated in the central nervous system (CNS). Impairments in proteostasis result in the accumulation of misfolded proteins as intracellular aggregates, such as neurofibrillary tangles and Lewy bodies, or extracellular plaques, such as senile and prion plaques, which ultimately lead to conditions termed "proteopathies." Alzheimer's disease (AD) is diagnosed with the development of two unique pathologies, senile plaques and neurofibrillary tangles. A comprehensive understanding of the brain cells responsible for the clearance of protein aggregation due to dysfunction is critical to fully elucidate the etiology of AD. This mechanism is largely understood to be a cell autonomous process, namely executed by neurons. However, non-autonomous processes that may also be involved have recently become the subject of extensive investigation. One representative cell type controlling brain proteostasis is microglia. Interestingly, their functions are largely affected by aging. This is genetically supported by the significant genome-wide association of microglia-specific *TREM2* gene with LOAD (Guerreiro et al., 2013; Jonsson et al., 2013). Microglia are the resident phagocytes of the CNS and are implicated in the pathogenesis of many neurocognitive disorders, including neurodevelopmental and neurodegenerative diseases. They are implicated in the phagocytosis and degradation of pathological protein aggregates. Numerous studies have been published recently

depicting the changes that cause microglia to become dysfunctional during aging and disease. Once microglia become dysfunctional, they further contribute to CNS destabilization in response to protein aggregates, which ultimately leads to brain degeneration. One prominent aspect of microglial dysfunction is their role in chronic neuroinflammation, a phenomenon in which immune cells recognize and pervade the ailing tissue causing damage through both antigen-specific and non-specific mechanisms. Several groups have recently provided a comprehensive characterization of microglial phenotype in order to elucidate the mechanisms by which microglial dysfunction disrupts the CNS microenvironment (Matcovitch-Natan et al., 2016; Keren-Shaul et al., 2017; Krasemann et al., 2017).

These new concepts considering the causal relationships between microglial dysfunction, neuroinflammation, and protein aging, introduce the question of how novel therapies may halt or reverse the contribution of microglia to the spread of proteopathy and neurodegeneration. Here, we summarize clinical and preclinical studies aimed to prevent protein aggregation or restore homeostatic microglial function. Furthermore, we overview the physiological function of microglia, their changes in response to aging, and their specific neurodegenerative phenotype leading to proteopathy in AD.

Aging and Proteopathies

Most neurodegenerative disorders are pathologically characterized as proteopathies (Walker and LeVine, 2000). Aging can impact multiple aspects of proteostasis: production, folding, posttranslational modification, and clearance in several pathways, including secretion and autophagosomal, endolysosomal, and proteasomal degradation (Kaushik and Cuervo, 2015), all of which are demonstrated to affect protein aggregation when impaired. Aggregated proteins, such as amyloid-beta peptides (Aβ), are inherently cytotoxic *in vitro*, causing stress and stimulating synaptic loss, mitochondrial dysfunction, and eventually apoptosis in neurons (Sakono and Zako, 2010). We will mainly describe the metabolism of Aβ and tau in this review.

The production of Aβ from amyloid precursor protein (APP) is the most well-studied component of AD development, especially in early-onset Alzheimer's disease (EOAD) (Rovelet-Lecrux et al., 2006; Sleegers et al., 2006; McNaughton et al., 2012). In addition to the well-known mutations proximal to the α, β, and γ-processing of APP, several mutations in the promoter region of *APP* have been reported and contribute to enhanced *APP* gene expression (Athan et al., 2002; Theuns et al., 2006; Hooli et al., 2012; Rodgers et al., 2012). However, the majority of sporadic cases do not show increased expression of APP by aging. Rather, there is a reduction in the amount of Aβ in the cerebrospinal fluid (CSF), suggesting its absorption into amyloid plaques, rather than export to the periphery. Researchers have increasingly argued that sporadic or late-onset AD is more likely caused by a reduction in clearance of Aβ than by its overproduction (Mawuenyega et al., 2010).

There is also a possibility for an age-related shift in APP processing toward the amyloidogenic rather than non-amyloidogenic pathway. This results in the production of pathogenic Aβ, as opposed to the non-pathogenic p3 peptide. One study reported that age did not have an effect on γ-secretase production of Aβ42 (Dewachter et al., 2000). However, the expression of beta-site APP converting enzyme 1 (BACE1), the enzyme designated as β-secretase, is elevated in the AD brain (Li et al., 2004; Zhao et al., 2007). Furthermore, primary cortical neurons were shown to up-regulate *BACE1* expression in response to Aβ42 exposure (Mamada et al., 2015). This suggests that Aβ42 production may be self-perpetuating via up-regulation of BACE1 expression in neurons. Given that BACE1 acts on APP primarily in endosomal compartments, age-related increases in early endosome volume could result in increased BACE1 processing of APP (Cataldo et al., 2000). Another possibility is the reduced activity or expression of α-secretase, ADAM10, a component of the non-amyloidogenic pathway. Reduced non-amyloidogenic processing of APP was reported to occur as a result of cellular aging (Kern et al., 2006), although overall activity and expression was increased in cognitively normal subjects (Schuck et al., 2016). This suggests that an age-dependent reduction of ADAM10 function is specific to AD subjects.

Reduced clearance of Aβ has emerged as the central mechanism of amyloid plaque formation in AD. Aβ is thought to be cleared via interstitial fluid (ISF) drainage into the blood vessels, and brought across the blood brain barrier (BBB) into the peripheral bloodstream. There are mutations in APP reported in AD cases that appear to reduce transport of Aβ from the CSF into the blood (Monro et al., 2002). Receptor for advanced glycation end products (RAGE) is proposed to be expressed in the BBB and responsible for shuttling Aβ from the bloodstream into the brain, while LRP1 is responsible for efflux of Aβ42 out of the brain (Deane et al., 2009). However, LRP1 expression in the BBB is reduced in rodents, primates, and humans (Shibata et al., 2000; Deane et al., 2004; Zerbinatti et al., 2004; Donahue et al., 2006). For this reason, RAGE antagonists, which have already been proposed to have effective anti-inflammatory properties, are being further explored for clinical development (see **Table 1**). In addition to the transport of Aβ out of the ISF to the blood, the CNS is equipped with several other clearance mechanisms, principally mediated via Aβ degrading enzymes. These include enzymes derived from the M13 zinc-binding membrane metalloendopeptidase (such as insulin degrading enzyme), Type II integral membrane bound glycoproteins (NEP-2, ECE-1), membrane-bound zinc metalloproteinase (such as matrix metalloproteinase 2 and 9), thiol-metalloendopeptidase, matrix metalloproteinase, and members of the serine and cysteine protease families (see Miners et al., 2011 for a complete list). One well-investigated protease, neprilysin (NEP), appears to be critical in this pathway, demonstrated by the effectiveness of a combination of NEP inhibitors, over-expression of *NEP*, and genetic disruption of *NEP* in increasing proteolytic cleavage and clearance of Aβ (Marr et al., 2003; Dolev and Michaelson, 2004; Nisemblat et al., 2008; Hafez et al., 2011; Takamatsu et al., 2014). Aβ clearance also occurs extracellularly, via microglia-mediated phagocytosis. The effect of aging on this process is further discussed in following sections.

TABLE 1 | A comprehensive list of all of the drugs in clinical development that aim to reduce either Aβ pathology, tau pathology, or inflammation within the past five years categorized by treatment strategy and drug class.

Category	Drug class	Mechanism	Compound name	Current status
Inflammation	Anti-inflammatories (Ferretti et al., 2012; Tawakol et al., 2014; Hori et al., 2015)	Anti-inflammatories act through a variety of interactions.	Cromoglicic acid	Approved (alternate indication)
			ALZT-OP1	Approved (alternate indication)
			CHF 5074	Phase 2
	RAGE Antagonists (Srikanth et al., 2011; Gilham et al., 2016)	RAGE increases pathogenic pro-inflammatory signaling in diabetes, AD, and cancer. Antagonists may alleviate the deleterious effects, but may also reduce amyloid deposition.	Rilapladib	Phase 2
			ALZT-OP1	Phase 3
			GSK2647544	Phase 1
			Minocycline	Approved (alternate indication)
			Azeliragon	Phase 3
	Tumor necrosis factor alpha inhibitor (Butchart et al., 2015; Gilham et al., 2016)	Traditionally a cancer drug, Etanercept may lower the effects of heightened levels of tumor necrosis factor alpha and deleterious inflammation.	Etanercept	Approved (alternate indication)
Tau-related pathology	Microtubule Stabilizers (Mitchell et al., 2016)	Dysfunction of phosphorylated tau results in impaired microtubule stabilizing function, synaptic shrinkage, and eventually neuronal death. Microtubule-stabilizing agents may alleviate the deficit caused by tau phosphorylation.	TPI-287	Phase 1
	Inhibitors of Tau Aggregation (Harrington et al., 2015)	Small molecules that bind pathological versions of tau and prevent aggregation may help reduce overall toxicity.	TRx0237	Phase 3
	Vaccine against Tau (Theunis et al., 2013; Kontsekova et al., 2014)	Use second-generation immunotherapy to stimulate the brains innate immune system to increase neurofibrillary tangle clearance.	AADvac1	Phase 2
			ACI-35	Phase 1
	Src/abl family of kinases inhibitor (Nygaard et al., 2014)	Fyn phosphorylates tau after exposure to pathogenic Aβ. Therefore, inhibitors may prevent or reduce the generation of pathological tau.	Saracatinib	Phase 2
	Antibodies against Tau	Antibodies against pathogenic Tau seek to utilize the brain's natural immune system to clear Aβ faster.	ABBV-8E12	Phase 2
			RO7105705	Phase 1
Reduction in Aβ	BACE Inhibitors (He et al., 2013; Eketjäll et al., 2016)	Inhibits the action of pathogenic β-secretase cleavage of APP, reducing overall amyloid burden.	AZD3293	Phase 3
			JNJ-54861911	Phase 2/3
			LY3202626	Phase 2
			CNP520	Phase 2/3
			E2609	Phase 3
	Antibodies against Aβ (Bard et al., 2000; Dodel et al., 2013)	Antibodies against pathogenic Aβ seek to utilize the brain's natural immune system to clear Aβ faster.	BAN2401	Phase 2
			Gantenerumab	Phase 3
			GSK933776	Phase 2
			LY3002813	Phase 1
			LY3303560	Phase 1
			MEDI1814	Phase 1
			SAR228810	Phase 1
			AAB-003	Phase 1
			Aducanumab	Phase 3
			Crenezumab	Phase 3
			Gamunex	Approved (alternate indication)
			KHK6640	Phase 1
	Small Molecule Aβ inhibitors (McLaurin et al., 2006; Habchi et al., 2016)	Small molecules are believed to either bind Aβ42 and Aβ40 peptides early, preventing nucleation, or inhibiting organization of higher-level tertiary and quaternary structures.	ELND005	Phase 2

(Continued)

TABLE 1 | Continued

Category	Drug class	Mechanism	Compound name	Current status
	RXR-selective analogues (Tai et al., 2014)	These receptors ameliorate loss-of-function associated with ApoE, decreasing Aβ burden and improving synaptic viability.	Bexarotene	Approved (alternate indication)
	Phosphodiesterase 9 Inhibitors (Su et al., 2016)	PDE9 inhibitors halt Aβ aggregation, thus reducing abundance and associated toxicity of senile plaques.	BI 409306 BPN14770	Phase 2 Phase 1
	Beta amyloid vaccines (Wiessner et al., 2011)	Using second-generation immunotherapy to stimulate the brain's innate immune system to increase Aβ clearance.	CAD106 MER5101 UB-311 ACI-24	Phase 2/3 Phase 1 Phase 2 Phase 1/2
	Purinoceptor P2Y6 agonists (Koizumi et al., 2007)	Stimulation of the P2Y6 receptor increases microglia phagocytosis and associated clearance of Aβ.	GC021109	Phase 1
	Gamma Secretase Modulators (Imbimbo et al., 2009; Imbimbo and Giardina, 2011)	Modulate γ-secretase to process pathological Aβ42 more readily into non-toxic forms.	NGP 555 CHF 5074 EVP-0962	Phase 1 Phase 2 Phase 2
	Inhibitors of Aβ synthesis (Maccecchini et al., 2012)	Binding of APP mRNA prevents translation, thus reducing amyloid burden in the subject.	Posiphen	Phase 1/2
	Sigma 2 receptor ligands (Izzo et al., 2014)	These ligands bind to the sigma 2 receptor, inhibiting binding of Aβ fragments and associated synaptic toxicity.	CT1812	Phase 1/2
	Glutaminyl cyclase inhibitors (Morawski et al., 2014)	Glutaminyl cyclase is a metalloenzyme that catalyzes the cyclization of pathogenic Aβ, forming pGlu-Ab, which is a highly toxic constituent of senile plaques.	PQ912	Phase 2
	Dihydropyridine calcium channel blocker	Serves as an anti-hypertensive with Aβ deposition prevention properties (Paris, 2010).	Nilvadine	Phase 3
	SNRI (Chalermpalanupap et al., 2013)	Reducing NET activity has the potential to reduce amyloid burden.	Atomoxetine	Phase 2

Drugs in green are already approved by the FDA for a condition separate from AD. Drugs in red have been granted Fast Track privileges for AD clinical development.

Microglial Origin and Presence in the CNS

This first reports of cells exhibiting microglia-like phenotypes came from the work of Nissl and Robertson in the late nineteenth century (Gomez-Nicola and Perry, 2015). It wasn't until the late 1930's that these cells were differentiated from other glial cells and received the name of "microglia" by Pio del Rio-Hortega. Hortega used silver staining techniques to describe microglial morphology and introduced the idea of microglia as ramified resting cells (Ginhoux et al., 2013). He pioneered the idea that microglia have the ability to change morphology, migrate, and proliferate in response to their microenvironment and described their basic functional roles as phagocytic cells (Ginhoux et al., 2013). Although Hortega introduced the idea of a mesodermal origin of microglia, a more recent study showed that microglia differentiate from yolk-sac derived myeloid precursor cells (Ginhoux et al., 2010). Utilizing fate mapping technology, Ginhoux et al. have demonstrated that microglia progenitor cells infiltrate into the brain from the yolk sac during early embryonic development and continue to migrate and mature in the early stages of post-natal brain development. Support for the yolk sac hypothesis of microglia origin has prompted scientists to investigate the mechanisms by which microglia maintain homeostatic presence in the CNS throughout the lifetime. Several studies have found that microglia are largely maintained by proliferation, while circulating peripheral monocytes only contribute to the microglia population in disease conditions (Ginhoux et al., 2010; Bruttger et al., 2015). In adulthood, microglia make up approximately 0.5–16.6% of all cells in the brain, depending on brain sub-regional variations (Mittelbronn et al., 2001). They are widely present in the entire CNS, including the brain and spinal cord.

Microglia Morphology: a Correlation with Functional Profiles?

One particularly essential characteristic of microglia is their ability to rapidly change morphology and function in response to changes in their microenvironment (Karperien et al., 2013). Several studies have suggested that microglia morphology falls on a spectrum, ranging from amoeboid to ramified (Stence et al., 2001; Fontainhas et al., 2011). Additionally, newer studies have introduced a third morphological classification; reactive or "alternatively" activated microglia, characterized by thick retracted processes, typically directed toward a lesion or site of protein aggregation (Franco and Fernández-Suárez, 2015). Morphologically, this state falls in between amoeboid and ramified. Ramified microglia, frequently defined as homeostatic

or surveying microglia, are characterized by dynamic thin processes extending out from a relatively circular-shaped soma (Kreutzberg, 1996; Fontainhas et al., 2011; Karperien et al., 2013). Surveying microglia are involved in CNS homeostasis by actively making contacts with surrounding synaptic elements. Interestingly, several studies have demonstrated that the most complex microglia appear to be seen in compromised conditions and may be subtly activated, suggesting that ramified microglia may also be slightly reactive (Hinwood et al., 2012; Karperien et al., 2013). Amoeboid microglia display the greatest level of motility, facilitated by a retraction and reduction of processes (Kreutzberg, 1996; Karperien et al., 2013). Amoeboid microglia are most commonly found during the early stages of brain development, before they undergo morphological differentiation to ramified microglia during brain maturation (Harry and Kraft, 2012; Ginhoux et al., 2013). They are also occasionally reported in inflammatory and phagocytic conditions, although their specific function in these states remains unclear (Karperien et al., 2013). Microglia morphology is strongly influenced by neurotransmitter activity. Excitatory neurotransmission significantly increases the ramification of microglia via ATP signaling (Fontainhas et al., 2011). This evidence suggests that microglial processes are highly susceptible to external cues. Although numerous studies have attempted to elucidate the correlation between amoeboid and ramified microglia and their roles in physiological and pathological conditions, the exact functional profiles of different morphological states remain widely debated.

The Function of Microglia in Synaptogenesis and Synaptic Plasticity

Microglia are known to play an important role in synaptogenesis and synaptic wiring and maintenance, which is crucial for functional brain connectivity (Ginhoux et al., 2010; Paolicelli et al., 2011). Lim et al. have recently shown that microglia-mediated release of IL-10, a pro-inflammatory molecule, led to an increase in dendritic spines (Lim et al., 2013). Concurrently, in a second study, they demonstrated that hippocampal neurons expressed IL-10 receptors during the early stages of brain maturation (Lim et al., 2013). Together, these studies suggest a causal role of microglia in synaptogenesis through microglia-mediated IL-10 signaling. Microglia maintain the ability to modulate synaptic circuits into early adulthood. A study by Parkhurst et al. revealed a microglia-dependent effect on learning-related synaptogenesis (Parkhurst et al., 2013). In addition to their role in synaptic wiring and refinement, microglia are also key modulators of synaptic plasticity. In a study investigating plasticity in the visual system, microglia-mediated synaptic remodeling in layers II/III of the V1 was shown to be activity-dependent (Tremblay et al., 2012). Additional studies have focused on other synaptic functions, such as long term potentiation (LTP), suggesting that microglia actively participate in strengthening neuronal connections through Hebbian plasticity (Penn et al., 1998). Furthermore, several studies have been published highlighting chemokine fractalkine receptor (CX3CR1) signaling and secretion of soluble molecules enhancing NMDA receptor function as key effectors in microglia-mediated modulation of synaptic plasticity (Hayashi et al., 2006; Justin et al., 2011). A study investigating the role of microglia in ocular dominance columns found that microglia modulate experience-driven plasticity in the monocular deprivation model through synaptic pruning (Sipe et al., 2016). Moreover, microglia were shown to have an indirect effect on synaptic strength through upregulation of *TNF*-α (Lewitus et al., 2016). Together, these findings reinforce the role of microglia in modulating cortical plasticity throughout the lifetime.

Pruning: Microglia-Mediated Phagocytosis of Excess, Inactive or Dysfunctional Synapses

Microglia provide crucial supportive functions in the CNS development starting early embryonic stages and persisting into adulthood. In their steady state, microglia play important roles in synaptic maintenance by serving as phagocytic cells, pruning excess or dysfunctional synapses (Tremblay et al., 2010). These processes are controlled by three principal mechanisms: the complement system, chemokine pathway, and activity-dependent signaling.

The complement system, a part of the innate immune response, facilitates phagocytosis in response to antigens. Complement proteins are highly expressed in neurons and glia, but selectively localized to immature synapses (Stevens et al., 2007). Microglia express complement C3 receptor CR3 (aka CD11b, Itgam, and Mac-1), which recognizes activated C3 fragments tagged to excess, immature, or dysfunctional synapses, consequently initiating phagocytosis (Carroll, 2004; Gasque, 2004; Ransohoff and Perry, 2009).

Several studies have found that microglia-mediated pruning is dependent on fractalkine signaling, which promotes survival in monocytes (Landsman et al., 2009). *CX3CR1* is specific to microglia in the brain and subset of peripheral monocytes, and responds to pruning cues from surrounding neurons. Knock out (KO) of *CX3CR1* was associated with a brief reduction in microglia and subsequent deficit in synaptic pruning, which resulted in an excess of excitatory synapses, as well as an increase in spine density and PSD95 expression (Paolicelli et al., 2011). These findings suggest that disruptions in microglia-mediated synaptic pruning are sufficient to induce deficits in brain maturation, resulting in impaired functional connectivity.

Additionally, studies have shown that pruning is activity-dependent and persists into adulthood (Tremblay et al., 2010; Schafer et al., 2012). Recently, one study has found that synaptic pruning is negatively altered in disease conditions and results in microglia-mediated synaptic loss (Hong et al., 2016). This evidence confirms the crucial role microglia play in shaping neuronal circuits throughout the lifetime, in both physiological and pathological conditions.

Microglial Phagocytosis of Cellular Debris

Microglia are known to phagocytose biological waste and a variety of pathogens, including apoptotic bodies, cellular

debris, and exogenous particles, through various well-established phagocytic pathways (Chan et al., 2001; Fu et al., 2014). This phagocytic function is crucial in both health and disease (Aderem and Underhill, 1999). Ravishadran has established a four-step model for the phagocytosis of apoptotic neurons: apoptotic cells first release "find me" signals attracting microglia, followed by the "eat me" process, mediated by specific receptors expressed by targets, the "digest me" phase, resulting in degradation of cellular materials, and finally, the post-phagocytic phase, which involves inflammatory consequences, such as cytokine and chemokine release (Ravichandran, 2010). Additionally, the fifth step, which occurs in proteopathies, has been proposed (**Figure 1**). Different signaling pathways are implicated in the phagocytosis of various targets (Fu et al., 2014). Extracellular nucleotides, such as ATP and UTP, are the most common "find me" signals released by apoptotic cells. UTP degradation yields UDP, which interacts directly with microglia via P2Y6 receptors (Nimmerjahn and Ravetch, 2006; Koizumi et al., 2007). Fractalkine signaling has also been shown to contribute to microglia-mediated phagocytosis of apoptotic cells (Truman et al., 2008; Noda et al., 2011; Sierra et al., 2013). "Eat me" signals are expressed by targets to initiate recognition by receptors expressed on the microglial cell surface. Toll-like receptors (TLRs) and Fc receptors are commonly implicated in microglia-mediated phagocytosis of α–synuclein (Okun et al., 2010; Hanke and Kielian, 2011; Cao et al., 2012), whereas triggering receptor expressed on myeloid cells 2 (TREM2), is known to control microglia-mediated Aβ compaction, and phagocytosis of apoptotic neurons (Piccio et al., 2007; Takahashi et al., 2007; Yuan et al., 2016). Complement and scavenger receptors are expressed by microglia and astrocytes, specifically in the pathophysiology of AD, multiple sclerosis, and amyotrophic lateral sclerosis (Husemann et al., 2002; Alarcón et al., 2005; Keren-Shaul et al., 2017). Together, these studies indicate that various types of stimulus are able to differentially trigger microglia-mediated phagocytosis via a wide range of signaling pathways. In addition to their role in phagocytosing apoptotic cells, microglia also have an established role in initiating cell death, in a process termed "phagoptosis" (Brown and Neher, 2012). Interestingly, some studies have shown that microglia-mediated "phagoptosis" can have deleterious effects in neurodegenerative diseases by triggering phagocytosis of viable neurons (Kao et al., 2011). These findings suggest that microglia-mediated phagocytosis can have both protective and deleterious effects in disease states (Fu et al., 2014).

Microglial Antigen Presentation

In homeostatic physiological conditions, the blood brain barrier (BBB) prevents most peripheral infectious agents, as well as peripheral immune cells, from reaching the CNS. Consequently, the brain depends on its' own immune cells, microglia, to fulfill the roll of peripheral immune cells. As such, microglia have been shown to act as antigen presenting cells (APCs) upon activation in response to immune-related insults (Gottfried-Blackmore et al., 2009). In homeostatic conditions, major histocompatibility complex class II (MHC-II) expression is virtually non-existent in microglial populations (Ford et al., 1995). In inflammatory or neurodegenerative conditions, however, microglial MHC- II expression is quickly upregulated (Perry et al., 1987; Kreutzberg, 1996; Gottfried-Blackmore et al., 2009). One of the largest barriers to comprehending this mechanism comes from the observation that microglia are unable to travel to the lymph nodes, limiting their ability to act as APCs. Several studies have proposed that the CNS fulfills the role of a functional lymphatic system, where antigen-presenting microglia can come into contact with peripheral APCs in the meninges and choroid plexus, effectively playing an active role in T-cell mediated acquired immunity in the CNS (Louveau et al., 2015). However, recently it is speculated that antigens can be delivered to meningeal lymphatic vessels, where meningeal macrophages reside (Raper et al., 2016). There is no evidence of microglial presence in this region, suggesting their limited role for antigen presentation (Mildner et al., 2017).

Microglial Chemotaxis

Resting microglia are known to exhibit dynamic behavior, surveying their environment and making contacts with surrounding cells in order to execute a variety of functions. When activated, microglia become highly motile cells, migrating toward pathological stimuli such as debris and lesions. Chemotaxis from chemo- (chemical) and -taxis (movement), defines the ability of a cell to move in response to chemical triggers. Microglial migration is modulated by microglia-expressed receptors and gradients of different chemoattractant chemokines released by targets in inflammatory conditions (Dijkstra et al., 2004; Wang et al., 2008). The signaling pathways involved in microglia chemotaxis are highly complex. Briefly, studies have highlighted the specific roles of extracellular signal–regulated kinases (ERK1/2), protein kinase A (PKA), phospholipase A2 (PLA2), phosphoinositide 3-kinase (PI3K), and ATP/purinergic receptor signaling pathways in regulating microglial migration (Fan et al., 2017). Monocyte chemoattractant proteins (MCPs) are of particular interest in neuroinflammatory conditions. The expression of CCL2, aka MCP-1, has been associated with microglia activation in the pathogenesis of multiple sclerosis (Simpson et al., 2000) and AD (Conductier et al., 2010). Additionally, neuron-derived Fractalkine (CXCL1) stimulates microglia migration through CX3CR1 receptors (Harrison et al., 1998). Interestingly, CXCL1 is implicated in a variety of neurodegenerative disorders by acting as an anti-inflammatory agent, which may prove to be an interesting therapeutic target (Desforges et al., 2012).

A Role of Microglia in Neuroinflammatory Conditions

A key function of microglia is their ability to respond rapidly to immune-mediated insults and physical damage in the brain. Microglia modulate the stress response to a variety of pathological triggers in CNS diseases reviewed extensively by Streit and Graeber et al. (Streit et al., 2004; Graeber et al., 2011). It is well-established that physiological responses to infection in the periphery are propagated through microglia in the CNS directly without the help of a cellular messenger (Chen et al., 2012), a response that is largely reduced after microglia depletion (Elmore et al., 2014). The propensity of

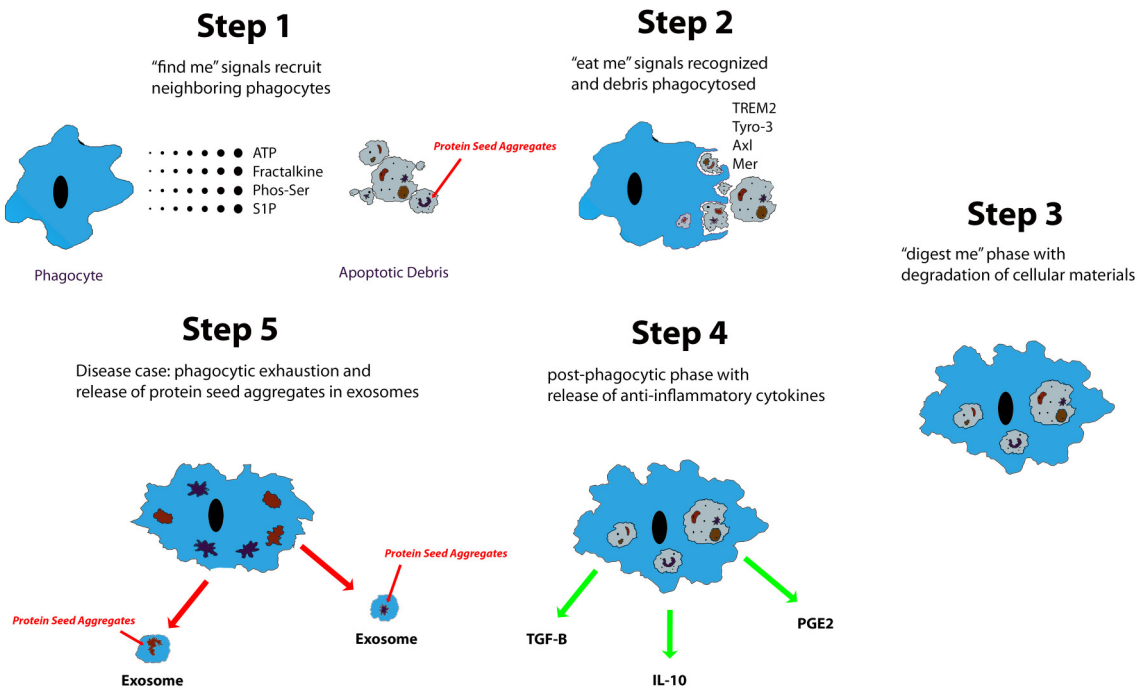

FIGURE 1 | Described are five steps of apoptotic cell clearance via phagocytes. Trace chemicals and molecules associated with cell necrosis and apoptosis stimulate the chemotaxis of phagocytes up their concentration gradient to the source. From there, the phagocyte engulfs the apoptotic debris and begins degradation. Eventually, it will release anti-inflammatory and reparative signals such as TGF-β, IL-10, and PGE2. In neurodegenerative diseases of protein aggregation, protein seed aggregates are packaged into exosomes where they can be shuttled to different regions of the CNS.

the brain to propagate an inflammatory response is increased naturally due to aging (Rosczyk et al., 2008). These triggers range from autoimmune damage, such as demyelination from multiple sclerosis (Vowinckel et al., 1997; Ponomarev et al., 2005), CNS infection (Rock et al., 2004), protein aggregation (such as amyloid plaques) (Kamphuis et al., 2012), or cellular debris from neurodegeneration (Fraser et al., 2010), to physical damage from trauma or ischemia. Microglia also contain a number of purinergic receptors that respond to extracellular ATP and ADP, which are signs of possible necrosis and cellular injury (Inoue and Tsuda, 2012). Upon activation, microglial physiological function is altered, characterized by changes in morphology, coupled with upregulation of cell surface receptors and expression of chemokines and cytokines, all dependent on the triggering event (Perry and Teeling, 2013). The have been a subject of intense debate for the past few decades. Studies have demonstrated that microglia activation, independent of other cytotoxic elements, impacts synaptic function (Selkoe, 2002; Di Filippo et al., 2008) and has neurotoxic effects (von Bernhardi et al., 2015b) that correlate with neurodegeneration and decline in cognitive abilities (Cagnin et al., 2001; Kim and de Vellis, 2005). However, it is also widely believed that transient microglia activation is beneficial in neuroinflammatory conditions by promoting neuron survival (Neumann et al., 2006) and repair after brain injury (Kitamura et al., 2004) through anti-inflammatory signaling.

How Do Microglia Sense Damage?

Microglia activation in neuroinflammatory conditions is mediated by a variety of complex signaling pathways, recently reviewed in Kaminska et al. (2016). Pathogen associated molecular patterns (PAMPs) and damage or danger -associated molecular patterns (DAMPs) activate PRRs (pattern recognition receptors) (Janeway, 1992; Kigerl et al., 2014), triggering crucial responses to immune-related insults and physical injury. PAMPs are expressed by microorganisms and play a critical role in innate immunity. DAMPs are produced by damaged cells and trigger a microglial response to brain injury. PAMPs and DAMPs have been reported to mediate microglia activation and immune response via a variety of PRRs, including Toll-like receptors (TLRs) and nucleotide oligomerization domain (NOD)-like receptors (NLRs) (Kigerl et al., 2014). TLRs are commonly activated in CNS injury and promote transcription of pro-inflammatory cytokines via activation of NF-κB and MAP kinase signaling pathways (Akira and Takeda, 2004). Lipopolysaccharide (LPS) is a PAMP of particular relevance to neurodegenerative diseases. It exerts its function through TLR4 and results in the production of several pro-inflammatory cytokines (Lu et al., 2008). *TLR4* mutations were shown to reduce microglia activation, while stimulation of TLR4 modulated cytokine expression in AD models (Jin et al., 2008). NLRs trigger the formation of large protein complexes that activate caspace-1, an essential molecule in the production of pro-inflammatory cytokines (Martinon

et al., 2002; Kigerl et al., 2014). NLRP3 is expressed on microglia and participates in microglia activation in AD and several prion diseases (Halle et al., 2008; Kigerl et al., 2014). Microglia activation is also mediated by purines, such as ATP and UTP, released by apoptotic cells. These induce chemotaxis and phagocytosis via ubiquitously expressed purinergic receptors on microglial cell surfaces (Koizumi et al., 2013). Additionally, research has shown that in neuroinflammatory conditions, neurotransmitters have the capacity to mediate microglia-neuron interactions (Mead et al., 2012). Microglia express glutamate receptors, which allows them to sense neuron-released extracellular glutamate, a potent neurotoxic factor (Taylor et al., 2005). Interestingly, studies have reported that upon activation, microglia are self-producers of glutamate, which induces excito-neurotoxicity in neurons and contributes to the pathology of several neurodegenerative diseases (Takeuchi et al., 2006). This suggests that microglia are capable of autocrine signaling and supports the idea of a self-renewing neurotoxic cycle in chronic inflammatory conditions. Microglia activation is also initiated by the absence of certain signaling pathways. CD200 is expressed by neurons and interacts via CD200R expressed on microglial cell surfaces. This interaction maintains microglia in a resting, inactive state (Hoek et al., 2000). CD200 expression is downregulated with age and contributes to increased microglia activation and neuroinflammation (Lyons et al., 2007).

Brain Aging

Aging is the single most dominant risk factor for all neurodegenerative disorders, resulting in an impairment in protein production, homeostasis, chaperone-mediated folding, trafficking, stability, clearance, and autophagy. It is important to note that the CNS undergoes several changes during aging including, the shrinking of cortical areas (Salat et al., 2004; Raz et al., 2005), restricted neurogenesis (Praag et al., 2005), reduction in synaptic density, reduction in cognitive and psychomotor function in both in humans and in mice (Godbout et al., 2008; Hayashi et al., 2008), and reduction in glucose metabolism in various regions (Salmon et al., 2003; Kalpouzos et al., 2009; Hsieh, 2012). Additionally, aging also typically leads to an overall increase in the level of proinflammatory cytokines, such as IL-1β, IL-6, CD68, CD11b, and Toll-like receptors (TLRs) (Maher et al., 2004; Godbout et al., 2005), and a decrease in anti-inflammatory cytokines, such as IL-10 and IL-4 (Maher et al., 2005; Nolan et al., 2005). Furthermore, overall brain volume normally decreases by approximately 20% by the time a person turns 100 years old. It is also worth noting that the aged brain frequently has impaired vasculature, resulting in reduced oxygen and nutrient delivery to the CNS that may be exacerbated in certain brain regions (Montagne et al., 2015). Moreover, studies have suggested that blood-brain-barrier (BBB) permeability is increased by aging (Blau et al., 2012; Enciu et al., 2013), suggesting a greater susceptibility to external factors.

The natural propensity of the CNS to adopt a more inflammatory microenvironment during aging earned it the nickname "inflamm-aging" (Franceschi et al., 2000; De Martinis et al., 2005). This may be due in part to the increase in reactive oxygen species (ROS) that is evident in the aged brain. Microglia are largely responsible for the production of these species, which include lipid peroxides, superoxide anions, and hydroxyl radicals (Coatrieux et al., 2007). These molecules, in turn, lead to increased oxidative stress and elicit neurotoxic effects. Oxidative stress is known to initiate neuronal cell death *in vitro* and via a high calorie diet *in vivo* (Bros et al., 2014; Treviño et al., 2015). Conversely, some anti-inflammatory factors are known to also increase in concentration in the aged CNS. For example, TGF-β1 is a potent anti-inflammatory factor upregulated in the aged brain (Blobe et al., 2000; Tichauer et al., 2014). TGF-β1 has been shown to promote microglial phagocytosis of Aβ (Wyss-Coray et al., 2001). When considering the effect of age on various CNS responses to different stressors, aged mice, in comparison to young mice, appeared to frequently exhibit exaggerated or prolonged release of proinflammatory cytokines, worsened cognitive decline, as well as age-dependent anxiety-like behavior and sociability changes (Shoji et al., 2016).

Microglia in Aging

Microglia undergo changes in their morphology, phagocytic activity, chemotactic activity, surveying activity, and inflammatory responses that could be relevant to their involvement in disease. Research suggests age-related changes prime microglia to polarize and cause damage in response to disease-related insults. When trying to understand the true nature of pathological conditions, it is important to distinguish the changes resulting from the disease itself, vs. normal age-related variations.

Microglia undergo key morphological changes during aging. Microglial surveying processes are reported to be less dynamic, less complex, and to travel more slowly as mice age (Sierra et al., 2007; Damani et al., 2011). This suggests that responses to pathogens, aggregated proteins, or injury will be delayed in aging brains in comparison to younger mouse brains. In the aged brain, microglia appear to have enhanced proliferation in response to injury, shown in a facial nerve axotomy study in rats (Conde and Streit, 2006). Migration velocity of microglia in response to injury also appears to be affected by aging (Damani et al., 2011; Hefendehl et al., 2014). Studies have shown that in aged animals, microglia survey the environment at a lower speed (Hefendehl et al., 2014), possess thinner and fewer distal branches, and contain spheroids within the major processes (Egensperger et al., 1998; Simmons et al., 2007; Streit et al., 2009). It is possible that in these conditions, myelin fragmentation significantly contributes to the formation of these spheroid inclusions in microglia (Safaiyan et al., 2016). Furthermore, aging reduces microglia cell soma volume and results in decreased tissue distribution homogeneity. (Euler and Schuitemaker, 2012; von Bernhardi et al., 2015b). These characteristics are typically referred to as microglial dystrophy, and are considered to be a normal age-dependent phenotypic state. Recently, a new characterization termed "dark microglia" was established (Bisht et al., 2016). These microglia, identified by their extremely electron-dense soma, become more prominent with age and are especially present in disease states. It is suggested that this may represent a senescent state of microglia. Dark microglia are thought to be caused by a

build-up of lipofuscin and increased mtDNA mutations (Wong, 2013).

As microglia age, they undergo many changes at the expression level that confer a heightened inflammatory response. For instance, aged microglia express more MHC-II, as well as mouse CD68 (Godbout et al., 2005; Henry et al., 2009). CD200, a membrane glycoprotein expressed on neurons, astrocytes, and oligodendrocytes, acts as a resting or pro-ramification signal for microglia, which express CD200R. Research has shown that CD200 is decreased in the human AD brain (Walker et al., 2009). CX3CL1 is a cytokine present in neurons that appears to have similar functions as CD200 in promoting microglial ramification. CX3CL1 interacts with CX3CR1, which is also widely expressed in microglia (Fuhrmann et al., 2010). Several studies have suggested that Fractalkine signaling appears to be reduced in the aged brain (Lyons et al., 2009; Bachstetter et al., 2011; Vukovic et al., 2012). Smad3, responsible for the canonical signaling pathway for TGFβ and its anti-inflammatory effects, is reduced in the aged brain (von Bernhardi et al., 2015a). Furthermore, IFN-γ, a potent activator of microglia and initiator of pro-inflammatory gene transcription (Rock et al., 2004; Klegeris et al., 2005), is increased in the aged brain. Genes conventionally known to influence microglia maturation were found to be master regulators of age-dependent changes in microglial phenotype (Wehrspaun et al., 2015). In many species, Iba-1 expression is increased in microglia due to age, often accompanied by a less ramified morphology (Streit et al., 2004), suggesting a more proliferative microglial state. It is also important to note age-related changes in astrocytes, which include an increase in glial fibrillary acidic protein (GFAP) expression, indicating a more pro-inflammatory phenotypic state (Godbout et al., 2005).

Researchers have sought to further elucidate age-associated changes by investigating the number and dynamics of existing microglia in the CNS. There does not appear to be a change in the overall number of microglia as the brain ages. However, during aging, as microglia generally become dysfunctional, they remain in the brain for longer periods of time (Mosher and Wyss-Coray, 2014). A recent study suggested that some microglia can live to be as much as 40 years old, with an average lifespan of 4.2 years and typical yearly turnover rate of 28% (Réu et al., 2017). Furthermore, the effect of peripheral monocyte infiltration on microglia phenotype must be taken into account, given that the cytokine-release profile can differ between the two (Ritzel et al., 2015). A previous study in rats has shown an age-associated increase in blood-derived monocytes, identified as CD11b+ $CD45^{high}$ cells (Blau et al., 2012).

Research investigating the effect of long-term intraperitoneal LPS injection has suggested that some of these changes may be more prominent in certain brain regions (Hart et al., 2012). Indeed, recent studies have revealed that the effect of aging on the transcriptome of microglia is highly dependent upon location within the CNS (Grabert et al., 2016). Given that neurodegenerative diseases frequently follow a region-specific onset, it is important to consider the idea that region-specific microglia priming could contribute to this phenomenon. The fact that the cerebellum is significantly less susceptible to amyloid deposition (Johnson-Wood et al., 1997), while microglia appear to exhibit a hyper immune-alert phenotype (Grabert et al., 2016) during aging in this region, supports this notion.

During aging, microglia generally seem to exhibit an enhanced response to both CNS and peripheral insults. *In vivo*, aged mice appear to undergo an exaggerated inflammatory response to peripheral LPS injection, defined as an increased release of pro-inflammatory cytokine IL-1β (Godbout et al., 2005). Although immunoreactivity of microglia seems to be increased, age also appears to promote a senescent phenotype in microglia that reduces their functional capabilities, which appears to be accentuated *in vitro*. One study pointed out the propensity of isolated microglia to be more ramified, and exhibit a reduction in chemotaxis, phagocytosis, autophagic capacity, and overall reactivity (Caldeira et al., 2014) after aging *in vitro*. These findings were recently reproduced in the context of amyloid pathology, where microglia exhibited reduced phagocytic capabilities after 2 weeks in culture (Caldeira et al., 2017). Primary microglia isolated from 15 month old C57BL/6 were shown to have increased secretion of IL-6 in response to LPS, as well as a reduced ability to phagocytose Aβ oligomers, when compared to younger mice (Njie et al., 2012). A decrease in the ability to migrate was also noted, along with a more senescent phenotype, and less complicated inflammatory response. Furthermore, primary microglia isolated from aged mice exhibit increased release of pro-inflammatory TNF-α, IL-1β, IL-6, and IL-10 in response to challenge with LPS (Sierra et al., 2007). Aged microglia also tend to secrete more ROS, while those from young animals predominantly secrete NO (Tichauer et al., 2014). It can be difficult to distinguish whether these established changes in microglia *in vitro* are due to age or due to the effects of changing from the *in vivo* to *in vitro* environment. Nonetheless, these findings present strong evidence that aged microglia are more readily primed for activation, may be easily triggered by pathological elements in neurodegenerative diseases.

Microglial Polarization

Microglia activation *in vitro* is often classified into two categories, M1 pro-inflammatory classical activation and M2 anti-inflammatory alternative activation (Colton, 2009). This bipolar model has evolved and is now understood to represent a spectrum, where activation status can fall anywhere between M1 and M2 (Mantovani et al., 2005; Martinez and Gordon, 2014). Pro-inflammatory molecules, such as IFN-γ, TNFα, and LPS, induce the M1 classical activation of microglia (Delgado and Ganea, 2003; Martinez and Gordon, 2014). Microglia in the pro-inflammatory state secrete a variety of inflammatory cytokines, including TNF, IL-6, IL-12, IL-23, IL-1β, as well as other cytotoxic molecules, such as ROS and NO, all of which promote neurotoxicity and reinforce the inflammatory response (Delgado and Ganea, 2003; Cherry et al., 2014). Oxidative stress is implicated in nearly all neurodegenerative disorders (Gandhi and Abramov, 2012). Studies have suggested that the accumulation of reactive oxidative species results in neuronal damage and triggers apoptosis (Gilgun-Sherki et al., 2001). LPS has been show to mediate activation-induced production and secretion of ROS and reactive nitrogen species (RNS) in microglia (Dimayuga et al., 2007). Using a co-culture system of microglia and fetal neuronal

cells, Chao and collaborators revealed that both LPS and IFN-γ stimulation resulted in the production of NO, which induced neurotoxicity in neuronal cells. The production of ROS and NOS was later shown to be dependent on nicotinamide adenine dinucleotide phosphate (NADPH) oxidase activity in microglia (Qin et al., 2004; Block and Hong, 2007). *In vivo,* mice deficient of NADPH oxidase were demonstrated to experience reduced nigrostriatal degeneration in response to systemic LPS injection (Qin et al., 2013), suggesting that microglia are capable of being modulated to prevent harmful activation.

The M1 pro-inflammatory profile of microglia is counter to the M2, anti-inflammatory activation state. Stein and collaborators first reported the ability of microglia to adopt anti-inflammatory properties upon stimulation by IL-4 (Stein et al., 1992). Microglia activation by IL-4 has been shown to upregulate IGF-1 production, leading to neuroprotective and regenerative effects (Butovsky et al., 2006). Additionally, other Th2-associated cytokines, such as, IL-10 and TGFα, as well as glucocorticoids, have been reported to promote M2 activation in microglia (Goerdt et al., 1999). M2 microglia have further been subdivided into three functional subclasses: M2a, M2b, and M2c (Mantovani et al., 2004; Chhor et al., 2013). M2a is induced in microglia via IL-13 and IL-4 signaling and is primarily responsible for Arg-1 production, a molecule known to participate in collagen formation facilitating tissue repair (Chhor et al., 2013). Arg1 was also recently shown to increase uptake of Aβ (Cherry et al., 2015). Microglia M2b phenotype is triggered by TLR agonists. Interestingly, the M2b subtype is capable of producing both pro- and anti-inflammatory cytokines (Bell-Temin et al., 2015). The M2c subtype, induced by IL-10, TGFα, and glucocorticoids, have two key functions following brain injury; termination of the pro-inflammatory immune response (Bell-Temin et al., 2015) and repair and regeneration after brain injury (Mantovani et al., 2004). A more recent study validated microglia's regenerative role in disease states by showing that TGFα derived from M2 microglia encourages proliferation and maturation of neural precursor cells in tissue damaged from ischemic stroke (Choi et al., 2017).

The M1/M2 classification scheme contributes to a basic understanding of well-defined microglia-mediated immunological responses *in vitro*. Several experts, however, have questioned its comprehensiveness in describing *in vivo* processes and its validity in disease states (Butovsky et al., 2014; Martinez and Gordon, 2014; Ransohoff, 2016). Microglia are thought to be particularly hard to research, given that their gene expression profiles can change fairly dramatically when taken from the CNS and placed into the *in vitro* environment (Gosselin et al., 2017). Particularly, there appears to be an increase in the expression of genes associated with inflammation and stress. SORL1, the receptor for APOE protein whose deficiency has been noted in AD patients (Scherzer et al., 2004), appears to be under-expressed in the *in vitro* environment (Gosselin et al., 2017). Isolation of primary microglia is a tenuous and complicated process. Immunohistochemistry in microglia is also noted amongst researchers to be challenging, due to issues with granular staining and autofluorescence (Koellhoffer et al., 2017). Microglia are identified by a variety of markers to distinguish them from other glial cells and neurons. Unfortunately, they share a number of these markers with peripheral macrophages, making them hard to distinguish. Recent research suggests a third, new classification of microglia, may better reflect their *in vivo* phenotypes, specifically in disease states.

Microglia in Neurodegeneration

Beyond normal aging, microglia in neurodegenerative conditions experience a specific change in phenotypic state, which researchers have struggled to characterize. Given that there are clear distinctions between microglia that promote neurogenesis and reverse atrophy, and those that release ROS and pro-inflammatory cytokines, understanding the phenotypic state responsible for mediating neuroinflammatory damage is of paramount importance. Potential therapeutic interventions should target the specific deleterious activities of harmful microglia, while leaving beneficial neuroprotective mechanisms unhindered.

Microglia activation is a necessary and beneficial function in response to acute neuro-inflammatory events and aids in sustaining brain homeostasis. Chronic activation, however, can occur from excessive neuronal or immune-related damage in various CNS diseases (Polazzi and Monti, 2010). This can lead to the sustained release of pro-inflammatory molecules and harmful production of ROS which results in detrimental effects. Moderate increases in these cytokines are generally considered a normal part of aging. However, large increases, as observed in AD, lead to excessive neurotoxicity (Giunta et al., 2008; Glass et al., 2010). In turn, increased neurotoxicity triggers additional microglial activation, initiating a harmful loop of inflammation and neuronal damage termed "reactive microgliosis" (Streit et al., 1999). Microglia have been shown to be activated in nearly all neurological disorders (Neumann et al., 2009). Signs of microglia activation have been reported in autoimmune diseases, such as multiple sclerosis (Goldmann and Prinz, 2013; Luo et al., 2017), prion diseases, such as Creutzfeldt-Jakob Disease (CJD) (Aguzzi and Zhu, 2017), neurodegenerative diseases, such as Parkinson's Disease (PD) and AD, as well as traumatic brain injury (TBI) and ischemia (Jassam et al., 2017; Liu et al., 2017). Their implication in the pathophysiology of such a wide variety of neurological disorders has made them an interesting target for potential therapeutic approaches.

With regards to AD, some observations can be confusing. As mentioned in the previous section, aged microglia frequently become "dystrophic" and are highly immunoreactive. However, studies have reported reduced phagocytosis of Aβ in older AD mice (Floden and Combs, 2011), which may be caused by decreased expression of CD36, an Aβ interacting protein. In AD patients, as well as mouse models of AD, Smad3 signaling appears to be reduced (Tesseur et al., 2006; Ueberham et al., 2006), likely resulting in the pathological activation of microglia. Overall microglia number in both Alzheimer's patients and AD mouse models is increased and correlates with disease severity (Olmos-Alonso et al., 2016). This suggests that disease pathology promotes microglia proliferation. Microglia behavior in AD may also depend heavily upon the stage of the disease. One study reported that Aβ fibrils enhance microglia phagocytosis, while

Aβ oligomers attenuate phagocytosis (Pan et al., 2011). This finding suggests that microglia presence is more significant after considerable protein deposition.

A recent study expanded current microglia classification beyond the typical M1/M2 scheme. Researchers in this study named this third category of microglia, "disease-associated" microglia (MGnD), using a gene expression profile revealed through K-means clustering. These microglia revealed a reduction in the expression of 68 homeostatic microglial genes and upregulation of 28 inflammatory molecules (Krasemann et al., 2017). A large portion of these responses were eliminated due to microglia-specific KO of *APOE*, suggesting that APOE potently induces phenotypic changes in disease-associated microglia and is up-regulated in the presence of plaques (Krasemann et al., 2017). MGnD microglia also exhibited a significant increase in miR-155 expression. MiR-155, a significantly up-regulated microRNA in microglia after challenge with an insult, is largely responsible for the release of pro-inflammatory cytokines IL-6, IL-1β, NOS2, and TNFα (Woodbury et al., 2015). Beyond microglia interaction, APOE is important for maintaining hippocampal neurogenesis and suppressing astrogenesis in mice, both of which are reduced via APOE4 mutation (Li et al., 2009). *TREM2* KO was shown to have very similar effects on the gene expression profile as the *APOE* KO, suggesting these two molecules work concurrently to determine microglia phenotype. Another large study utilizing single-cell RNA-seq to identify unique microglia subpopulations present in 5XFAD mice found gene expression profiles associated with increase in APOE, TREM2, and Cst7 expression, amongst others, in disease-associated microglia, referred to as "DAM." These same microglia exhibited decreased expression of homeostatic genes *P2RY12* and *CX3CR1* (Keren-Shaul et al., 2017). Lpl was selected as a consistent marker for the disease associated microglia subtype, and found to be present on phagocytic plaque-associated microglia positive for Thioflavin-S. The expression of genes known to influence microglia maturation and ramification such as *RUNX1, SALL 1, TAL1,* and *IRF8* is also affected by AD pathology (Olmos-Alonso et al., 2016). It is important to recognize the differences between MGnD and classically activated M1 or M2 microglia (**Figure 2**). MGnD are a result of chronic exposure to disease pathology and can be distinguished from M1 microglia by the presence APOE, TREM2, and M2-associated anti-inflammatory markers such as arginase 1 (Arg1) and chitinase-3-like protein (Ym1), as well as the absence of homeostatic transcription factor Egr1 (Krasemann et al., 2017). In contrast, M1 microglia activated through LPS down-regulate TREM2 expression (Kleinberger et al., 2017; Zhong et al., 2017b). Furthermore, plaque-associated microglia exhibit a hyperactive immune response to LPS injection in comparison to non-plaque-associated microglia (Yin et al., 2017), suggesting their contribution to neuroinflammation in disease states is more detrimental.

The MGnD and DAM phenotypes are largely dependent on TREM2 expression, which is up-regulated in the microglia of diseased brains and MGnD microglia specifically (Ofengeim et al., 2017; Yin et al., 2017). This evidence suggests that the APOE-TREM2 signaling cascade is responsible for the changes in gene expression profile which induce the MGnD phenotype in microglia (Keren-Shaul et al., 2017; Krasemann et al., 2017; Yin et al., 2017). Two papers recently reported conflicting results of *TREM2* KO in different mouse models of tauopathy. In hTau mice, prior to the time of expected significant neuronal loss, *TREM2* KO was reported to increase the deposition of hyperphosphorylated tau and promote a less homeostatic microglial phenotype (Bemiller et al., 2017). However, in a study investigating PS19 mice with *TREM2* KO, researchers found a reduction in brain atrophy in the absence of any changes in tauopathy or a reduction of MGnD-associated markers APOE and Cst7 (Krasemann et al., 2017; Leyns et al., 2017). Collectively, these recent studies support the idea that the APOE-TREM2 signaling pathway shifts microglia toward an MGnD phenotype, which actively contributes to the tauopathy-induced reduction of neuropil space in the entorhinal cortex of PS19 mice. During aging in the CNS, microglia become more dystrophic, suffer a reduction in functional characteristics, and begin to exhibit a gene expression signature similar to that of MGnD microglia. Although age is not required for the generation of the MGnD phenotype, aged microglia are primed to make this transition. Further research is necessary to generate a more concrete and time-dependent understanding of the APOE-TREM2 signaling complex as it relates to the MGnD phenotype.

Therapeutics Targeting Protein Misfolding

Several techniques exist allowing researchers to design pharmacological agents aimed at reducing the buildup of pathological Aβ. One validated method is to focus on developing inhibitors of BACE1, which is the membrane protease responsible for the beta-site cleavage of APP (Eketjäll et al., 2016). Several of these compounds have been in clinical trials in recent years, such as the Merck EPOCH trial in patients with mild to moderate AD. This trial was speculated to have failed because the drug was administered too late to substantially address the pathology. Another obstacle in clinical trials is heterogeneous patient enrollment, which introduces the possibility of including patients that do not have AD, but suffer from dementia due to a different disease. Instead of inhibiting Aβ production, some compounds are being designed to address the prion-like properties of amyloid aggregation itself. This concept uses a small molecule, which binds to nascent amyloid fibrils or aggregates, preventing nucleation or further accumulation (McLaurin et al., 2006; Habchi et al., 2016). Additionally, there are also antibodies designed to bind pathological Aβ protofibrils, a passive immunization technique in which the antigen, Aβ, is bound, leading to complement activation and phagocytosis by neighboring phagocytes (Bard et al., 2000). However, considerable evidence has suggested this pursuit may be clinically ineffective—decreasing amyloid burden in patients with an already significant degree of cognitive deficits, and hence neurodegeneration, does not appear to dampen the rate of decline (Holmes et al., 2008). This was most recently found during Phase 3 of a clinical trial for Solanezumab (Doody et al., 2014). Aducanumab, a fully human IgG isolated from cognitively normal donors that binds a

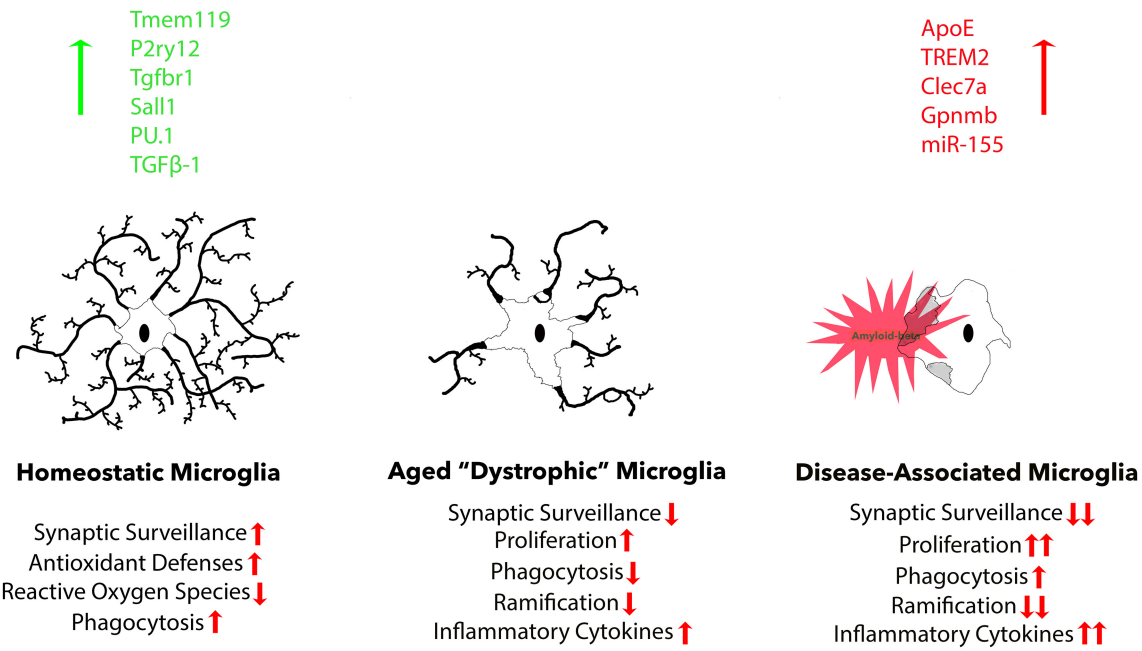

FIGURE 2 | Three common microglia phenotypes are described. Homeostatic microglia are found in the adult brain under non-infectious, non-diseased, and non-aged conditions, exhibiting robust expression of homeostatic microglial markers: Tmem119, P2ry12, Tgfbr1, and transcription factor Sall1. During normal aging, homeostatic markers gradually decline, resulting in reduced functional aspects, including proliferation, phagocytosis, ramification, and cytokine secretion. Finally, there is a distinct microglia phenotype that is associated with neurodegeneration that possesses a more exacerbated dystrophic phenotype, but is specifically associated with plaques and dystrophic neurites that cause neurodegeneration.

conformational epitope of Aβ, is currently in Phase 3 trials (Sevigny et al., 2016). Neurofibrillary tangles (NFTs), the second pathological hallmark of AD, are another promising target for pharmacological intervention. Several classes of pharmacologic agents may be effective in preventing both the aggregation and spread of NFTs in AD. Small molecule drugs, that work by binding to tau to inhibit its aggregation, are currently being developed (Harrington et al., 2015). Additionally, several tau vaccines are also currently in development, with one entering Phase II of clinical trial (Theunis et al., 2013; Kontsekova et al., 2014).

Pharmacological modulation targeting the intracellular trafficking of APP via intervention on the enzymes involved in its cleavage may also be successful in regulating Aβ accumulation. APP is not exclusively found on the cell surface; it is most frequently localized to the trans-Golgi network (TGN) (Caporaso et al., 1994; Hartmann et al., 1997; Xu et al., 1997). After shuttling to the plasma membrane, APP is reinternalized into endosomes and, eventually, lysosomes (Haass et al., 1993a,b; Koo and Squazzo, 1994), where Aβ production primarily occurs (Huse et al., 2000, 2002). Therefore, enhanced sequestering of APP to the plasma membrane and out of the TGN is a potential therapeutic venue for AD. Currently, there are no drugs in development targeting this mechanism. TPI-287, a microtubule-stabilizing agent, is a unique drug, which influences APP intracellular trafficking, and may also facilitate kinesin-mediated axonal transport of APP (Zempel and Mandelkow, 2014).

Strategies for Targeting Microglia and Neuroinflammation

Given the overwhelming evidence supporting the role of microglia in the pathogenesis of neurodegenerative functions, it is of interest to discuss potential therapeutic interventions targeting the neurotoxic effects of microglia.

One strategy is to pharmacologically enhance microglial clearance of protein aggregates. Sargramostim is a synthetic form of the hematopoietic growth factor granulocyte-macrophage colony-stimulating factor (GM-CSF), which is FDA approved to increase white blood cell count after chemotherapy (Markovic et al., 2008). Evidence suggests that GM-CSF stimulates phagocytosis of Aβ via bone-marrow derived macrophages and microglia (Mitrasinovic et al., 2001), although GM-CSF may also potentially exacerbate their inflammatory response. Sargramostim was entered into two Phase 2 clinical trials to assess treatment and safety in patients with mild cognitive impairment or AD. One of these trials has since been withdrawn. Valproic acid, an anticonvulsant medication which exerts its function via inhibition of voltage-gated sodium channels and increases levels of gamma-aminobutyric acid (Löscher, 2002), can enhance microglial phagocytosis of Aβ, although it has not yet been tested in clinical trials. Additionally, vasoactive intestinal peptide, a multifunctional neuropeptide, which can enhance microglial phagocytosis, while suppressing the production of TNF-α and ROS (Song et al., 2012), could also be effective for restoring homeostatic microglial functions.

Gotz et al. previously demonstrates the acceleration of NFT formation by Aβ injection into the mouse brain (Götz et al., 2001). This finding was validated in a double transgenic mouse model. The model was created by crossing P301L tau mice with APP mice expressing the familial Swedish mutations of APP (K670N and M671L), resulting in a marked acceleration in tau pathology development (Lewis et al., 2001). The same result was reported in a different double transgenic model, created by crossed PS19 mice with APPV717F mice (Hurtado et al., 2010). The potential contribution of microglia to accelerate tau pathology in the presence of Aβ accumulation has yet to be tested. The spread of pathogenic tau protein may be facilitated by phagocytic microglia, which are activated by Aβ accumulation in the brain.

Immune cells, including microglia, are highly efficient in secreting extracellular vesicles, such as exosomes and ectosomes (Robbins and Morelli, 2014; Greening et al., 2015). Research has shown that microglia promote the spread of pathological protein aggregates through exosomes (Sarko and McKinney, 2017; Soria et al., 2017). Exosomes are extracellular vesicles that are between 30 and 150 nm in size (Zomer et al., 2010; Vlassov et al., 2012; Thompson et al., 2016) and possess a myriad of roles in the CNS and periphery (Budnik et al., 2016). They are frequently excreted by antigen-presenting cells, such as microglia (Nair-Gupta et al., 2014), but are also secreted by all other cells of the CNS (Frühbeis et al., 2012). In AD, microglia have been shown to congregate around senile plaques in order to phagocytose them, consequently secreting Aβ oligomer-containing exosomes (Rajendran et al., 2006). Exosomes isolated from AD brains also contain hyper-phosphorylated tau oligomers (Saman et al., 2012), which are interestingly found in the CSF of AD patients (Saman et al., 2012; Fiandaca et al., 2015). In ALS, exosomal TDP-43 is increased, suggesting that pathological protein-containing exosomes play a role in several neurodegenerative disorders (Iguchi et al., 2016). Exosomal spread is the proposed mechanism through which microglia enhance tau propagation in mouse models of AD (Asai et al., 2015). In this study, depletion of microglia was demonstrated to reduce the spread of AAV-induced tau pathology from the medial entorhinal cortex to the dentate gyrus.

Inhibiting microglia-mediated exosome excretion may show promising results in halting disease progression in neurodegenerative disorders. Pharmacological inhibition, via GW4869, of neutral sphingomyelinase 2 (nSMase2), which synthesizes ceramide from sphingomyelin and is critical for exosome synthesis, successfully halted the packaging of human tau into exosomes in microglia (Asai et al., 2015). In addition to preventing exosome-mediated tau propagation, GW4869 also attenuates the release of pro-inflammatory cytokines in macrophages in response to LPS, while not appearing to have potent cytotoxic affects (Essandoh et al., 2015). Increased exosome secretion was demonstrated to enhance spread of prion protein in cell culture (Guo et al., 2016), which was prevented via treatment with GW4869. Evidence for the role of exosomes in prion disease, including ALS, have been presented (Vella et al., 2007; Guo et al., 2016; Iguchi et al., 2016). However, administration of GW4869 in a mouse model of ALS expressing human mutant TDP-43^{A315T} (autosomal mutation of ALS), appeared to worsen disease phenotypes, increase levels of insoluble TDP-43, and cause cytoplasmic accumulation of TDP-43 in neurons (Iguchi et al., 2016). GW4869 was also reported to disrupt synaptic connections (Tabatadze et al., 2010), suggesting potential CNS damage with this compound. The compound impaired spatial memory, as assessed via the Morris Water maze, but not spatial recognition memory, tested in the Y maze. Chronic exposure of GW4869 was also reported to have no effect on novel object recognition (Iguchi et al., 2016), suggesting inconclusive results. An alternative strategy is necessary for regulating exosomes synthesis and secretion.

Preventing the pathogenic change in microglial phenotype and infiltration of peripheral monocytes in neurodegenerative conditions is another promising strategy. Long-term use of non-steroidal anti-inflammatory drugs (NSAIDs) was classically recognized to reduce the risk of developing AD and PD by two meta-analysis studies (Chen et al., 2005; Vlad et al., 2008). However, this was not fully reproduced in clinical trials (Vlad et al., 2008; Imbimbo et al., 2010; Breitner et al., 2011).

Cumulatively, these studies have led scientists to question whether microglia are insufficient for clearing proteinopathies, or if they engage in a mechanism that progresses the pathology. This question is complex and must incorporate the findings of cutting-edge studies, which have used the depletion of microglia via CSF1R inhibitors (PLX3397 and PLX5622 among others), to assess the role of microglia in proteinopathies and disease pathogenesis. These compounds are able to deplete virtually all microglia in the CNS after as little as 1 week of oral administration without significant side effects (Elmore et al., 2014; Dagher et al., 2015; Olmos-Alonso et al., 2016). No abnormal behaviors were observed in wild type mice, even after two months of treatment with PLX3397, as evaluated by contextual fear conditioning, elevated plus maze, open field, and Barnes maze (Elmore et al., 2014). Microglia depletion appeared to block disease-mediated increases in exploratory activity of mice, suggesting this may have a beneficial effect on cognition without significantly affecting amyloid burden (Grathwohl et al., 2009; Dagher et al., 2015; Olmos-Alonso et al., 2016; Spangenberg et al., 2016). CSF1R inhibitors are currently on clinical trials for oncology and joint neoplasm indications, but not for AD or other neurodegenerative disorders. No apparent side effects were detected in treated groups. Cognitive evaluations of patients in these trials will provide us with better information on the effects of microglia have on mental capacity.

Interestingly, replacement of microglia was tested as a means of protecting against excitotoxic injury with success (Vinet et al., 2012). In this study, microglia-deprived hippocampal slice cultures where infiltrated by exogenous microglia. Given that ROS production in microglia is deleterious, one therapeutic strategy may be to inhibit NOX (Altenhöfer et al., 2015). NADPH oxidase is largely responsible for ROS production in microglia in response to LPS (Qin et al., 2004). Furthermore, NOX activity was found to correlate with cognitive impairment

in AD, while KO of *NOX* was associated with a reduction in cognitive impairment (Bordt and Polster, 2014). Studies have reported that treatment with the NOX inhibitor apocymin leads to a reduction in amyloid burden, reduced overall microglia number, and reduced cerebral amyloid angiopathy in an AD mouse model (Han et al., 2015). In addition, delivery of adeno-associated virus (AAV) containing CD200, a glycoprotein involved in maintaining a quiescent state in microglia, into the hippocampus of 6-month old Tg2576 APP mice resulted in increased neurogenesis and reduced amyloidosis (Varnum et al., 2015). Microglia were also treated with CD200 *in vitro*, which enhanced their phagocytosis and promoted an M2-like phenotype. These studies support the notion that aged microglia are largely ineffective in the brain and are incapable of significantly reducing amyloid burden. Furthermore, their inflammatory presence serves only to exacerbate cytotoxicity of neurons, leading to increased neuronal loss and cognitive impairment. More thorough assessment of these findings may be necessary, but ample evidence exists to suggest that microglia presence in the CNS is detrimental in the context of neurodegenerative disease.

This notion should be considered when interpreting AD research assessing microglial dysfunction, such as studies examining the effect of TREM2 disruption in animal models of amyloidosis. Results of these studies were controversial, with some stipulating that TREM2 in microglia increase phagocytosis and clearance of Aβ (Wang et al., 2015; Xiang et al., 2016; Yuan et al., 2016), while others have suggested that disruption of TREM2 reduces amyloid plaque load (Ulrich et al., 2014; Jay et al., 2015; Krasemann et al., 2017). These differences could be caused by the different functional role of TREM2 at the various stages of Aβ accumulation in the brain. TREM2 is up-regulated in the brains of AD patients and several mutations have been identified risk factors for late-onset AD (Frischmeyer-Guerrerio et al., 2013). TREM2 expression is increased in plaque-associated microglia (Guerreiro et al., 2013) and in particular, in the processes of microglia which are in direct contact with plaques (Yuan et al., 2016). TREM2 disruption has also been shown to reduce the overall amount of plaque-associated microglia (Krasemann et al., 2017). These were unexpected results since phagocytosis of not only Aβ, but a number of other molecules recognized by phagocytes, is dependent on TREM2 (Kleinberger et al., 2014; Xiang et al., 2016; Yuan et al., 2016; Varnum et al., 2017). However, it is important to note that complete depletion of microglia has repeatedly failed to influence overall amyloid deposition (Grathwohl et al., 2009; Dagher et al., 2015; Olmos-Alonso et al., 2016). If *TREM2* KO confers a dysfunctional microglia phenotype, which results in increased amyloid burden, then this effect is likely to be caused by the functional activity of microglia (Krasemann et al., 2017). One possibility is the anti-inflammatory effect of TREM2 signaling. Expression of pro-inflammatory cytokines IL-1β, IL-6, and TNF-α in response to challenge with Aβ42 was shown to be drastically increased due to knockdown with DAP12/TYROBP and synergized with *TREM2* KO (Zhong et al., 2017a). This also supports the notion that Aβ42 is a ligand for TREM2, although one study reported that the TREM2-TYROBP association is not affected by Aβ presence in cell culture. However, it has also been shown that TREM2 is down-regulated in primary microglia cultures in response to Aβ42 (Zheng et al., 2016), which was prevented with treatment with a JNK inhibitor (Zhong et al., 2017a). JNK inhibitors are proposed as a possible therapeutic target for AD (Yarza et al., 2015) and have entered clinical trials for a number of indications, but have no approvals to date. Nonetheless, research has repeatedly suggested that TREM2 is upregulated in disease-associated microglia (Frank et al., 2008; Frischmeyer-Guerrerio et al., 2013; Krasemann et al., 2017). These findings support the notion that dysfunctional microglia in disease contribute to a cytotoxic environment through the release of pro-inflammatory cytokines and ROS. The connection between APOE, TREM2, and microglia will continue to be investigated.

The contribution of circulating peripheral monocytes to the microglia population in the CNS has been thoroughly investigated and shown to function through parabiotic mechanisms. In these experiments, the blood streams of two mice are connected, where one mouse contains a reporter in circulating monocytes that allows them to be distinguished from those of the partner. One study found low levels of monocyte infiltration after full body irradiation in mice (Hess et al., 2004), while another study attempted the same experiment and did not find evidence of any CNS penetration (Ajami et al., 2007). Two mouse models of microgliosis, facial nerve axotomy and mSOD, did not provide any evidence of CNS penetration either. Reports were also released with evidence suggesting that bone-marrow transplanted myeloid cells can penetrate the CNS mainly when the BBB is compromised (Eglitis and Mezey, 1997; Brazelton et al., 2000; Ajami et al., 2007; Mildner et al., 2009). To test the effect of peripheral lymphocytes on amyloid clearance in brain, parabiosis experiments have been conducted in which the blood supply of young WT mice was connected to that of older APP mice. These experiments did not result in a reduction in amyloid burden, suggesting that immune infiltration of circulating monocytes is not a significant factor (Middeldorp et al., 2016). If circulating monocytes are unable to penetrate the BBB without significant damage to the BBB, this is unlikely to be a factor in neurodegenerative diseases, but could be applicable to other neurologic disorders with BBB impairment, such as traumatic brain injury or stroke.

CONCLUSION

Microglia are an important aspect of CNS homeostasis, damage repair, proteinostasis, and proteopathy in aging. The aged brain shows changes in microglial phenotype, which are associated with changes in protein clearance, misfolding, aggregation, and spread. Proteopathy and neuronal cell loss in neurodegenerative conditions also contribute to a shift in microglial phenotype from homeostatic to pathological, which permanently leads to harmful inflammatory responses and further promotes

cortical degeneration. This mechanism provides us with novel therapeutic targets for AD and related proteopathies.

AUTHOR CONTRIBUTIONS

KC and AV contributed equally to the manuscript. TI wrote and edited the manuscript. All authors listed have approved this work for publication.

ACKNOWLEDGMENTS

This work is in funded in part by National Institute of Health grants 5T32GM008541 (KC), 1RF1AG05419 and 1R01AG054672 (TI), Alzheimer's Association DVT-14-320835 (TI), BrightFocus Foundation A2016551S (TI), and Massachusetts Neuroscience Consortium (TI).

REFERENCES

Aderem, A., and Underhill, D. M. (1999). Mechanisms of Phagocytosis in Macrophages. *Annu. Rev. Immunol.* 17, 593–623. doi: 10.1146/annurev.immunol.17.1.593

Aguzzi, A., and Zhu, C. (2017). Microglia in prion diseases. *J. Clin. Invest.* 127, 3230–3239. doi: 10.1172/JCI90605

Ajami, B., Bennett, J. L., Krieger, C., Tetzlaff, W., and Rossi, F. M. V. (2007). Local self-renewal can sustain CNS microglia maintenance and function throughout adult life. *Nat. Neurosci.* 10, 1538–1543. doi: 10.1038/nn2014

Akira, S., and Takeda, K. (2004). Toll-like receptor signalling. *Nat. Rev. Immunol.* 4, 499–511. doi: 10.1038/nri1391

Alarcón, R., Fuenzalida, C., Santibá-ez, M., and von Bernhardi, R. (2005). Expression of scavenger receptors in glial cells: comparing the adhesion of astrocytes and microglia from neonatal rats to surface-bound β-amyloid. *J. Biol. Chem.* 280, 30406–30415. doi: 10.1074/jbc.M414686200

Altenhöfer, S., Radermacher, K. A., Kleikers, P. W. M., Wingler, K., and Schmidt, H. H. (2015). Evolution of NADPH oxidase inhibitors: selectivity and mechanisms for target engagement. *Antioxid. Redox Signal.* 23, 406–427. doi: 10.1089/ars.2013.5814

Asai, H., Ikezu, S., Tsunoda, S., Medalla, M., Luebke, J., Haydar, T., et al. (2015). Depletion of microglia and inhibition of exosome synthesis halt tau propagation. *Nat. Neurosci.* 18, 1584–1593. doi: 10.1038/nn.4132

Athan, E. S., Lee, J. H., Arriaga, A., Mayeux, R. P., and Tycko, B. (2002). Polymorphisms in the promoter of the human app gene: functional evaluation and allele frequencies in Alzheimer disease. *Arch. Neurol.* 59, 1793–1799. doi: 10.1001/archneur.59.11.1793

Bachstetter, A. D., Morganti, J. M., Jernberg, J., Schlunk, A., Mitchell, S. H., Brewster, K. W., et al. (2011). Fractalkine and CX(3)CR1 regulate hippocampal neurogenesis in adult and aged rats. *Neurobiol. Aging* 32, 2030–2044. doi: 10.1016/j.neurobiolaging.2009.11.022

Bard, F., Cannon, C., Barbour, R., Burke, R.-L., Games, D., Grajeda, H., et al. (2000). Peripherally administered antibodies against amyloid [beta]-peptide enter the central nervous system and reduce pathology in a mouse model of Alzheimer disease. *Nat. Med.* 6, 916–919. doi: 10.1038/78682

Bell-Temin, H., Culver-Cochran, A. E., Chaput, D., Carlson, C. M., Kuehl, M., Burkhardt, B. R., et al. (2015). Novel molecular insights into classical and alternative activation states of microglia as revealed by stable isotope labeling by Amino Acids in Cell Culture (SILAC)-based Proteomics. *Mol. Cell. Proteom.* 14, 3173–3184. doi: 10.1074/mcp.M115.053926

Bemiller, S. M., McCray, T. J., Allan, K., Formica, S. V., Xu, G., Wilson, G., et al. (2017). TREM2 deficiency exacerbates tau pathology through dysregulated kinase signaling in a mouse model of tauopathy. *Mol. Neurodegener.* 12:74. doi: 10.1186/s13024-017-0216-6

Bisht, K., Sharma, K. P., Lecours, C., Gabriela Sánchez, M., El Hajj, H., Milior, G., et al. (2016). Dark microglia: a new phenotype predominantly associated with pathological states. *Glia* 64, 826–839. doi: 10.1002/glia.22966

Blau, C. W., Cowley, T. R., O'Sullivan, J., Grehan, B., Browne, T. C., Kelly, L., et al. (2012). The age-related deficit in LTP is associated with changes in perfusion and blood-brain barrier permeability. *Neurobiol. Aging* 33, 1005.e23–1005.e35. doi: 10.1016/j.neurobiolaging.2011.09.035

Blobe, G. C., Schiemann, W. P., and Lodish, H. F. (2000). Role of Transforming Growth Factor β in Human Disease. *N. Eng. J. Med.* 342, 1350–1358. doi: 10.1056/NEJM200005043421807

Block, M. L., and Hong, J. S. (2007). Chronic microglial activation and progressive dopaminergic neurotoxicity. *Biochem. Soc. Trans.* 35:1127. doi: 10.1042/BST0351127

Bordt, E. A., and Polster, B. M. (2014). NADPH oxidase- and mitochondria-derived reactive oxygen species in proinflammatory microglial activation: a bipartisan affair? *Free Radic. Biol. Med.* 76, 34–46. doi: 10.1016/j.freeradbiomed.2014.07.033

Brazelton, T. R., Rossi, F. M. V., Keshet, G. I., and Blau, H. M. (2000). From marrow to brain: expression of neuronal phenotypes in adult mice. *Science* 290:1775. doi: 10.1126/science.290.5497.1775

Breitner, J. C., Baker, L. D., Montine, T. J., Meinert, C. L., Lyketsos, C. G., Ashe, K. H., et al. (2011). Extended results of the Alzheimer disease anti-inflammatory prevention trial (ADAPT). *Alzheim. Dement.* 7, 402–411. doi: 10.1016/j.jalz.2010.12.014

Bros, H., Millward, J. M., Paul, F., Niesner, R., and Infante-Duarte, C. (2014). Oxidative damage to mitochondria at the nodes of Ranvier precedes axon degeneration in *ex vivo* transected axons. *Exp. Neurol.* 261, 127–135. doi: 10.1016/j.expneurol.2014.06.018

Brown, G. C., and Neher, J. J. (2012). Eaten alive! Cell death by primary phagocytosis: 'phagoptosis'. *Trends Biochem. Sci.* 37, 325–332. doi: 10.1016/j.tibs.2012.05.002

Bruttger, J., Karram, K., Wörtge, S., Regen, T., Marini, F., Hoppmann, N., et al. (2015). Genetic cell ablation reveals clusters of local self-renewing microglia in the mammalian central nervous system. *Immunity* 43, 92–106. doi: 10.1016/j.immuni.2015.06.012

Budnik, V., Ruiz-Canada, C., and Wendler, F. (2016). Extracellular vesicles round off communication in the nervous system. *Nat. Rev. Neurosci.* 17, 160–172. doi: 10.1038/nrn.2015.29

Butchart, J., Brook, L., Hopkins, V., Teeling, J., Püntener, U., Culliford, D., et al. (2015). Etanercept in Alzheimer disease: a randomized, placebo-controlled, double-blind, phase 2 trial. *Neurology* 84, 2161–2168. doi: 10.1212/WNL.0000000000001617

Butovsky, O., Jedrychowski, M. P., Moore, C. S., Cialic, R., Lanser, A. J., Gabriely, G., et al. (2014). Identification of a unique TGF-β dependent molecular and functional signature in Microglia. *Nat. Neurosci.* 17, 131–143. doi: 10.1038/nn0914-1286d

Butovsky, O., Ziv, Y., Schwartz, A., Landa, G., Talpalar, A. E., Pluchino, S., et al. (2006). Microglia activated by IL-4 or IFN-γ differentially induce neurogenesis and oligodendrogenesis from adult stem/progenitor cells. *Mol. Cell. Neurosci.* 31, 149–160. doi: 10.1016/j.mcn.2005.10.006

Cagnin, A., Brooks, D. J., Kennedy, A. M., Gunn, R. N., Myers, R., Turkheimer, F. E., et al. (2001). *In-vivo* measurement of activated microglia in dementia. *Lancet* 358, 461–467. doi: 10.1016/S0140-6736(01)05625-2

Caldeira, C., Cunha, C., Vaz, A. R., Falcão, A. S., Barateiro, A., Seixas, E., et al. (2017). Key aging-associated alterations in primary Microglia response to beta-amyloid stimulation. *Front. Aging Neurosci.* 9:277. doi: 10.3389/fnagi.2017.00277

Caldeira, C., Oliveira, A. F., Cunha, C., Vaz, A. R., Falcão, A. S., Fernandes, A., et al. (2014). Microglia change from a reactive to an age-like phenotype with the time in culture. *Front. Cell. Neurosci.* 8:152. doi: 10.3389/fncel.2014.00152

Cao, T., Thomas, T. C., Ziebell, J. M., Pauly, J. R., and Lifshitz, J. (2012). Morphological and genetic activation of microglia after diffuse traumatic brain injury in the rat. *Neuroscience* 225, 65–75. doi: 10.1016/j.neuroscience.2012.08.058

Caporaso, G. L., Takei, K., Gandy, S. E., Matteoli, M., Mundigl, O., Greengard, P., et al. (1994). Morphologic and biochemical analysis of the intracellular

trafficking of the Alzheimer beta/A4 amyloid precursor protein. *J. Neurosci.* 14, 3122.

Carroll, M. C. (2004). The complement system in B cell regulation. *Mol. Immunol.* 41, 141–146. doi: 10.1016/j.molimm.2004.03.017

Cataldo, A. M., Peterhoff, C. M., Troncoso, J. C., Gomez-Isla, T., Hyman, B. T., and Nixon, R. A. (2000). Endocytic pathway abnormalities precede amyloid β deposition in sporadic Alzheimer's disease and down syndrome : differential effects of APOE genotype and presenilin mutations. *Am. J. Pathol.* 157, 277–286. doi: 10.1016/S0002-9440(10)64538-5

Chalermpalanupap, T., Kinkead, B., Hu, W. T., Kummer, M. P., Hammerschmidt, T., Heneka, M. T., et al. (2013). Targeting norepinephrine in mild cognitive impairment and Alzheimer's disease. *Alzheim. Res. Ther.* 5:21. doi: 10.1186/alzrt175

Chan, A., Magnus, T., and Gold, R. (2001). Phagocytosis of apoptotic inflammatory cells by microglia and modulation by different cytokines: mechanism for removal of apoptotic cells in the inflamed nervous system. *Glia* 33, 87–95. doi: 10.1002/1098-1136(20010101)33:1<87::AID-GLIA1008>3.0.CO;2-S

Chen, H., Cúrdia, V., and Ferrero, A. (2012). The macroeconomic effects of large-scale asset purchase programmes∗. *Econ. J.* 122, F289–F315. doi: 10.1111/j.1468-0297.2012.02549.x

Chen, H., Jacobs, E., Schwarzschild, M. A., McCullough, M. L., Calle, E. E., Thun, M. J., et al. (2005). Nonsteroidal antiinflammatory drug use and the risk for Parkinson's disease. *Ann. Neurol.* 58, 963–967. doi: 10.1002/ana.20682

Cherry, J. D., Olschowka, J. A., and O'Banion, M. K. (2014). Neuroinflammation and M2 microglia: the good, the bad, and the inflamed. *J. Neuroinflam.* 11:98. doi: 10.1186/1742-2094-11-98

Cherry, J. D., Olschowka, J. A., and O'Banion, M. K. (2015). Arginase 1+ microglia reduce Aβ plaque deposition during IL-1β-dependent neuroinflammation. *J. Neuroinflam.* 12:203. doi: 10.1186/s12974-015-0411-8

Chhor, V., Le Charpentier, T., Lebon, S., Oré, M.-V., Celador, I. L., Josserand, J., et al. (2013). Characterization of phenotype markers and neuronotoxic potential of polarised primary microglia *in vitro*. *Brain Behav. Immun.* 32, 70–85. doi: 10.1016/j.bbi.2013.02.005

Choi, J. Y., Kim, J. Y., Kim, J. Y., Park, J., Lee, W. T., and Lee, J. E. (2017). M2 phenotype microglia-derived cytokine stimulates proliferation and neuronal differentiation of endogenous stem cells in ischemic brain. *Exp. Neurobiol.* 26, 33–41. doi: 10.5607/en.2017.26.1.33

Coatrieux, C., Sanson, M., Negre-Salvayre, A., Parini, A., Hannun, Y., Itohara, S., et al. (2007). MAO-A-induced mitogenic signaling is mediated by reactive oxygen species, MMP-2, and the sphingolipid pathway. *Free Rad. Biol. Med.* 43, 80–89. doi: 10.1016/j.freeradbiomed.2007.03.036

Colton, C. A. (2009). Heterogeneity of microglial activation in the innate immune response in the brain. *J. Neuroimmune Pharmacol.* 4, 399–418. doi: 10.1007/s11481-009-9164-4

Conde, J. R., and Streit, W. J. (2006). Effect of aging on the microglial response to peripheral nerve injury. *Neurobiol. Aging.* 27, 1451–1461. doi: 10.1016/j.neurobiolaging.2005.07.012

Conductier, G., Blondeau, N., Guyon, A., Nahon, J.-L., and Rovère, C. (2010). The role of monocyte chemoattractant protein MCP1/CCL2 in neuroinflammatory diseases. *J. Neuroimmunol.* 224, 93–100. doi: 10.1016/j.jneuroim.2010.05.010

Dagher, N. N., Najafi, A. R., Kayala, K. M. N., Elmore, M. R. P., White, T. E., Medeiros, R., et al. (2015). Colony-stimulating factor 1 receptor inhibition prevents microglial plaque association and improves cognition in 3xTg-AD mice. *J. Neuroinflam.* 12:139. doi: 10.1186/s12974-015-0366-9

Damani, M. R., Zhao, L., Fontainhas, A. M., Amaral, J., Fariss, R. N., and Wong, W. T. (2011). Age-related alterations in the dynamic behavior of Microglia. *Aging Cell* 10, 263–276. doi: 10.1111/j.1474-9726.2010.00660.x

De Martinis, M., Franceschi, C., Monti, D., and Ginaldi, L. (2005). Inflamm-ageing and lifelong antigenic load as major determinants of ageing rate and longevity. *FEBS Lett.* 579, 2035–2039. doi: 10.1016/j.febslet.2005.02.055

Deane, R., Bell, R. D., Sagare, A., and Zlokovic, B. V. (2009). Clearance of amyloid-β peptide across the blood-brain barrier: implication for therapies in Alzheimer's disease. *CNS Neurol. Disord. Drug Targets* 8, 16–30. doi: 10.2174/187152709787601867

Deane, R., Wu, Z., Sagare, A., Davis, J., Du Yan, S., Hamm, K., et al. (2004). LRP/Amyloid β-Peptide interaction mediates differential brain efflux of Aβ isoforms. *Neuron* 43, 333–344. doi: 10.1016/j.neuron.2004.07.017

Delgado, M., and Ganea, D. (2003). Vasoactive intestinal peptide prevents activated microglia-induced neurodegeneration under inflammatory conditions: potential therapeutic role in brain trauma. *FASEB J.* 17, 1922–1924. doi: 10.1096/fj.02-1029fje

Desforges, N. M., Hebron, M. L., Algarzae, N. K., Lonskaya, I., and Moussa, C. E. H. (2012). Fractalkine mediates communication between pathogenic proteins and microglia: implications of anti-inflammatory treatments in different stages of neurodegenerative diseases. *Int. J. Alzheim. Dis.* 2012:345472. doi: 10.1155/2012/345472

Dewachter, I., Van Dorpe, J., Smeijers, L., Gilis, M., Kuipéri, C., Laenen, I., et al. (2000). Aging increased amyloid peptide and caused amyloid plaques in brain of old APP/V717I transgenic mice by a different mechanism than mutant Presenilin1. *J. Neurosci.* 20, 6452–6458.

Di Filippo, M., Tozzi, A., Costa, C., Belcastro, V., Tantucci, M., Picconi, B., et al. (2008). Plasticity and repair in the post-ischemic brain. *Neuropharmacology* 55, 353–362. doi: 10.1016/j.neuropharm.2008.01.012

Dijkstra, F. A., Hobbie, S. E., Knops, J. M. H., and Reich, P. B. (2004). Nitrogen deposition and plant species interact to influence soil carbon stabilization. *Ecol. Lett.* 7, 1192–1198. doi: 10.1111/j.1461-0248.2004.00679.x

Dimayuga, F. O., Wang, C., Clark, J. M., Dimayuga, E. R., Dimayuga, V. M., and Bruce-Keller, A. J. (2007). SOD1 overexpression alters ROS production and reduces neurotoxic inflammatory signaling in microglial cells. *J. Neuroimmunol.* 182, 89–99. doi: 10.1016/j.jneuroim.2006.10.003

Dodel, R., Rominger, A., Bartenstein, P., Barkhof, F., Blennow, K., Förster, S., et al. (2013). Intravenous immunoglobulin for treatment of mild-to-moderate Alzheimer's disease: a phase 2, randomised, double-blind, placebo-controlled, dose-finding trial. *Lancet Neurol.* 12, 233–243. doi: 10.1016/S1474-4422(13)70014-0

Dolev, I., and Michaelson, D. M. (2004). A nontransgenic mouse model shows inducible amyloid-β (Aβ) peptide deposition and elucidates the role of apolipoprotein E in the amyloid cascade. *Proc. Natl. Acad. Sci. U.S.A.* 101, 13909–13914. doi: 10.1073/pnas.0404458101

Donahue, J. E., Flaherty, S. L., Johanson, C. E., Duncan, J. A., Silverberg, G. D., Miller, M. C., et al. (2006). RAGE, LRP-1, and amyloid-beta protein in Alzheimer's disease. *Acta Neuropathol.* 112, 405–415. doi: 10.1007/s00401-006-0115-3

Doody, R. S., Thomas, R. G., Farlow, M., Iwatsubo, T., Vellas, B., Joffe, S., et al. (2014). Phase 3 Trials of Solanezumab for Mild-to-Moderate Alzheimer's Disease. *N. Engl. J. Med.* 370, 311–321. doi: 10.1056/NEJMoa1312889

Egensperger, R., Kösel, S., von Eitzen, U., and Graeber, M. B. (1998). Microglial activation in Alzheimer disease: association with APOE genotype. *Brain Pathol.* 8, 439–447. doi: 10.1111/j.1750-3639.1998.tb00166.x

Eglitis, M. A., and Mezey, É. (1997). Hematopoietic cells differentiate into both microglia and macroglia in the brains of adult mice. *Proc. Natl. Acad. Sci. U.S.A.* 94, 4080–4085. doi: 10.1073/pnas.94.8.4080

Eketjäll, S., Janson, J., Kaspersson, K., Bogstedt, A., Jeppsson, F., Fälting, J., et al. (2016). AZD3293: a novel, orally active BACE1 inhibitor with high potency and permeability and markedly slow off-rate kinetics. *J. Alzheim. Dis.* 50, 1109–1123. doi: 10.3233/JAD-150834

Elmore, M. R. P., Najafi, A. R., Koike, M. A., Dagher, N. N., Spangenberg, E. E., Rice, R. A., et al. (2014). CSF1 receptor signaling is necessary for microglia viability, which unmasks a cell that rapidly repopulates the microglia-depleted adult brain. *Neuron* 82, 380–397. doi: 10.1016/j.neuron.2014.02.040

Enciu, A.-M., Gherghiceanu, M., and Popescu, B. O. (2013). Triggers and effectors of oxidative stress at blood-brain barrier level: relevance for brain ageing and neurodegeneration. *Oxid. Med. Cell. Longev.* 2013:297512. doi: 10.1155/2013/297512

Essandoh, K., Yang, L., Wang, X., Huang, W., Qin, D., Hao, J., et al. (2015). Blockade of exosome generation with GW4869 dampens the sepsis-induced inflammation and cardiac dysfunction. *Biochim. Biophys. Acta* 1852, 2362–2371. doi: 10.1016/j.bbadis.2015.08.010

Euler, Z., and Schuitemaker, H. (2012). Cross-reactive broadly neutralizing antibodies: timing is everything. *Front. Immunol.* 3:215. doi: 10.3389/fimmu.2012.00215

Fan, Y., Xie, L., and Chung, C. Y. (2017). Signaling pathways controlling Microglia chemotaxis. *Mol. Cells* 40, 163–168. doi: 10.14348/molcells.2017.0011

Ferretti, M. T., Allard, S., Partridge, V., Ducatenzeiler, A., and Cuello, A. C. (2012). Minocycline corrects early, pre-plaque neuroinflammation and inhibits

BACE-1 in a transgenic model of Alzheimer's disease-like amyloid pathology. *J. Neuroinflammation* 9, 1–16. doi: 10.1186/1742-2094-9-62

Fiandaca, M. S., Kapogiannis, D., Mapstone, M., Boxer, A., Eitan, E., Schwartz, J. B., et al. (2015). Identification of pre-clinical Alzheimer's disease by a profile of pathogenic proteins in neurally-derived blood exosomes: a case-control study. *Alzheim. Dement.* 11, 600–607.e1. doi: 10.1016/j.jalz.2014.06.008

Floden, A. M., and Combs, C. K. (2011). Microglia demonstrate age-dependent interaction with Beta-amyloid fibrils. *J. Alzheim. Dis.* 25, 279–293. doi: 10.3233/JAD-2011-101014

Fontainhas, A. M., Wang, M., Liang, K. J., Chen, S., Mettu, P., Damani, M., et al. (2011). Microglial morphology and dynamic behavior is regulated by ionotropic glutamatergic and GABAergic neurotransmission. *PLoS ONE* 6:e15973. doi: 10.1371/journal.pone.0015973

Ford, A. L., Goodsall, A. L., Hickey, W. F., and Sedgwick, J. D. (1995). Normal adult ramified microglia separated from other central nervous system macrophages by flow cytometric sorting. Phenotypic differences defined and direct *ex vivo* antigen presentation to myelin basic protein-reactive CD4+ T cells compared. *J. Immunol.* 154:4309.

Franceschi, C., BonafÈ, M., Valensin, S., Olivieri, F., De Luca, M., Ottaviani, E., et al. (2000). Inflamm-aging: an evolutionary perspective on immunosenescence. *Ann. N.Y. Acad. Sci.* 908, 244–254. doi: 10.1111/j.1749-6632.2000.tb06651.x

Franco, R., and Fernández-Suárez, D. (2015). Alternatively activated microglia and macrophages in the central nervous system. *Progr. Neurobiol.* 131(Suppl. C), 65–86. doi: 10.1016/j.pneurobio.2015.05.003

Frank, S., Burbach, G. J., Bonin, M., Walter, M., Streit, W., Bechmann, I., et al. (2008). TREM2 is upregulated in amyloid plaque-associated microglia in aged APP23 transgenic mice. *Glia* 56, 1438–1447. doi: 10.1002/glia.20710

Fraser, H. B., Moses, A. M., and Schadt, E. E. (2010). Evidence for widespread adaptive evolution of gene expression in budding yeast. *Proc. Natl. Acad. Sci. U.S.A.* 107, 2977–2982. doi: 10.1073/pnas.0912245107

Frischmeyer-Guerrerio, P. A., Guerrerio, A. L., Oswald, G., Chichester, K., Myers, L., Halushka, M. K., et al. (2013). TGFβ receptor mutations impose a strong predisposition for Human Allergic Disease. *Sci. Transl. Med.* 5:195ra94. doi: 10.1126/scitranslmed.3006448

Frühbeis, C., Fröhlich, D., and Krämer-Albers, E.-M. (2012). Emerging roles of exosomes in Neuron–Glia communication. *Front. Physiol.* 3:119. doi: 10.3389/fphys.2012.00119

Fu, R., Shen, Q., Xu, P., Luo, J. J., and Tang, Y. (2014). Phagocytosis of microglia in the central nervous system diseases. *Mol. Neurobiol.* 49, 1422–1434. doi: 10.1007/s12035-013-8620-6

Fuhrmann, M., Bittner, T., Jung, C. K. E., Burgold, S., Page, R. M., Mitteregger, G., et al. (2010). Microglial Cx3cr1 knockout prevents neuron loss in a mouse model of Alzheimer's disease. *Nat. Neurosci.* 13, 411–413. doi: 10.1038/nn.2511

Gandhi, S., and Abramov, A. Y. (2012). Mechanism of oxidative stress in neurodegeneration. *Oxid. Med. Cell. Longev.* 2012:428010. doi: 10.1155/2012/428010

Gasque, P. (2004). Complement: a unique innate immune sensor for danger signals. *Mol. Immunol.* 41, 1089–1098. doi: 10.1016/j.molimm.2004.06.011

Gilgun-Sherki, Y., Melamed, E., and Offen, D. (2001). Oxidative stress induced-neurodegenerative diseases: the need for antioxidants that penetrate the blood brain barrier. *Neuropharmacology* 40, 959–975. doi: 10.1016/S0028-3908(01)00019-3

Gilham, D., Wasiak, S., Tsujikawa, L. M., Halliday, C., Norek, K., Patel, R. G., et al. (2016). RVX-208, a BET-inhibitor for treating atherosclerotic cardiovascular disease, raises ApoA-I/HDL and represses pathways that contribute to cardiovascular disease. *Atherosclerosis* 247, 48–57. doi: 10.1016/j.atherosclerosis.2016.01.036

Ginhoux, F., Greter, M., Leboeuf, M., Nandi, S., See, P., Gokhan, S., et al. (2010). Fate mapping analysis reveals that adult microglia derive from primitive macrophages. *Science* 330, 841–845. doi: 10.1126/science.1194637

Ginhoux, F., Lim, S., Hoeffel, G., Low, D., and Huber, T. (2013). Origin and differentiation of microglia. *Front. Cell. Neurosci.* 7:45. doi: 10.3389/fncel.2013.00045

Giunta, B., Fernandez, F., Nikolic, W. V., Obregon, D., Rrapo, E., Town, T., et al. (2008). Inflammaging as a prodrome to Alzheimer's disease. *J. Neuroinflam.* 5:51. doi: 10.1186/1742-2094-5-51

Glass, C. K., Saijo, K., Winner, B., Marchetto, M. C., and Gage, F. H. (2010). Mechanisms Underlying Inflammation in Neurodegeneration. *Cell* 140, 918–934. doi: 10.1016/j.cell.2010.02.016

Godbout, J. P., Chen, J., Abraham, J., Richwine, A. F., Berg, B. M., Kelley, K. W., et al. (2005). Exaggerated neuroinflammation and sickness behavior in aged mice after activation of the peripheral innate immune system. *FASEB J.* 19, 1329–1331. doi: 10.1096/fj.05-3776fje

Godbout, J. P., Moreau, M., Lestage, J., Chen, J., Sparkman, N. L., O'Connor, J., et al. (2008). Aging exacerbates depressive-like behavior in mice in response to activation of the peripheral innate immune system. *Neuropsychopharmacology* 33, 2341–2351. doi: 10.1038/sj.npp.1301649

Goerdt, S., Politz, O., Schledzewski, K., Birk, R., Gratchev, A., Guillot, P., et al. (1999). Alternative versus classical activation of macrophages. *Pathobiology* 67, 222–226. doi: 10.1159/000028096

Goldmann, T., and Prinz, M. (2013). Role of Microglia in CNS Autoimmunity. *Clin. Develop. Immunol.* 2013:208093. doi: 10.1155/2013/208093

Gomez-Nicola, D., and Perry, V. H. (2015). Microglial dynamics and role in the healthy and diseased brain: a paradigm of functional plasticity. *Neuroscientist* 21, 169–184. doi: 10.1177/1073858414530512

Gosselin, D., Skola, D., Coufal, N. G., Holtman, I. R., Schlachetzki, J. C. M., Sajti, E., et al. (2017). An environment-dependent transcriptional network specifies human microglia identity. *Science* 356:eaal3222. doi: 10.1126/science.aal3222

Gottfried-Blackmore, A., Kaunzner, U. W., Idoyaga, J., Felger, J. C., McEwen, B. S., and Bulloch, K. (2009). Acute *in vivo* exposure to interferon-γ enables resident brain dendritic cells to become effective antigen presenting cells. *Proc. Natl. Acad. Sci. U.S.A.* 106, 20918–20923. doi: 10.1073/pnas.0911509106

Götz, J., Chen, F., van Dorpe, J., and Nitsch, R. M. (2001). Formation of neurofibrillary tangles in P301L Tau Transgenic mice induced by Aβ42 fibrils. *Science* 293:1491. doi: 10.1126/science.1062097

Grabert, K., Michoel, T., Karavolos, M. H., Clohisey, S., Baillie, J. K., Stevens, M. P., et al. (2016). Microglial brain region-dependent diversity and selective regional sensitivities to ageing. *Nat. Neurosci.* 19, 504–516. doi: 10.1038/nn.4222

Graeber, M. B., Li, W., and Rodriguez, M. L. (2011). Role of microglia in CNS inflammation. *FEBS Lett.* 585, 3798–3805. doi: 10.1016/j.febslet.2011.08.033

Grathwohl, S. A., Kälin, R. E., Bolmont, T., Prokop, S., Winkelmann, G., Kaeser, S. A., et al. (2009). Formation and maintenance of Alzheimer's disease β-amyloid plaques in the absence of microglia. *Nat. Neurosci.* 12, 1361–1363. doi: 10.1038/nn.2432

Greening, D. W., Gopal, S. K., Xu, R., Simpson, R. J., and Chen, W. (2015). Exosomes and their roles in immune regulation and cancer. *Sem. Cell Develop. Biol.* 40(Suppl. C), 72–81. doi: 10.1016/j.semcdb.2015.02.009

Guerreiro, R., Wojtas, A., Bras, J., Carrasquillo, M., Rogaeva, E., Majounie, E., et al. (2013). TREM2 Variants in Alzheimer's Disease. *N. Engl. J. Med.* 368, 117–127. doi: 10.1056/NEJMoa1211851

Guo, B. B., Bellingham, S. A., and Hill, A. F. (2016). Stimulating the release of exosomes increases the intercellular transfer of prions. *J. Biol. Chem.* 291, 5128–5137. doi: 10.1074/jbc.M115.684258

Haass, C., Hung, A. Y., Schlossmacher, M. G., Oltersdorf, T., Teplow, D. B., and Selkoe, D. J. (1993a). Normal cellular processing of the β-Amyloid precursor protein results in the secretion of the Amyloid β Peptide and related moleculesa. *Ann. N.Y. Acad. Sci.* 695, 109–116. doi: 10.1111/j.1749-6632.1993.tb23037.x

Haass, C., Hung, A. Y., Schlossmacher, M. G., Teplow, D. B., and Selkoe, D. J. (1993b). beta-Amyloid peptide and a 3-kDa fragment are derived by distinct cellular mechanisms. *J. Biol. Chem.* 268, 3021–3024.

Habchi, J., Arosio, P., Perni, M., Costa, A. R., Yagi-Utsumi, M., Joshi, P., et al. (2016). An anticancer drug suppresses the primary nucleation reaction that initiates the production of the toxic Aβ42 aggregates linked with Alzheimer's disease. *Sci. Adv.* 2:e1501244. doi: 10.1126/sciadv.1501244

Hafez, D., Huang, J. Y., Huynh, A. M., Valtierra, S., Rockenstein, E., Bruno, A. M., et al. (2011). Neprilysin-2 Is an important β-Amyloid degrading enzyme. *Am. J. Pathol.* 178, 306–312. doi: 10.1016/j.ajpath.2010.11.012

Halle, A., Hornung, V., Petzold, G. C., Stewart, C. R., Monks, B. G., Reinheckel, T., et al. (2008). The NALP3 inflammasome is involved in the innate immune response to amyloid-β. *Nat. Immunol.* 9, 857–865. doi: 10.1038/ni.1636

Han, B. H., Zhou, M.-L. Johnson, A. W., Singh, I., Liao, F., Vellimana, A. K., et al. (2015). Contribution of reactive oxygen species to cerebral amyloid angiopathy, vasomotor dysfunction, and microhemorrhage in aged Tg2576 mice. *Proc. Natl. Acad. Sci. U.S.A.* 112, E881–E890. doi: 10.1073/pnas.1414930112

Hanke, M. L., and Kielian, T. (2011). Toll-like receptors in health and disease in the brain: mechanisms and therapeutic potential. *Clin. Sci.* 121, 367–387. doi: 10.1042/CS20110164

Harrington, C. R., Storey, J. M. D., Clunas, S., Harrington, K. A., Horsley, D., Ishaq, A., et al. (2015). Cellular models of aggregation-dependent template-directed proteolysis to characterize tau aggregation inhibitors for treatment of Alzheimer disease. *J. Biol. Chem.* 290, 10862–10875. doi: 10.1074/jbc.M114.616029

Harrison, J. K., Jiang, Y., Chen, S., Xia, Y., Maciejewski, D., McNamara, R. K., et al. (1998). Role for neuronally derived fractalkine in mediating interactions between neurons and CX3CR1-expressing microglia. *Proc. Natl. Acad. Sci. U.S.A.* 95, 10896–10901. doi: 10.1073/pnas.95.18.10896

Harry, G. J., and Kraft, A. D. (2012). Microglia in the developing brain: a potential target with lifetime effects. *Neurotoxicology* 33, 191–206. doi: 10.1016/j.neuro.2012.01.012

Hart, A. D., Wyttenbach, A., Hugh Perry, V., and Teeling, J. L. (2012). Age related changes in microglial phenotype vary between CNS regions: grey versus white matter differences. *Brain Behav. Immun.* 26, 754–765. doi: 10.1016/j.bbi.2011.11.006

Hartmann, T., Bieger, S. C., Bruhl, B., Tienari, P. J., Ida, N., Allsop, D., et al. (1997). Distinct sites of intracellular production for Alzheimer's disease A[beta]40/42 amyloid peptides. *Nat. Med.* 3, 1016–1020. doi: 10.1038/nm0997-1016

Hayashi, Y., Ishibashi, H., Hashimoto, K., and Nakanishi, H. (2006). Potentiation of the NMDA receptor-mediated responses through the activation of the glycine site by microglia secreting soluble factors. *Glia* 53, 660–668. doi: 10.1002/glia.20322

Hayashi, Y., Yoshida, M., Yamato, M., Ide, T., Wu, Z., Ochi-Shindou, M., et al. (2008). Reverse of age-dependent memory impairment and mitochondrial DNA damage in microglia by an overexpression of human mitochondrial transcription factor A in mice. *J. Neurosci.* 28:8624. doi: 10.1523/JNEUROSCI.1957-08.2008

He, P., Cheng, X., Staufenbiel, M., Li, R., and Shen, Y. (2013). Long-term treatment of thalidomide ameliorates amyloid-like pathology through inhibition of β-secretase in a mouse model of Alzheimer's Disease. *PLoS ONE* 8:e55091. doi: 10.1371/journal.pone.0055091

Hefendehl, J. K., Neher, J. J., Sühs, R. B., Kohsaka, S., Skodras, A., and Jucker, M. (2014). Homeostatic and injury-induced microglia behavior in the aging brain. *Aging Cell* 13, 60–69. doi: 10.1111/acel.12149

Henry, C. J., Huang, Y., Wynne, A. M., and Godbout, J. P. (2009). Peripheral Lipopolysaccharide (LPS) challenge promotes microglial hyperactivity in aged mice that is associated with exaggerated induction of both pro-inflammatory IL-1β and anti-inflammatory IL-10 cytokines. *Brain Behav. Immun.* 23, 309–317. doi: 10.1016/j.bbi.2008.09.002

Hess, D. C., Abe, T., Hill, W. D., Studdard, A. M., Carothers, J., Masuya, M., et al. (2004). Hematopoietic origin of microglial and perivascular cells in brain. *Exp. Neurol.* 186, 134–144. doi: 10.1016/j.expneurol.2003.11.005

Hinwood, M., Morandini, J., Day, T. A., and Walker, F. R. (2012). Evidence that microglia mediate the neurobiological effects of chronic psychological stress on the medial prefrontal cortex. *Cereb. Cortex* 22, 1442–1454. doi: 10.1093/cercor/bhr229

Hoek, R. M., Ruuls, S. R., Murphy, C. A., Wright, G. J., Goddard, R., Zurawski, S. M., et al. (2000). Down-regulation of the macrophage lineage through interaction with OX2 (CD200). *Science* 290, 1768–1771. doi: 10.1126/science.290.5497.1768

Holmes, C., Boche, D., Wilkinson, D., Yadegarfar, G., Hopkins, V., Bayer, A., et al. (2008). Long-term effects of Aβ42 immunisation in Alzheimer's disease: follow-up of a randomised, placebo-controlled phase I trial. *Lancet* 372, 216–223. doi: 10.1016/S0140-6736(08)61075-2

Hong, S., Beja-Glasser, V. F., Nfonoyim, B. M., Frouin, A., Li, S., Ramakrishnan, S., et al. (2016). Complement and microglia mediate early synapse loss in alzheimer mouse models. *Science* 352, 712–716. doi: 10.1126/science.aad8373

Hooli, B. V., Mohapatra, G., Mattheisen, M., Parrado, A. R., Roehr, J. T., Shen, Y., et al. (2012). Role of common and rare APP DNA sequence variants in Alzheimer disease. *Neurology* 78, 1250–1257. doi: 10.1212/WNL.0b013e3182515972

Hori, Y., Takeda, S., Cho, H., Wegmann, S., Shoup, T. M., Takahashi, K., et al. (2015). A Food and Drug Administration-approved Asthma Therapeutic Agent Impacts Amyloid β in the Brain in a Transgenic Model of Alzheimer Disease. *J. Biol. Chem.* 290, 1966–1978. doi: 10.1074/jbc.M114.586602

Hsieh, J. (2012). Orchestrating transcriptional control of adult neurogenesis. *Genes Dev.* 26, 1010–1021. doi: 10.1101/gad.187336.112

Hurtado, D. E., Molina-Porcel, L., Iba, M., Aboagye, A. K., Paul, S. M., Trojanowski, J. Q., et al. (2010). Aβ accelerates the spatiotemporal progression of tau pathology and Augments Tau Amyloidosis in an Alzheimer Mouse Model. *Am. J. Pathol.* 177, 1977–1988. doi: 10.2353/ajpath.2010.100346

Huse, J. T., Liu, K., Pijak, D. S., Carlin, D., Lee, V. M. Y., and Doms, R. W. (2002). β-Secretase processing in the trans-golgi network preferentially generates truncated amyloid species that accumulate in Alzheimer's disease brain. *J. Biol. Chem.* 277, 16278–16284. doi: 10.1074/jbc.M111141200

Huse, J. T., Pijak, D. S., Leslie, G. J., Lee, V. M. Y., and Doms, R. W. (2000). Maturation and endosomal targeting of β-Site amyloid precursor protein-cleaving enzyme: the Alzheimer's disease β-secretase. *J. Biol. Chem.* 275, 33729–33737. doi: 10.1074/jbc.M004175200

Husemann, J., Loike, J. D., Anankov, R., Febbraio, M., and Silverstein, S. C. (2002). Scavenger receptors in neurobiology and neuropathology: their role on microglia and other cells of the nervous system. *Glia* 40, 195–205. doi: 10.1002/glia.10148

Iguchi, Y., Eid, L., Parent, M., Soucy, G., Bareil, C., Riku, Y., et al. (2016). Exosome secretion is a key pathway for clearance of pathological TDP-43. *Brain* 139, 3187–3201. doi: 10.1093/brain/aww237

Imbimbo, B. P., and Giardina, G. A. (2011). γ-Secretase Inhibitors and Modulators for the Treatment of Alzheimer's Disease: disappointments and hopes. *Curr. Top. Med. Chem.* 11, 1555–1570. doi: 10.2174/156802611795860942

Imbimbo, B. P., Hutter-Paier, B., Villetti, G., Facchinetti, F., Cenacchi, V., Volta, R., et al. (2009). CHF5074, a novel γ-secretase modulator, attenuates brain β-amyloid pathology and learning deficit in a mouse model of Alzheimer's disease. *Br. J. Pharmacol.* 156, 982–993. doi: 10.1111/j.1476-5381.2008.00097.x

Imbimbo, B. P., Solfrizzi, V., and Panza, F. (2010). Are NSAIDs useful to treat Alzheimer's disease or mild cognitive impairment? *Front. Aging Neurosci.* 2:19. doi: 10.3389/fnagi.2010.00019

Inoue, K., and Tsuda, M. (2012). Purinergic systems, neuropathic pain and the role of microglia. *Exp. Neurol.* 234, 293–301. doi: 10.1016/j.expneurol.2011.09.016

Izzo, N. J., Xu, J., Zeng, C., Kirk, M. J., Mozzoni, K., Silky, C., et al. (2014). Alzheimer's Therapeutics Targeting Amyloid Beta 1–42 Oligomers II: sigma-2/PGRMC1 Receptors Mediate Abeta 42 Oligomer Binding and Synaptotoxicity. *PLoS ONE* 9:e111899. doi: 10.1371/journal.pone.0111899

Janeway, C. A. (1992). The immune system evolved to discriminate infectious nonself from noninfectious self. *Immunol. Tod.* 13, 11–16. doi: 10.1016/0167-5699(92)90198-G

Jassam, Y. N., Izzy, S., Whalen, M., McGavern, D. B., and El Khoury, J. (2017). Neuroimmunology of traumatic brain injury: time for a paradigm shift. *Neuron* 95, 1246–1265. doi: 10.1016/j.neuron.2017.07.010

Jay, T. R., Miller, C. M., Cheng, P. J., Graham, L. C., Bemiller, S., and Broihier, M. L. (2015). TREM2 deficiency eliminates TREM2+ inflammatory macrophages and ameliorates pathology in Alzheimer's disease mouse models. *J. Exp. Med.* 212. doi: 10.1084/jem.20142322

Jin, J.-J., Kim, H.-D., Maxwell, J. A., Li, L., and Fukuchi, K.-I. (2008). Toll-like receptor 4-dependent upregulation of cytokines in a transgenic mouse model of Alzheimer's disease. *J. Neuroinflam.* 5, 23–23. doi: 10.1186/1742-2094-5-23

Johnson-Wood, K., Lee, M., Motter, R., Hu, K., Gordon, G., Barbour, R., et al. (1997). Amyloid precursor protein processing and Aβ(42) deposition in a transgenic mouse model of Alzheimer disease. *Proc. Natl. Acad. Sci. U.S.A.* 94, 1550–1555. doi: 10.1073/pnas.94.4.1550

Jonsson, T., Stefansson, H., Steinberg, S., Jonsdottir, I., Jonsson, P. V., Snaedal, J., et al. (2013). Variant of TREM2 associated with the risk of Alzheimer's disease. *N. Engl. J. Med.* 368, 107–116. doi: 10.1056/NEJMoa1211103

Justin, T. R., Josh, M. M., Adam, D. B., Charles, E. H., Melinda, M. P., Bethany, A. G., et al. (2011). CX3CR1 deficiency leads to impairment of hippocampal cognitive function and synaptic plasticity. *J. Neurosci.* 31, 16241–16250. doi: 10.1523/JNEUROSCI.3667-11.2011

Kalpouzos, G., Chételat, G., Baron, J.-C., Landeau, B., Mevel, K., Godeau, C., et al. (2009). Voxel-based mapping of brain gray matter volume and glucose metabolism profiles in normal aging. *Neurobiol. Aging* 30, 112–124. doi: 10.1016/j.neurobiolaging.2007.05.019

Kaminska, B., Mota, M., and Pizzi, M. (2016). Signal transduction and epigenetic mechanisms in the control of microglia activation during neuroinflammation. *Biochim. Biophys. Acta* 1862, 339–351. doi: 10.1016/j.bbadis.2015.10.026

Kamphuis, W., Mamber, C., Moeton, M., Kooijman, L., Sluijs, J. A., Jansen, A. H. P., et al. (2012). GFAP isoforms in adult mouse brain with a focus on neurogenic astrocytes and reactive astrogliosis in mouse models of Alzheimer disease. *PLoS ONE* 7:e42823. doi: 10.1371/journal.pone.0042823

Kao, A. W., Eisenhut, R. J., Martens, L. H., Nakamura, A., Huang, A., Bagley, J. A., et al. (2011). A neurodegenerative disease mutation that accelerates the clearance of apoptotic cells. *Proc. Natl. Acad. Sci. U.S.A.* 108, 4441–4446. doi: 10.1073/pnas.1100650108

Karperien, A., Ahammer, H., and Jelinek, H. (2013). Quantitating the subtleties of microglial morphology with fractal analysis. *Front. Cell. Neurosci.* 7:3. doi: 10.3389/fncel.2013.00003

Kaushik, S., and Cuervo, A. M. (2015). Proteostasis and aging. *Nat. Med.* 21, 1406–1415. doi: 10.1038/nm.4001

Keren-Shaul, H., Spinrad, A., Weiner, A., Matcovitch-Natan, O., Dvir-Szternfeld, R., Ulland, T. K., et al. (2017). A unique microglia type associated with restricting development of Alzheimer's disease. *Cell* 169, 1276–1290.e17. doi: 10.1016/j.cell.2017.05.018

Kern, A., Roempp, B., Prager, K., Walter, J., and Behl, C. (2006). Down-regulation of endogenous amyloid precursor protein processing due to cellular aging. *J. Biol. Chem.* 281, 2405–2413. doi: 10.1074/jbc.M505625200

Kigerl, K. A., de Rivero Vaccari, J. P., Dietrich, W. D., Popovich, P. G., and Keane, R. W. (2014). Pattern recognition receptors and central nervous system repair. *Exp. Neurol.* 258, 5–16. doi: 10.1016/j.expneurol.2014.01.001

Kim, S. U., and de Vellis, J. (2005). Microglia in health and disease. *J. Neurosci. Res.* 81, 302–313. doi: 10.1002/jnr.20562

Kitamura, R., Tsukamoto, K., Harada, K., Shimizu, A., Shimada, S., Kobayashi, T., et al. (2004). Mechanisms underlying the dysfunction of melanocytes in vitiligo epidermis: role of SCF/KIT protein interactions and the downstream effector, MITF-M. *J. Pathol.* 202, 463–475. doi: 10.1002/path.1538

Klegeris, A., Bissonnette, C. J., and McGeer, P. L. (2005). Modulation of human microglia and THP-1 cell toxicity by cytokines endogenous to the nervous system. *Neurobiol. Aging* 26, 673–682. doi: 10.1016/j.neurobiolaging.2004.06.012

Kleinberger, G., Brendel, M., Mracsko, E., Wefers, B., Groeneweg, L., Xiang, X., et al. (2017). The FTD-like syndrome causing TREM2 T66M mutation impairs microglia function, brain perfusion, and glucose metabolism. *EMBO J.* 36, 1837–1853. doi: 10.15252/embj.201796516

Kleinberger, G., Yamanishi, Y., Suárez-Calvet, M., Czirr, E., Lohmann, E., Cuyvers, E., et al. (2014). TREM2 mutations implicated in neurodegeneration impair cell surface transport and phagocytosis. *Sci. Transl. Med.* 6:243ra86. doi: 10.1126/scitranslmed.3009093

Koellhoffer, E. C., McCullough, L. D., and Ritzel, R. M. (2017). Old maids: aging and its impact on Microglia function. *Int. J. Mol. Sci.* 18:769. doi: 10.3390/ijms18040769

Koizumi, S., Ohsawa, K., Inoue, K., and Kohsaka, S. (2013). Purinergic receptors in microglia: functional modal shifts of microglia mediated by P2 and P1 receptors. *Glia* 61, 47–54. doi: 10.1002/glia.22358

Koizumi, S., Shigemoto-Mogami, Y., Nasu-Tada, K., Shinozaki, Y., Ohsawa, K., Tsuda, M., et al. (2007). UDP acting at P2Y(6) receptors is a mediator of microglial phagocytosis. *Nature* 446, 1091–1095. doi: 10.1038/nature05704

Kontsekova, E., Zilka, N., Kovacech, B., Novak, P., and Novak, M. (2014). First-in-man tau vaccine targeting structural determinants essential for pathological tau–tau interaction reduces tau oligomerisation and neurofibrillary degeneration in an Alzheimer's disease model. *Alzheim. Res. Ther.* 6, 44–44. doi: 10.1186/alzrt278

Koo, E. H., and Squazzo, S. L. (1994). Evidence that production and release of amyloid beta-protein involves the endocytic pathway. *J. Biol. Chem.* 269, 17386–17389.

Krasemann, S., Madore, C., Cialic, R., Baufeld, C., Calcagno, N., El Fatimy, R., et al. (2017). The TREM2-APOE pathway drives the transcriptional phenotype of dysfunctional microglia in neurodegenerative diseases. *Immunity* 47, 566–581.e9. doi: 10.1016/j.immuni.2017.08.008.

Kreutzberg, G. W. (1996). Microglia: a sensor for pathological events in the CNS. *Trends Neurosci.* 19, 312–318. doi: 10.1016/0166-2236(96)10049-7

Landsman, L., Bar-On, L., Zernecke, A., Kim, K.-W., Krauthgamer, R., Shagdarsuren, E., et al. (2009). CX3CR1 is required for monocyte homeostasis and atherogenesis by promoting cell survival. *Blood* 113:963. doi: 10.1182/blood-2008-07-170787

Lewis, J., Dickson, D. W., Lin, W.-L., Chisholm, L., Corral, A., Jones, G., et al. (2001). Enhanced Neurofibrillary Degeneration in Transgenic Mice Expressing Mutant Tau and APP. *Science* 293:1487. doi: 10.1126/science.1058189

Lewitus, G. M., Konefal, S. C., Greenhalgh, A. D., Pribiag, H., Augereau, K., and Stellwagen, D. (2016). Microglial TNFα suppresses cocaine-induced plasticity and behavioral sensitization. *Neuron* 90, 483–491. doi: 10.1016/j.neuron.2016.03.030

Leyns, C. E. G., Ulrich, J. D., Finn, M. B., Stewart, F. R., Koscal, L. J., Remolina Serrano, J., et al. (2017). TREM2 deficiency attenuates neuroinflammation and protects against neurodegeneration in a mouse model of tauopathy. *Proc. Natl. Acad. Sci. U.S.A.* 114, 11524–11529. doi: 10.1073/pnas.1710311114

Li, G., Bien-Ly, N., Andrews-Zwilling, Y., Xu, Q., Bernardo, A., Ring, K., et al. (2009). GABAergic interneuron dysfunction impairs hippocampal neurogenesis in adult apolipoprotein E4 knock-in mice. *Cell Stem Cell* 5, 634–645. doi: 10.1016/j.stem.2009.10.015

Li, R., Lindholm, K., Yang, L. B., Yue, X.,Citron, M., Yan, R., et al. (2004). Amyloid β peptide load is correlated with increased β-secretase activity in sporadic Alzheimer's disease patients. *Proc. Natl. Acad. Sci. U.S.A.* 101, 3632–3637. doi: 10.1073/pnas.0205689101

Lim, S.-H., Park, E., You, B., Jung, Y., Park, A. R., Park, S. G., et al. (2013). Neuronal Synapse Formation Induced by Microglia and Interleukin 10. *PLoS ONE* 8:e81218. doi: 10.1371/journal.pone.0081218

Liu, Z., Ran, Y., Huang, S., Wen, S., Zhang, W., Liu, X., et al. (2017). Curcumin protects against ischemic stroke by Titrating microglia/macrophage polarization. *Front. Aging Neurosci.* 9:233. doi: 10.3389/fnagi.2017.00233

Löscher, W. (2002). Animal models of epilepsy for the development of antiepileptogenic and disease-modifying drugs. A comparison of the pharmacology of kindling and post-status epilepticus models of temporal lobe epilepsy. *Epil. Res.* 50, 105–123.

Louveau, A., Smirnov, I., Keyes, T. J., Eccles, J. D., Rouhani, S. J., Peske, J. D., et al. (2015). Structural and functional features of central nervous system lymphatics. *Nature* 523, 337–341. doi: 10.1038/nature14432

Lu, Y.-C., Yeh, W.-C., and Ohashi, P. S. (2008). LPS/TLR4 signal transduction pathway. *Cytokine* 42, 145–151. doi: 10.1016/j.cyto.2008.01.006

Luo, C., Jian, C., Liao, Y., Huang, Q., Wu, Y., Liu, X., et al. (2017). The role of microglia in multiple sclerosis. *Neuropsychiatr. Dis. Treat.* 13, 1661–1667. doi: 10.2147/NDT.S140634

Lyons, A., Downer, E. J., Crotty, S., Nolan, Y. M., Mills, K. H. G., and Lynch, M. A. (2007). CD200 ligand–receptor interaction modulates microglial activation *in vivo* and *in vitro*: a role for IL-4. *J. Neurosci.* 27:8309. doi: 10.1523/JNEUROSCI.1781-07.2007

Lyons, A., Lynch, A. M., Downer, E. J., Hanley, R., O'Sullivan, J. B., Smith, A., et al. (2009). Fractalkine-induced activation of the phosphatidylinositol-3 kinase pathway attentuates microglial activation *in vivo* and *in vitro*. *J. Neurochem.* 110, 1547–1556. doi: 10.1111/j.1471-4159.2009.06253.x

Maccecchini, M. L., Chang, M. Y., Pan, C., John, V., Zetterberg, H., and Greig, N. H. (2012). Posiphen as a candidate drug to lower CSF amyloid precursor protein, amyloid-β peptide and τ levels: target engagement, tolerability and pharmacokinetics in humans. *J. Neurol. Neurosurg. Psychiatr.* 83, 894–902. doi: 10.1136/jnnp-2012-302589

Maher, F. O., Martin, D. S. D., and Lynch, M. A. (2004). Increased IL-1beta in cortex of aged rats is accompanied by downregulation of ERK and PI-3 kinase. *Neurobiol. Aging* 25, 795–806. doi: 10.1016/j.neurobiolaging.2003.08.007

Maher, F. O., Nolan, Y., and Lynch, M. A. (2005). Downregulation of IL-4-induced signalling in hippocampus contributes to deficits in LTP in the aged rat. *Neurobiol. Aging* 26, 717–728. doi: 10.1016/j.neurobiolaging.2004.07.002

Mamada, N., Tanokashira, D., Hosaka, A., Kametani, F., Tamaoka, A., and Araki, W. (2015). Amyloid β-protein oligomers upregulate the β-secretase, BACE1, through a post-translational mechanism involving its altered subcellular distribution in neurons. *Mol. Brain* 8:73. doi: 10.1186/s13041-015-0163-5

Mantovani, A., Sica, A., and Locati, M. (2005). Macrophage polarization comes of age. *Immunity* 23, 344–346. doi: 10.1016/j.immuni.2005.10.001

Mantovani, A., Sica, A., Sozzani, S., Allavena, P., Vecchi, A., and Locati, M. (2004). The chemokine system in diverse forms of macrophage activation and polarization. *Trends Immunol.* 25, 677–686. doi: 10.1016/j.it.2004.09.015

Markovic, S. N., Suman, V. J., Nevala, W. K., Geeraerts, L., Creagan, E. T., Erickson, L. A., et al. (2008). A dose-escalation study of aerosolized sargramostim in the treatment of metastatic melanoma: an NCCTG study. *Am. J. Clin. Oncol.* 31, 573–579. doi: 10.1097/COC.0b013e318173a536

Marr, R. A., Rockenstein, E., Mukherjee, A., Kindy, M. S., Hersh, L. B., Gage, F. H., et al. (2003). Neprilysin gene transfer reduces human amyloid pathology in transgenic mice. *J. Neurosci.* 23, 1992–1996.

Martinez, F. O., and Gordon, S. (2014). The M1 and M2 paradigm of macrophage activation: time for reassessment. *F1000Prime Rep.* 6:13. doi: 10.12703/P6-13

Martinon, F., Burns, K., and Tschopp, J. (2002). The Inflammasome: a molecular platform triggering activation of inflammatory caspases and processing of proIL-beta. *Mol. Cell* 10, 417–426.

Matcovitch-Natan, O., Winter, D. R., Giladi, A., Vargas Aguilar, S., Spinrad, A., Sarrazin, S., et al. (2016). Microglia development follows a stepwise program to regulate brain homeostasis. *Science* 353:aad8670. doi: 10.1126/science.aad8670

Mawuenyega, K. G., Sigurdson, W., Ovod, V., Munsell, L., Kasten, T., Morris, J. C., et al. (2010). Decreased clearance of CNS amyloid-β in Alzheimer's disease. *Science* 330, 1774–1774. doi: 10.1126/science.1197623

McLaurin, J., Kierstead, M. E., Brown, M. E., Hawkes, C. A., Lambermon, M. H. L., Phinney, A. L., et al. (2006). Cyclohexanehexol inhibitors of A[beta] aggregation prevent and reverse Alzheimer phenotype in a mouse model. *Nat. Med.* 12, 801–808. doi: 10.1038/nm1423

McNaughton, D., Knight, W., Guerreiro, R., Ryan, N., Lowe, J., Poulter, M., et al. (2012). Duplication of amyloid precursor protein (APP), but not prion protein (PRNP) gene is a significant cause of early onset dementia in a large UK series. *Neurobiol. Aging* 33:426.e13-426.e21. doi: 10.1016/j.neurobiolaging.2010.10.010

Mead, E. L., Mosley, A., Eaton, S., Dobson, L., Heales, S. J., and Pocock, J. M. (2012). Microglial neurotransmitter receptors trigger superoxide production in microglia; consequences for microglial–neuronal interactions. *J. Neurochem.* 121, 287–301. doi: 10.1111/j.1471-4159.2012.07659.x

Middeldorp, J., Lehallier, B., Villeda, S. A., Miedema, S. S., Evans, E., Czirr, E., et al. (2016). Preclinical assessment of young blood plasma for alzheimer disease. *JAMA Neurol.* 73, 1325–1333. doi: 10.1001/jamaneurol.2016.3185

Mildner, A., Huang, H., Radke, J., Stenzel, W., and Priller, J. (2017). P2Y12 receptor is expressed on human microglia under physiological conditions throughout development and is sensitive to neuroinflammatory diseases. *Glia* 65, 375–387. doi: 10.1002/glia.23097

Mildner, A., Mack, M., Schmidt, H., Brück, W., Djukic, M., Zabel, M. D., et al. (2009). CCR2+Ly-6Chi monocytes are crucial for the effector phase of autoimmunity in the central nervous system. *Brain* 132, 2487–2500. doi: 10.1093/brain/awp144

Miners, J. S., Barua, N., Kehoe, P. G., Gill, S., and Love, S. (2011). Aβ-degrading enzymes: potential for treatment of Alzheimer disease. *J. Neuropathol.Exp. Neurol.* 70, 944–959. doi: 10.1097/NEN.0b013e3182345e46

Mitchell, D., Bergendahl, G., Ferguson, W., Roberts, W., Higgins, T., Ashikaga, T., et al. (2016). A phase 1 trial of TPI 287 as a single agent and in combination with temozolomide in patients with refractory or recurrent neuroblastoma or medulloblastoma. *Pediatr. Blood Cancer* 63, 39–46. doi: 10.1002/pbc.25687

Mitrasinovic, O. M., Perez, G. V., Zhao, F., Lee, Y. L., Poon, C., and Murphy, G. M. (2001). Overexpression of Macrophage Colony-stimulating Factor Receptor on Microglial Cells Induces an Inflammatory Response. *J. Biol. Chem.* 276, 30142–30149. doi: 10.1074/jbc.M104265200

Mittelbronn, M., Dietz, K., J., Schluesener, H., and Meyermann, R. (2001). Local distribution of microglia in the normal adult human central nervous system differs by up to one order of magnitude. *Acta Neuropathol.* 101, 249–255.

Monro, O. R., Mackic, J. B., Yamada, S., Segal, M. B., Ghiso, J., Maurer, C., et al. (2002). Substitution at codon 22 reduces clearance of Alzheimer's amyloid-β peptide from the cerebrospinal fluid and prevents its transport from the central nervous system into blood. *Neurobiol. Aging* 23, 405–412. doi: 10.1016/S0197-4580(01)00317-7

Montagne, A., Barnes, S. R., Sweeney, M. D., Halliday, M. R., Sagare, A. P., Zhao, Z., et al. (2015). Blood-brain barrier breakdown in the aging human hippocampus. *Neuron* 85, 296–302. doi: 10.1016/j.neuron.2014.12.032

Morawski, M., Schilling, S., Kreuzberger, M., Waniek, A., Jäger, C., Koch, B. et al. (2014). Glutaminyl cyclase in human cortex: correlation with (pGlu)-Amyloid-β Load and cognitive decline in Alzheimer's disease. *J. Alzheim. Dis.* 39, 385–400. doi: 10.3233/JAD-131535

Mosher, K. I., and Wyss-Coray, T. (2014). Microglial dysfunction in brain aging and Alzheimer's disease. *Biochem. Pharmacol.* 88, 594–604. doi: 10.1016/j.bcp.2014.01.008

Nair-Gupta, P., Baccarini, A., Tung, N., Seyffer, F., Florey, O., Huang, Y., et al. (2014). TLR signals induce phagosomal MHC-I delivery from the endosomal recycling compartment to allow cross-presentation. *Cell* 158, 506–521. doi: 10.1016/j.cell.2014.04.054

Neumann, G., Noda, T., and Kawaoka, Y. (2009). Emergence and pandemic potential of swine-origin H1N1 influenza virus. *Nature* 459, 931–939. doi: 10.1038/nature08157

Neumann, M., Sampathu, D. M., Kwong, L. K., Truax, A. C., Micsenyi, M. C., Chou, T. T., et al. (2006). Ubiquitinated TDP-43 in frontotemporal lobar degeneration and amyotrophic lateral sclerosis. *Science* 314:130. doi: 10.1126/science.1134108

Nimmerjahn, F., and Ravetch, J. V. (2006). Fcγ receptors: old friends and new family members. *Immunity* 24, 19–28. doi: 10.1016/j.immuni.2005.11.010

Nisemblat, Y., Belinson, H., Dolev, I., and Michaelson, D. M. (2008). Activation of the Amyloid cascade by intracerebroventricular injection of the protease inhibitor phosphoramidon. *Neurodegener. Dis. Manag.* 5, 166–169. doi: 10.1159/000113692

Njie, e., G., Boelen, E., Stassen, F. R., Steinbusch, H. W. M., Borchelt, D. R., and Streit, W. J. (2012). *Ex vivo* cultures of microglia from young and aged rodent brain reveal age-related changes in microglial function. *Neurobiol. Aging* 33, 195.e1–195.12. doi: 10.1016/j.neurobiolaging.2010.05.008

Noda, M., Doi, Y., Liang, J., Kawanokuchi, J., Sonobe, Y., Takeuchi, H., et al. (2011). Fractalkine attenuates excito-neurotoxicity via microglial clearance of damaged neurons and antioxidant enzyme heme oxygenase-1 expression. *J. Biol. Chem.* 286, 2308–2319. doi: 10.1074/jbc.M110.169839

Nolan, Y., Maher, F. O., Martin, D. S., Clarke, R. M., Brady, M. T., Bolton, A. E., et al. (2005). Role of Interleukin-4 in regulation of age-related inflammatory changes in the Hippocampus. *J. Biol. Chem.* 280, 9354–9362. doi: 10.1074/jbc.M412170200

Nygaard, H. B., van Dyck, C. H., and Strittmatter, S. M. (2014). Fyn kinase inhibition as a novel therapy for Alzheimer's disease. *Alzheim. Res. Ther.* 6:8. doi: 10.1186/alzrt238

Ofengeim, D., Mazzitelli, S., Ito, Y., DeWitt, J. P., Mifflin, L., Zou, C., et al. (2017). RIPK1 mediates a disease-associated microglial response in Alzheimer's disease. *Proc. Natl. Acad. Sci. U.S.A.* 114, E8788–E8797. doi: 10.1073/pnas.1714175114

Okun, E., Griffioen, K. J., Gen Son, T., Lee, J.-H., Roberts, N. J., Mughal, M. R., et al. (2010). TLR2 activation inhibits embryonic neural progenitor cell proliferation. *J. Neurochem.* 114, 462–474. doi: 10.1111/j.1471-4159.2010.06778.x

Olmos-Alonso, A., Schetters, S. T. T., Sri, S., Askew, K., Mancuso, R., Vargas-Caballero, M., et al. (2016). Pharmacological targeting of CSF1R inhibits microglial proliferation and prevents the progression of Alzheimer's-like pathology. *Brain* 139, 891–907. doi: 10.1093/brain/awv379

Pan, X.-D., Zhu, Y.-G., Lin, N., Zhang, J., Ye, Q.-Y. Huang, H.-P., et al. (2011). Microglial phagocytosis induced by fibrillar β-amyloid is attenuated by oligomeric β-amyloid: implications for Alzheimer's disease. *Mol. Neurodegener.* 6:45. doi: 10.1186/1750-1326-6-45

Paolicelli, R. C., Bolasco, G., Pagani, F., Maggi, L., Scianni, M., Panzanelli, P., et al. (2011). Synaptic pruning by microglia is necessary for normal brain development. *Science* 333:1456. doi: 10.1126/science.1202529

Parkhurst, C. N., Yang, G., Ninan, I., Savas, J. N., Yates, J. R., Lafaille, J. J., et al. (2013). Microglia promote learning-dependent synapse formation through BDNF. *Cell* 155, 1596–1609. doi: 10.1016/j.cell.2013.11.030

Penn, A. A., Riquelme, P. A., Feller, M. B., and Shatz, C. J. (1998). Competition in retinogeniculate patterning driven by spontaneous activity. *Science* 279:2108. doi: 10.1126/science.279.5359.2108

Perry, V. H., and Teeling, J. (2013). Microglia and macrophages of the central nervous system: the contribution of microglia priming and systemic inflammation to chronic neurodegeneration. *Semin. Immunopathol.* 35, 601–612. doi: 10.1007/s00281-013-0382-8

Perry, V. H., Brown, M. C., and Gordon, S. (1987). The macrophage response to central and peripheral nerve injury. A possible role for macrophages in regeneration. *J. Exp. Med.* 165, 1218–1223.

Piccio, L., Buonsanti, C., Mariani, M., Cella, M., Gilfillan, S., Cross, A. H., et al. (2007). Blockade of TREM-2 exacerbates experimental autoimmune encephalomyelitis. *Eur. J. Immunol.* 37, 1290–1301. doi: 10.1002/eji.200636837

Polazzi, E., and Monti, B. (2010). Microglia and neuroprotection: from *in vitro* studies to therapeutic applications. *Progr. Neurobiol.* 92, 293–315. doi: 10.1016/j.pneurobio.2010.06.009

Ponomarev, E. D., Shriver, L. P., Maresz, K., and Dittel, B. N. (2005). Microglial cell activation and proliferation precedes the onset of CNS autoimmunity. *J. Neurosci. Res.* 81, 374–389. doi: 10.1002/jnr.20488

Praag, H. V., Shubert, T., Zhao, C., and Gage, F. H. (2005). Exercise enhances learning and hippocampal neurogenesis in aged mice. *J. Neurosci.* 25, 8680–8685. doi: 10.1523/JNEUROSCI.1731-05.2005

Qin, L., Liu, Y., Hong, J.-S., and Crews, F. T. (2013). NADPH oxidase and aging drive microglial activation, oxidative stress and dopaminergic neurodegeneration following systemic LPS administration. *Glia* 61, 855–868. doi: 10.1002/glia.22479

Qin, L., Liu, Y., Wang, T., Wei, S.-J., Block, M. L., Wilson, B., et al. (2004). NADPH oxidase mediates lipopolysaccharide-induced neurotoxicity and proinflammatory gene expression in activated Microglia. *J. Biol. Chem.* 279, 1415–1421. doi: 10.1074/jbc.M307657200

Rajendran, L., Honsho, M., Zahn, T. R., Keller, P., Geiger, K. D., Verkade, P., et al. (2006). Alzheimer's disease β-amyloid peptides are released in association with exosomes. *Proc. Natl. Acad. Sci. U.S.A.* 103, 11172–11177. doi: 10.1073/pnas.0603838103

Ransohoff, R. M. (2016). A polarizing question: do M1 and M2 microglia exist? *Nat. Neurosci.* 19, 987–991. doi: 10.1038/nn.4338

Ransohoff, R. M., and Perry, V. H. (2009). Microglial physiology: unique stimuli, specialized responses. *Annu. Rev. Immunol.* 27, 119–145. doi: 10.1146/annurev.immunol.021908.132528

Raper, D., Louveau, A., and Kipnis, J. (2016). How do meningeal lymphatic vessels drain the CNS? *Trends Neurosci.* 39, 581–586. doi: 10.1016/j.tins.2016.07.001

Ravichandran, K. S. (2010). Find-me and eat-me signals in apoptotic cell clearance: progress and conundrums. *J. Exp. Med.* 207, 1807–1817. doi: 10.1084/jem.20101157

Raz, N., Lindenberger, U., Rodrigue, K. M., Kennedy, K. M., Head, D., Williamson, A., et al. (2005). Regional brain changes in aging healthy adults: general trends, individual differences and modifiers. *Cereb. Cortex* 15, 1676–1689. doi: 10.1093/cercor/bhi044

Réu, P., Khosravi, A., Bernard, S., Mold, J. E., Salehpour, M., Alkass, K., et al. (2017). The lifespan and turnover of microglia in the human brain. *Cell Rep.* 20, 779–784. doi: 10.1016/j.celrep.2017.07.004

Ritzel, R. M., Patel, A. R., Pan, S., Crapser, J., Hammond, M., Jellison, E., et al. (2015). Age- and location-related changes in microglial function. *Neurobiol. Aging* 36, 2153–2163. doi: 10.1016/j.neurobiolaging.2015.02.016

Robbins, P. D., and Morelli, A. E. (2014). Regulation of immune responses by extracellular vesicles. *Nat. Rev. Immunol.* 14, 195–208. doi: 10.1038/nri3622

Rock, R. B., Gekker, G., Hu, S., Sheng, W. S., Cheeran, M., Lokensgard, J. R., et al. (2004). Role of Microglia in central nervous system infections. *Clin. Microbiol. Rev.* 17, 942–964. doi: 10.1128/CMR.17.4.942-964.2004

Rodgers, S. P., Born, H. A., Das, P., and Jankowsky, J. L. (2012). Transgenic APP expression during postnatal development causes persistent locomotor hyperactivity in the adult. *Mol. Neurodegener.* 7:28. doi: 10.1186/1750-1326-7-28

Rosczyk, H. A., Sparkman, N. L., and Johnson, R. W. (2008). Neuroinflammation and cognitive function in aged mice following minor surgery. *Exp. Gerontol.* 43, 840–846. doi: 10.1016/j.exger.2008.06.004

Rovelet-Lecrux, A., Hannequin, D., Raux, G., Meur, N. L., Laquerriere, A., Vital, A., et al. (2006). APP locus duplication causes autosomal dominant early-onset Alzheimer disease with cerebral amyloid angiopathy. *Nat. Genet.* 38, 24–26. doi: 10.1038/ng1718

Safaiyan, S., Kannaiyan, N., Snaidero, N., Brioschi, S., Biber, K., Yona, S., et al. (2016). Age-related myelin degradation burdens the clearance function of microglia during aging. *Nat. Neurosci.* 19, 995–998. doi: 10.1038/nn.4325

Sakono, M., and Zako, T. (2010). Amyloid oligomers: formation and toxicity of Aβ oligomers. *FEBS J.* 277, 1348–1358. doi: 10.1111/j.1742-4658.2010.07568.x

Salat, D. H., Buckner, R. L., Snyder, A. Z., Greve, D. N., Desikan, R. S. R., Busa, E., et al. (2004). Thinning of the cerebral cortex in aging. *Cereb. Cortex* 14, 721–730. doi: 10.1093/cercor/bhh032

Salmon, E., Garraux, G., Delbeuck, X., Collette, F., Kalbe, E., Zuendorf, G., et al. (2003). Predominant ventromedial frontopolar metabolic impairment in frontotemporal dementia. *Neuroimage* 20, 435–440. doi: 10.1016/S1053-8119(03)00346-X

Saman, S., Kim, W., Raya, M., Visnick, Y., Miro, S., Saman, S., et al. (2012). Exosome-associated Tau Is Secreted in Tauopathy Models and Is Selectively Phosphorylated in Cerebrospinal Fluid in Early Alzheimer Disease. *J. Biol. Chem.* 287, 3842–3849. doi: 10.1074/jbc.M111.277061

Sarko, D. K., and McKinney, C. E. (2017). Exosomes: origins and therapeutic potential for neurodegenerative disease. *Front. Neurosci.* 11:82. doi: 10.3389/fnins.2017.00082

Schafer, D. P., Lehrman, E. K., Kautzman, A. G., Koyama, R., Mardinly, A. R., Yamasaki, R., et al. (2012). Microglia sculpt postnatal neural circuits in an activity and complement-dependent manner. *Neuron* 74, 691–705. doi: 10.1016/j.neuron.2012.03.026

Scherzer, C. R., Offe, K., Gearing, M., Rees, H. D., Fang, G., Heilman, C. J., et al. (2004). Loss of apolipoprotein e receptor lr11 in alzheimer disease. *Arch. Neurol.* 61, 1200–1205. doi: 10.1001/archneur.61.8.1200

Schuck, F., Wolf, D., Fellgiebel, A., and Endres, K. (2016). Increase of α-secretase ADAM10 in platelets along cognitively healthy aging. *J. Alzheimers Dis.* 50, 817–826. doi: 10.3233/JAD-150737

Selkoe, D. J. (2002). Alzheimer's disease is a synaptic failure. *Science*, 298:789. doi: 10.1126/science.1074069

Sevigny, J., Chiao, P., Bussière, T., Weinreb, P. H., Williams, L., Maier, M., et al. (2016). The antibody aducanumab reduces Aβ plaques in Alzheimer's disease. *Nature* 537, 50–56. doi: 10.1038/nature19323

Shibata, M., Yamada, S., Kumar, S. R., Calero, M., Bading, J., Frangione, B., et al. (2000). Clearance of Alzheimer's amyloid-β(1-40) peptide from brain by LDL receptor–related protein-1 at the blood-brain barrier. *J. Clin. Invest.* 106, 1489–1499. doi: 10.1172/JCI10498

Shoji, H., Takao, K., Hattori, S., and Miyakawa, T. (2016). Age-related changes in behavior in C57BL/6J mice from young adulthood to middle age. *Mol. Brain* 9:11. doi: 10.1186/s13041-016-0191-9

Sierra, A., Abiega, O., Shahraz, A., and Neumann, H. (2013). Janus-faced microglia: beneficial and detrimental consequences of microglial phagocytosis. *Front. Cell. Neurosci.* 7:6. doi: 10.3389/fncel.2013.00006

Sierra, A., Gottfried-Blackmore, A. C., McEwen, B. S., and Bulloch, K. (2007). Microglia derived from aging mice exhibit an altered inflammatory profile. *Glia* 55, 412–424. doi: 10.1002/glia.20468

Simmons, D. A., Casale, M., Alcon, B., Pham, N., Narayan, N., and Lynch, G. (2007). Ferritin accumulation in dystrophic microglia is an early event in the development of Huntington's disease. *Glia* 55, 1074–1084. doi: 10.1002/glia.20526

Simpson, J., Rezaie, P., Newcombe, J., Cuzner, M. L., Male, D., and Woodroofe, M. N. (2000). Expression of the beta-chemokine receptors CCR2, CCR3 and CCR5 in multiple sclerosis central nervous system tissue. *J. Neuroimmunol.* 108, 192–200. doi: 10.1016/S0165-5728(00)00274-5

Sipe, G. O., Lowery, R. L., Tremblay, M. È., Kelly, E. A., Lamantia, C. E., and Majewska, A. K. (2016). Microglial P2Y12 is necessary for synaptic plasticity in mouse visual cortex. *Nat. Commun.* 7:10905. doi: 10.1038/ncomms10905

Sleegers, K., Brouwers, N., Gijselinck, I., Theuns, J., Goossens, D., Wauters, J., et al. (2006). APP duplication is sufficient to cause early onset Alzheimer's dementia with cerebral amyloid angiopathy. *Brain* 129, 2977–2983. doi: 10.1093/brain/awl203

Song, J., Shu, L., Zhang, Z., Tan, X., Sun, E., Jin, X., et al. (2012). Reactive oxygen species-mediated mitochondrial pathway is involved in Baohuoside I-induced apoptosis in human non-small cell lung cancer. *Chem. Biol. Interact.* 199, 9–17. doi: 10.1016/j.cbi.2012.05.005

Soria, F. N., Pampliega, O., Bourdenx, M., Meissner, W. G., Bezard, E., and Dehay, B. (2017). Exosomes, an unmasked culprit in neurodegenerative diseases. *Front. Neurosci.* 11:26. doi: 10.3389/fnins.2017.00026

Spangenberg, E. E., Lee, R. J., Najafi, A. R., Rice, R. A., Elmore, M. R. P., Blurton-Jones, M., et al. (2016). Eliminating microglia in Alzheimer's mice prevents

neuronal loss without modulating amyloid-β pathology. *Brain* 139, 1265–1281. doi: 10.1093/brain/aww016

Srikanth, V., Maczurek, A., Phan, T., Steele, M., Westcott, B., Juskiw, D., et al. (2011). Advanced glycation endproducts and their receptor RAGE in Alzheimer's disease. *Neurobiol. Aging* 32, 763–777. doi: 10.1016/j.neurobiolaging.2009.04.016

Stein, M., Keshav, S., Harris, N., and Gordon, S. (1992). Interleukin 4 potently enhances murine macrophage mannose receptor activity: a marker of alternative immunologic macrophage activation. *J. Exp. Med.* 176, 287–292. doi: 10.1084/jem.176.1.287

Stence, N., Waite, M., and Dailey, M. E. (2001). Dynamics of microglial activation: a confocal time-lapse analysis in hippocampal slices. *Glia* 33, 256–266. doi: 10.1002/1098-1136(200103)33:3<256::AID-GLIA1024>3.0.CO;2-J

Stevens, B., Allen, N. J., Vazquez, L. E., Howell, G. R., Christopherson, K. S., Nouri, N., et al. (2007). The classical complement cascade mediates CNS synapse elimination. *Cell* 131, 1164–1178. doi: 10.1016/j.cell.2007.10.036

Streit, W. J., Braak, H., Xue, Q.-S., and Bechmann, I. (2009). Dystrophic (senescent) rather than activated microglial cells are associated with tau pathology and likely precede neurodegeneration in Alzheimer's disease. *Acta Neuropathol.* 118, 475–485. doi: 10.1007/s00401-009-0556-6

Streit, W. J., Mrak, R. E., and Griffin, W. S. T. (2004). Microglia and neuroinflammation: a pathological perspective. *J. Neuroinflammation* 1:14. doi: 10.1186/1742-2094-1-14

Streit, W. J., Walter, S. A., and Pennell, N. A. (1999). Reactive microgliosis. *Progr. Neurobiol.* 57, 563–581. doi: 10.1016/S0301-0082(98)00069-0

Su, T., Zhang, T., Xie, S., Yan, J., Wu, Y., Li, X., et al. (2016). Discovery of novel PDE9 inhibitors capable of inhibiting Aβ aggregation as potential candidates for the treatment of Alzheimer's disease. *Sci. Rep.* 6:21826. doi: 10.1038/srep21826

Tabatadze, N., Savonenko, A., Song, H., Bandaru, V. V. R., Chu, M., and Haughey, N. J. (2010). Inhibition of neutral sphingomyelinase-2 perturbs brain sphingolipid balance and spatial memory in mice. *J. Neurosci. Res.* 88, 2940–2951. doi: 10.1002/jnr.22438

Tai, L. M., Koster, K. P., Luo, J., Lee, S. H., Wang, Y.-T., Collins, N. C., et al. (2014). Amyloid-β pathology and APOE genotype modulate retinoid X receptor agonist activity *in vivo*. *J. Biol. Chem.* 289, 30538–30555. doi: 10.1074/jbc.M114.600833

Takahashi, K., Prinz, M., Stagi, M., Chechneva, O., and Neumann, H. (2007). TREM2-transduced myeloid precursors mediate nervous tissue debris clearance and facilitate recovery in an animal model of multiple sclerosis. *PLoS Med.* 4:e124. doi: 10.1371/journal.pmed.0040124

Takamatsu, K., Ikeda, T., Haruta, M., Matsumura, K., Ogi, Y., Nakagata, N., et al. (2014). Degradation of amyloid beta by human induced pluripotent stem cell-derived macrophages expressing Neprilysin-2. *Stem Cell Res.* 13, 442–453. doi: 10.1016/j.scr.2014.10.001

Takeuchi, H., Jin, S., Wang, J., Zhang, G., Kawanokuchi, J., Kuno, R., et al. (2006). Tumor necrosis factor-α induces neurotoxicity via glutamate release from hemichannels of activated Microglia in an autocrine manner. *J. Biol. Chem.* 281, 21362–21368. doi: 10.1074/jbc.M600504200

Tawakol, A., Singh, P., Rudd, J. H. F., Soffer, J., Cai, G., Vucic, E., et al. (2014). Effect of treatment for 12 weeks with Rilapladib, a lipoprotein-associated phospholipase A2 inhibitor, on arterial inflammation as assessed with 18F-fluorodeoxyglucose-positron emission tomography imaging. *J. Am. Coll. Cardiol.* 63, 86–88. doi: 10.1016/j.jacc.2013.07.050

Taylor, D. L., Jones, F., Kubota, E. S., F. C. S., and Pocock, J. M. (2005). Stimulation of microglial metabotropic glutamate receptor mGlu2 triggers tumor necrosis factor α-induced neurotoxicity in concert with microglial-derived fas ligand. *J. Neurosci.* 25:2952. doi: 10.1523/JNEUROSCI.4456-04.2005

Tesseur, I., Zou, K., Esposito, L., Bard, F., Berber, E., Can, J. V., et al. (2006). Deficiency in neuronal TGF-β signaling promotes neurodegeneration and Alzheimer's pathology. *J. Clin. Invest.* 116, 3060–3069. doi: 10.1172/JCI27341

Theunis, C., Crespo-Biel, N., Gafner, V., Pihlgren, M., López-Deber, M. P., Reis, P., et al. (2013). Efficacy and Safety of A Liposome-Based Vaccine against Protein Tau, Assessed in Tau.P301L Mice That Model Tauopathy. *PLoS ONE* 8:e72301. doi: 10.1371/journal.pone.0072301

Theuns, J., Marjaux, E., Vandenbulcke, M., Van Laere, K., Kumar-Singh, S., Bormans, G., et al. (2006). Alzheimer dementia caused by a novel mutation located in the APP C-terminal intracytosolic fragment. *Hum. Mutat.* 27, 888–896. doi: 10.1002/humu.20402

Thompson, A. G., Gray, E., Heman-Ackah, S. M., Mager, I., Talbot, K., Andaloussi, S. E., et al. (2016). Extracellular vesicles in neurodegenerative disease [mdash] pathogenesis to biomarkers. *Nat. Rev. Neurol.* 12, 346–357. doi: 10.1038/nrneurol.2016.68

Tichauer, J. E., Flores, B., Soler, B., Bernhardi, L. E.-V., Ramírez, G., and von Bernhardi, R. (2014). Age-dependent changes on TGFβ1 Smad3 pathway modify the pattern of microglial cell activation. *Brain Behav. Immun.* 37, 187–196. doi: 10.1016/j.bbi.2013.12.018

Tremblay, M. S., Colley, R. C., Saunders, T. J., Healy, G. N., and Owen, N. (2010). Physiological and health implications of a sedentary lifestyle. *Appl. Physiol. Nutr. Metab.* 35, 725–740. doi: 10.1139/H10-079

Tremblay, M.-È., Zettel, M. L., Ison, J. R., Allen, P. D., and Majewska, A. K. (2012). Effects of aging and sensory loss on glial cells in mouse visual and auditory cortices. *Glia* 60, 541–558. doi: 10.1002/glia.22287

Treviño, S., Aguilar-Alonso, P., Flores Hernandez, J. A., Brambila, E., Guevara, J., Flores, G., et al. (2015). A high calorie diet causes memory loss, metabolic syndrome and oxidative stress into hippocampus and temporal cortex of rats. *Synapse* 69, 421–433. doi: 10.1002/syn.21832

Truman, L. A., Ford, C. A., Pasikowska, M., Pound, J. D., Wilkinson, S. J., Dumitriu, I. E., et al. (2008). CX3CL1/fractalkine is released from apoptotic lymphocytes to stimulate macrophage chemotaxis. *Blood* 112:5026. doi: 10.1182/blood-2008-06-162404

Ueberham, U., Ueberham, E., Gruschka, H., and Arendt, T. (2006). Altered subcellular location of phosphorylated Smads in Alzheimer's disease. *Euro. J. Neurosci.* 24, 2327–2334. doi: 10.1111/j.1460-9568.2006.05109.x

Ulrich, J. D., Finn, M. B., Wang, Y., Shen, A., Mahan, T. E., Jiang, H., et al. (2014). Altered microglial response to Aβ plaques in APPPS1-21 mice heterozygous for TREM2. *Mol. Neurodegener.* 9, 20–20. doi: 10.1186/1750-1326-9-20

Varnum, M. M., Clayton, K. A., Yoshii-Kitahara, A., Yonemoto, G., Koro, L., Ikezu, S., et al. (2017). A split-luciferase complementation, real-time reporting assay enables monitoring of the disease-associated transmembrane protein TREM2 in live cells. *J. Biol. Chem.* 292, 10651–10663. doi: 10.1074/jbc.M116.759159

Varnum, M. M., Kiyota, T., Ingraham, K. L., Ikezu, S., and Ikezu, T. (2015). The Anti-inflammatory glycoprotein, cd200, restores neurogenesis and enhances amyloid phagocytosis in a mouse model of Alzheimer's disease. *Neurobiol. Aging* 36, 2995–3007. doi: 10.1016/j.neurobiolaging.2015.07.027

Vella, L. J., Sharples, R. A., Lawson, V. A., Masters, C. L., Cappai, R., and Hill, A. F. (2007). Packaging of prions into exosomes is associated with a novel pathway of PrP processing. *J. Pathol.* 211, 582–590. doi: 10.1002/path.2145

Vinet, J., van Weering, H. R. J., Heinrich, A., Kälin, R. E., Wegner, A., Brouwer, N., et al. (2012). Neuroprotective function for ramified microglia in hippocampal excitotoxicity. *J. Neuroinflam.* 9, 27–27. doi: 10.1186/1742-2094-9-27

Vlad, S. C., Miller, D. R., Kowall, N. W., and Felson, D. T. (2008). Protective effects of NSAIDs on the development of Alzheimer disease. *Neurology* 70, 1672–1677. doi: 10.1212/01.wnl.0000311269.57716.63

Vlassov, A. V., Magdaleno, S., Setterquist, R., and Conrad, R. (2012). Exosomes: current knowledge of their composition, biological functions, and diagnostic and therapeutic potentials. *Biochim. Biophys. Acta* 1820, 940–948. doi: 10.1016/j.bbagen.2012.03.017

von Bernhardi, R., Cornejo, F., Parada, G. E., and Eugenín, J. (2015a). Role of TGFβ signaling in the pathogenesis of Alzheimer's disease. *Front. Cell. Neurosci.* 9:426. doi: 10.3389/fncel.2015.00426

von Bernhardi, R., Eugenín-von Bernhardi, L., and Eugenín, J. (2015b). Microglial cell dysregulation in brain aging and neurodegeneration. *Front. Aging Neurosci.* 7:124. doi: 10.3389/fnagi.2015.00124

Vowinckel, E., Reutens, D., Becher, B., Verge, G., Evans, A., Owens, T., et al. (1997). PK11195 binding to the peripheral benzodiazepine receptor as a marker of microglia activation in multiple sclerosis and experimental autoimmune encephalomyelitis. *J. Neurosci. Res.* 50, 345–353. doi: 10.1002/(SICI)1097-4547(19971015)50:2<345::AID-JNR22>3.0.CO;2-5

Vukovic, J., Colditz, M. J., Blackmore, D. G., Ruitenberg, M. J., and Bartlett, P. F. (2012). Microglia modulate hippocampal neural precursor activity in response to exercise and aging. *J. Neurosci.* 32:6435. doi: 10.1523/JNEUROSCI.5925-11.2012

Walker, D. G., Dalsing-Hernandez, J. E., Campbell, N. A., and Lue, L.-F. (2009). Decreased expression of CD200 and CD200 receptor in Alzheimer's disease: a potential mechanism leading to chronic inflammation. *Exp. Neurol.* 215, 5–19. doi: 10.1016/j.expneurol.2008.09.003

Walker, L. C., and LeVine, H. (2000). The cerebral proteopathies. *Mol. Neurobiol.* 21, 83–95. doi: 10.1385/MN:21:1-2:083

Wang, J., Shiozawa, Y., Wang, J., Wang, Y., Jung, Y., Pienta, K. J., et al. (2008). The role of CXCR7/RDC1 as a chemokine receptor for CXCL12/SDF-1 in prostate cancer. *J. Biol. Chem.* 283, 4283–4294. doi: 10.1074/jbc.M707465200

Wang, Y., Cella, M., Mallinson, K., Ulrich, J. D., Young, K. L., and Robinette, M. L. (2015). TREM2 lipid sensing sustains the microglial response in an Alzheimer's disease model. *Cell* 160, 1061–1071. doi: 10.1016/j.cell.2015.01.049

Wehrspaun, C. C., Haerty, W., and Ponting, C. P. (2015). Microglia recapitulate a hematopoietic master regulator network in the aging human frontal cortex. *Neurobiol. Aging* 36, 2443.e9–2443.e20. doi: 10.1016/j.neurobiolaging.2015.04.008

Wiessner, C., Wiederhold, K. H., Tissot, A. C., Frey, P., Danner, S., Jacobson, L. H., et al. (2011). The second-generation active Aβ immunotherapy CAD106 reduces amyloid accumulation in APP transgenic mice while minimizing potential side effects. *J. Neurosci.* 31, 9323–9331. doi: 10.1523/JNEUROSCI.0293-11.2011

Wong, W. T. (2013). Microglial aging in the healthy CNS: phenotypes, drivers, and rejuvenation. *Front. Cell. Neurosci.* 7:22. doi: 10.3389/fncel.2013.00022

Woodbury, M. E., Freilich, R. W., Cheng, C. J., Asai, H., Ikezu, S., Boucher, J. D., et al. (2015). miR-155 is essential for inflammation-induced hippocampal neurogenic dysfunction. *J. Neurosci.* 35, 9764–9781. doi: 10.1523/JNEUROSCI.4790-14.2015

Wyss-Coray, T., Lin, C., Yan, F.,Yu, G. Q., Rohde, M., McConlogue, L., et al. (2001). TGF-[beta]1 promotes microglial amyloid-[beta] clearance and reduces plaque burden in transgenic mice. *Nat. Med.* 7, 612–618. doi: 10.1038/87945

Xiang, X., Werner, G., Bohrmann, B., Liesz, A., Mazaheri, F., Capell, A., et al. (2016). TREM2 deficiency reduces the efficacy of immunotherapeutic amyloid clearance. *EMBO Mol. Med.* 8, 992–1004. doi: 10.15252/emmm.201606370

Xu, H., Sweeney, D., Wang, R., Thinakaran, G., Lo, A. C. Y., Sisodia, S. S., et al. (1997). Generation of Alzheimer β-amyloid protein in the trans-Golgi network in the apparent absence of vesicle formation. *Proc. Natl. Acad. Sci. U.S.A.* 94, 3748–3752. doi: 10.1073/pnas.94.8.3748

Yarza, R., Vela, S., Solas, M., and Ramirez, M. J. (2015). c-Jun N-terminal Kinase (JNK) signaling as a therapeutic target for Alzheimer's disease. *Front. Pharmacol.* 6:321. doi: 10.3389/fphar.2015.00321

Yin, Z., Raj, D., Saiepour, N., Van Dam, D., Brouwer, N., Holtman, I. R., et al. (2017). Immune hyperreactivity of Aβ plaque-associated microglia in Alzheimer's disease. *Neurobiol. Aging* 55, 115–122. doi: 10.1016/j.neurobiolaging.2017.03.021

Yuan, P., Condello, C., Keene, C. D., Wang, Y., Bird, T. D., Paul, S. M., et al. (2016). TREM2 haplodeficiency in mice and humans impairs the microglia barrier function leading to decreased amyloid compaction and severe axonal dystrophy. *Neuron* 90, 724–739. doi: 10.1016/j.neuron.2016.05.003

Zempel, H., and Mandelkow, E. (2014). Lost after translation: missorting of Tau protein and consequences for Alzheimer disease. *Trends Neurosci.* 37, 721–732. doi: 10.1016/j.tins.2014.08.004

Zerbinatti, C. V., Wozniak, D. F., Cirrito, J., Cam, J. A., Osaka, H., Bales, K. R., et al. (2004). Increased soluble amyloid-β peptide and memory deficits in amyloid model mice overexpressing the low-density lipoprotein receptor-related protein. *Proc. Natl. Acad. Sci. U.S.A.* 101, 1075–1080. doi: 10.1073/pnas.0305803101

Zhao, J., Fu, Y., Yasvoina, M., Shao, P., Hitt, B., and O'Connor, T. (2007). Beta-site amyloid precursor protein cleaving enzyme 1 levels become elevated in neurons around amyloid plaques: implications for Alzheimer's disease pathogenesis. *J. Neurosci.* 27, 3639–3649. doi: 10.1523/JNEUROSCI.4396-06.2007

Zheng, H., Liu, C.-C., Atagi, Y., Chen, X.-F., Jia, L., Yang, L., et al. (2016). Opposing roles of the triggering receptor expressed on Myeloid Cells 2 (TREM2) and TREM-like Transcript 2 (TREML2) in Microglia Activation. *Neurobiol. Aging* 42, 132–141. doi: 10.1016/j.neurobiolaging.2016.03.004

Zhong, L., Chen, X.-F., Wang, T., Wang, Z., Liao, C., Wang, Z., et al. (2017a). Soluble TREM2 induces inflammatory responses and enhances microglial survival. *J. Exp. Med.* 214, 597–607. doi: 10.1084/jem.20160844

Zhong, L., Zhang, Z.-L., Li, X., Liao, C., Mou, P., Wang, T., et al. (2017b). TREM2/DAP12 complex regulates inflammatory responses in Microglia via the JNK signaling pathway. *Front. Aging Neurosci.* 9:204. doi: 10.3389/fnagi.2017.00204

Zomer, A., Vendrig, T., Hopmans, E. S., van Eijndhoven, M., Middeldorp, J. M., and Pegtel, D. M. (2010). Exosomes: fit to deliver small RNA. *Commun. Integr. Biol.* 3, 447–450. doi: 10.4161/cib.3.5.12339

Conflict of Interest Statement: The authors declare that the research was conducted in the absence of any commercial or financial relationships that could be construed as a potential conflict of interest.

frontiers in Neuroscience

REVIEW
published: 22 December 2017
doi: 10.3389/fnins.2017.00724

Imbalances in the Hsp90 Chaperone Machinery: Implications for Tauopathies

*Lindsey B. Shelton, John Koren III and Laura J. Blair**

Department of Molecular Medicine and USF Health Byrd Institute, University of South Florida, Tampa, FL, United States

The ATP-dependent 90 kDa heat shock protein, Hsp90, is a major regulator of protein triage, from assisting in nascent protein folding to refolding or degrading aberrant proteins. Tau, a microtubule associated protein, aberrantly accumulates in Alzheimer's disease (AD) and other neurodegenerative diseases, deemed tauopathies. Hsp90 binds to and regulates tau fate in coordination with a diverse group of co-chaperones. Imbalances in chaperone levels and activity, as found in the aging brain, can contribute to disease onset and progression. For example, the levels of the Hsp90 co-chaperone, FK506-binding protein 51 kDa (FKBP51), progressively increase with age. *In vitro* and *in vivo* tau models demonstrated that FKBP51 synergizes with Hsp90 to increase neurotoxic tau oligomer production. Inversely, protein phosphatase 5 (PP5), which dephosphorylates tau to restore microtubule-binding function, is repressed with aging and activity is further repressed in AD. Similarly, levels of cyclophilin 40 (CyP40) are reduced in the aged brain and further repressed in AD. Interestingly, CyP40 was shown to breakup tau aggregates *in vitro* and prevent tau-induced neurotoxicity *in vivo*. Moreover, the only known stimulator of Hsp90 ATPase activity, Aha1, increases tau aggregation and toxicity. While the levels of Aha1 are not significantly altered with aging, increased levels have been found in AD brains. Overall, these changes in the Hsp90 heterocomplex could drive tau deposition and neurotoxicity. While the relationship of tau and Hsp90 in coordination with these co-chaperones is still under investigation, it is clear that imbalances in these proteins with aging can contribute to disease onset and progression. This review highlights the current understanding of how the Hsp90 family of molecular chaperones regulates tau or other misfolded proteins in neurodegenerative diseases with a particular emphasis on the impact of aging.

Keywords: Hsp90, aging, tau, chaperones, co-chaperones, proteostasis

OPEN ACCESS

Edited by:
Naruhiko Sahara,
National Institute of Radiological Sciences (NIRS), Japan

Reviewed by:
Shin-ichi Hisanaga,
Tokyo Metropolitan University, Japan
Jason Eriksen,
University of Houston, United States

****Correspondence:***
Laura J. Blair
lblair@health.usf.edu

Specialty section:
This article was submitted to Neurodegeneration, a section of the journal Frontiers in Neuroscience

Received: *30 September 2017*
Accepted: *12 December 2017*
Published: *22 December 2017*

Citation:
Shelton LB, Koren J III and Blair LJ (2017) Imbalances in the Hsp90 Chaperone Machinery: Implications for Tauopathies. Front. Neurosci. 11:724. doi: 10.3389/fnins.2017.00724

INTRODUCTION

Aging is the biggest risk factor for developing a neurodegenerative disease, but the specific factors which cause these predominantly sporadic diseases are still under investigation (Reeve et al., 2014). As cells within the body age, the cellular homeostasis network must deal with an increasing amount of misfolded and aggregated proteins that can pathogenically accumulate leading to cell

death. Aging is caused by compromised cellular homeostasis, fitness, and plasticity, leading to degeneration and cell death in vital organs. According to the "garbage catastrophe" hypothesis, aged differentiated cells lose the capacity to dispose of damaged and malfunctioning proteins (Terman, 2001). Such damaged proteins can assume cytotoxic properties, and their constant removal is thus essential for cell survival. Not only does aging lead to an increased likelihood of protein misfolding and aggregation, it is compounded by a decrease in the efficiency of the protein degradation machinery. The activity of both the proteasome, which is the main mechanism of protein degradation (Rock et al., 1994; Conconi et al., 1996), and chaperone-mediated autophagy (CMA; Cuervo and Dice, 2000b) is significantly impaired with aging and is especially pronounced in post-mitotic cells, such as neurons, potentially resulting in neurodegenerative disease (Terman, 2001). Fortunately, there is a system in place to help the body maintain proteostasis in times of stress and disease: the molecular chaperone network (Söti and Csermely, 2002). This network is comprised of a diverse family of proteins which contains members that are constitutively expressed to help in normal cell maintenance as well as members that become activated during times of stress. All of these chaperones assist in various ways to help fold, refold and degrade misfolded proteins.

The molecular chaperone network is comprised of diverse families of heat shock proteins (Hsps) that are divided based on their molecular mass. The small Hsps regulate general protein aggregation, Hsp40s regulate Hsp70 ATP hydrolysis, Hsp70 folds proteins during translation, and Hsp90 maintains and triages a subset of clients (Liberek et al., 2008; Miyata et al., 2011). While Hsp70 and Hsp90 perform many overlapping roles in the cell, Hsp90 shows more client selectivity. Hsp90 requires ATP to perform these functions including protein degradation, protein folding, prevention of protein aggregation, and protein modification (Echeverría et al., 2011). These regulatory processes are particularly important for intrinsically disordered proteins (IDPs) which have a high propensity to aggregate (Schopf et al., 2017).

Hsp90 binds to one of these IDPs, tau, in a broad region that includes aggregation prone areas (Karagöz et al., 2014). Tau normally functions to stabilize the microtubules and regulate axonal transport (Guo et al., 2017). The pathological accumulation of tau is a hallmark in several neurodegenerative disorders collectively termed tauopathies (Kovacs, 2015); a series of diseases including Alzheimer's disease (AD), progressive supranuclear palsy (PSP), Pick's disease, and chronic traumatic encephalopathy (CTE; Guo et al., 2017). Currently there are no treatment options available which regulate tau pathogenesis (Orr et al., 2017), therefore more work needs to be done to identify potential tau regulating therapeutic strategies.

A promising avenue to target tau is through Hsp90 inhibition. In fact, Hsp90 ATPase-inhibitors rapidly degrade tau aggregates *in vivo* (Dickey et al., 2007a; Luo et al., 2007), but these inhibitors have not yet been successful in clinical trials due to lack of efficacy and associated toxicities (Bhat et al., 2014; Renouf et al., 2016; Thakur et al., 2016). However, Hsp90 regulates tau and other aggregating proteins in coordination with a diverse group of co-chaperones (Schopf et al., 2017). In fact, the levels of many of these co-chaperones have been shown to change with aging, which can alter the fate of tau and potentially contribute to disease onset or severity (Blair et al., 2013; Brehme et al., 2014). It is possible that a more successful treatment strategy may be found by a therapeutic aimed toward regulating these co-chaperones or Hsp90/co-chaperone heterocomplexes (Kamal et al., 2003; Rodina et al., 2016). This review discusses the involvement of Hsp90 and its co-chaperones in disease and how alterations in levels and activity with aging can affect this process (**Table 1**). Current Hsp90 therapeutic interventions for neurodegenerative diseases will also be reviewed.

HSP90

Hsp90 is critical to maintaining proteostasis (Brehme et al., 2014) and accounts for up to 6% of all protein within the cell during times of stress (Picard, 2002; Prodromou, 2016). Hsp90 consists of three domains: an N-terminal ATP-binding domain, a middle domain, and a C-terminal domain responsible for the inherent dimerization of the protein (Li and Buchner, 2013). Hsp90 requires ATP in order to dimerize and properly assist in protein folding. The Hsp90 ATPase cycle consists of four stages: the ATP-bound state, an initial intermediate state (I1), a second intermediate state (I2), and finally a closed state in which ATP hydrolysis occurs (Li and Buchner, 2013). There are several different isoforms of Hsp90, however this review will only focus on Hsp90 in the cytosol, which includes Hsp90α (stress-inducible) and Hsp90β (constitutively active) (Li et al., 2012).

The two different cytosolic forms of Hsp90 are 86% genetically identical and have 93% amino acid sequence homology, showing lots of similarities in structure and function. However, there are some differences that set these two isoforms apart. The first difference is the viability of Hsp90 knock-out mice. Mice lacking Hsp90β are embryonically lethal and do not survive past day 9, whereas mice lacking Hsp90α are viable but leads to sterility in male mouse (**Table 2**; Voss et al., 2000; Grad et al., 2010). There are also some differences in the cellular functions of Hsp90α and Hsp90β. Hsp90α is involved in growth promotion, cell cycle regulation, stress-induced cytoprotection, and cancer cell invasiveness; whereas Hsp90β is involved with early embryonic development, germ cell maturation, cytoskeletal stabilization, cellular transformation, signal transduction, and long-term cell adaptation (Eustace et al., 2004; Sreedhar et al., 2004). While there are some general functional differences between the two cytosolic isoforms more studies are needed to better understand the role of these different isoforms on tau pathology.

Alterations in chaperone expression are commonly seen in aging, leading to complications within the Hsp90 chaperone network. In fact, recent work has shown the levels of many Hsp90 co-chaperones are also altered in the aged brain (Brehme et al., 2014). These co-chaperones are necessary for client selection and triage. There are two main categories

TABLE 1 | Summary of Hsp90 and Hsp90 co-chaperone levels in aging and Alzheimer's disease (AD).

Chaperone	Gene	Function	Aging	AD	References
Hsp90α	*HSP90AA1*	Chaperone	Repressed	No Data	Brehme et al., 2014
Hsp90ß	*HSP90AB1*	Chaperone	Repressed	Repressed	Brehme et al., 2014
CyP40	*CYP40*	Peptidyl-prolyl isomerase	Repressed	Repressed	Brehme et al., 2014
FKBP51	*FKBP5*	Peptidyl-prolyl isomerase	Induced	Induced	Blair et al., 2013; Brehme et al., 2014
FKBP52	*FKBP4*	Peptidyl-prolyl isomerase	Repressed	Repressed'	Brehme et al., 2014; Meduri et al., 2016
Xap2	*AIP*	Co-chaperone	Slightly Repressed	No Data	Brehme et al., 2014
PP5	*PPP5*	Ser/Thr phosphatase	Repressed	Activity repressed	Liu et al., 2005; Brehme et al., 2014
FKBP38	*FKBP8*	Peptidyl-prolyl isomerase	Unchanged	No Data	Brehme et al., 2014
FKBP36	*FKBP6*	Peptidyl-prolyl isomerase	Unchanged	No Data	Brehme et al., 2014
WISp39	*FKBPL*	Peptidyl-prolyl isomerase	Unchanged	Repressed	Brehme et al., 2014
Hop	*STIP1*	Client protein maturation	Slightly Repressed	No Data	Brehme et al., 2014
CHIP	*STUB1*	E3 ubiquitin ligase	Unchanged	Unchanged	Brehme et al., 2014
DNAJC7	*DNAJC7*	Steroid receptor co-chaperone	Repressed	Repressed	Brehme et al., 2014
Tom34	*TOMM34*	Mitochondrial import protein	Unchanged	No Data	Brehme et al., 2014
UNC-45A	*UNC45A*	Myosin chaperone	Slightly Induced	Unchanged	Brehme et al., 2014
Tom70	*TOMM70*	Mitochondrial import protein	Repressed	Repressed	Loerch et al., 2008; Brehme et al., 2014
NASP	*NASP*	Co-chaperone	Slightly Induced	Induced	Brehme et al., 2014
SGTA	*SGTA*	Co-chaperone	Unchanged	No Data	Brehme et al., 2014
SGTB	*SGTB*	Co-chaperone	Repressed	Repressed	Loerch et al., 2008; Brehme et al., 2014
Cns1	*TTC4*	Co-chaperone	Induced	No Data	Brehme et al., 2014
CRN	*CRNKL1*	Co-chaperone	Slightly Repressed	No Data	Brehme et al., 2014
Tah1	*RPAP3*	RNA Polymerase II-associated protein	Repressed	No Data	Brehme et al., 2014
TPR1	*TTC1*	Co-chaperone	Unchanged	No Data	Brehme et al., 2014
DYX1C1	*DNAAF4*	Co-chaperone	Induced	No Data	Brehme et al., 2014
AIPL1	*AIPL1*	Co-chaperone	Unchanged	No Data	Brehme et al., 2014
Cdc37	*CDC37*	Inhibits ATPase activity	Unchanged	Repressed	Brehme et al., 2014
Aha1	*AHSA1*	Stimulates ATPase activity	Slightly Repressed	Induced	Brehme et al., 2014; Shelton et al., 2017
p23	*PTGES3*	Inhibits ATPase activity	Slightly Repressed	Unchanged	Brehme et al., 2014
S100A1	*S100A1*	Co-chaperone	No Data	No Data	
FNIP1	*FNIP1*	Co-chaperone	No Data	No Data	

A summary of the levels of the Hsp90 chaperone network in both aging and AD human samples.

of Hsp90 co-chaperones: tetratricopeptide repeat (TPR) and non-TPR containing (Prodromou et al., 2000). Therefore, changes in Hsp90 levels are part of a larger imbalance in the chaperone network which contribute to aging and age-related neurodegenerative disorders.

TPR CO-CHAPERONES

TPR-containing Hsp90 co-chaperones interact with the C-terminal MEEVD peptide motif on Hsp90 (Li et al., 2012). Since Hsp90 functions as a dimer, two TPR-containing co-chaperones could interact simultaneously. However, these interactions are dependent on the isoform of Hsp90 and the repertoire of expressed co-chaperones. In fact, co-chaperones do compete for binding to Hsp90 (Harst et al., 2005; Hildenbrand et al., 2011). This competition can have beneficial or detrimental effects on tau pathology. Known examples include co-chaperones which interact with Hsp90 to promote the degradation of aberrant tau or others which drive tau oligomerization and aggregation. Therefore, an imbalance in protein levels with aging and AD compound this already complex competition for binding Hsp90 to regulate tau fate (**Figure 1**). Here, we will describe these TPR-co-chaperones, and how their interaction with Hsp90 regulates tau.

Immunophilins and Immunophilin Homologs

Hsp90 interacts with six immunophilins that display peptidyl-prolyl isomerase (PPIase) activity through TPR domains including cyclophilin 40 (CyP40) and five FK506-binding proteins: FKBP51, FKBP52, FKBP36, FKBP38, FKBPL/WISp39 (Jascur et al., 2005; Jarczowski et al., 2009; Guy et al., 2015; Blundell et al., 2017). These PPIases regulate the twisting of proline bonds through stabilization of the *cis-trans* transition state and accelerate the isomerization process. This is particularly important for tau, which has 40 proline residues that regulate phosphorylation and aggregation propensity (Mandelkow and Mandelkow, 2012). Hsp90

TABLE 2 | Summary of Hsp90 and Hsp90 co-chaperone knockout mice.

	Protein	Gene	KO model	Viable	Phenotype	References
Hsp90	Hsp90α	Hsp90aa1	Mouse	Yes	Male mice, failure of spermatogenesis; viable and phenotypically normal into adulthood	Grad et al., 2010
	Hsp90β	*Hsp90ab1*	*Mouse*	No	Early embryonic lethality (day E9)	Voss et al., 2000
	Cyp40	*Cyp40*	*Mouse*	Yes	Phenotypically normal	Periyasamy et al., 2010
	FKBP51	*Fkbp5*	*Mouse*	Yes	Resilliant to stress-induced depression-like behavior	Yong et al., 2007; O'Leary et al., 2011; Touma et al., 2011
TPR co-chaperones	FKBP52	*Fkbp4*	*Mouse*	∼50% are embryonic lethal	Reduced fertility in both males and females	Cheung-Flynn et al., 2005; Tranguch et al., 2005; Yang et al., 2006
	Xap2	*AIP*	*Mouse*	No	Embryonic lethality	Raitila et al., 2010
	PP5	*Ppp5*	*Mouse*	Yes	Mice survive both embryonic development and into postnatal mice; defect in DNA damage checkpoint after ionizing radiation	Yong et al., 2007
	FKBP38	*Fkbp8*	*Mouse*	No	Embryonically lethal	Bulgakov et al., 2004
	FKBP36	*Fkbp6*	*Mouse*	Yes	Both male and female mice are healthy and live normal lifespans; male mice are sterile	Crackower et al., 2003
	WISp39	*Fkbpl*	*Mouse*	No	Heterozygous FKBPL mice appear normal	Yakkundi et al., 2015
	Hop	*Stip1*	*Mouse*	No	Embryonically lethal around day E9.5-10.5	Beraldo et al., 2013
	CHIP	*Stub1*	*Mouse*	Yes	Develop normally but are susceptible to stress-induced apoptosis of multiple organs; increased peri- and postnatal lethality	Dai et al., 2003
	DnaJC7	*Dnajc7*	*Mouse*	Yes	No information on phenotype	Dickinson et al., 2016
	Tom34	*TOMM34*	*Mouse*	Yes	Phenotypically normal	Terada et al., 2003
	UNC-45A	*UNC45A*	*Mouse*	No	Embryonic lethality	Dickinson et al., 2016
	Tom70	*TOMM70*	*No*	N/A		
	NASP	*NASP*	*Mouse*	No	Embryonic lethality	Richardson et al., 2006
	SGTA	*SGTA*	*Mouse*	Yes	Less fertile with small liters and higher neonatal death rates; smaller body size in both males and females	Philp et al., 2016
	SGTB	*SGTB*	*No*	N/A		
	Cns1	*TTC4*	*Mouse*	Yes	Phenotypically normal	Josefowicz et al., 2012
	CRN	*CRNKL1*	*No*	N/A		
	Tah1	*RPAP3*	*No*	N/A		
	TPR1	*TTC1*	*No*	N/A		
	DYX1C1	*DYX1C1*	*Mouse*	Yes	Embryonic lethality in approx. 2/3; surviving mice develop severe hydrocephalus by postnatal day 16 and died by P21	Tarkar et al., 2013
	AIPL1	*AIPL1*	*Mouse*	Yes	Phenotypically normal	Ramamurthy et al., 2003
Non TPR co-chaperones	Cdc37	*Cdc37*	*C. elegan*	No	Embryonically lethal in C. elegans	Beers and Kemphues, 2006
	Aha1	*Ahsa1*	*Mouse*	Yes	No information on phenotype	The Jackson Laboratory: Stock No: 029805
	p23	*Ptges3*	*Mouse*	No	Perinatal lethality resulting from defective lung development; Abnormal skin and reduced expression of GR markers	Grad et al., 2006; Lovgren et al., 2007; Nakatani et al., 2007
	S100A1	*S100A1*	*Mouse*	Yes	Phenotypically normal	Du et al., 2002
	FNIP1	*FNIP1*	*Mouse*	Yes	Phenotypically normal	Hasumi et al., 2015

This table contains information on the available knock-out mouse lines for the Hsp90 chaperone family.

also interacts with two immunophilin homologs: protein phosphatase 5 (PP5) and XAP2/FKBP37. Altered levels of many of these immunophilins and immunophilin-like proteins have been found in aging and AD (**Table 1**), which could skew the competition dynamics for Hsp90 binding (discussed later in this review) and may promote toxic tau accumulation.

CyP40

An interesting PPIase, CyP40, decreases in aging and is further repressed in AD (**Table 1**; Brehme et al., 2014). CyP40 was recently shown to disaggregate tau fibrils *in vitro* and prevents toxic tau accumulation *in vivo* preserving memory, demonstrating a neuroprotective role for CyP40 in the brain (Baker et al., 2017). The PPIase activity of CyP40 is slightly

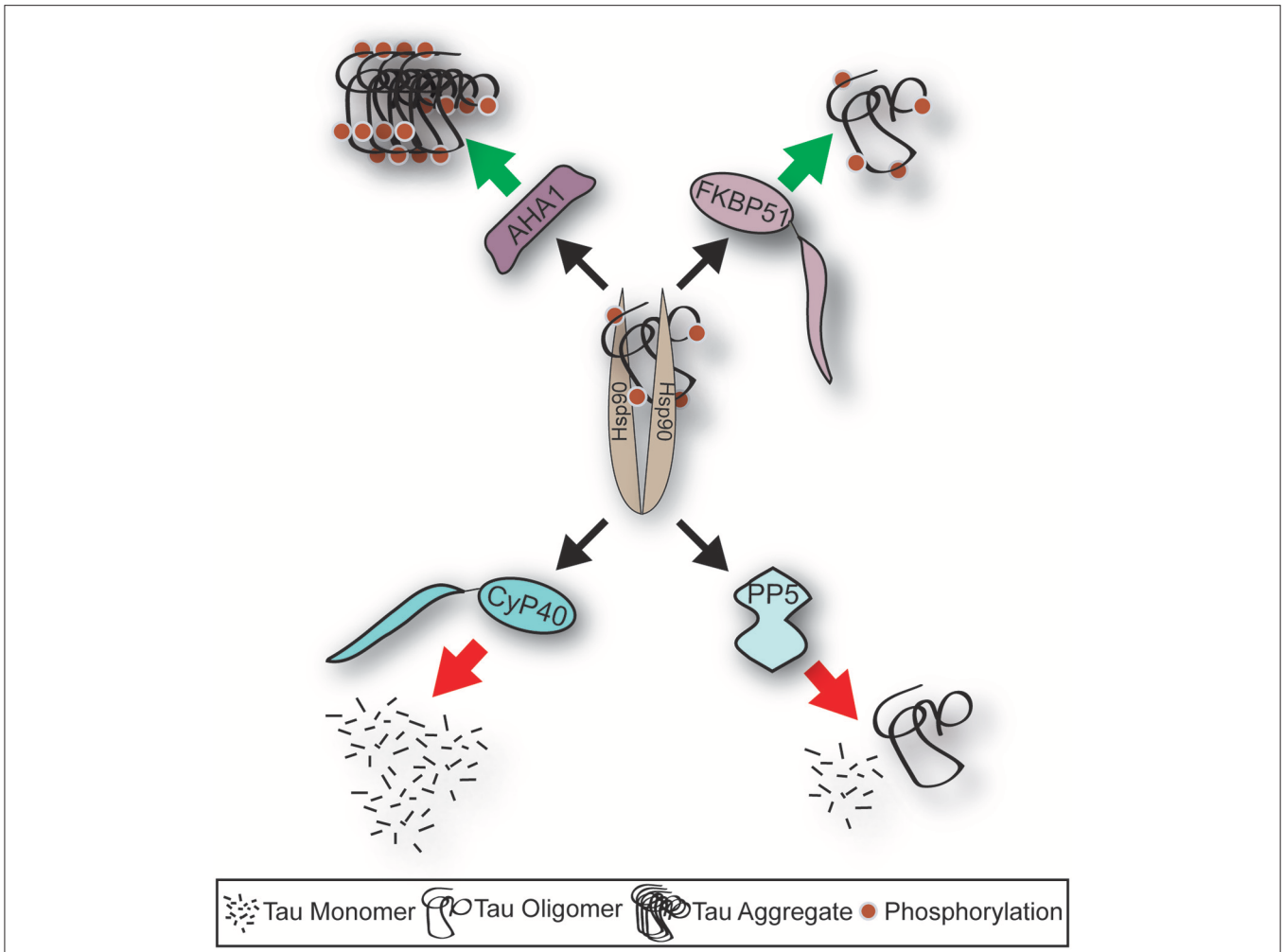

FIGURE 1 | Schematic depicting fate of tau following Hsp90 interaction with distinct co-chaperone; the impact of Alzheimer's disease on the levels of co-chaperones. Aha1 and FKBP51 protein levels are induced in AD, and their association to tau leads to increased aggregation. Whereas, CyP40 and PP5 levels are repressed in AD, and their association to tau leads to reduced tau aggregation. This schematic highlights the important role of co-chaperones in AD.

repressed when bound to Hsp90, but under cellular stress CyP40 can release from Hsp90 increasing its isomerase and chaperone activity (Blackburn et al., 2015). However, as CyP40 levels decrease with aging, it is possible that the pool of free CyP40 is not sufficient to help disentangle aggregating proteins, like tau.

FKBP51

Contrary to the neuroprotective effects of CyP40, two FK506-binding proteins (FKBPs) have been shown to stimulate toxic tau aggregation (Blair et al., 2013; Giustiniani et al., 2015; Kamah et al., 2016). One of these, FKBP51, coordinates with Hsp90 to preserve toxic tau oligomers *in vivo* (Blair et al., 2013). In fact, mice lacking FKBP51 have decreased tau levels in the brain (Jinwal et al., 2010; Blair et al., 2013). However, throughout aging, FKBP51 levels progressively increase and are further increased in AD brain samples (**Table 1**; Blair et al., 2013; Sabbagh et al., 2014). Previous studies have also shown that FKBP51 can form complexes with tau in both human AD brain samples and control samples (Jinwal et al., 2010). Additionally, this study showed that FKBP51 was able to stabilize microtubules, suggesting a novel and unique function for FKBP51 (Jinwal et al., 2010). Taken together, the increase in FKBP51 in aging and AD suggest that targeting FKBP51 could offer a potential therapeutic strategy for tauopathies such as AD.

FKBP52

FKBP52 interacts both physically and functionally with tau and promotes tau aggregation *in vitro* (Giustiniani et al., 2015; Meduri et al., 2016). FKBP52 induces oligomers from both P301L and truncated wild-type tau. Interestingly, this oligomerization is not due to the PPIase activity of FKBP52, instead the oligomerization of tau appears to occur via molecular interaction (Kamah et al., 2016). FKBP52 can also induce aggregation of a truncated form of tau that appears to have prion like behavior, suggesting a possible mechanism for the spread of tau pathology throughout the brain in diseases such as AD (Giustiniani et al.,

2015). However, it is interesting to note that FKBP52 levels are lower in the cortex of AD patients' brains (**Table 1**; Brehme et al., 2014; Meduri et al., 2016).

FKBP36, FKBP38, and FKBPL

There are several other FKBPs that act as co-chaperones to Hsp90 including FKBP36, FKBP38, and FKBPL (WISp39), however their relationship to tau, if any, is still unknown at this point and so they will not be discussed in detail.

XAP2

XAP2, otherwise known as FKBP37 or Aryl hydrocarbon receptor interacting protein (AIP), contains a PPIase homologous domain. While a direct role of XAP2 in tau pathogenesis has not been described, studies have shown that XAP2 is activated by histone deacetylase (HDAC) 6, which has been linked to pathogenic tau (Kekatpure et al., 2009; Cook et al., 2012; Selenica et al., 2014). In addition, XAP2 coordinates with Hsp90 to regulate glucocorticoid receptor signaling (Laenger et al., 2009), which has also been implicated in the production of pathogenic tau (Pinheiro et al., 2016). Additional studies are needed to determine the direct or indirect effects of XAP2 on tau pathology.

PP5

Another member of this family, protein phosphatase 5 (PP5), is repressed in aging. PP5 is contains a PPIase homology domain, but does not display classical PPIase activity, since it can bind FK506 (Silverstein et al., 1997). Instead, PP5 acts as a Ser/Thr phosphatase, which activates when bound to Hsp90 (Conde et al., 2005). PP5 activity has been shown to be repressed in AD (**Table 1**; Liu et al., 2005). Studies have shown that PP5 is able to dephosphorylate tau at several phosphorylation sites connected to AD pathology (Gong et al., 2004). Further studies are needed to better understand if the upregulation of PP5 could be used to slow or prevent tau pathogenesis.

Hop

The Hsp70-Hsp90 organizing protein, otherwise known as Hop and sometimes STIP1 (stress inducible protein 1), is involved in helping transfer client proteins from the early stages of protein maturation involving Hsp70 and Hsp40 to the later stages of the cycle involving Hsp90 (Baindur-Hudson et al., 2015). As such, Hop plays a crucial role in the maturation of client proteins, like tau. A previous study found that when Hop was depleted using siRNA, there was an accumulation of tau (Jinwal et al., 2013). This suggests that Hop is necessary for tau clearance via Hsp70/Hsp90. In fact, loss-of-function mutations in Hop drive toxic tau accumulation in a fly model of tauopathy (Ambegaokar and Jackson, 2011). Together these studies demonstrate a protective role of Hop in a tauopathic brain.

CHIP

C-terminus of Hsc70-interacting protein (CHIP) is highly involved in the Hsp70-Hsp90 machinery acting not only as a co-chaperone, but also as an E3 ubiquitin ligase responsible for ubiquitin-dependent proteasomal degradation (Edkins, 2015). CHIP has many roles within the cell including stress-response activation, protein triage, and restitution of the stress response (Dickey et al., 2007b). CHIP has been linked to several neurodegenerative disorders including Huntington's disease, Parkinson's disease and AD as well as other diseases such as cystic fibrosis and cancer (Dickey et al., 2007b; Edkins, 2015). In tauopathic mice, CHIP regulates the removal of tau species that have undergone abnormal phosphorylation and folding (Dickey et al., 2007b). Additionally, silencing CHIP via siRNA, led to a massive increase in tau levels (Dickey et al., 2008). Similarly, CHIP/*Stub1*-knockout mice have increased accumulation of phospho- and total tau species (**Table 2**; Palubinsky et al., 2015). Overexpression of CHIP could represent a therapeutic strategy to prevent neuronal cell death and improve outcomes of neurodegenerative diseases by promoting the degradation of tau.

DnaJC7

DnaJC7, also known as Tpr2, simultaneously binds Hsp70 and Hsp90 via its two TPR domains (Brychzy et al., 2003). To date, a link between DnaJC7 and tau has not been investigated. However, it is known that DnaJC7 plays an important role in steroid receptor chaperoning, as well as recycling substrates from Hsp90 back to Hsp70 via this unique TPR interaction (Brychzy et al., 2003; Moffatt et al., 2008). Additional studies are needed to understand if DnaJC7 regulates tau pathogenesis.

Tom34

Tom34 is a co-chaperone involved in mitochondrial protein import. One study found that in *Drosophila*, impaired Tom34 gene function led to enhanced tau pathology (Ambegaokar and Jackson, 2011). Conversely, the same study demonstrated Tom34 overexpression was able to suppress tau toxicity elucidating a role for Tom34 in tau pathology in *Drosophila*. The mechanism by which Tom34 promotes tau pathology remains unclear. It is possible that mitochondrial dysfunction could lead to cellular stress which, in turn, could enhance tau pathology. Additional studies are needed to fully elucidate this interaction.

In addition, there are other TPR-containing Hsp90 co-chaperones such as UNC-45, Tom70, NASP, SGTA, SGTB, Cns1, CRN, Tah1, TPR1, DYX1C1, and AIPL1. However, very little is known about most of these co-chaperones in the brain and even less is known about their interactions with tau, therefore they will not be discussed in detail in this review.

Non-TPR Co-chaperones

Cdc37

Cell division cycle 37 (Cdc37) slows the ATPase activity of Hsp90 allowing a prolonged interaction between Hsp90 and its client proteins (Cox and Johnson, 2011). Cdc37 is also required for the stable folding of protein kinases in coordination with Hsp90 (Calderwood, 2015). Many of these kinases are known to phosphorylate tau at sites associated with AD, such as GSK3β and MAPK13 (Taipale et al., 2012; Jin et al., 2016). Interestingly, overexpression of Cdc37 preserves tau, and its suppression reduces tau (Jinwal et al., 2012). However, additional studies are needed to better understand the dynamics between Cdc37 and tau phosphorylation.

Aha1

The activator of Hsp90 ATPase homolog 1 (Aha1) works as a co-chaperone to stimulate the ATPase function of Hsp90 to regulate the folding and activation of client proteins. Aha1 interacts with Hsp90 independent of its nucleotide status and allows the Hsp90 ATPase cycle to skip the I1 phase, thus accelerating the progression of the ATPase cycle dramatically (Li and Buchner, 2013; Wolmarans et al., 2016). Aha1 levels have been shown to increase with AD. In fact, we have found that Aha1 levels in the medial temporal gyrus of human brain correlated with increased tau Braak staging (Shelton et al., 2017). In the same study, we found that high levels of Aha1 in a tau transgenic mouse model increased tau oligomers as well as neuronal loss concomitant with cognitive deficits (Shelton et al., 2017). Since Aha1 levels are repressed in aging, but are abnormally preserved in AD, tau aggregation could be accelerated in part by Aha1 in the AD brain. Previous studies have also implicated Aha1 for a role in cystic fibrosis. In fact, one study showed that knockdown of Aha1 promotes the translocation of the disease-related mutant of cystic fibrosis transmembrane conductance receptor, CFTR, to the plasma membrane, allowing it to properly function (Wang et al., 2006). Thus, treatments which reduce Aha1 may be beneficial for both AD and cystic fibrosis.

p23

p23 has an opposing effect on Hsp90 compared to Aha1. p23 works by inhibiting the ATPase activity of Hsp90. The interaction between Hsp90 and p23 is nucleotide-dependent meaning that p23 can only interact with Hsp90 when ATP is bound (Sullivan et al., 1997). p23 works in a unique way to inhibit ATPase activity, it can either inhibit the hydrolysis process or it can impede the release of ADP and Pi (Rehn and Buchner, 2015). As a co-chaperone, p23 works to suppress protein aggregation and exhibits chaperoning activity, although p23 is not able to refold proteins on its own (Freeman et al., 1996). Inhibition of p23 in an siRNA screen of Hsp90 co-chaperones showed that silencing p23 reduced both total and phospho-tau (Jinwal et al., 2012, 2013). p23 also plays an important role in preventing endoplasmic reticulum (ER) stress-induced cell death, which can be triggered by misfolded proteins, like tau (Rao et al., 2006; Abisambra et al., 2013). However, p23 can be cleaved during ER stress-induced cell death into a smaller p19 fragment which is then unable to exert its anti-apoptotic effects (Zhang et al., 2013). A mutant p23 (p23D142N) that is uncleavable was shown to ameliorate the ER stress-induced cell death *in vitro* and suggests that this mutant p23 could be a potential therapeutic target in neurodegenerative diseases (Zhang et al., 2013).

S100A1

S100 calcium-binding protein A1 (S100A1) interacts with Hsp90. One study used siRNA to screen several Hsp90 co-chaperones to investigate the effect on tau. This study found that reductions in S100A1 also led to massive reductions in both phospho- and total tau levels in cells (Jinwal et al., 2013). S100A1 could play a role in stabilizing tau, thus leading to a worsening of tau pathology. Therefore, silencing or knocking down S100A1 could offer a potential therapeutic strategy for tauopathies.

FNIP1

The folliculin-interacting protein 1 (FNIP1) is able to interact with Hsp90 as a co-chaperone in order to inhibit its ATPase activity. One study found that FNIP1, in complex with FNIP2 and Hsp90, was able to stabilize the tumor suppressor folliculin (FLCN; Woodford et al., 2016). FNIP1 was shown to interact directly with Hsp90, and it can also interact with other co-chaperones such as p23, Hop and Cdc37 (Woodford et al., 2016). FNIP1 was also shown to compete for binding with Aha1 suggesting an important role for FNIP1 in the Hsp90 chaperone network (Woodford et al., 2016). Additional studies are needed to determine if FNIP1 could regulate tau directly or potentially through competition with Aha1 to bind Hsp90 and alter its ATPase activity.

Aging in the Hsp90 Chaperone Network

All of the above mentioned co-chaperones interact with Hsp90 in order to form diverse heterocomplexes, however, changes in Hsp90 expression with aging can alter their composition. There is conflicting data on Hsp90 levels with age in both human and animal studies. One study focused on the basal levels of cytosolic Hsp90 in peripheral blood mononuclear cells (PBMC) and found that in aged human samples there was an increase in Hsp90 under normal physiological conditions when compared to young samples (Njemini et al., 2007). Another study had similar findings in the hippocampus of aged gerbils. This study demonstrated that cytosolic Hsp90 levels were significantly increased in the hippocampus of aged gerbils (24 months) compared to adult gerbils (6 months) (Lee et al., 2011). Conversely, there are also studies showing decreased levels of Hsp90 in aged human brain samples. For instance, two other studies investigated the levels of chaperone proteins in the human brain. One study found that cytosolic Hsp90 was repressed in the superior frontal gyrus, while another demonstrated a similar repression in the prefrontal cortex of aged patients compared to controls (Berchtold et al., 2008; Loerch et al., 2008; Brehme et al., 2014). Taken together, this data suggests that alterations in Hsp90 levels do not occur uniformly and that changes in the expression of Hsp90 with aging may vary between cell types and brain regions (Berchtold et al., 2008). While Hsp90 protein levels are an important factor with aging, co-chaperone expression levels could be equally important in heterocomplex formation.

In addition to the differences in expression levels of Hsp90, there are also changes in expression levels of co-chaperone proteins during the aging process. Almost all of the Hsp90 co-chaperones are repressed in aging, suggesting that these proteins could play important roles in maintaining homeostasis within the cell (Brehme et al., 2014). For instance, CyP40, FKBP52, PP5, Hop, p23, and Aha1 are all repressed in the aged brain. All of these proteins are integral to the Hsp90 chaperone system and when levels of these proteins go down the Hsp90 chaperone network can no longer function normally, which can lead to an increased risk of developing a neurodegenerative disease. Interestingly, one co-chaperone is significantly induced in the aged brain and that is FKBP51. FKBP51 has several important roles within the cell including immunoregulation as well as helping with protein folding and trafficking in complex with

Hsp90. Because FKBP51 is induced in aging, while many other co-chaperones are reduced, this suggests that the imbalance seen in these proteins during aging could lead to completely different Hsp90 heterocomplexes resulting in the dysfunction of cellular homeostasis during aging.

Hsp90 is able to form many unique heterocomplexes with different co-chaperones in order to regulate protein triage. Hsp90 heterocomplexes are unique in that there is usually a specific progression of co-chaperones that interact with Hsp90 (Schopf et al., 2017). One interesting aspect to these heterocomplexes is the fact that Hsp90 can bind multiple co-chaperones simultaneously. One study found that Hsp90 could form stable complexes with Hsp90, FKBP52, Hop, and p23 (Hildenbrand et al., 2011). There does appear to be a hierarchy though, with some co-chaperones able to bind more strongly than others. For example, Aha1 has been shown to compete with Hop, FNIP1, and p23 for the ability to bind with Hsp90 (Harst et al., 2005; Woodford et al., 2016). These competition dynamics between Aha1 and p23/FNIP1 suggest that there is a constant battle for control of the ATPase activity of Hsp90. Additionally, FKBP51 and FKBP52 have been shown to have greater relative binding to Hsp90 compared to other TPR co-chaperones (Schülke et al., 2010). While not as strong as FKBP51 and FKBP52, PP5 forms more complexes with Hsp90 than most other TPR co-chaperones. Taken together, increased FKBP51 and decreased PP5 and CyP40 could contribute to an imbalance in Hsp90 heterocomplexes which may promote increased tau phosphorylation and aggregation causing neurotoxicity (Blair et al., 2013). This suggests an even more complex system in place because depending on the amount of certain co-chaperones and their relative ability to bind to Hsp90; certain maladaptive complexes could be more abundant than others with aging.

In addition to altering Hsp90 heterocomplex composition and client selection, altered Hsp90 co-chaperone expression can interfere with degradation of aberrant proteins via the proteasome or autophagy. As mentioned above, aged cells are often inundated with misfolded and aggregated proteins, which can overload the Hsp90 chaperone network causing a negative spiral where there are not enough healthy chaperone molecules to refold or degrade aberrant proteins. In addition to the problems faced with an overwhelmed chaperone network, the proteolytic activity of the proteasome also declines with aging, and in fact Hsp90 has been shown to protect the proteasome from age-related, oxidative-dependent decline (Conconi and Friguet, 1997). However, with advanced aging, the association between Hsp90 and the proteasome drastically decreases (Conconi et al., 1996). This suggests that because the Hsp90 chaperone system and the proteasome are so connected, when one starts to fail the other will fail as well leading to cytotoxicity and cell death. Proteins can also be degraded by CMA; however, CMA activity also decreases with age (Cuervo and Dice, 2000a). Hsp90 and Hop are both involved in the CMA system; helping to unfold the target substrate before it can translocate into the lysosome for degradation. As mentioned previously, both Hsp90 and Hop are repressed in aging and therefore may not be able to assist in the translocation of substrates, leading to a buildup of misfolded or aggregated proteins. Post-translational modifications (PTMs) of Hsp90 can also complicate the matter further.

There are many different PTMs that can affect Hsp90 including phosphorylation, acetylation, S-nitrosylation, oxidation, and ubiquitination; and all of these PTMs can impact the chaperoning function of Hsp90. Phosphorylation of Hsp90 leads to reduced chaperoning ability and phosphorylation of specific tyrosine residues can affect the ability of Hsp90 to interact with distinct client proteins (Zhao et al., 2001; Mollapour and Neckers, 2012). Acetylation of Hsp90 affects client protein interaction and also decreases binding of Hsp90 to ATP (Yu et al., 2002; Mollapour and Neckers, 2012). S-nitrosylation, oxidation and ubiquitination also inhibit Hsp90 chaperone activity (Blank et al., 2003; Martínez-Ruiz et al., 2005; Chen et al., 2008). These PTMs increase with aging and can alter the ability of Hsp90 to function properly as well as change the ability of different co-chaperones to bind. As the chaperone network declines with aging, so does the ability of the cell to recover from damaged proteins and stress, thus leading to an environment which promotes aberrant protein accumulation and neurotoxicity.

Targeting the Hsp90 Chaperone Network

Inhibition of the ATPase activity of Hsp90 has been shown to have positive outcomes in cell culture and animal models of tauopathy. Hsp90 ATPase inhibitors have been developed to target each of the three domains; with the majority of Hsp90 inhibitors targeting the N-terminal domain (Bhat et al., 2014). Inhibition of Hsp90 induces the expression of protective chaperones, Hsp70 and Hsp40, further promoting the degradation of aberrant proteins (Carman et al., 2013). Previous studies have shown that Hsp90 inhibition decreased the levels of hyperphosphorylated and/or mutated tau species both in cells and mice. The Hsp90 N-terminal domain inhibitor, EC102, was used to demonstrate degradation of hyperphosphorylated pathologically relevant tau in cells (Dickey et al., 2007a). Another N-terminal Hsp90 ATPase inhibitor, 17-AAG, was shown to decrease levels of phosphorylated tau in cells, and a related N-terminal Hsp90 ATPase inhibitor, PU-DZ8, reduced soluble and insoluble tau in tauP301L mice (Luo et al., 2007). Although Hsp90 inhibitors have been in clinical development since 1999, none have reached New Drug Application (NDA) status (Bhat et al., 2014). All of these clinical trials were focused on investigating Hsp90 inhibitors on various cancers. Hsp90 plays a similar role in both neurodegenerative disorders and cancer, however because of the complexity of the brain and the need for a blood-brain barrier (BBB) permeable drug, the clinical development of Hsp90 inhibitors for neurodegenerative diseases has been even less successful. While the development of Hsp90 inhibitors is still underway, it is possible that the development of therapeutics which target Hsp90 heterocomplexes or discrete Hsp90 co-chaperones could open up additional avenues for success in developing a BBB-permeable drug.

In addition to offering more potential therapeutic targets, small molecules which modify Hsp90/co-chaperone interactions may also show more specificity for a specific pool of Hsp90 which may reduce the number of on-target side effects. There

are very few Hsp90 co-chaperone targeting small molecules, and of these, only a handful of these have been investigated for their role in effecting tau. There is a Hop/Hsp90 complex specific inhibitor, C9, however, there is no available data on how chemical inhibition of this complex affects tau accumulation (Pimienta et al., 2011). The Cdc37/Hsp90 inhibitors, Celasterol and Withaferin A (Zhang et al., 2008; Yu et al., 2010), reduce tau levels and a new compound, platycodin D has just been discovered (Li et al., 2017). Platycodin D does not affect the ATPase activity of Hsp90, but instead disrupts the interaction between Hsp90 and Cdc37 leading to client protein degradation without an increase in Hsp70 (Li et al., 2017). More work still needs to be done to better understand the role of Cdc37 in tau phosphorylation to determine if targeting this complex is of therapeutic benefit. Developing drugs to target discrete FKBPs has been challenging due to their homology, however, despite their structural similarity they do display differences in conformational flexibility which could be a way to potentially target specific FKBPs in the future (LeMaster and Hernandez, 2015). Interestingly, one study demonstrated that patients chronically treated with FK506, which inhibits the PPIase domain of many of the FKBPs, significantly reduced the incidence of AD (Taglialatela et al., 2015). The targeting FKBP51 is of great interest for the treatment of tauopathies as well as mood disorders (Zannas and Binder, 2014). Recently a PPIase antagonist has been developed which shows selectivity for FKBP51, but additional studies are needed to determine if targeting the PPIase domain of FKBP51 will be effective in regulating tau accumulation (Jinwal et al., 2010). There is one compound, MJC13, which targets the FKBP52-Hsp90-androgen receptor complex (De Leon et al., 2011). MJC13 results in a reduced stress response which has demonstrated therapeutic potential in cancer, but so far MJC13 has not been investigated for a role in tau pathology (De Leon et al., 2011). Additionally, Aha1-specific inhibitors have been recently developed (Hall et al., 2014). One of these inhibitors, KU-177, reduced insoluble tauP301L levels in cells (Shelton et al., 2017). While this is an exciting result, more studies are needed to determine if Aha1 inhibitors regulate tau similarly *in vivo*. There is still much to be done to develop compounds which target the Hsp90 chaperone network, but there are a lot of promising leads which can be targeted to develop disease-modifying therapeutics.

CONCLUSIONS

The Hsp90 chaperone machinery plays a huge role in both aging and neurodegenerative diseases. Hsp90 is one of the most highly expressed proteins in the cell and is involved in a myriad of cellular processes. Previous work has focused on inhibition of Hsp90 to triage misfolded proteins. There are also many co-chaperones that associate with Hsp90 and play their own roles in aging and neurodegeneration. As these Hsp90 co-chaperones change with age they can significantly impact the propensity for certain neurodegenerative diseases. FKBP51 steadily increases with age and both FKBP51 and Aha1 are induced in the AD brain suggesting that these two co-chaperones negatively affect tau pathology. On the other hand, both CyP40 and PP5 are repressed in aged and AD brains. CyP40 disaggregates tau fibrils *in vitro* and PP5 dephosphorylates tau restoring microtubule binding, suggesting that increasing the levels or activity of these co-chaperones could have a beneficial, neuroprotective role in diseases such as AD. These are just a few examples of how important maintaining the balance of Hsp90 co-chaperones is to homeostasis, and what can happen when they are altered in aging and disease. Hsp90 co-chaperones offer a unique target for potential therapeutics due to their specific roles within the Hsp90 machinery. Overall, more work needs to be done to develop BBB-permeable therapeutics to target discrete Hsp90 co-chaperones for the treatment of AD and other tauopathies.

AUTHOR CONTRIBUTIONS

LS wrote the manuscript. JK created the figures and edited the manuscript. LB critiqued and edited the manuscript drafts.

FUNDING

This work was supported by NIH Grants NS073899 and MH103848.

REFERENCES

Abisambra, J. F., Jinwal, U. K., Blair, L. J., O'Leary, J. C., Li, Q., Brady, S., et al. (2013). Tau accumulation activates the unfolded protein response by impairing endoplasmic reticulum-associated degradation. *J. Neurosci. Off. J. Soc. Neurosci.* 33, 9498–9507. doi: 10.1523/JNEUROSCI.5397-12.2013

Ambegaokar, S. S., and Jackson, G. R. (2011). Functional genomic screen and network analysis reveal novel modifiers of tauopathy dissociated from tau phosphorylation. *Hum. Mol. Genet.* 20, 4947–4977. doi: 10.1093/hmg/ddr432

Baindur-Hudson, S., Edkins, A. L., and Blatch, G. L. (2015). Hsp70/Hsp90 organising protein (hop): beyond interactions with chaperones and prion proteins. *Subcell. Biochem.* 78, 69–90. doi: 10.1007/978-3-319-11731-7_3

Baker, J. D., Shelton, L. B., Zheng, D., Favretto, F., Nordhues, B. A., Darling, A., et al. (2017). Human cyclophilin 40 unravels neurotoxic amyloids. *PLoS Biol.* 15:e2001336. doi: 10.1371/journal.pbio.2001336

Beers, M., and Kemphues, K. (2006). Depletion of the co-chaperone CDC-37 reveals two modes of PAR-6 cortical association in *C. elegans* embryos. *Dev. Camb. Engl.* 133, 3745–3754. doi: 10.1242/dev.02544

Beraldo, F. H., Soares, I. N., Goncalves, D. F., Fan, J., Thomas, A. A., Santos, T. G., et al. (2013). Stress-inducible phosphoprotein 1 has unique cochaperone activity during development and regulates cellular response to ischemia via the prion protein. *FASEB J. Off. Publ. Fed. Am. Soc. Exp. Biol.* 27, 3594–3607. doi: 10.1096/fj.13-232280

Berchtold, N. C., Cribbs, D. H., Coleman, P. D., Rogers, J., Head, E., Kim, R., et al. (2008). Gene expression changes in the course of normal brain aging are sexually dimorphic. *Proc. Natl. Acad. Sci. U.S.A.* 105, 15605–15610. doi: 10.1073/pnas.0806883105

Bhat, R., Tummalapalli, S. R., and Rotella, D. P. (2014). Progress in the discovery and development of heat shock protein 90 (Hsp90) inhibitors. *J. Med. Chem.* 57, 8718–8728. doi: 10.1021/jm500823a

Blackburn, E. A., Wear, M. A., Landré, V., Narayan, V., Ning, J., Erman, B., et al. (2015). Cyclophilin40 isomerase activity is regulated by a temperature-dependent allosteric interaction with Hsp90. *Biosci. Rep.* 35:e00258. doi: 10.1042/BSR20150124

Blair, L. J., Nordhues, B. A., Hill, S. E., Scaglione, K. M., O'Leary, J. C., Fontaine, S. N., et al. (2013). Accelerated neurodegeneration through chaperone-mediated oligomerization of tau. *J. Clin. Invest.* 123, 4158–4169. doi: 10.1172/JCI69003

Blank, M., Mandel, M., Keisari, Y., Meruelo, D., and Lavie, G. (2003). Enhanced ubiquitinylation of heat shock protein 90 as a potential mechanism for mitotic cell death in cancer cells induced with hypericin. *Cancer Res.* 63, 8241–8247.

Blundell, K. L., Pal, M., Roe, S. M., Pearl, L. H., and Prodromou, C. (2017). The structure of FKBP38 in complex with the MEEVD tetratricopeptide binding-motif of Hsp90. *PLoS ONE* 12:e0173543. doi: 10.1371/journal.pone.0173543

Brehme, M., Voisine, C., Rolland, T., Wachi, S., Soper, J. H., Zhu, Y., et al. (2014). A chaperome subnetwork safeguards proteostasis in aging and neurodegenerative disease. *Cell Rep.* 9, 1135–1150. doi: 10.1016/j.celrep.2014.09.042

Brychzy, A., Rein, T., Winklhofer, K. F., Hartl, F. U., Young, J. C., and Obermann, W. M. J. (2003). Cofactor Tpr2 combines two TPR domains and a J domain to regulate the Hsp70/Hsp90 chaperone system. *EMBO J.* 22, 3613–3623. doi: 10.1093/emboj/cdg362

Bulgakov, O. V., Eggenschwiler, J. T., Hong, D.-H., Anderson, K. V., and Li, T. (2004). FKBP8 is a negative regulator of mouse sonic hedgehog signaling in neural tissues. *Dev. Camb. Engl.* 131, 2149–2159. doi: 10.1242/dev.01122

Calderwood, S. K. (2015). Cdc37 as a co-chaperone to Hsp90. *Subcell. Biochem.* 78, 103–112. doi: 10.1007/978-3-319-11731-7_5

Carman, A., Kishinevsky, S., Koren, J., Lou, W., and Chiosis, G. (2013). Chaperone-dependent neurodegeneration: a molecular perspective on therapeutic intervention. *J. Alzheimers Dis. Park.* 2013:007. doi: 10.4172/2161-0460.S10-007

Chen, W.-Y., Chang, F.-R., Huang, Z.-Y., Chen, J.-H., Wu, Y.-C., and Wu, C.-C. (2008). Tubocapsenolide A, a novel withanolide, inhibits proliferation and induces apoptosis in MDA-MB-231 cells by thiol oxidation of heat shock proteins. *J. Biol. Chem.* 283, 17184–17193. doi: 10.1074/jbc.M709447200

Cheung-Flynn, J., Prapapanich, V., Cox, M. B., Riggs, D. L., Suarez-Quian, C., and Smith, D. F. (2005). Physiological role for the cochaperone FKBP52 in androgen receptor signaling. *Mol. Endocrinol. Baltim. Md* 19, 1654–1666. doi: 10.1210/me.2005-0071

Conconi, M., and Friguet, B. (1997). Proteasome inactivation upon aging and on oxidation-effect of HSP 90. *Mol. Biol. Rep.* 24, 45–50. doi: 10.1023/A:1006852506884

Conconi, M., Szweda, L. I., Levine, R. L., Stadtman, E. R., and Friguet, B. (1996). Age-related decline of rat liver multicatalytic proteinase activity and protection from oxidative inactivation by heat-shock protein 90. *Arch. Biochem. Biophys.* 331, 232–240. doi: 10.1006/abbi.1996.0303

Conde, R., Xavier, J., McLoughlin, C., Chinkers, M., and Ovsenek, N. (2005). Protein phosphatase 5 is a negative modulator of heat shock factor 1. *J. Biol. Chem.* 280, 28989–28996. doi: 10.1074/jbc.M503594200

Cook, C., Gendron, T. F., Scheffel, K., Carlomagno, Y., Dunmore, J., DeTure, M., et al. (2012). Loss of HDAC6, a novel CHIP substrate, alleviates abnormal tau accumulation. *Hum. Mol. Genet.* 21, 2936–2945. doi: 10.1093/hmg/dds125

Cox, M. B., and Johnson, J. L. (2011). The role of p23, Hop, immunophilins, and other co-chaperones in regulating Hsp90 function. *Methods Mol. Biol. Clifton NJ* 787, 45–66. doi: 10.1007/978-1-61779-295-3_4

Crackower, M. A., Kolas, N. K., Noguchi, J., Sarao, R., Kikuchi, K., Kaneko, H., et al. (2003). Essential role of Fkbp6 in male fertility and homologous chromosome pairing in meiosis. *Science* 300, 1291–1295. doi: 10.1126/science.1083022

Cuervo, A. M., and Dice, J. F. (2000a). Age-related decline in chaperone-mediated autophagy. *J. Biol. Chem.* 275, 31505–31513. doi: 10.1074/jbc.M002102200

Cuervo, A. M., and Dice, J. F. (2000b). When lysosomes get old. *Exp. Gerontol.* 35, 119–131. doi: 10.1016/S0531-5565(00)00075-9

Dai, Q., Zhang, C., Wu, Y., McDonough, H., Whaley, R. A., Godfrey, V., et al. (2003). CHIP activates HSF1 and confers protection against apoptosis and cellular stress. *EMBO J.* 22, 5446–5458. doi: 10.1093/emboj/cdg529

De Leon, J. T., Iwai, A., Feau, C., Garcia, Y., Balsiger, H. A., Storer, C. L., et al. (2011). Targeting the regulation of androgen receptor signaling by the heat shock protein 90 cochaperone FKBP52 in prostate cancer cells. *Proc. Natl. Acad. Sci. U.S.A.* 108, 11878–11883. doi: 10.1073/pnas.1105160108

Dickey, C. A., Kamal, A., Lundgren, K., Klosak, N., Bailey, R. M., Dunmore, J., et al. (2007a). The high-affinity HSP90-CHIP complex recognizes and selectively degrades phosphorylated tau client proteins. *J. Clin. Invest.* 117, 648–658. doi: 10.1172/JCI29715

Dickey, C. A., Koren, J., Zhang, Y.-J., Xu, Y.-F., Jinwal, U. K., Birnbaum, M. J., et al. (2008). Akt and CHIP coregulate tau degradation through coordinated interactions. *Proc. Natl. Acad. Sci. U.S.A.* 105, 3622–3627. doi: 10.1073/pnas.0709180105

Dickey, C. A., Patterson, C., Dickson, D., and Petrucelli, L. (2007b). Brain CHIP: removing the culprits in neurodegenerative disease. *Trends Mol. Med.* 13, 32–38. doi: 10.1016/j.molmed.2006.11.003

Dickinson, M. E., Flenniken, A. M., Ji, X., Teboul, L., Wong, M. D., White, J. K., et al. (2016). High-throughput discovery of novel developmental phenotypes. *Nature* 537, 508–514. doi: 10.1038/nature19356

Du, X.-J., Cole, T. J., Tenis, N., Gao, X.-M., Köntgen, F., Kemp, B. E., et al. (2002). Impaired cardiac contractility response to hemodynamic stress in S100A1-deficient mice. *Mol. Cell. Biol.* 22, 2821–2829. doi: 10.1128/MCB.22.8.2821-2829.2002

Echeverría, P. C., Bernthaler, A., Dupuis, P., Mayer, B., and Picard, D. (2011). An interaction network predicted from public data as a discovery tool: application to the Hsp90 molecular chaperone machine. *PLoS ONE.* 6:e26044. doi: 10.1371/journal.pone.0026044

Edkins, A. L. (2015). CHIP: a co-chaperone for degradation by the proteasome. *Subcell. Biochem.* 78, 219–242. doi: 10.1007/978-3-319-11731-7_11

Eustace, B. K., Sakurai, T., Stewart, J. K., Yimlamai, D., Unger, C., Zehetmeier, C., et al. (2004). Functional proteomic screens reveal an essential extracellular role for hsp90 alpha in cancer cell invasiveness. *Nat. Cell Biol.* 6, 507–514. doi: 10.1038/ncb1131

Freeman, B. C., Toft, D. O., and Morimoto, R. I. (1996). Molecular chaperone machines: chaperone activities of the cyclophilin Cyp-40 and the steroid aporeceptor-associated protein p23. *Science* 274, 1718–1720. doi: 10.1126/science.274.5293.1718

Giustiniani, J., Guillemeau, K., Dounane, O., Sardin, E., Huvent, I., Schmitt, A., et al. (2015). The FK506-binding protein FKBP52 *in vitro* induces aggregation of truncated Tau forms with prion-like behavior. *FASEB J. Off. Publ. Fed. Am. Soc. Exp. Biol.* 29, 3171–3181. doi: 10.1096/fj.14-268243

Gong, C.-X., Liu, F., Wu, G., Rossie, S., Wegiel, J., Li, L., et al. (2004). Dephosphorylation of microtubule-associated protein tau by protein phosphatase 5. *J. Neurochem.* 88, 298–310. doi: 10.1111/j.1471-4159.2004.02147.x

Grad, I., Cederroth, C. R., Walicki, J., Grey, C., Barluenga, S., Winssinger, N., et al. (2010). The molecular chaperone Hsp90α is required for meiotic progression of spermatocytes beyond pachytene in the mouse. *PLoS ONE* 5:e15770. doi: 10.1371/journal.pone.0015770

Grad, I., McKee, T. A., Ludwig, S. M., Hoyle, G. W., Ruiz, P., Wurst, W., et al. (2006). The Hsp90 cochaperone p23 is essential for perinatal survival. *Mol. Cell. Biol.* 26, 8976–8983. doi: 10.1128/MCB.00734-06

Guo, T., Noble, W., and Hanger, D. P. (2017). Roles of tau protein in health and disease. *Acta Neuropathol. (Berl.)* 133, 665–704. doi: 10.1007/s00401-017-1707-9

Guy, N. C., Garcia, Y. A., Sivils, J. C., Galigniana, M. D., and Cox, M. B. (2015). Functions of the Hsp90-binding FKBP immunophilins. *Subcell. Biochem.* 78, 35–68. doi: 10.1007/978-3-319-11731-7_2

Hall, J. A., Forsberg, L. K., and Blagg, B. S. J. (2014). Alternative approaches to Hsp90 modulation for the treatment of cancer. *Future Med. Chem.* 6, 1587–1605. doi: 10.4155/fmc.14.89

Harst, A., Lin, H., and Obermann, W. M. J. (2005). Aha1 competes with Hop, p50 and p23 for binding to the molecular chaperone Hsp90 and contributes to kinase and hormone receptor activation. *Biochem. J.* 387, 789–796. doi: 10.1042/BJ20041283

Hasumi, H., Baba, M., Hasumi, Y., Lang, M., Huang, Y., Oh, H. F., et al. (2015). Folliculin-interacting proteins Fnip1 and Fnip2 play critical roles in kidney tumor suppression in cooperation with Flcn. *Proc. Natl. Acad. Sci. U.S.A.* 112, E1624–E1631. doi: 10.1073/pnas.1419502112

Hildenbrand, Z. L., Molugu, S. K., Herrera, N., Ramirez, C., Xiao, C., and Bernal, R. A. (2011). Hsp90 can accommodate the simultaneous binding of the FKBP52 and HOP proteins. *Oncotarget* 2, 43–58. doi: 10.18632/oncotarget.225

Jarczowski, F., Jahreis, G., Erdmann, F., Schierhorn, A., Fischer, G., and Edlich, F. (2009). FKBP36 is an inherent multifunctional glyceraldehyde-3-phosphate dehydrogenase inhibitor. *J. Biol. Chem.* 284, 766–773. doi: 10.1074/jbc.M709779200

Jascur, T., Brickner, H., Salles-Passador, I., Barbier, V., El Khissiin, A., Smith, B., et al. (2005). Regulation of p21(WAF1/CIP1) stability by WISp39, a Hsp90 binding TPR protein. *Mol. Cell* 17, 237–249. doi: 10.1016/j.molcel.2004.11.049

Jin, J., Tian, R., Pasculescu, A., Dai, A. Y., Williton, K., Taylor, L., et al. (2016). Mutational analysis of glycogen synthase kinase 3β protein kinase together with kinome-wide binding and stability studies suggests context-dependent recognition of kinases by the chaperone heat shock protein 90. *Mol. Cell. Biol.* 36, 1007–1018. doi: 10.1128/MCB.01045-15

Jinwal, U. K., Abisambra, J. F., Zhang, J., Dharia, S., O'Leary, J. C., Patel, T., et al. (2012). Cdc37/Hsp90 protein complex disruption triggers an autophagic clearance cascade for TDP-43 protein. *J. Biol. Chem.* 287, 24814–24820. doi: 10.1074/jbc.M112.367268

Jinwal, U. K., Koren, J., Borysov, S. I., Schmid, A. B., Abisambra, J. F., Blair, L. J., et al. (2010). The Hsp90 cochaperone, FKBP51, increases Tau stability and polymerizes microtubules. *J. Neurosci. Off. J. Soc. Neurosci.* 30, 591–599. doi: 10.1523/JNEUROSCI.4815-09.2010

Jinwal, U. K., Koren, J., and Dickey, C. A. (2013). Reconstructing the Hsp90/Tau machine. *Curr. Enzyme Inhib.* 9, 41–45. doi: 10.2174/1573408011309010006

Josefowicz, S. Z., Niec, R. E., Kim, H. Y., Treuting, P., Chinen, T., Zheng, Y., et al. (2012). Extrathymically generated regulatory T cells control mucosal TH2 inflammation. *Nature* 482, 395–399. doi: 10.1038/nature10772

Kamah, A., Cantrelle, F. X., Huvent, I., Giustiniani, J., Guillemeau, K., Byrne, C., et al. (2016). Isomerization and oligomerization of truncated and mutated tau forms by FKBP52 are independent processes. *J. Mol. Biol.* 428, 1080–1090. doi: 10.1016/j.jmb.2016.02.015

Kamal, A., Thao, L., Sensintaffar, J., Zhang, L., Boehm, M. F., Fritz, L. C., et al. (2003). A high-affinity conformation of Hsp90 confers tumour selectivity on Hsp90 inhibitors. *Nature* 425, 407–410. doi: 10.1038/nature01913

Karagöz, G. E., Duarte, A. M. S., Akoury, E., Ippel, H., Biernat, J., Morán Luengo, T. et al. (2014). Hsp90-tau complex reveals molecular basis for specificity in chaperone action. *Cell* 156, 963–974. doi: 10.1016/j.cell.2014.01.037

Kekatpure, V. D., Dannenberg, A. J., and Subbaramaiah, K. (2009). HDAC6 modulates Hsp90 chaperone activity and regulates activation of aryl hydrocarbon receptor signaling. *J. Biol. Chem.* 284, 7436–7445. doi: 10.1074/jbc.M808999200

Kovacs, G. G. (2015). Invited review: neuropathology of tauopathies: principles and practice. *Neuropathol. Appl. Neurobiol.* 41, 3–23. doi: 10.1111/nan.12208

Laenger, A., Lang-Rollin, I., Kozany, C., Zschocke, J., Zimmermann, N., Rüegg, J., et al. (2009). XAP2 inhibits glucocorticoid receptor activity in mammalian cells. *FEBS Lett.* 583, 1493–1498. doi: 10.1016/j.febslet.2009.03.072

Lee, C. H., Park, J. H., Choi, J. H., Yoo, K.-Y., Ryu, P. D., and Won, M.-H. (2011). Heat shock protein 90 and its cochaperone, p23, are markedly increased in the aged gerbil hippocampus. *Exp. Gerontol.* 46, 768–772. doi: 10.1016/j.exger.2011.05.002

LeMaster, D. M., and Hernandez, G. (2015). Conformational dynamics in FKBP domains: relevance to molecular signaling and drug design. *Curr. Mol. Pharmacol.* 9, 5–26. doi: 10.2174/1874467208666150519113146

Li, J., and Buchner, J. (2013). Structure, function and regulation of the hsp90 machinery. *Biomed. J.* 36, 106–117. doi: 10.4103/2319-4170.113230

Li, J., Soroka, J., and Buchner, J. (2012). The Hsp90 chaperone machinery: conformational dynamics and regulation by co-chaperones. *Biochim. Biophys. Acta* 1823, 624–635. doi: 10.1016/j.bbamcr.2011.09.003

Li, T., Chen, X., Dai, X.-Y., Wei, B., Weng, Q.-J., Chen, X., et al. (2017). Novel Hsp90 inhibitor platycodin D disrupts Hsp90/Cdc37 complex and enhances the anticancer effect of mTOR inhibitor. *Toxicol. Appl. Pharmacol.* 330, 65–73. doi: 10.1016/j.taap.2017.07.006

Liberek, K., Lewandowska, A., and Zietkiewicz, S. (2008). Chaperones in control of protein disaggregation. *EMBO J.* 27, 328–335. doi: 10.1038/sj.emboj.7601970

Liu, F., Iqbal, K., Grundke-Iqbal, I., Rossie, S., and Gong, C.-X. (2005). Dephosphorylation of tau by protein phosphatase 5: impairment in Alzheimer's disease. *J. Biol. Chem.* 280, 1790–1796. doi: 10.1074/jbc.M410775200

Loerch, P. M., Lu, T., Dakin, K. A., Vann, J. M., Isaacs, A., Geula, C., et al. (2008). Evolution of the aging brain transcriptome and synaptic regulation. *PLoS ONE* 3:e3329. doi: 10.1371/journal.pone.0003329

Lovgren, A. K., Kovarova, M., and Koller, B. H. (2007). cPGES/p23 is required for glucocorticoid receptor function and embryonic growth but not prostaglandin E2 synthesis. *Mol. Cell. Biol.* 27, 4416–4430. doi: 10.1128/MCB.02314-06

Luo, W., Dou, F., Rodina, A., Chip, S., Kim, J., Zhao, Q., et al. (2007). Roles of heat-shock protein 90 in maintaining and facilitating the neurodegenerative phenotype in tauopathies. *Proc. Natl. Acad. Sci. U.S.A.* 104, 9511–9516. doi: 10.1073/pnas.0701055104

Mandelkow, E.-M., and Mandelkow, E. (2012). Biochemistry and cell biology of tau protein in neurofibrillary degeneration. *Cold Spring Harb. Perspect. Med.* 2:a006247. doi: 10.1101/cshperspect.a006247

Martínez-Ruiz, A., Villanueva, L., González de Orduña, C., López-Ferrer, D., Higueras, M. A., Tarín, C., et al. (2005). S-nitrosylation of Hsp90 promotes the inhibition of its ATPase and endothelial nitric oxide synthase regulatory activities. *Proc. Natl. Acad. Sci. U.S.A.* 102, 8525–8530. doi: 10.1073/pnas.0407294102

Meduri, G., Guillemeau, K., Dounane, O., Sazdovitch, V., Duyckaerts, C., Chambraud, B., et al. (2016). Caspase-cleaved Tau-D(421) is colocalized with the immunophilin FKBP52 in the autophagy-endolysosomal system of Alzheimer's disease neurons. *Neurobiol. Aging* 46, 124–137. doi: 10.1016/j.neurobiolaging.2016.06.017

Miyata, Y., Koren, J., Kiray, J., Dickey, C. A., and Gestwicki, J. E. (2011). Molecular chaperones and regulation of tau quality control: strategies for drug discovery in tauopathies. *Future Med. Chem.* 3, 1523–1537. doi: 10.4155/fmc.11.88

Moffatt, N. S., Bruinsma, E., Uhl, C., Obermann, W. M., and Toft, D. (2008). Role of the cochaperone Tpr2 in Hsp90 chaperoning. *Biochemistry (Mosc.)* 47, 8203–8213. doi: 10.1021/bi800770g

Mollapour, M., and Neckers, L. (2012). Post-translational modifications of Hsp90 and their contributions to chaperone regulation. *Biochim. Biophys. Acta* 1823, 648–655. doi: 10.1016/j.bbamcr.2011.07.018

Nakatani, Y., Hokonohara, Y., Kakuta, S., Sudo, K., Iwakura, Y., and Kudo, I. (2007). Knockout mice lacking cPGES/p23, a constitutively expressed PGE2 synthetic enzyme, are peri-natally lethal. *Biochem. Biophys. Res. Commun.* 362, 387–392. doi: 10.1016/j.bbrc.2007.07.180

Njemini, R., Lambert, M., Demanet, C., Kooijman, R., and Mets, T. (2007). Basal and infection-induced levels of heat shock proteins in human aging. *Biogerontology* 8, 353–364. doi: 10.1007/s10522-006-9078-y

O'Leary, J. C., Dharia, S., Blair, L. J., Brady, S., Johnson, A. G., Peters, M., et al. (2011). A new anti-depressive strategy for the elderly: ablation of FKBP5/FKBP51. *PLoS ONE* 6:e24840. doi: 10.1371/journal.pone.0024840

Orr, M. E., Sullivan, A. C., and Frost, B. (2017). A brief overview of tauopathy: causes, consequences, and therapeutic strategies. *Trends Pharmacol. Sci.* 38, 637–648. doi: 10.1016/j.tips.2017.03.011

Palubinsky, A. M., Stankowski, J. N., Kale, A. C., Codreanu, S. G., Singer, R. J., Liebler, D. C., et al. (2015). CHIP is an essential determinant of neuronal mitochondrial stress signaling. *Antioxid. Redox Signal.* 23, 535–549. doi: 10.1089/ars.2014.6102

Periyasamy, S., Hinds, T., Shemshedini, L., Shou, W., and Sanchez, E. R. (2010). FKBP51 and Cyp40 are positive regulators of androgen-dependent prostate cancer cell growth and the targets of FK506 and cyclosporin A. *Oncogene* 29, 1691–1701. doi: 10.1038/onc.2009.458

Philp, L. K., Day, T. K., Butler, M. S., Laven-Law, G., Jindal, S., Hickey, T. E., et al. (2016). Small glutamine-rich tetratricopeptide repeat-containing protein alpha (SGTA) ablation limits offspring viability and growth in mice. *Sci. Rep.* 6:28950. doi: 10.1038/srep28950

Picard, D. (2002). Heat-shock protein 90, a chaperone for folding and regulation. *Cell. Mol. Life Sci. CMLS* 59, 1640–1648. doi: 10.1007/PL00012491

Pimienta, G., Herbert, K. M., and Regan, L. (2011). A compound that inhibits the HOP-Hsp90 complex formation and has unique killing effects in breast cancer cell lines. *Mol. Pharm.* 8, 2252–2261. doi: 10.1021/mp200346y

Pinheiro, S., Silva, J., Mota, C., Vaz-Silva, J., Veloso, A., Pinto, V., et al. (2016). Tau mislocation in glucocorticoid-triggered hippocampal pathology. *Mol. Neurobiol.* 53, 4745–4753. doi: 10.1007/s12035-015-9356-2

Prodromou, C. (2016). Mechanisms of Hsp90 regulation. *Biochem. J.* 473, 2439–2452. doi: 10.1042/BCJ20160005

Prodromou, C., Panaretou, B., Chohan, S., Siligardi, G., O'Brien, R., Ladbury, J. E., et al. (2000). The ATPase cycle of Hsp90 drives a molecular 'clamp' via transient dimerization of the N-terminal domains. *EMBO J.* 19, 4383–4392. doi: 10.1093/emboj/19.16.4383

Raitila, A., Lehtonen, H. J., Arola, J., Heliövaara, E., Ahlsten, M., Georgitsi, M., et al. (2010). Mice with inactivation of aryl hydrocarbon receptor-interacting protein (Aip) display complete penetrance of pituitary adenomas with aberrant ARNT expression. *Am. J. Pathol.* 177, 1969–1976. doi: 10.2353/ajpath.2010.100138

Ramamurthy, V., Roberts, M., van den Akker, F., Niemi, G., Reh, T. A., and Hurley, J. B. (2003). AIPL1, a protein implicated in Leber's congenital amaurosis, interacts with and aids in processing of farnesylated proteins. *Proc. Natl. Acad. Sci. U.S.A.* 100, 12630–12635. doi: 10.1073/pnas.2134194100

Rao, R. V., Niazi, K., Mollahan, P., Mao, X., Crippen, D., Poksay, K. S., et al. (2006). Coupling endoplasmic reticulum stress to the cell-death program: a novel HSP90-independent role for the small chaperone protein p23. *Cell Death Differ.* 13, 415–425. doi: 10.1038/sj.cdd.4401761

Reeve, A., Simcox, E., and Turnbull, D. (2014). Ageing and Parkinson's disease: why is advancing age the biggest risk factor? *Ageing Res. Rev.* 14, 19–30. doi: 10.1016/j.arr.2014.01.004

Rehn, A. B., and Buchner, J. (2015). p23 and Aha1. *Subcell. Biochem.* 78, 113–131. doi: 10.1007/978-3-319-11731-7_6

Renouf, D. J., Hedley, D., Krzyzanowska, M. K., Schmuck, M., Wang, L., and Moore, M. J. (2016). A phase II study of the HSP90 inhibitor AUY922 in chemotherapy refractory advanced pancreatic cancer. *Cancer Chemother. Pharmacol.* 78, 541–545. doi: 10.1007/s00280-016-3102-y

Richardson, R. T., Alekseev, O. M., Grossman, G., Widgren, E. E., Thresher, R., Wagner, E. J., et al. (2006). Nuclear autoantigenic sperm protein (NASP), a linker histone chaperone that is required for cell proliferation. *J. Biol. Chem.* 281, 21526–21534. doi: 10.1074/jbc.M603816200

Rock, K. L., Gramm, C., Rothstein, L., Clark, K., Stein, R., Dick, L., et al. (1994). Inhibitors of the proteasome block the degradation of most cell proteins and the generation of peptides presented on MHC class I molecules. *Cell* 78, 761–771. doi: 10.1016/S0092-8674(94)90462-6

Rodina, A., Wang, T., Yan, P., Gomes, E. D., Dunphy, M. P. S., Pillarsetty, N., et al. (2016). The epichaperome is an integrated chaperome network that facilitates tumour survival. *Nature* 538, 397–401. doi: 10.1038/nature19807

Sabbagh, J. J., O'Leary, J. C., Blair, L. J., Klengel, T., Nordhues, B. A., Fontaine, S. N., et al. (2014). Age-associated epigenetic upregulation of the FKBP5 gene selectively impairs stress resiliency. *PLoS ONE* 9:e107241. doi: 10.1371/journal.pone.0107241

Schopf, F. H., Biebl, M. M., and Buchner, J. (2017). The HSP90 chaperone machinery. *Nat. Rev. Mol. Cell Biol.* 18, 345–360. doi: 10.1038/nrm.2017.20

Schülke, J.-P., Wochnik, G. M., Lang-Rollin, I., Gassen, N. C., Knapp, R. T., Berning, B., et al. (2010). Differential impact of tetratricopeptide repeat proteins on the steroid hormone receptors. *PLoS ONE* 5:e11717. doi: 10.1371/journal.pone.0011717

Selenica, M.-L., Benner, L., Housley, S. B., Manchec, B., Lee, D. C., Nash, K. R., et al. (2014). Histone deacetylase 6 inhibition improves memory and reduces total tau levels in a mouse model of tau deposition. *Alzheimers Res. Ther.* 6:12. doi: 10.1186/alzrt241

Shelton, L. B., Baker, J. D., Zheng, D., Sullivan, L. E., Solanki, P. K., Webster, J. M., et al. (2017). Hsp90 activator Aha1 drives production of pathological tau aggregates. *Proc. Natl. Acad. Sci. U.S.A.* 114, 9707–9712. doi: 10.1073/pnas.1707039114

Silverstein, A. M., Galigniana, M. D., Chen, M. S., Owens-Grillo, J. K., Chinkers, M., and Pratt, W. B. (1997). Protein phosphatase 5 is a major component of glucocorticoid receptor.hsp90 complexes with properties of an FK506-binding immunophilin. *J. Biol. Chem.* 272, 16224–16230. doi: 10.1074/jbc.272.26.16224

Söti, C., and Csermely, P. (2002). Chaperones and aging: role in neurodegeneration and in other civilizational diseases. *Neurochem. Int.* 41, 383–389. doi: 10.1016/S0197-0186(02)00043-8

Sreedhar, A. S., Kalmár, E., Csermely, P., and Shen, Y.-F. (2004). Hsp90 isoforms: functions, expression and clinical importance. *FEBS Lett.* 562, 11–15. doi: 10.1016/S0014-5793(04)00229-7

Sullivan, W., Stensgard, B., Caucutt, G., Bartha, B., McMahon, N., Alnemri, E. S., et al. (1997). Nucleotides and two functional states of hsp90. *J. Biol. Chem.* 272, 8007–8012. doi: 10.1074/jbc.272.12.8007

Taglialatela, G., Rastellini, C., and Cicalese, L. (2015). Reduced incidence of dementia in solid organ transplant patients treated with calcineurin inhibitors. *J. Alzheimers Dis. JAD* 47, 329–333. doi: 10.3233/JAD-150065

Taipale, M., Krykbaeva, I., Koeva, M., Kayatekin, C., Westover, K. D., Karras, G. I., et al. (2012). Quantitative analysis of HSP90-client interactions reveals principles of substrate recognition. *Cell* 150, 987–1001. doi: 10.1016/j.cell.2012.06.047

Tarkar, A., Loges, N. T., Slagle, C. E., Francis, R., Dougherty, G. W., Tamayo, J. V., et al. (2013). DYX1C1 is required for axonemal dynein assembly and ciliary motility. *Nat. Genet.* 45, 995–1003. doi: 10.1038/ng.2707

Terada, K., Ueno, S., Yomogida, K., Imai, T., Kiyonari, H., Takeda, N., et al. (2003). Expression of Tom34 splicing isoforms in mouse testis and knockout of Tom34 in mice. *J. Biochem.* 133, 625–631.

Terman, A. (2001). Garbage catastrophe theory of aging: imperfect removal of oxidative damage? *Redox Rep. Commun. Free Radic. Res.* 6, 15–26. doi: 10.1179/135100001101535996

Thakur, M. K., Heilbrun, L. K., Sheng, S., Stein, M., Liu, G., Antonarakis, E. S., et al. (2016). A phase II trial of ganetespib, a heat shock protein 90 Hsp90) inhibitor, in patients with docetaxel-pretreated metastatic castrate-resistant prostate cancer (CRPC)-a prostate cancer clinical trials consortium (PCCTC) study. *Invest. New Drugs* 34, 112–118. doi: 10.1007/s10637-015-0307-6

Touma, C., Gassen, N. C., Herrmann, L., Cheung-Flynn, J., Büll, D. R., Ionescu, I. A., et al. (2011). FK506 binding protein 5 shapes stress responsiveness: modulation of neuroendocrine reactivity and coping behavior. *Biol. Psychiatry* 70, 928–936. doi: 10.1016/j.biopsych.2011.07.023

Tranguch, S., Cheung-Flynn, J., Daikoku, T., Prapapanich, V., Cox, M. B., Xie, H., et al. (2005). Cochaperone immunophilin FKBP52 is critical to uterine receptivity for embryo implantation. *Proc. Natl. Acad. Sci. U.S.A.* 102, 14326–14331. doi: 10.1073/pnas.0505775102

Voss, A. K., Thomas, T., and Gruss, P. (2000). Mice lacking HSP90beta fail to develop a placental labyrinth. *Dev. Camb. Engl.* 127, 1–11.

Wang, X., Venable, J., LaPointe, P., Hutt, D. M., Koulov, A. V., Coppinger, J., et al. (2006). Hsp90 cochaperone Aha1 downregulation rescues misfolding of CFTR in cystic fibrosis. *Cell* 127, 803–815. doi: 10.1016/j.cell.2006.09.043

Wolmarans, A., Lee, B., Spyracopoulos, L., and LaPointe, P. (2016). The mechanism of Hsp90 ATPase stimulation by Aha1. *Sci. Rep.* 6, 33179. doi: 10.1038/srep33179

Woodford, M. R., Dunn, D. M., Blanden, A. R., Capriotti, D., Loiselle, D., Prodromou, C., et al. (2016). The FNIP co-chaperones decelerate the Hsp90 chaperone cycle and enhance drug binding. *Nat. Commun.* 7:12037. doi: 10.1038/ncomms12037

Yakkundi, A., Bennett, R., Hernández-Negrete, I., Delalande, J.-M., Hanna, M., Lyubomska, O., et al. (2015). FKBPL is a critical antiangiogenic regulator of developmental and pathological angiogenesis. *Arterioscler. Thromb. Vasc. Biol.* 35, 845–854. doi: 10.1161/ATVBAHA.114.304539

Yang, Z., Wolf, I. M., Chen, H., Periyasamy, S., Chen, Z., Yong, W., et al. (2006). FK506-binding protein 52 is essential to uterine reproductive physiology controlled by the progesterone receptor A isoform. *Mol. Endocrinol. Baltim. Md* 20, 2682–2694. doi: 10.1210/me.2006-0024

Yong, W., Yang, Z., Periyasamy, S., Chen, H., Yucel, S., Li, W., et al. (2007). Essential role for co-chaperone FKBP52 but not FKBP51 in androgen receptor-mediated signaling and physiology. *J. Biol. Chem.* 282, 5026–5036. doi: 10.1074/jbc.M609360200

Yu, X., Guo, Z. S., Marcu, M. G., Neckers, L., Nguyen, D. M., Chen, G. A., et al. (2002). Modulation of p53, ErbB1, ErbB2, and Raf-1 expression in lung cancer cells by depsipeptide FR901228. *J. Natl. Cancer Inst.* 94, 504–513. doi: 10.1093/jnci/94.7.504

Yu, Y., Hamza, A., Zhang, T., Gu, M., Zou, P., Newman, B., et al. (2010). Withaferin A targets heat shock protein 90 in pancreatic cancer cells. *Biochem. Pharmacol.* 79, 542–551. doi: 10.1016/j.bcp.2009.09.017

Zannas, A. S., and Binder, E. B. (2014). Gene-environment interactions at the FKBP5 locus: sensitive periods, mechanisms and pleiotropism. *Genes Brain Behav.* 13, 25–37. doi: 10.1111/gbb.12104

Zhang, J., Spilman, P., Chen, S., Gorostiza, O., Matalis, A., Niazi, K., et al. (2013). The small co-chaperone p23 overexpressing transgenic mouse. *J. Neurosci. Methods* 212, 190–194. doi: 10.1016/j.jneumeth.2012.09.022

Zhang, T., Hamza, A., Cao, X., Wang, B., Yu, S., Zhan, C.-G., et al. (2008). A novel Hsp90 inhibitor to disrupt Hsp90/Cdc37 complex against pancreatic cancer cells. *Mol. Cancer Ther.* 7, 162–170. doi: 10.1158/1535-7163.MCT-07-0484

Zhao, Y. G., Gilmore, R., Leone, G., Coffey, M. C., Weber, B., and Lee, P. W. (2001). Hsp90 phosphorylation is linked to its chaperoning function. Assembly of the reovirus cell attachment protein. *J. Biol. Chem.* 276, 32822–32827. doi: 10.1074/jbc.M105562200

Conflict of Interest Statement: The authors declare that the research was conducted in the absence of any commercial or financial relationships that could be construed as a potential conflict of interest.

frontiers in Neuroscience

MINI REVIEW
published: 10 November 2017
doi: 10.3389/fnins.2017.00626

Cognitive Decline in Neuronal Aging and Alzheimer's Disease: Role of NMDA Receptors and Associated Proteins

Jesús Avila[1,2]*, *María Llorens-Martín*[1,2], *Noemí Pallas-Bazarra*[1,2], *Marta Bolós*[1,2], *Juan R. Perea*[1,2], *Alberto Rodríguez-Matellán*[1,2] and *Félix Hernández*[1,2]

[1] Centro de Biología Molecular Severo Ochoa, Consejo Superior de Investigaciones Científicas, Universidad Autonoma de Madrid (CSIC-UAM), Madrid, Spain, [2] Centro de Investigación Biomédica en Red de Enfermedades Neurodegenerativas, Instituto de Salud Carlos III (ISCIII), Madrid, Spain

Molecular changes associated with neuronal aging lead to a decrease in cognitive capacity. Here we discuss these alterations at the level of brain regions, brain cells, and brain membrane and cytoskeletal proteins with an special focus in NMDA molecular changes through aging and its effect in cognitive decline and Alzheimer disease. Here, we propose that some neurodegenerative disorders, like Alzheimer's disease (AD), are characterized by an increase and acceleration of some of these changes.

Keywords: tau proteins, neurotransmitter agents, dendritic spines, cognition, therapies

OPEN ACCESS

Edited by:
Naruhiko Sahara,
National Institute of Radiological Sciences (NIRS), Japan

Reviewed by:
Shinsuke Ishigaki,
Nagoya University, Japan
Irving E. Vega,
Michigan State University, United States

***Correspondence:**
Jesús Avila
javila@cbm.csic.es

Specialty section:
This article was submitted to Neurodegeneration, a section of the journal Frontiers in Neuroscience

Received: *13 September 2017*
Accepted: *26 October 2017*
Published: *10 November 2017*

Citation:
Avila J, Llorens-Martín M, Pallas-Bazarra N, Bolós M, Perea JR, Rodríguez-Matellán A and Hernández F (2017) Cognitive Decline in Neuronal Aging and Alzheimer's Disease: Role of NMDA Receptors and Associated Proteins. Front. Neurosci. 11:626. doi: 10.3389/fnins.2017.00626

INTRODUCTION

Human development and maturation are characterized by various stages, the final one being aging. The different stages are characterized by different cellular and molecular changes. The changes that occur during the final phase may, in part, result from the accumulation of alterations that have taken place in previous phases.

Aging is influenced not only by the programmed developmental process from gestation through to the final stages of human life but also by the environment (see Figure 2 of reference Sharon et al., 2016). Some of the hallmarks of aging in peripheral tissues are also common to aged brain cells (**Table 1**). These include an increase in reactive oxygen species production, together with a decrease in the removal of these species (Espinet et al., 2015; Yuan et al., 2015; Zhang et al., 2016), mitochondrial alterations (Santos et al., 2013; He et al., 2016), and the deterioration of neuronal stem cells (Licht et al., 2016; **Table 2**). Recently, a growing amount of literature demonstrates that alterations in peripheral tissues affect brain aging, being an example the influence of the gut microbiome (Lustgarten, 2016; Schroeder and Backhed, 2016; Sharon et al., 2016).

All of these changes can favor the development of neurodegenerative diseases. Indeed, aging is the main risk for Alzheimer's disease (AD), and it has been proposed that therapies seeking to slow down aging may also delay the onset of this condition. An example are blood factors that are able to revitalize hippocampal function (Wyss-Coray, 2016; Castellano et al., 2017). In this review, we address the aging-dependent alterations of the morphology of neurons and glia (mainly microglia), of a cytoskeletal component (microtubules), and of a cytoskeletal microtubule-associated protein (tau), and how these changes contribute to aging-dependent cognitive decline. To this end, here we focus on neurons present in brain regions, such as the hippocampus and cortex, which are involved mainly in memory and learning.

TABLE 1 | Some hallmarks of aging in peripheral tissues that are also present in brain tissue.

	Hallmarks of aging in peripheral tissues
1	Genomic instability
2	Epigenetic alterations
3	Decrease in growth factors
4	Mitochondrial dysfunction
5	Loss of proteostasis
6	Stem cell exhaustion
7	Cellular senescence

TABLE 2 | Some hallmarks of brain aging.

	Hallmarks for brain aging
1	Neuron senescence
2	Microglia activation and senescence
3	Changes in spine plasticity
4	Cytoskeletal changes
5	Changes in the amount and localization of neurotransmitter receptors

AGING IN NEURONS

The main risk factor for several neurodegenerative disorders, including AD, is aging. However, these disorders can be triggered by inherited mutations, environmental factors, and somatic mutations in the cells present in the central nervous system (CNS) (see for example Gomez-Ramos et al., 2017; Hoch et al., 2017) or read the proposed unifying mechanism in neurodegeneration that involves DNA damage and DNA repair errors in aged neurons (Ross and Truant, 2017).

Neuron morphology is characterized by the presence of several short and wide cytoplasmic extensions (dendrites), which may have some protrusions (dendritic spines), and a long and thin cytoplasmatic extension (axon), which may be wrapped by some glia (oligodendrocytes) structures. At the cellular (cytoskeleton) level, neurons display an age-dependent reduction in microtubules (Cash et al., 2003). It has also been proposed that the actin cytoskeleton contributes to aging (Gourlay et al., 2004; Mattson and Magnus, 2006). At cellular-molecular level, neuronal aging can be visualized by mean of universal biomarkers of cell senescence (Evangelou et al., 2017), namely lipofuscin (a fluorescent aggregate of oxidized proteins, metals and lipids) (Jung et al., 2007) and β-galactosidase activity (Dimri et al., 1995; Munoz-Espin and Serrano, 2014).

A main feature related to brain aging is cognitive decline. Cognitive capacity has been related to neuron number and function. Humans have around 86 billion neurons (Herculano-Houzel, 2012), and this number decreases during aging as a result of various factors. Selective neuronal susceptibility due to calcium dysregulation, mitochondrial perturbations, lack of neurotrophic factors, and cytoskeletal disruption, among others, may account for this decrease (Mattson and Magnus, 2006). Thus, brain atrophy occurs during aging (O'Shea et al., 2016; Pini et al., 2016). A recent study indicates that two components related to neurodegenerative disorders, namely tau and amyloid beta (Aβ) peptide, are associated with memory encoding during normal aging (Marks et al., 2017).

Nevertheless, changes in neuronal function may occur prior to neurodegeneration as a result of a decrease in neuron-neuron connectivity through synapses. In this regard, analysis of such alterations is now unfeasible, given that it has been postulated that the number of synapses in humans could amount to around 11.5×10^{14} (Herculano-Houzel, 2012).

DENDRITIC SPINES

There are several types of synapses, some are excitatory while others are inhibitory. The former can be identified on the basis of a spine-like shape, and since their discovery by Cajal they are referred to as dendritic spines (Ramon y Cajal, 1888 quoted in Yuste, 2015). The structure, dynamics and regulation of these spines are summarized in Hering and Sheng (2001).

The molecular scaffold of these spines is related to an actin cytoskeleton, composed of actin and actin binding proteins (Mattson and Magnus, 2006; **Figure 1**). Some of these proteins, like debrin (Hayashi and Shirao, 1999), bind to microtubule-binding proteins like EB3 (Dent, 2017). These in turn bind to other microtubule-binding proteins, like tau (Ramirez-Rios et al., 2016), a molecule that is also present in the spines (Ittner et al., 2010). Some of these proteins, together with small GTPases like Rac1 (Luo et al., 1996), RhoA (Mattson and Magnus, 2006), or SPAR (Naisbitt et al., 1999; Pak et al., 2001), regulate spine shape and function (Mattson and Magnus, 2006), through the formation of protein complexes with structural proteins like PSD95, Shank and Homer, among others (Naisbitt et al., 1999).

CHANGES IN DENDRITIC SPINES WITH AGING

Dendrites show progressive regression with increasing age in several brain regions (de Brabander et al., 1998; Kabaso et al., 2009). In a mouse model of aging, this regression occurs mainly in apical dendrites (Shimada et al., 2006). Glutamatergic receptors are among the key membrane proteins located on the surface of dendritic spines, and they participate in processes like learning and memory (Kumar, 2015). Glutamate acts on various membrane neuron receptors: NMDA, AMPA and ionotropic glutamate receptors (Dingledine et al., 1999; Conn et al., 2005). Here we will focus on NMDA receptors, which are found not only at the (synaptic) spine dendrites but also at extrasynaptic sites (Sun et al., 2016; **Figure 2**) although trafficking of AMPA receptors is also essential for synaptic plasticity and cognitive aging as well (Cantanelli et al., 2014).

NMDA RECEPTORS

NMDA receptors are diverse in their subunit composition (GluN1, GluN2, and GluN3) (Paoletti et al., 2013). Combinations of GluN1 with a mixture of GluN2 or GluN3 subunits can build a

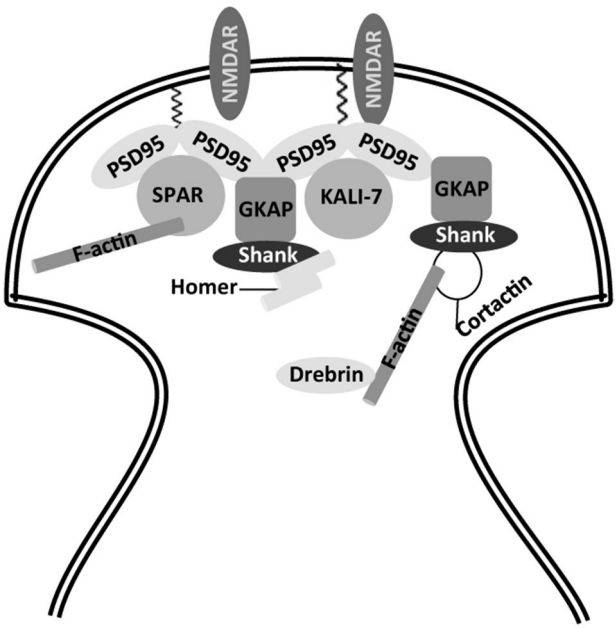

FIGURE 1 | Partial view of actin cytoskeleton in dendritic spines. Scaffold proteins involved in anchoring of NMDA receptors to actin cytoskeleton. NMDAR, N-methyl-D-aspartate receptor; PSD-95, post-synaptic density protein 95; GKAP, guanylate kinase-associated protein; Shank, SH3 and ankyrin repeat-containing protein; SPAR, spine-associated RapGAP; KALI-7, kalirin-7.

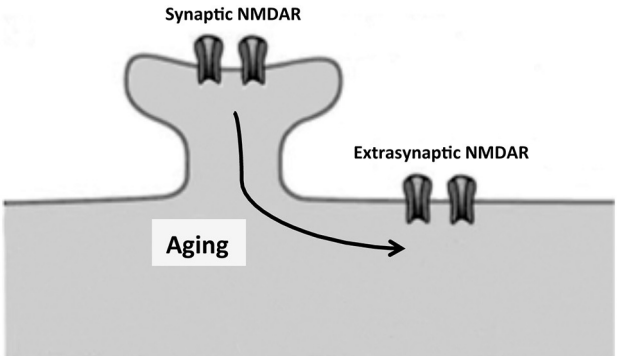

FIGURE 2 | Proposed movement, by lateral diffusion, of NMDA receptors from dendritic spines to extrasynaptic sites. Unbalance between synaptic and extrasynaptic NMDAR may contribute to cognitive decline in neuronal aging and neurodegenerative diseases as Alzheimer disease.

functional NMDA tetramer (Paoletti et al., 2013). Four distinct GluN2 subunits (GluN2A, GluN2B, GluN2C, or GluN2D) can be present in this tetramer. Also, there are two distinct GluN3 subunits (GluN3A and GluN3B) (Paoletti et al., 2013).

GluN2 and GluN3 subunits differ in temporal expression. In the embryonic brain, GluN2B and GluN2D are present, while GluN2A and GluN2C expression starts after birth. After this point, GluN2D, and GluN2B expression decreases, the latter remaining mainly in the adult forebrain. GluN2C expression is found mainly in the cerebellum and olfactory bulb. In the case of GluN3 subunits, the expression of GluN3A occurs earlier than that of GluN3B, which is expressed mainly in motor neurons (for a comprehensive review on this subject, see reference Paoletti et al., 2013).

The function of GluN subunits may be related to their localization. GluN2A and GluN2B, present in hippocampus and cortex (Watanabe et al., 1993; Monyer et al., 1994; Laurie et al., 1997), have been associated with processes like learning and memory (Woodhall et al., 2001; Bidoret et al., 2009). Also, GluN2A, present in prefrontal cortex, may be required for working memory and its decrease is associated with age-related cognitive decline (McQuail et al., 2016). GluN2B appears to be crucial for channel function and post-synaptic macromolecular organization (Akashi et al., 2009). In the prefrontal cortex, this subunit may be involved in contextual fear memory (Zhao et al., 2005). In addition, GluN2B has been postulated to participate in depression (Tannenholz et al., 2016) and addictive behavior (Hopf, 2017).

NMDA receptors containing GluN2B are particularly mobile and segregate outside synapses to extrasynaptic sites (Triller and Choquet, 2005; Groc et al., 2006). This process may increase with aging (see below) (**Figure 2**).

NMDA RECEPTORS DURING SENESCENCE

A possible relationship between impaired memory function and a decrease in NMDA receptors (Kumar, 2015) during senescence has been proposed. Thus, a decrease in NMDA receptor protein expression in regions like the hippocampus occurs during senescence (Magnusson, 1998). This decrease involve a reduction in GluN1 (Gazzaley et al., 1996; Liu et al., 2008). Also, an age-related decrease in the expression of GluN2A and GluN2B occurs in the hippocampus (Sonntag et al., 2000; Zhao et al., 2009). This decrease occurs together with a change in the localization of GluN2B from the synapse to extrasynaptic sites (Potier et al., 2010). A reduction in glutamate uptake has been associated with extrasynaptic NMDA receptors at the hippocampal CA1 synapse of aged rats (Potier et al., 2010). Recently, it has been reported that activation of extrasynaptic NMDA receptors induces tau overexpression (Sun et al., 2016). Since, the GluN2B subunit is present (Rammes et al., 2017) in extrasynaptic NMDA receptors, it has been considered a potential target for the treatment of neurodegenerative disorders related to aging, such as AD. In this context, it is especially interesting that in AD Aβ oligomers interact with the exposed regions of the subunit GluN1 (see for example Amar et al., 2017).

NMDA RECEPTOR–TAU INTERACTION

Synaptic GluN2B is phosphorylated by the tyrosine kinase fyn in a process regulated by tau (a protein present at dendritic spines Ittner et al., 2010). This phosphorylation is specific for this subunit and, upon phosphorylation, the NMDA receptor forms a complex with the post-synaptic density protein 95 (PSD95)

(Ittner et al., 2010). Whether this complex favors the final morphology of dendritic spines remains unknown. However, the NMDA receptor-PSD95 interaction may be required for the toxic effect of Aβ peptide through its interaction with the NMDA receptor (Ittner et al., 2010), a toxic effect that could take place in AD (**Figure 3**). In addition, Aβ soluble oligomers (known as ADDLs) may interact with synaptic EphB2 receptors, proteins that are crucial for maintaining the integrity of NMDA receptors. Thus, loss of EphB2 mediated by ADDLs results in a decrease in surface localization of NMDA receptor subunits like GluN2B (Shi et al., 2016).

In hippocampal neurons, spines present at distal dendritic regions may have a larger window for long-term depression (LTD) than the proximal ones (Walker et al., 2017). Also, a decrease in the number of spines at distal dendritic regions in tau k.o. mice was found (Pallas-Bazarra et al., 2016). Taken together, these two results may explain in part the decrease in LTD found in tau k.o. animals (Regan et al., 2015). However, further research is needed to draw a clear conclusion since other factors, such as tau phosphorylation at Ser 396, are required for LTD (Regan et al., 2015).

TAU AND AGING

The posttranslational modifications of tau, like phosphorylation, or its aggregation (Avila et al., 2013), can serve as a molecular marker of development, aging and neurodegenerative disorders (Hernandez et al., 2008). Also, a tau-like protein, present in C. *elegans*, could regulate neuronal integrity during aging (Chew et al., 2014).

Tau is a microtubule-associated protein and a microtubular reduction in this protein occurs in aging, as shown by analyzing pyramidal neurons of individuals of different ages (Cash et al., 2003). However, this reduction is not dependent on tau abnormalities that occur during aging, such as its aggregation (Cash et al., 2003), but on other unknown factors.

On the other hand, age-dependent changes in synaptic plasticity may enhance tau aggregation in mouse hippocampus (Kimura et al., 2017). Also, pathological aggregation of tau, in glia cells, could be a feature of aging in brain. An example is in aging-related tau astrogliopathy (ARTAG) (Liu et al., 2016).

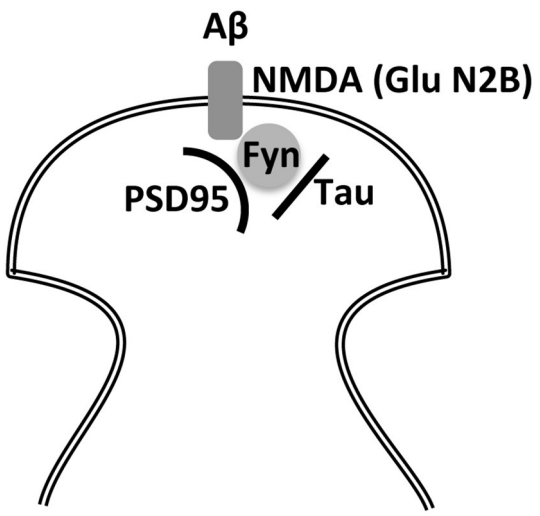

FIGURE 3 | Indirect interaction between Aβ and tau through the NMDA receptor and fyn kinase. Two of the main molecular markers involved in Alzheimer disease, Aβ and tau, may require for their toxic effects of NMDAR-PSD-95 playing a role the kinase Fyn to alter post-synaptic density.

NMDA RECEPTOR–REELIN INTERACTION

Some proteins modify the age-dependent risk of cognitive impairment. One such protein, the apolipoliprotein isoform 4 (ApoE4), is a major risk factor for sporadic AD (Strittmatter et al., 1993). Furthermore, another protein, reelin, may exert a different role (Senkov et al., 2014). Both apoE and reelin share some cell receptors (Bal et al., 2013) and, one of them, ApoER2, appears to stimulate the coupling of the Dab1-Src/Fyn complex to the GluN2A and GluN2B subunits of the NMDA receptor, thereby facilitating the tyrosine phosphorylation of GluN2B (Doehner and Knuesel, 2010). A reduction of reelin expression during aging may contribute to cognitive impairment; however, appropriate reelin-mediated signaling may delay the shift to mainly pathological aging (Doehner and Knuesel, 2010). Of note, in AD, reelin expression is reduced in regions like the entorhinal cortex (Chin et al., 2007), which plays a role in cognitive capacity. Moreover, several relationships have been reported between reelin, the actin cytoskeleton, and dendrite spine growth (Chai et al., 2009; Caroni et al., 2014).

NMDA RECEPTOR, MICROGLIA, DENDRITIC SPINES AND AGING

In the aging brain, alterations occur not only in neurons but also in glia. Indeed, major shifts in glial regional identity are a transcriptional hallmark of aging in the human brain (Soreq et al., 2017). With respect to microglia, a link has been reported with the NMDA receptor. Microglia release D-serine, which may strengthen the synaptic response of NMDA receptor through the activation of its glycine site (Dhami et al., 2013). This process is altered in aged microglia (Hayashi et al., 2006). Furthermore, aging leads to impaired microglial function, which results in reduced brain resiliency, thereby increasing susceptibility to neurodegenerative diseases (Bickford et al., 2017).

However, a more relevant interaction takes place between microglia and dendritic spines. Microglia participate in the elimination of synapses—a process known as synaptic pruning (Paolicelli et al., 2011; Schafer et al., 2012), which takes place via complement activation (Hong et al., 2016; Lui et al., 2016). This and other microglia functions are altered with aging, thereby contributing to neurodegeneration as a function of age (Harry, 2013). Also, microglia show altered morphology and reduced arborization in the aged human brain

(Davies et al., 2016). In addition, microglia transformation during aging results in changes in immune-modulatory functions of secreted factors showing a pro-inflammatory phenotype that favors neurodegeneration (Udeochu et al., 2016).

AGING AS A MAIN RISK FACTOR FOR COGNITIVE DECLINE AND DEMENTIA

The main risk factor for senile dementia like sporadic AD is aging. In fact, to study centenarians and their cognitive function would be a valuable manner to identify factors involved in healthy aging (Lavrencic et al., 2017). Despite neuronal death, AD is characterized by an increase in Aβ peptide, which could be toxic through its interaction (probably in oligomeric form) with a NMDA receptor subunit, GluN1 (Amar et al., 2017) present at the dendritic spines but also when it interacts with the glutamate receptor subunits present at extrasynaptic sites. The latter process of toxicity may involve tau protein in its modified form, which is also present in a higher proportion in the brains of AD patients. **Figure 3** shows how these two molecules may exert a toxic effect on a dendritic spine. In this regard, Tyrosine kinase Fyn plays an important role (Ittner et al., 2010) by phosphorylating NMDA receptor subunit GluN2B. It could be postulated that, in the absence of this phosphorylation, the toxic effect of Aβ (which may occur in AD) will not take place. Little is known about the interaction of GluN2B with fyn-tau at extracellular synaptic sites and whether the presence of Aβ peptide has a toxic effect through its interaction at these sites by a mechanism involving the fyn-tau complex.

Table 2 shows some of the events that take place during aging and that are accelerated in neurological disorders like AD. These events include the following: neuron senescence in a hostile microglia environment; alterations in dendritic spines and in neurotransmission; and changes in the localization of neurotransmitter receptor from synapses to extrasynaptic sites. The latter alterations refer mainly to neurotransmitter receptors like NMDA receptors bearing a GluN2B subunit present at extrasynaptic sites, where they can interact with toxic ligands like Aβ peptide. The final result of the process at the functional level may be cognitive decline.

Therefore, changes in tau protein at the molecular level may contribute to the formation of protein complex (tau-fyn-PSD95-NMDAr). This complex may modify the shape or number of dendritic spines and/or the morphology of the neurons. Such alterations may lead to impaired neuronal function, thus promoting neurodegeneration (**Figure 4**).

THERAPIES

Figure 4 indicates the different levels at which to analyze aging: the whole organism, brain regions, neurons, dendritic spines, NMDA receptors, and cytoskeleton, mainly tau proteins.

Adult hippocampal neurogenesis is linked to cognition and memory (Anacker and Hen, 2017). In the mouse, this process decreases with age (Sirerol-Piquer et al., 2011). It has recently been shown that treatment with Δ9-tetrahydrocannabinal (THC), a substance present in cannabis, enhances learning capacity and memory in aged mice (Bilkei-Gorzo et al., 2017). The administration of THC increases histone H3 and H4 acetylation at the klotho (an anti-aging protein) and BNDF promoters. Interestingly, a decrease in histone deacetylase HDAC3 improves memory capacity in older mice (Kwapis et al., 2017). In addition, the presence of some klotho fragments may enhance congnition in a mouse model (Leon et al., 2017).

On the other hand, transient overexpression of a negative regulator of dendritic spines, kruppel-like factor 9 (kef9), enhances the integration of newborn dentate granule cells into the neuronal network and may rejuvenate aged memory circuits (McAvoy et al., 2016). However, little is known about how to modulate the dynamics of dendritic spines and the role of microglia in synaptic pruning or in neuroinflamation (Ardestani et al., 2017).

Aging appears to be partly encoded in a blood-base signature, and it has been proposed that blood factors modulate aging and could find application for the rejuvenation of some organs, including brain (Wyss-Coray, 2016). The mechanisms of hippocampal aging and the potential for rejuvenation have been covered in an excellent review (Fan et al., 2017) and, recently, it has been reported that human umbilical cord plasma proteins revitalize hippocampal function in aged mice (Castellano et al., 2017). Indeed, the tissue inhibitor of metalloproteinase 2 (TIMP2), a factor in umbilical cord plasma, increases hippocampal-dependent cognition in these animals. At the neuronal level, it should be addressed whether abrogate senescent cells decrease aging in the surrounding cells (Baker et al., 2016). Also, it has been described that the presence of senescent cells contributes to tissue damage. A new technique through which to clear senescent cells without affecting non-senescent ones has been described (Baar et al., 2017). Brain regions, for example in the hippocampal zones CA1 and CA3, differ in their susceptibility to distinct components, such as zinc, which may affect subcellular structures like mitochondria (Medvedeva et al., 2017). In this regard, the chelation of zinc

FIGURE 4 | Different levels to study the changes that occur in the brain during aging. An alteration at any of these levels can cause cognitive impairment.

has been shown to enhance long-term potentiation in the CA1 neurons of aged rats (Shetty et al., 2017).

Also, an increase in growth factor expression could support neuron health. In this regard, methods to stimulate insulin production may prevent neuron aging (Hansen et al., 2015). In addition, the capacity of a modified peptide of the cilary neurotrophic factor to prevent synaptic deficits has also been tested with promising results (Baazaoui and Iqbal, 2017). Also recently, anti-aging strategies based on cellular reprograming have been tested in peripheral tissue (Ocampo et al., 2016). However, the effects of such strategies on neuronal tissue have not been addressed.

Little is known about how to modulate the dynamics of dendritic spines and the role of microglia in synaptic pruning or in neuroinflamation (Ardestani et al., 2017).

Also, effort should be channeled into the possible modulation of NMDA receptors subunits like GluN2B and their modification at tyrosine residues by fyn kinase. In this regard, memantine, an NMDA receptor antagonist, is currently used for the treatment of AD (Greig, 2015). Also, other NMDA receptor antagonists are under study (Raybuck et al., 2017).

Regarding the use of therapies targeting tau, mainly in modified forms, or Aβ in aging-related disorders like AD, there are abundant references. An example is a recent review that describes therapeutic strategies for restoring tau homeostasis to treat tauopathies like AD (Young et al., 2017).

In summary, the search for suitable treatments for aging-dependent cognitive decline continues at many levels.

AUTHOR CONTRIBUTIONS

JA and FH: Conception and design, manuscript writing, editing and figure design. ML-M, NP-B, MB, JP, and AR-M: Manuscript writing, editing and synthesis of previous literature.

FUNDING

This study was funded by grants from the Spanish Ministry of Economy and Competitiveness [SAF-2014-53,040-P (JA); BFU2016-77885-P (FH)] and the Centro de Investigasción Biomédica en Red sobre Enfermedades Neurodegeneritivas (CIBERNED, ISCIII) (JA).

REFERENCES

Akashi, K., Kakizaki, T., Kamiya, H., Fukaya, M., Yamasaki, M., Abe, M., et al. (2009). NMDA receptor GluN2B (GluR epsilon 2/NR2B) subunit is crucial for channel function, post-synaptic macromolecular organization, and actin cytoskeleton at hippocampal CA3 synapses. *J. Neurosci.* 29, 10869–10882. doi: 10.1523/JNEUROSCI.5531-08.2009

Amar, F., Sherman, M. A., Rush, T., Larson, M., Boyle, G., Chang, L., et al. (2017). The amyloid-β oligomer Aβ*56 induces specific alterations in neuronal signaling that lead to tau phosphorylation and aggregation. *Sci. Signal.* 10:eaal2021. doi: 10.1126/scisignal.aal2021

Anacker, C. and Hen, R. (2017). Adult hippocampal neurogenesis and cognitive flexibility-linking memory and mood. *Nat. Rev. Neurosci.* 18, 335–346. doi: 10.1038/nrn.2017.45

Ardestani, P. M., Evans, A. K., Yi, B., Nguyen, T., Coutellier, L., and Shamloo, M. (2017). Modulation of neuroinflammation and pathology in the 5XFAD mouse model of Alzheimer's disease using a biased and selective beta-1 adrenergic receptor partial agonist. *Neuropharmacology* 116, 371–386. doi: 10.1016/j.neuropharm.2017.01.010

Avila, J., de Barreda, E. G., Pallas-Bazarra, N., and Hernandez, F. (2013). Tau and neuron aging. *Aging Dis.* 4, 23–28.

Baar, M. P., Brandt, R. M., Putavet, D. A., Klein, J. D., Derks, K. W., Bourgeois, B. R., et al. (2017). Targeted apoptosis of senescent cells restores tissue homeostasis in response to chemotoxicity and aging. *Cell* 169, 132.e16–147.e16. doi: 10.1016/j.cell.2017.02.031

Baazaoui, N., and Iqbal, K. (2017). Prevention of dendritic and synaptic deficits and cognitive impairment with a neurotrophic compound. *Alzheimers Res. Ther.* 9:45. doi: 10.1186/s13195-017-0273-7

Baker, D. J., Childs, B. G., Durik, M., Wijers, M. E., Sieben, C. J., Zhong, J., et al. (2016). Naturally occurring p16(Ink4a)-positive cells shorten healthy lifespan. *Nature* 530, 184–189. doi: 10.1038/nature16932

Bal, M., Leitz, J., Reese, A. L., Ramirez, D. M., Durakoglugil, M., Herz, J., et al. (2013). Reelin mobilizes a VAMP7-dependent synaptic vesicle pool and selectively augments spontaneous neurotransmission. *Neuron* 80, 934–946. doi: 10.1016/j.neuron.2013.08.024

Bickford, P. C., Flowers, A., and Grimmig, B. (2017). Aging leads to altered microglial function that reduces brain resiliency increasing vulnerability to neurodegenerative diseases. *Exp. Gerontol.* 94, 4–8. doi: 10.1016/j.exger.2017.01.027

Bidoret, C., Ayon, A., Barbour, B., and Casado, M. (2009). Presynaptic NR2A-containing NMDA receptors implement a high-pass filter synaptic plasticity rule. *Proc. Natl. Acad. Sci. U.S.A.* 106, 14126–14131. doi: 10.1073/pnas.0904284106

Bilkei-Gorzo, A., Albayram, O., Draffehn, A., Michel, K., Piyanova, A., Oppenheimer, H., et al. (2017). A chronic low dose of delta9-tetrahydrocannabinol (THC) restores cognitive function in old mice. *Nat. Med.* 23, 782–787. doi: 10.1038/nm.4311

Cantanelli, P., Sperduti, S., Ciavardelli, D., Stuppia, L., Gatta, V., and Sensi, S. L. (2014). Age-dependent modifications of ampa receptor subunit expression levels and related cognitive effects in 3xTg-AD mice. *Front. Aging Neurosci.* 6:200. doi: 10.3389/fnagi.2014.00200

Caroni, P., Chowdhury, A., and Lahr, M. (2014). Synapse rearrangements upon learning: from divergent-sparse connectivity to dedicated sub-circuits. *Trends Neurosci.* 37, 604–614. doi: 10.1016/j.tins.2014.08.011

Cash, A. D., Aliev, G., Siedlak, S. L., Nunomura, A., Fujioka, H., Zhu, X., et al. (2003). Microtubule reduction in Alzheimer's disease and aging is independent of tau filament formation. *Am. J. Pathol.* 162, 1623–1627. doi: 10.1016/S0002-9440(10)64296-4

Castellano, J. M., Mosher, K. I., Abbey, R. J., McBride, A. A., James, M. L., Berdnik, D., et al. (2017). Human umbilical cord plasma proteins revitalize hippocampal function in aged mice. *Nature* 544, 488–492. doi: 10.1038/nature22067

Chai, X., Förster, E., Zhao, S., Bock, H. H., and Frotscher, M. (2009). Reelin stabilizes the actin cytoskeleton of neuronal processes by inducing n-cofilin phosphorylation at serine3. *J. Neurosci.* 29, 288–299. doi: 10.1523/JNEUROSCI.2934-08.2009

Chew, Y. L., Fan, X., Götz, J., and Nicholas, H. R. (2014). Regulation of age-related structural integrity in neurons by protein with tau-like repeats (PTL-1) is cell autonomous. *Sci. Rep.* 4:5185. doi: 10.1038/srep05185

Chin, J., Massaro, C. M., Palop, J. J., Thwin, M. T., Yu, G. Q., Bien-Ly, N., et al. (2007). Reelin depletion in the entorhinal cortex of human amyloid precursor protein transgenic mice and humans with Alzheimer's disease. *J. Neurosci.* 27, 2727–2733. doi: 10.1523/JNEUROSCI.3758-06.2007

Conn, P. J., Battaglia, G., Marino, M. J., and Nicoletti, F. (2005). Metabotropic glutamate receptors in the basal ganglia motor circuit. *Nat. Rev. Neurosci.* 6, 787–798. doi: 10.1038/nrn1763

Davies, D. S., Ma, J., Jegathees, T., and Goldsbury, C. (2016). Microglia show altered morphology and reduced arborization in human brain during aging and Alzheimer's disease. *Brain Pathol.* 27, 795–808. doi: 10.1111/bpa.12456

de Brabander, J. M., Kramers, R. J., and Uylings, H. B. (1998). Layer-specific dendritic regression of pyramidal cells with ageing in the human prefrontal cortex. *Eur. J. Neurosci.* 10, 1261–1269. doi: 10.1046/j.1460-9568.1998.00137.x

Dent, E. W. (2017). Of microtubules and memory: implications for microtubule dynamics in dendrites and spines. *Mol. Biol. Cell* 28, 1–8. doi: 10.1091/mbc.E15-11-0769

Dhami, K. S., Churchward, M. A., Baker, G. B., and Todd, K. G. (2013). Fluoxetine and citalopram decrease microglial release of glutamate and D-serine to promote cortical neuronal viability following ischemic insult. *Mol. Cell Neurosci.* 56, 365–374. doi: 10.1016/j.mcn.2013.07.006

Dimri, G. P., Lee, X., Basile, G., Acosta, M., Scott, G., Roskelley, C., et al. (1995). A biomarker that identifies senescent human cells in culture and in aging skin *in vivo*. *Proc. Natl. Acad. Sci. U.S.A.* 92, 9363–9367. doi: 10.1073/pnas.92.20.9363

Dingledine, R., Borges, K., Bowie, D., and Traynelis, S. F. (1999). The glutamate receptor ion channels. *Pharmacol. Rev.* 51, 7–61.

Doehner, J., and Knuesel, I. (2010). Reelin-mediated signaling during normal and pathological forms of aging. *Aging Dis.* 1, 12–29.

Espinet, C., Gonzalo, H., Fleitas, C., Menal, M. J., and Egea, J. (2015). Oxidative stress and neurodegenerative diseases: a neurotrophic approach. *Curr. Drug Targets* 16, 20–30. doi: 10.2174/1389450116666150107153233

Evangelou, K., Lougiakis, N., Rizou, S. V., Kotsinas, A., Kletsas, D., Muñoz-Espín, D., et al. (2017). Robust, universal biomarker assay to detect senescent cells in biological specimens. *Aging Cell* 16, 192–197. doi: 10.1111/acel.12545

Fan, X., Wheatley, E. G., and Villeda, S. A. (2017). Mechanisms of hippocampal aging and the potential for rejuvenation. *Annu. Rev. Neurosci.* 40, 251–272. doi: 10.1146/annurev-neuro-072116-031357

Gazzaley, A. H., Weiland, N. G., McEwen, B. S., and Morrison, J. H. (1996). Differential regulation of NMDAR1 mRNA and protein by estradiol in the rat hippocampus. *J. Neurosci.* 16, 6830–6838.

Gomez-Ramos, A., Picher, A. J., García, E., Garrido, P., Hernandez, F., Soriano, E., et al. (2017). Validation of suspected somatic single nucleotide variations in the brain of Alzheimer's disease patients. *J. Alzheimers Dis.* 56, 977–990. doi: 10.3233/JAD-161053

Gourlay, C. W., Carpp, L. N., Timpson, P., Winder, S. J., and Ayscough, K. R. (2004). A role for the actin cytoskeleton in cell death and aging in yeast. *J. Cell Biol.* 164, 803–809. doi: 10.1083/jcb.200310148

Greig, S. L. (2015). Memantine ER/Donepezil: a review in Alzheimer's disease. *CNS Drugs* 29, 963–970. doi: 10.1007/s40263-015-0287-2

Groc, L., Heine, M., Cousins, S. L., Stephenson, F. A., Lounis, B., Cognet, L., et al. (2006). NMDA receptor surface mobility depends on NR2A-2B subunits. *Proc. Natl. Acad. Sci. U.S.A.* 103, 18769–18774. doi: 10.1073/pnas.0605238103

Hansen, H. H., Fabricius, K., Barkholt, P., Niehoff, M. L., Morley, J. E., Jelsing, J., et al. (2015). The GLP-1 receptor agonist liraglutide improves memory function and increases hippocampal CA1 neuronal numbers in a senescence-accelerated mouse model of Alzheimer's disease. *J. Alzheimers Dis.* 46, 877–888. doi: 10.3233/JAD-143090

Harry, G. J. (2013). Microglia during development and aging. *Pharmacol. Ther.* 139, 313–326. doi: 10.1016/j.pharmthera.2013.04.013

Hayashi, K., and Shirao, T. (1999). Change in the shape of dendritic spines caused by overexpression of drebrin in cultured cortical neurons. *J. Neurosci.* 19, 3918–3925.

Hayashi, Y., Ishibashi, H., Hashimoto, K., and Nakanishi, H. (2006). Potentiation of the NMDA receptor-mediated responses through the activation of the glycine site by microglia secreting soluble factors. *Glia* 53, 660–668. doi: 10.1002/glia.20322

He, Y. H., Chen, X. Q., Yan, D. J., Xiao, F. H., Lin, R., Liao, X. P., et al. (2016). Familial longevity study reveals a significant association of mitochondrial DNA copy number between centenarians and their offspring. *Neurobiol. Aging* 47, 218.e11–218.e18. doi: 10.1016/j.neurobiolaging.2016.07.026

Herculano-Houzel, S. (2012). The remarkable, yet not extraordinary, human brain as a scaled-up primate brain and its associated cost. *Proc. Natl. Acad. Sci. U.S.A.* 109(Suppl. 1), 10661–10668. doi: 10.1073/pnas.1201895109

Hering, H., and Sheng, M. (2001). Dendritic spines: structure, dynamics and regulation. *Nat. Rev. Neurosci.* 2, 880–888. doi: 10.1038/35104061

Hernández, F., Pérez, M., de Barreda, E. G., Goñi-Oliver, P., and Avila, J. (2008). Tau as a molecular marker of development, aging and neurodegenerative disorders. *Curr. Aging Sci.* 1, 56–61. doi: 10.2174/1874609810801010056

Hoch, N. C., Hanzlikova, H., Rulten, S. L., Tétreault, M., Komulainen, E., Ju, L., et al. (2017). XRCC1 mutation is associated with PARP1 hyperactivation and cerebellar ataxia. *Nature* 541, 87–91. doi: 10.1038/nature20790

Hong, S., Beja-Glasser, V. F., Nfonoyim, B. M., Frouin, A., Li, S., Ramakrishnan, S., et al. (2016). Complement and microglia mediate early synapse loss in Alzheimer mouse models. *Science* 352, 712–716. doi: 10.1126/science.aad8373

Hopf, F. W. (2017). Do specific NMDA receptor subunits act as gateways for addictive behaviors? *Genes Brain Behav.* 16, 118–138. doi: 10.1111/gbb.12348

Ittner, L. M., Ke, Y. D., Delerue, F., Bi, M., Gladbach, A., van Eersel, J., et al. (2010). Dendritic function of tau mediates amyloid-beta toxicity in Alzheimer's disease mouse models. *Cell* 142, 387–397. doi: 10.1016/j.cell.2010.06.036

Jung, T., Bader, N., and Grune, T. (2007). Lipofuscin: formation, distribution, and metabolic consequences. *Ann. N. Y. Acad. Sci.* 1119, 97–111. doi: 10.1196/annals.1404.008

Kabaso, D., Coskren, P. J., Henry, B. I., Hof, P. R., and Wearne, S. L. (2009). The electrotonic structure of pyramidal neurons contributing to prefrontal cortical circuits in macaque monkeys is significantly altered in aging. *Cereb. Cortex* 19, 2248–2268. doi: 10.1093/cercor/bhn242

Kimura, T., Suzuki, M., and Akagi, T. (2017). Age-dependent changes in synaptic plasticity enhance tau oligomerization in the mouse hippocampus. *Acta Neuropathol. Commun.* 5:67. doi: 10.1186/s40478-017-0469-x

Kumar, A. (2015). NMDA Receptor Function during senescence: implication on cognitive performance. *Front. Neurosci.* 9:473. doi: 10.3389/fnins.2015.00473

Kwapis, J. L., Alaghband, Y., López, A. J., White, A. O., Campbell, R. R., Dang, R. T., et al. (2017). Context and auditory fear are differentially regulated by HDAC3 activity in the lateral and basal subnuclei of the amygdala. *Neuropsychopharmacology* 42, 1284–1294. doi: 10.1038/npp.2016.274

Laurie, D. J., Bartke, I., Schoepfer, R., Naujoks, K., and Seeburg, P. H. (1997). Regional, developmental and interspecies expression of the four NMDAR2 subunits, examined using monoclonal antibodies. *Brain Res. Mol. Brain Res.* 51, 23–32. doi: 10.1016/S0169-328X(97)00206-4

Lavrencic, L. M., Richardson, C., Harrison, S. L., Muniz-Terrera, G., Keage, H. A. D., Brittain, K., et al. (2017). Is there a link between cognitive reserve and cognitive function in the oldest-old? *J. Gerontol. A Biol. Sci. Med. Sci.* doi: 10.1093/gerona/glx140. [Epub ahead of print].

Leon, J., Moreno, A. J., Garay, B. I., Chalkley, R. J., Burlingame, A. L., Wang, D., et al. (2017). Peripheral elevation of a klotho fragment enhances brain function and resilience in young, aging, and alpha-synuclein transgenic mice. *Cell Rep.* 20, 1360–1371. doi: 10.1016/j.celrep.2017.07.024

Licht, T., Rothe, G., Kreisel, T., Wolf, B., Benny, O., Rooney, A. G., et al. (2016). VEGF preconditioning leads to stem cell remodeling and attenuates age-related decay of adult hippocampal neurogenesis. *Proc. Natl. Acad. Sci. U.S.A.* 113, E7828–E7836. doi: 10.1073/pnas.1609592113

Liu, A. K., Goldfinger, M. H., Questari, H. E., Pearce, R. K., and Gentleman, S. M. (2016). ARTAG in the basal forebrain: widening the constellation of astrocytic tau pathology. *Acta Neuropathol. Commun.* 4:59. doi: 10.1186/s40478-016-0330-7

Liu, P., Smith, P. F., and Darlington, C. L. (2008). Glutamate receptor subunits expression in memory-associated brain structures: regional variations and effects of aging. *Synapse* 62, 834–841. doi: 10.1002/syn.20563

Lui, H., Zhang, J., Makinson, S. R., Cahill, M. K., Kelley, K. W., Huang, H. Y., et al. (2016). Progranulin deficiency promotes circuit-specific synaptic pruning by microglia via complement activation. *Cell* 165, 921–935. doi: 10.1016/j.cell.2016.04.001

Luo, L., Hensch, T. K., Ackerman, L., Barbel, S., Jan, L. Y., and Jan, Y. N. (1996). Differential effects of the Rac GTPase on Purkinje cell axons and dendritic trunks and spines. *Nature* 379, 837–840. doi: 10.1038/379837a0

Lustgarten, M. S. (2016). Classifying aging as a disease: the role of microbes. *Front. Genet.* 7:212. doi: 10.3389/fgene.2016.00212

Magnusson, K. R. (1998). The aging of the NMDA receptor complex. *Front. Biosci.* 3, e70–80. doi: 10.2741/A368

Marks, S. M., Lockhart, S. N., Baker, S. L., and Jagust, W. J. (2017). Tau and beta-amyloid are associated with medial temporal lobe structure, function and memory encoding in normal aging. *J. Neurosci.* 37, 3192–3201. doi: 10.1523/JNEUROSCI.3769-16.2017

Mattson, M. P., and Magnus, T. (2006). Ageing and neuronal vulnerability. *Nat. Rev. Neurosci.* 7, 278–294. doi: 10.1038/nrn1886

McAvoy, K. M., Scobie, K. N., Berger, S., Russo, C., Guo, N., Decharatanachart, P., et al. (2016). Modulating neuronal competition dynamics in the dentate gyrus to rejuvenate aging memory circuits. *Neuron* 91, 1356–1373. doi: 10.1016/j.neuron.2016.08.009

McQuail, J. A., Beas, B. S., Kelly, K. B., Simpson, K. L., Frazier, C. J., Setlow, B., et al. (2016). NR2A-Containing NMDARs in the prefrontal cortex are required for working memory and associated with age-related cognitive decline. *J. Neurosci.* 36, 12537–12548. doi: 10.1523/JNEUROSCI.2332-16.2016

Medvedeva, Y. V., Ji, S. G., Yin, H. Z., and Weiss, J. H. (2017). Differential vulnerability of CA1 versus CA3 pyramidal neurons after ischemia: possible relationship to sources of Zn^{2+} accumulation and its entry into and prolonged effects on mitochondria. *J. Neurosci.* 37, 726–737. doi: 10.1523/JNEUROSCI.3270-16.2016

Monyer, H., Burnashev, N., Laurie, D. J., Sakmann, B., and Seeburg, P. H. (1994). Developmental and regional expression in the rat brain and functional properties of four NMDA receptors. *Neuron* 12, 529–540. doi: 10.1016/0896-6273(94)90210-0

Muñoz-Espín, D., and Serrano, M. (2014). Cellular senescence: from physiology to pathology. *Nat. Rev. Mol. Cell Biol.* 15, 482–496. doi: 10.1038/nrm3823

Naisbitt, S., Kim, E., Tu, J. C., Xiao, B., Sala, C., Valtschanoff, J., et al. (1999). Shank, a novel family of post-synaptic density proteins that binds to the NMDA receptor/PSD-95/GKAP complex and cortactin. *Neuron* 23, 569–582. doi: 10.1016/S0896-6273(00)80809-0

Ocampo, A., Reddy, P., Martinez-Redondo, P., Platero-Luengo, A., Hatanaka, F., Hishida, T., et al. (2016). *In vivo* amelioration of age-associated hallmarks by partial reprogramming. *Cell* 167, 1719.e12–1733.e12. doi: 10.1016/j.cell.2016.11.052

O'Shea, A., Cohen, R. A., Porges, E. C., Nissim, N. R., and Woods, A. J. (2016). Cognitive aging and the hippocampus in older adults. *Front. Aging Neurosci.* 8:298. doi: 10.3389/fnagi.2016.00298

Pak, D. T., Yang, S., Rudolph-Correia, S., Kim, E., and Sheng, M. (2001). Regulation of dendritic spine morphology by SPAR, a PSD-95-associated RapGAP. *Neuron* 31, 289–303. doi: 10.1016/S0896-6273(01)00355-5

Pallas-Bazarra, N., Jurado-Arjona, J., Navarrete, M., Esteban, J. A., Hernández, F., Ávila, J., et al. (2016). Novel function of Tau in regulating the effects of external stimuli on adult hippocampal neurogenesis. *EMBO J.* 35, 1417–1436. doi: 10.15252/embj.201593518

Paoletti, P., Bellone, C., and Zhou, Q. (2013). NMDA receptor subunit diversity: impact on receptor properties, synaptic plasticity and disease. *Nat. Rev. Neurosci.* 14, 383–400. doi: 10.1038/nrn3504

Paolicelli, R. C., Bolasco, G., Pagani, F., Maggi, L., Scianni, M., Panzanelli, P., et al. (2011). Synaptic pruning by microglia is necessary for normal brain development. *Science* 333, 1456–1458. doi: 10.1126/science.1202529

Pini, L., Pievani, M., Bocchetta, M., Altomare, D., Bosco, P., Cavedo, E., et al. (2016). Brain atrophy in Alzheimer's disease and aging. *Ageing Res. Rev.* 30, 25–48. doi: 10.1016/j.arr.2016.01.002

Potier, B., Billard, J. M., Rivière, S., Sinet, P. M., Denis, I., Champeil-Potokar, G., et al. (2010). Reduction in glutamate uptake is associated with extrasynaptic NMDA and metabotropic glutamate receptor activation at the hippocampal CA1 synapse of aged rats. *Aging Cell* 9, 722–735. doi: 10.1111/j.1474-9726.2010.00593.x

Ramirez-Rios, S., Denarier, E., Prezel, E., Vinit, A., Stoppin-Mellet, V., Devred, F., et al. (2016). Tau antagonizes end-binding protein tracking at microtubule ends through a phosphorylation-dependent mechanism. *Mol. Biol. Cell* 27, 2924–2934. doi: 10.1091/mbc.E16-01-0029

Rammes, G., Mattusch, C., Wulff, M., Seeser, F., Kreuzer, M., Zhu, K., et al. (2017). Involvement of GluN2B subunit containing N-methyl-d-aspartate (NMDA) receptors in mediating the acute and chronic synaptotoxic effects of oligomeric amyloid-beta (Abeta) in murine models of Alzheimer's disease (AD). *Neuropharmacology* 123, 100–115. doi: 10.1016/j.neuropharm.2017.02.003

Ramon y Cajal, S. (1888). Estructura de los centros nerviosos de las aves. *Rev. Trim. Histol. Norm. Pat.* 1, 1–10.

Raybuck, J. D., Hargus, N. J., and Thayer, S. A. (2017). A GluN2B-Selective NMDAR antagonist reverses synapse loss and cognitive impairment produced by the HIV-1 protein tat. *J. Neurosci.* 37, 7837–7847. doi: 10.1523/JNEUROSCI.0226-17.2017

Regan, P., Piers, T., Yi, J. H., Kim, D. H., Huh, S., Park, S. J., et al. (2015). Tau phosphorylation at serine 396 residue is required for hippocampal LTD. *J. Neurosci.* 35, 4804–4812. doi: 10.1523/JNEUROSCI.2842-14.2015

Ross, C. A., and Truant, R. (2017). DNA repair: a unifying mechanism in neurodegeneration. *Nature* 541, 34–35. doi: 10.1038/nature21107

Santos, R. X., Correia, S. C., Zhu, X., Smith, M. A., Moreira, P. I., Castellani, R. J., et al. (2013). Mitochondrial DNA oxidative damage and repair in aging and Alzheimer's disease. *Antioxid. Redox Signal.* 18, 2444–2457. doi: 10.1089/ars.2012.5039

Schafer, D. P., Lehrman, E. K., Kautzman, A. G., Koyama, R., Mardinly, A. R., Yamasaki, R., et al. (2012). Microglia sculpt postnatal neural circuits in an activity and complement-dependent manner. *Neuron* 74, 691–705. doi: 10.1016/j.neuron.2012.03.026

Schroeder, B. O., and Bäckhed, F. (2016). Signals from the gut microbiota to distant organs in physiology and disease. *Nat. Med.* 22, 1079–1089. doi: 10.1038/nm.4185

Senkov, O., Andjus, P., Radenovic, L., Soriano, E., and Dityatev, A. (2014). Neural ECM molecules in synaptic plasticity, learning, and memory. *Prog. Brain Res.* 214, 53–80. doi: 10.1016/B978-0-444-63486-3.00003-7

Sharon, G., Sampson, T. R., Geschwind, D. H., and Mazmanian, S. K. (2016). The central nervous system and the gut microbiome. *Cell* 167, 915–932. doi: 10.1016/j.cell.2016.10.027

Shetty, M. S., Sharma, M., and Sajikumar, S. (2017). Chelation of hippocampal zinc enhances long-term potentiation and synaptic tagging/capture in CA1 pyramidal neurons of aged rats: implications to aging and memory. *Aging Cell* 16, 136–148. doi: 10.1111/acel.12537

Shi, X. D., Sun, K., Hu, R., Liu, X. Y., Hu, Q. M., Sun, X. Y., et al. (2016). Blocking the interaction between EphB2 and ADDLs by a small peptide rescues impaired synaptic plasticity and memory deficits in a mouse model of Alzheimer's disease. *J. Neurosci.* 36, 11959–11973. doi: 10.1523/JNEUROSCI.1327-16.2016

Shimada, A., Tsuzuki, M., Keino, H., Satoh, M., Chiba, Y., Saitoh, Y., et al. (2006). Apical vulnerability to dendritic retraction in prefrontal neurones of ageing SAMP10 mouse: a model of cerebral degeneration. *Neuropathol. Appl. Neurobiol.* 32, 1–14. doi: 10.1111/j.1365-2990.2006.00632.x

Sirerol-Piquer, M., Gomez-Ramos, P., Hernández, F., Perez, M., Morán, M. A., Fuster-Matanzo, A., et al. (2011). GSK3β overexpression induces neuronal death and a depletion of the neurogenic niches in the dentate gyrus. *Hippocampus* 21, 910–922. doi: 10.1002/hipo.20805

Sonntag, W. E., Bennett, S. A., Khan, A. S., Thornton, P. L., Xu, X., Ingram, R. L., et al. (2000). Age and insulin-like growth factor-1 modulate N-methyl-D-aspartate receptor subtype expression in rats. *Brain Res. Bull.* 51, 331–338. doi: 10.1016/S0361-9230(99)00259-2

Soreq, L., UK Brain Expression Consortium., North American Brain Expression Consortium., Rose, J., Soreq, E., Hardy, J., et al. (2017). Major shifts in glial regional identity are a transcriptional hallmark of human brain aging. *Cell Rep.* 18, 557–570. doi: 10.1016/j.celrep.2016.12.011

Strittmatter, W. J., Saunders, A. M., Schmechel, D., Pericak-Vance, M., Enghild, J., Salvesen, G. S., et al. (1993). Apolipoprotein E: high-avidity binding to beta-amyloid and increased frequency of type 4 allele in late-onset familial Alzheimer disease. *Proc. Natl. Acad. Sci. U.S.A.* 90, 1977–1981. doi: 10.1073/pnas.90.5.1977

Sun, X. Y., Tuo, Q. Z., Liuyang, Z. Y., Xie, A. J., Feng, X. L., Yan, X., et al. (2016). Extrasynaptic NMDA receptor-induced tau overexpression mediates neuronal death through suppressing survival signaling ERK phosphorylation. *Cell Death Dis.* 7:e2449. doi: 10.1038/cddis.2016.329

Tannenholz, L., Hen, R., and Kheirbek, M. A. (2016). GluN2B-Containg NMDA receptors on adult-born granule cells contribute to the antidepressant action of fluoxetine. *Front. Neurosci.* 10:242. doi: 10.3389/fnins.2016.00242

Triller, A., and Choquet, D. (2005). Surface trafficking of receptors between synaptic and extrasynaptic membranes: and yet they do move! *Trends Neurosci.* 28, 133–139. doi: 10.1016/j.tins.2005.01.001

Udeochu, J. C., Shea, J. M., and Villeda, S. A. (2016). Microglia communication: parallels between aging and Alzheimer's disease. *Clin. Exp. Neuroimmunol.* 7, 114–125. doi: 10.1111/cen3.12307

Walker, A. S., Neves, G., Grillo, F., Jackson, R. E., Rigby, M., O'Donnell, C., et al. (2017). Distance-dependent gradient in NMDAR-driven spine calcium signals along tapering dendrites. *Proc. Natl. Acad. Sci. U.S.A.* 114, E1986–E1995. doi: 10.1073/pnas.1607462114

Watanabe, M., Inoue, Y., Sakimura, K., and Mishina, M. (1993). Distinct distributions of five N-methyl-D-aspartate receptor channel subunit mRNAs in the forebrain. *J. Comp. Neurol.* 338, 377–390. doi: 10.1002/cne.903380305

Woodhall, G., Evans, D. I., Cunningham, M. O., and Jones, R. S. (2001). NR2B-containing NMDA autoreceptors at synapses on entorhinal cortical neurons. *J. Neurophysiol.* 86, 1644–1651.

Wyss-Coray, T. (2016). Ageing, neurodegeneration and brain rejuvenation. *Nature* 539, 180–186. doi: 10.1038/nature20411

Young, Z. T., Mok, S. A., and Gestwicki, J. E. (2017). Therapeutic strategies for restoring tau homeostasis. *Cold Spring Harb. Perspect. Med.* doi: 10.1101/cshperspect.a024612. [Epub ahead of print].

Yuan, T. F., Gu, S., Shan, C., Marchado, S., and Arias-Carrion, O. (2015). Oxidative stress and adult neurogenesis. *Stem Cell Rev.* 11, 706–709. doi: 10.1007/s12015-015-9603-y

Yuste, R. (2015). The discovery of dendritic spines by Cajal. *Front. Neuroanat.* 9:18. doi: 10.3389/fnana.2015.00018

Zhang, B., Bailey, W. M., McVicar, A. L., and Gensel, J. C. (2016). Age increases reactive oxygen species production in macrophages and potentiates oxidative damage after spinal cord injury. *Neurobiol. Aging* 47, 157–167. doi: 10.1016/j.neurobiolaging.2016.07.029

Zhao, M. G., Toyoda, H., Lee, Y. S., Wu, L. J., Ko, S. W., Zhang, X. H., et al. (2005). Roles of NMDA NR2B subtype receptor in prefrontal long-term potentiation and contextual fear memory. *Neuron* 47, 859–872. doi: 10.1016/j.neuron.2005.08.014

Zhao, X., Rosenke, R., Kronemann, D., Brim, B., Das, S. R., Dunah, A. W., et al. (2009). The effects of aging on N-methyl-D-aspartate receptor subunits in the synaptic membrane and relationships to long-term spatial memory. *Neuroscience* 162, 933–945. doi: 10.1016/j.neuroscience.2009.05.018

Conflict of Interest Statement: The authors declare that the research was conducted in the absence of any commercial or financial relationships that could be construed as a potential conflict of interest.

frontiers in Neurology

REVIEW
published: 15 February 2018
doi: 10.3389/fneur.2018.00070

Tau Filaments and the Development of Positron Emission Tomography Tracers

Michel Goedert[1], Yoshiki Yamaguchi[2], Sushil K. Mishra[2], Makoto Higuchi[3] and Naruhiko Sahara[3]**

[1] *MRC Laboratory of Molecular Biology, Cambridge, United Kingdom,* [2] *RIKEN Global Research Cluster, Wako, Japan,* [3] *National Institute of Radiological Sciences, Chiba, Japan*

A pathological pathway leading from soluble, monomeric to insoluble, filamentous Tau, is believed to underlie human Tauopathies. Cases of frontotemporal dementia are caused by dominantly inherited mutations in *MAPT*, the Tau gene. They show that dysfunction of Tau protein is sufficient to cause neurodegeneration and dementia. Extrapolation to the more common sporadic Tauopathies leads one to conclude that the pathological pathway is central to the development of all cases of disease, even if there are multiple reasons for Tau assembly. These findings are conceptually similar to those reported for beta-amyloid, alpha-synuclein and prion protein. Here, we provide an overview of Tau filaments and their positron emission tomography ligands.

Keywords: tau protein, Tauopathy, tau isoform, filamentous tau aggregate, cryo-electron microscopy, positron emission tomography ligand

OPEN ACCESS

Edited by:
Emmanuel Planel, Laval University, Canada

Reviewed by:
Michal Novak, Slovak Academy of Sciences (SAS), Slovakia
Roland Brandt, University of Osnabrück, Germany

****Correspondence:***
Michel Goedert
mg@mrc-lmb.cam.ac.uk;
Naruhiko Sahara
sahara.naruhiko@qst.go.jp

Specialty section:
This article was submitted to Neurodegeneration, a section of the journal Frontiers in Neurology

Received: *08 December 2017*
Accepted: *30 January 2018*
Published: *15 February 2018*

Citation:
Goedert M, Yamaguchi Y, Mishra SK, Higuchi M and Sahara N (2018) Tau Filaments and the Development of Positron Emission Tomography Tracers. Front. Neurol. 9:70. doi: 10.3389/fneur.2018.00070

INTRODUCTION

Neurofibrillary lesions strongly correlate with cognitive deficits, making them an important therapeutic target for Alzheimer's disease (AD) (1, 2). Dominantly inherited mutations in *MAPT*, the Tau gene, cause a form of frontotemporal dementia that can be associated with parkinsonism (FTDP-17T), showing that dysfunction of Tau protein is sufficient to cause neurodegeneration and dementia (3). In FTDP-17T, abundant filamentous Tau inclusions are present in either nerve cells or in both nerve cells and glial cells. Aβ deposits, a defining feature of AD, are not characteristic of FTDP-17T. However, there are many similarities between cases of FTDP-17T and other pure Tauopathies, such as sporadic progressive supranuclear palsy (PSP), corticobasal degeneration (CBD), argyrophilic grain disease (AGD), and Pick's disease, especially with regard to the isoform composition of Tau filaments.

TAU ISOFORMS

Tau is expressed predominantly in the central and peripheral nervous systems, where it is most abundant in nerve cell axons. It belongs to the family of Tau/MAP2/MAP4 microtubule-associated proteins. Tau is natively unfolded with a low content of secondary structure (4, 5). However, long-range contacts between N- and C-termini, as well as between both termini and the repeats (i.e., paperclip conformation), have been described (5, 6). Using single-molecule Förster resonance energy transfer, it has been shown that upon tubulin binding the repeats expand and long-range contacts between both termini and the repeats are reduced (7).

Tau can be divided into an N-terminal domain, a proline-rich region, the repeat region, and a C-terminal domain (2). The N-terminal domain projects away from microtubules (8). Residues 2–18 have been shown to be involved in a signaling cascade that inhibits axonal transport (9). The N-terminal region also binds to the C-terminus of the p150 subunit of the dynactin complex (10). The proline-rich region has seven PXXP motifs, which provide recognition sites for SH3 domain-containing proteins of the Src family of non-receptor tyrosine kinases, such as Fyn (11). Its interaction with Tau may regulate the targeting of Fyn and thereby mediate beta-amyloid-induced toxicity (12). It has been reported that the proline-rich region of Tau also mediates binding to other proteins, including bridging integrator 1 and peptidyl-prolyl *cis/trans* isomerases (13). Interactions between Tau and microtubules are mediated through the repeats and some adjoining sequences (2). Less is known about the role of the C-terminal region. Tau belongs to the family of intrinsically disordered proteins, which have many interaction partners and are commonly implicated in neurodegenerative diseases (14). Theoretical calculations have estimated that more than 70 different binding partners of tau may exist (14).

Six Tau isoforms ranging from 352 to 441 amino acids in length are expressed in adult human brain (**Figure 1A**) (15). They are produced by alternative mRNA splicing of transcripts from *MAPT* and differ by the presence or absence of inserts of 29 or 58 amino acids (encoded by exons 2 and 3 of *MAPT*, with exon 3 being only transcribed in conjunction with exon 2) in the N-terminal half, and the inclusion, or not, of the 31 amino acid microtubule-binding repeat, encoded by exon 10, in the C-terminal half. Inclusion of exon 10 results in the production of three Tau isoforms with four repeats each (4R) and its exclusion in a further three isoforms with three repeats each (3R). The repeats comprise residues 244–368 of Tau, in the numbering of the 441 amino acid isoform. The N-terminal inserts are not believed to play an active role in Tau aggregation, but the insert encoded by exon 10 is important. In adult human brain, similar levels of 3R and 4R Tau are expressed (16), and the finding that a correct isoform ratio is essential for preventing neurodegeneration (17, 18) came as a surprise. Inclusion of exons 2 and 3, giving rise to 2N isoforms, is relatively underrepresented in comparison with inclusion of exon 2 and exclusion of exons 2 and 3, such that 2N, 1N, and 0N Tau isoforms make up 9, 54, and 37% of the total.

Why six Tau isoforms are found in adult human brain is not known. Isoform expression is not conserved between species (19–22). Thus, in adult mouse brains, 4R Tau isoforms are almost exclusively present, whereas adult chicken brains express 3R, 4R, and 5R Tau isoforms. However, what is conserved is the expression of one hyperphosphorylated 3R Tau isoform lacking N-terminal repeats during vertebrate development. In mice the switch from 3R to 4R Tau occurs between postnatal days 9 and 18, with Tau phosphorylation also decreasing during that time (23). However, isoform switching and phosphorylation are regulated differently. Adult Tau isoforms with 4R are better at promoting microtubule assembly and binding to microtubules than the fetal 3R Tau isoform (16). This is consistent with the need for a more dynamic cytoskeleton during the development of nerve cells.

The repeats and some adjoining sequences constitute the microtubule-binding domains of Tau. Single-molecule tracking revealed a kiss-and-hop mechanism, with a dwell time of Tau on individual microtubules of only about 40 ms (24, 25). Isoform differences did not influence this interaction. Despite these rapid dynamics, Tau promoted microtubule assembly. It remains to be seen if microtubules were also stabilized. In brain, Tau is subject to a large number of posttranslational modifications, including phosphorylation, acetylation, methylation, glycation, isomerization, *O*-GlcNAcylation, nitration, sumoylation, ubiquitination, and truncation (26–28). Big Tau, which carries an additional large exon in the N-terminal half, is only expressed in the peripheral nervous system (29, 30). Several structural models have been put forward for the binding of Tau to microtubules (31–33), but there is no consensus. Overall, it appears that the microtubule-bound conformation of Tau may delay aggregation. Cryogenic electron microscopy (cryo-EM) is bound to provide atomic structures of Tau bound to microtubules that were assembled from tubulin in different ways (34).

TAU FILAMENTS

Full-length Tau assembles into filaments through its repeats, with the N-terminal half and the C-terminus forming the fuzzy coat (35–38). Tau filaments from human brain and those assembled from expressed protein have a cross-β structure characteristic of amyloid fibrils, with their cores consisting of approximately 90 amino acids (39). The region of Tau that binds to microtubules also forms the core of Tau filaments, suggesting that physiological function and pathological assembly are mutually exclusive.

Phosphorylation of Tau negatively regulates its ability to interact with microtubules, and filamentous Tau is abnormally hyperphosphorylated (40). However, it remains to be proved that phosphorylation is the trigger for aggregation in human diseases. Alternatively, a conformational change in Tau arising from assembly may cause its hyperphosphorylation. Recombinant Tau assembles in bulk into filaments when incubated with heparin, in the absence of phosphorylation (41, 42). However, it has also been shown that recombinant S262A 4R Tau assembled into filaments following incubation with brain extracts from adult rats (43). Other posttranslational modifications may also be involved. Initial studies on Tau acetylation reported that it promoted phosphorylation and aggregation (44, 45). However, subsequent work has suggested that an inverse correlation exists between Tau acetylation and phosphorylation, with acetylation inhibiting Tau assembly (46, 47). Unlike phosphorylation, acetylation occurs on lysine residues, as do glycation, ubiquitination, and methylation.

Many publications equate Tau phosphorylation with aggregation. This is probably not correct. Although aggregated Tau is heavily phosphorylated in human brain, not all phosphorylated Tau is aggregated or on its way to aggregation. For instance, highly phosphorylated Tau forms during hibernation, in the absence of aggregation (48). There is substantial overlap between the phosphorylation of Tau during development and its hyperphosphorylation in disease. However, some Tau phosphorylation, such as that at T212, S214, and T217 detected by antibody AT100, is pathological (49). Antibody AT8 has been used to detect both

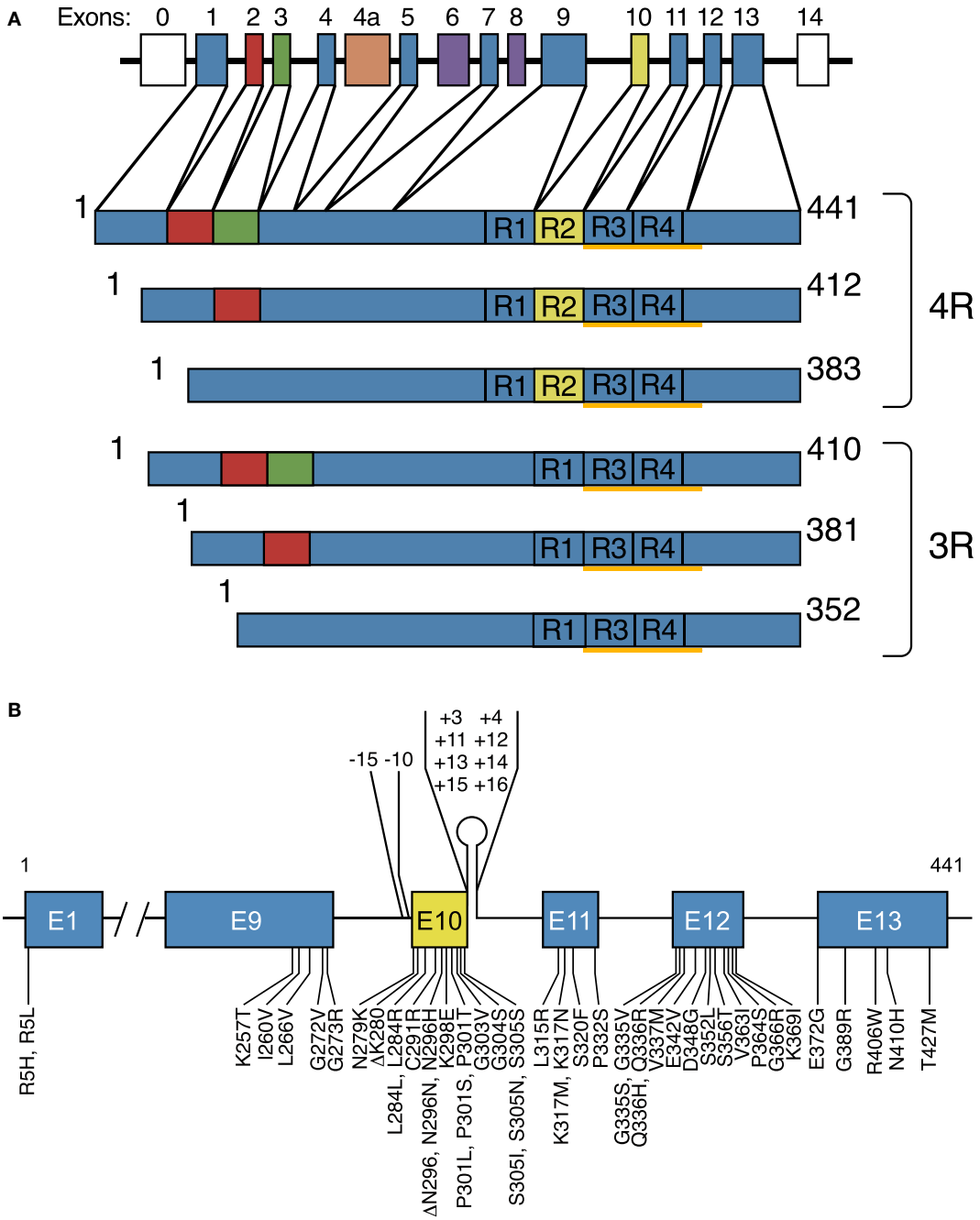

FIGURE 1 | Human brain Tau isoforms and disease-causing *MAPT* mutations. **(A)** *MAPT* and the six Tau isoforms expressed in adult human brain. *MAPT* consists of 16 exons (E). Alternative mRNA splicing of E2 (red), E3 (green), and E10 (yellow) gives rise to six Tau isoforms (352–441 amino acids). The constitutively spliced exons (E1, E4, E5, E7, E9, E11, E12, and E13) are shown in blue. E0, which is part of the promoter, and E14 are non-coding (white). E6 and E8 (violet) are not transcribed in human brain. E4a (orange) is only expressed in the peripheral nervous system. The repeats (R1–R4) are shown, with three isoforms having four repeats each (4R) and three isoforms having three repeats each (3R). The core sequences of the Tau filaments from Alzheimer's disease brain (V306-F378) determined by cryo-EM are underlined. **(B)**, Mutations in *MAPT* in cases of frontotemporal dementia and parkinsonism linked to chromosome 17 (FTDP-17T). Forty-nine coding region mutations and 10 intronic mutations flanking E10 are shown.

physiologically and pathologically phosphorylated Tau. It was recently shown that it recognizes triply phosphorylated Tau (S202, T205, and S208) better than doubly phosphorylated protein (S202 andT205), raising the possibility of differential phosphorylation of pathologically and physiologically phosphorylated Tau at the AT8 epitope (50).

In AD, chronic traumatic encephalopathy, postencephalitic parkinsonism, and many other Tauopathies, all six isoforms are

present in the disease filaments (**Table 1**) (2). They are either paired helical (PHFs) or straight (SFs) and contain both 3R and 4R Tau isoforms in a one-to-one ratio, similar to the isoform composition and relative abundance of the six isoforms in soluble Tau from normal human brain. By cryo-EM, the cores of Tau filaments from AD are made of two identical protofilaments consisting of residues V306-F378 of Tau, which adopt a combined cross-β/β-helix structure, possibly defining the seed for Tau aggregation (51). The N-terminal part of the cross-β structure is formed by the hexapeptide ^{306}VQIVYK^{311} (PHF6), which is essential for the oligomerization of Tau and its assembly into filaments (52, 53). It packs through a heterotypic, non-staggered interface with the opposing residues 373–378. The same packing interface is absent in the widely used K18 and K19 proteins, which span three or four repeat domains of recombinantly expressed Tau, and end at E372 (54). Therefore, filaments made of K18 and K19 proteins cannot represent the complete core structure of PHFs and SFs from the brains of individuals with AD. The second hexapeptide motif ^{275}VQIINK^{280} (PHF6*) that is required for filament assembly (55) does not form part of the core of Tau filaments from AD brain. However, inhibitors of the PHF6* motif have been shown to reduce the heparin-induced assembly of 4R Tau (56). Both hexapeptide motifs were required for the seeded aggregation of mutant human Tau in transfected non-neuronal cells (57). It remains to be seen if PHF6 and PHF6* are required for the assembly of Tau in human brain.

TABLE 1 | Neurodegenerative diseases with abundant tau inclusions.

3R + 4R Tauopathies
Alzheimer's disease
Amyotrophic lateral sclerosis/parkinsonism-dementia complex
Anti-IgLON5-related Tauopathy
Chronic traumatic encephalopathy
Diffuse neurofibrillary tangles with calcification
Down's syndrome
Familial British dementia
Familial Danish dementia
Gerstmann–Sträussler–Scheinker disease
Niemann–Pick disease, type C
Non-Guamanian motor neuron disease with neurofibrillary tangles
Postencephalitic parkinsonism
Progressive ataxia and palatal tremor
Tangle-only dementia
Familial frontotemporal dementia and parkinsonism (some *MAPT* mutations, such as V337M and R406W)
3R Tauopathies
Pick's disease
Familial frontotemporal dementia and parkinsonism (some *MAPT* mutations, such as G272V and Q336R)
4R Tauopathies
Argyrophilic grain disease
Corticobasal degeneration
Guadeloupean parkinsonism
Globular glial Tauopathy
Huntington's disease
Progressive supranuclear palsy
SLC9A6-related parkinsonism
Tau astrogliopathy
Familial frontotemporal dementia and parkinsonism (some *MAPT* mutations, such as P301L and P301S, all known intronic mutations, and many coding region mutations in exon 10)

Each protofilament contains eight β-strands, five of which give rise to two pairs of anti-parallel β-sheets, with the other three forming a β-helix. PHFs and SFs differ in their inter-protofilament packing, showing that they are ultrastructural polymorphs. The protofilaments of PHFs are arranged base-to-base, whereas those of SFs are arranged back-to-base. These findings do not explain why all six Tau isoforms are found in PHFs and SFs. However, a less ordered β-sheet is present upstream of V306; it can accommodate an additional 16 amino acids, which probably correspond to a mixture of residues 259–274 (R1) from 3R Tau and 290–305 (R2) from 4R Tau.

In other diseases, such as PSP, CBD, AGD, globular glial Tauopathy, and aging-related Tau astrogliopathy, isoforms with 4R Tau are found in the filaments (**Table 1**) (3), but the presence of 3R Tau-positive neuronal inclusions has also been reported in PSP and CBD (58, 59). The Pick bodies of Pick's disease are only made of 3R Tau (**Table 1**) (60). The morphologies of Tau filaments in different diseases vary, even when they are made of the same isoforms. Silver staining can also detect these differences (61). Inclusions made of all six Tau isoforms stain with Gallyas–Braak and Campbell–Switzer. Those made of 4R Tau are only positive with Gallyas–Braak, whereas those made of 3R Tau stain only with Campbell–Switzer. It remains to be seen if the cores of filaments made of 3R or 4R Tau differ structurally from those of AD, which are made of 3R + 4R Tau isoforms.

The specificity of antibodies Alz50 and MC-1 for assembled Tau relies on a conformation that all isoforms can undergo and which requires two discontinuous intramolecular epitopes separated by almost 300 amino acids (62, 63). They are ^{7}EFE^{9} in the N-terminus and ^{313}VDLSKVTSKC^{322} in R3. MC-1 staining is one of the earliest markers of misfolded Tau. NMR experiments using heparin-induced filaments of 4R Tau also provided evidence for an interaction between the N-terminus and residues 313–322 of the structured core (64). Moreover, the cryo-EM structures of Tau filaments from AD brain showed a density consistent with ^{7}EFE^{9} contacting K317 and K321 in the protofilament core (51). These electrostatic interactions may be essential for Tau filament formation, implying that acetylation of K317 and/or K321 might protect against aggregation. The only known disease-causing mutations in *MAPT* that are located outside the repeats and the C-terminus (R5H and R5L) (3) are close to ^{7}EFE^{9}.

Fifty-nine different mutations in *MAPT* have been identified in FTDP-17T (**Figure 1B**) (3). The filaments consist of 3R, 4R, or 3R + 4R Tau (**Figure 2**) (65). *MAPT* mutations account for approximately 5% of cases of frontotemporal dementia and are concentrated in exons 9–12 (encoding R1–R4) and the introns flanking exon 10. They can be divided into those with a primary effect at the protein level and those affecting the alternative splicing of Tau pre-mRNA. There is no obvious correlation between known mutations and posttranslational modifications of Tau.

It has been suggested that patients with AD-type neurofibrillary degeneration restricted to hippocampus and medial temporal lobe, who lack Aβ deposits, suffer from primary age-related Tauopathy (PART), a condition that differs from AD (70). Tangle-only dementia, a rare form of dementia, may represent a severe form of PART (71). However, the view that PART is

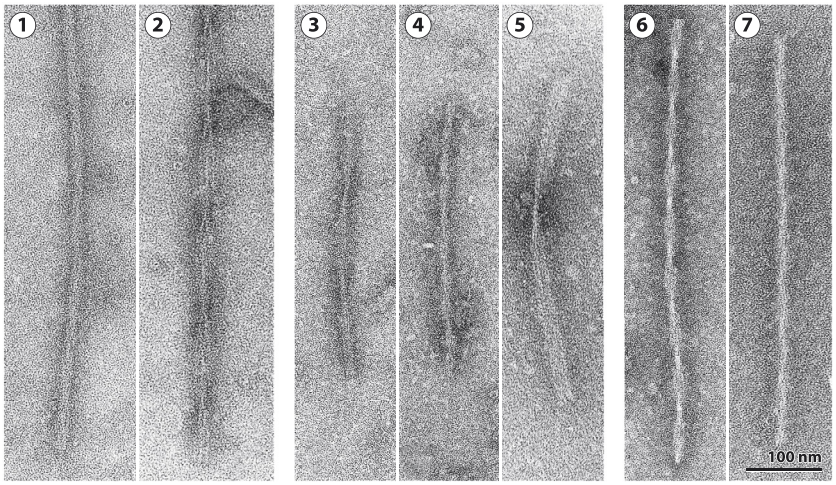

FIGURE 2 | Tau filaments from FTDP-17T. [1,2] Neuronal Tau filaments from a case with abundant Pick body-like inclusions and a G389R mutation in *MAPT* (66). [1] Straight filaments form the majority species and [2] strongly stranded twisted filaments are in the minority. [3–5] Tau filaments from cases with neuronal and glial inclusions and a P301L mutation in *MAPT* or an intronic mutation [from Ref. (67, 68)]. [3] Narrow twisted ribbons and [4] occasional rope-like filaments. [5] Familial multiple system Tauopathy with presenile dementia and other cases caused by *MAPT* mutations in the intron after E10 are characterized by wide twisted ribbons and neuronal and glial Tau inclusions. The filaments in [3–5] are made of 4R Tau. [6,7] Tau filaments from a case with a V337M mutation in *MAPT* [from Ref. (69)]. [6] Paired helical and [7] straight filaments are present as in Alzheimer's disease. Tau inclusions are largely neuronal, and filaments in [6] and [7] are made of 3R and 4R Tau.

different from AD has been challenged, because it is clinically and neuropathologically similar to what appear to be the early stages of the Tau pathology of AD (72).

In AD, following the death of tangle-bearing cells, Tau filaments can remain in the extracellular space as ghost tangles, which consist largely of Tau repeats that have lost their fuzzy coat through proteolysis. In Pick's disease, PSP, CBD, and most cases caused by *MAPT* mutations, Tau filaments do not accumulate to a significant extent in the extracellular space following the death of aggregate-bearing cells. The reasons why Tau filaments from AD brain are less soluble remain to be established (2).

TAU AGGREGATE-BINDING LIGANDS AND THE DEVELOPMENT OF POSITRON EMISSION TOMOGRAPHY (PET) TRACERS

Monomeric Tau assembles into filaments through oligomerization (1, 2). In tissue sections, filamentous Tau aggregates are labeled by amyloid-binding dyes, such as Congo red, thioflavins, and some luminescent conjugated oligothiophenes (2, 73). These dyes appear to bind to both intra- and extracellular Tau deposits. They are useful for cross-sectional studies but require the availability of brain tissue.

To perform longitudinal studies and to assess the effects of treatments on the level of aggregates, one needs to be able to visualize Tau inclusions repeatedly in the living human nervous system. The field of PET imaging of brain inclusions characteristic of human neurodegenerative diseases started with the development of [^{11}C]Pittsburgh compound B ([^{11}C]PIB), a derivative of thioflavin T, which detects β-amyloid deposits in the living brain (74). Subsequently, several PET tracers for aggregated Tau, such as [^{11}C]PBB3, [^{18}F]PM-PBB3, [^{18}F]AV-1451, [^{18}F]THK5351, [^{18}F]MK-6240, [^{18}F]R06958948, [^{18}F]GTP-1, and [^{18}F]PI-2620, were developed and are currently being tested in humans (75–81). Most tracers show a high affinity for Tau inclusions and recognize β-amyloid deposits less well (79, 81). However, some off-target effects have also been described. Thus, non-specific retention of [^{11}C]PBB3 was seen in the dural venous sinuses (75). *In vitro* studies have shown that [^{18}F]AV-1451 can bind to monoamine oxidase (MAO)-A, as well as to pigmented and mineralized vascular structures (82). Retention of [^{18}F]AV-1451 in the choroid plexus of control individuals also reflected off-target binding (83). Age-related, off-target effects of [^{18}F]AV-1451 binding in the basal ganglia closely correlated with iron accumulation (84). Selegiline, a MAO-B inhibitor, reduced [^{18}F]THK5351 signal in basal ganglia and neocortex (85). Moreover, an *in vitro* study confirmed that MAO-B was an off-target binding substrate for [^{18}F]THK5351 (86). Perhaps most worryingly, elevated binding of [^{18}F]AV-1451 and [^{18}F]THK5351 has been described in the semantic variant of primary progressive aphasia, a form of frontotemporal dementia that is consistently associated with assembled TDP-43, but not with Tau inclusions (87–89). Where studied, second generation Tau PET tracers ([^{18}F]PM-PBB3, [^{18}F]MK-6240, [^{18}F]R06958948, [^{18}F]GTP-1, and [^{18}F]Pl-2620) have shown less off-target binding than the first generation of tracers. Future autopsy studies are needed to identify the binding targets of these ligands. On the other hand, the distribution of [^{18}F]AV-1451 binding, a first generation tracer, recapitulated Braak staging in AD brain (90). Moreover, a combination of PET imaging with [^{18}F]AV-1451 and graph theory supported the view that

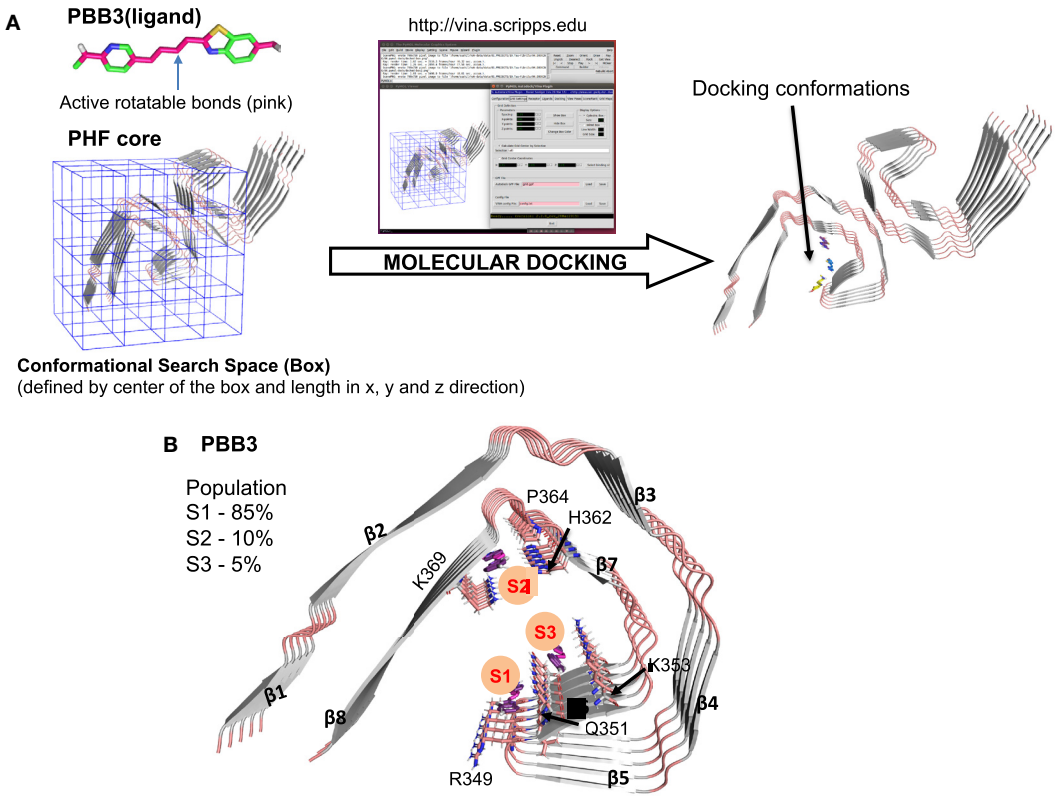

FIGURE 3 | Molecular docking of PBB3 to paired helical Tau filaments (PHFs) from Alzheimer's disease brain. **(A)** Schematic representation of the docking process using Pymol and AutoDock Vina. The PHF core structure was from Ref. (51) (PDB ID: 503L). Out of 100 docking conformations, the top 20 were selected for further analysis. **(B)** Molecular docking of PBB3 into the PHF protofilament core structure. The top 20 conformations distributed into three clusters (S1, S2, and S3). S1 had the highest affinity for the Tau filament, followed by S2 and S3.

tau pathology can undergo transneuronal spread (91), consistent with experimental studies (92, 93).

To develop more specific and selective ligands, it is important to determine where in the structured cores of Tau filaments PET ligands bind. Recent advances in cryo-EM, which have resulted in the determination of the high-resolution structures of Tau filaments from AD brain (51), have made this possible in principle. We used this information, together with molecular docking (94), to study the binding of PBB3 to the protofilament core of Tau filaments from AD (**Figure 3A**). As shown in **Figure 3**, PBB3 bound in a perpendicular manner to a high-affinity site (S1) in the C-shaped part of the protofilament, which includes residues 349–351 (RVQ) of Tau (**Figure 3B**). Two lower affinity binding sites were also detected, at residues 364–369 (PGGGNK) (S2) and 351–353 (QSK) (S3) (**Figure 3B**).

PBB3 visualizes the Tau pathologies of AD and non-AD Tauopathies (75, 95, 96). Unlike PBB3, previous *in vitro* and *in vivo* studies have shown that AV-1451 binds only with low-affinity to filaments from non-AD Tauopathies (95, 97, 98). It has been reported that AV-1451 and its lead compound failed to visualize Tau inclusions in a mouse line transgenic for human P301L Tau (76). However, using [^{11}C]PBB3, it was possible to image Tau inclusions in mouse models of Tauopathy (lines PS19 and Tg4510) (75, 99). These findings further support the view that AV-1451 recognizes Tau inclusions made of 3R or 4R Tau with lower affinity than those made of 3R + 4R Tau. It will be interesting to obtain cryo-EM structures of the cores of Tau filaments from AD and other Tauopathies with bound PET ligands. One cannot exclude that high-affinity binding sites exist in the "fuzzy coat" of human brain Tau filaments. However, both AV-1451 and PBB3 have been shown to detect extracellular Tau inclusions in AD brain (95). We believe that the aggregated Tau in extracellular tangles corresponds closely to the structured filament cores.

CONCLUSION

The determination of high-resolution structures of Tau filaments by cryo-EM has opened the way for elucidating the structures of other amyloid filaments from human brain. Future work will tell what the differences between morphotypes of amyloid filaments are, which will in turn inform the mechanisms underlying the prion-like propagation of protein aggregates. Perhaps most importantly, cryo-EM will make it possible to relate mechanisms of amyloid formation of recombinant proteins to those in human brain.

AUTHOR CONTRIBUTIONS

MG and NS wrote the manuscript; YY and SM analyzed the molecular docking simulation; and MH critiqued the manuscript.

FUNDING

MG is an Honorary Professor in the Department of Clinical Neurosciences of the University of Cambridge, UK. This work was supported by the UK Medical Research Council (MC_U105184291 to MG) and the European Union (Joint Programme-Neurodegeneration Research REfrAME to MG and Horizon 2020 IMPRiND to MG). This work was also supported by grants from the Japanese Ministry of Education, Culture, Sports, Science and Technology (26117001 and 15K06793 to NS) and the Strategic Research Program for Brain Sciences of the Japan Agency for Medical Research and Development (to NS). MH holds a patent on compounds including PBB3 (JP 5422782/EP 12 844 742.3).

REFERENCES

1. Sahara N, Avila J. "Tau oligomers," what we know and what we don't know. *Front Neurol* (2014) 5:1. doi:10.3389/fneur.2014.00001
2. Goedert M, Eisenberg DS, Crowther RA. Propagation of Tau aggregates and neurodegeneration. *Annu Rev Neurosci* (2017) 40:189–210. doi:10.1146/annurev-neuro-072116-031153
3. Ghetti B, Oblak AL, Boeve BF, Johnson KA, Dickerson BC, Goedert M. Invited review: frontotemporal dementia caused by microtubule-associated protein tau gene (MAPT) mutations: a chameleon for neuropathology and neuroimaging. *Neuropathol Appl Neurobiol* (2015) 41:24–46. doi:10.1111/nan.12213
4. Cleveland DW, Hwo SY, Kirschner MW. Physical and chemical properties of purified tau factor and the role of tau in microtubule assembly. *J Mol Biol* (1977) 116:227–47. doi:10.1016/0022-2836(77)90214-5
5. Jeganathan S, von Bergen M, Brutlach H, Steinhoff HJ, Mandelkow E. Global hairpin folding of tau in solution. *Biochemistry* (2006) 45:2283–93. doi:10.1021/bi0521543
6. Wang Y, Mandelkow E. Tau in physiology and pathology. *Nat Rev Neurosci* (2016) 17:5–21. doi:10.1038/nrn.2015.1
7. Melo AM, Coraor J, Alpha-Cobb G, Elbaum-Garfinkle S, Nath A, Rhoades E. A functional role for intrinsic disorder in the tau-tubulin complex. *Proc Natl Acad Sci U S A* (2016) 113:14336–41. doi:10.1073/pnas.1610137113
8. Chen J, Kanai Y, Cowan NJ, Hirokawa N. Projection domains of MAP2 and tau determine spacings between microtubules in dendrites and axons. *Nature* (1992) 360:674–7. doi:10.1038/360674a0
9. Kanaan NM, Morfini GA, Lapointe NE, Pigino GF, Patterson KR, Song Y, et al. Pathogenic forms of tau inhibit kinesin-dependent axonal transport through a mechanism involving activation of axonal phosphotransferases. *J Neurosci* (2011) 31:9858–68. doi:10.1523/JNEUROSCI.0560-11.2011
10. Magnani E, Fan J, Gasparini L, Golding M, Williams M, Schiavo G, et al. Interaction of tau protein with the dynactin complex. *EMBO J* (2007) 26:4546–54. doi:10.1038/sj.emboj.7601878
11. Lee G, Newman ST, Gard DL, Band H, Panchamoorthy G. Tau interacts with src-family non-receptor tyrosine kinases. *J Cell Sci* (1998) 111(Pt 21):3167–77.
12. Ittner LM, Ke YD, Delerue F, Bi M, Gladbach A, Van Eersel J, et al. Dendritic function of tau mediates amyloid-beta toxicity in Alzheimer's disease mouse models. *Cell* (2010) 142:387–97. doi:10.1016/j.cell.2010.06.036
13. Morris M, Maeda S, Vossel K, Mucke L. The many faces of tau. *Neuron* (2011) 70:410–26. doi:10.1016/j.neuron.2011.04.009
14. Uversky VN. Intrinsically disordered proteins and their (disordered) proteomes in neurodegenerative disorders. *Front Aging Neurosci* (2015) 7:18. doi:10.3389/fnagi.2015.00018
15. Goedert M, Spillantini MG, Jakes R, Rutherford D, Crowther RA. Multiple isoforms of human microtubule-associated protein tau: sequences and localization in neurofibrillary tangles of Alzheimer's disease. *Neuron* (1989) 3:519–26. doi:10.1016/0896-6273(89)90210-9
16. Goedert M, Jakes R. Expression of separate isoforms of human tau protein: correlation with the tau pattern in brain and effects on tubulin polymerization. *EMBO J* (1990) 9:4225–30.
17. Hutton M, Lendon CL, Rizzu P, Baker M, Froelich S, Houlden H, et al. Association of missense and 5'-splice-site mutations in tau with the inherited dementia FTDP-17. *Nature* (1998) 393:702–5. doi:10.1038/31508
18. Spillantini MG, Murrell JR, Goedert M, Farlow MR, Klug A, Ghetti B. Mutation in the tau gene in familial multiple system tauopathy with presenile dementia. *Proc Natl Acad Sci U S A* (1998) 95:7737–41. doi:10.1073/pnas.95.13.7737
19. Kosik KS, Orecchio LD, Bakalis S, Neve RL. Developmentally regulated expression of specific tau sequences. *Neuron* (1989) 2:1389–97. doi:10.1016/0896-6273(89)90077-9
20. Janke C, Beck M, Stahl T, Holzer M, Brauer K, Bigl V, et al. Phylogenetic diversity of the expression of the microtubule-associated protein tau: implications for neurodegenerative disorders. *Brain Res Mol Brain Res* (1999) 68:119–28. doi:10.1016/S0169-328X(99)00079-0
21. Yoshida H, Goedert M. Molecular cloning and functional characterization of chicken brain tau: isoforms with up to five tandem repeats. *Biochemistry* (2002) 41:15203–11. doi:10.1021/bi026464m
22. Takuma H, Arawaka S, Mori H. Isoform changes of tau protein during development in various species. *Brain Res Dev Brain Res* (2003) 142:121–7. doi:10.1016/S0165-3806(03)00056-7
23. Tuerde D, Kimura T, Miyasaka T, Furusawa K, Shimozawa A, Hasegawa M, et al. Isoform-independent and -dependent phosphorylation of microtubule-associated protein tau in mouse brain during postnatal development. *J Biol Chem* (2018) 293:1781–93. doi:10.1074/jbc.M117.798918
24. Janning D, Igaev M, Sündermann F, Bruhmann J, Beutel O, Heinisch JJ, et al. Single-molecule tracking of tau reveals fast kiss-and-hop interaction with microtubules in living neurons. *Mol Biol Cell* (2014) 25:3541–51. doi:10.1091/mbc.E14-06-1099
25. Niewidok B, Igaev M, Sündermann F, Janning D, Bakota L, Brandt R. Presence of a carboxy-terminal pseudorepeat and disease-like pseudohyperphosphorylation critically influence tau's interaction with microtubules in axon-like processes. *Mol Biol Cell* (2016) 27:3537–49. doi:10.1091/mbc.E16-06-0402
26. Spillantini MG, Goedert M. Tau pathology and neurodegeneration. *Lancet Neurol* (2013) 12:609–22. doi:10.1016/S1474-4422(13)70090-5
27. Morris M, Knudsen GM, Maeda S, Trinidad JC, Ioanoviciu A, Burlingame AL, et al. Tau post-translational modifications in wild-type and human amyloid precursor protein transgenic mice. *Nat Neurosci* (2015) 18:1183–9. doi:10.1038/nn.4067
28. Mair W, Muntel J, Tepper K, Tang S, Biernat J, Seeley WW, et al. FLEXITau: quantifying post-translational modifications of Tau protein in vitro and in human disease. *Anal Chem* (2016) 88:3704–14. doi:10.1021/acs.analchem.5b04509
29. Couchie D, Mavilia C, Georgieff IS, Liem RK, Shelanski ML, Nunez J. Primary structure of high molecular weight tau present in the peripheral nervous system. *Proc Natl Acad Sci U S A* (1992) 89:4378–81. doi:10.1073/pnas.89.10.4378
30. Goedert M, Spillantini MG, Crowther RA. Cloning of a big tau microtubule-associated protein characteristic of the peripheral nervous system. *Proc Natl Acad Sci U S A* (1992) 89:1983–7. doi:10.1073/pnas.89.5.1983
31. Al-Bassam J, Ozer RS, Safer D, Halpain S, Milligan RA. MAP2 and tau bind longitudinally along the outer ridges of microtubule protofilaments. *J Cell Biol* (2002) 157:1187–96. doi:10.1083/jcb.200201048
32. Kar S, Fan J, Smith MJ, Goedert M, Amos LA. Repeat motifs of tau bind to the insides of microtubules in the absence of taxol. *EMBO J* (2003) 22:70–7. doi:10.1093/emboj/cdg001
33. Kadavath H, Höfele RV, Biernat J, Kumar S, Tepper K, Urlaub H, et al. Tau stabilizes microtubules by binding at the interface between tubulin heterodimers. *Proc Natl Acad Sci U S A* (2015) 112:7501–6. doi:10.1073/pnas.1504081112
34. Nogales E, Kellogg EH. Challenges and opportunities in the high-resolution cryo-EM visualization of microtubules and their binding partners. *Curr Opin Struct Biol* (2017) 46:65–70. doi:10.1016/j.sbi.2017.06.003
35. Goedert M, Wischik CM, Crowther RA, Walker JE, Klug A. Cloning and sequencing of the cDNA encoding a core protein of the paired helical filament

of Alzheimer disease: identification as the microtubule-associated protein tau. *Proc Natl Acad Sci U S A* (1988) 85:4051–5. doi:10.1073/pnas.85.11.4051
36. Wischik CM, Novak M, Edwards PC, Klug A, Tichelaar W, Crowther RA. Structural characterization of the core of the paired helical filament of Alzheimer disease. *Proc Natl Acad Sci U S A* (1988) 85:4884–8.
37. Wischik CM, Novak M, Thogersen HC, Edwards PC, Runswick MJ, Jakes R, et al. Isolation of a fragment of tau derived from the core of the paired helical filament of Alzheimer disease. *Proc Natl Acad Sci U S A* (1988) 85:4506–10.
38. Lee VM, Balin BJ, Otvos L, Trojanowski JQ. A68: a major subunit of paired helical filaments and derivatized forms of normal Tau. *Science* (1991) 251:675–8. doi:10.1126/science.1899488
39. Berriman J, Serpell LC, Oberg KA, Fink AL, Goedert M, Crowther RA. Tau filaments from human brain and from in vitro assembly of recombinant protein show cross-beta structure. *Proc Natl Acad Sci U S A* (2003) 100:9034–8. doi:10.1073/pnas.1530287100
40. Iqbal K, Liu F, Gong CX. Tau and neurodegenerative disease: the story so far. *Nat Rev Neurol* (2016) 12:15–27. doi:10.1038/nrneurol.2015.225
41. Goedert M, Jakes R, Spillantini MG, Hasegawa M, Smith MJ, Crowther RA. Assembly of microtubule-associated protein tau into Alzheimer-like filaments induced by sulphated glycosaminoglycans. *Nature* (1996) 383:550–3. doi:10.1038/383550a0
42. Perez M, Valpuesta JM, Medina M, Montejo De Garcini E, Avila J. Polymerization of tau into filaments in the presence of heparin: the minimal sequence required for tau-tau interaction. *J Neurochem* (1996) 67:1183–90. doi:10.1046/j.1471-4159.1996.67031183.x
43. Despres C, Byrne C, Qi H, Cantrelle FX, Huvent I, Chambraud B, et al. Identification of the Tau phosphorylation pattern that drives its aggregation. *Proc Natl Acad Sci U S A* (2017) 114:9080–5. doi:10.1073/pnas.1708448114
44. Min SW, Cho SH, Zhou Y, Schroeder S, Haroutunian V, Seeley WW, et al. Acetylation of tau inhibits its degradation and contributes to tauopathy. *Neuron* (2010) 67:953–66. doi:10.1016/j.neuron.2010.08.044
45. Cohen TJ, Guo JL, Hurtado DE, Kwong LK, Mills IP, Trojanowski JQ, et al. The acetylation of tau inhibits its function and promotes pathological tau aggregation. *Nat Commun* (2011) 2:252. doi:10.1038/ncomms1255
46. Cook C, Carlomagno Y, Gendron TF, Dunmore J, Scheffel K, Stetler C, et al. Acetylation of the KXGS motifs in tau is a critical determinant in modulation of tau aggregation and clearance. *Hum Mol Genet* (2014) 23:104–16. doi:10.1093/hmg/ddt402
47. Carlomagno Y, Chung DC, Yue M, Castanedes-Casey M, Madden BJ, Dunmore J, et al. An acetylation-phosphorylation switch that regulates tau aggregation propensity and function. *J Biol Chem* (2017) 292:15277–86. doi:10.1074/jbc.M117.794602
48. Arendt T, Stieler J, Strijkstra AM, Hut RA, Rüdiger J, Van Der Zee EA, et al. Reversible paired helical filament-like phosphorylation of tau is an adaptive process associated with neuronal plasticity in hibernating animals. *J Neurosci* (2003) 23:6972–81.
49. Yoshida H, Goedert M. Sequential phosphorylation of tau protein by cAMP-dependent protein kinase and SAPK4/p38delta or JNK2 in the presence of heparin generates the AT100 epitope. *J Neurochem* (2006) 99:154–64. doi:10.1111/j.1471-4159.2006.04052.x
50. Malia TJ, Teplyakov A, Ernst R, Wu SJ, Lacy ER, Liu X, et al. Epitope mapping and structural basis for the recognition of phosphorylated tau by the anti-tau antibody AT8. *Proteins* (2016) 84:427–34. doi:10.1002/prot.24988
51. Fitzpatrick AWP, Falcon B, He S, Murzin AG, Murshudov G, Garringer HJ, et al. Cryo-EM structures of tau filaments from Alzheimer's disease. *Nature* (2017) 547:185–90. doi:10.1038/nature23002
52. Von Bergen M, Friedhoff P, Biernat J, Heberle J, Mandelkow EM, Mandelkow E. Assembly of tau protein into Alzheimer paired helical filaments depends on a local sequence motif (^{306}VQIVYK^{311}) forming beta structure. *Proc Natl Acad Sci U S A* (2000) 97:5129–34. doi:10.1073/pnas.97.10.5129
53. Sahara N, Maeda S, Murayama M, Suzuki T, Dohmae N, Yen SH, et al. Assembly of two distinct dimers and higher-order oligomers from full-length tau. *Eur J Neurosci* (2007) 25:3020–9. doi:10.1111/j.1460-9568.2007.05555.x
54. Gustke N, Trinczek B, Biernat J, Mandelkow EM, Mandelkow E. Domains of tau protein and interactions with microtubules. *Biochemistry* (1994) 33:9511–22. doi:10.1021/bi00198a017
55. Von Bergen M, Barghorn S, Li L, Marx A, Biernat J, Mandelkow EM, et al. Mutations of tau protein in frontotemporal dementia promote aggregation of paired helical filaments by enhancing local beta-structure. *J Biol Chem* (2001) 276:48165–74. doi:10.1074/jbc.M105196200
56. Seidler PM, Boyer DR, Rodriguez JA, Sawaya MR, Cascio D, Murray K, et al. Structure-based inhibitors of tau aggregation. *Nat Chem* (2018) 10(2):170–6. doi:10.1038/nchem.2889
57. Falcon B, Cavallini A, Angers R, Glover S, Murray TK, Barnham L, et al. Conformation determines the seeding potencies of native and recombinant Tau aggregates. *J Biol Chem* (2015) 290:1049–65. doi:10.1074/jbc.M114.589309
58. Uchihara T, Nakamura A, Shibuya K, Yagishita S. Specific detection of pathological three-repeat tau after pretreatment with potassium permanganate and oxalic acid in PSP/CBD brains. *Brain Pathol* (2011) 21:180–8. doi:10.1111/j.1750-3639.2010.00433.x
59. Uchihara T, Hara M, Nakamura A, Hirokawa K. Tangle evolution linked to differential 3- and 4-repeat tau isoform deposition: a double immunofluorolabeling study using two monoclonal antibodies. *Histochem Cell Biol* (2012) 137:261–7. doi:10.1007/s00418-011-0891-2
60. De Silva R, Lashley T, Strand C, Shiarli AM, Shi J, Tian J, et al. An immunohistochemical study of cases of sporadic and inherited frontotemporal lobar degeneration using 3R- and 4R-specific tau monoclonal antibodies. *Acta Neuropathol* (2006) 111:329–40. doi:10.1007/s00401-006-0048-x
61. Uchihara T, Tsuchiya K, Nakamura A, Akiyama H. Argyrophilic grains are not always argyrophilic-distinction from neurofibrillary tangles of diffuse neurofibrillary tangles with calcification revealed by comparison between Gallyas and Campbell-Switzer methods. *Acta Neuropathol* (2005) 110:158–64. doi:10.1007/s00401-005-1031-7
62. Carmel G, Mager EM, Binder LI, Kuret J. The structural basis of monoclonal antibody Alz50's selectivity for Alzheimer's disease pathology. *J Biol Chem* (1996) 271:32789–95. doi:10.1074/jbc.271.51.32789
63. Jicha GA, Bowser R, Kazam IG, Davies P. Alz-50 and MC-1, a new monoclonal antibody raised to paired helical filaments, recognize conformational epitopes on recombinant tau. *J Neurosci Res* (1997) 48:128–32. doi:10.1002/(SICI)1097-4547(19970415)48:2<128::AID-JNR5>3.0.CO;2-E
64. Bibow S, Mukrasch MD, Chinnathambi S, Biernat J, Griesinger C, Mandelkow E, et al. The dynamic structure of filamentous tau. *Angew Chem Int Ed Engl* (2011) 50:11520–4. doi:10.1002/anie.201105493
65. Crowther RA, Goedert M. Abnormal tau-containing filaments in neurodegenerative diseases. *J Struct Biol* (2000) 130:271–9. doi:10.1006/jsbi.2000.4270
66. Murrell JR, Spillantini MG, Zolo P, Guazzelli M, Smith MJ, Hasegawa M, et al. Tau gene mutation G389R causes a tauopathy with abundant pick body-like inclusions and axonal deposits. *J Neuropathol Exp Neurol* (1999) 58:1207–26. doi:10.1097/00005072-199912000-00002
67. Spillantini MG, Goedert M, Crowther RA, Murrell JR, Farlow MR, Ghetti B. Familial multiple system tauopathy with presenile dementia: a disease with abundant neuronal and glial tau filaments. *Proc Natl Acad Sci U S A* (1997) 94:4113–8. doi:10.1073/pnas.94.8.4113
68. Spillantini MG, Crowther RA, Kamphorst W, Heutink P, Van Swieten JC. Tau pathology in two Dutch families with mutations in the microtubule-binding region of tau. *Am J Pathol* (1998) 153:1359–63. doi:10.1016/S0002-9440(10)65721-5
69. Spillantini MG, Crowther RA, Goedert M. Comparison of the neurofibrillary pathology in Alzheimer's disease and familial presenile dementia with tangles. *Acta Neuropathol* (1996) 92:42–8. doi:10.1007/s004010050487
70. Crary JF, Trojanowski JQ, Schneider JA, Abisambra JF, Abner EL, Alafuzoff I, et al. Primary age-related tauopathy (PART): a common pathology associated with human aging. *Acta Neuropathol* (2014) 128:755–66. doi:10.1007/s00401-014-1349-0
71. Ulrich J, Spillantini MG, Goedert M, Dukas L, Stähelin HB. Abundant neurofibrillary tangles without senile plaques in a subset of patients with senile dementia. *Neurodegeneration* (1992) 1:257–64.
72. Duyckaerts C, Braak H, Brion JP, Buée L, Del Tredici K, Goedert M, et al. PART is part of Alzheimer disease. *Acta Neuropathol* (2015) 129:749–56. doi:10.1007/s00401-015-1390-7
73. Shirani H, Appelqvist H, Back M, Klingstedt T, Cairns NJ, Nilsson KPR. Synthesis of thiophene-based optical ligands that selectively detect tau pathology in Alzheimer's disease. *Chemistry* (2017) 23:17127–35. doi:10.1002/chem.201703846
74. Klunk WE, Engler H, Nordberg A, Wang Y, Blomqvist G, Holt DP, et al. Imaging brain amyloid in Alzheimer's disease with Pittsburgh compound-B. *Ann Neurol* (2004) 55:306–19. doi:10.1002/ana.20009

75. Maruyama M, Shimada H, Suhara T, Shinotoh H, Ji B, Maeda J, et al. Imaging of tau pathology in a tauopathy mouse model and in Alzheimer patients compared to normal controls. *Neuron* (2013) 79:1094–108. doi:10.1016/j.neuron.2013.07.037
76. Xia CF, Arteaga J, Chen G, Gangadharmath U, Gomez LF, Kasi D, et al. [^{18}F] T807, a novel tau positron emission tomography imaging agent for Alzheimer's disease. *Alzheimers Dement* (2013) 9:666–76. doi:10.1016/j.jalz.2012.11.008
77. Hostetler ED, Walji AM, Zeng Z, Miller P, Bennacef I, Salinas C, et al. Preclinical characterization of ^{18}F-MK-6240, a promising PET tracer for in vivo quantification of human neurofibrillary tangles. *J Nucl Med* (2016) 57:1599–606. doi:10.2967/jnumed.115.171678
78. Walji AM, Hostetler ED, Selnick H, Zeng Z, Miller P, Bennacef I, et al. Discovery of 6-(Fluoro-^{18}F)-3-(1H-pyrrolo[2,3-c]pyridin-1-yl)isoquinolin-5-amine ([^{18}F]-MK-6240): a positron emission tomography (PET) imaging agent for quantification of neurofibrillary tangles (NFTs). *J Med Chem* (2016) 59:4778–89. doi:10.1021/acs.jmedchem.6b00166
79. Hall B, Mak E, Cervenka S, Aigbirhio FI, Rowe JB, O'Brien JT. In vivo tau PET imaging in dementia: pathophysiology, radiotracer quantification, and a systematic review of clinical findings. *Ageing Res Rev* (2017) 36:50–63. doi:10.1016/j.arr.2017.03.002
80. Mueller A, Kroth H, Schieferstein H, Berndt M, Oden F, Capotosti F, et al. Preclinical characterization of PI-2620, a novel tau PET tracer for detection of tau in AD and other tauopathies. *Alzheimer Dement* (2017) 13:141–2. doi:10.1016/j.jalz.2017.06.2567
81. Saint-Aubert L, Lemoine L, Chiotis K, Leuzy A, Rodriguez-Vieitez E, Nordberg A. Tau PET imaging: present and future directions. *Mol Neurodegener* (2017) 12:19. doi:10.1186/s13024-017-0162-3
82. Lowe VJ, Curran G, Fang P, Liesinger AM, Josephs KA, Parisi JE, et al. An autoradiographic evaluation of AV-1451 Tau PET in dementia. *Acta Neuropathol Commun* (2016) 4:58. doi:10.1186/s40478-016-0315-6
83. Marquie M, Normandin MD, Vanderburg CR, Costantino IM, Bien EA, Rycyna LG, et al. Validating novel tau positron emission tomography tracer [F-18]-AV-1451 (T807) on postmortem brain tissue. *Ann Neurol* (2015) 78:787–800. doi:10.1002/ana.24517
84. Choi JY, Cho H, Ahn SJ, Lee JH, Ryu YH, Lee MS, et al. Off-target ^{18}F-AV-1451 binding in the basal ganglia correlates with age-related iron accumulation. *J Nucl Med* (2018) 59:117–20. doi:10.2967/jnumed.117.195248
85. Ng KP, Pascoal TA, Mathotaarachchi S, Therriault J, Kang MS, Shin M, et al. Monoamine oxidase B inhibitor, selegiline, reduces ^{18}F-THK5351 uptake in the human brain. *Alzheimers Res Ther* (2017) 9:25. doi:10.1186/s13195-017-0253-y
86. Harada R, Ishiki A, Kai H, Sato N, Furukawa K, Furumoto S, et al. Correlations of ^{18}F-THK5351 PET with post-mortem burden of tau and astrogliosis in Alzheimer's disease. *J Nucl Med* (2017). doi:10.2967/jnumed.117.197426
87. Bevan-Jones WR, Cope TE, Jones PS, Passamonti L, Hong YT, Fryer TD, et al. [(18)F]AV-1451 binding in vivo mirrors the expected distribution of TDP-43 pathology in the semantic variant of primary progressive aphasia. *J Neurol Neurosurg Psychiatry* (2017). doi:10.1136/jnnp-2017-316402
88. Lee H, Seo S, Lee SY, Jeong HJ, Woo SH, Lee KM, et al. [^{18}F]-THK5351 PET Imaging in patients with semantic variant primary progressive aphasia. *Alzheimer Dis Assoc Disord* (2017). doi:10.1097/WAD.0000000000000216
89. Makaretz SJ, Quimby M, Collins J, Makris N, McGinnis S, Schultz A, et al. Flortaucipir tau PET imaging in semantic variant primary progressive aphasia. *J Neurol Neurosurg Psychiatry* (2017). doi:10.1136/jnnp-2017-316409
90. Schwarz AJ, Yu P, Miller BB, Shcherbinin S, Dickson J, Navitsky M, et al. Regional profiles of the candidate tau PET ligand ^{18}F-AV-1451 recapitulate key features of Braak histopathological stages. *Brain* (2016) 139:1539–50. doi:10.1093/brain/aww023
91. Cope TE, Rittman T, Borchert RJ, Jones PS, Vatansever D, Allinson K, et al. Tau burden and the functional connectome in Alzheimer's disease and progressive supranuclear palsy. *Brain* (2018) 141:550–67. doi:10.1093/brain/awx347
92. Clavaguera F, Bolmont T, Crowther RA, Abramowski D, Frank S, Probst A, et al. Transmission and spreading of tauopathy in transgenic mouse brain. *Nat Cell Biol* (2009) 11:909–13. doi:10.1038/ncb1901
93. He Z, Guo JL, Mcbride JD, Narasimhan S, Kim H, Changolkar L, et al. Amyloid-β plaques enhance Alzheimer's brain tau-seeded pathologies by facilitating neuritic plaque tau aggregation. *Nat Med* (2018) 24:29–38. doi:10.1038/nm.4443
94. Trott O, Olson AJ. AutoDock Vina: improving the speed and accuracy of docking with a new scoring function, efficient optimization, and multithreading. *J Comput Chem* (2010) 31:455–61. doi:10.1002/jcc.21334
95. Ono M, Sahara N, Kumata K, Ji B, Ni R, Koga S, et al. Distinct binding of PET ligands PBB3 and AV-1451 to tau fibril strains in neurodegenerative tauopathies. *Brain* (2017) 140:764–80. doi:10.1093/brain/aww339
96. Shimada H, Kitamura S, Shinotoh H, Endo H, Niwa F, Hirano S, et al. Association between Abeta and tau accumulations and their influence on clinical features in aging and Alzheimer's disease spectrum brains: a [^{11}C] PBB3-PET study. *Alzheimers Dement (Amst)* (2017) 6:11–20. doi:10.1016/j.dadm.2016.12.009
97. Marquie M, Normandin MD, Meltzer AC, Siao Tick Chong M, Andrea NV, Anton-Fernandez A, et al. Pathological correlations of [F-18]-AV-1451 imaging in non-Alzheimer tauopathies. *Ann Neurol* (2017) 81:117–28. doi:10.1002/ana.24844
98. Smith R, Schöll M, Honer M, Nilsson CF, Englund E, Hansson O. Tau neuropathology correlates with FDG-PET, but not AV-1451-PET, in progressive supranuclear palsy. *Acta Neuropathol* (2017) 133:149–51. doi:10.1007/s00401-016-1650-1
99. Ishikawa I, Tokunaga M, Maeda J, Minamihisamatsu T, Shimojo M, Takuwa H, et al. In vivo visualization of tau accumulation, microglial activation and brain atrophy in a mouse model of tauopathy rTg4510. *J Alzheimers Dis* (2018) 61:1037–52. doi:10.3233/JAD-170509

Conflict of Interest Statement: The authors declare that the research was conducted in the absence of any commercial or financial relationships that could be construed as a potential conflict of interest.

Advantages of publishing in Frontiers

OPEN ACCESS
Articles are free to read for greatest visibility and readership

FAST PUBLICATION
Around 90 days from submission to decision

HIGH QUALITY PEER-REVIEW
Rigorous, collaborative, and constructive peer-review

TRANSPARENT PEER-REVIEW
Editors and reviewers acknowledged by name on published articles

Frontiers
Avenue du Tribunal-Fédéral 34
1005 Lausanne | Switzerland

Visit us: www.frontiersin.org
Contact us: info@frontiersin.org | +41 21 510 17 00

REPRODUCIBILITY OF RESEARCH
Support open data and methods to enhance research reproducibility

DIGITAL PUBLISHING
Articles designed for optimal readership across devices

FOLLOW US
@frontiersin

IMPACT METRICS
Advanced article metrics track visibility across digital media

EXTENSIVE PROMOTION
Marketing and promotion of impactful research

LOOP RESEARCH NETWORK
Our network increases your article's readership